U.S. DEPARTMENT OF COMMERCE
NATIONAL OCEANIC AND
ATMOSPHERIC ADMINISTRATION

U.S. DEPARTMENT OF ARMY
CORPS OF ENGINEERS

HYDROMETEOROLOGICAL REPORT NO. 59

(SUPERCEDES HYDROMETEOROLOGICAL REPORT NO. 36)

PROBABLE MAXIMUM PRECIPITATION FOR CALIFORNIA

Prepared By

P. Corrigan, D.D. Fenn, D. R. Kluck, and J.L. Vogel
Hydrometeorological Design Studies Center
Office of Hydrology
National Weather Service

Published By
National Weather Service
Silver Spring, MD
February 1999

TABLE OF CONTENTS

LIST OF FIGURES

LIST OF TABLES

PROBABLE MAXIMUM PRECIPITATION FOR CALIFORNIA

P. Corrigan, D.D. Fenn, D. R. Kluck, and J. L. Vogel
Hydrometeorological Design Studies Center
Office of Hydrology
National Weather Service

ABSTRACT

This study provides estimates of general-storm probable maximum precipitation (PMP) for drainages in the state of California for durations of 1 to 72 hours, for areas of 10 to 10,000 mi^2, and during any month of the year. The report also provides estimates of local-storm PMP for durations of 15 minutes to 6 hours in drainages of 1 to 500 mi^2. Step-by-step procedures are given along with example calculations.

Comparisons are made to its predecessors, Hydrometeorological Report No. 36 (1961) and Hydrometeorological Report No. 49 (California area, 1977); to extreme precipitation values from major storms in California; to record-setting rainfalls at individual locations; and to 100-year rainfall frequency values from NOAA Atlas 2 (1973). The comparisons indicate that the PMP estimates of this report are consistent and reasonable.

A computerized storm analysis scheme was developed and implemented to examine 31 major storms. Updated maximum persisting dewpoints and sea surface temperatures were used in the storm analyses. Many of the calculations, comparisons, and analyses involving spatial relations were facilitated by using a geographical information system (GIS). The plates accompanying the report and all of the figures are digital products.

1. INTRODUCTION

1.1 Background

Generalized estimates of probable maximum precipitation (PMP) for Pacific Ocean drainages of California were first published by the National Weather Service (NWS) as Technical Paper No. 38 in 1960, and followed by Hydrometeorological Report No. 36 (1961), which was printed with revisions in October 1969. PMP estimates were provided for general storms from October through April. General-storm estimates of PMP for southeast California (mostly desert) were presented in Hydrometeorological Report No. 49 (1977). Hydrometeorological Report No. 49, which examined the Colorado River and Great Basin Drainages, also provided estimates of local-storm PMP for all of California. None of the reports provided general-storm PMP estimates for most of northeast California. In this report, publications in the Hydrometeorological Report series, such as Hydrometeorological Reports No. 36 and 49, will be abbreviated as HMR 36 and HMR 49.

HMR 36 used a mass-conservation model as a primary tool to develop estimates of general-storm PMP in topographic regions, but was unable to account for local convergence, convection, and synergistic effects caused by natural upper-level seeding of low-level clouds in orographic regions (Browning 1980, Hobbs 1989). This last effect is sometimes called the *seeder-feeder* effect. It is caused by convergence of moisture and upward vertical motion on the windward side of a mountain, with precipitation from the upper levels seeding and feeding (enhancing) the lower levels, resulting in increased precipitation on the ground. Presently, no numerical model of atmospheric processes can completely replicate orographic precipitation, especially quantitative amounts, in a reliable manner, especially for extreme general storms (Cotton and Anthes 1989, Katzfey 1995).

HMR 57 (1994), a recent PMP study for the Pacific Northwest, showed some major differences between general-storm PMP estimates at the California-Oregon border, and local-storm values, especially in the western half of California. In addition, some intense storms that occurred since the publication of HMR 36 had many precipitation amounts that approached, and in a few instances surpassed the PMP estimates given in HMR 36. As a

result, it was decided that PMP estimates for California needed to be examined using new storm data and new techniques for an orographic region, which uses storms as the basis for establishing PMP.

Due to continued and strong interest in the operational products (maps, tables, diagrams, etc.) and techniques developed in this study, expressed to the Hydrometeorological Design Studies Center by some within the hydroelectric and hydrometeorological community, it was decided to present the calculation procedures in a separate report, HMR 58 (1998), prior to release here. Chapter 13 and Appendix 4 of HMR 59 constitute the preponderance of material in HMR 58. Chapters 2 through 9 of the present report provide the rationale for the computational procedures described in HMR 58.

1.2 Authorization

The authorization to develop new PMP estimates for California was given by the United States Army Corps of Engineers Office of Civil Works. Funding for this work was received from the United States Army Corps of Engineers and the Corps of Engineers Los Angeles District Office, South Pacific Division. Appropriations supporting the National Weather Service (NWS) effort were provided through a continuing Memorandum of Understanding between the NWS and the Corps of Engineers (COE). The Bureau of Reclamation (BOR), through its Flood Hydrology Group in Denver, provided insight, ideas, and reviewed the work throughout the study, giving many helpful suggestions and comparisons.

Many review meetings were held from 1992 to 1997 to share the progress being made in the development of California PMP estimates. Regular attendees, known as the Federal Interagency Team, were representatives of the COE (Office of the Chief Engineer, South Pacific Division, and the Los Angeles and Sacramento Districts of the South Pacific Division), BOR, Federal Energy Regulatory Commission, and the NWS. Many comments and suggestions made by this group improved the final estimates presented in this report.

1.3 PMP Definition and Philosophy

The PMP definition used for this report was given in HMR 55A (1988) as

"theoretically, the greatest depth of precipitation for a given duration that is physically possible over a given storm area at a particular geographical location at a certain time of the year." This is slightly different from the previous definition (American Meteorological Society 1959), which was used in HMR 36. The HMR 36 definition stressed that the estimate was for a particular drainage area. The current definition is more generalized, and emphasizes the control the atmosphere has over a broad geographic region. At the same time, the techniques from this report provide estimates of PMP for specific basins.

Intense storms are the building blocks of PMP estimations (Schreiner and Riedel 1978, Hansen et al. 1988, Vogel 1993, Hansen et al. 1994). Precipitation totals from the most intense storms of a region represent the lowest potential levels of PMP, and provide a first measure of an optimum set of atmospheric moisture and dynamics that can produce intense precipitation rates and amounts. A basic assumption is that the record of intense storms is sufficiently large that an efficient *storm mechanism* has been identified, but the observed storms have not attained the optimum moisture and energy levels necessary to produce a PMP event (Showalter and Solot 1942, Cudworth 1989).

The atmospheric conditions considered important to the formation of storms used in the estimation of PMP are: 1) abundant atmospheric moisture, 2) an efficient precipitation-producing mechanism, and 3) an intense storm system. Another assumption is that there is a sufficiently large catalog of such storms to describe the optimum storm mechanism for producing a PMP event. However, even though about 100 years of intense storm information is available, such storms have not been observed over all areas of a region. To overcome this lack of storms, three important tools are used in the estimation of PMP: moisture maximization, storm transposition, and envelopment.

Both moisture maximization and storm transposition consider the moisture content of the atmosphere and the efficiency of the storm mechanism that produces the precipitation. *Moisture maximization* is the process by which extreme observed precipitation is increased to a value consistent with the maximum potential moisture in the atmosphere for that storm location at that time of the year. A ratio is formed between the maximum moisture the atmosphere could hold at that time of the year and the actual moisture observed in the storm, and becomes a multiplier of the precipitation. This assumes that the storm would produce precipitation at the same efficiency.

Storm transposition is the relocation of the precipitation from an intense storm to another area that is climatically and geographically homogeneous with regard to extreme precipitation. Again, because of the inadequate sample of intense storms, it is necessary to assume that an extreme storm can be moved from its original location to a region in which climatology shows that similar storms, possibly of lesser intensity, could occur. This assumes that at least one storm in the sample has achieved maximum precipitation efficiency.

Envelopment is required because even some of the most intense storms have not reached maximum intensity over all areal sizes and durations. As a result, more than one storm is used over a region to define the temporal, areal, and seasonal distribution of PMP. During PMP development, where envelopment occurs, every effort is made to keep envelopment of values to a minimum. The method is primarily used to keep discontinuities to a minimum. In some instances there are areas where no major storms have been recorded. In such cases, it is necessary to infer PMP characteristics between regions, and this is done by smoothing gradients from one region to another.

The PMP storm for a region is considered the upper limit of precipitation. Moisture maximization, storm transposition, and envelopment are tools that provide estimates of the upper limits of precipitation for a region from intense storms. However, the remaining procedures used to develop a PMP design storm do not maximize the other factors involved in the estimation of these potential storms. Moisture is maximized, but other factors are allowed to act in a lesser manner, so that an unreasonable compounding of extremes does not occur. These procedures produce a PMP design storm. For orographic regions, only that portion of the precipitation that can be considered non-orographic is transposed. No attempt is made to transpose the orographic components of a storm.

1.4 California Terrain and Climate Influences

California provides several interesting challenges for estimating PMP. First, there are a complex series of mountains and valleys. Often the mountains act to enhance precipitation, but sometimes they shield areas from intense precipitation, and precipitation on the lee side quickly decreases. Both of these effects must be considered. Precipitation in the Central Valley behaves very differently than the rains in the surrounding orographic

regions. Furthermore, the rainfall in the northern and southern parts of the Valley has quite different influences on it, depending upon the season. The most intense storms in the Pacific drainage region occur during winter. However, southern California is also affected by decaying tropical storms that form off the western coast of Mexico and move into the region. Over the desert areas of southeastern California the maximum PMP is caused by decaying tropical storms from July through September. Further challenges occur because the warm season produces severe local storms over all of California. These storms produce intense heavy rains over areas of 500 mi^2 or less and occur in 6 hours or less. Such estimates are especially important over small basins. Like the Pacific Northwest, California has varied sets of terrain, storm, and climatic relations that makes the estimation of PMP, or any other climatic factor a challenge.

1.5 Scope of Study

The entire state of California is considered in this study. HMR 36 only developed general storm PMP estimates for the Pacific drainages. As a result neither Northeast nor Southeast California were considered. General storm PMP estimates for the desert regions were defined in HMR 49. The only generalized PMP that was previously defined for Northeast California was compiled by Riedel (1985). Local-storm PMP for California was not defined in HMR 36, but was included in HMR 49. For this report estimates of PMP for both general and local storms are provided.

General storms are major synoptic events that have intense precipitation for durations from 6 to 72 hours or longer, and cover areas greater than 500 mi^2, often more than 10,000 mi^2. Local storms occur individually or are embedded in a larger storm system, and are characterized by intense precipitation in 6 hours or less and over 500 mi^2 or less. Most often these rains occur in thunderstorms. Observations indicate that both general and local storms can occur anytime of the year. However, general-storm precipitation maximizes during the winter months; maximum local-storm rainfall occurs most often during the warm months. In the Southeast desert, the dominant general storms are decaying tropical storms that occur from July through October. Over the Pacific drainages of California, local storms very seldom occur during the height of summer (July and August).

It was agreed by the Federal Interagency Study Team that the PMP general storm

estimates would be limited to 72 hours or less and the areal coverage would be 10,000 mi^2 or less. Local-storm rainfall would be limited to areas of 500 mi^2 or less and durations of 6 hours or less. General-storm PMPIndex maps (Plates 1 and 2) give the all-season estimates. Methods to obtain seasonal estimates for general storms are provided in Chapter 13. Local-storm estimates of PMP are given in Chapter 9, Figure 9.23 (same as Figure 13.21), and the method to obtain estimates of the local-storm 1-hour PMP are given in Chapter 13.

1.6 Method of Study

General and local all-season PMP estimates and their seasonal variation were determined primarily by an intense study of extreme storm events that have occurred over California and nearby states with similar climatic regimes. In addition, climatic studies of various precipitation-related parameters were also performed. General-storm PMP estimates were developed using the *storm separation* technique. This technique was originally developed and used in the area between the 103rd Meridian and the crest of the Rocky Mountains in HMR 55A, and then again for the Pacific Northwest HMR 57. The storm separation technique provides a way of maximizing and transposing storms by separating the dynamically-forced precipitation from the orographically-forced precipitation. This allows only the dynamic part of the precipitation to be maximized and transposed to other regions.

Extreme storms of record are used for this analysis. The precipitation in these storms is divided into convergence (non-terrain influenced) and orographic (terrain-influenced) components. The convergence component of precipitation in a storm, that part of precipitation due to atmospheric forcing, is used to estimate the convergence PMP within the region where this storm occurred. This is the value that is maximized and transposed. The orographic component of the storm is not used to compute the total PMP in other parts of the region. Rather the total PMP is established by defining an orographic factor or ratio (T/C), which is derived from the 100-year, 24-hour maps of NOAA Atlas 2. The T is the Total storm precipitation at a point, while C represents the Convergence component, or that part of the precipitation that would be expected if there were no orographic component. If there is no orographic component acting on the precipitation at a point, then T/C is equal to

one. The storm separation analysis procedure is summarized in Chapter 6, and fully described in HMR 55A and HMR 57.

Many of the calculations, comparisons, and analyses involving spatial characteristics of PMP were performed via computer. A geographic information system (GIS) called GRASS (Geographical Resources Analysis Support System), was used extensively throughout the study to create maps which could then be combined with other maps (GRASS Version 4.0, Users Reference Manual, U.S. Army Corps of Engineers, Construction Engineering Research Laboratory, Champaign, Illinois, 1991). The process consisted of digitizing isolines which are considered vectors in a GIS. Vectors are the computer interpretation of an isoline. An interpolation between vectors forms a continuous field of values called a raster field in which each point (or raster) on the map has a value. Sometimes the individual rasters are called cells or raster cells. Each raster cell was a 15 second by 15 second region (about 0.08 mi^2) and had a interpolated value related to it. Raster fields or layers can be manipulated mathematically with other layers covering the same geographic region, usually by multiplying or dividing one layer by another. The final PMP Index map was produced from many such calculations and combinations of raster layers. It was found that the GIS was very useful in expediting preparation of the many maps that would have taken much more time to produce manually.

1.7 Peer Review

In the past, peer review of these reports was limited to personnel in the Hydrometeorological Branch and the Joint Study Team. Interest in PMP has grown over the years because of the National Dam Inspection Act of 1972, which required certain dams to meet safety standards imposed by PMP events. As a result, many more people are interested in PMP analysis, as evidenced by a number of conferences and studies: Australian National Committee on Large Dams 1988; Federal Emergency Management Agency 1990; National Research Council 1985; National Research Council 1988; National Research Council 1994; Office of Water Data Coordination 1986. This report was submitted to and reviewed by the following: Catalino Cecilio, Robert Collins, Dennis Marfice, Douglas Morris, John Riedel, Maurice Roos, Louis Schreiner, Ronald Spath, and Richard Stodt. The following individuals from the U.S. Army Corps of Engineers provided valuable insights and guidance during review of this report: Earl Eiker, Richard DiBuono, Frank Krhoun. We extend our

sincere appreciation for the competent and constructive reviews given by all reviewers. It is hoped that this report has been strengthened by the inter-action with such a cross section of the hydroelectric and hydrometeorologic community.

1.8 Report Organization

Chapters 2 through 8 present discussions of procedures and data used to obtain general-storm PMP estimates for California. Chapter 9 provides background, storms, and procedures used to develop local-storm PMP. Chapter 10 gives comparisons of general-storm PMP for individual drainages between HMR 36 and the present study. Chapter 11 contains comparisons to other HMR 36 PMP estimates, the 100-year return-frequency precipitation event, other adjoining PMP studies, and observed extreme rainfall amounts in California. Chapter 12 provides conclusions and recommendations from this study, and Chapter 13 presents the computational procedures, with examples. As mentioned in Section 1.1, Chapter 13 and Appendix 4 are the essential contents of HMR 58.

References follow the computational procedures in Chapter 13. Appendix 1 provides depth-area-duration tables of storms used in this study. Appendix 2 gives a discussion of the storms and their precipitation mechanisms that caused the intense rainfalls. Appendix 3 contains a list of 137 local storms. Appendix 4 contains information and all tables necessary to compute the snowmelt associated with a PMP storm. Appendix 5 reproduces information about the storm separation method from earlier hydrometeorological reports.

1.9 Definitions

All-season. The largest or smallest value of a meteorological variable without regard to the time of the year it occurred. In this report, the largest PMP estimate determined without regard to the time of the year it may occur.

Among-storm. A storm characteristic determined when values of various parameters may be determined from different storms. For example, a 6-hour/24-hour ratio, where the 6-hour value is taken from a different storm than the 24-hour value.

Atmospheric Forces. The forces that result only from the pressure, temperature and moisture gradients and their relative changes with time over a particular location.

Barrier Elevation. The height assigned to a location which reflects the presence (or absence) of terrain features that have a significant effect on the broad-scale moisture flow and precipitation processes.

Basin Shape/Drainage Outline. The physical outline of the basin as determined from topographic charts or field survey.

Dewpoint. The temperature to which a given parcel of air must be cooled at constant pressure and constant water-vapor content in order for saturation to occur.

Envelopment. The process of selecting the largest value from any set of data. By so doing, consistency is maintained among charts depicting data for a variety of area sizes or durations.

Generalized. When used as an adjective to modify names such as PMP or estimates or charts, it is to be taken in the sense of *comprehensive*, i.e., pertaining to all things belonging to a group or category. Thus, a generalized PMP map for a specific area and duration defines PMP for all points in the region; no location is excluded.

General Storm. A storm event which usually produces precipitation over areas larger than 500 mi^2 and durations longer than 6 hours, and is associated with a major synoptic weather feature.

Implicit Transposition. The regional, areal or durational smoothing used to eliminate the discontinuity created (during transposition of non-orographic components of precipitation) by limitations of storm history, quantity and quality of observations, and transposition boundaries.

Individualized. As applied to drainage estimates, indicates studies for specific drainages that include considerations for possible local influences. In the sense of applications to specific basins, it is commonly implied that information obtained from a generalized study will be processed and result in specific drainage-averaged values.

Local Storm. A storm event restricted in time and space. Precipitation rarely exceeds 6 hours in duration and the area covered by precipitation is less than 500 mi^2. Frequently local storms will last only 1 to 2 hours and precipitation will occur over only 100 or 200 mi^2. Precipitation in local storms is considered isolated from general-storm rainfall.

Probable Maximum Precipitation (PMP). Theoretically, the greatest depth of precipitation for a given duration that is physically possible over a given storm area at a particular geographic location at a certain time of the year.

Spatial Distribution. The geographic distribution of PMP for a storm area based on a storm with an idealized pattern.

Storm-centered. A characteristic of a storm that is always determined in relation to the maximum observed value in the storm as compared to the same factor for some other duration and/or area of the storm. For example, a storm-centered depth-area ratio relates the average depth over some specific isohyetal area of the storm to the amount at the storm center.

Temporal Distribution. The order in which incremental PMP amounts are arranged within the PMP storm.

Within-storm. A storm characteristic determined when values of various parameters are required to be from the same storm. For example, a 6-hour/24-hour ratio where the values for each duration are always selected as the maximum values for the particular duration in the same storm (see also Among-storm).

2. SIGNIFICANT GENERAL STORMS

2.1 Major General Storms of Record

A review of storms was performed to determine the largest precipitation events on record. Various data sources were examined to create a master list of storms in the period from about 1900 to 1990. Initially, the United States Corps of Engineers (USCOE) Storm Rainfall Catalog (USCOE 1945-) provided a foundation for much depth-area-duration (DAD) data information. Most of the older storms (1901-1945) came from this Storm Catalog, while Bureau of Reclamation and National Weather Service files were used to supplement the list. In an effort to define other important storms, a search was made of digital rainfall data from California, and were compared to the 100-year, 24-hour precipitation frequency of NOAA Atlas 2 (1973). Individual amounts from stations were put in chronological order to define other potential storms. In addition, extreme storms identified by Goodridge (1992) were examined to uncover other potential storms. Finally, those storms used in HMR 36 (1961), HMR 49 (1977), and HMR 57 (1994) were reviewed to assure continuity between studies as far as the storm sample was concerned.

These storms were primarily general storms; they had durations of 12 hours or more, and precipitation was widespread as a result of a major synoptic-scale disturbance, such as a low pressure system, strong frontal activity or remnant tropical moisture from a decaying tropical system. Other short-duration (6 hours or less), small-area (less than 500 mi^2) storms were considered for local-storm analysis, and are discussed in Chapter 9. The general storms are listed in Table 2.1, and geographic distribution of all but three are shown in Figure 2.1. Five of these storms: December 1921 (40), December 1937 (88), November 1961 (149), December 1980 (175), and June 1958 (1013) occurred outside of California, but within a few degrees north. Of these five storms, three (40, 88, and 175) are north of the region shown on Figure 2.1. The latitudes and longitudes indicated in Table 2.1, are for the maximum point rainfall for the storm.

A number of storms from Figure 2.1 are centered just north and east of Los Angeles in the San Gabriel - San Bernardino mountains, and another storm group is located in the

Table 2.1. *California general and seasonal storms.*

Storm Number	Date	Latitude	Longitude	Barrier Elevation (ft)	24-hr/10-mi^2 Precipitation (in)	Area (mi^2)/ Duration (hr)
40	12/9 - 12/1921	48°01'	-121°32'	3200	8.58	27253/72
88	12/26 - 30/1937	44°55'	-123°38'	1500	10.76	13869/96
126	10/26 - 29/1950	41°52'	-123°58'	2000	15.84	80511/72
149	11/21 - 24/1961	42°10'	-123°56'	2700	10.90	20850/48
156	12/19 - 24/1964	41°52'	-123°40'	2500	16.23	1932/72
165	1/11 - 18/1974	41°08'	-122°16'	1900	10.63	2272/72
175	12/24 - 26/1980	44°55'	-123°44'	1400	9.22	24865/48
508	1/15 - 19/1906	39°54'	-121°34'	2600	14.77	10000/84
523	5/8 - 10/1915	40°42'	-122°26'	1800	10.51	20000/72
525	1/1 - 4/1916	39°48'	-121°36'	2000	10.12	30000/72
544	12/9 - 12/1937	40°11'	-121°26'	5500	15.29	20000/72
572	12/21 - 24/1955	37°59'	-119°20'	10500	13.42	30000/72
575	10/11 - 13/1962	40°02'	-121°29'	5500	19.71	10000/96
630	1/3 - 5/1982	37°05'	-122°01'	950	20.65	20000/60
1000	2/1 - 6/1905	34°30'	-119°10'	3000	9.34	20000/96
1002	2/27 - 3/3/1938	34°14'	-117°32'	4400	20.25	20000/96
1003	1/20 - 24/1943	34°12'	-118°03'	2100	22.90	30000/96
1004	11/17 - 21/1950	39°08'	-120°20'	6900	11.90	20000/102
1005	1/25 - 27/1956	34°13'	-117°31'	3900	11.45	10000/48
1006	9/17 - 20/1959	40°43'	-122°16'	1000	17.83	30000/48
1007	12/4 - 6/1966	36°17'	-118°36'	8000	21.69	30000/54
1008	1/23 - 26/1969	34°13'	-117°35'	5500	19.07	20000/80
1010	2/14 - 19/1986	39°54'	-121°12'	5200	18.12	30000/120
1011	9/25 - 26/1939	34°16'	-118°04'	2500	10.08	5000/42
1012	5/18 - 19/1957	39°57'	-121°27'	5200	7.23	20000/60
1013	6/1 - 2/1958	42°15'	-123°25'	3500	4.33	5000/48
1014	7/8 - 10/1974	38°50'	-120°41'	2100	6.85	10000/48
1015	8/13 - 16/1976	40°43'	-122°16'	1200	5.11	10000/48
1016	9/9 - 11/1976	34°20'	-117°03'	6000	15.10	20000/48
1017	8/15 - 17/1977	34°50'	-115°41'	3600	5.70	20000/60
1018	7/27 - 29/1984	34°58'	-115°31'	3900	5.79	20000/36

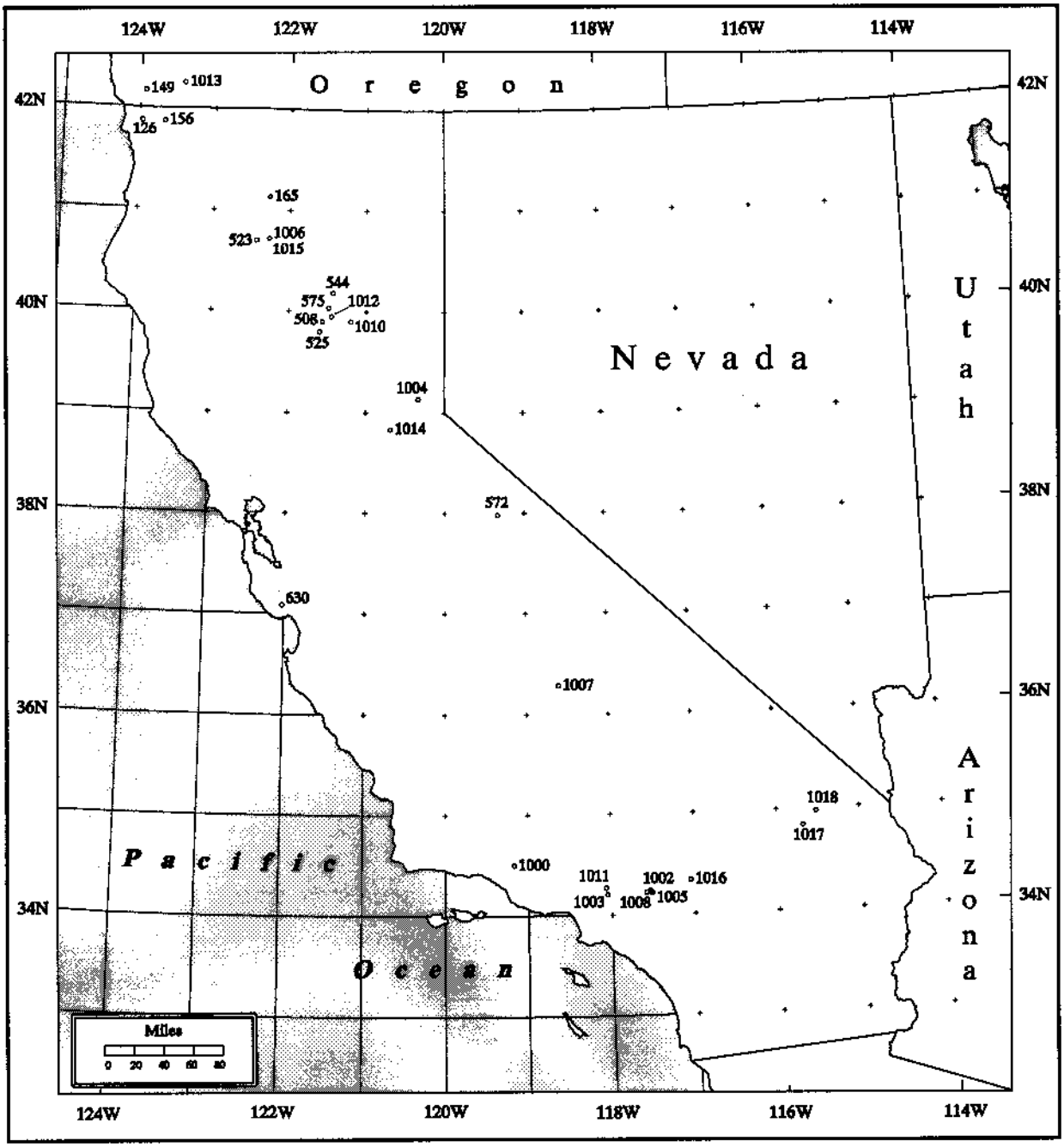

Figure 2.1. *Location of general storms of record from Table 2.1.*

northern Sierra Nevada mountains. In both locations terrain features served to focus and enhance precipitation in the passing storms. It is also true that, at least around Los Angeles, the raingage density is relatively high compared to the rest of the state. At the same time, there are immense areas where few storms are recorded due to a lack of systematic raingage records, most notably in the deserts of eastern California. Furthermore, many of the heavy rainfalls in the Central Valley are associated with storms centered in orographic regions.

2.2 Storm Data Analysis

An important part of the procedure to develop probable maximum precipitation (PMP) estimates is the analysis of the major storms in Table 2.1. Analysis includes: collecting precipitation data from various sources; applying quality control that identifies incorrect data; handling missing data; and compiling the data into a format for automated processing. The inclusion of a synoptic weather analysis for each storm is important to understand the timing and precipitation pattern for each storm. The synoptic analysis for each storm examines the surface and upper-air features, precipitation, and dewpoints and/or temperatures pertinent to the storm. Appendix 2 provides excerpts from the synoptic analyses for the most significant storms. Some of the other storms are discussed in HMR 36 and HMR 57.

The objective of the storm analysis was to obtain DAD information upon which to base PMP estimates, as well as generalized relations for other areas with similar climatic and topographic characteristics. The DAD information was used in the storm-separation process in Chapter 5, Section 5.4, and for the derivation of enveloped regionalized DAD relations in Chapter 8, Section 8.2. The numbers associated with the storms were assigned in no particular order. They are reference numbers that have been given to storms for filing and tracking purposes only. Storms with numbers less than 1000 were storms used in the derivation of PMP for the Pacific Northwest (HMR 57). Numbers greater than 1000 are an internal Hydro-meteorological Design Studies Center ordering system. All storms from Table 2.1 were analyzed to obtain DAD relations. In some cases, previously published pertinent data sheets, from the Storm Rainfall Catalog (USCOE 1945-), were re-analyzed. The procedure used to determine DAD for each of the storms is described in Chapter 5.

2.3 Characteristics of Wintertime and Summertime Extreme Storms

The analysis of synoptic weather relations for a PMP study is similar to the analysis used in the preparation of a weather forecast. *Synoptic knowledge* is applied to transpose storms and to regionalize DAD relations. The information required to calculate PMP for a region, does not depend directly on special insights about synoptic (or any other) scale atmospheric patterns, but is used to define the extreme storm types of a region and the generalized relations for similar regions.

The characteristics of various synoptic patterns associated with major precipitation-producing general storms in California are well-recognized and understood, and were described for all but southeast California in HMR 37 (1962). In 1981 the meteorology of important rainstorms was published in HMR 50 (1981) for the southwestern United States, and included storms from southeast of California. HMR 50 provides a thorough discussion of the observed and hypothesized sets of atmospheric patterns associated with extreme precipitation. Since publication of these reports, knowledge of the associations between weather and the structure of cyclonic storms and fronts has been much improved, e.g., Browning et al. 1973, Hobbs 1978, Shapiro and Keyser 1990, Martin et al. 1995. This increased understanding has provided added insight into the atmospheric structure for use in transposition and regionalization of storms.

A distinction is made in HMR 37 between summertime tropical and convective-like PMP storms, and wintertime orographic and convergence combined with convection PMP storm. This distinction remains relevant today. The summertime storms establish the annual or all-season levels of PMP for southeastern California; the wintertime storms set the upper limits for precipitation for the remainder of California. The conclusions related to the optimum wintertime atmospheric features expressed succinctly in HMR 37, have withstood the test of time. There is a basis to conclude:

> "that in the optimum storm, the band of high moisture transport has a degree of both persistence and stability of position which concentrates storm orographic precipitation totals. To this is added the conclusion that convergence precipitation characteristic of this storm may be centered within this band and that the most intense convergence precipitation may occur simultaneously with that of orographic precipitation."

Information from major storms occurring since 1962, remote-sensing data defining the storm environment, and storm simulation via numerical modeling have not changed or undermined these conclusions. The wintertime optimum conditions can be found everywhere except southeast California in varying degrees of strength and complexity. This is the basis for having only marginal differences in the DAD relations for all regions of the state except for the Southeast and to a lesser extent the Central Valley. These matters are discussed again in Chapters 6 and 7.

The atmospheric characteristics for all-season PMP storms in southeastern California were summarized in HMR 50. These characteristics include: 1) greater than customary amounts of moisture available for precipitation preceding the PMP storm, 2) maximum or near maximum values of sea surface temperatures off the west coast of Baja California, 3) an optimal track (both direction and speed) for tropical cyclones approaching southeastern California, and 4) an interaction with a *digging and deepening* cold trough or low pressure system aloft after the tropical cyclone arrives. However, not all of these features have been observed and recorded in southeastern California, but have been observed in Arizona. In the optimum PMP case these conditions could be assembled anywhere in southeastern California.

3. TERRAIN

3.1 Introduction

The climate and terrain of California are highly varied. The orographic complexity is largely responsible for the broad range of precipitation across the state. For example, Mount Whitney at 14,494 feet above sea level (ASL) in the Sierra Nevada is the highest mountain in the contiguous 48 states, and Badwater basin at 282 feet below sea level in Death Valley National Park is the lowest elevation in the United States. Several major mountain chains and many smaller ridges cover much of the region. Three notable mountain chains, the Sierra Nevada, the Coastal Range, and the San Gabriel-San Bernardino mountains have an especially important impact on precipitation. The Sierra Nevada chain has some of the highest mountains in California, with elevations surpassing 10,000 feet ASL, and runs north-south along the Nevada border. The Coastal Range, a much lower conglomeration of mountains ranging from 3000 to 6000 feet ASL, stretches the length of California along the Pacific Ocean with only minor breaks. Finally, the San Gabriel-San Bernardino mountains lie just north and east of the Los Angeles metropolitan area, with elevations above 10,000 feet ASL.

Surrounded by the various mountain ranges, the Central Valley extends from the Sacramento River basin in the north to the Imperial Valley in the south. Other notable low-level areas are found near Los Angeles and San Diego, nestled into areas bounded by mountains or the Pacific Ocean. Southeast California lies east of the major mountain areas, but contains a number of minor ridges and valleys. Another area of interest is the Salton Sea, surrounded by low-lying mountain ridges (3000 to 4000 feet) with some peaks to the west above 6000 feet ASL. Overall the mountains, valleys, and the Pacific Ocean make the climate of California unique and varied. Figure 3.1 shows the principal mountain ranges and major low-elevation areas in California.

All three mountain ranges block in substantial ways the dominant westerly or southwesterly moisture inflow. This leads to greatly enhanced precipitation along the windward side of these ranges and rainshadow effects downwind. Some of these

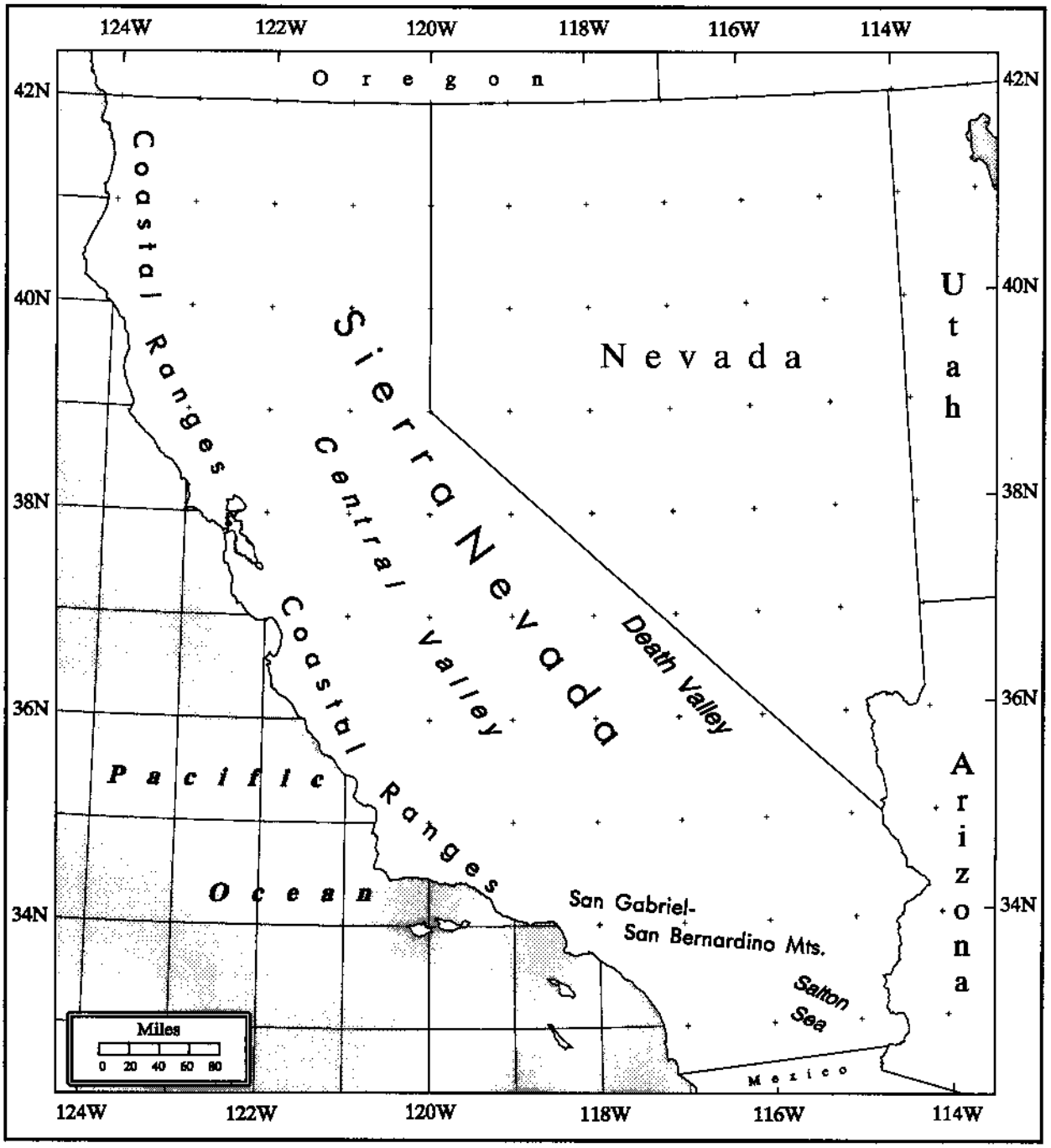

Figure 3.1. *Locations of principal mountain ranges and low-elevation valleys in California.*

characteristics are shown in the mean annual precipitation map (National Climatic Data Center 1992) in Figure 3.2. Average annual totals exceeding 70 inches are observed in the Sierra Nevada and along the Coastal Range in northern California. Average annual precipitation values exceeding 40 inches are found in the San Gabriel-San Bernardino mountains to the south. Note the relative lack of rainfall in the lee of orographic terrain. A large portion of California in the Central Valley and southeast California has yearly averages of less than 10 inches of rainfall. While Figure 3.2 includes the latest data updates, it is a computerized map that does not take into account the complex terrain of the region, but provides a generalized picture of mean annual precipitation.

3.2 Regional Analysis

Due to the widely differing terrain and orographic influences on precipitation California was divided into several regions shown in Figure 3.3. The regions were based upon terrain, similar climate zones, similar storm types, and precipitation characteristics. The regions also reflect variations in depth-area-duration (DAD) relations in California.

In order to represent meteorologically homogeneous regions several specific factors were considered. First and foremost, the individual storm DAD relations were analyzed and compared to one another to see how DAD relations vary by region. Second, obvious topographic differences provided guidance on how and where the boundary lines between regions were drawn. Third, the pattern of the 100-year, 24-hour rainfall frequency map from NOAA Atlas 2 (1973) shows the spatial variations in precipitation, thus providing a climatology.

The analysis resulted in seven distinct regions: Northwest (region 1), Northeast (region 2), Midcoastal (region 3), Central Valley (region 4), Sierra (region 5), Southwest (region 6) and Southeast (region 7). The Northwest region encompasses the relatively wet, rolling mountainous terrain of coastal northern California. The Northeast region represents the drier downwind zone of northern California, just north of the Sierra region. The Midcoastal region represents the low coastal mountains running along the California coast between the Central Valley and the Pacific Ocean. Sandwiched between the Midcoastal and the Sierra regions is the Central Valley region, constituting the flat, wide north-south plain of California. The final two regions include the Southwest, which is the mountainous area

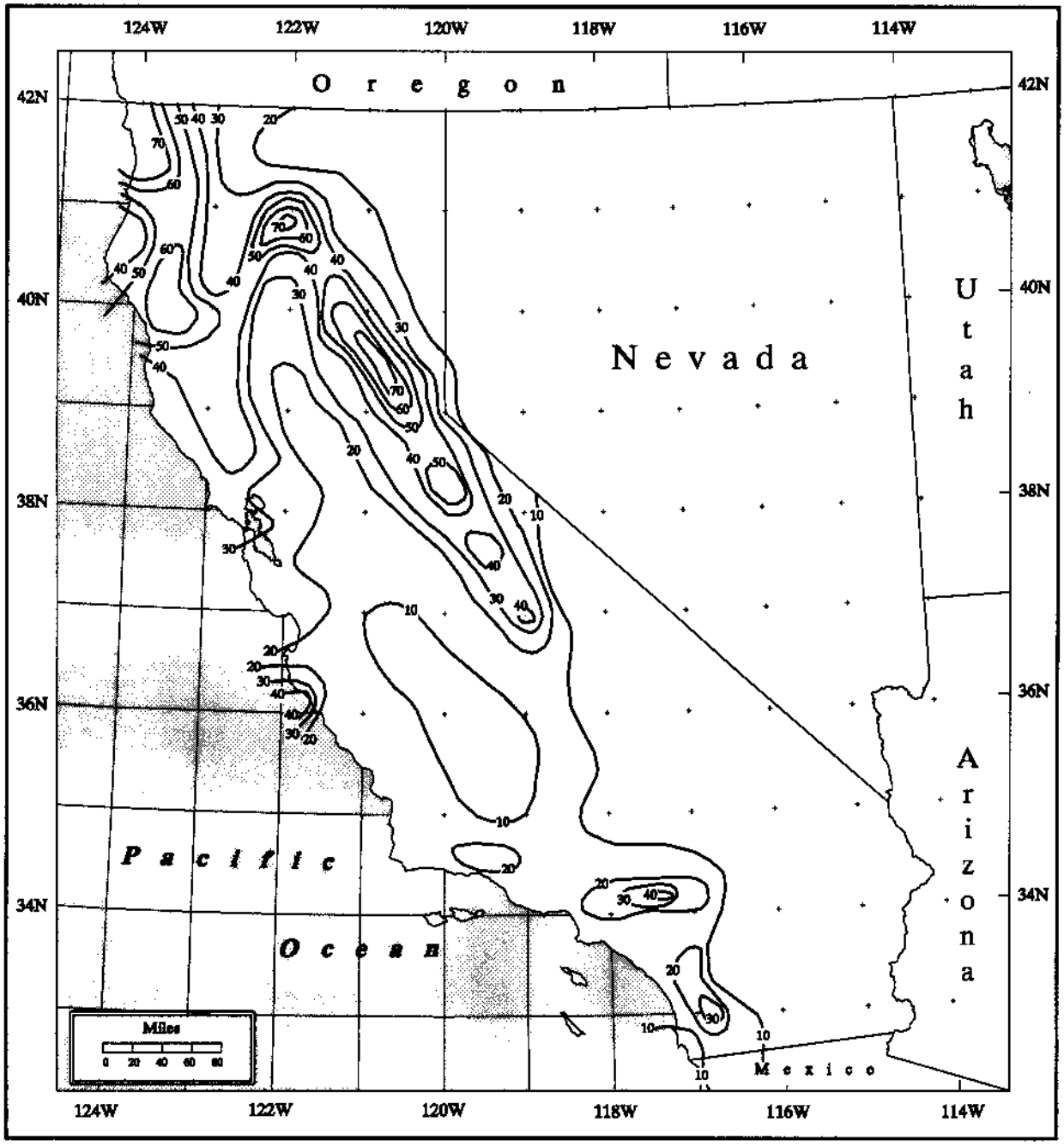

Figure 3.2. *Mean annual precipitation (inches) based on 1961-1990 normals (National Climatic Data Center 1992).*

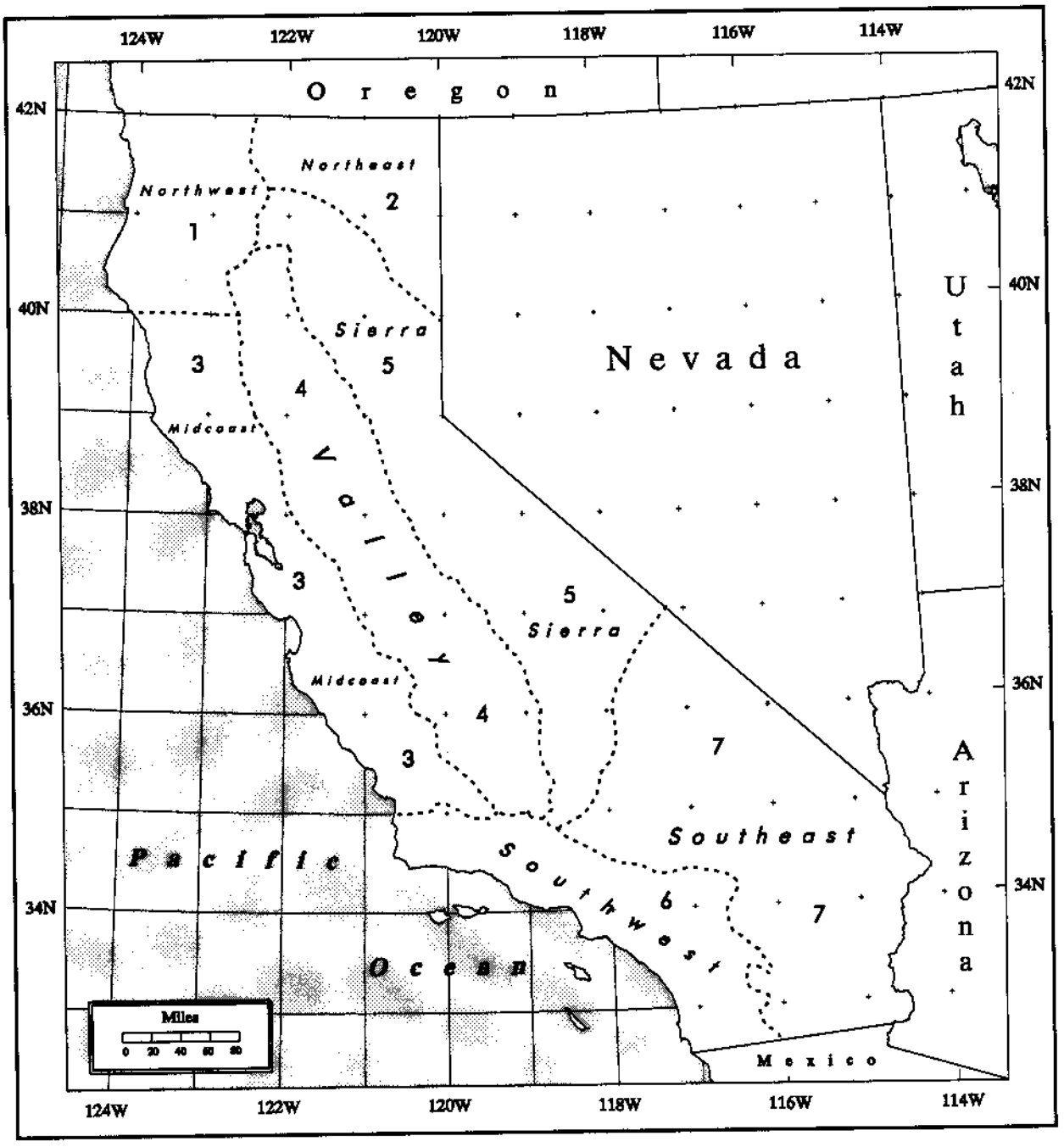

Figure 3.3. *Regional boundaries for development of depth-area-duration relations. Same as Figure 13.11.*

between the Pacific ocean and the deserts to the east, and the Southeast which encompasses the deserts of California. A complete discussion on the DAD relationships, and their derivation is found in Chapter 8, Section 8.2.

3.3 Barrier-Elevation

In this study, as in other studies, probable maximum precipitation (PMP) adjustments in the vertical must be made to precipitation and moisture values (dewpoints) to: 1) calculate orographic influence (K-factors), 2) define moisture maximization, and 3) adjust storm rainfall depths as the result of transposition. This adjustment is required because terrain interacts with the broad-scale winds and accompanying moisture flow when they encounter or are forced to bypass terrain features that act as barriers. The technique used to make barrier elevation maps has been discussed extensively in previously issued reports, (e.g., HMR 36 (1961), HMR 43 (1966), HMR 49 (1977) and HMR 55A (1988)). No changes from previous studies were made to derive barrier elevations.

The inflow wind directions used to construct the barrier elevation map ranged from south-southeast to west-southwest for PMP storms in the Central Valley, Sierra, and Midcoastal regions of the state and, from east through south for PMP storms in the Southeast region. The final barrier elevation map was hand-drawn at the 1:1,000,000 map scale, with topographic features less than 10 miles in width disregarded. The barrier elevation map is shown in Figure 3.4.

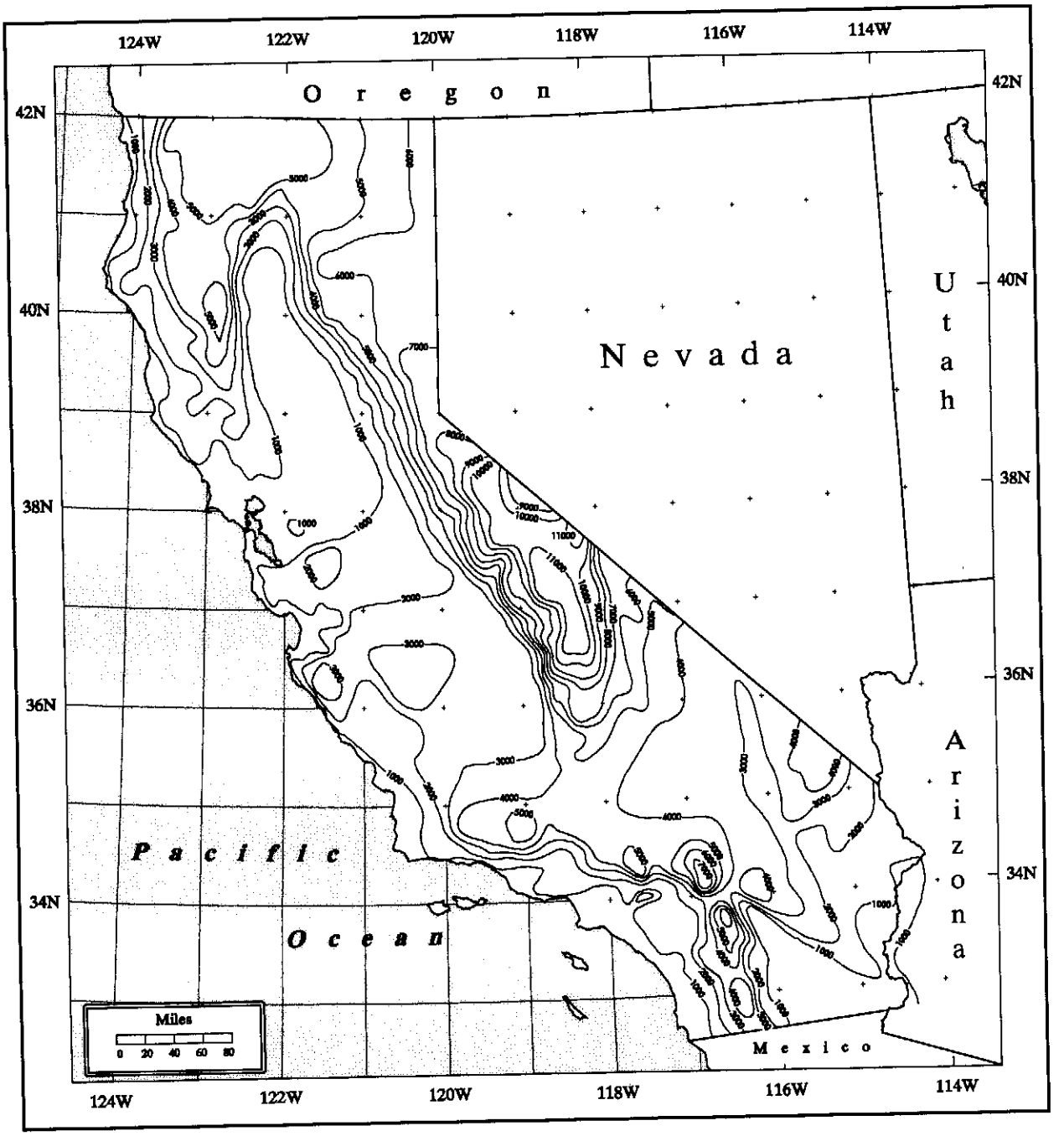

Figure 3.4. *Barrier elevations (whole feet MSL) for California.*

4. MOISTURE

4.1 Introduction

There are a number of ways to provide atmospheric moisture information for input into the calculation of probable maximum precipitation (PMP). The longest available record of moisture measurements are from surface observations. Early in the 20th century observations were only taken 2 or 3 times a day. In an effort to obtain the maximum possible record of extreme atmospheric moisture, these early measurements are used with more modern observations to provide a measure of extreme atmospheric moisture. A 12-hour duration was chosen to represent the general broad-scale flow into a storm with precipitation covering an area greater than several thousand square miles. Because of the limited observations taken each day in the early part of the century, a persisting dewpoint value was used to define maximum moisture. A maximum persisting dewpoint is the highest dewpoint equaled or exceeded throughout a given duration. It can be considered to be the highest, as indicated by the record, that can persist for various durations. Generally, the persisting value provides a lower value than a 12-hour average dewpoint. Surface values are observed at a number of different elevations. In order to compare values from different locations, the 12-hour persisting dewpoint is normalized or adjusted to the 1000-mb pressure level, or essentially sea level. This allows these values to be compared across the United States, in spite of large differences in the elevation of observations.

Charts of 12-hour maximum persisting dewpoint temperatures have been used in many HMRs including those for the western United States: HMR 36 (1961), HMR 43 (1966), HMR 49 (1977), HMR 55A (1988), and HMR 57 (1994). This extreme atmospheric moisture information is used to maximize observed storm precipitation, and to adjust storm precipitation for horizontal and vertical changes in storm location (transposition). Several studies (e.g., Reitan 1963; Bolsenga 1995) have shown that surface dewpoint temperature is an acceptable measure of water vapor aloft in the saturated atmosphere during storm periods. In addition, Kuo et al. 1996 indicates that the inclusion of surface moisture measurements in a variational data assimilation system can be "quite effective in...improving the quality of moisture analysis in the lower troposphere."

4.2 Dewpoint Analysis

In this study, we used monthly analyses of 12-hour maximum persisting 1000-mb dewpoints developed for the United States west of the Continental Divide for HMR 57. These analyses used synoptic time observations of dewpoint temperatures for 36 locations (Peck et al. 1977) as well as hourly dewpoint observations for 23 California locations obtained on tape from the National Climatic Data Center (NCDC) for the years 1948 to 1983. These data were examined for possible exceedances to the 1905-1959 set of data used in HMR 36. When such exceedances occurred, they were verified against values in the Local Climatological Data (NCDC 1948-). They were also checked with synoptic weather information to ensure that the new records occurred with conditions favorable for precipitation. When new dewpoint records occurred during precipitation sequences, the dewpoints were accepted, provided that upwind trajectories from the site showed increasing dewpoints over time. Once the new records were determined, new annual curves were drawn for these stations. Values from these curves were plotted on monthly maps and new analyses were drawn. Maps of month-to-month changes of persisting dewpoint values were made and individual monthly maps redrawn to obtain a smooth monthly transition of 12-hour persisting dewpoints across California. Monthly differences from the earlier reports were usually less than 2°F and none exceeded 3°F.

The dewpoint analyses shown in Figures 4.1 to 4.12 reflect seasonal-scale atmospheric changes or adjustments. The contours in these figures depict mid-monthly values. The contour configuration for November through April in Figures 4.11, 4.12, 4.1 to 4.4 (albeit weakly in April) reflects the persistent presence of (relatively dry) continental polar and mixed maritime and continental polar air masses in eastern California. The warmer land area in the central and western regions sustain a *wedge* of higher dewpoints during the *wintertime* months. The cold, off-shore ocean currents affect the recurvature of the contours along the coast line. May is seen as a transition month between these characteristic *wintertime* and *summertime* regimes (Figure 4.5.) Then the contour pattern for June through September in Figures 4.6 to 4.9 and weakly in October (Figure 4.10) is forced by circulation patterns which bring in high-moisture content air originating over the regions with high sea-surface temperatures (SST) in the Gulfs of California and Mexico.

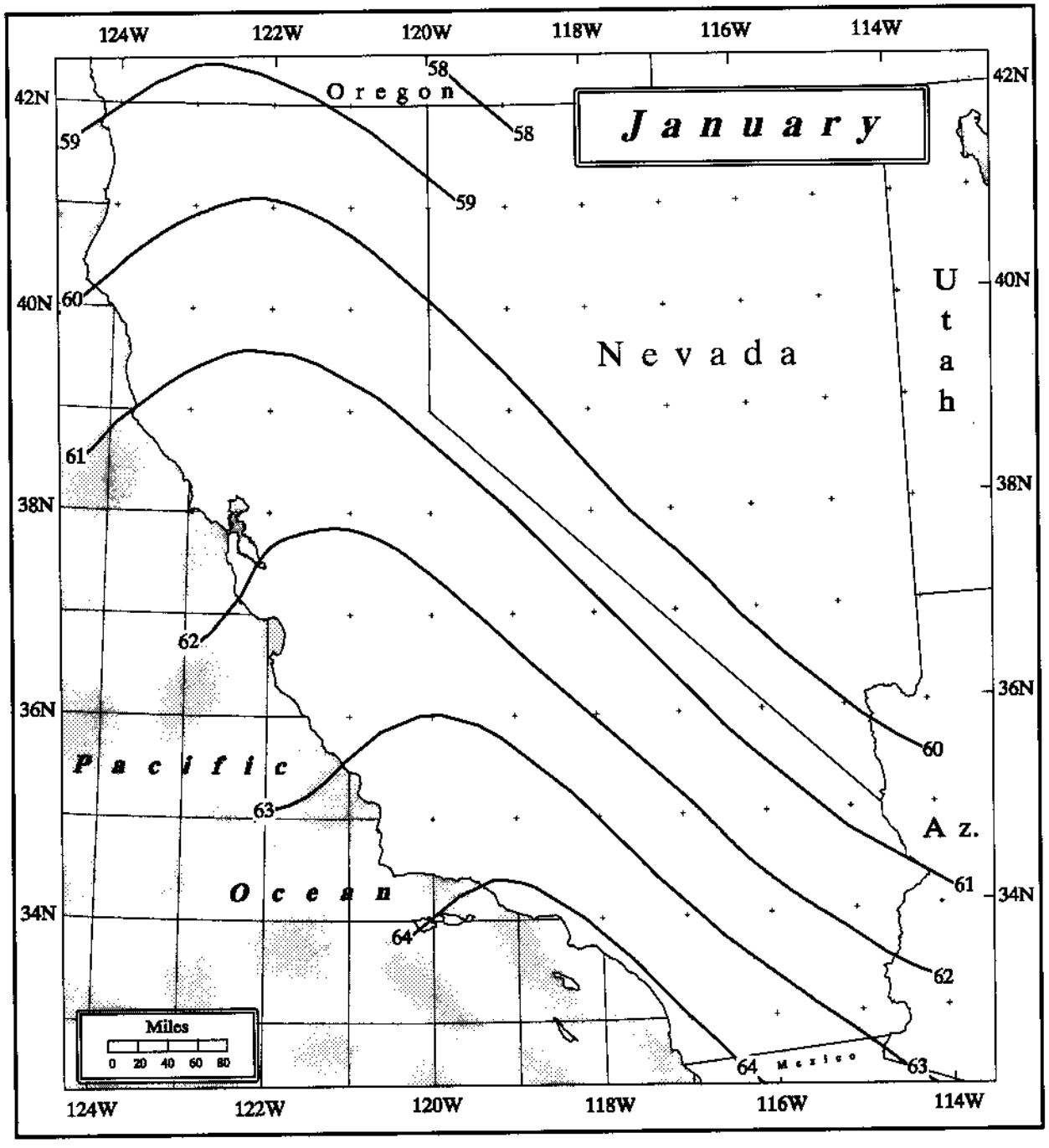

Figure 4.1. *Twelve-hour maximum persisting 1000-mb dewpoints for January (°F).*

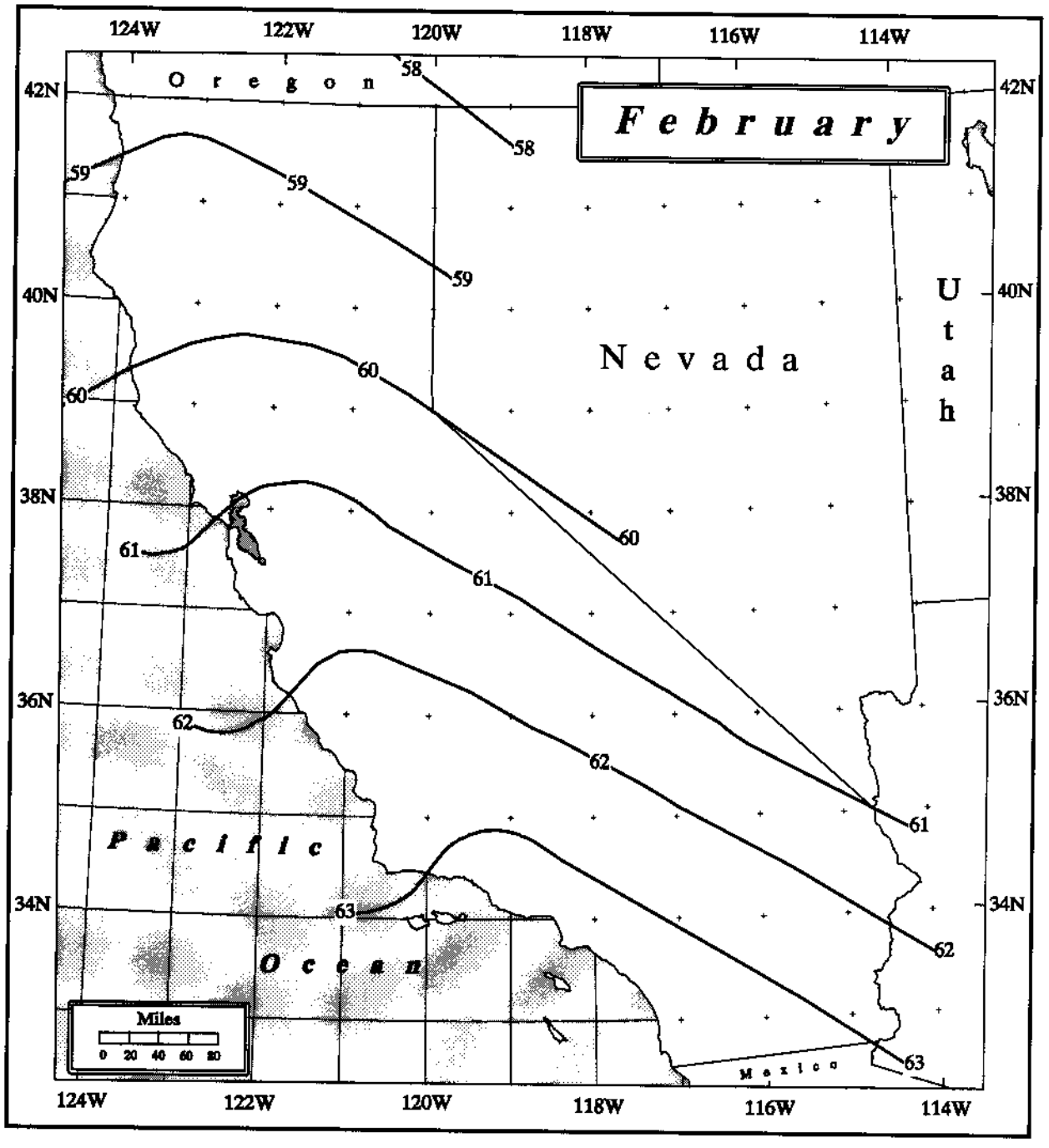

Figure 4.2. *Twelve-hour maximum persisting 1000-mb dewpoints for February (°F).*

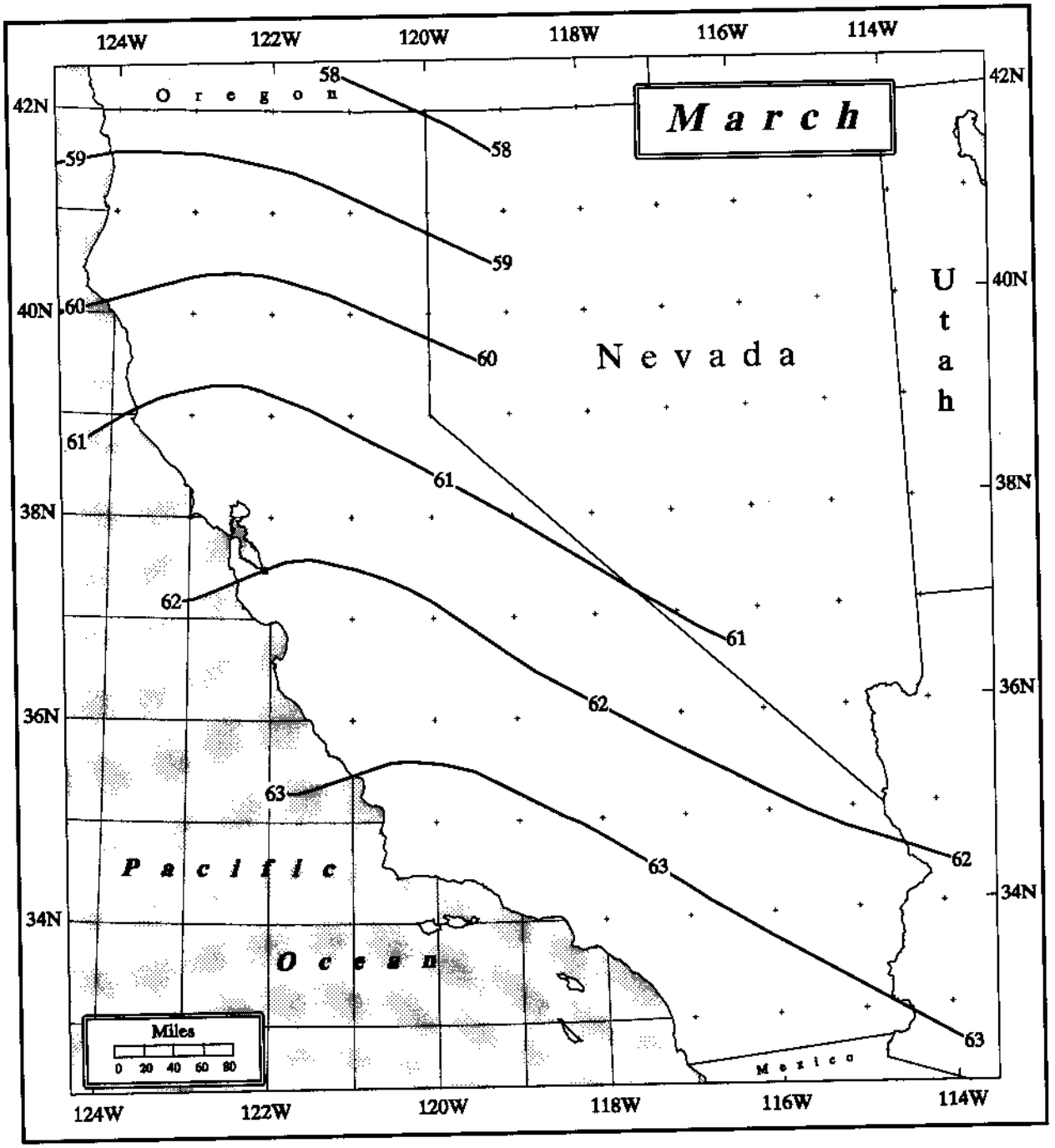

Figure 4.3. *Twelve-hour maximum persisting 1000-mb dewpoints for March (°F).*

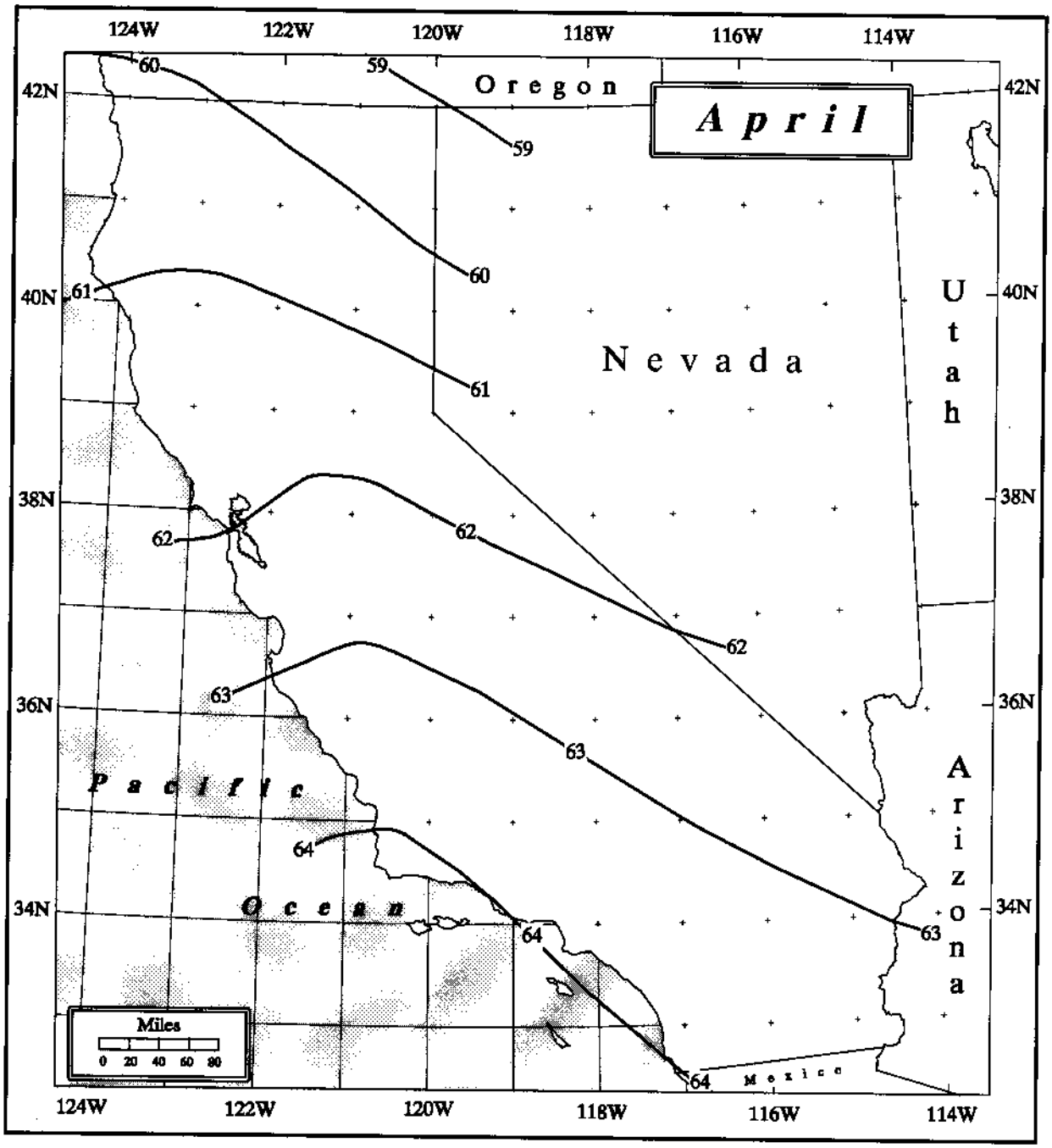

Figure 4.4. *Twelve-hour maximum persisting 1000-mb dewpoints for April (°F).*

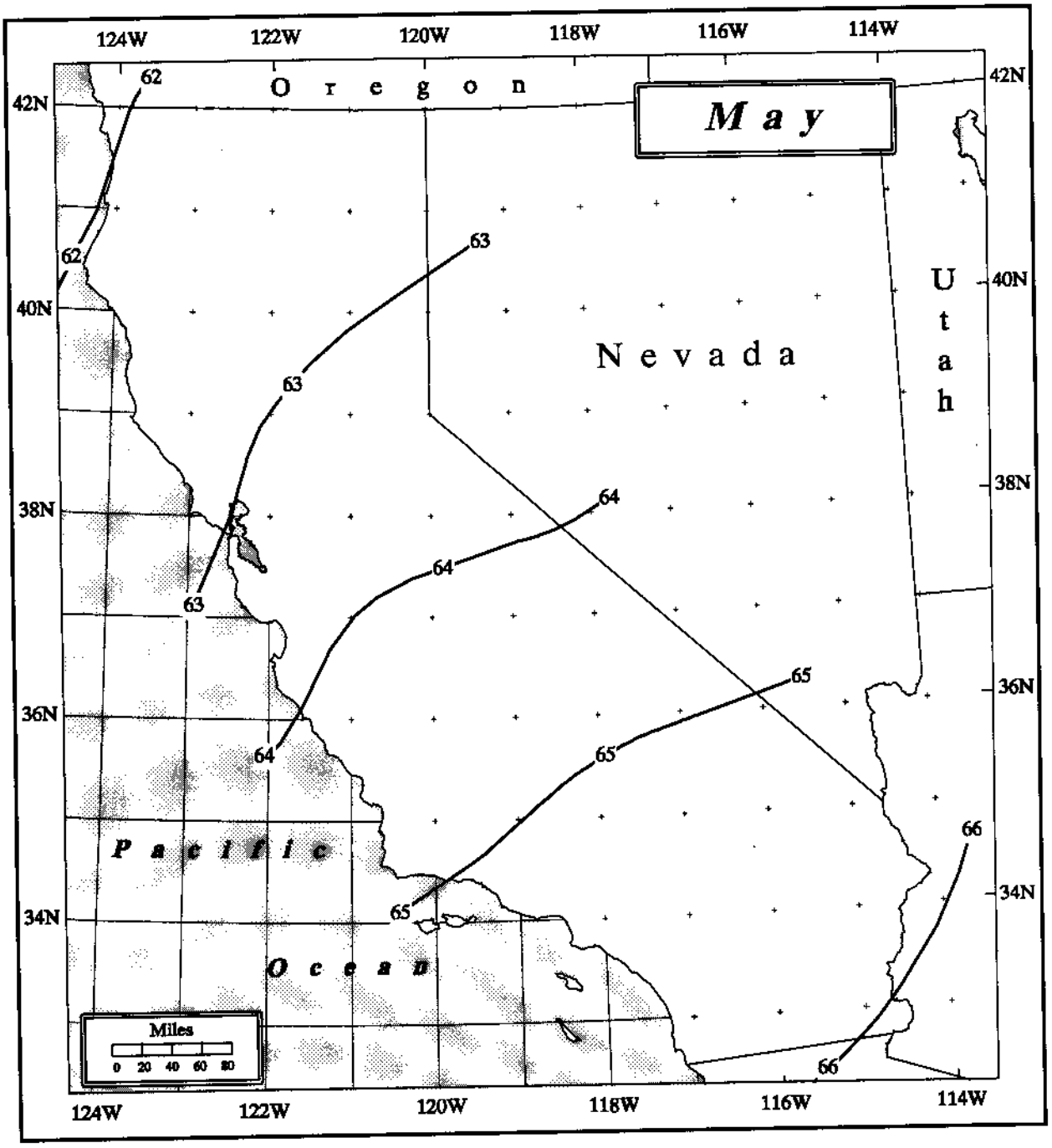

Figure 4.5. *Twelve-hour maximum persisting 1000-mb dewpoints for May (°F).*

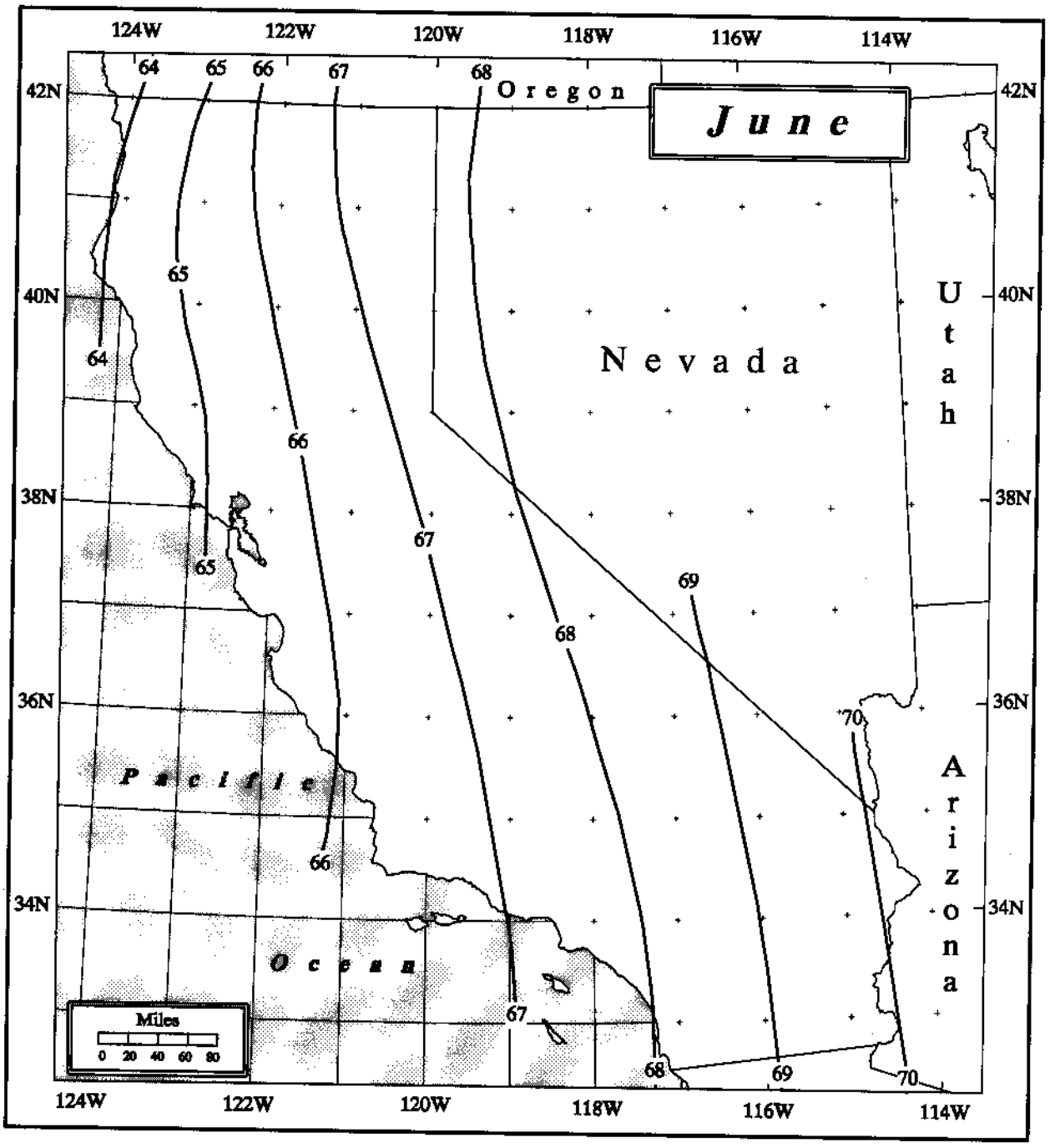

Figure 4.6. *Twelve-hour maximum persisting 1000-mb dewpoints for June (°F).*

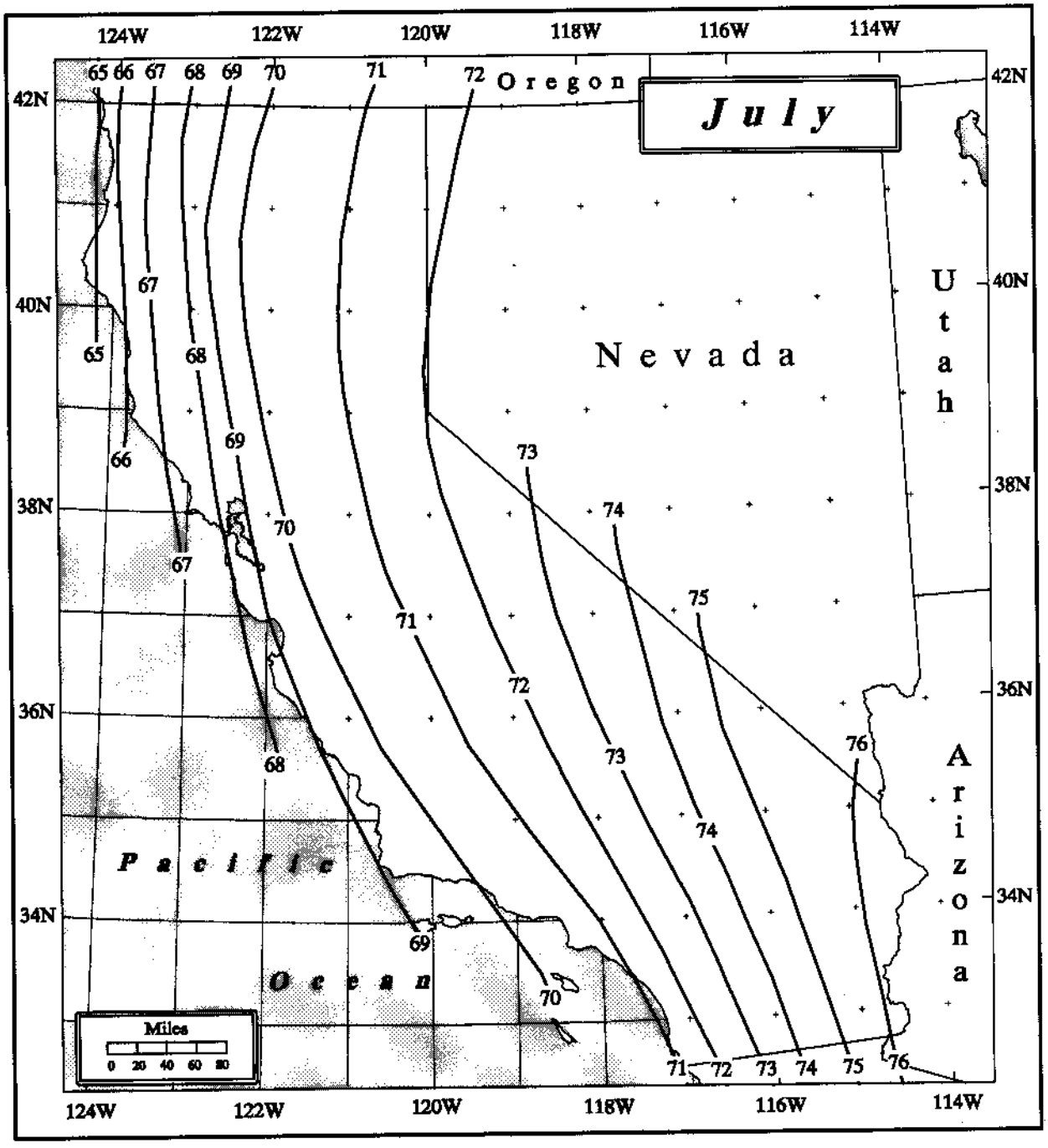

Figure 4.7. *Twelve-hour maximum persisting 1000-mb dewpoints for July (°F).*

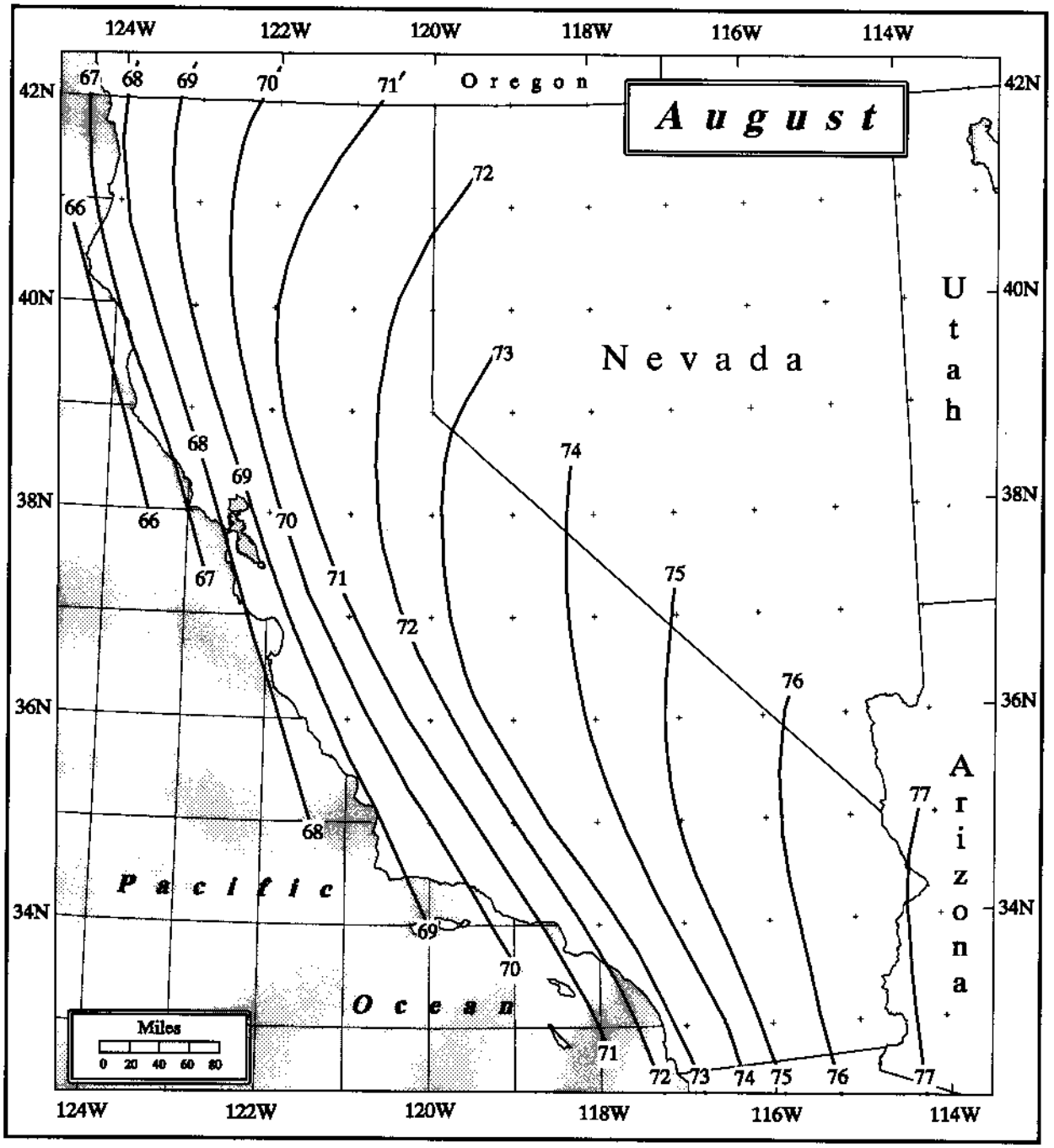

Figure 4.8. *Twelve-hour maximum persisting 1000-mb dewpoints for August (°F).*

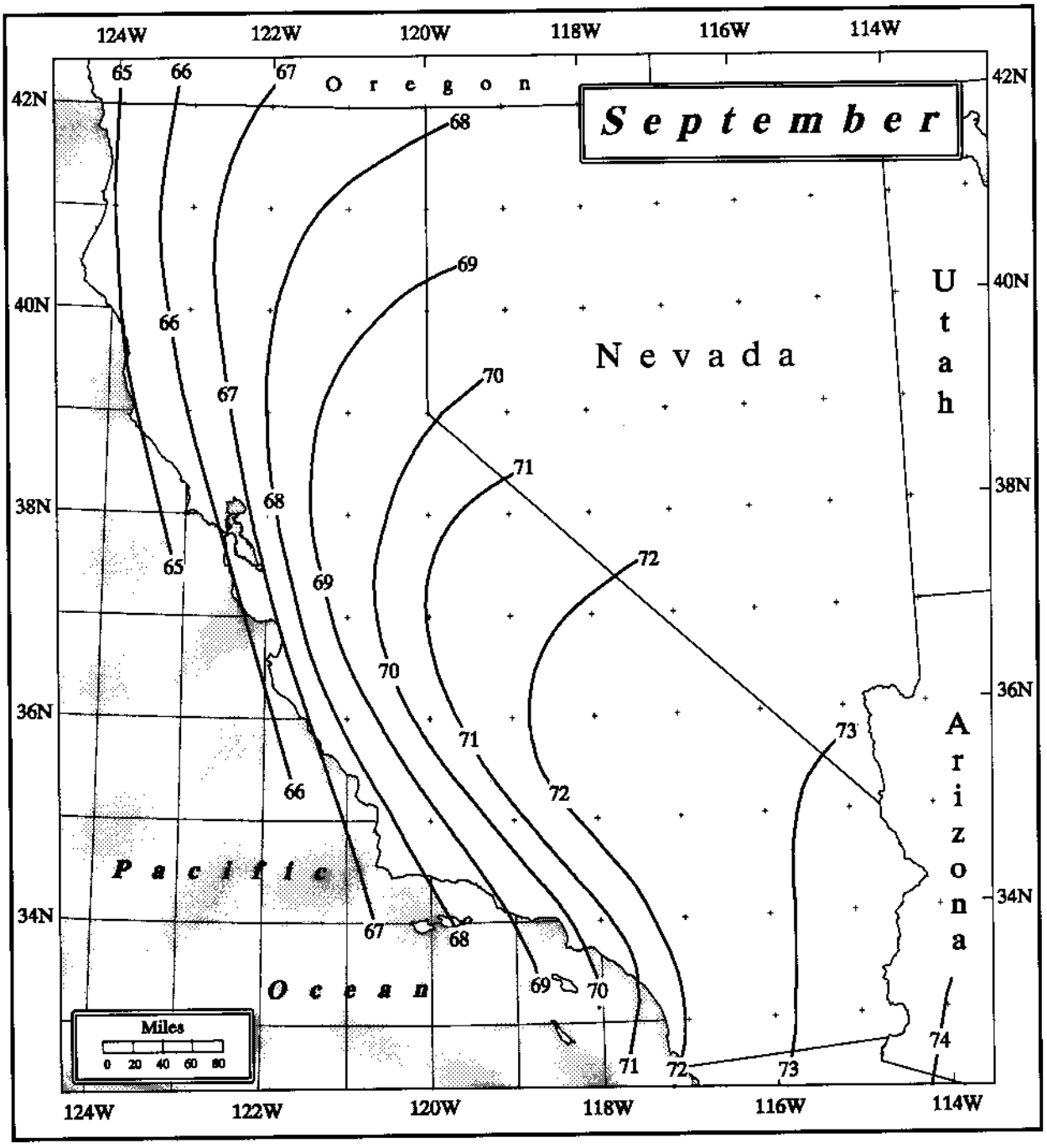

Figure 4.9. *Twelve-hour maximum persisting 1000-mb dewpoints for September (°F).*

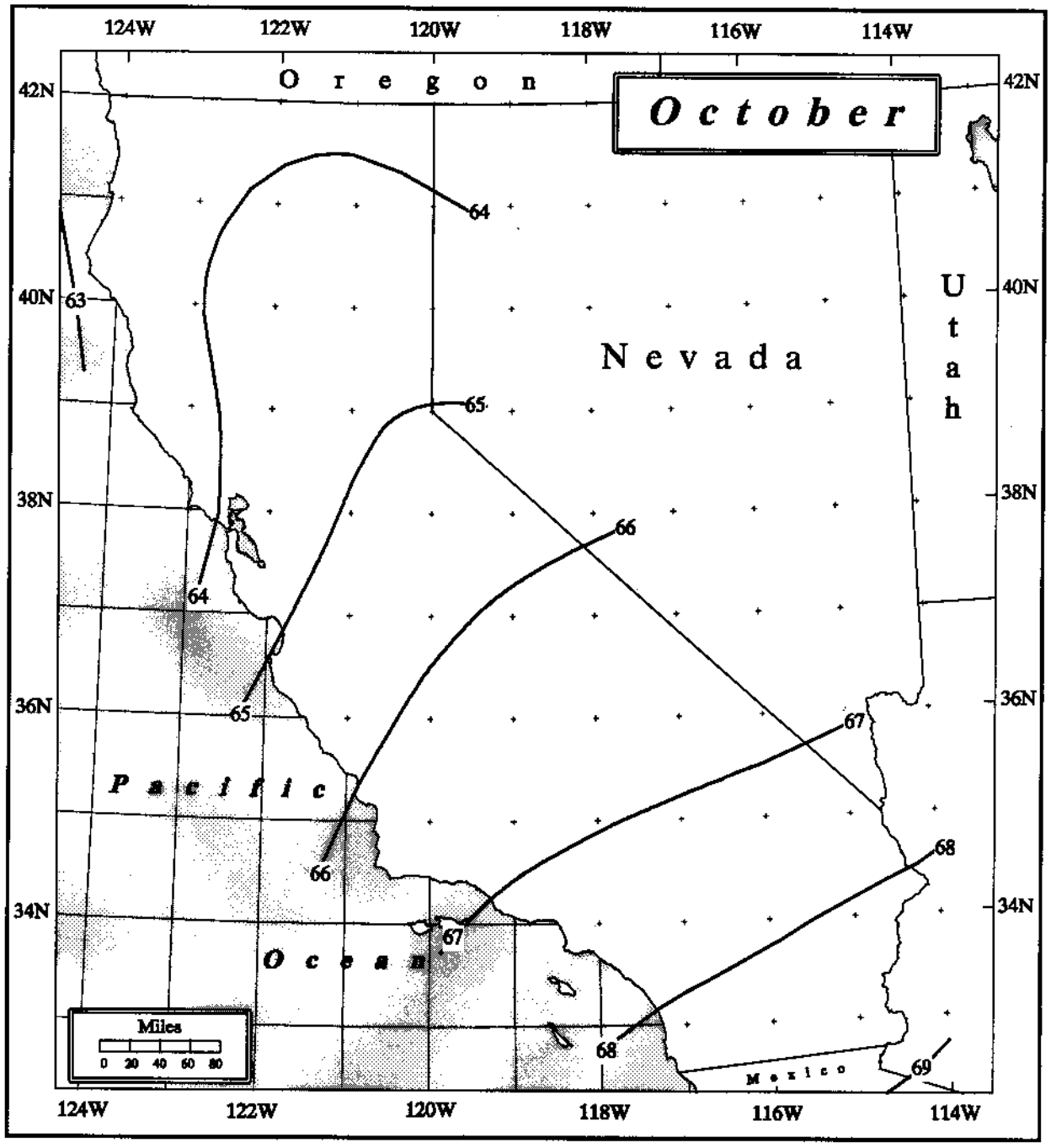

Figure 4.10. *Twelve-hour maximum persisting 1000-mb dewpoints for October (°F).*

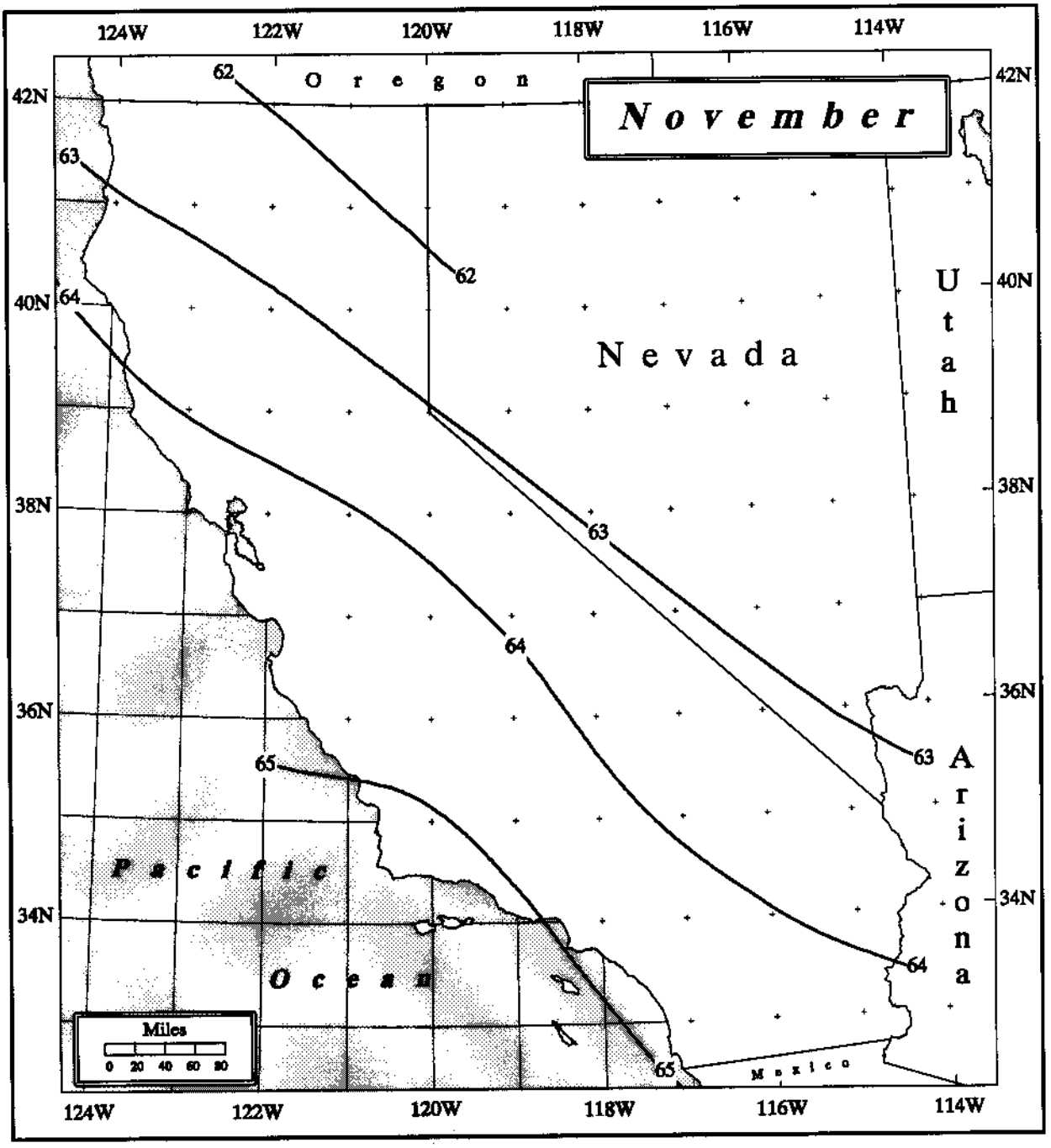

Figure 4.11. *Twelve-hour maximum persisting 1000-mb dewpoints for November (°F).*

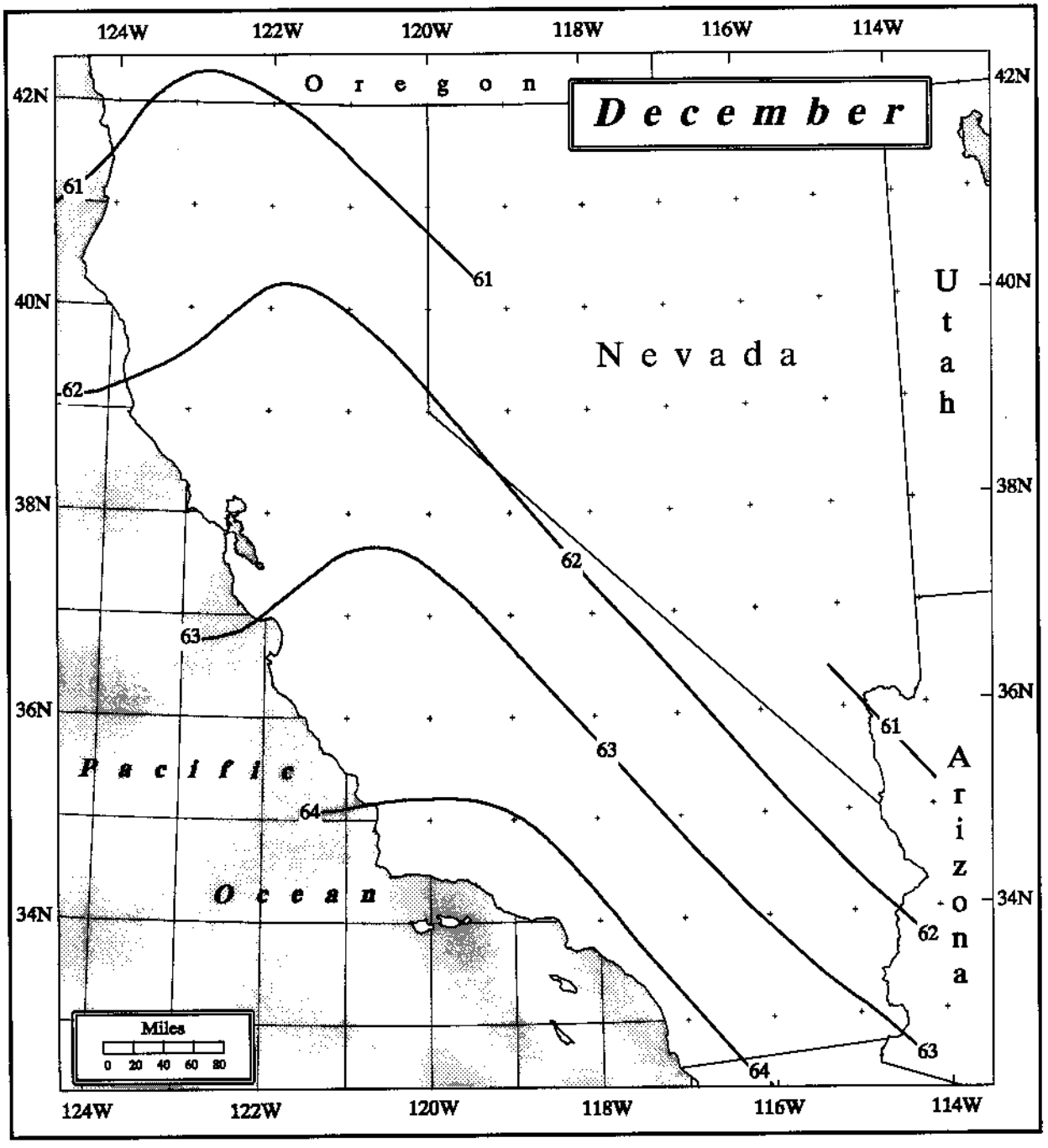

Figure 4.12. *Twelve-hour maximum persisting 1000-mb dewpoints for December (°F).*

Four locations indicated by A, B, C, and D in Figure 4.13 were selected to monitor the monthly transition. Figure 4.14 shows the monthly variations in 1000-mb 12-hour persisting dewpoint temperatures for four locations in California. All four locations show maximum dewpoints in July to August and minimums in January or February and a smooth transition from month to month and across the year. The largest 1000-mb persisting dewpoint is over southeast California.

Figure 4.15 partitions California into three regions, each defining the months in which the largest daily precipitation amounts have been observed most frequently. The California partitions are continuous with the partitioning for Washington and Oregon shown in Figure 4.14 in HMR 57. The months with the potential of having the greatest rainstorms are: October through March in most of western California; July through October in extreme southeast California; and any month for the remainder of California. Isodrosotherms were drawn by averaging monthly dewpoint for the indicated months within the three sections. The analyses were combined by smoothing across sectional boundaries. The result was the *multi-seasonal* 12-hour maximum persisting dewpoint map shown in Figure 4.16. In the process of deriving all-season PMP values shown in Plates 1 and 2, this map was used to adjust all transposed 1000-mb free-atmospheric-forced precipitation (FAFP) values in the region to their respective barrier elevations. FAFP is convergence or non-orographic precipitation (see Chapter 6 for more explanation). The dewpoint map was also used to adjust the 100-year, non-orographic precipitation values to create the orographic parameter, T/C (Chapter 6).

Except for HMR 57, previous HMRs for the western United States have used land-based observed and maximum persisting dewpoints for storm maximization. In HMR 57, it was decided to use SST as a proxy for the *traditional* maximization factor for many storms. Many of the storms have up-wind regions with only ocean surface, and consequently no possible upwind measurements of dewpoint temperatures. For such storms SSTs were used. All these storms, had moisture trajectories originating in the Pacific Ocean. The proxy factor was based on a comparison between an observed SST and an estimated maximum SST. The maximum SST (or upper limit SST) was estimated from two standard deviations above climatology, which was at a point sufficiently upwind of the cold coastal current to be unaffected by it and along the moisture trajectory into the storm center. In HMR 57, it was

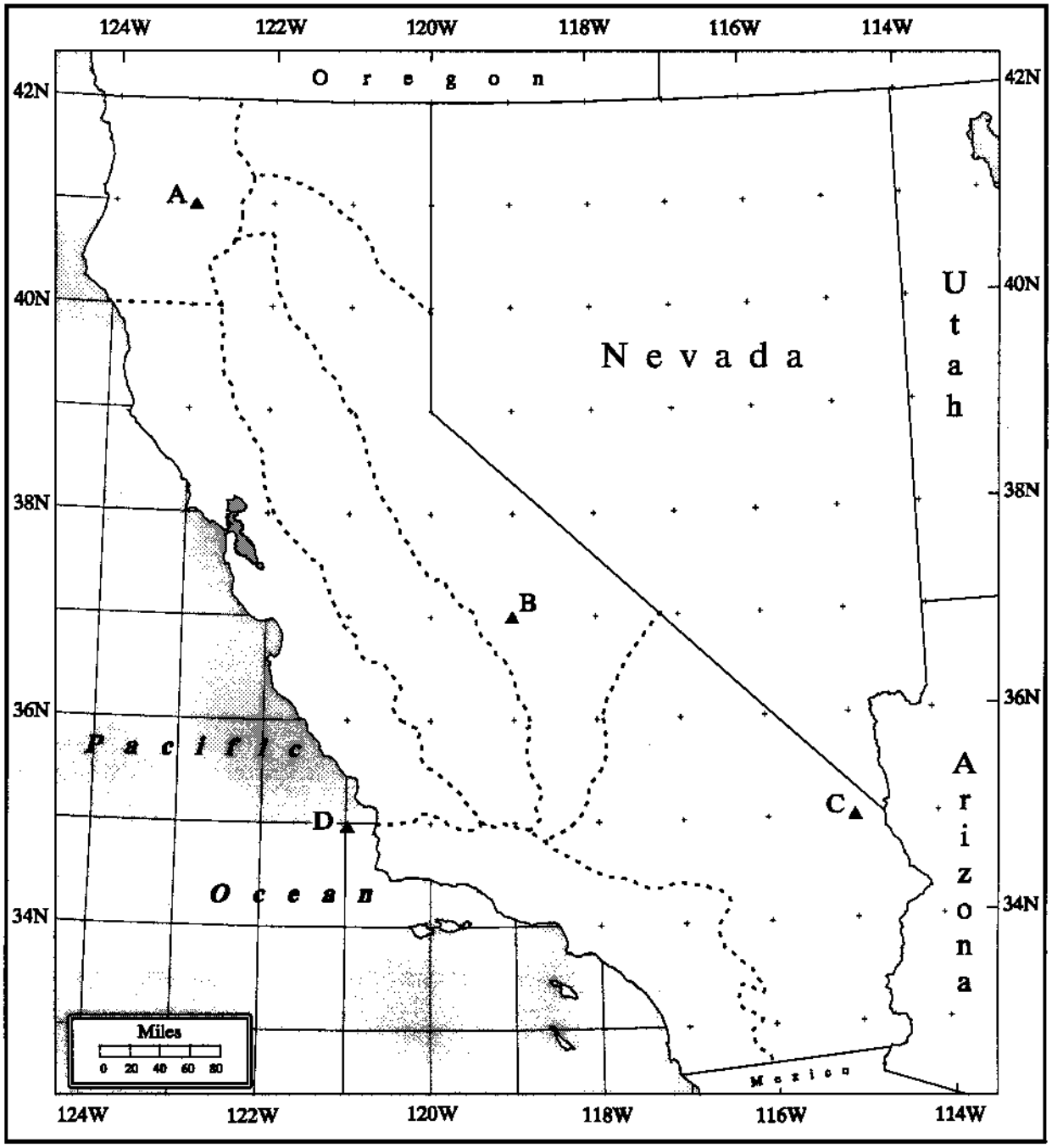

Figure 4.13. *Locations (A, B, C, D) shown for the month-to-month continuity check from January to December. Regional boundaries are shown.*

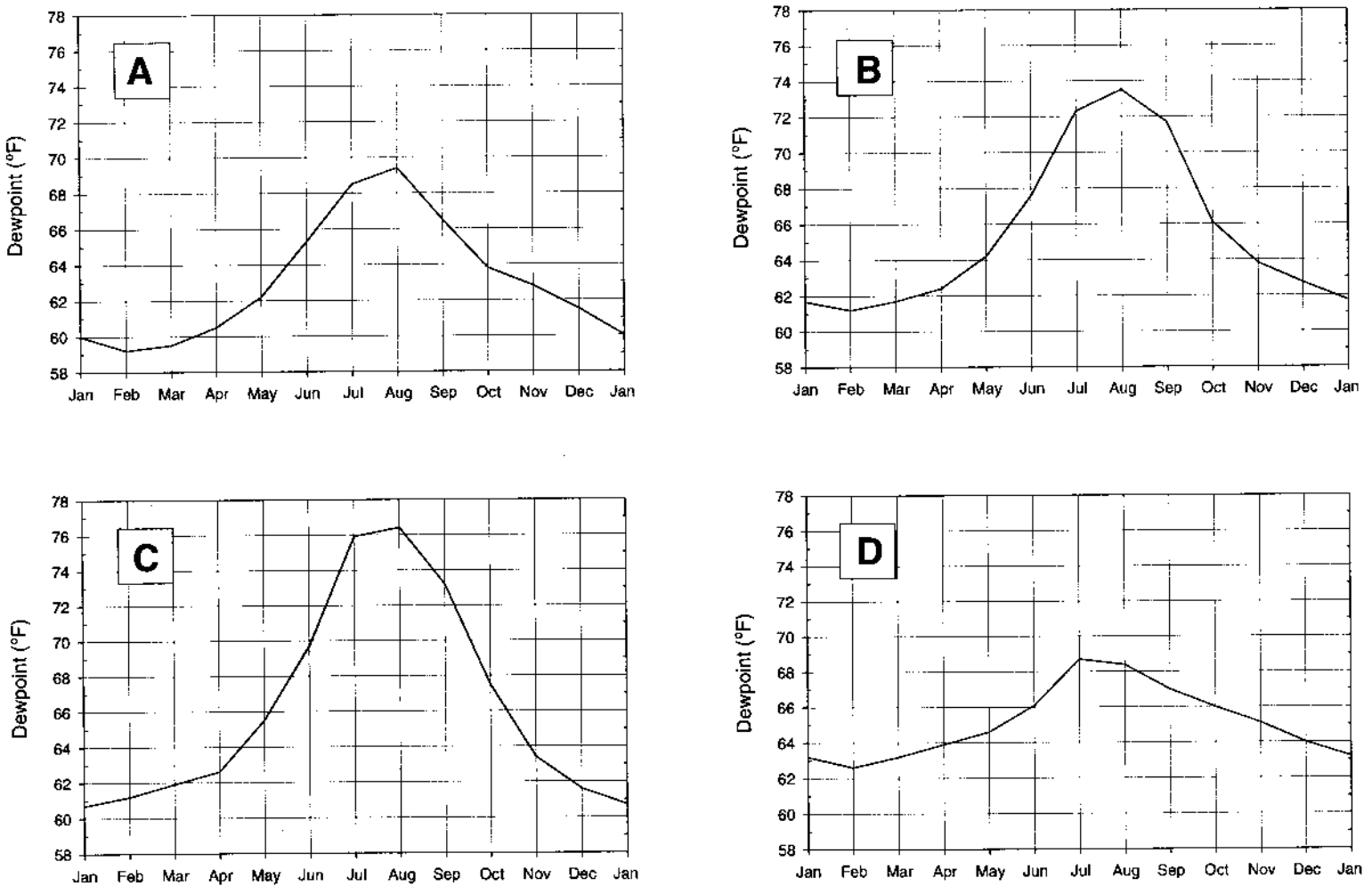

Figure 4.14. *Example of consistency and smoothness checks for 12-hour maximum persisting 1000-mb dewpoint temperatures (°F) at the locations shown in Figure 4.13.*

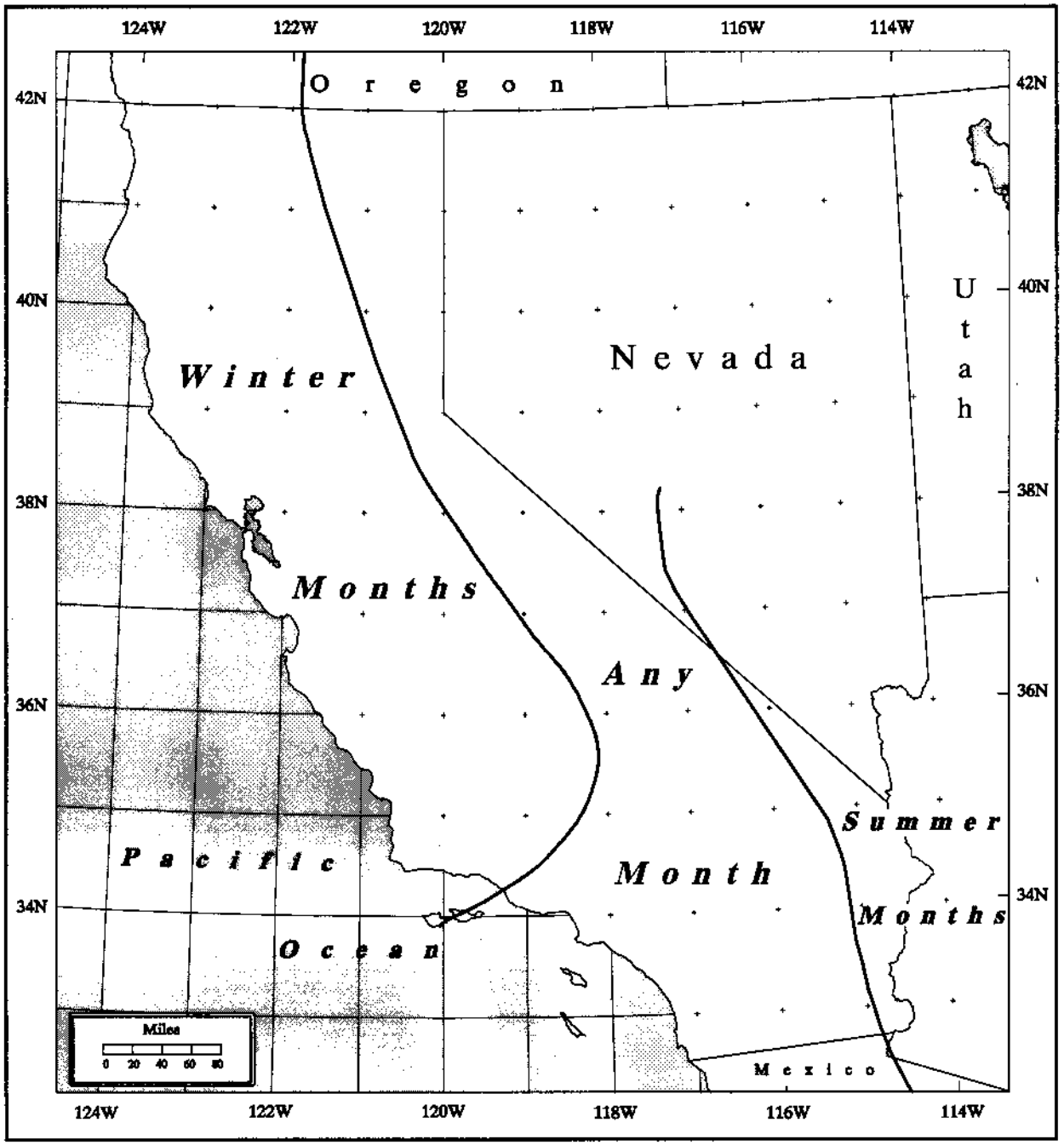

Figure 4.15. *Regions and months used in developing the multi-seasonal dewpoint maps in Figure 4.16.*

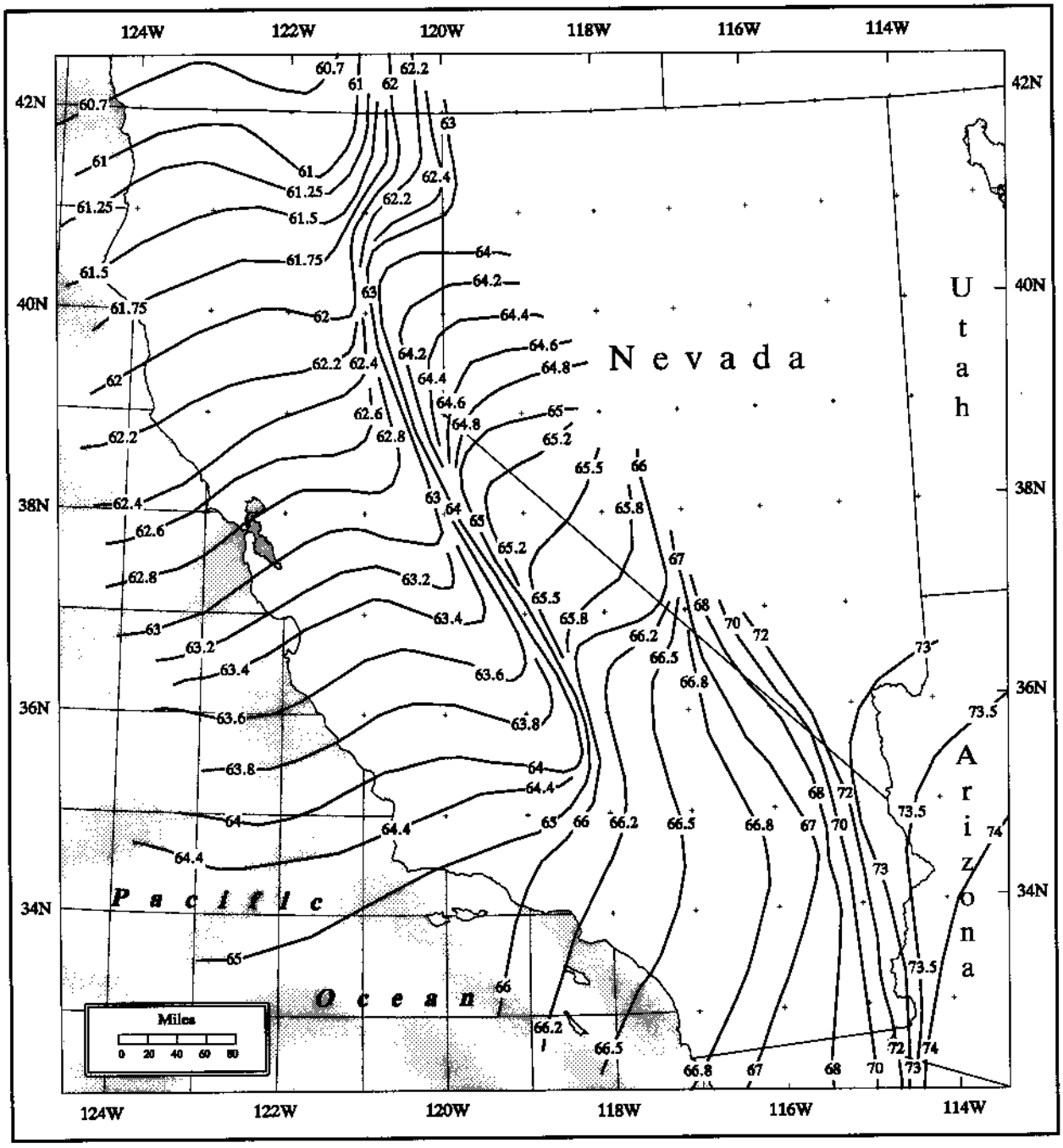

Figure 4.16. *Multi-seasonal, 12-hour maximum persisting 1000-mb dewpoints used for calculating vertical adjustments (°F).*

demonstrated that the proxy maximization factor remains nearly constant regardless of the amount of moisture scavenged from a parcel of air, as it crosses the cold coastal current. Therefore, it was considered reliable for setting precipitation depth for a PMP storm, as long as the assumption that the amount of scavenging in the PMP storm was the same as in an observed record-setting storm.

The Marine Climatic Atlas of the World (U.S. Navy 1981), was used to obtain the mean SSTs and standard deviations. To determine the maximum SST it was assumed that the mean SST plus two standard deviations would adequately set the upper limit for moisture *charge* or availability. The same procedures and assumptions used in HMR 57 were followed in this study. Thus, two SSTs were estimated for each storm - one for the storm being analyzed; the other, the maximum SST for the same location.

Essentially, the steps are: for the storm SST 1) a trajectory was extended upwind and backward in time from the storm center to a moisture source region in the Pacific Ocean; and then 2) a best estimate SST within the source region, based upon ship reports, was used as long as synoptic characteristics and distance from trajectory were consistent; and 3) for the maximum SST for approximately the same location, the mean SST and standard deviation were derived from the Marine Climatic Atlas for the same month, with a 15-day adjustment toward the warmest time of year (World Meteorological Organization 1986). For the September 1959 (1006) and the August 1977 (1017) storms, that do not have extended inflow trajectories, the traditional National Weather Service procedures were followed as described in the Manual for Estimation of Probable Maximum Precipitation (World Meteorological Organization 1986). Calculations of maximizing factors were made with temperatures to the nearest tenth of a degree Fahrenheit and precipitable water amounts from interpolation in precipitable water tables (U.S. Weather Bureau 1951).

All trajectories were drawn using archived surface weather maps. For storms before 1950, SST measurements came from archived ship reports from the NOAA Environmental Research Laboratory (1985), Boulder, Colorado, and the National Oceanic Data Center, Washington, DC. The analyses were supplemented by the daily weather maps (Environmental Data Services 1899-1971). The records of land station observations from the Local Climatological Data Series (NCDC 1948-) were used to obtain persisting dewpoints for traditional maximization.

Within the process of determining the appropriate SST for individual storms, some complications arose that influenced the values adopted in this study. These complications typically involved decisions about the timing of the moist air inflow. Relatively small differences in time (order of hours) could result in widely different source regions (order of degrees of latitude/longitude). Additional analysis was used to resolve any inconsistencies.

5. STORM ANALYSIS

5.1 Introduction

A complete analysis of 31 storms listed in Chapter 2, Table 2.1 was done to produce depth-area-duration (DAD) relations. Although the procedure is similar to past storm studies and hydrometeorological reports, no previous DAD relations were accepted for this study, except from storms used in HMR 57 (1994); otherwise, uniformity of analysis could not be assured. Each storm was individually examined and analyzed based upon all available data. Although previous storm DADs were available from the Corps of Engineers Storm Rainfall Catalog and from unofficial DAD studies completed by the National Weather Service (NWS), new DADs were developed. Previous storm analysis procedures were labor-intensive and time-consuming. However, with the help of a geographic information system (GIS) the storm studies were completed more expeditiously and efficiently.

As a result of using a more automated approach to calculate DAD for the storms, less time was spent in routine procedures and manual drawing of various maps. The use of a GIS system (GRASS 4.0 1991) and computer spreadsheets minimized many of the computational aspects. For instance, data tabulation for specific storm periods, mass curves for each station (hourly and daily), DAD analysis, and pertinent data sheet preparation were all done by computer. However, much time was still needed for quality control, formatting, and entering supplemental data (data not part of the regular NWS network of stations, such as bucket survey data).

As in HMR 57, the spatial distribution of storm rainfall was determined by comparing the proportion of storm rainfall to the 100-year frequency analyses in NOAA Atlas 2 (1973). The 100-year precipitation analysis shows considerable correlation with the underlying terrain, and the choice was made for this very reason. But it is also understood that individual storm precipitation could have different spatial distributions than shown in the atlas.

5.2 Precipitation Data

Precipitation data come from various sources and are the foundation for all storm DAD results and eventually PMP estimates. A thorough search was made for all recorder (hourly), non-recorder (daily), and supplemental (bucket survey and partial record stations) data available for all storms on the storm list (Chapter 2, Table 2.1). The majority of the data came from official NWS sites, both first order and cooperative stations. Supplemental data are data not normally archived by the NWS. For example, bucket surveys may be conducted by local, state, or federal officials. Such surveys provide invaluable data sets for a storm, especially in areas of limited information. The post-1948 NWS data were in digital form and converted to a standard internal format. The supplemental data and observation times for each observation were entered manually. Occasionally observation times, especially for older storms, were not extremely precise. For example, some observation times are given as sunrise or sunset, or as morning or evening with no set time indicated. Timing for these observations were determined by checking with nearby stations. The observation-entering stage was also the beginning of the quality-control as every station was examined for anomalous and incorrect information. Problems with accumulated amounts (precipitation for a multi-day storm period totaled into one observation usually at the end of the storm), missing data, and incorrect or ambiguous observation times, were addressed. Missing observations during the storm period usually caused the station to be discarded. Accumulated precipitation amounts for the storm period were useable if the observation began and ended within the storm period.

Once all of the quality-controlled data were put into a common format, each daily and supplemental station was timed. Timing provides a consistent temporal and spatial precipitation distribution for all stations within a storm. Thus, instead of just a few stations with hourly records, now all stations have an hourly distribution. A station was timed by assigning each daily station to an hourly station in order to distribute the daily station's rainfall in the same manner as the hourly station. The hourly station controls the hour when the rainfall began, the intensity of rainfall during the rain event, and when the rainfall ended at each of the daily stations assigned to it. In other words, the hourly station defines how the daily precipitation fell during the storm period at the daily stations.

Criteria for timing the stations included: distance between the hourly and daily

stations, topography, and the precipitation observed at the hourly and daily stations assigned to each other. Topographical considerations included the closeness of stations, valley/slope relations, and the location of crestlines. After all daily stations were assigned to an hourly station, daily precipitation was distributed into hourly increments across the storm period. Using the hourly distribution of rainfall, the observation times, and the amounts at the daily stations, the rainfall at the daily and supplemental stations was allocated according to the hourly station distribution. This process was done iteratively so that if an hourly distribution failed to provide adequate or realistic results, another nearby hourly station could be used instead. The distributions were compared by graphing the results, using mass curves, and examining them for consistency.

Figure 5.1 shows an example of one of the mass curves, for the January 20-24, 1943 storm (1003), and illustrates the consistency between the daily and hourly stations. Hoegees Camp was the hourly station used to time the other stations. For this set of stations, little or no rain was observed in the first 24 hours of the storm period. The rains began at hour 26 and continued to accumulate through hour 78. A total 37.34 inches was observed at Hoegees Camp and Camp Leroy Hoegees. These 2 stations are less than a mile apart. Lesser rainfall amounts were observed at the other stations. Daily total amounts were used for each of the other stations, and the daily totals were timed individually for each day. Most general storms exhibit a fairly uniform temporal distribution.

5.3 Storm Depth-Area-Duration Analysis Procedure

The first step in defining the development of DAD relations requires that rainfall amounts be assigned to all areas in the storm. In the past, point precipitation amounts were interpolated by assigning a particular precipitation gauge to a region. Usually the rain gage was centered in the domain. Once the entire storm area was assigned to particular gages, the rainfall distribution of those gages was used to determine the precipitation sequence for each individual region (Thiessen 1911). The Thiessen technique works well in non-orographic terrain. However, in mountainous areas, such as California, a modified approach was used to describe or develop likely rainfall patterns that fell over varying topographic features. The technique used here is similar to that in HMR 57. In order to construct a model for California and distribute rainfall over areas lacking in observations, a detailed map of the percent of total storm precipitation to the 100-year, 24-hour precipitation frequency (NOAA

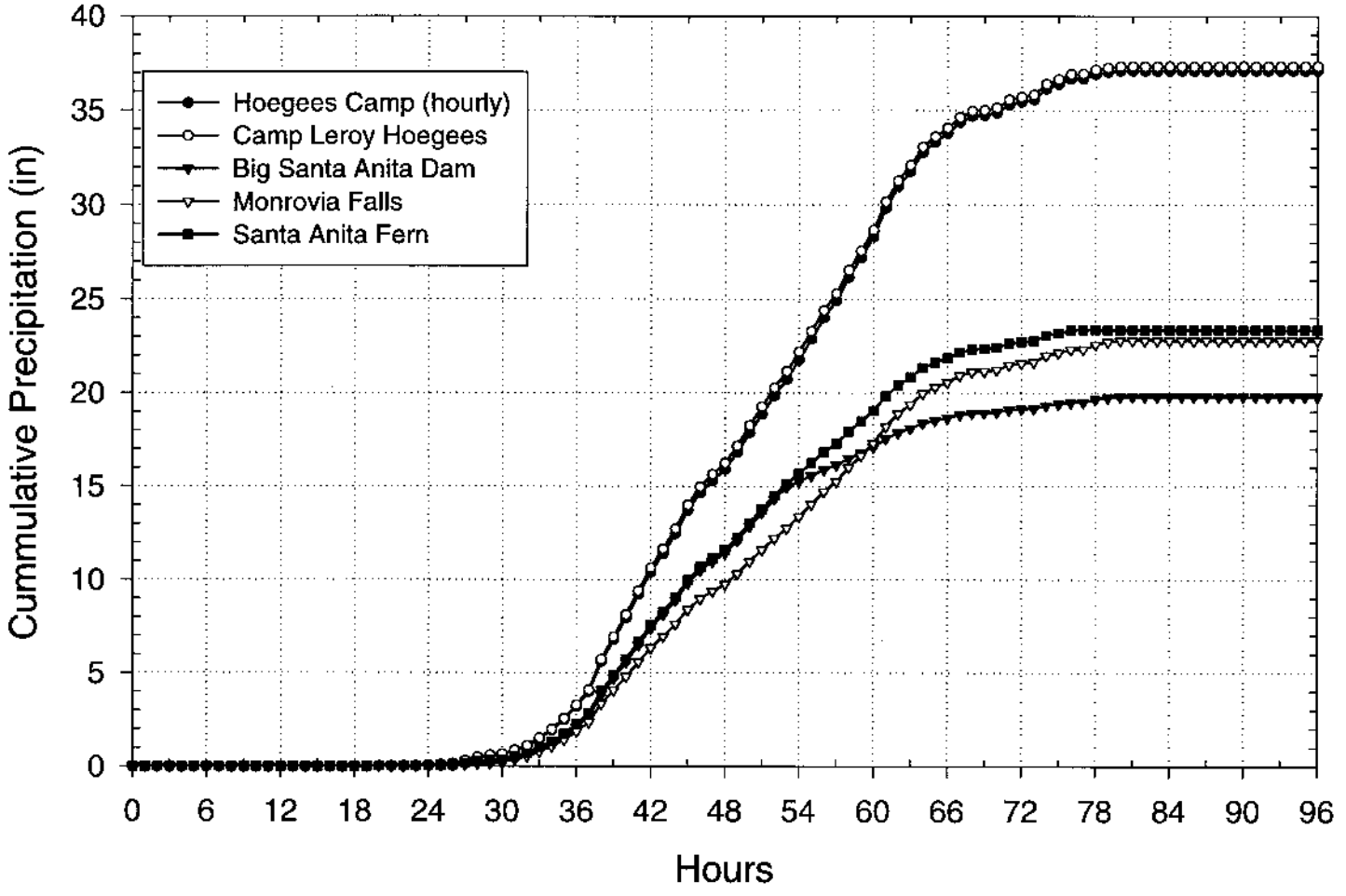

Figure 5.1. *Mass curves for four daily stations using Hoegees Camp as the hourly recorder for the January 20-24, 1943 storm (1003).*

Atlas 2) was produced. This map, called an isopercental map, represents the percentage of total storm rainfall to the 100-year, 24-hour analysis. Figure 5.2 shows a portion of an isopercental map from the January 20-24, 1943 storm (1003). The map was digitized using a GIS, and then interpolated, resulting in a raster field of percentals for the storm region. The process consisted of digitizing isolines which are considered vectors in a GIS. Vectors are the computer interpretation of an isoline. An interpolation between vectors forms a continuous field of values called a raster field in which each point (or raster) on the map has a value. Each raster cell was a 15 second by 15 second region (about 0.08 mi^2) and had a interpolated value related to it. Next, the rainfall over the whole area is distributed temporally. Individual subareas of the total storm pattern are delineated, with a representative individual station mass curve. Representative subareas or polygons were drawn by first choosing the station that best represented the total precipitation and rainfall distribution for the area. Then, a border was drawn that encompasses that region which is meteorologically and topographically homogeneous. A portion of the polygon map for the January 20-24, 1943 storm (1003), is shown in Figure 5.3. The polygons were drawn with the synoptic situation, terrain, and station type (hourly, daily, or supplemental) taken into consideration. There is no uniform rule as to the number of sides or the size of the polygon as long as the station chosen represents the precipitation distribution for that area. Drawing to terrain features often produces polygons that are not like those in a classic Thiessen polygon analysis since those Thiessen polygons do not follow the terrain features.

With the completion of the polygons, total storm precipitation values and their appropriate hourly distribution were determined using a GIS. A total storm precipitation map for the area was created by multiplying the isopercental raster layer by the 100-year, 24-hour precipitation frequency raster layer from NOAA Atlas 2. The temporal distribution of precipitation at each point within the storm area was then calculated by combining the polygon raster layer, containing the temporal distribution of the previously assigned station, and the total precipitation raster layer. Once the temporal distribution field was defined, total storm precipitation was distributed into a field of hourly values for the storm. All computations were done using GRASS 4.0 (1991) GIS at 15-second intervals (0.08 mi^2).

An isohyetal map was made for total storm rainfall for each storm, based on the total storm precipitation layer. Figure 5.4 shows a portion of the isohyetal map for the January 20-24, 1943 storm (1003). The isohyetal map identifies regions of peak precipitation. It is

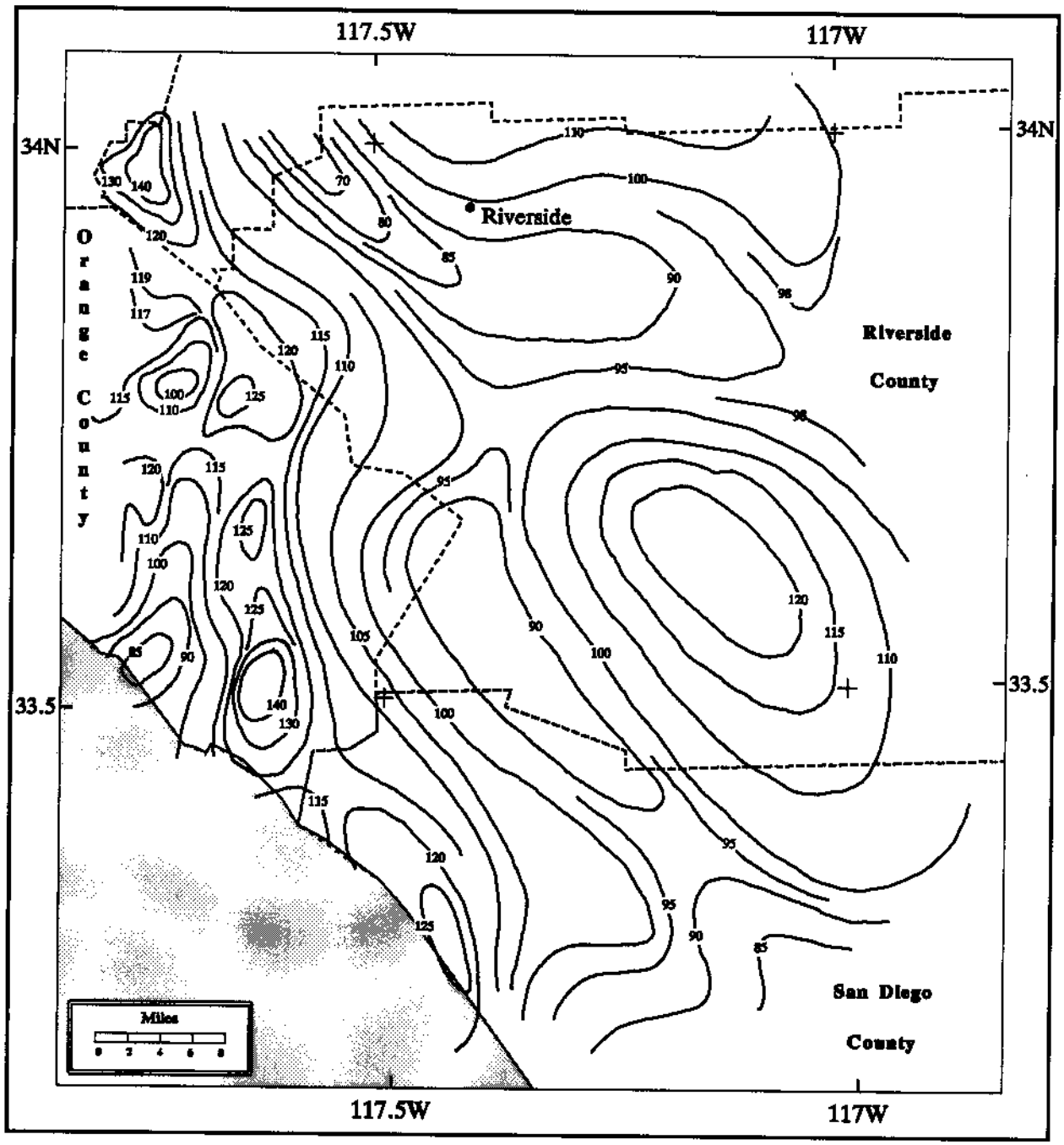

Figure 5.2. *An example of isopercental lines drawn for the January 20-24, 1943 storm (1003). The values represent the percent of the total storm rainfall to the 100-year, 24-hour precipitation frequency (NOAA Atlas 2, 1973).*

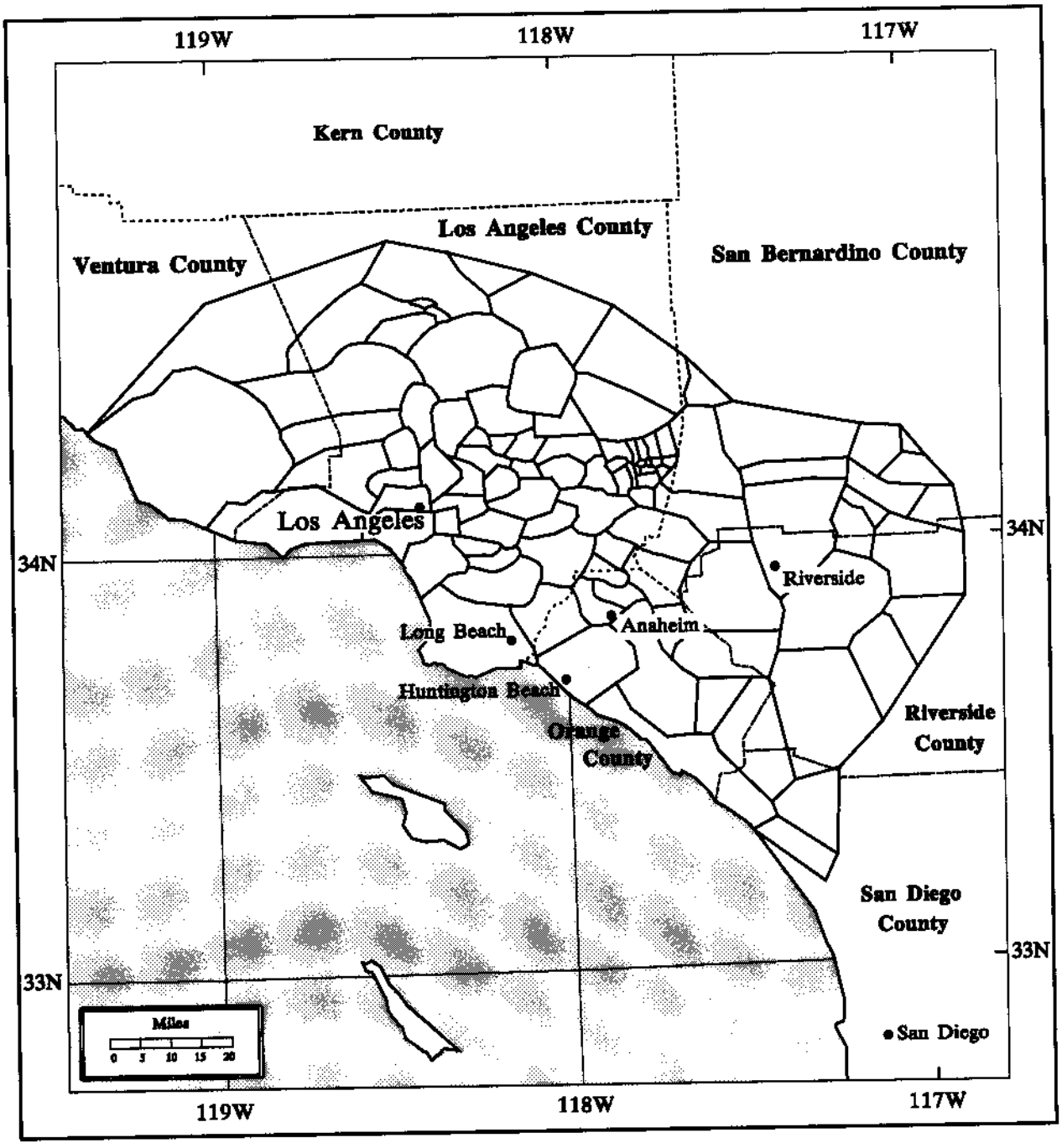

Figure 5.3. *An example of a polygon map used for analysis in the January 20-24, 1943 storm (1003).*

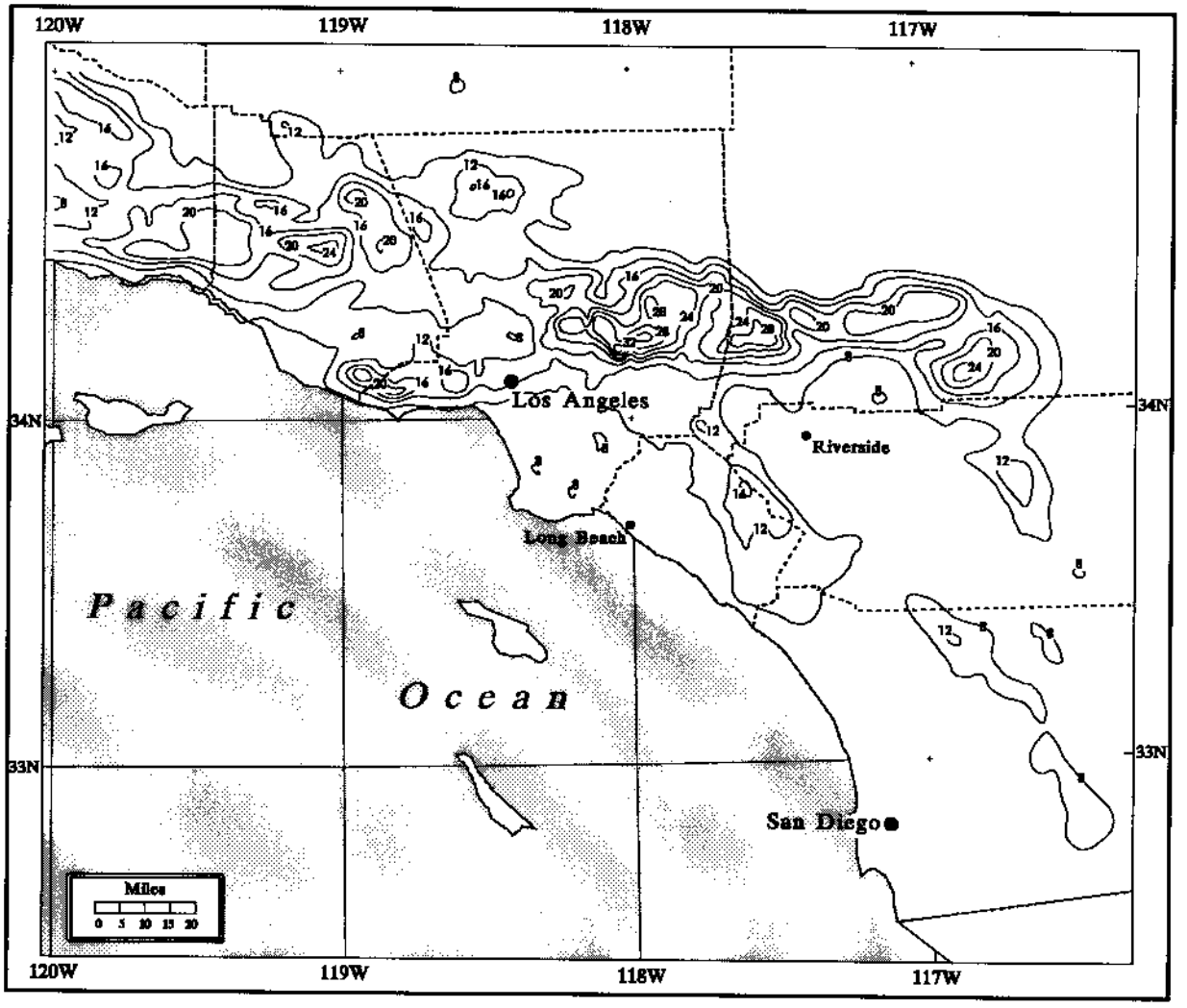

Figure 5.4. *Precipitation for the January 20-24, 1943 storm (1003). Isolines begin at 8 inches with 4-inch intervals up to 32 inches.*

important to identify the maximum precipitation center(s) for determining the DAD for a storm. Often in complex terrain, several significant precipitation peaks occur. Since combining precipitation centers miles apart is akin to combining nonhomogeneous meteorological factors and/or moisture supply, only those centers that were judged to be from the same dynamic mechanisms and moisture supply were combined. To choose which precipitation center would provide the maximum depth at a given area size and for a particular duration, several centers were examined separately. Precipitation centers occurring near one another were consolidated if the same convergence/orographic mechanisms appeared responsible for the precipitation. Multi-center storms normally occur along mountain chains where nearby peaks become precipitation centers. A common example of a split center is one center along the Coastal range and a secondary maximum over the Sierra Nevada mountains. The Coastal range center(s) almost certainly had differing orographic and convergence components than the Sierra center and therefore differing dynamic mechanisms. Split centers of this type occurred in more than half of the storms examined.

Storm DAD was calculated with a program developed with a C-language interface provided with GRASS 4.0. The output from the DAD program was plotted and examined on semi-log paper with the precipitation depth on the x-axis and the area on the y-axis. A graph was made for each duration interval (1, 6, 12, 24, 36, 48, 60, and 72 hours). The values on the graph reflect the greatest precipitation depth for various area sizes and for various durations of the storm based upon a particular storm center. The maximum depth for various area sizes was determined for each duration. Care was taken to insure spatial and temporal consistency with the storm center. A line was drawn to connect those points with the same center from 1 mi^2 to beyond 10,000 mi^2 at the upper areal limit.

Finally, after the DAD lines connecting all of the maximum precipitation amounts were drawn for the storm, precipitation values were extracted for selected durations and area sizes and placed on a pertinent data sheet. Table 5.1 presents the results for the January 20-24, 1943 storm (1003). This pertinent data sheet was the culmination of the entire storm analysis procedure.

Table 5.1. *Precipitation from the January 20-24, 1943 storm (1003) by area and duration (inches.)*

	Duration (hours)											
Area (mi^2)	**1**	**3**	**6**	**12**	**18**	**24**	**36**	**48**	**60**	**72**	**84**	**96**
1	2.90	5.50	9.50	16.05	20.52	25.70	33.18	36.10	36.51	36.52	36.54	36.65
10	2.43	4.78	8.55	14.62	17.80	22.90	28.76	31.60	32.28	32.30	32.86	33.00
50	2.14	4.25	7.85	13.15	16.38	20.62	26.32	28.82	29.91	30.63	30.81	30.95
100	1.97	3.92	7.25	11.77	15.42	19.60	24.96	27.63	28.56	29.19	29.25	29.38
200	1.80	3.57	6.63	10.80	14.70	18.38	23.41	26.18	26.91	27.11	27.23	27.31
500	1.65	3.20	5.91	10.28	13.38	16.62	21.13	23.55	24.16	24.52	24.62	24.65
1000	1.30	2.78	5.02	8.60	11.25	14.25	18.45	20.51	21.27	21.54	21.55	21.56
2000	0.97	2.04	4.59	7.55	9.70	12.00	16.02	17.33	18.69	18.79	18.83	18.84
5000	0.62	1.80	3.50	5.78	7.50	9.50	13.32	14.79	15.60	15.78	15.86	15.88
10000			2.67	4.38	5.75	7.25	10.21	11.45	12.01	12.40	12.78	12.80
20000				3.00	4.17	4.92	7.14	7.90	8.77	9.05	9.28	9.45
30000					3.00	3.20	5.36	6.30	6.78	7.20	7.32	7.40

The final numbers were normalized and compared with other storms in the same region to create DAD curves for each region. To normalize the pertinent data sheet values for each storm, each depth at each duration was divided by the 10-mi^2 value at that duration. Table 5.2 contains the normalized values for the January 20-24, 1943 storm (1003).

Table 5.2. *Ratio of DAD rainfall to the 10-mi² DAD rainfall for the January 20-24, 1943 storm (1003).*

	Duration (hours)											
Area (mi²)	**1**	**3**	**6**	**12**	**18**	**24**	**36**	**48**	**60**	**72**	**84**	**96**
1	119	115	111	110	115	112	115	114	113	113	111	111
10	100	100	100	100	100	100	100	100	100	100	100	100
50	88	89	92	90	92	90	92	91	93	95	94	94
100	81	82	85	81	87	86	87	87	88	90	89	89
200	74	75	78	74	83	80	81	83	83	84	83	83
500	68	67	69	70	75	73	73	75	75	76	75	75
1000	53	58	59	59	63	62	64	65	66	67	66	65
2000	40	43	54	52	54	52	56	55	58	58	57	57
5000	26	38	41	40	42	41	46	47	48	49	48	48
10000			31	30	32	32	36	36	37	38	39	39
20000				21	23	21	25	25	27	28	28	29
30000					17	14	19	20	21	22	22	22

5.4 Storm Separation Analysis

The Storm Separation Method (SSM) is used in hydrometeorological analysis to arrive at an approximation of the non-orographic component of precipitation from storms centered in orographic areas. The SSM was originally developed for HMR 55A (1988) as a standardized procedure to isolate and quantify orographic from non-orographic factors in record-setting storms. The SSM incorporates both the moisture-maximizing process and the adjustment of dewpoints to a common reference level of 1000 mb as described in Chapter 4. The technique is fully described in Chapter 7 of HMR 55A and in Chapter 6 and Appendix 3 of HMR 57. The values produced by the SSM provide the starting point for making an index map of non-orographic PMP or free-atmospheric-forced precipitation (FAFP) to be discussed in Chapter 6. The FAFP index map, when modified by orographic factors, becomes the first approximation to the PMP Index map discussed in Chapter 7.

The SSM was performed on all storms listed in Chapter 2, Table 2.1. However, only 19 of those storms plus two Arizona storms (September 1939 (3) and September 1980 (8)) proved to have large enough index values of FAFP to warrant their transposition. Of the 21 storms of Table 5.3 only nine provided controlling values across California. The areas controlled by these nine storms are found in the next chapter in Figure 6.2. The controlling storms are noted by asterisks in Table 5.3.

Table 5.3 contains a variety of information for the 21 most significant storms. The FAFP point values from these storms were used to develop an areal analysis of FAFP for California which in turn is a component of the final PMP index values for the state.

It may be of interest to note that, the FAFP (adjusted to 1000 mb) for the December 1921 (40), November 1961 (149), and August 1977 (1017) storms was larger than the observed amount. Causitive factors for these high FAFP values include: the observed highly non-orographic precipitation at storm centers, and the substantial effects of both the moisture maximization and the vertical adjustment factors.

Table 5.3. *Storms studied using the storm separation method (SSM). The 9 controlling storms are indicated by *.*

Storm ID #	Storm Dates	Storm Center (decimal degrees)	10-mi², 24-hour precip. (inches)	1000-mb, 10-mi², 24-hour FAFP (inches)
508	1/15-19/1906	39.9 / 121.6	14.8	6.7
525	1/1-4/1916	39.8 / 121.6	10.1	7.6
544	12/9-12/1937	40.2 / 121.4	15.3	10.8
572	12/21-24/1955	38.0 / 119.3	13.4	7.2
575	10/11-13/1962	40.0 / 121.5	19.7	7.6
* 630	1/3-5/1982	37.1 / 122.0	20.7	10.8
1002	2/27-3/3/1938	34.2 / 117.5	20.3	7.1
* 1003	1/20-24/1943	34.2 / 118.0	22.9	9.1
* 1004	11/17-21/1950	39.2 / 120.5	12.0	9.8
1005	1/25-27/1956	34.2 / 117.5	11.5	8.1
1006	9/17-20/1959	40.7 / 122.3	17.8	7.8
1007	12/4-6/1966	36.3 / 118.6	21.7	4.3
1008	1/23-26/1969	34.2 / 117.6	19.1	4.1
* 1010	2/14-19/1986	39.9 / 121.2	18.1	11.7
* 1017	8/15-17/1977	34.8 / 115.7	5.7	9.1
Other Storms				
* 40	12/9-12/1921	48.0 / 121.4	8.1	8.7
* 88	12/26-30/1937	44.9 / 123.6	10.8	7.6
* 149	11/21-24/1961	42.2 / 123.9	10.9	12.7
* 165	1/14-17/1974	41.1 / 122.3	10.3	7.6
3	9/3-7/1939	34.7 / 113.2	4.6	1.9
8	9/4-7/1970	33.8 / 110.9	10.6	3.5

6. CONVERGENCE AND OROGRAPHIC COMPONENTS OF PMP

6.1 Introduction

The rationale for estimating a convergence or non-orographic component of precipitation in record-setting storms in regions of significant topography is that precipitation in extreme storms there is so tied to topographic variation that re-creation of the same set of record-storm conditions is unlikely anywhere else. The Storm Separation Method (SSM) addresses this theory by extracting the influence of topography from the observed precipitation, thereby permitting more extensive transposition of the storm *mechanism* responsible for the remaining non-orographic precipitation. Thus, the creation of a non-orographic probable maximum precipitation (PMP) map within extensive orographic areas is made possible.

6.2 Moisture Maximization

Both the traditional approach to moisture maximization using dewpoint observations from coastal or inland locations (WMO Operational Hydrology Report No. 1 (1986), Chapter 2, and HMR 51 (1994), Chapter 2) and maximization based on a climatology of sea surface temperatures (SST) upflow of storms (HMR 57 (1994), Chapter 4) were employed in this study. Table 6.1 shows the moisture maximization factors for the SSM analyses for 21 storms. Dewpoints with an asterisk are land-based, maximum 12-hour persisting dewpoints adjusted to 1000-mb; all others are mean SSTs plus two standard deviations from the Marine Climatic Atlas of the World (U.S. Navy 1981). Although some of the same storms were used in HMR 57, there were slight differences in method. In HMR 57 the December 1921 (40), November 1961 (149), and January 1974 (165) storms were analyzed using land-based extreme dewpoints at the storm center; for HMR 59, the SSTs were taken at a reference location upflow of the cold Pacific coastal current. The moisture maximization factor is calculated from the following expression:

Table 6.1. *In-place maximization factors from storms used to prepare the free-atmospheric forced-precipitation map. Asterisks indicate land-based dewpoints; all others are sea surface temperatures (SST).*

Storm ID	Date	Maxi-mization factor	Barrier Elevation (ft)	Observed Temp. (°F)	Upper Limit Temp. (°F)	Land-Based Reference Location
Storms						
508	1/15-19/1906	1.24	2600	70	74	
525	1/1-4/1916	1.39	2000	69	76	
544	12/9-12/1937	1.39	5500	66	72	
572	12/21-24/1955	1.58	10,500	72	78	
575	10/11-13/1962	1.19	5500	72	75	
630	1/3-5/1982	1.35	950	66	72	
1002	2/27-3/3/1938	1.48	4400	70	77	
1003	1/20-24/1943	1.37	2100	69	75	
1004	11/17-21/1950	1.29	6900	71	75	
1005	1/25-27/1956	1.22	3900	66	70	
1006	9/17-20/1959	1.50	1000	*38	*69	Red Bluff, CA
1007	12/4-6/1966	1.39	8000	70	75	
1008	1/23-26/1969	1.33	5500	72	77	
1010	2/14-19/1986	1.26	5200	66	70	
1017	8/15-17/1977	1.39	3750	*73	*79	Phoenix, AZ
Storms used in other HMR studies						
40	12/9-12/1921	1.42	500	64	71	
88	12/26-30/1937	1.54	1500	*60	*68	Valsetz, OR
149	11/21-24/1961	1.47	2700	60	67	
165	1/14-17/1974	1.23	3300	66	70	
3	9/3-7/1939	1.30	2200	*72	*77	Gila Bend 30 SW, AZ
8	9/4-7/1970	1.32	4400	*73	*78	Phoenix 55 SW, AZ

$$R_{Ip} = \frac{W_{p,\ SL,\ SE}}{W_{ps,\ SL,\ SE}} \qquad (6\text{-}1)$$

where,

R_{Ip}	=	In-place maximization factor
W_p	=	precipitable water associated with 12-hour maximum persisting dewpoint
W_{ps}	=	precipitable water associated with 12-hour persisting dewpoint for storm 's'
SL	=	storm location
SE	=	storm barrier elevation

6.3 Horizontal and Vertical Adjustment Factors

Horizontal transpositions were done on a 1000-mb surface, and therefore, the SSM-derived, in-place maximized, non-orographic moisture was adjusted to 1000 mb. The adjustment factor is based on the difference in moisture available for precipitation between the storm's barrier elevation and 1000-mb, in a saturated pseudoadiabatic atmosphere (U.S. Weather Bureau 1951). No changes were made in the first 1000 feet of vertical transposition. All vertical adjustments were *downward* and were, therefore, equal to or greater than 100 percent. The adjustment is calculated from the following expression:

$$R_{vt} = \frac{W_{p\ max,\ SL,\ SE,\ 1000\ mb}}{W_{p\ max,\ SL,\ SE\ \pm 1000\ feet}} \qquad (6\text{-}2)$$

where,

R_{vt}	=	vertical adjustment factor
$W_{p\ max}$	=	precipitable water associated with 12-hour maximum persisting dewpoint
SL	=	storm location
SE	=	storm barrier elevation
1000 mb	=	sea-level equivalent height
SE±1000	=	1000-foot exclusion from adjustment

Figure 6.1 is a graphical representation of this expression for selected dewpoints.

The maximized, non-orographic record-setting storm amounts were adjusted from their elevations of occurrence to a common surface at 1000 mb. Next they were transposed along the 1000-mb surface within certain meteorological and orographic constraints, more fully described in Section 6.3. When a storm is transposed it is assumed that the same meteorological dynamics can be assembled in another location. The only difference between the vertically-adjusted and maximized observed precipitation amount at its origin, and the precipitation amount at the transposed location is from differences in moisture availability between the two locations, i.e., the differences would be based on the climatology of moisture for the region involved.. The gradients of maximum 12-hour persisting dewpoints at 1000 mb are the basis for the horizontal adjustments. Figures 4.1 to 4.12 (Chapter 4) show the fields of dewpoints involved in this adjustment. The adjustment is calculated from the following expression:

$$R_{HT} = \frac{W_{p\ max,\ TL,\ 1000\ mb}}{W_{p\ max,\ SL,\ 1000\ mb}} \qquad (6\text{-}3)$$

where,

R_{HT} = horizontal transposition adjustment factor

W_{pmax} = precipitable water associated with 12-hour maximum persisting dewpoint

TL = transposed location

SL = storm location

The date of the storm determines which monthly dewpoint chart is to be used.

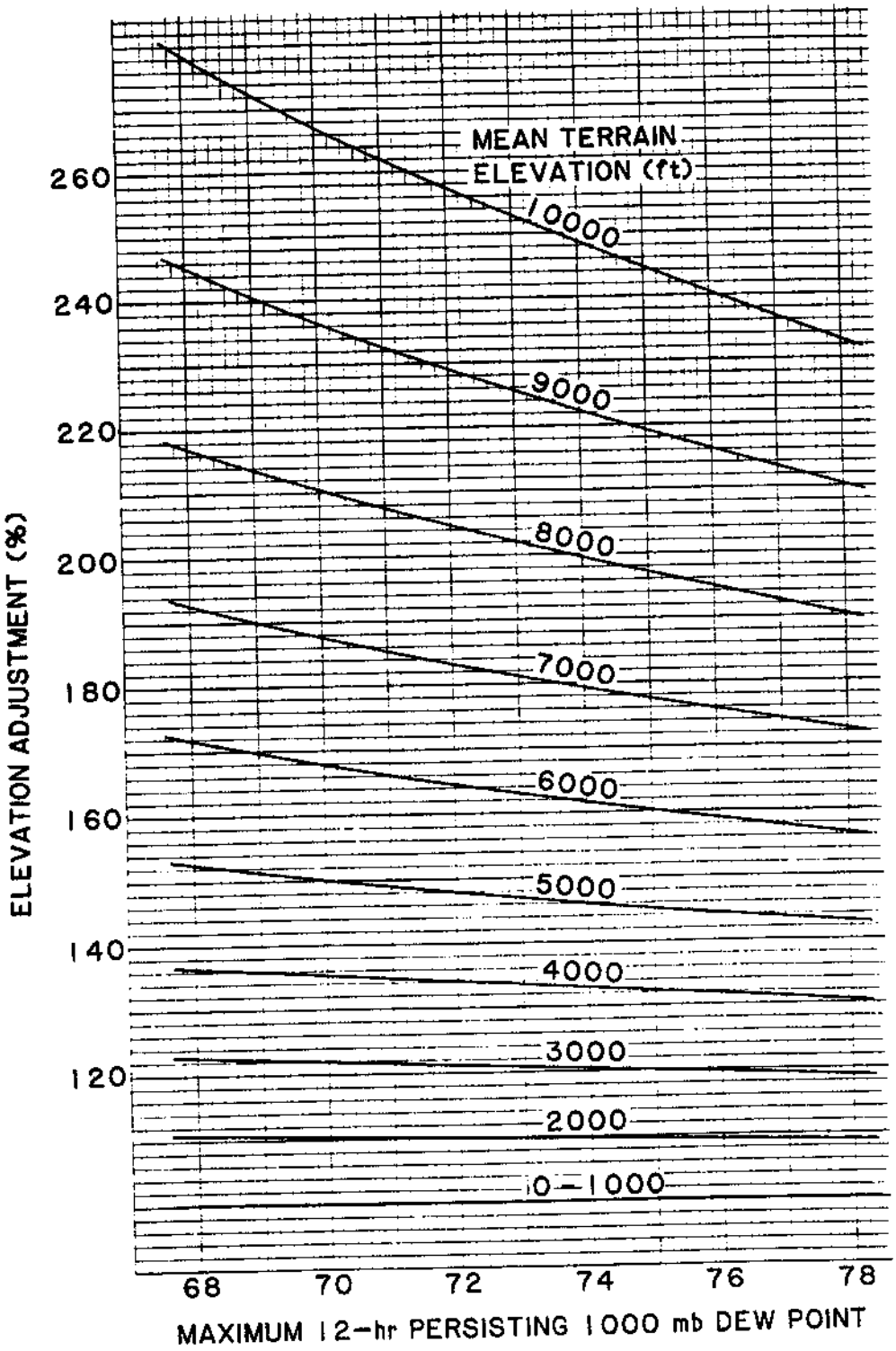

Figure 6.1. *Factors (%) for vertical adjustment of storm amounts at selected barrier elevations and dewpoint temperatures.*

6.4 Vertical and Horizontal Range of Transposition

Storm transposition involves relocating the atmospheric features of a storm from the place where they occurred to places where these features could be reassembled in the same way. It is not the storm precipitation as such which is transposed, rather it is the thermal and dynamic properties of the atmosphere responsible for the precipitation that are transposed.

The first step used to set the horizontal limits of transposition was a meteorological classification of each storm. Storm classification system was based on the factors most important for occurrence of extreme rainfall and is the same as the system developed for HMR 55A. In California the classification contains two major groups, general cyclonic and convective. The convective group is divided into complex and simple systems; cyclonic storms are divided into tropical and extratropical. And finally, extratropical storms are divided into frontal and convergence events (HMR 55A (1988), Chapter 2 and HMR 57, Chapter 7). Table 6.1 shows 21 storms that were classified, 19 as cyclonic and 2 as convective. The cyclonic storms were extratropical except for the September 3-7, 1939 storm (3). The principal forcing factor in 7 of the 19 storms was the circulation and associated convergence/divergence fields, whereas thermal contrasts and frontal displacements were paramount in the other 12 storms. Cyclonic storms were found in all regions of California, except the Northeast. It was determined that the November 1950 storm (1004) was transposable to the Northeast since it was north of the 39th parallel, and occurred at a significantly more remote site than other Sierra storms. The January 1974 storm (165), originally analyzed for HMR 57, occurred near the border between the Northeast and Sierra regions and was also considered transposable to the Northeast. Thus, at the first stage of transposition, all of California was covered by storm mechanisms classified as cyclonic.

The September 1959 (1006) and August 1977 (1017) storms were convectively driven. Although they were found in the extreme northern Central Valley and in the Southeast region, respectively, it is believed that such storms could occur anywhere in California. However, it was judged that only in the Southeast and in the northern Central Valley could convection develop well enough to become the mechanism responsible for non-orographic PMP at 10-mi^2 and 24-hours, regardless of season. Hence, at the first approximation of transposition limits, these two storms were confined to their region of

occurrence. Even though the September 1959 storm (1006) was estimated to have produced the largest non-orographic amount of precipitation in the northern Central Valley among storms occurring in California, it is the adjusted non-orographic amount from the December 1937 storm (88) transposed from Oregon to the northern end of the Central Valley, which controls FAFP there by approximately 20 percent over the September 1959 storm (1006).

At the second refining stage of transposition, the horizontal range set during the first stage is limited by: 1) the specific thermal and moisture inflow characteristics of each storm, 2) a reasonable latitude range over which the absolute vorticity of the flow about the storm would remain virtually unchanged, and 3) the distribution of record-setting storms across California. The way in which such considerations are handled in setting horizontal transposition limits has been widely discussed, most recently in HMR 57, Chapter 7.4.

The limit to vertical transposition of the non-orographic storm mechanism is defined as the elevation at which mixed (liquid and forzen) precipitation in a probable maximum storm begins. Mixed precipitation is generally observed at and below 2° Celsius. The procedure to define this elevation is slightly different than used in HMR 57. An upper air climatology (Crutcher and Meserve 1970) was used to determine an elevation at which the ambient air temperature becomes 2° C. This *climatological* elevation was compared with printed records which showed the level where liquid precipitation became frozen during the given storm. The *climatological* elevation is important because the storm mechanism produces only liquid precipitation below it and mixed (freezing, frozen) states of precipitation above it. Climatological elevation considerations mentioned here apply only to techniques relating to the vertical component of transposition. For transposition purposes, the higher of the two elevations was used. Steps in determining the *climatological* elevation are as follows:

A. At one or more points taken to represent either the whole or a subregion of the horizontal range of transposition of a storm mechanism, find the mean and standard deviation of the geopotential height and ambient air temperature of the 700-mb surface.

B. Increase the means of the geopotential height and the temperature, obtained by A, by two standard deviations.

C. Starting with the (increased) height and (increased) temperature from B, and assuming the atmosphere to be saturated and pseudoadiabatic, increase or decrease the starting temperature until a value of 2° C is achieved. Increase or decrease the height by the amount to achieve the required temperature change. The final height is the required *climatological* elevation. The height and temperature changes were performed here using a USAF Skew T, log P Diagram.

6.5 Controlling Storms

Once all the storms had been analyzed using the above procedures the final adjusted values were transposed to a sufficient number of points so that gradients of non-orographic PMP could be defined for all of California. Table 6.1 shows all of the storms from Chapter 5, Table 5.3 and as mentioned in Chapter 5, Section 5.4, only 9 of these storms provided controlling values of FAFP. Figure 6.2 shows regions where the indicated storm *controlled* the convergence component of PMP. In other words, the storm had a higher value of FAFP than any other storm observed or transposed in the region. A storm could be transposed over a wider range than indicated, but in such extended areas its transposed FAFP value would be exceeded by another storm.

There are two stippled areas, one in the high Sierra, and the other along and leeward of the peaks rimming the southern edge of the Mojave Desert and the western edge of the Imperial Valley. These areas are not *controlled* by any of the storms listed in Table 6.1. Instead they are areas in which FAFP is set through implicit transposition. A portion of the FAFP field in California is shown as Figure 6.3. In this figure, the values of FAFP near the 42nd parallel were constrained to the same values as in HMR 57 in that vicinity.

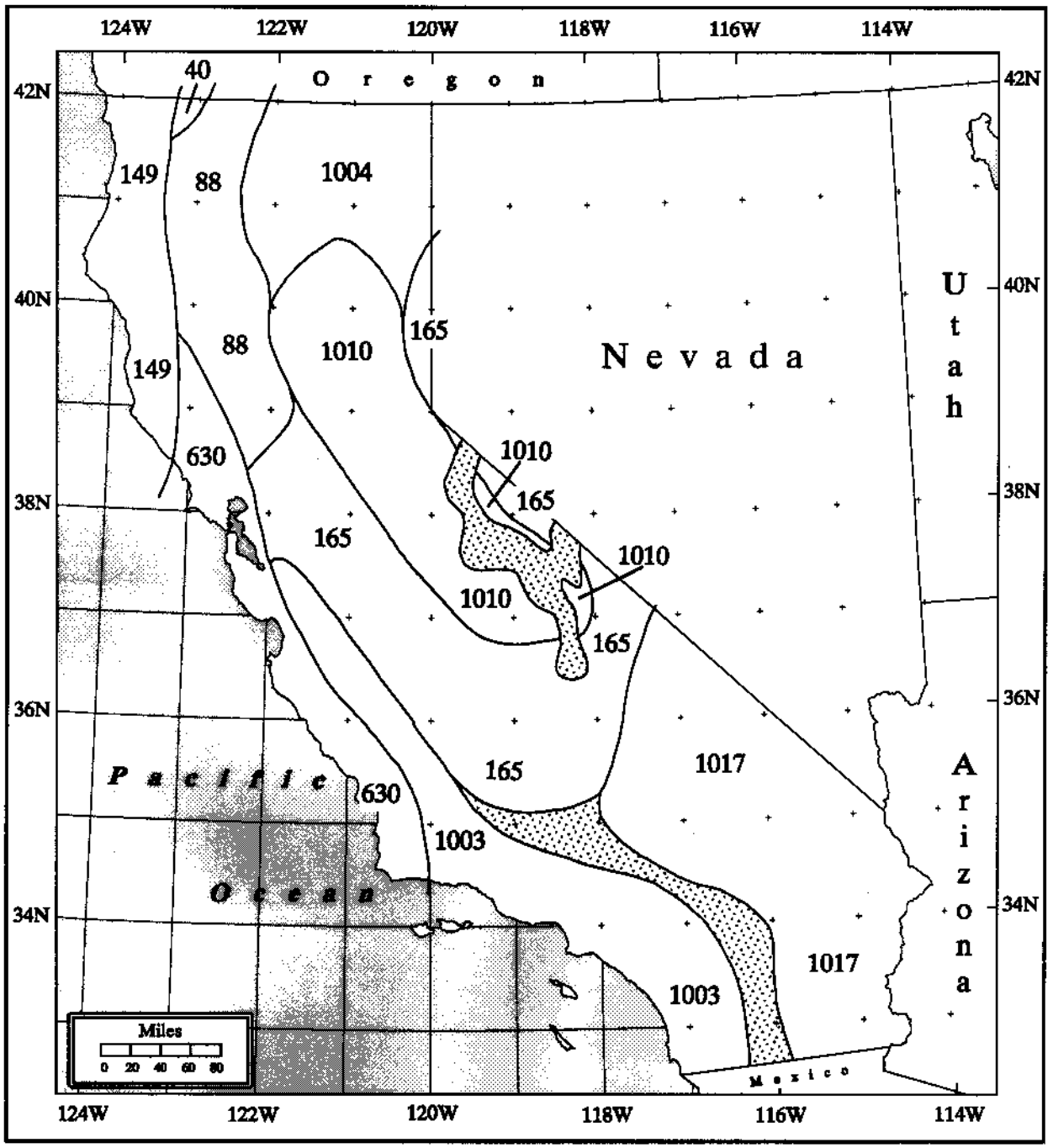

Figure 6.2. *Controlling subregions for 1000-mb, 10-mi^2, 24-hour maximized convergence storm component (storm identification numbers in Table 6.1). The stippled area represents areas that have FAFP set through implicit transposition.*

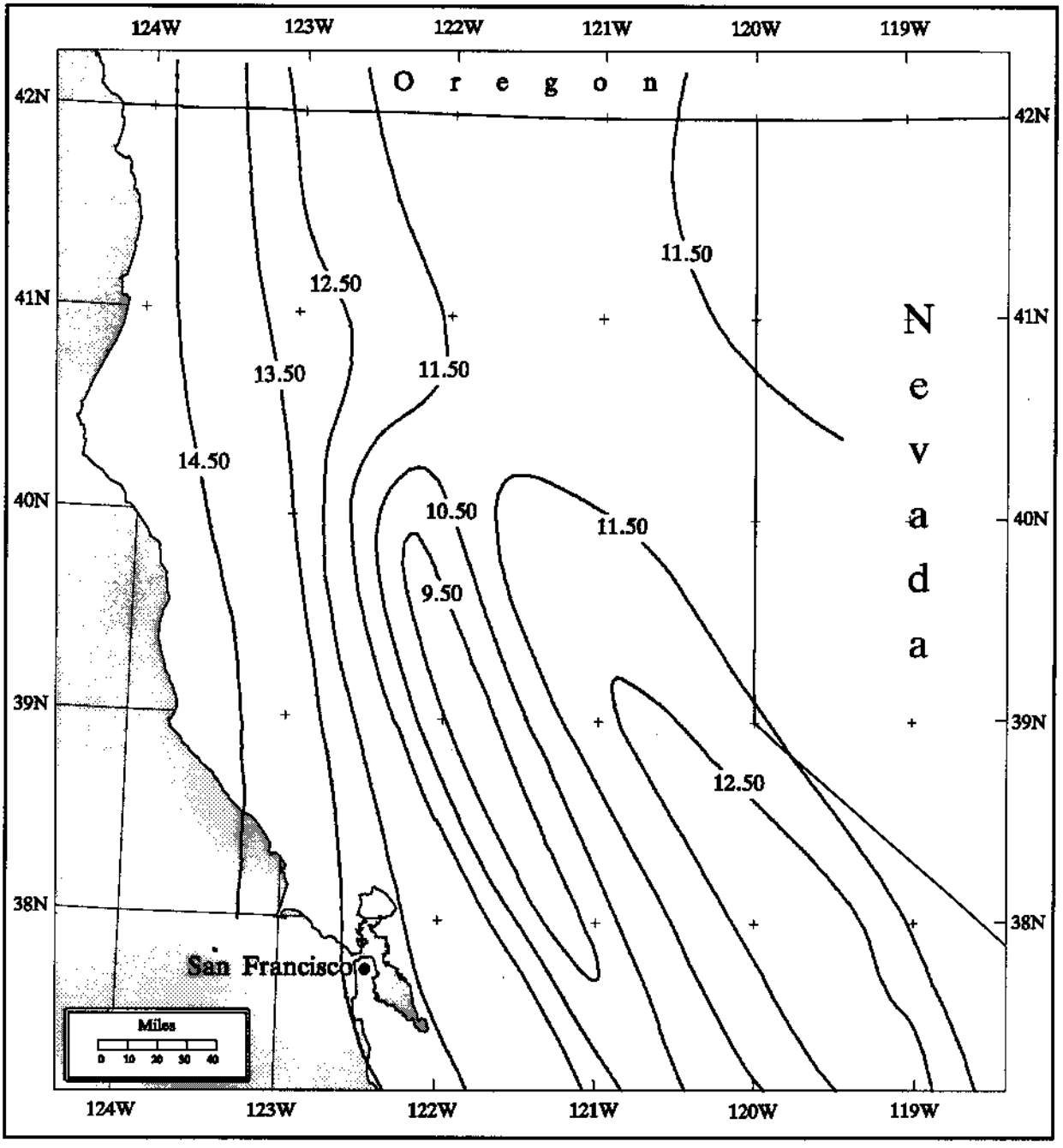

Figure 6.3. *Non-orographic PMP (FAFP) at 1000 mb (inches of rainfall).*

6.6 Determining the Orographic Influence (K) Factor

6.6.1 Introduction

The topographic effect on convergence precipitation, is expressed as a percent increase or decrease of convergence precipitation. Thus:

$$PMP = K * FAFP \qquad (6\text{-}4)$$

where,

K is the orographic factor for the same area and duration, and

FAFP is convergence precipitation for an *index area size* and *index duration*, usually 10-mi^2 and 24-hour

The K-factor is derived from two relationships: 1) The first involves the one-percent chance (100-year return period) precipitation amount in proximate areas of large and small topographic variation. This relationship is represented by T/C where T is the 100-year, 24-hour return-frequency precipitation; and C is the non-orographic (convergence) component of T. 2) The second concerns the accumulation rate and absolute depth of non-orographic precipitation from record-setting storms. It is represented by M which is the ratio of the precipitation depth of in a *core* period to the depth during the *index duration*. The *core* period is the longest, contiguous of time interval within an *index duration* during which:

A. The accumulated *core* precipitation equals or exceeds some arbitrarily long return period (usually 100 years), and also

B. The ratio of the proposed *core* amount (as a percent of the index amount) to the proposed *core* duration (as a percent of the index duration) equals or exceeds 2.

The depths used in A and B above are obtained from the mass curves of precipitation at locations of minimal topographic variation. It is assumed that those precipitation rates are representative of the non-orographic rain rates at the storm center. The K-factor is evaluated from the expression:

$$K = M^2 (1 - (T/C)) + (T/C) \qquad (6\text{-}5)$$

where,

K is the orographic factor,
M is the storm intensification factor,
T is the 100-year, 24-hour precipitation value, and
C is the 100-year convergence component.

This expression has been discussed in HMR 55A and other reports (Fenn 1985, Miller et al. 1984, WMO 1986).

6.6.2 Determining the (T/C) Ratio

The denominator (C) of the ratio was determined in two steps:

A. 100-year, 24-hour values from areas of non-orographic topographic characteristics were adjusted to a 1000-mb reference level using the 12-hour maximum persisting dewpoints from Chapter 4, Figure 4.16, and smooth analysis of these values drawn. The analysis near the 42nd parallel in California was made to match the analysis in Oregon used in HMR 57. The vertical adjustments were based on the barrier elevations (Chapter 3, Figure 3.4) and a 1000-mb persisting dewpoint field, representative of the season in which storms produce precipitation depths near the 100-year level. The analysis was interpolated smoothly from the calculated values unless modification of the field were indicated by climatology or by physiographic features.

B. The results from Step A are then adjusted from 1000 mb to the barrier elevation using the same persisting dewpoint field as in Step A. The resulting values are the calculated point values for the denominator (C) of the ratio.

Figure 6.4 is the T/C field for California. In some places, the calculated value of T/C was less than one. When physiographic features explained the low values, they were accepted; otherwise, values were set to one.

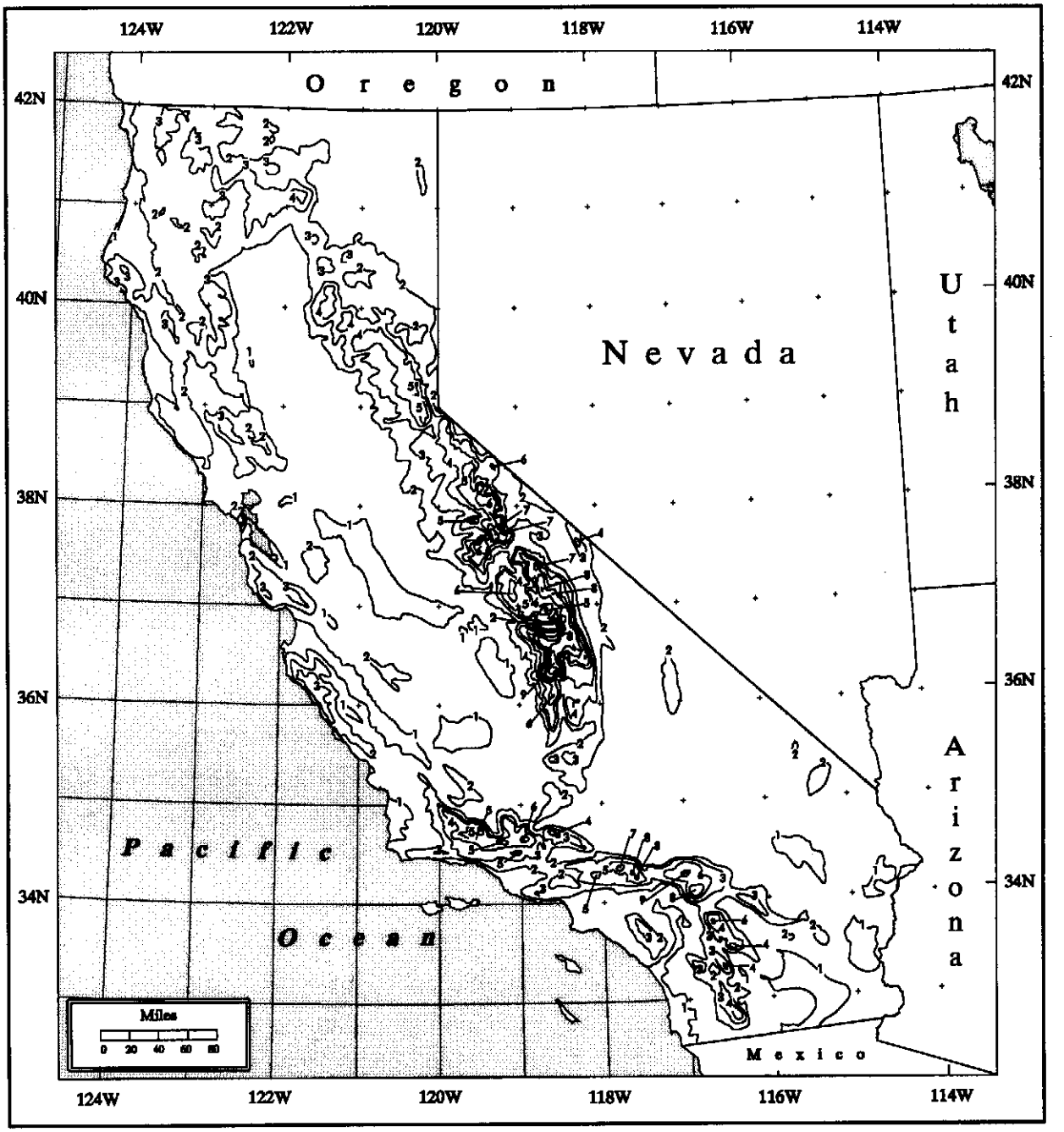

Figure 6.4. *Computer produced analysis of the orographic factor, T/C.*

In Chapter 7, a number of subjective changes made to preliminary versions of the 10-mi^2, 24-hour Index map of PMP are discussed. Some of these changes were prompted by examination of the T/C parameter, the principal determinant of the K-factor. In some instances, low NOAA Atlas 2 (1973) 100-year, 24-hour depths were believed to underestimate the orographic potential for enhancement of convergence precipitation. In other instances, it was an overestimate of the convergence component of the 100-year, 24-hour depths, which then caused the underestimation first of T/C, then of the K-factor and finally of index PMP. At other times, unusually high index PMP depths may have resulted from underestimation of the convergence component. A rule was adopted, that when the orographic factor was the causative factor in an untenable estimate of index PMP and where NOAA Atlas 2 100-year, 24-hour depths in an area were valid, changes to the denominator, C, of the T/C ratios were made as long as the changes did not result in anomalous localized values in the analyzed field of C.

6.6.3 Determining the M-factor

Table 6.2 lists the storms controlling the level of FAFP in California, along with the M-factor associated with each of these storms. The storm intensification factor, M, relates the precipitation in the most intense rain period to the total rainfall within the storm period, and therefore varies with storm type. Only two of these storms the February 1986 (1010) and the January 1974 (165) events have intensification factors that are not zero. The M-factor for the January 1974 storm (165) was a compromise value of 0.24. The compromise arose because the M-factor requires that not only the normalized rain rate exceed an acceptable level, but also that the precipitation depth during a *core* period exceed another acceptable level. This storm had a slightly shorter return-period definition for the depth and yielded an intensification factor of 0.38, while strict adherence to a 100-year level definition caused the M-factor to drop to zero. This instance highlights just one of the problems associated with defining a physically meaningful factor by arbitrarily set levels. Somewhat the same situation exists for storm 1003 where both the rain rate and the level of core precipitation are both below the acceptable level. Storm 1010 poses a different problem in that its intensification factor of 0.65 is achieved by having acceptably large values for rain rate and level of core precipitation, but an M-factor this large is more representative of a warm, moist season PMP storm which is not the season for the maximum, all-season storm in the Sierra. It was determined that an M-factor with a lesser, more winter-

like value in the range of 0.30 to 0.40 in the Sierra region would be used for storm 1010. Using a higher value would have resulted in a 29 to 37 percent reduction in total PMP in the more highly orographic sections of the region. Reduction of PMP to this extent was considered untenable.

Table 6.2. *Value of storm intensification factor M for storms setting the level of FAFP.*

Storm ID	Date	M-Factor
630	1/3-5/1982	0.0
1003	1/20-24/1943	0.0
1004	11/17-21/1950	0.0
1010	2/14-19/1986	0.65
1017	8/15-17/1977	0.0
Storms used in other HMR studies		
40	12/9-12/1921	0.0
88	12/26-30/1937	0.0
149	11/21-24/1961	0.0
165	1/14-17/1974	0.38

It will be recalled from Section 6.4 that transposed values from the (winter-time) January storm 1937 (88) with an M-factor of zero, set the FAFP level in the northern Central Valley. The September 1959 storm (1006) had a lower transposed value of FAFP and an M-factor of 0.59. However, storm 1006 is considered to be an *off-season* storm and so its M-factor was not weighted as highly as that of the January 1937 storm (88) when setting values in the northern end of the Central Valley. Compromise values between 0.25 and 0.32 are used in this region rather than a value exactly as observed. Thus, the analysis of the storm intensification parameter incorporates considerable modification to the directly calculated M-factors based on the profiles (mass curves) of the largest observed non-orographic precipitation from record-setting storms across the state. Figure 6.5 shows the storm intensity or M-factor analysis. The largest values of the M-factor for all of California approach 0.55 in the extreme southeastern part of the state. Minimum storm-intensity potential (low M-factor)is along the Pacific coastline, with a secondary minimum in a quite narrow zone to the lee of the Sierra crests along the Nevada border. The all-season PMP storm in this secondary area is a winter-time phenomenon, as will be seen in Chapter 7, Figures 7.2 through 7.11.

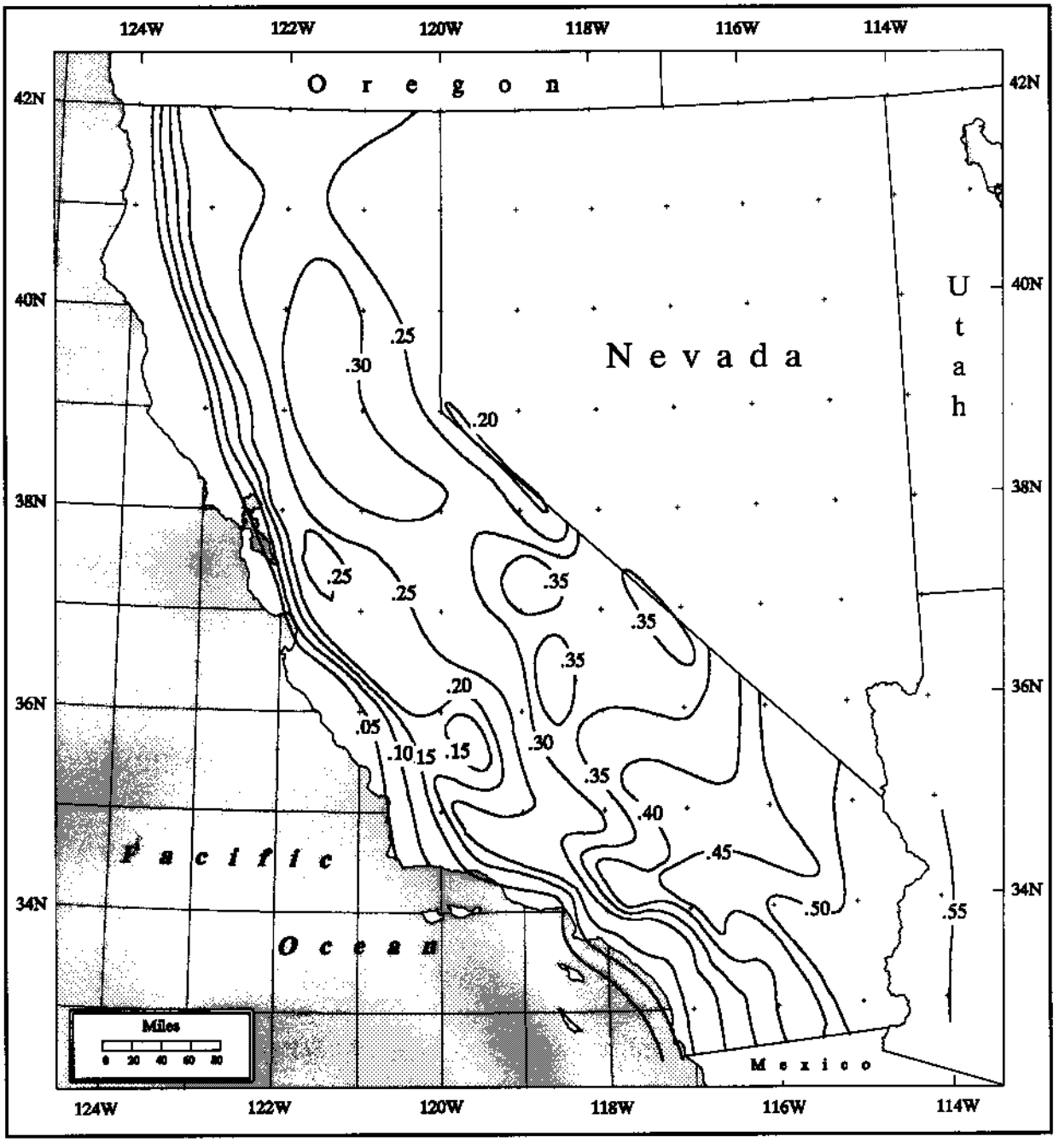

Figure 6.5. *Storm intensity (M-factor) map.*

During peer review concern was expressed that the somewhat subjective modifications made to M-factors, based on meteorological judgement, threatened the credibility of the (orographic) K-factor calculations. Unfortunately, many of the major California storm centers are not found in unambiguously non-orographic areas. The M-factor is a non-orographic storm property which should be determined as close as possible to the storm center. Consequently, varying degrees of uncertainty are associated with M-factors for those storms where the mass curves of rainfall come from non-orographic locations considerably removed from the storm center. In such cases when available mass curves indicate M-factors out-of-line with values found in other storms, meteorological judgement was exercised.

K-factors are not as sensitive to variation in M-factor as they are to variation in T/C, as can be seen in Table 6.3. A three-fold *uncertainty* as to the *correct* T/C produces an approximate 250 to 300 percent change in the resulting K-factor (over the range of M-factors shown), whereas, a three-fold *uncertainty* in the M-factor (over the range of T/C shown) produces only a 20 to 40 percent change in the resulting K-factor. In other words, if we are quite confident in our value for T/C, that should mitigate considerably our uncertainties in the resulting K-factor. But, alas, a variation of *only* 20 percent in a K-factor is not insignificant in absolute terms. We believe that our exercise of meteorological judgement has kept our uncertainties about the K-factors used in this report to a minimum and has produced far better results than would have been the case had we not modified what we believed were unrepresentative M-factors for certain storms.

Table 6.3 *Sample K-factors resulting from indicated values of (T/C) and M.*

M T/C	2.00	3.00	6.00
0	2.00	3.00	6.00
.1	1.99	2.98	5.95
.2	1.96	2.92	5.80
.3	1.91	2.82	5.55
.4	1.84	2.68	5.20
.5	1.75	2.50	4.75
.6	1.64	2.28	4.20

6.6.4 Analysis of the K-factor

After modifications to the analysis of the storm intensification factor M and the convergence component of the 100-year level of precipitation were finalized, the orographic intensification factor K was calculated using equation 6-5. The K-factor analysis for California is shown in Figure 6.6. In some instances, PMP calculated from equation 6.4 was considered too high or too low within an area, and slight modifications were made to the non-orographic fields to rectify the anomalies. In this situation percent changes were incorporated into the existing K-factor field in order that PMP values be adjusted to an acceptable level. In other circumstances where the calculated K-factors (usually at centers of maximum or minimum values) were at a level believed to be reasonable, but where the particular maximum or minimum was slightly offset with respect to a topographic feature to which it was related, changes were made to the K-factor field to achieve proper alignment. The PMP Index map was calculated using a K-factor field which includes percentage changes in limited areas and alignment corrections.

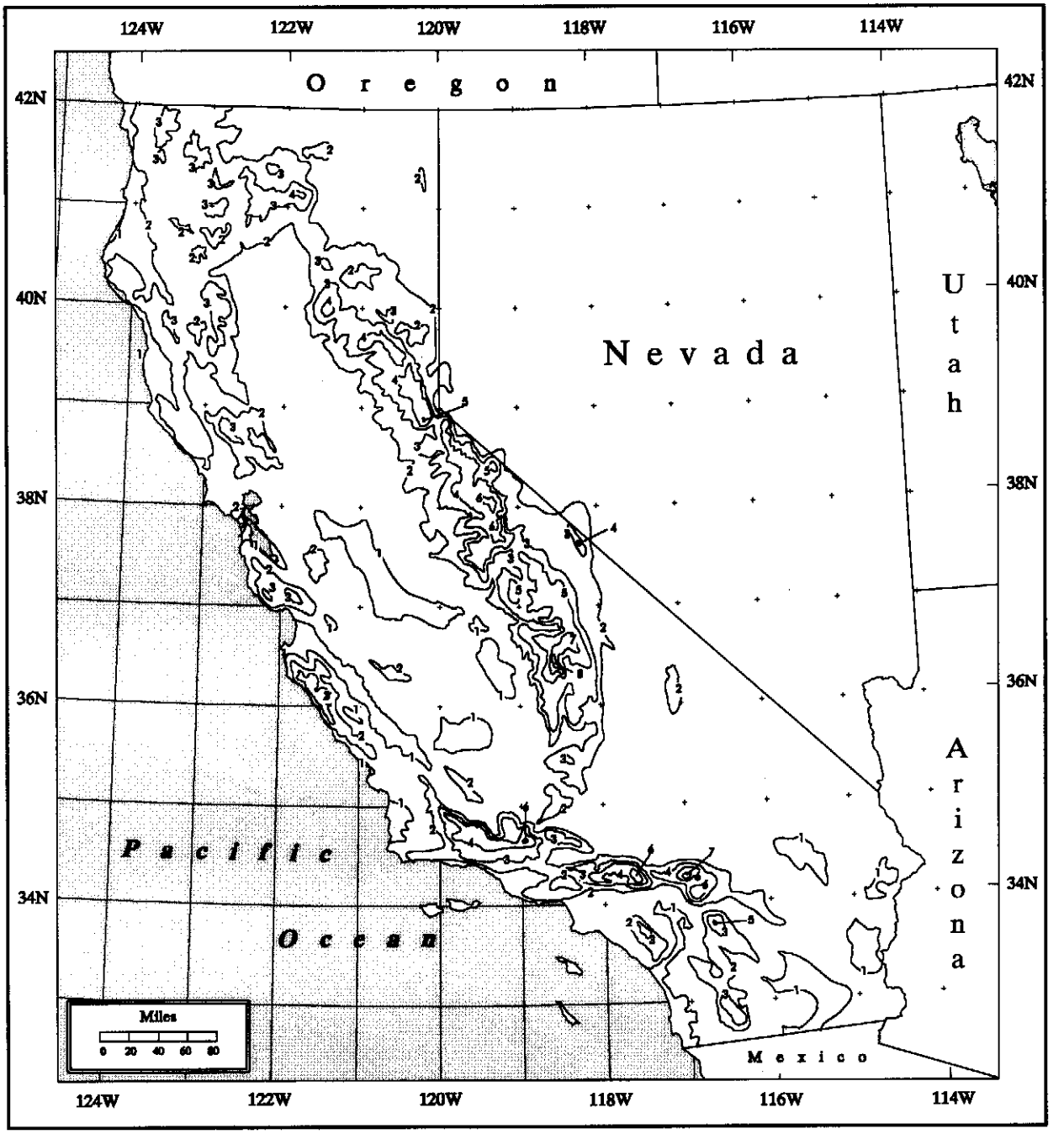

Figure 6.6. *The orographic influence (K-factors) for California.*

7. GENERAL-STORM PMP INDEX MAP AND SEASONAL VARIATION

7.1 Introduction

A general-storm Index map of California probable maximum precipitation (PMP) was developed for 24 hours and 10 mi^2. Calculations were done using a combination of a Geographical Information System (GIS) application (GRASS 4.0, 1991) and software developed exclusively for the task. The result was a 15 by 15 second grid of raster values which completely cover the study area. Adjustments were made to both the grid point values and the contours of PMP by making percentage changes to selected sets of grid points, redrawing contours and re-analyzing them. The finished analyses are printed as Plates 1 and 2 for southern and northern California, respectively.

The standard contour intervals in the Plates are as follows: every half-inch up to 11 inches, every inch between 12 and 15 inches, and every 3 inches above 15 inches. The larger contour interval above the 15 inch depth was required to preserve visible separation between adjacent contours at the map scale of 1:1,000,000. A consequence of using the provided PMP Index maps is that the interpolated values may differ from user to user. One advantage of constructing a digital PMP index field is that identical results can be found by different users. The digital ascii version of the map is available at the Hydrometeorological Design Studies Center web site. Of course, GIS software must be in place to use these data.

An example of the contour field from the PMP Index map, as originally calculated from equation 6.4 and adjusted where deemed necessary is shown in Figure 7.1. The adjustments for all of California are discussed in the next section. The main features of the PMP Index map are quite similar to the isopluvial features of the 100-year, 24-hour precipitation map for California in NOAA Atlas 2 (1973), even though the level of PMP varies from about twice to over 4.5 times the 100-year level. A ratio map of PMP to the 100-year 24-hour values is shown in Chapter 11, Figure 11.1.

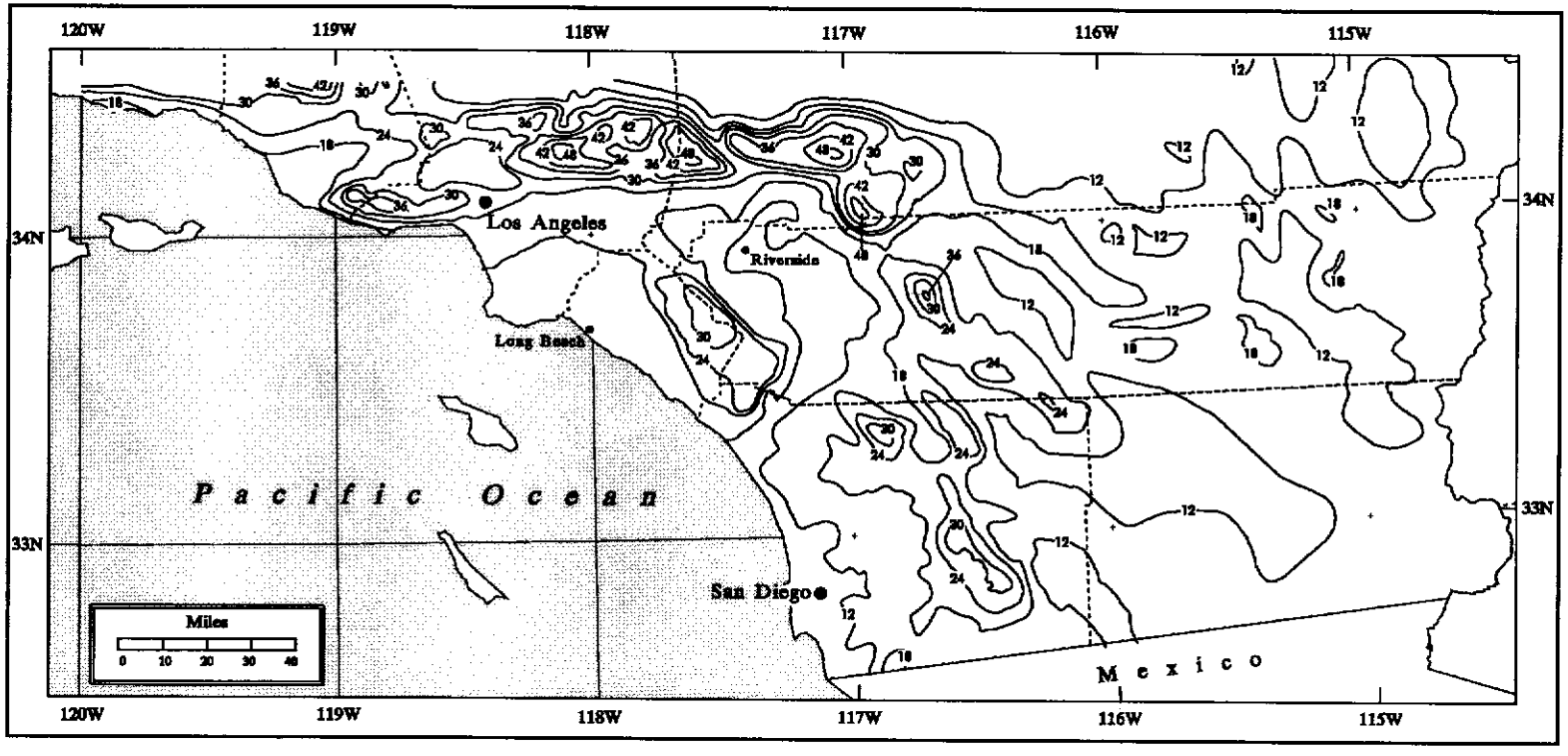

Figure 7.1. *HMR 59 PMP estimates for a portion of southern California at 10 mi^2, 24 hours. Contours are at 6 inch intervals.*

7.2 Adjustments to the General Storm Index Map

Several comparisons were made between the index values of PMP and the following: the 100-year and longer return-period precipitation; PMP index values from HMR 36 (1961); and the greatest recorded 1-day and 24-hour amounts for California. These comparisons indicated a need for adjustments to the calculated index PMP depths at some locations and across some regions. Examples of these adjustments follow.

As a result of the comparison with NOAA Atlas 2, north of the 35th meridian the largest values in the Sierra Nevada mountains were increased by up to 25 percent, while similar maxima along the coastal ridges were decreased up to 12 percent, so that the relations of the PMP values to one another would more closely resemble the relations in NOAA Atlas 2 for the 100-year level of precipitation. Within the area of percentage increases in the Sierra, an area in the vicinity of Sirretta Peak, northeast of Bakersfield, showed a total increase of about 40 percent due to an undervaluation of orographic enhancement in the original calculations. The under-enhancement arose from what was perceived to be an underestimate of the 100-year level of precipitation in that location. In the Coastal mountains to the northwest and northeast of Santa Barbara, the gradient of PMP was relaxed on the slopes of these mountains so that it would more closely resemble the gradient of the 100-year return period precipitation shown in NOAA Atlas 2.

In comparisons with draft PMP values, an observed daily storm amount reached 94 percent of PMP in the northern Central Valley. A decision was made to increase the Index map by up to 10 percent in this region to decrease the ratio of the observed value to PMP and bring it more into line with other values in the area.

Decreases up to 22 percent in the draft PMP estimates were made in the area around Stockton and San Jose, based on comparisons with HMR 36 and by concluding that the 1000-mb, non-orographic PMP pattern in that area reflected the values from the Central Valley more closely. In the mountains east of Riverside the draft value of PMP calculated as a maximum near the crest of the San Gorgonio Mountain, was reduced by around 25 percent. Furthermore, the maximum was relocated further downslope on the windward side to conform more closely with patterns established for PMP in the Sierra. Maximum levels of PMP were increased up to 12 percent near the crests of isolated mountain peaks in the

desert region of southeastern California to bring their levels into closer conformity with the (adjusted) levels at the southern end of the Sierra Nevada. Finally, very small adjustments were made near the 42nd meridian so that there would be very close agreement with the PMP index level in HMR 57 (1994).

The calculation of PMP involves the interaction of four independent variables: the 100-year level of precipitation from NOAA Atlas 2 (T), the non-orographic component of the 100-year level of precipitation (C), non-orographic PMP (FAFP), and the storm intensity factor (M). A given percentage change in any one of the first three independent variables will produce an equal percentage change in the dependent variable (PMP). A given percentage change in the M factor will produce a smaller percentage change in PMP for the range of M factors in California (which range from 0.0 to 0.55). Because of the sparseness of extreme-storm data, and since the data that are available tend to be concentrated in densely populated areas, a degree of analytical discretion was used in performing the analysis of C, FAFP, and M. Changes of 5 to 10 percent in the value of C, FAFP and M can account for a 20 to 25 percent change in PMP. When comparisons with the 100-year precipitation frequency, HMR 36 PMP values, or the greatest one-day and 24-hour amounts dictated changes in PMP of 20 to 25 percent, we reviewed the original analyses of C, FAFP, and M to determine whether changes of 5 to 10 percent could be justified. If so, the changes were accepted.

This practice should not be taken to imply that the finalized index PMP values of this report can be lowered or raised by 25 percent anywhere a user chooses, but only that changes of this order were justified during preparation of the final product where the low density of extreme-storm data makes such choices reasonable. In the very few instances when adjustments in excess of 25 percent were deemed necessary, it was assumed that the orographic factor K alone was responsible for any unrepresentativeness in the calculation of PMP.

7.3 Monthly Variation of PMP Index Values

Monthly PMP values were constructed based upon the all-season 10-mi^2, 24-hour PMP index values. Monthly PMP index amounts are shown as a percentage of all-season general storm PMP in Figures 7.2 to 7.11. The monthly index values are to be used with the

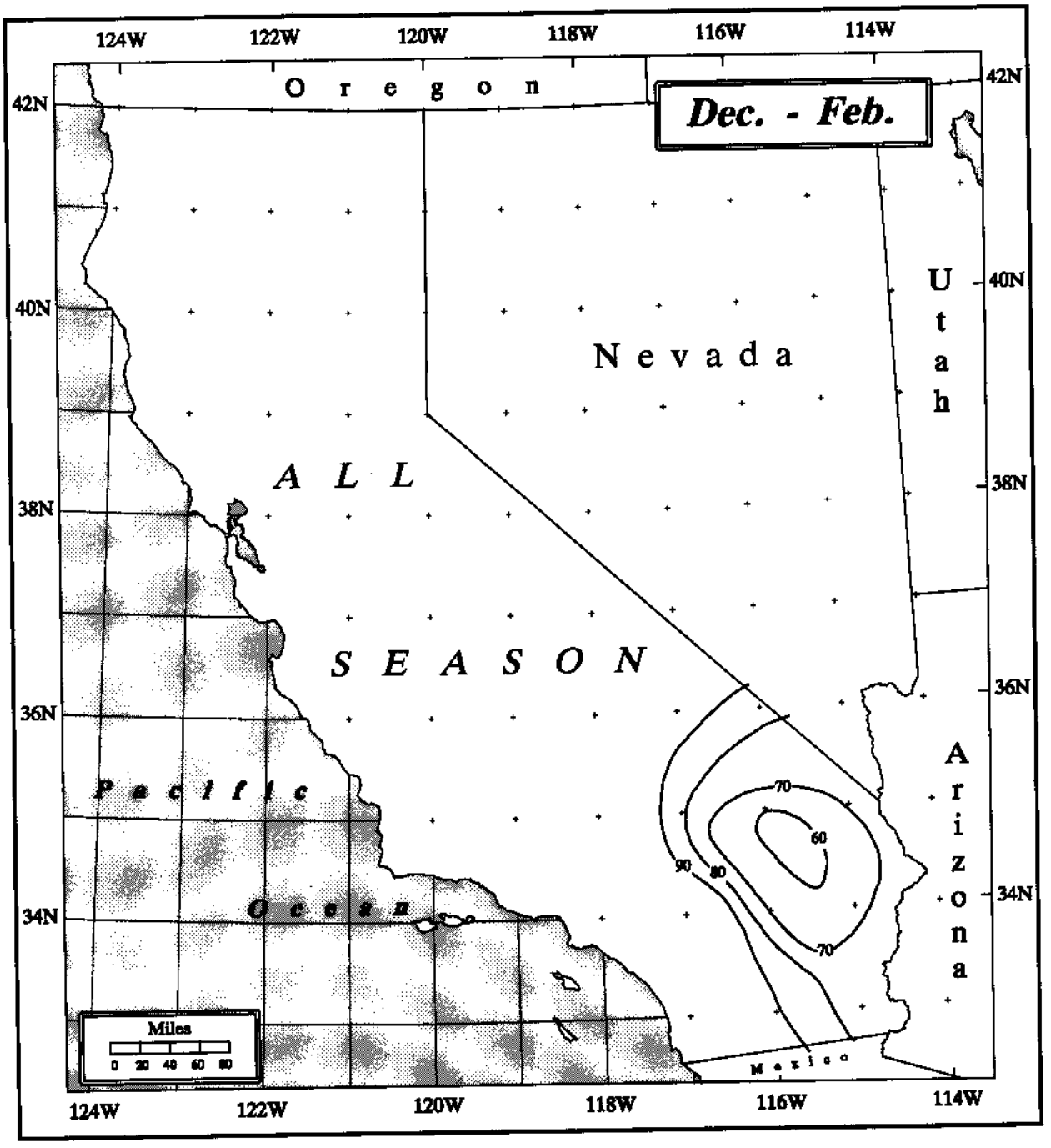

Figure 7.2. *10-mi² 24-hour general-storm PMP for December through February in California as a percent of all-season PMP (Plates 1 and 2). Same as Figure 13.1.*

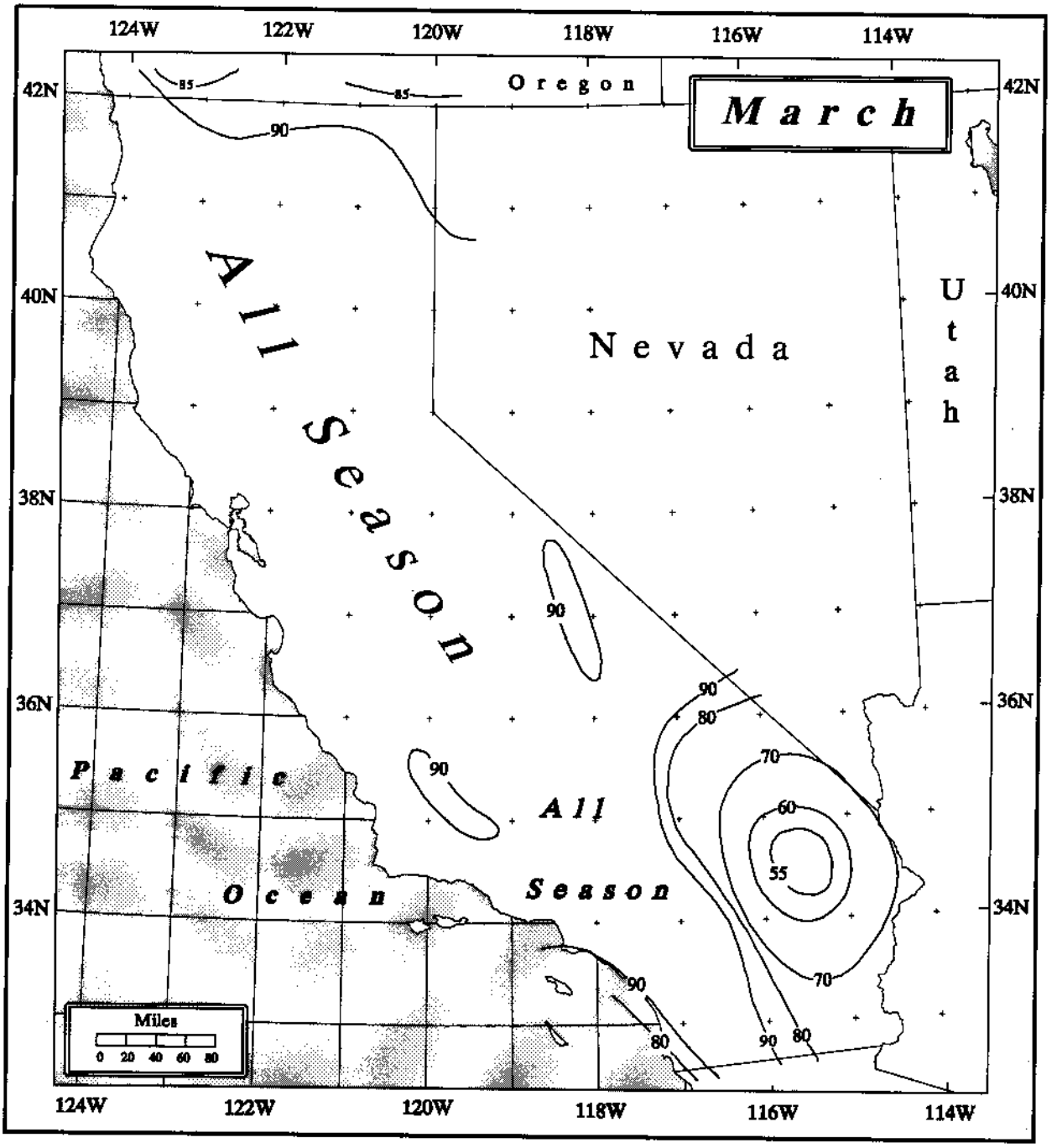

Figure 7.3. *10-mi² 24-hour general-storm PMP for March in California as a percent of all-season PMP (Plates 1 and 2). Same as Figure 13.2.*

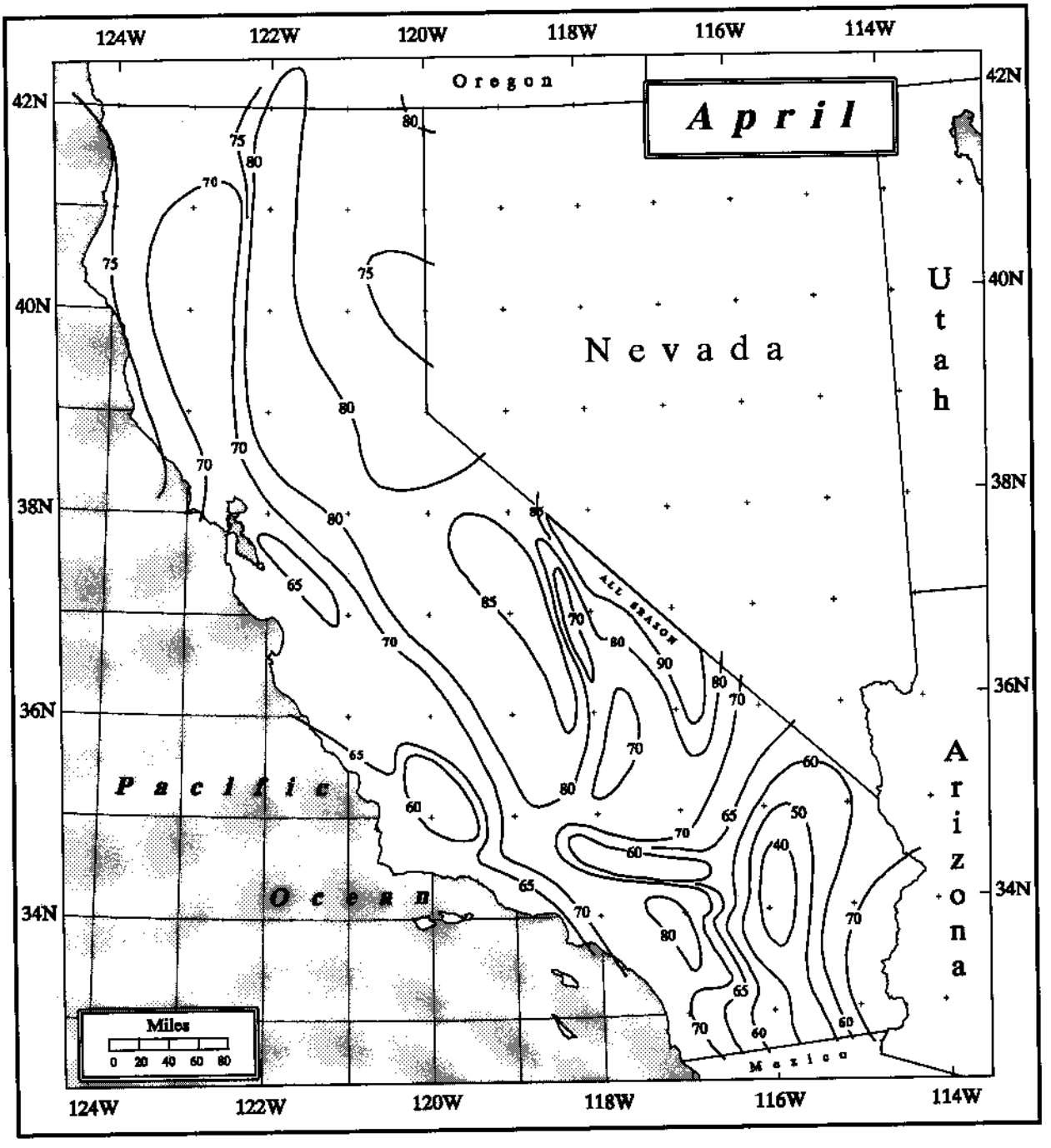

Figure 7.4. *10-mi² 24-hour general-storm PMP for April in California as a percent of all-season PMP (Plates 1 and 2). Same as Figure 13.3.*

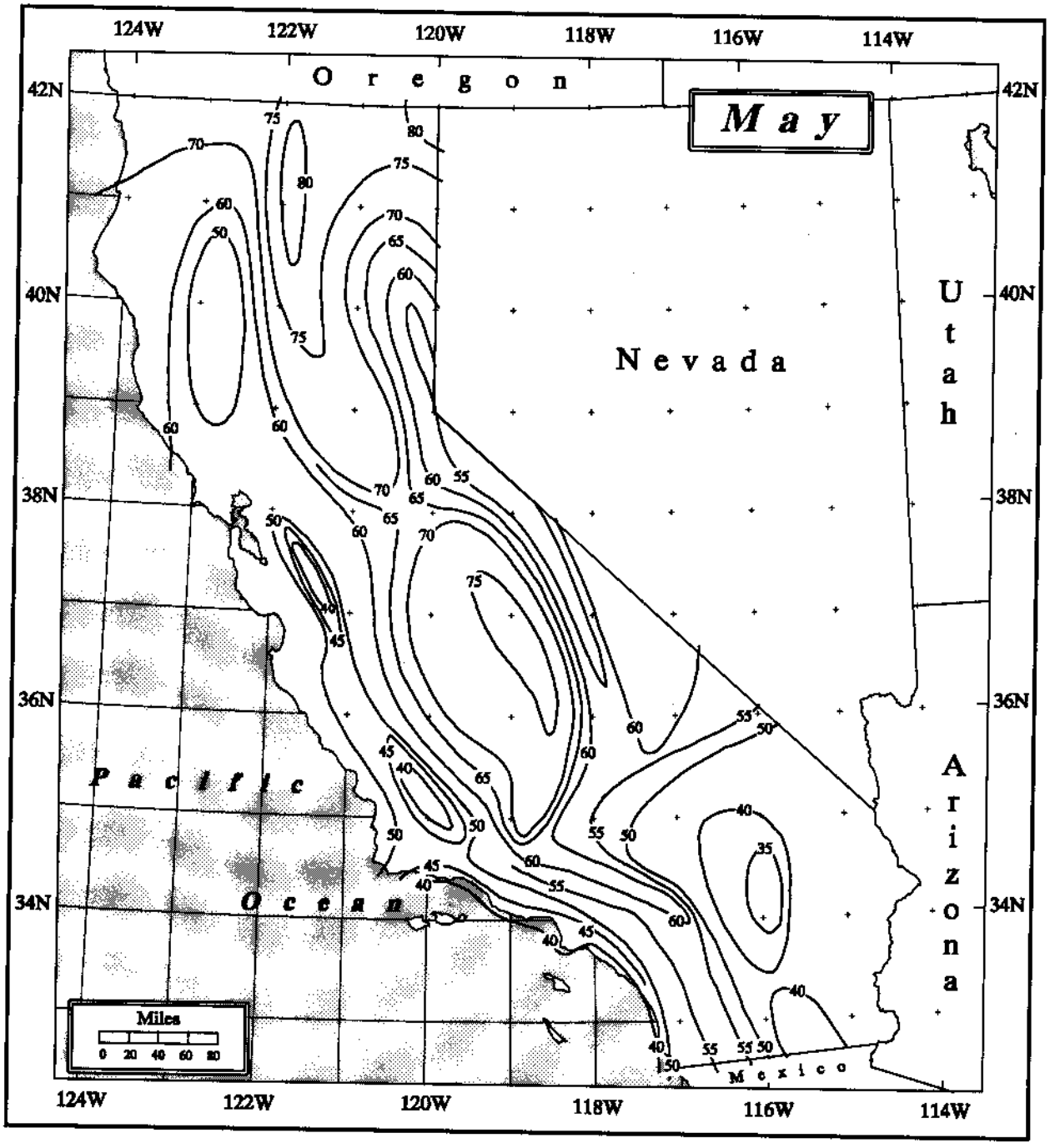

Figure 7.5. *10-mi² 24-hour general-storm PMP for May in California as a percent of all-season PMP (Plates 1 and 2). Same as Figure 13.4.*

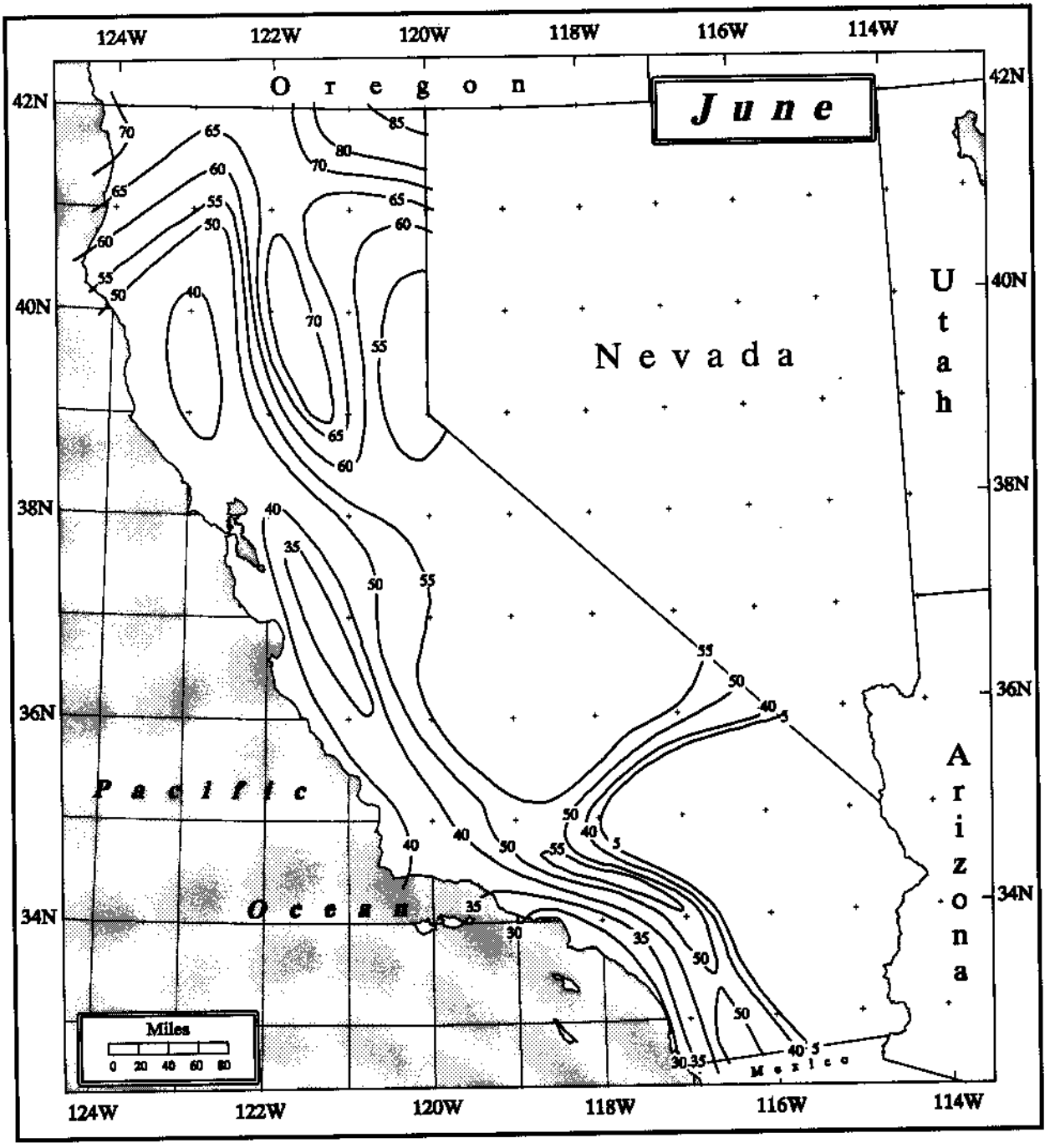

Figure 7.6. *10-mi² 24-hour general-storm PMP for June in California as a percent of all-season PMP (Plates 1 and 2). Same as Figure 13.5.*

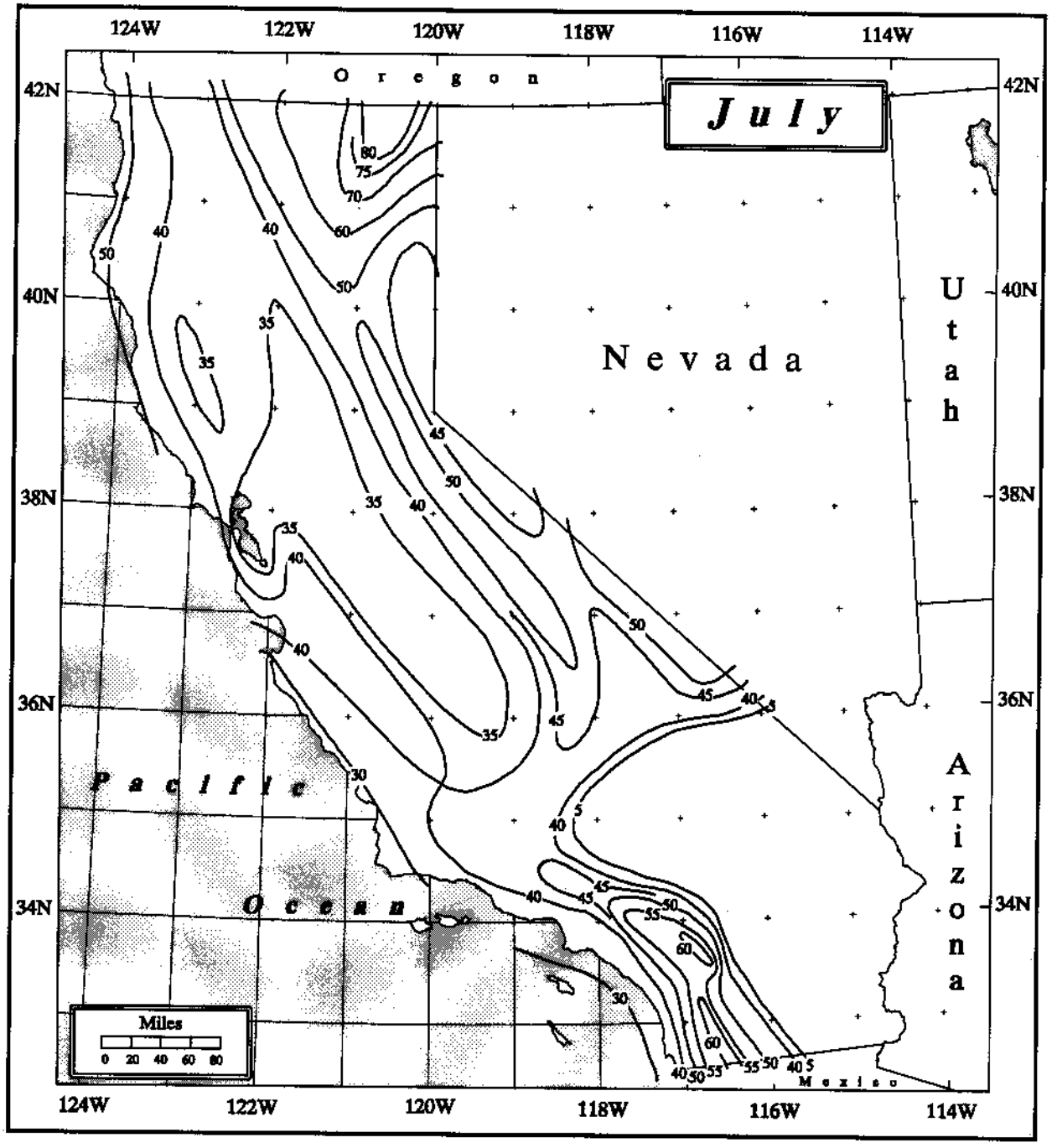

Figure 7.7. *10-mi² 24-hour general-storm PMP for July in California as a percent of all-season PMP (Plates 1 and 2). Same as Figure 13.6.*

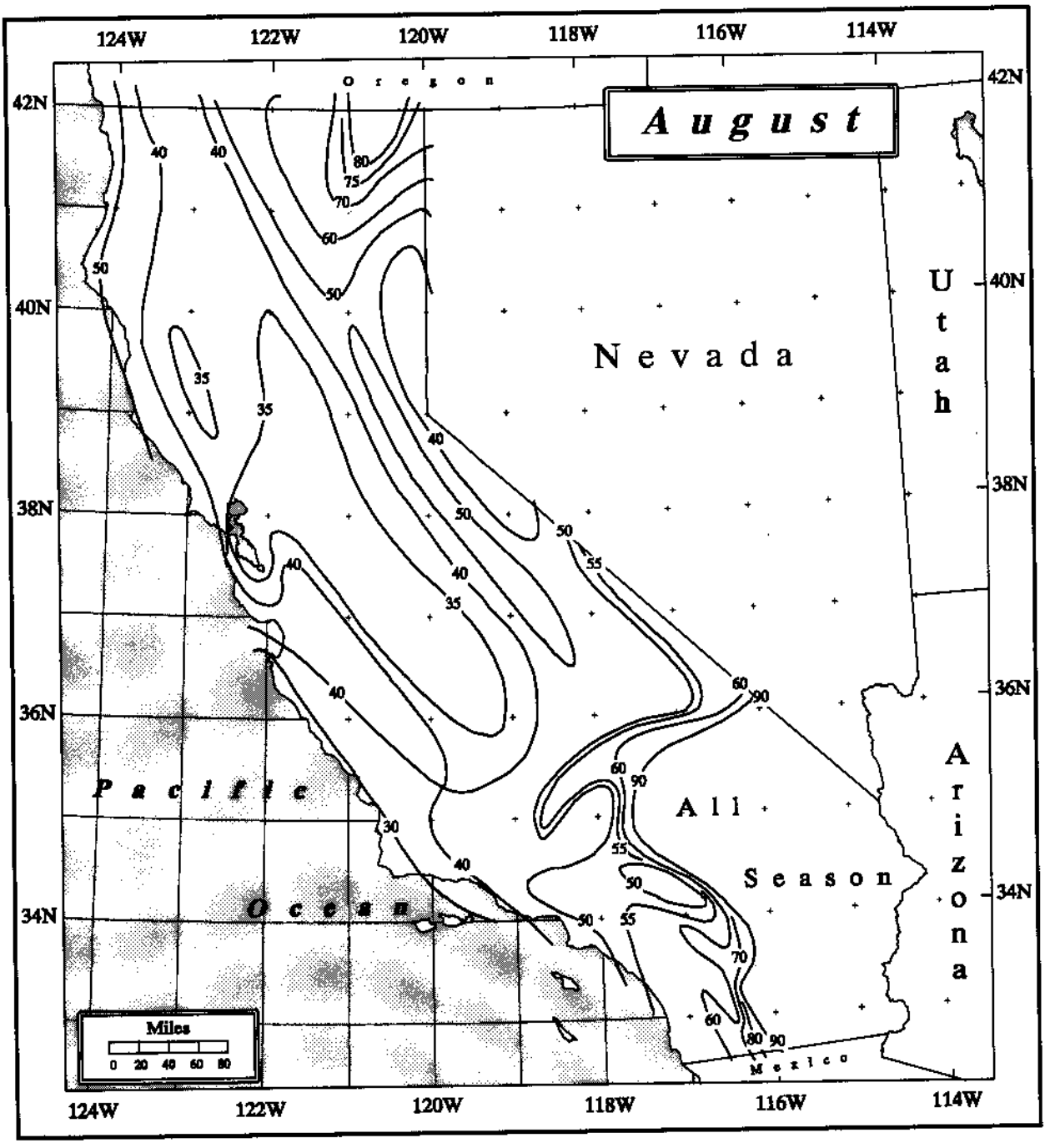

Figure 7.8. *10-mi² 24-hour general-storm PMP for August in California as a percent of all-season PMP (Plates 1 and 2). Same as Figure 13.7.*

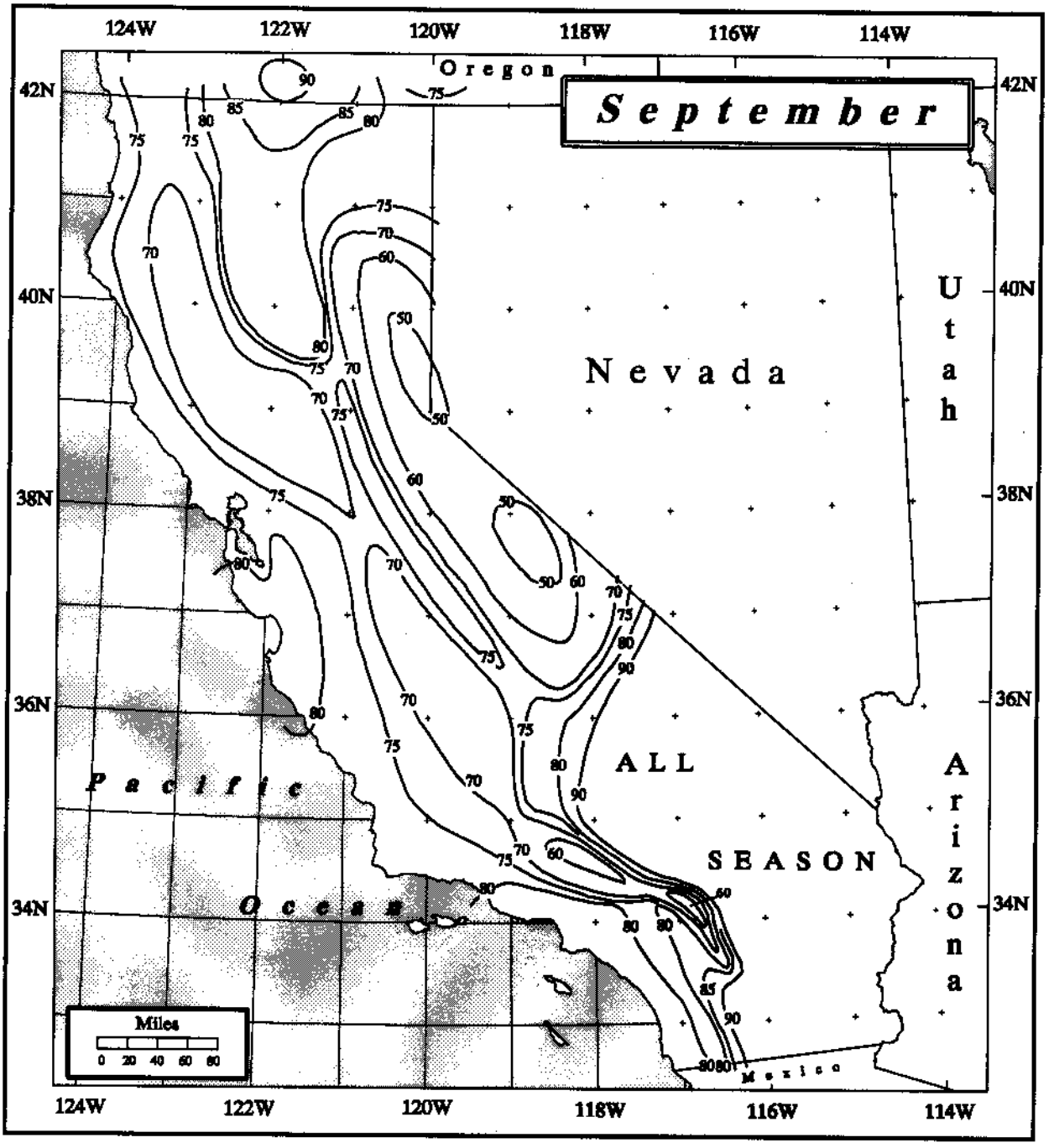

Figure 7.9. *10-mi² 24-hour general-storm PMP for September in California as a percent of all-season PMP (Plates 1 and 2). Same as Figure 13.8.*

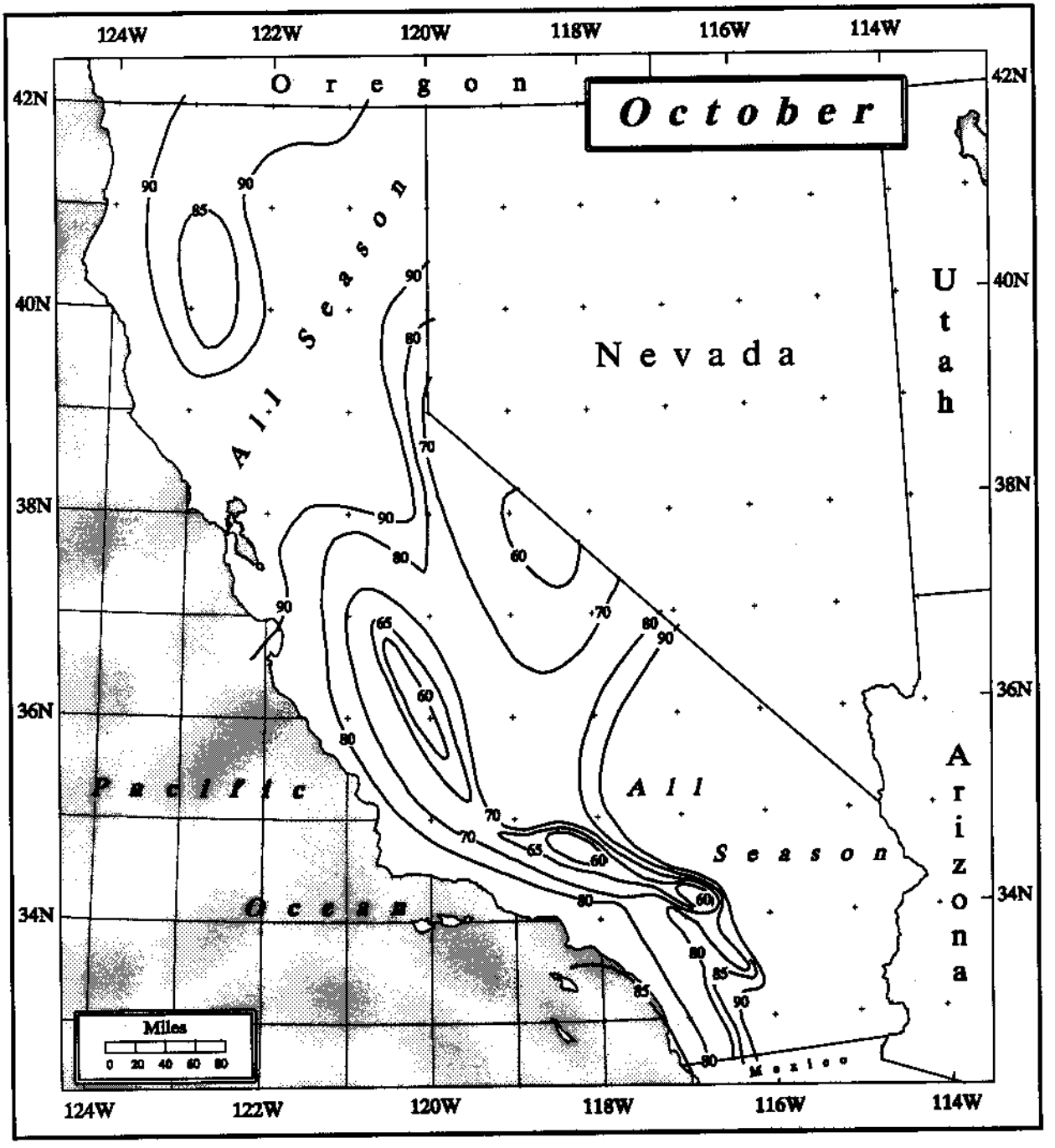

Figure 7.10. *10-mi² 24-hour general-storm PMP for October in California as a percent of all-season PMP (Plates 1 and 2). Same as Figure 13.9.*

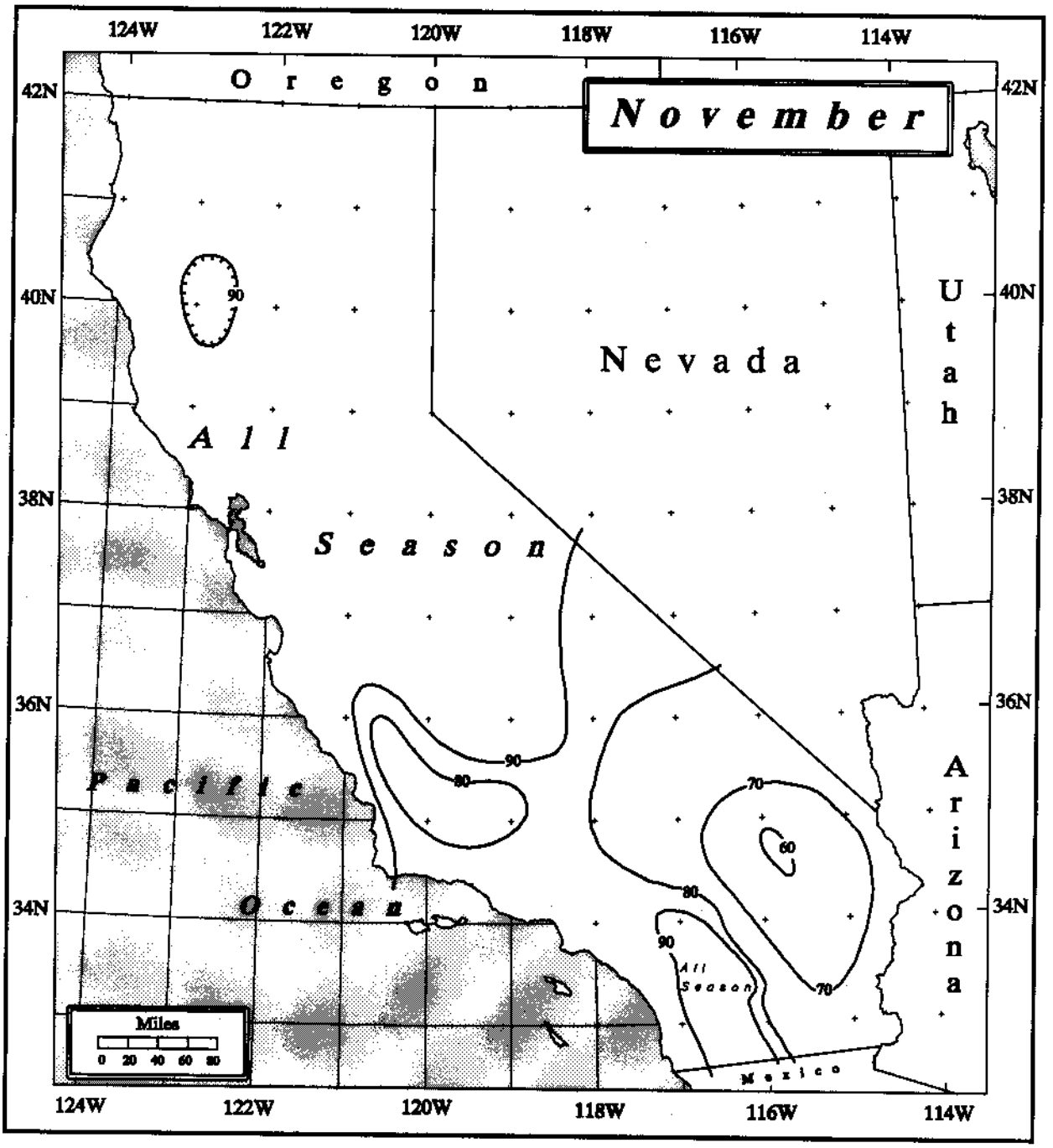

Figure 7.11. *10-mi² 24-hour general-storm PMP for November in California as a percent of all-season PMP (Plates 1 and 2). Same as Figure 13.10.*

seasonally-adjusted depth-area-duration (DAD) relations which are discussed in Chapter 8.

The key notion involved with the seasonality maps is that monthly variation of index PMP is well-represented by the monthly variation of maximum recorded daily precipitation. Over 400 locations across California had precipitation records of sufficient length to be useful. Forty-eight percent of these locations had records of at least 40 years, while close to 10 percent (or 38 locations) had records of at least 50 years. Sixty-four percent of these locations were below 2,000 feet elevation, 29 percent were at 2,000 to 5,000 feet, and only 5 locations were above 7,000 feet.

The daily maximum precipitation amounts for each month were normalized by dividing each month's amount by the largest annual maximum at each site. For instance, if the maximum 24-hour precipitation recorded at a site in August was 5 inches and the all-time maximum 24-hour precipitation at the same site was 10 inches the resulting ratio would be .5 or 50 percent. The resulting ratios, coded at 1,000-foot intervals above 2,000 feet, were then plotted on the maps for analysis. No month showed any apparent elevation-ratio dependency within the regions used to establish DAD uniformity. The regional boundaries for DAD are shown in Chapter 3, Figure 3.3. A degree of dependency was discernable, however, between the ratio and latitude. The southeastern region showed the strongest physiographic influence on the distribution of ratio values on seasonality. This region contains the Mojave Desert and its attendant northward extending valleys, and the desert surrounding the Salton Sea eastward to Arizona. The ratios at the crests of the mountains essentially define the northern and western edge of the southeastern DAD region. In Figures 7.6 and 7.7 a strong gradient of percentage (from 5 to 40 percent) can be seen across the western and northern edge of the Southeast region and is well-supported by observations. An average value of 22.5 percent is recommended for use with basins located between these two isopercental contours. The southeastern region experiences its largest PMP storm in late summer, whereas the rest of California experiences their PMP storms in winter. Of some interest is the observation that the months of maximum and minimum general-storm PMP potential are juxtaposed in the southeastern region, whereas they are separated by 5-6 months for the rest of the state. The temporal transition in the Southeast region changing from 5 to 90 percent is exceptionally abrupt in the month of July. When constructing a smooth curve of annual variation of percentage (see discussion below), the curve will be very sharply pitched for the transition from July to August for locations in the Southeast

region. We recommend such curves indicate a value of 85 percent for the dates July 31 and August 1.

The analysis of the monthly percentages in Figures 7.2 to 7.11 was guided by the following principles:

1. Within each DAD regions and for a given month, it is assumed that the location of the largest observed percentage is a matter of chance, given that the period of record is relatively long and that the maximum percentage could, therefore, have occurred anywhere in the region.

2. If adjacent DAD regions for a given month have significantly different maximum percentages found within their boundaries, then a gradient of percentage is assumed to exist along the periphery of the regions for that month.

3. In deciding the level of percentage to assign across all or part of a region, greater influence was given to those observations associated with: longer period of record, associated largest depth, and fewer nearby observations.

4. In the Southeast region, large general-storm precipitation was not observed for the greater portion of June and July. During these months, 10-mi^2, 6-hour PMP is produced by the local storm. The percentage of all-season general storm PMP may reach zero percent, but was set at 5 percent since the period of recorded observations in this region is on the order of a quite short 100 years.

5. When spot checks of the annual cycle of percentages revealed a brief monthly departure from a trend not observed elsewhere in the vicinity, the monthly isopercental analyses were revised at that location to eliminate the irregularity.

6. Although local storms produced some of the large percentage values found in the Southeast region during the months of maximum convective potential, there were enough instances of large percentages associated with general storms to justify the all-season categorization for this region in August and September.

Figures 7.2 to 7.11 contain no isopercental contours labeled greater than 90. Places where the percentages exceeded 90 have been identified as *all-season* for the given month(s) because it was assumed that at such times and places, the full 100-percent index amount of general-storm PMP should be expected. To assure that any irregularities in the annual cycle of percentages which remain are removed, we recommend that when setting the annual cycle for any location, all 12 monthly percentages be plotted at the mid-point of each month and smoothed if necessary. To achieve this, adjustment of plus or minus 5 percent may be employed, except when an all-season value (> 90 percent) is indicated.

Finally, when deciding on an off-season, drainage-average index value of general-storm PMP for a specific drainage across which there is a gradient of percentages for any month, it is recommended that an average percentage within the drainage be selected to represent the whole drainage for that month. Percentages so obtained would be used to represent the annual cycle of percentages for the specific drainage. These average values could be smoothed under the constraints mentioned above.

8. GENERAL-STORM DEPTH-AREA-DURATION

8.1 Introduction

Depth-area-duration (DAD) data from storm events are the basis for development of depth-duration and depth-area relations. Those depth-duration and depth-area relations are then used with the 10-mi^2, 24-hour probable maximum precipitation (PMP) Index map (Plates 1 and 2) to develop storm-centered average depths of PMP for a selected duration and area size. Development of the PMP Index map is discussed in Chapter 7. Both the depth-duration and depth-area relations were a product of the combination and comparison of storm events occurring in or transposed to a particular region. The depth-duration and depth-area relations were normalized to 10 mi^2. They are based on highly smoothed within-storm depth-area-duration data from important storms, as well as on continuity with relations developed for adjacent areas. The term within-storm is a storm characteristic determined when values of various parameters are required to be from the same storm.

The depth-duration and depth-area relations vary within the state and were assigned to regions. The regional boundaries were determined from major topographic features and precipitation climatology (regional DAD boundaries are shown in Chapter 3, Figure 3.3).

8.2 Adopted Relations

Table 8.1 defines the depth-duration relations for general-storm, all-season PMP at 10 mi^2 in California. To obtain depth-duration ratios for durations other than those in the table, the user should draw a smooth curve connecting the listed values on semi-log graph paper (a ratio value of 0 at a duration of 0 hours) extracting the ratio at the desired duration. The value for depth-duration is just one factor that will eventually be multiplied by the PMP index value (see Chapter 13).

Regional depth-area reduction percentages for the all-season PMP storm are listed in Table 8.2 for selected area sizes durations and regions. The data from Table 8.2 are presented graphically in Figures 8.1 to 8.6. Examples of data from several record-setting

storms and the relationship between the adopted DAD for two of these regions are shown in Figures 8.7 to 8.10. These examples show that the smoothly varying sets of DAD relationships describing a PMP storm are not found throughout all area sizes and durations in some of the outstanding storms within a region. However, some of the storms characteristics are quite close to those anticipated in a PMP storm. Figures 8.7 to 8.10 are based on the data in Tables 8.3 and 8.4. In a few instances, the percentages in Table 8.4 for a fixed area size will decrease as duration increases, eg. the storm 575 at 500 mi^2 and between 6 and 24 hours. The respective depths corresponding to these percentages (68, 61), however, are 4.67 and 11.95 inches (see Appendix 1) so no violation of depth-area rules has occurred. Seasonally adjusted depth-duration relations for California general storms are discussed in Section 8.3. All DAD relations presented in this chapter are expressed as percentages of an index value of general-storm PMP averaged across an area, typically that of a particular drainage.

Table 8.1. *All-season PMP depth-duration ratios for 10 mi^2 for California regions.*

	Duration (hours)					
Region	**1**	**6**	**12**	**24**	**48**	**72**
Northwest	0.10	0.40	0.73	1.00	1.49	1.77
Northeast	0.16	0.52	0.69	1.00	1.40	1.55
Midcoastal	0.13	0.45	0.74	1.00	1.45	1.70
C. Valley	0.13	0.42	0.65	1.00	1.48	1.75
Sierra	0.14	0.42	0.65	1.00	1.56	1.76
Southwest	0.14	0.48	0.76	1.00	1.41	1.59
Southeast	0.30	0.60	0.86	1.00	1.17	1.28

Table 8.2. *All-season depth-area relations for California by region (percent of 10 mi²).*

Northwest / Northeast

Area (mi²)	1 hr	6 hr	12 hr	24 hr	48 hr	72 hr
10	100.00	100.00	100.00	100.00	100.00	100.00
50	87.50	88.50	90.00	91.50	93.00	94.00
100	82.00	84.00	86.00	88.00	89.50	91.00
200	77.00	79.50	82.00	84.00	86.00	87.75
500	69.50	73.00	76.25	78.25	81.00	83.00
1000	63.00	67.50	71.00	73.50	76.50	79.00
2000	55.50	60.50	64.00	67.00	69.50	72.00
5000	42.50	49.50	52.50	56.00	59.00	62.00
10000	32.00	40.00	43.50	47.00	51.00	54.00

Midcoastal

Area (mi²)	1 hr	6 hr	12 hr	24 hr	48 hr	72 hr
10	100.00	100.00	100.00	100.00	100.00	100.00
50	87.50	88.75	90.00	91.00	92.00	93.00
100	81.75	83.75	85.50	87.00	88.50	90.00
200	75.75	78.25	80.50	82.50	84.50	86.25
500	67.50	71.00	73.50	76.00	78.50	80.50
1000	60.75	65.50	68.00	70.50	73.00	75.50
2000	53.00	58.50	61.50	64.00	67.00	70.00
5000	38.00	44.50	48.50	52.00	55.00	59.00

Central Valley

Area (mi²)	1 hr	6 hr	12 hr	24 hr	48 hr	72 hr
10	100.00	100.00	100.00	100.00	100.00	100.00
50	84.50	87.25	89.50	91.50	92.75	94.00
100	77.25	81.00	84.00	86.50	88.50	90.50
200	70.00	74.50	78.00	81.00	83.00	85.00
500	59.75	64.75	68.75	72.00	74.50	77.00
1000	51.00	56.50	61.00	64.50	67.00	69.50
2000	41.00	47.50	52.00	55.50	58.50	61.50
5000	27.00	33.75	38.50	42.00	45.25	48.50
10000	14.00	21.00	26.00	30.00	33.00	36.50
10000	25.00	34.00	38.00	42.00	45.00	49.00

Table 8.2 (cont.) *All-season depth-area relations for California by region (percent of 10 mi^2).*

Sierra						
Area (mi^2)	**1 hr**	**6 hr**	**12 hr**	**24 hr**	**48 hr**	**72 hr**
10	100.00	100.00	100.00	100.00	100.00	100.00
50	88.00	89.00	90.00	91.00	92.50	94.00
100	82.50	84.00	85.50	87.00	89.25	91.25
200	76.75	78.75	80.75	82.75	85.50	88.25
500	69.25	71.75	74.25	77.00	80.50	83.50
1000	63.25	66.25	69.25	72.25	76.25	79.75
2000	57.00	60.00	63.50	67.00	71.25	75.25
5000	47.50	51.00	55.00	59.00	63.50	68.00
10000	40.00	44.00	48.00	52.50	57.50	62.00
Southwest						
Area (mi^2)	**1 hr**	**6 hr**	**12 hr**	**24 hr**	**48 hr**	**72 hr**
10	100.00	100.00	100.00	100.00	100.00	100.00
50	87.75	88.50	89.50	90.50	91.75	92.75
100	81.75	83.25	84.75	86.25	87.75	89.25
200	75.75	78.00	79.75	81.50	83.75	85.75
500	67.50	70.50	72.50	75.00	77.50	80.00
1000	60.00	63.50	66.00	69.00	71.75	74.75
2000	51.00	56.00	59.00	62.00	65.00	68.00
5000	35.00	41.00	46.00	50.00	52.50	56.00
10000	22.00	30.00	34.00	38.00	42.00	46.00
Southeast						
Area (mi^2)	**1 hr**	**6 hr**	**12 hr**	**24 hr**	**48 hr**	**72 hr**
10	100.00	100.00	100.00	100.00	100.00	100.00
50	89.00	90.50	91.75	93.00	94.50	96.00
100	83.50	85.25	87.25	89.00	90.75	92.50
200	76.50	79.75	82.00	84.00	86.00	88.00
500	66.00	70.75	74.00	76.50	78.75	81.00
1000	56.50	63.25	67.00	70.00	72.50	75.00
2000	46.00	54.75	59.00	62.00	64.75	67.50
5000	31.25	41.50	47.00	50.00	52.50	55.50
10000	19.00	30.00	36.00	39.50	42.50	45.00

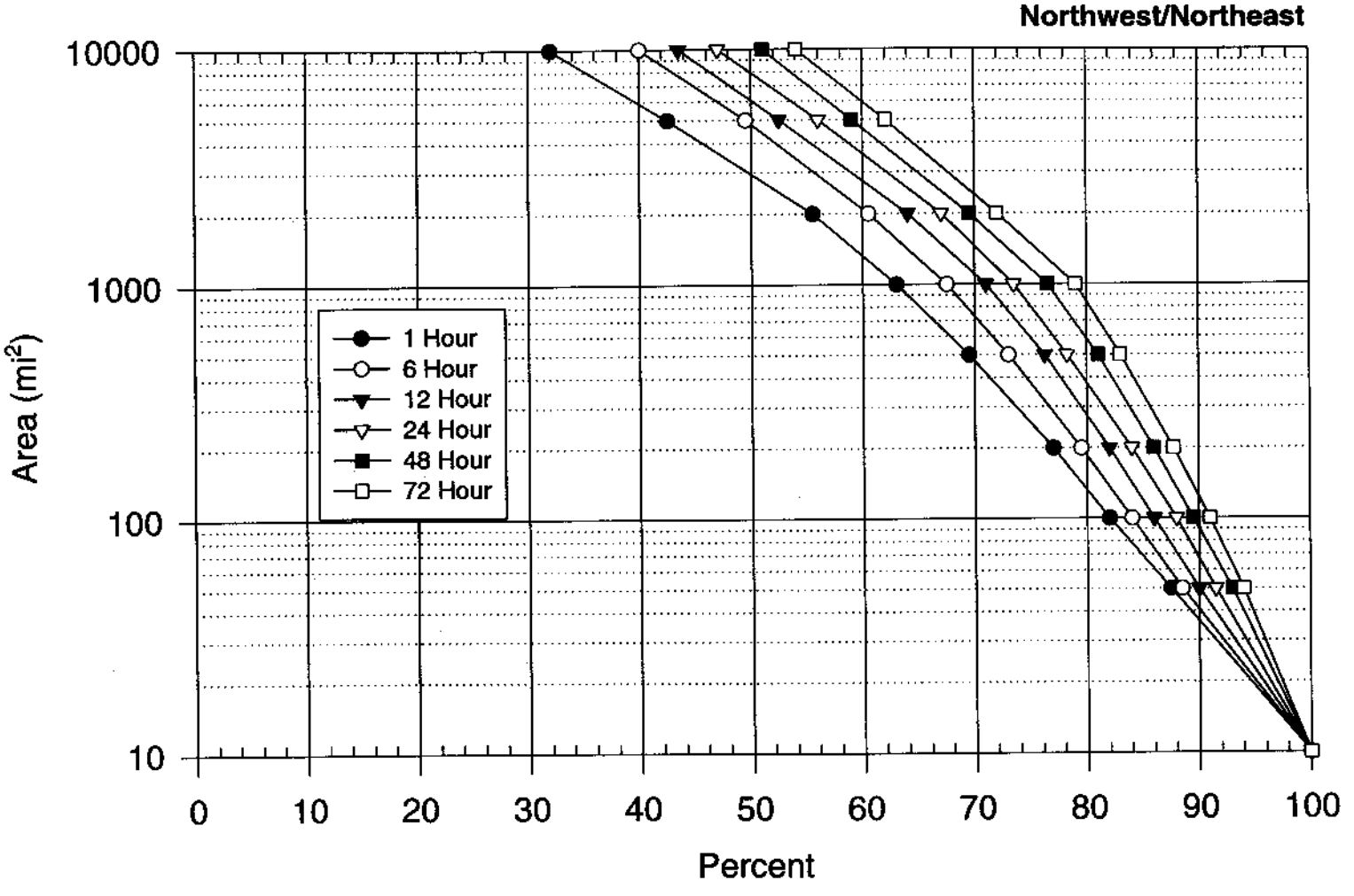

Figure 8.1. *Depth-area relations for the California Northwest/Northeast region for 1 to 72 hour durations. Same as Figure 13.12.*

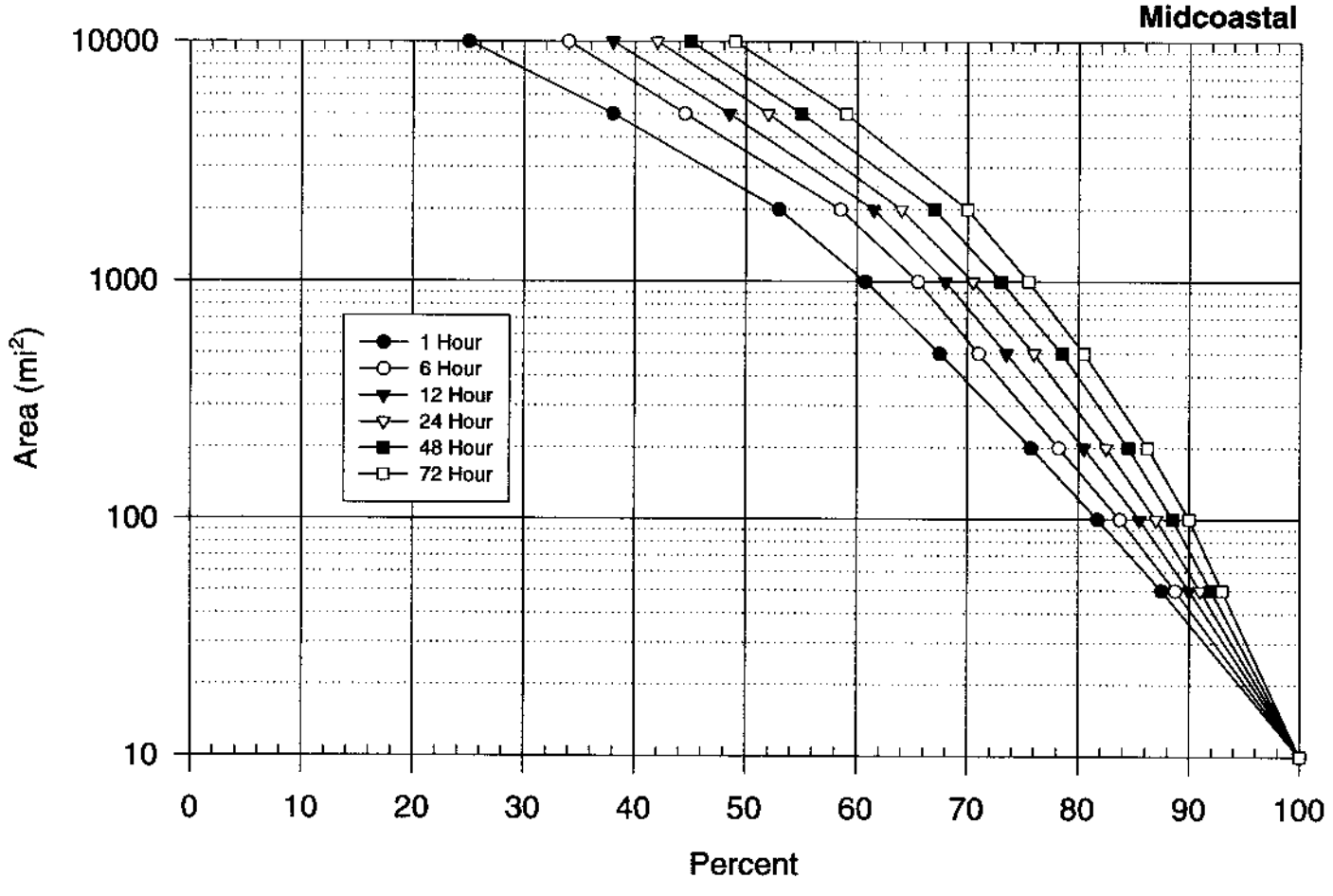

Figure 8.2. *Depth-area relations for the California Midcoastal region for 1 to 72 hour durations. Same as Figure 13.13.*

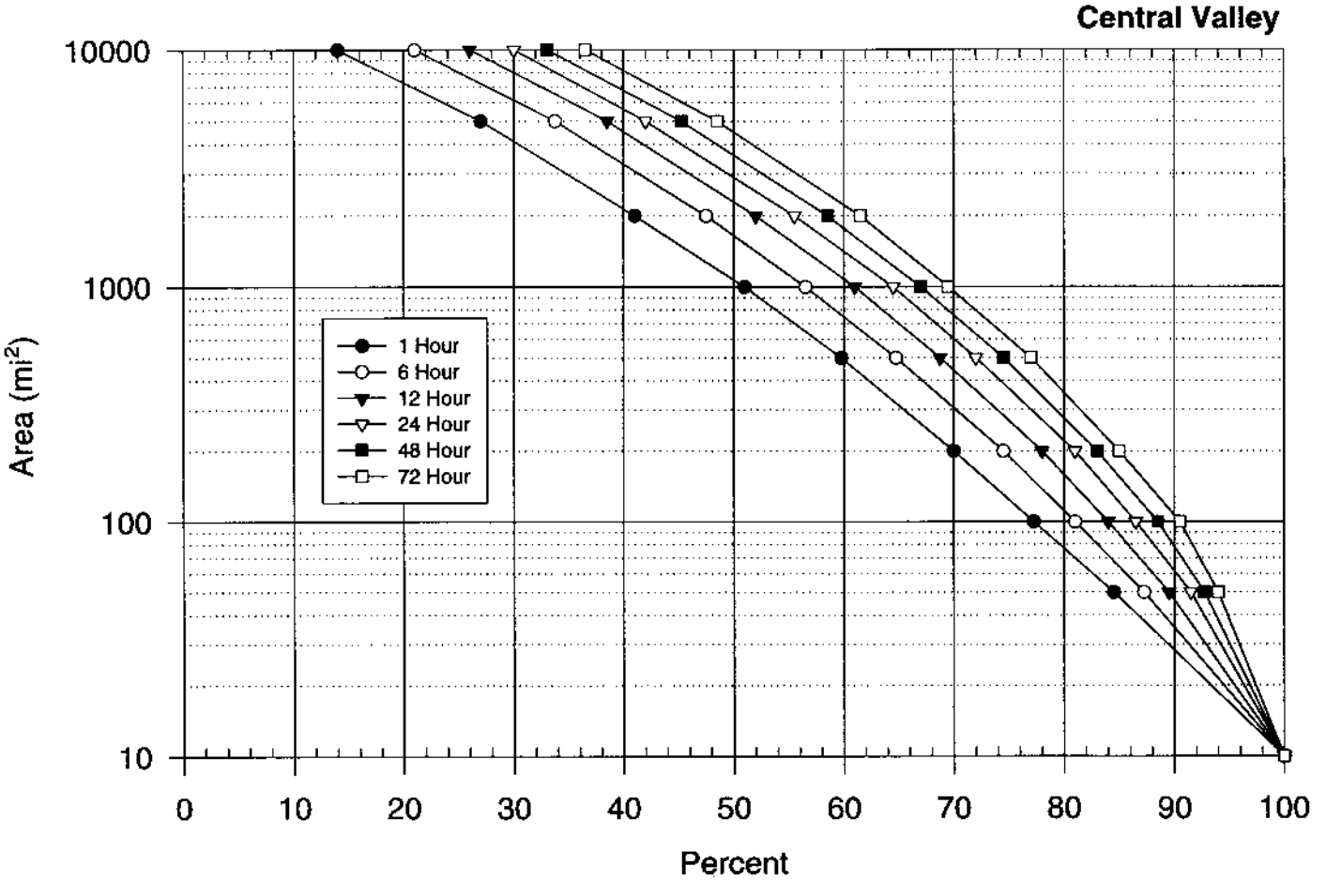

Figure 8.3. *Depth-area relations for the California Central Valley region for 1 to 72 hour durations. Same as Figure 13.14.*

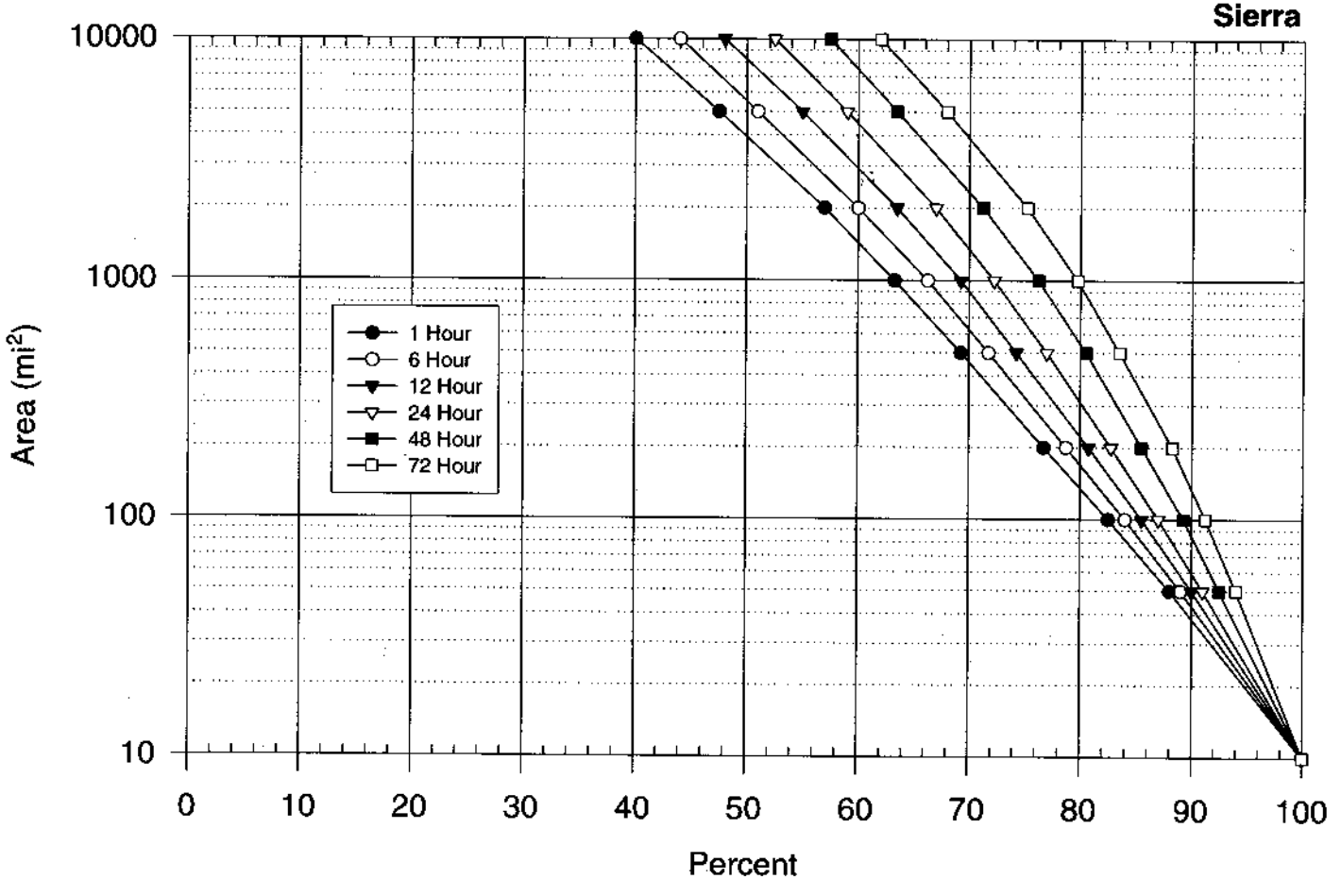

Figure 8.4. *Depth-area relations for the California Sierra region for 1 to 72 hour durations. Same as Figure 13.15.*

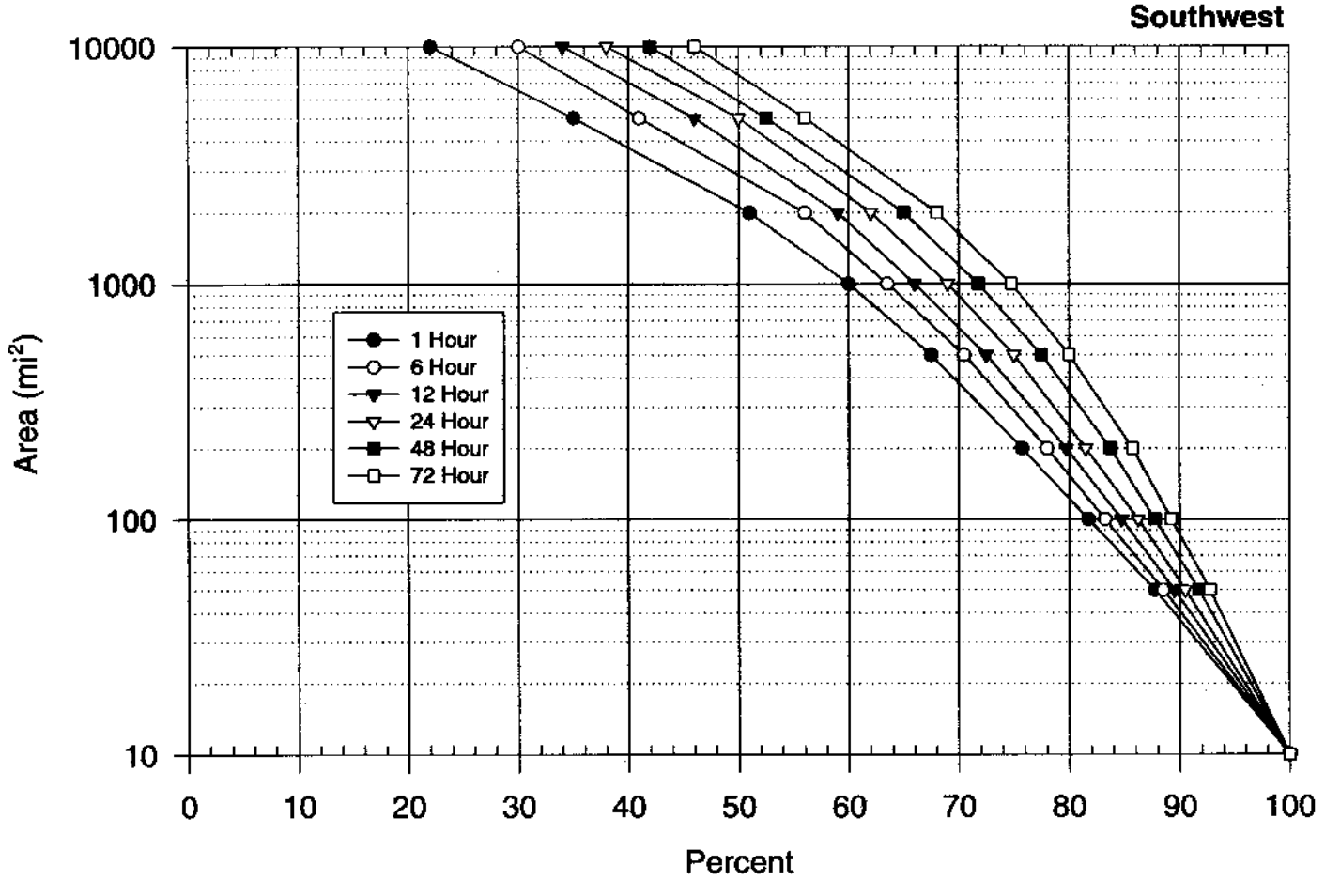

Figure 8.5. *Depth-area relations for the California Southwest region for 1 to 72 hour durations. Same as Figure 13.16.*

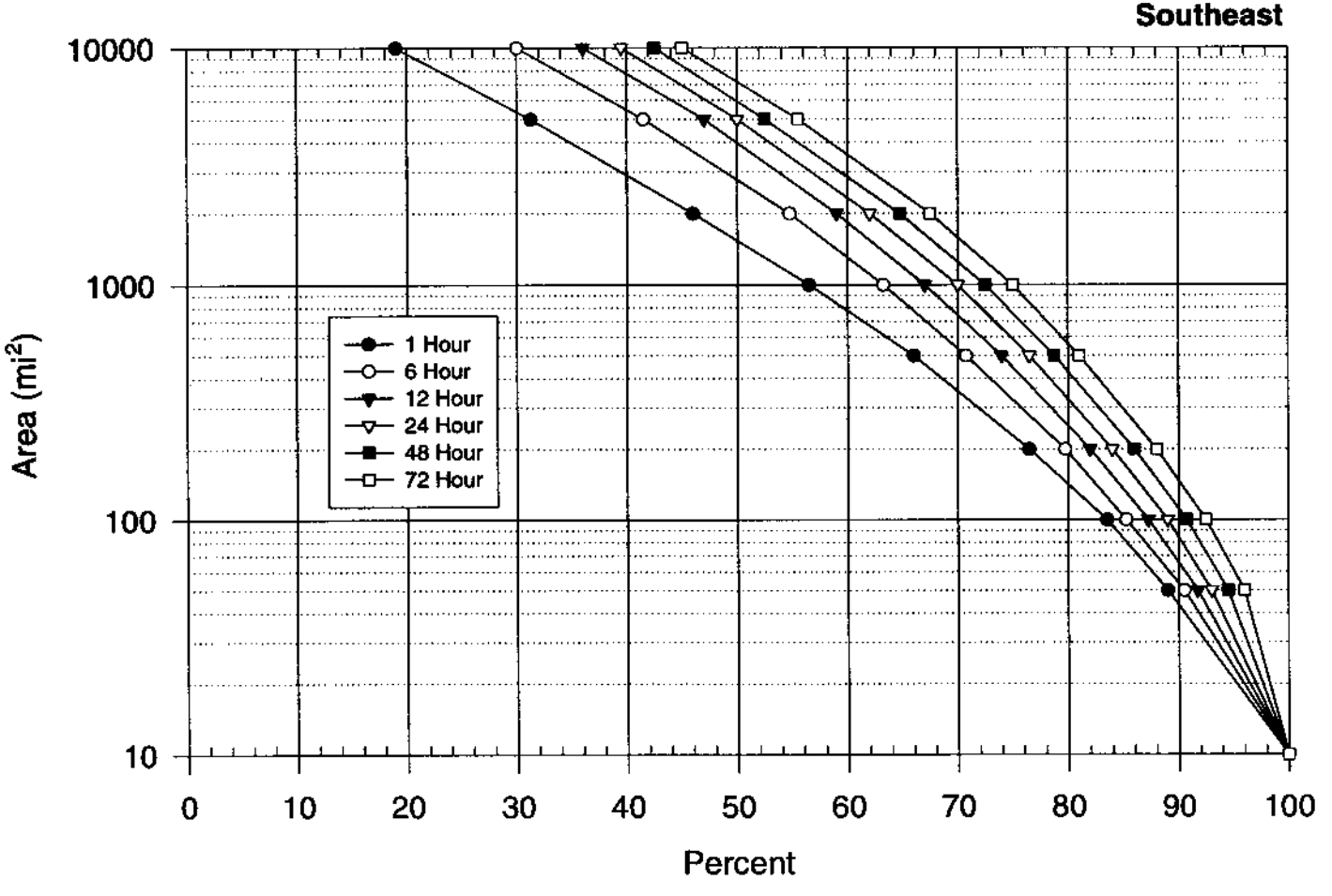

Figure 8.6. *Depth-area relations for the California Southeast region for 1 to 72 hour durations. Same as Figure 13.17.*

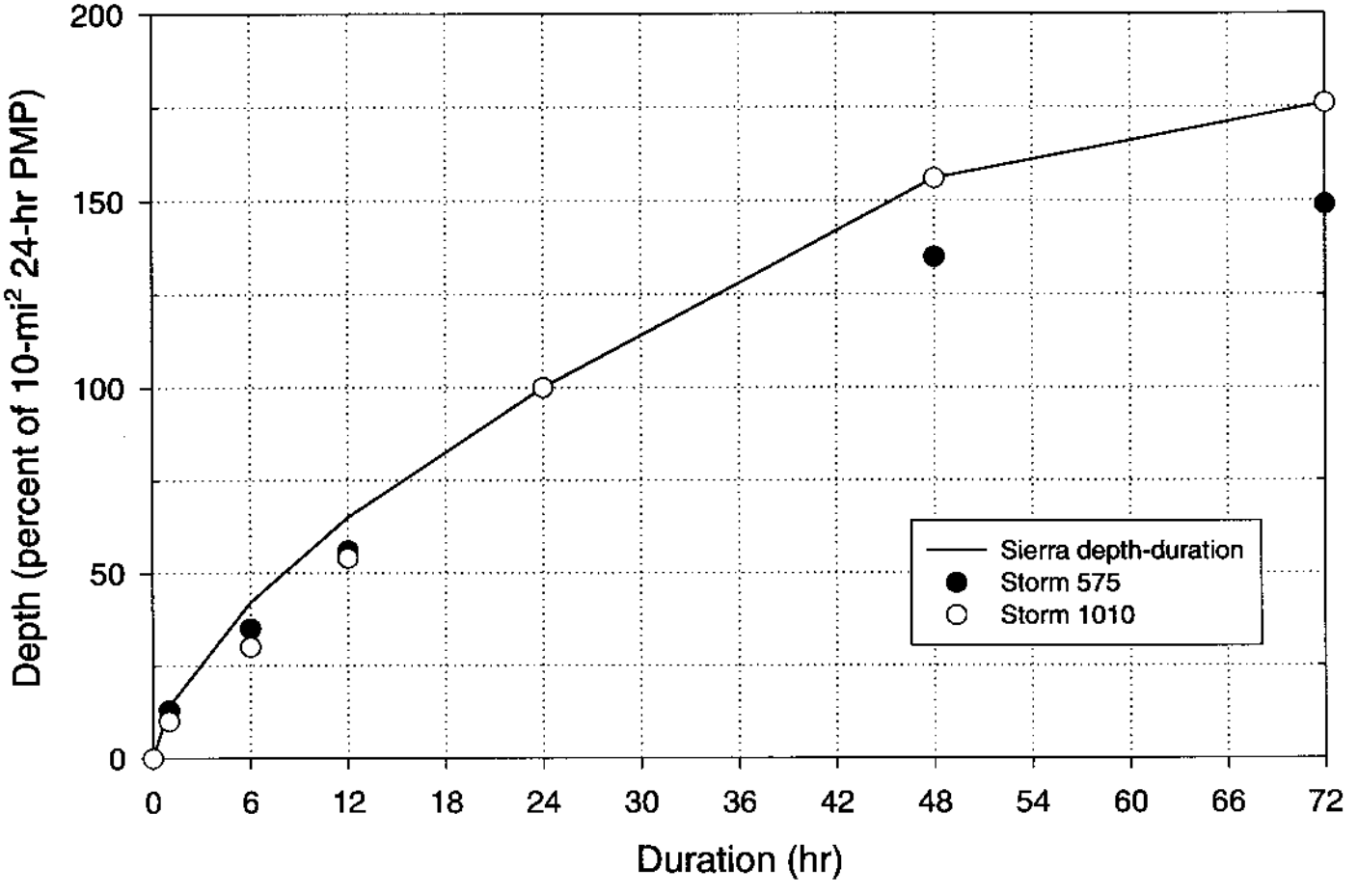

Figure 8.7. *10-mi² depth-duration relation (solid line) for the Sierra region of California. Filled symbols represent calculated storm 575 (October, 1962) values and open symbols represent calculated storm 1010 (February, 1986) values.*

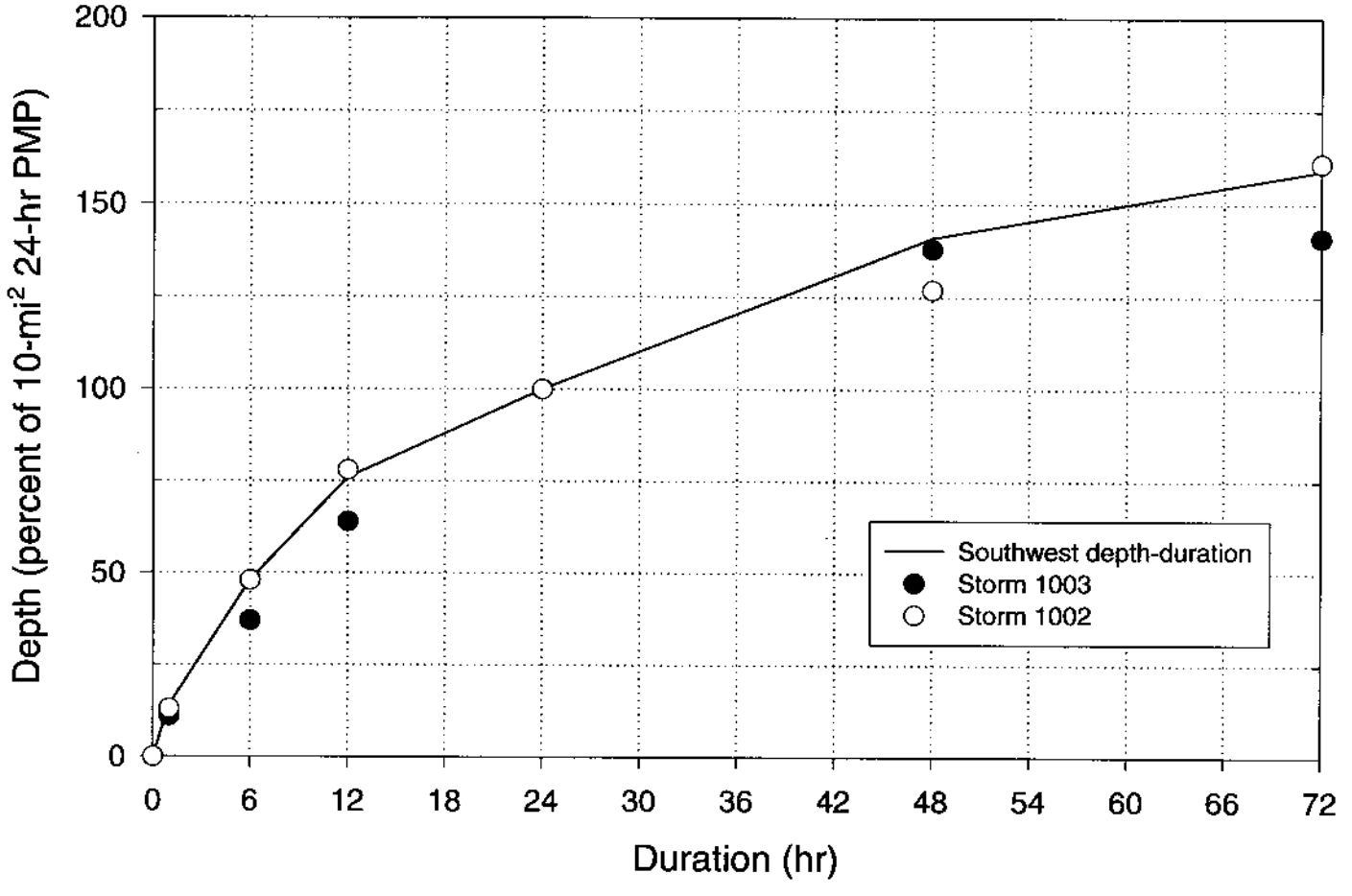

Figure 8.8. *10-mi² depth-duration relation (solid line for the Southwest region of California. Filled symbols represent calculated storm 1003 (January, 1943) values and open symbols represent calculated storm 1002 (February, 1938) values.*

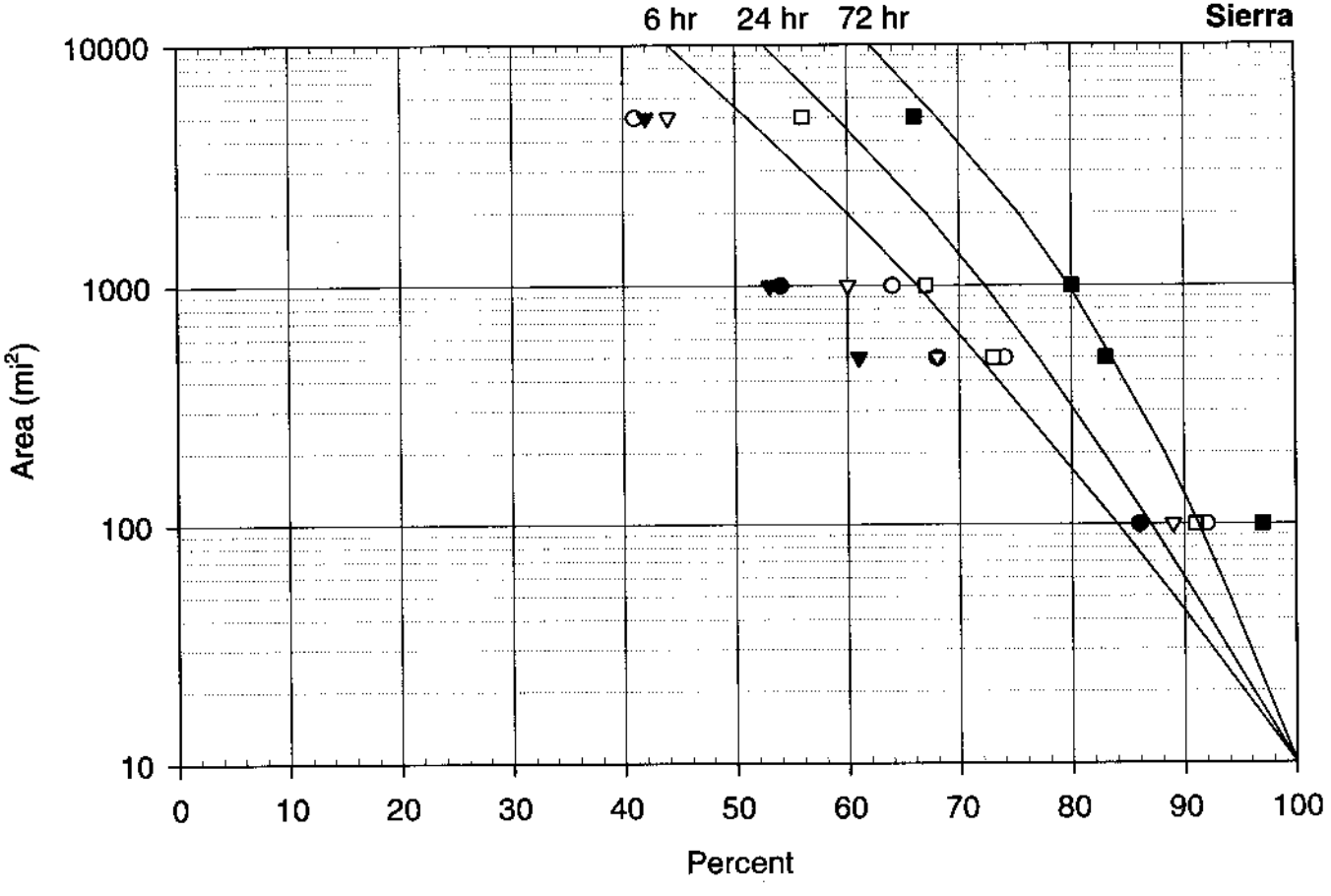

Figure 8.9. *Probable maximum storm depth-area relation (solid lines labeled 6, 24, and 72 hr) for the Sierra region. Open symbols are reduction ratios for storm 1010 (February, 1986); filled symbols are reduction ratios for storm 575 (October, 1962). Circles, triangles and squares represent 6-, 24-, and 72-hr storm values, respectively.*

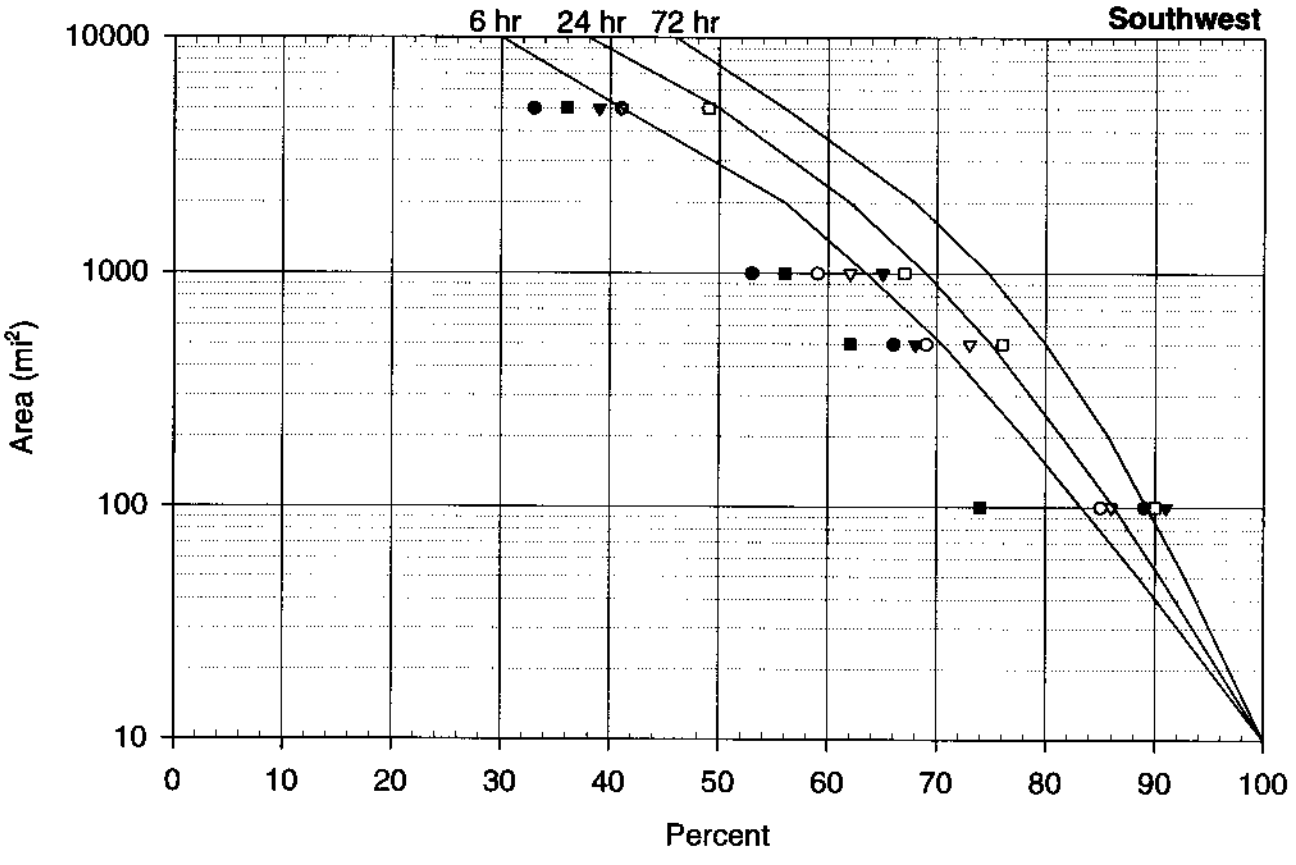

Figure 8.10. *Probable maximum storm depth-area relation (solid lines labeled 6, 24, and 72 hr) for the Southwest region. Open symbols are reduction ratios for storm 1010 (February, 1986); filled symbols are reduction ratios for storm 575 (October 1962). Circles, triangles and squares represent 6-, 24-, and 72-hr storm values, respectively.*

Table 8.3. *Depth-duration values as used in Figures 8.7 and 8.8 for two regions (enveloped) and for two storms found in each region. Values are for 10-mi^2 PMP and individual storm depths, expressed as a percent of 10-mi^2, 24-hour depth.*

Region/ Storm ID No.	Duration (hours) 1	6	12	24	48	72
Sierra	14	42	65	100	156	176
575	13	35	56	100	135	149
1010	10	30	54	100	156	176
Southwest	14	48	76	100	141	159
1002	13	48	78	100	127	161
1003	11	37	64	100	138	141

Table 8.4. *Depth-area values for individual storms (indicated by storm reference number) found in indicated regions. Values are for depth of precipitation at the indicated area size and duration, expressed as a percent of each storm's depth at 10-mi^2. "m" indicates a missing depth. Values are found in Figures 8.9 and 8.10.*

	Sierra Region						Southwest Region					
	Storm 575			Storm 1010			Storm 1002			Storm 1003		
	Duration (Hours)											
Area (mi^2)	6	24	72	6	24	72	6	24	72	6	24	72
5,000	m	42	66	41	44	56	33	39	36	41	41	49
1,000	54	53	80	64	60	67	53	65	56	59	62	67
500	68	61	83	74	68	73	66	68	62	69	73	76
100	86	86	97	92	89	91	89	91	74	85	86	90

8.3 Seasonal Adjustments to General-Storm DAD Curves

Once the all-season DAD relations had been agreed upon, normalized DAD relations from the outstanding seasonal storms were smoothed for durational consistency and then expressed as a percentage of the all-season values. These off-season percentages (referenced as "factors" in this section) fell into two classes: off-season depth-duration factors for 10-mi^2 and off-season depth-area factors for selected durations. The factors were plotted for each class. The y-axis on each diagram was in units of percentage; the x-axis for the depth-duration factors was in units of months away from the envelope of all-season months, and for the depth-area factors it was in units of area size. In the depth-duration factor diagram, the plotted points from the outstanding off-season storms were values (of percentage) for durations of 1-, 6-, 12-, 24-, 36-, 48-, and 72-hours at monthly offsets from the all-season envelope. Contours of percentage were drawn on the diagram for each duration. For the depth-area factor diagram, the plotted percentages were at selected area sizes and for monthly offsets from the all-season envelope. Contours of percentage were also drawn. The results are shown in Table 8.5.

A monthly offset or departure from the all-season envelope of months was considered positive if it followed the last month in the envelope and considered negative if it preceded the first month in the envelope. For example, if the all-season envelope for some location (as determined from Chapter 7, Figures 7.2 to 7.11) extends from October through March, then the "off-season" months of April, May, and June are designated as +1, +2, and +3 months respectively away from the all-season envelope of DAD relations; while September, August, and July are designated as -1, -2, and -3 months offset, respectively, from the envelope of all-season DAD relations. Furthermore, an even number of off-season months can be divided evenly between positive and negative offsets; while for an odd number of off-season months, the remaining month is given a negative offset. The values of the factors are symmetric about the all-season envelope of months. The factors were derived from the four largest (at 10-mi^2, 24-hours) off-season storms (numbers 575, 1012, 1015, and 1016), none of which were located in the southeast DAD region. At the places where the four storms were centered, their dates of occurrence (in units of months departure from the all-season envelope at that site) were -0.5, +2, -3, and -3 months, respectively. Furthermore, these four storms took place in just 3 of the 6 non-southeastern DAD regions. It was therefore decided to group the depth-area and depth-duration factors derived from these

Table 8.5. *Seasonally adjusted 10-mi² depth-duration ratios (monthly offsets).*

Northwest

Offset	1 hr	6 hr	12 hr	24 hr	48 hr	72 hr
1	0.102	0.404	0.734	1.000	1.445	1.682
2	0.106	0.416	0.745	1.000	1.386	1.558
3	0.112	0.428	0.759	1.000	1.341	1.469
4	0.121	0.448	0.774	1.000	1.296	1.416
5	0.127	0.464	0.788	1.000	1.267	1.381

Northeast

Offset	1 hr	6 hr	12 hr	24 hr	48 hr	72 hr
1	0.163	0.525	0.693	1.000	1.358	1.473
2	0.170	0.541	0.704	1.000	1.302	1.364
3	0.179	0.556	0.718	1.000	1.260	1.287
4	0.194	0.582	0.731	1.000	1.218	1.240
5	0.203	0.603	0.745	1.000	1.190	1.209

Midcoastal

Offset	1 hr	6 hr	12 hr	24 hr	48 hr	72 hr
1	0.133	0.455	0.744	1.000	1.407	1.615
2	0.138	0.468	0.755	1.000	1.349	1.496
3	0.146	0.482	0.770	1.000	1.305	1.411
4	0.157	0.504	0.784	1.000	1.262	1.360
5	0.165	0.522	0.799	1.000	1.233	1.326

Central Valley

Offset	1 hr	6 hr	12 hr	24 hr	48 hr	72 hr
1	0.133	0.424	0.653	1.000	1.436	1.663
2	0.138	0.437	0.663	1.000	1.376	1.540
3	0.146	0.449	0.676	1.000	1.332	1.453
4	0.157	0.470	0.689	1.000	1.288	1.400
5	0.165	0.487	0.702	1.000	1.258	1.365

Table 8.5. (cont.) *Seasonally adjusted 10-mi² depth-duration ratios (monthly offsets).*

Sierra

Offset	1 hr	6 hr	12 hr	24 hr	48 hr	72 hr
1	0.143	0.424	0.653	1.000	1.513	1.672
2	0.148	0.437	0.663	1.000	1.451	1.549
3	0.157	0.449	0.676	1.000	1.404	1.461
4	0.169	0.470	0.689	1.000	1.357	1.408
5	0.178	0.487	0.702	1.000	1.326	1.373

Southwest

Offset	1 hr	6 hr	12 hr	24 hr	48 hr	72 hr
1	0.143	0.485	0.764	1.000	1.368	1.511
2	0.148	0.499	0.775	1.000	1.311	1.399
3	0.157	0.514	0.790	1.000	1.269	1.320
4	0.169	0.538	0.806	1.000	1.227	1.272
5	0.178	0.557	0.821	1.000	1.199	1.240

Southeast

Offset	1 hr	6 hr	12 hr	24 hr	48 hr	72 hr
1	0.294	0.594	0.856	1.000	1.206	1.347
2	0.283	0.577	0.843	1.000	1.258	1.455
3	0.268	0.561	0.827	1.000	1.300	1.542
4	0.248	0.536	0.811	1.000	1.345	1.600
5	0.236	0.517	0.796	1.000	1.376	1.641

storms into only 2 regional groups: a non-southeastern and southeastern. The values of the depth-area and depth-duration percentage factors for the southeast region are the inverse of the percentages derived from the rest of California. The contours drawn on the depth-area and depth-duration factor diagrams were, of necessity, based on significant extrapolation from a limited amount of information.

Once the contours were completed, values were extracted to form an array for selected area sizes, durations and monthly departures for the two off-season regions. These percentages were then multiplied with corresponding all-season, regional DAD to produce an array of seasonally-adjusted, regional DAD. These DAD are found in Tables 8.6 to 8.11. Because of the multiplicity of the DAD relations, it was decided not to present them here as plotted curves. The reader who requires values of off-season PMP for a drainage area in one of the DAD regions should plot the appropriate depth-area-duration information, from Tables 8.6 to 8.11, and interpolate as required.

For a particular application, when deciding whether the month of interest should begin with a plus or minus designator, we recommend the user to "take the shorter path" from the edge of the all-season envelope of months to the month of interest, i.e., choose the value which is smaller in absolute value. For example, if the all-season envelope extends from October to March and the month of interest is July, one might choose either -3 or +4. The "shorter path" to July is from October not March so the recommended choice is -3. This kind of decision comes into play only when the all-season envelope of months is an even number.

In most situations it is likely that there is some month in which the average monthly percentage of all-season index PMP for a drainage is 100 percent. However, this might not always be the case. When there is no month in which the average percentage for a drainage is 100 percent, the all-season month or envelope of months is defined as that month or months in which the average percentage is at a maximum. Average percentages within one percent of each other should be regarded as the same.

An example for a particular drainage area will help bring together the several strands developed above. Table 8.12 contains the information needed to calculate PMP for an off-season month at Auburn, a 973-mi^2 drainage located between Sacramento and Lake

Table 8.6. *Seasonally adjusted areal reduction factors for the Northeast and Northwest regions.*

Offset 1 Month						
Area (mi^2)	**1 hr**	**6 hr**	**12 hr**	**24 hr**	**48 hr**	**72 hr**
10	1.000	1.000	1.000	1.000	1.000	1.000
50	0.913	0.930	0.948	0.960	0.967	0.975
100	0.861	0.883	0.905	0.928	0.945	0.960
200	0.785	0.818	0.847	0.871	0.900	0.919
500	0.677	0.725	0.769	0.798	0.835	0.859
1000	0.582	0.644	0.690	0.730	0.762	0.790
2000	0.480	0.559	0.608	0.650	0.680	0.709
5000	0.340	0.436	0.478	0.524	0.561	0.595
10000	0.240	0.338	0.372	0.418	0.467	0.502
Offset 2 Months						
Area (mi^2)	**1 hr**	**6 hr**	**12 hr**	**24 hr**	**48 hr**	**72 hr**
10	1.000	1.000	1.000	1.000	1.000	1.000
50	0.894	0.921	0.939	0.952	0.959	0.965
100	0.831	0.868	0.892	0.916	0.929	0.941
200	0.753	0.802	0.834	0.858	0.880	0.892
500	0.641	0.702	0.746	0.778	0.806	0.825
1000	0.544	0.617	0.658	0.697	0.728	0.751
2000	0.447	0.528	0.570	0.610	0.639	0.666
5000	0.313	0.401	0.436	0.484	0.519	0.552
10000	0.218	0.302	0.335	0.381	0.428	0.459
Offset 3 Months						
Area (mi^2)	**1 hr**	**6 hr**	**12 hr**	**24 hr**	**48 hr**	**72 hr**
10	1.000	1.000	1.000	1.000	1.000	1.000
50	0.883	0.916	0.933	0.944	0.950	0.955
100	0.809	0.859	0.882	0.904	0.916	0.926
200	0.729	0.789	0.821	0.844	0.867	0.878
500	0.619	0.687	0.726	0.757	0.785	0.803
1000	0.522	0.596	0.636	0.671	0.697	0.719
2000	0.425	0.500	0.541	0.576	0.605	0.634
5000	0.294	0.374	0.412	0.451	0.481	0.512
10000	0.205	0.284	0.320	0.355	0.393	0.424

Table 8.6. (cont.) *Seasonally adjusted areal reduction factors for the Northeast and Northwest regions.*

Offset 4 Months

Area (mi^2)	1 hr	6 hr	12 hr	24 hr	48 hr	72 hr
10	1.000	1.000	1.000	1.000	1.000	1.000
50	0.865	0.902	0.926	0.940	0.946	0.952
100	0.787	0.837	0.869	0.890	0.901	0.913
200	0.696	0.760	0.800	0.821	0.842	0.853
500	0.576	0.649	0.695	0.721	0.747	0.765
1000	0.474	0.555	0.601	0.633	0.658	0.679
2000	0.375	0.464	0.502	0.536	0.563	0.590
5000	0.244	0.337	0.375	0.412	0.435	0.459
10000	0.162	0.248	0.283	0.317	0.354	0.383

Offset 5 Months

Area (mi^2)	1 hr	6 hr	12 hr	24 hr	48 hr	72 hr
10	1.000	1.000	1.000	1.000	1.000	1.000
50	0.851	0.893	0.917	0.931	0.946	0.955
100	0.770	0.823	0.851	0.874	0.886	0.898
200	0.672	0.743	0.778	0.801	0.822	0.833
500	0.551	0.627	0.667	0.697	0.722	0.740
1000	0.448	0.538	0.572	0.607	0.635	0.660
2000	0.347	0.445	0.480	0.516	0.546	0.572
5000	0.216	0.322	0.352	0.392	0.425	0.453
10000	0.141	0.228	0.261	0.298	0.339	0.367

Table 8.7. *Seasonally adjusted areal reduction factors for the Midcoastal region.*

Offset 1 Month

Area (mi^2)	1 hr	6 hr	12 hr	24 hr	48 hr	72 hr
10	1.000	1.000	1.000	1.000	1.000	1.000
50	0.903	0.915	0.928	0.943	0.957	0.975
100	0.846	0.868	0.886	0.908	0.930	0.949
200	0.775	0.804	0.832	0.856	0.885	0.909
500	0.663	0.710	0.750	0.778	0.815	0.838
1000	0.564	0.630	0.671	0.706	0.738	0.770
2000	0.458	0.536	0.584	0.621	0.655	0.690
5000	0.308	0.392	0.441	0.486	0.523	0.566
10000	0.188	0.287	0.325	0.374	0.412	0.456

Offset 2 Months

Area (mi^2)	1 hr	6 hr	12 hr	24 hr	48 hr	72 hr
10	1.000	1.000	1.000	1.000	1.000	1.000
50	0.885	0.906	0.919	0.935	0.949	0.965
100	0.817	0.853	0.872	0.896	0.914	0.931
200	0.743	0.787	0.820	0.843	0.866	0.882
500	0.627	0.688	0.727	0.758	0.786	0.805
1000	0.527	0.603	0.639	0.673	0.704	0.732
2000	0.427	0.506	0.547	0.582	0.616	0.648
5000	0.283	0.360	0.403	0.450	0.484	0.525
10000	0.170	0.257	0.293	0.340	0.378	0.417

Offset 3 Months

Area (mi^2)	1 hr	6 hr	12 hr	24 hr	48 hr	72 hr
10	1.000	1.000	1.000	1.000	1.000	1.000
50	0.874	0.902	0.913	0.927	0.940	0.955
100	0.795	0.844	0.862	0.885	0.901	0.917
200	0.719	0.775	0.807	0.830	0.852	0.869
500	0.606	0.673	0.708	0.739	0.766	0.784
1000	0.505	0.583	0.619	0.648	0.674	0.701
2000	0.405	0.480	0.520	0.550	0.583	0.616
5000	0.266	0.336	0.381	0.419	0.448	0.487
10000	0.160	0.241	0.279	0.317	0.347	0.385

Table 8.7. (cont.) *Seasonally adjusted areal reduction factors for the Midcoastal region.*

Offset 4 Months

Area (mi^2)	1 hr	6 hr	12 hr	24 hr	48 hr	72 hr
10	1.000	1.000	1.000	1.000	1.000	1.000
50	0.855	0.888	0.907	0.923	0.936	0.952
100	0.774	0.823	0.850	0.871	0.887	0.903
200	0.688	0.746	0.786	0.807	0.827	0.843
500	0.564	0.636	0.677	0.703	0.729	0.747
1000	0.459	0.543	0.584	0.612	0.637	0.662
2000	0.358	0.445	0.483	0.512	0.543	0.574
5000	0.220	0.303	0.347	0.382	0.406	0.437
10000	0.126	0.211	0.247	0.284	0.313	0.348

Offset 5 Months

Area (mi^2)	1 hr	6 hr	12 hr	24 hr	48 hr	72 hr
10	1.000	1.000	1.000	1.000	1.000	0.000
50	0.842	0.879	0.897	0.915	0.936	0.000
100	0.757	0.809	0.832	0.855	0.872	0.000
200	0.664	0.730	0.765	0.787	0.808	48.000
500	0.539	0.614	0.650	0.679	0.705	1.016
1000	0.434	0.526	0.556	0.587	0.615	0.919
2000	0.331	0.427	0.461	0.493	0.526	0.875
5000	0.196	0.289	0.325	0.364	0.396	0.834
10000	0.110	0.194	0.228	0.267	0.299	0.749

Table 8.8. *Seasonally adjusted areal reduction factors for the Central Valley region.*

Offset 1 Month

Area (mi^2)	1 hr	6 hr	12 hr	24 hr	48 hr	72 hr
10	1.000	1.000	1.000	1.000	1.000	1.000
50	0.828	0.886	0.918	0.940	0.952	0.970
100	0.752	0.823	0.866	0.893	0.915	0.934
200	0.663	0.750	0.798	0.832	0.860	0.889
500	0.536	0.638	0.701	0.739	0.775	0.803
1000	0.437	0.541	0.608	0.652	0.683	0.715
2000	0.333	0.440	0.504	0.548	0.582	0.616
5000	0.207	0.295	0.350	0.393	0.432	0.466
10000	0.113	0.182	0.222	0.267	0.302	0.339

Offset 2 Months

Area (mi^2)	1 hr	6 hr	12 hr	24 hr	48 hr	72 hr
10	1.000	1.000	1.000	1.000	1.000	1.000
50	0.812	0.877	0.909	0.932	0.944	0.960
100	0.726	0.809	0.853	0.882	0.899	0.916
200	0.636	0.734	0.786	0.819	0.841	0.862
500	0.507	0.618	0.679	0.720	0.748	0.771
1000	0.408	0.518	0.580	0.622	0.652	0.679
2000	0.310	0.415	0.472	0.514	0.547	0.578
5000	0.190	0.271	0.320	0.363	0.400	0.432
10000	0.102	0.162	0.200	0.243	0.277	0.310

Offset 3 Months

Area (mi^2)	1 hr	6 hr	12 hr	24 hr	48 hr	72 hr
10	1.000	1.000	1.000	1.000	1.000	1.000
50	0.802	0.872	0.903	0.924	0.935	0.951
100	0.707	0.801	0.843	0.870	0.886	0.902
200	0.615	0.723	0.774	0.806	0.828	0.849
500	0.490	0.605	0.661	0.701	0.729	0.751
1000	0.391	0.500	0.561	0.599	0.624	0.651
2000	0.295	0.394	0.448	0.486	0.518	0.550
5000	0.179	0.253	0.302	0.338	0.371	0.400
10000	0.096	0.153	0.191	0.227	0.254	0.287

Table 8.8. (cont.) *Seasonally adjusted areal reduction factors for the Central Valley region.*

Offset 4 Months

Area (mi^2)	1 hr	6 hr	12 hr	24 hr	48 hr	72 hr
10	1.000	1.000	1.000	1.000	1.000	1.000
50	0.785	0.859	0.897	0.920	0.931	0.947
100	0.688	0.780	0.831	0.857	0.873	0.889
200	0.588	0.696	0.753	0.784	0.804	0.825
500	0.456	0.572	0.633	0.668	0.694	0.716
1000	0.355	0.466	0.529	0.565	0.590	0.615
2000	0.260	0.365	0.416	0.452	0.482	0.513
5000	0.148	0.228	0.275	0.309	0.336	0.359
10000	0.076	0.133	0.169	0.203	0.229	0.259

Offset 5 Months

Area (mi^2)	1 hr	6 hr	12 hr	24 hr	48 hr	72 hr
10	1.000	1.000	1.000	1.000	1.000	1.000
50	0.772	0.850	0.888	0.912	0.931	0.951
100	0.673	0.768	0.813	0.841	0.858	0.874
200	0.568	0.681	0.733	0.764	0.785	0.805
500	0.436	0.552	0.608	0.645	0.670	0.692
1000	0.336	0.451	0.504	0.542	0.569	0.597
2000	0.241	0.350	0.398	0.435	0.467	0.497
5000	0.131	0.218	0.258	0.294	0.328	0.354
10000	0.066	0.123	0.156	0.191	0.219	0.248

Table 8.9. *Seasonally adjusted areal reduction factors for the Sierra region.*

Offset 1 Month

Area (mi^2)	1 hr	6 hr	12 hr	24 hr	48 hr	72 hr
10	1.000	1.000	1.000	1.000	1.000	1.000
50	0.908	0.920	0.933	0.950	0.962	0.985
100	0.851	0.868	0.886	0.908	0.930	0.960
200	0.775	0.799	0.822	0.851	0.880	0.919
500	0.667	0.706	0.745	0.778	0.820	0.859
1000	0.582	0.630	0.676	0.715	0.762	0.810
2000	0.493	0.550	0.603	0.650	0.699	0.749
5000	0.385	0.449	0.501	0.552	0.608	0.653
10000	0.300	0.372	0.410	0.472	0.531	0.577

Offset 2 Months

Area (mi^2)	1 hr	6 hr	12 hr	24 hr	48 hr	72 hr
10	1.000	1.000	1.000	1.000	1.000	1.000
50	0.889	0.911	0.924	0.942	0.954	0.975
100	0.821	0.853	0.872	0.896	0.914	0.941
200	0.743	0.782	0.810	0.839	0.861	0.892
500	0.632	0.684	0.722	0.758	0.791	0.825
1000	0.544	0.603	0.644	0.683	0.728	0.770
2000	0.459	0.519	0.565	0.610	0.658	0.703
5000	0.354	0.413	0.457	0.510	0.563	0.605
10000	0.272	0.332	0.370	0.429	0.487	0.527

Offset 3 Months

Area (mi^2)	1 hr	6 hr	12 hr	24 hr	48 hr	72 hr
10	1.000	1.000	1.000	1.000	1.000	1.000
50	0.878	0.907	0.918	0.934	0.945	0.965
100	0.800	0.844	0.862	0.885	0.901	0.926
200	0.719	0.770	0.797	0.825	0.847	0.878
500	0.611	0.669	0.703	0.739	0.771	0.803
1000	0.522	0.583	0.623	0.657	0.697	0.737
2000	0.436	0.492	0.537	0.576	0.622	0.669
5000	0.333	0.385	0.432	0.475	0.522	0.561
10000	0.256	0.312	0.353	0.400	0.447	0.487

Table 8.9. (cont.) *Seasonally adjusted areal reduction factors for the Sierra region.*

Offset 4 Months

Area (mi^2)	1 hr	6 hr	12 hr	24 hr	48 hr	72 hr
10	1.000	1.000	1.000	1.000	1.000	1.000
50	0.860	0.893	0.912	0.930	0.941	0.961
100	0.778	0.823	0.850	0.871	0.887	0.913
200	0.688	0.742	0.777	0.802	0.823	0.853
500	0.568	0.632	0.673	0.703	0.734	0.765
1000	0.474	0.543	0.588	0.621	0.658	0.697
2000	0.385	0.456	0.498	0.536	0.579	0.623
5000	0.276	0.347	0.393	0.434	0.472	0.503
10000	0.202	0.273	0.312	0.358	0.403	0.440

Offset 5 Months

Area (mi^2)	1 hr	6 hr	12 hr	24 hr	48 hr	72 hr
10	1.000	1.000	1.000	1.000	1.000	1.000
50	0.846	0.883	0.902	0.922	0.941	0.965
100	0.761	0.809	0.832	0.855	0.872	0.898
200	0.664	0.725	0.756	0.783	0.803	0.833
500	0.543	0.610	0.646	0.679	0.709	0.740
1000	0.448	0.526	0.560	0.595	0.635	0.676
2000	0.356	0.438	0.476	0.516	0.561	0.604
5000	0.245	0.332	0.369	0.413	0.461	0.496
10000	0.176	0.251	0.288	0.337	0.386	0.422

Table 8.10. *Seasonally adjusted areal reduction factors for the Southwest region.*

Offset 1 Month

Area (mi^2)	1 hr	6 hr	12 hr	24 hr	48 hr	72 hr
10	1.000	1.000	1.000	1.000	1.000	1.000
50	0.893	0.915	0.928	0.940	0.952	0.965
100	0.837	0.863	0.881	0.898	0.920	0.939
200	0.770	0.799	0.818	0.842	0.870	0.899
500	0.658	0.696	0.730	0.758	0.795	0.828
1000	0.555	0.611	0.647	0.686	0.723	0.760
2000	0.441	0.513	0.561	0.601	0.636	0.670
5000	0.284	0.361	0.419	0.468	0.499	0.538
10000	0.165	0.254	0.291	0.338	0.384	0.428

Offset 2 Months

Area (mi^2)	1 hr	6 hr	12 hr	24 hr	48 hr	72 hr
10	1.000	1.000	1.000	1.000	1.000	1.000
50	0.875	0.906	0.919	0.932	0.944	0.955
100	0.807	0.848	0.867	0.887	0.904	0.921
200	0.739	0.782	0.805	0.829	0.851	0.872
500	0.623	0.674	0.708	0.739	0.767	0.795
1000	0.519	0.585	0.616	0.655	0.690	0.722
2000	0.411	0.484	0.525	0.564	0.598	0.629
5000	0.261	0.332	0.382	0.433	0.462	0.498
10000	0.150	0.227	0.262	0.308	0.353	0.391

Offset 3 Months

Area (mi^2)	1 hr	6 hr	12 hr	24 hr	48 hr	72 hr
10	1.000	1.000	1.000	1.000	1.000	1.000
50	0.864	0.902	0.913	0.924	0.935	0.946
100	0.786	0.840	0.858	0.875	0.891	0.907
200	0.715	0.770	0.793	0.815	0.838	0.859
500	0.602	0.660	0.689	0.720	0.747	0.775
1000	0.497	0.566	0.596	0.630	0.661	0.692
2000	0.390	0.459	0.499	0.533	0.566	0.598
5000	0.245	0.310	0.361	0.403	0.428	0.462
10000	0.141	0.213	0.250	0.287	0.323	0.361

Table 8.10. (cont.) *Seasonally adjusted areal reduction factors for the Southwest region.*

Offset 4 Months

Area (mi^2)	1 hr	6 hr	12 hr	24 hr	48 hr	72 hr
10	1.000	1.000	1.000	1.000	1.000	1.000
50	0.846	0.888	0.907	0.920	0.931	0.942
100	0.765	0.818	0.845	0.861	0.877	0.894
200	0.683	0.742	0.772	0.793	0.813	0.834
500	0.560	0.624	0.659	0.685	0.712	0.738
1000	0.451	0.527	0.563	0.595	0.624	0.654
2000	0.344	0.426	0.463	0.496	0.527	0.558
5000	0.203	0.279	0.329	0.368	0.387	0.414
10000	0.111	0.186	0.221	0.257	0.292	0.327

Offset 5 Months

Area (mi^2)	1 hr	6 hr	12 hr	24 hr	48 hr	72 hr
10	1.000	1.000	1.000	1.000	1.000	1.000
50	0.833	0.879	0.897	0.912	0.931	0.946
100	0.748	0.805	0.827	0.846	0.863	0.879
200	0.660	0.725	0.751	0.774	0.794	0.814
500	0.536	0.602	0.633	0.662	0.688	0.713
1000	0.427	0.510	0.536	0.571	0.602	0.635
2000	0.319	0.409	0.443	0.477	0.510	0.541
5000	0.180	0.267	0.308	0.350	0.378	0.409
10000	0.097	0.171	0.204	0.241	0.279	0.313

Table 8.11. *Seasonally adjusted areal reduction factors for the Southeast region.*

Offset 1 Month

Area (mi^2)	1 hr	6 hr	12 hr	24 hr	48 hr	72 hr
10	1.000	1.000	1.000	1.000	1.000	1.000
50	0.902	0.935	0.945	0.952	0.964	0.970
100	0.838	0.877	0.894	0.912	0.920	0.929
200	0.779	0.832	0.848	0.874	0.880	0.891
500	0.713	0.760	0.776	0.807	0.820	0.837
1000	0.643	0.702	0.725	0.745	0.763	0.780
2000	0.561	0.622	0.647	0.655	0.675	0.690
5000	0.389	0.477	0.522	0.535	0.553	0.573
10000	0.253	0.355	0.427	0.444	0.464	0.484

Offset 2 Months

Area (mi^2)	1 hr	6 hr	12 hr	24 hr	48 hr	72 hr
10	1.000	1.000	1.000	1.000	1.000	1.000
50	0.921	0.944	0.954	0.960	0.972	0.980
100	0.869	0.892	0.908	0.924	0.936	0.947
200	0.813	0.849	0.861	0.887	0.900	0.918
500	0.753	0.785	0.800	0.828	0.850	0.871
1000	0.688	0.733	0.761	0.781	0.799	0.821
2000	0.602	0.659	0.691	0.698	0.717	0.735
5000	0.423	0.519	0.572	0.578	0.597	0.618
10000	0.279	0.397	0.474	0.488	0.506	0.529

Offset 3 Months

Area (mi^2)	1 hr	6 hr	12 hr	24 hr	48 hr	72 hr
10	1.000	1.000	1.000	1.000	1.000	1.000
50	0.932	0.949	0.960	0.968	0.982	0.990
100	0.892	0.902	0.918	0.936	0.950	0.962
200	0.840	0.862	0.874	0.902	0.914	0.933
500	0.779	0.802	0.822	0.850	0.872	0.894
1000	0.718	0.759	0.787	0.811	0.834	0.857
2000	0.634	0.695	0.728	0.738	0.759	0.773
5000	0.450	0.556	0.605	0.621	0.644	0.667
10000	0.297	0.423	0.497	0.523	0.552	0.573

Table 8.11. (cont.) *Seasonally adjusted areal reduction factors for the Southeast region.*

Offset 4 Months

Area (mi^2)	1 hr	6 hr	12 hr	24 hr	48 hr	72 hr
10	1.000	1.000	1.000	1.000	1.000	1.000
50	0.952	0.964	0.967	0.972	0.986	0.994
100	0.917	0.926	0.932	0.951	0.965	0.976
200	0.879	0.896	0.898	0.927	0.941	0.961
500	0.838	0.849	0.859	0.893	0.916	0.939
1000	0.791	0.815	0.833	0.859	0.883	0.907
2000	0.719	0.750	0.783	0.794	0.815	0.829
5000	0.543	0.618	0.664	0.680	0.711	0.743
10000	0.376	0.484	0.562	0.585	0.612	0.634

Offset 5 Months

Area (mi^2)	1 hr	6 hr	12 hr	24 hr	48 hr	72 hr
10	1.000	1.000	1.000	1.000	1.000	1.000
50	0.968	0.974	0.977	0.981	0.986	0.990
100	0.938	0.941	0.952	0.968	0.981	0.993
200	0.910	0.916	0.923	0.951	0.964	0.984
500	0.876	0.880	0.894	0.924	0.948	0.971
1000	0.836	0.841	0.875	0.896	0.915	0.934
2000	0.776	0.781	0.820	0.825	0.841	0.855
5000	0.612	0.646	0.709	0.714	0.729	0.753
10000	0.432	0.526	0.608	0.622	0.639	0.662

Table 8.12. *Comparison of all-season PMP with May PMP (2 month offset) in the 973-mi² Auburn drainage (Sierra region).*

	Duration	1 hr	6 hr	12 hr	24 hr	48 hr	72 hr
1.	All-season basin (973-mi²) average depth (in.) PMP from Chapter 10, Table 10.1.	2.20	6.90	11.21	17.72	29.56	34.64
2a.	Average PMP index (10-mi², 24-hour) value (in.) from Plate 2 for the basin.				24.6		
2b.	All-season Sierra depth-duration ratios from Table 8.3.	0.14	0.42	0.65	1.00	1.56	1.76
3.	All-season 10-mi² average depth (in.) PMP for the basin (line 2a times line 2b).	3.4	10.3	16.0	24.6	38.4	43.3
4.	May index PMP as a ratio of all-season index PMP from Chapter 7, Figure 7.5.				.68		
5.	May average PMP index value (in.) for the basin (line 4 times line 2a).				16.7		
6.	May depth-duration ratios for 10 mi² from Table 8.5.	0.148	0.437	0.663	1.000	1.451	1.549
7.	May 10-mi² average depth (in.) PMP for the basin (line 6 times line 5).	2.5	7.3	11.1	16.7	24.2	25.9
8.	Depth-area reduction ratios interpolated for the basin (973-mi²) from Table 8.9.	0.548	0.607	0.648	0.687	0.731	0.773
9.	May basin (973-mi²) average depth (in.) PMP (line 7 times line 8).	1.4	4.4	7.2	11.5	17.7	20.0
10.	Ratios of May 10-mi² average depth PMP for the basin to the all-season 10-mi² average depth PMP for the basin (line 7 divided by line 3).	0.735	0.709	0.694	0.679	0.630	0.598
11.	Ratios of May basin (973-mi²) average depth PMP to the all-season basin (973-mi²) average depth PMP (line 9 divided by line 1).	0.636	0.638	0.642	0.649	0.599	0.577

Tahoe. The Auburn drainage is shown on the map in Chapter 10, Figure 10.1 The procedure begins by obtaining the all-season PMP from Chapter 10, Table 10.1 (line 1 of Table 8.12). The values on line 1 are not needed in the process used to get PMP for an off-season month, but are included in the table so they may be compared with the derived off-season PMP. Next, we obtain the basin-average PMP from the PMP Index map using any well-established technique (line 2a). Multiplying line 2a by the all-season, depth-duration ratios (line 2b) for the Sierra region from Table 8.3 results in line 3. Line 3 will be used only to derive line 10 for comparison with line 11 in comment "A." below. Then Chapter 7, Figure 7.5 is used to get the average percentage value in the drainage for May (line 4). Multiplication of line 3 at 24 hours and line 4 provides us with the index value of PMP for May (line 5). Lines 6 and 8 contain the seasonally-adjusted DAD. Examination of Figures 7.2 through 7.11 reveals that the all-season envelope of months at Auburn runs from November through March. Thus May becomes a 2-month offset. The line 6 values are read directly from Table 8.5. Any reasonable interpolation scheme of the values in Table 8.9 may be used to get the values on line 8. The procedures followed in lines 2 through 10 would be used to obtain off-season PMP for any drainage.

As for the ratios on line 11 of Table 8.12, one should expect these values to reflect the peculiar circumstances of the drainage in question and the month under consideration. In the case illustrated here, *viz.* Auburn in May, it is of significance to note that:

A. Comparing lines 10 and 11, notice that for all durations, the reduction in PMP potential in May (spring) as compared with the all-season months - October through March (winter) - is greater at 973 mi^2 than at 10 mi^2. This would seem to indicate that there is a greater decrease in the capacity of the atmosphere to produce widespread, orographic precipitation in the spring, *vis a vis* winter, than in the atmosphere's capacity to produce smaller scale, intense precipitation during the same seasonal interval, at least in the Sierra of California.

B. The results in line 11 show that when the May basin average depth of PMP (line 9) is compared to the all-season (winter) basin average depth of PMP (line 1), the reduction potential in May is greater at 2 and 3 days than at 1 day. This reflects a lesser capacity of the atmosphere to produce consecutive (or

repeating) heavy precipitation episodes in the Spring in the California Sierra, *vis a vis* the winter.

C. Furthermore, why is the reduction in PMP potential in line 11 at 1 hour greater than at 6, 12, and 24 hours? Perhaps the answer lies in reframing the question to ask why the ratios at 6, 12, and 24 hours are greater than at 1 hour. We are not certain of the answer, but it can be speculated that in the durational range of 6 to 24 hours, atmospheric conditions in some manner in the spring are more favorable to synergistic interactions among the small-scale, heavy precipitation-producing elements than in the winter; while, at the same time, 1 hour is not sufficient time for such (speculative) interactions to take place regardless of season. Hence, there is a relative percentage increase at 6 through 24 hours, compared with the 1-hour percentage.

9. LOCAL-STORM PMP

9.1 Introduction

Local-storm probable maximum precipitation (PMP) estimates were developed to provide rainfall values for small basins and short-duration storms in California. HMR 49 (1977) was the first report to provide such estimates for the state. HMR 49 excluded the northwestern corner of California (see Figure 4.1 in HMR 49 for exact area) from local-storm PMP consideration. It was believed that the stable Pacific air usually predominating in this region precluded the development of excessive thunderstorm rainfall. However, the revised PMP for the northwestern United States, HMR 57 (1994) provides PMP estimates west of the Cascade mountain divide to the coast. In order to maintain continuity with HMR 57 the current study extends PMP to the northwest coast of California. This was done despite the fact that no major new storms were observed in that area since the publication of HMR 49. HMR 49 used data for the period from 1940-1972; an additional 25 years were available for the current study.

9.2 Definition and Methodology

The definition of local storms in the PMP process has remained relatively constant since the term was first applied in HMR 43 (1966), but the changes that were made are important. As defined in HMR 49 they are "unusually heavy rains exceeding 3 inches in 3 hours or less that are reasonably isolated from surrounding rains." The maximum duration allowed for such storms was increased to 6 hours in HMR 49 to account for the merging of several shorter duration events. In HMR 49 the areal coverage was defined for storms ranging up to a maximum of 500 mi^2, although the majority of storms cover an area substantially less than this. One of the biggest problems in defining local storms is the issue of "reasonably isolated" rainfall. Many times significant storms are embedded within a more widespread light or moderate rainfall pattern, and it is a matter of some debate as to which storms of this type to include. Several embedded locally heavy rains in California storms have been included in the list of record local storms, shown in Table 9.1. HMR 49 restricted such embedded storm types to the warm season, from about May through October. However,

Table 9.1. *Extreme local storms in California (rainfall in inches, duration in minutes).*

#	Location	Lat. Lon.	Elev	Date	Rainfall	Duration	References
1.	Encinitas	32°59' -117°15'	100	10/12/1889	7.58	8 hours	Pyke 1975
2.	Campo	32°36' -116°28'	2590	8/12/1891	11.5	80	HMR 37
3.	Kennett	40°45' -122°24'	730	5/9/1915	8.25	8 hours	HMR 37
4.	Wrights	37°08' -121°55'	1600	9/12/1918	3.5	60	HMR 37
5.	Red Bluff	40°09' -122°15'	340	9/14/1918	4.7	180	HMR 37
6.	Campo	32°36' -116°28'	2590	7/18/1922	7.1	120	CD 1922
7.	Squirrel Inn	34°14' -118°15'	5280	7/18/1922	5.01	90	CD 1922
8.	Tehachapi	35°08' -118°27'	3975	9/30/1932	10.6	5 hours	USCOE 1961; HMR 50
9.	Indio	33°43' -116°13'	-12	9/24/1939	6.75	6 hours	Pyke 1975
10.	Fullerton Creek	33°54' -117°55'	400	3/14/1941	2.51	40	USCOE 1941a.
11.	Needles	34°51' -114°36'	480	8/9/1941	2.00	60	USCOE 1941b.
12.	Avalon	33°21' -118°19'	10	10/21/1941	5.53	210	HMR 37
13	Los Angeles	34°00' -118°10'	500	3/3/1943	3.32	180	HMR 37
14.	Tehachapi	35°08' -118°27'	3975	10/6/1945	3.17	120	HMR 49
15.	Cucamonga	34°05' -117°25'	1650	9/29/1946	3.20	80	San Bernardino FCD
16.	La Quinta	33°40' -116°19'	50	7/22/1948	3.00	210	USCOE 1957
17.	Fresno (NE of)	37°09' -119°30'	1100	5/17/1949	2.26	60	USWB 1949
18.	Vallecito	32°58' -116°21'	1450	7/18/1955	7.1	70	USCOE 1955
19.	Chiatovich Flat	37°44' -118°15'	10320	7/19/1955	8.25	150	Kesseli & Beaty 1959
20.	Santa Barbara	34°26' -119°43'	10	2/4/1958	1.66	70	USCOE 1958
21.	Newton	40°42' -122°22'	700	9/18/1959	10.6	5 hours	HMR 37
22.	Darwin	36°16' -117°35'	4900	7/13/1967	3.35	20	Cal. DWR 1973
23.	Los Angeles	34°00' -118°10'	270	11/19/1967	1.51	30	CD 1967
24.	Bakersfield	35°25' -119°03'	475	6/7/1972	3.00	60	Bryant 1972
25.	Redding	40°34' -122°25'	580	8/14/1976	3.20	240	Fontana 1977
26.	Borrego	33°12' -116°20'	576	9/23/1976	4.00	180	USCOE 1977
27.	Goleta	34°26' -119°53'	10	10/1/1976	4.00	90	Santa Barbara FCD 1976
28.	Santa Barbara	34°25' -119°42'	100	1/10/1978	1.37	20	Santa Barbara FCD 1978
29.	Forni Ridge	38°48' -120°13'	7600	6/18/1982	5.76	6 hours	Kuehn 1983
30.	Palomar Mtn.	33°21' -116°52'	5550	8/13/1992	6.40	120	HPD 1992
31.	Copco	41°59' -122°21'	3000	7/21/1995	2.30	30	NWS 1995

the current study showed that some important local storms of the *embedded type* occurred in the cool season and are included here. As will be seen in this report, the former distinction between general- and local-storms has been blurred and a more complex array of storm types is recognized.

Local-storm PMP followed a methodology first used in the studies for the northwest United States, in HMR 43, HMR 49, HMR 55A (1988) and later in HMR 57.

9.3 Storm Record

The first and perhaps most important step in PMP development is the selection of the major local storms that will form the cornerstone for the calculation of PMP. One starting point was the list of major short-period rains contained in the PMP study for the Colorado River and Great Basin, HMR 49. The California major local storms, including those from HMR 49, are listed in chronological order in Table 9.1. The locations of the 31 storms are shown in Figure 9.1. Some minor corrections for latitude and longitude errors in the HMR 49 list were made, as well as the addition of 14 new storms. Seven of the *new* storms in Table 9.1 predate the 1975 data cutoff in HMR 49, but were not included in the HMR 49 list for a number of reasons. Either they had been overlooked completely, were examined and rejected due their *hybrid* nature, or did not quite meet the rainfall intensity criteria established in HMR 49. As a result of revised criteria and re-examination, seven storms which occurred prior to 1975 were added: 9. Indio, September 24,1939; 10. Fullerton, March 14, 1941; 11. Needles, August 9,1941; 17. Fresno, May 17, 1949; Santa Barbara, February 4, 1958; 22. Darwin, July 13, 1967; and 23. Los Angeles, November 19, 1967. The number are for reference in locating the storms on the map in Figure 9.1. Seven extreme local storms which occurred since the publication of HMR 49 were also added. The seven new storms include: 25. Redding, (Aug.14, 1976); 26. Borrego, (Sept.23, 1976); 27. Goleta, (Nov.1, 1976); 28. Santa Barbara, (Jan.10, 1978); 29. Forni Ridge, (June 18, 1982); 30. Palomar Mountain, (Aug.8, 1992); and 31. Copco, (July 21, 1995). Three of the most important new storms: Redding, Forni Ridge and Palomar Mountain, are discussed in detail later in this chapter.

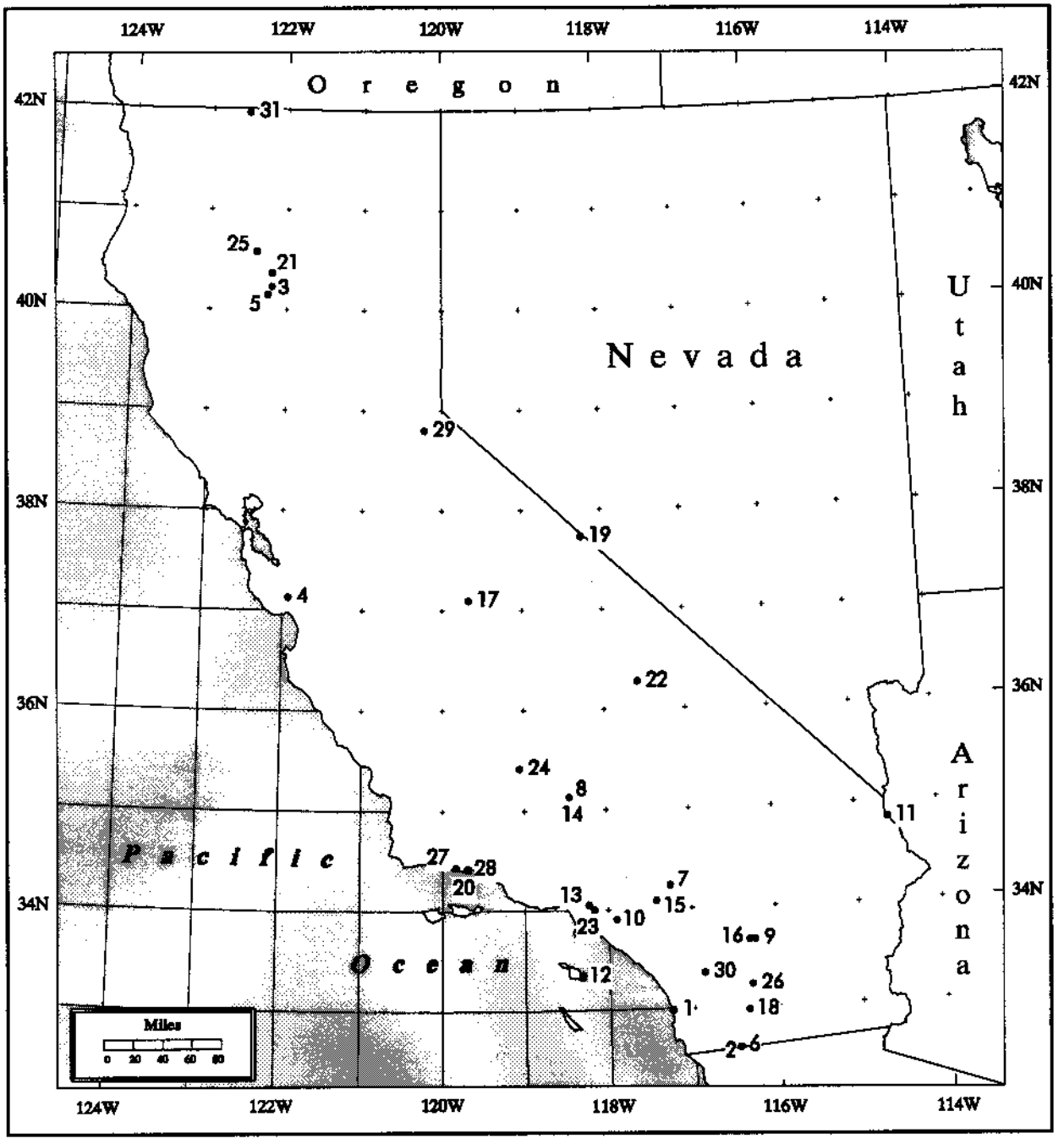

Figure 9.1. *Location of major local storms of record. The numbers refer to the list of storms found in Table 9.1.*

Several sources may be consulted for more information on the earlier storms listed in Table 9.1. HMR 37 (1962) contains detailed discussions on many of the storms which occurred up through 1960. HMR 50 (1981) also includes summaries of other major storms found in Table 9.1. Many of these storms have varied documentation; the references in Table 9.1 are to either original data sources or to the most comprehensive study which this office could locate. In cases where information is not available in the general literature, readers interested in complete documentation of a particular storm can contact the Hydrometeorological Design Studies Center where files on the storms are currently maintained.

In order to establish depth-duration and depth-area relations with a larger number of storms, a second list of local storms was also prepared. These storms did not generally meet the most extreme criteria, but were important nonetheless. They are listed in Appendix 3, Table A3.1 and consist of 137 storms from the National Weather Service Cooperative Station network. These storms cover the period from 1948-1992 and are considered very reliable in terms of depth and time measurements. The data were extracted from the National Climatic Data Center's (NCDC) Hourly Precipitation Data tapes. The relative sparseness of this network is illustrated by the fact that there is only one station for every 650 mi^2 in California. This presents a particular problem in the analysis of local storms, which by definition cover an area of 500 mi^2 or less, usually a much smaller area.

9.4 Meteorology of California Local Storms

The large-scale features that control the development and type of extreme storms affecting California are well-known, and are documented in HMR 37 and HMR 50. At the planetary scale, four or five Rossby waves are the most common flow configuration in the northern hemisphere, and both modes favor a long-wave ridge position over western United States. This *ridging* dampens the intensity of systems moving into the long-wave ridge. Of course large-scale troughs do develop and can help to intensify short-wave disturbances moving through them. An interesting and important exception to the *normal* flow pattern over the west occurs during El Niño events. The El Niño often causes a split flow in the westerlies and brings anomalously wet weather to much of southern California.

The climate of the western United States is also strongly influenced by large subtropical high pressure zones: the Bermuda High and the Pacific High. Subsidence along the east side of the Pacific High frequently affects western United States, bringing stable atmospheric conditions to coastal regions. Northwest flow also produces upwelling in the coastal water which further cools the lower levels of the atmosphere and enhances stability, thus producing a marine stratus layer and frequent coastal fog. This stable coastal air partially explains the relative lack of thunderstorm activity along the California coast (Changery 1981). Even though the Bermuda High is thousands of miles east of California, it also plays a role in the regional climate, as moist, unstable air along its western periphery can be pulled into the Southwest This pattern, often referred to as the Southwest summer monsoon, occurs most frequently from June through August. Recent research has increased understanding of the Southwest monsoon structure and of moisture sources for heavy rainfall in western United States (Carleton 1985, Douglas 1995), as will be discussed in the section on moisture, 9.5 of this chapter.

Local storm development is influenced to a large degree by the synoptic-scale patterns operating over California. As noted above, subsidence beneath the Pacific High is a frequent occurrence, and short waves moving into a ridge position are usually dampened, reducing the potential for strong storms. Significant troughs are often restricted to northern California and the cool season, which reduce the likelihood of strong convective activity. Several other synoptic features, however, can act to enhance local-storm potential. The so-called *thermal low* caused by intense summertime heating over the desert areas, produces an inverted trough that can reach from Mexico to Canada. This trough, enhanced by downslope warming from the mountains adjacent to the desert, can play a role in the initiation of convection, as will be seen in one of the case studies.

California terrain plays a critical role in determining frequency, location, and intensity of local storms in the state. The major features are well-known. A narrow coastal zone and long chain of north-south oriented coastal ranges block the inflow of Pacific moisture except at a few locations. A broad, flat interior valley, the Central Valley is bordered on the east by the massive Sierra Nevada mountains, on the north by the southern end of the Cascade range, and on the south by the Tehachapi mountains which separate divide the Central Valley from the deserts of southeast California. The terrain is somewhat more complex in southern California where the San Gabriels and San Bernardinos run west to east from Santa Barbara,

with more mountains extending south to the Mexican border. The only appreciable coastal plain in the south is the Los Angeles basin. The unique terrain of California has a strong impact on mesoscale and local-scale meteorological phenomena, and will be discussed at various points in this chapter.

Extreme local storms in California are usually convective storms, although not always of a classical, isolated thunderstorm type. Mesoscale convective features such as squall lines are sometimes embedded within cool season larger scale synoptic storms. Embedded local storms also result from eastern Pacific tropical cyclones which occasionally affect California. Some of the most intense short-duration rainfalls have occurred when a tropical cyclone or its remnant moisture has moved into California. One of the best recent examples was when the remnants of Tropical Storm Kathleen moved across southern California September 9-11, 1976. Widespread heavy rainfall fell across southern California from this storm, as well as intense short-duration rainfall, such as 4.8 inches in 3 hours at Mt. Laguna, San Diego County. This storm is not listed in Table 9.1, although a more localized event at Borrego on September 23, 1976 is included. The latter storm was the result of a tropical air incursion that resulted in very heavy rains. Although relatively rare, tropical disturbances can and do enter southern California and produce significant rainfall. The only tropical storm intense rainfall known to have entered central or northern California, although the center remained offshore, occurred during September 1918 and this storm produced two of the storms in Table 9.1, Wrights and Red Bluff. HMR 37 provides a detailed explanation of the meteorological aspects of this unique storm.

The so called *true* local storm is typically a very isolated thunderstorm, which develops without the strong, large-scale lifting mechanisms that produce widespread rainfall. These local storms can dump copious rainfall over a very small area, with little significant precipitation even a short distance away. The greatest recorded local storm in California history occurred on August 12, 1891 at Campo (Storm 6 in Fig. 9.1), where 11.50 inches fell in 80 minutes. Evidence gathered at the time of this storm indicates that this storm was very limited in area, although supporting information is scanty (HMR 50). The small scale of local storms means that they are very often missed by the conventional rain gage network. It is hoped that the advent of new observing systems, such as the WSR-88D radar and the Automated Surface Observing System (ASOS) will increase the likelihood of *catching* these local storms. In California they usually occur during the warm season, from April to

October, when moisture and solar energy are closer to their annual maxima. Another type of storm which has been less frequently recognized as affecting California is Mesoscale Convective Systems (MCSs). Each of these storm types: embedded storms, isolated thunderstorms, and MCSs will be discussed below with one or more examples to illustrate aspects of the various storm types.

In Section 9.5, which deals with maximum dewpoints, the discussion focuses on the spatial and temporal evolution of moisture fields across the state. In the current section (9.4) some of the dynamics of extreme storms which affect the state are examined. This will be important later in considering the question of transposing storms.

As stated earlier, several different storm types can produce extreme local storms in California. One of the seminal works on flash floods in the western United States (Maddox et al. 1980) showed that in California, the most common example is strong synoptic systems, or Type III. In this study, 8 out of 10 California flash flood events were Type III storms. All the Type III storms occurred during the cool-season months. These flash flood events are clear-cut cases of an embedded local storm. Rainfall rates can be quite intense in embedded storms, although not usually as intense as in more isolated storms. Among the reasons for this are: embedded type storms are cool-season phenomena and have lower moisture content; and the widespread nature of the rainfall means that several storms may be competing for a finite amount of water vapor. On the other hand, the precipitation in such storms is often organized into mesoscale rainbands and transient wave features that act to enhance rain rates. The combined effect of merging rainbands and transient waves produced hourly rainfall rates of 1.6 to 1.7 inches per hour over western Los Angeles County during the morning of February 10, 1978 (not listed). Several of the storms in Table 9.1 belong to this type of strong synoptic system with embedded convection, including the Los Angeles storm of November 19, 1967 and the Santa Barbara storm of January 10, 1978.

As noted earlier, another storm type which can produce very heavy rainfall is the MCS. Comparatively little research has been done on the existence or behavior of MCSs in California. However, recent research drawn from the Southwest Area Monsoon Project (SWAMP) (Meitin et al. 1991) has confirmed that MCSs occur in Arizona and it is very likely that they can and do migrate into southeastern California. The term MCS refers to any precipitation system with a spatial scale of 20-500 km that includes deep convection during

part of its life cycle (Zipser 1982). Confirmation of the existence of MCSs was only made possible by the advent of geostationary satellites, so they are a relatively *new* phenomenon, at least in terms of research.

Fleming and Spayd (1986) studied very heavy convective rainfall events (≥2 inches) in western United States and classified the storms according to various meteorological and satellite characteristics. From 1981-1983, 9 such events occurred in California, 6 of which were considered MCS-type systems. Two were synoptic-scale, overrunning events, and one was classified as a single-cluster convective storm, i.e., a *true* local storm. The California MCS systems were all smaller (area and duration) than the Mesoscale Convective Complexes (MCCs) in the central United States, and smaller than the MCS-alpha systems found over other parts of western United States The California MCSs were of two types; MCS-beta circular and MCS-beta linear storms, with length scales of 50 to 150 km (30-100 miles). The MCS-beta circular storms develop in environments of little or no vertical wind shear and appear as round or oval in satellite imagery. MCS-beta linear systems occur in environments with strong vertical wind shear and appear as wedge-, carrot- or diamond- shaped in satellite imagery. All the MCS systems in California were confined to either the elevated terrain east of Los Angeles and San Diego or the deserts of the southeast. It is interesting to note that the Lytle Creek Foothill Boulevard storm of August 17, 1983 (2.65 inches in 1 hour), one of the largest storms from the NCDC list in Appendix 3, Table A3.1, was classified in the Fleming and Spayd (1986) study as an MCS-beta circular system. The storm resulted in severe highway flooding and several fatalities. The Palomar Mountain storm of August 13, 1992 was also an MCS-beta circular system.

The full-blown mesoscale convective complex (MCC), which must fulfill certain size, duration and cloud-top temperature requirements to be classified as such, seems to be very rare in California (Maddox 1983). Very few full-blown MCCs have been documented anywhere in the western United States, but a relatively recent storm on August 10, 1981 did meet the criteria (Randerson 1986). The storm, centered near Ute, Nevada, about 30 miles northeast of Las Vegas, Nevada, affected a very wide area, but the very intense rainfall of more than 6 inches in several hours, occurred over a much smaller area. In terms of intensity and depth-area-duration characteristics, this storm can easily be classified as local, although the rainfall was not completely isolated. The proximity of this storm to the California border (the Ute storm center was approximately 75 miles northeast of the state border) makes it an

important addition to the catalog of significant local storms. The occurrence of this storm suggests the likelihood that even large MCSs or possibly even MCCs can affect the deserts of the Southwest and possibly California. The depth-area characteristics of the Ute storm are discussed in greater detail in the depth-area section of this chapter (Section 9.9).

Many of the storms listed in Table 9.1 have been discussed in detail in HMR 50 and in other sources and this information is not repeated in this report. Meteorological discussions of three important recent storms are provided in the following sections to give the reader some insight into the variety of processes and factors that lead to extreme local rainfall in California..

9.4.1 Redding - August 14, 1976

Heavy rainfall in and around Redding on the afternoon of August 14, 1976 provides one of the best examples of a strong synoptic system occurring in the summer season. The upper-air pattern is similar to the Type III flash flood-producing storm type cited earlier (Maddox et al. 1980). The Redding storm also illustrates some of the reasons for such a pronounced PMP maximum in the northern end of the Central Valley and surrounding foothills (see Figure 9.23).

The following description and analysis of the Redding storm draws heavily on a paper by Fontana (1977) who studied the storm in detail. According to surveys conducted after the storm by the United States Army Corps of Engineers, the maximum precipitation was 8.8 inches in a 24-hour period ending on the morning of August 15, although most of the rain fell in a five-hour period on the evening of August 14. The maximum-intensity report included a 2.5-inch amount in one hour on the evening of the 14th. Several other stations received over 3 inches in a three-hour period the same evening. The heaviest precipitation, an area of 8+ inches, fell in the higher terrain just west of downtown Redding, while the NWS cooperative station (Redding 5 SSE) southeast of town recorded less than one inch (0.85 inches) during the same time period.

The strong synoptic pattern within which this storm developed is far more typical of winter than summer. In this case, an unusually vigorous mid-level shortwave moved into the long-wave trough position located just off the Oregon-California border. Evidence for the

existence and movement of the short wave is given by the area of strong geopotential height decreases of over 120 meters, at the 500-mb level during the 24-hour period preceding the storm from 12 UTC on August 13 to 12 UTC on August 14. Intensification of a shortwave generally leads to increased divergence aloft and increased vertical motion. In addition, a strong wind maximum on the west side of the upper trough indicated that the system was undergoing intensification or continued deepening during this same period.

The strong dynamics aloft led to significant changes at the surface which also served to enhance the rainfall in the Redding area. Early on the morning of August 14 a cold front moved south, reaching a line from the San Francisco Bay area to just south of Sacramento. Over the course of the day, the front began to retreat north as a warm front and approached the Redding area during the afternoon. At the same time, a surface trough, a reflection of the shortwave aloft, developed along the Oregon coast and began a southeastward movement. By 00 UTC on August 15, frontogenesis took place along the trough line, and a weak low-pressure circulation developed along the front to the northwest of Redding. The newly developed cold front and the northward-moving warm front merged very close to Redding forming an instant occlusion or triple point low. As pointed out by Junker (1992), intersecting boundaries provide an area of maximized low-level convergence and enhance the potential for convective development. The location and movement of the short-wave trough is also confirmed by a surface isallobaric analysis, which showed sharply falling pressures in northern California where the frontal wave developed. These falling pressures are indicative of upper level divergence, which is expected ahead of the short-wave trough.

Radar analysis of the storm from the Medford, Oregon and Sacramento radar sites confirms the basic sequence of events outlined above. In the hour from 2230 UTC to 2330 UTC, there was an explosive increase in convective activity close to where the fronts intersected and the surface wave was forming. The strongest radar echoes occurred from 0030 UTC to 0330 UTC on August 15, with one cell west of Redding showing a VIP (video integrator and processor) intensity of 5. This intensity level (2.0 to 5.0 inches per hour) corresponds well with the observed rainfall intensities found in the Corps survey after the storm.

In looking at extreme precipitation events, very high moisture is usually a critical component in leading to the event. In the Redding storm, however, this was not one of the

major factors. As seen in Figure 9.11, the 3-hour maximum persisting dewpoint (at 1000-mb) for the northern end of the Sacramento Valley is close to 73°F. Dewpoint readings at Red Bluff and stations to the south (from which the inflow was occurring on the day of the storm) were in the upper 50's to low 60's most of the day. While these readings are well above average (mean August dewpoints range from the mid-40's to low 50's in the upper Sacramento Valley area), they do not come close to the maximum levels possible in the area. Although obviously adequate to support heavy precipitation, the relatively low moisture levels in this event imply that a significant increase in rainfall would be likely, given the same dynamics combined with higher moisture. The theoretical moisture maximization for the storm was 1.82, based on a storm dewpoint of 61°F and a maximum persisting dewpoint of 73°F. The actual in-place maximization was restricted to 1.50 in keeping with local-storm procedures outlined in Section 9.5.2. This limitation does indicate a level of conservatism in the PMP process which is not always recognized.

9.4.2 Forni Ridge - June 18, 1982

For a dramatic example of an isolated extreme local-storm, Forni Ridge provides one of the best recent cases in California. The storm on the afternoon of June 18, 1982 occurred within the headwaters of the South Fork of the American River (#29 in Figure 9.1) between the communities of Kyburz and Strawberry (Kuehn 1983). The six-hour rainfall total of 5.76 inches is intense, but the shorter duration amounts were extraordinary: 1.50 inches in 5 minutes; 2.20 in 10; 2.80 in 15; 4.02 in 30; and 4.42 in one hour. The rain was recorded in a United States Bureau of Reclamation tipping-bucket gage, allowing for the temporal resolution to be described accurately. As pointed out by Kuehn (1983) the short-duration rainfall actually **exceeded** PMP as given in HMR 49; the 15-minute PMP was 2.69 inches, 0.11 inches **less** than the 2.80 that fell in 15 minutes at Forni Ridge. The degree of exceedance was even greater at durations below 15 minutes. There was tremendous runoff from this storm, owing to both the intensity of the storm and the fact that much of the vegetation in the area had been burned off in a wildfire the previous summer. According to Kuehn (1983), the discharge magnitude was one of the highest ever recorded in California for that basin size.

Another important aspect of the Forni Ridge storm is the high elevation at which it occurred, approximately 7600 feet. This is well above the elevation at which PMP begins

to decrease in both HMR 49 and in this report. Using the formula in HMR 49 (see Section 4.3.2 for details) a 13-percent reduction in the PMP index level would be expected for a storm at this elevation. Using a slightly different formula than in HMR 49, the current report (Section 9.7 - Elevation) would allow a percentage reduction of 14 percent for a basin at an elevation at 7600 feet. The occurrence of this storm at such an elevation is strong confirmation of the ability of the atmosphere to produce very heavy rainfall at levels well above levels at which the reduction in moisture was formerly believed to diminish storm amounts.

The meteorological factors leading to the Forni Ridge deluge included unusually high moisture at the surface and aloft as well, a strong upper-level trough, and an extension of the summertime thermal trough well north of its usual position.

Surface dewpoints at the closest observing stations to the storm site reflect the high moisture available for storm inflow. Blue Canyon, the nearest observing station (approximately 40 miles north-northwest of Forni Ridge) experienced a dramatic influx of moisture late on June 17 and early June 18, as dewpoints surged from the low 40's to low 50's (°F). When reduced to a common reference level of 1000 mb, Blue Canyon recorded a 3-hour maximum persisting dewpoint of 66°F, only about five degrees less than the maximum persisting values for mid-June shown in Figure 9.9. At Reno, 55 miles northeast of the storm site, the readings were only slightly less extreme, reaching a 3-hour maximum persisting value of 64°F at 1000-mb (maximum persisting of 72°F - see Figure 9.9). At 12-hours, the persistence of high moisture was even more striking at these stations, coming within one degree of the maximum persisting 12-hour value. Extremely high moisture was also observed at Red Bluff, located in the northern end of the Sacramento Valley. The moisture surged into Red Bluff late on the 17th, as the dewpoint jumped 16°F in one hour from 48°F to 64°F. High dewpoints were maintained throughout the 18th, with a maximum 3-hour value of 65°F (at 1000-mb), versus the extreme of 71°F. It is highly likely that these high dewpoints also affected Forni Ridge on the afternoon of June 18th, providing abundant moisture for heavy rainfall.

This extremely high moisture was due to a combination of factors. First, the interaction between the thermal trough which extended north into southern Canada and the Pacific high, created an onshore pressure gradient between these two features, allowing some

inland penetration of marine air. Furthermore, this air was intensely heated by the strong June sun, raising temperatures to 108°F at Red Bluff on June 17. In addition, as noted by Hill (1993) when the signature of a thermal trough extends up to 850 mb or higher (as it did on June 17-18, 1982), the circulation pattern draws subtropical moisture northward. At upper levels of the atmosphere a split-flow pattern existed across the state, with a highly amplified ridge extending from California all the way to northern British Columbia. A trough associated with the subtropical jet stream existed well to the south over Baja California. The central Sierra were in a (*col-like*) area between these two features. Winds aloft were quite weak, generally 10 to 15 knots at 500 mb and 20 to 25 knots at 300 mb. This upper-level weak flow slowed the movement of any thunderstorms that did form. Causes for convection on the scale of the Forni Ridge storm are often unresolvable on synoptic-scale maps, and there was not any strong synoptic feature, such as a short wave, to which this storm can be attributed. The complex terrain of the Sierra Nevada creates differential heating and cooling of slopes with resultant thermal circulations. In the daytime, upslope winds create areas of moisture convergence, which can lead to convective cloud formation and thunderstorms. The thermal trough itself is also known to initiate convection, as convergence into it forces lifting of air parcels. Instability was also clearly enhanced by the strong solar insolation on the day of the storm. Any of these factors could have led to the development of convective activity on a limited scale, but with very high moisture to draw on, an extremely unusual event unfolded.

9.4.3 Palomar Mountain - August 13, 1992

The storm at Palomar Mountain Observatory was one of the rare instances where extremely heavy rainfall was recorded in an NWS cooperative network rain gage. A two-hour storm total rainfall of 6.40 inches fell at this site on the afternoon of August 13, 1992. In the first hour of the storm, from 12:15 to 1:15 local standard time (2015 UTC to 2115 UTC), 4.70 inches fell. This was an amount far in excess of the 100-year return frequency amount of 1.80 inches. The two-hour amount at Palomar is very close to 50 percent of the two-hour PMP for this location. An isohyetal map of the Palomar storm is shown in Figure 9.2. Of interest as well is the rainfall center at Mt. Laguna, where 4.70 inches fell in less than four hours during about the same time period as the Palomar rainfall. The existence of two intense rainfall centers occurring so far apart (approximately 40 miles), but taking place almost concurrently indicates that there was more

than one thunderstorm involved in the storm system. This suggests that the storm is properly classified as an MCS, and satellite imagery confirms it as an MCS-beta circular type.

Palomar Mountain Observatory is located at 33° 21' N, 116° 52' W, at an elevation of 5548 feet. Although Palomar Mountain is one of the higher points in the local area, the terrain is quite mountainous, especially to the east. The mountain ranges of southern California, east of the San Diego metropolitan area, extend north-south in a nearly unbroken chain, separating the coastal plain from the interior deserts of the southeastern part of the state. As shown in the isohyetal map, heavy rainfall was confined to the higher terrain, with much lower amounts in the coastal plain and in the deserts just to the east.

The hemispheric flow pattern prior to the Palomar storm featured a meridional pattern, with an unusually amplified ridge at upper levels over the western United States, especially for August. Geopotential heights at 500-mb in this ridge centered over Nevada, reached a maximum of 5940 meters on the morning of August 13, and built somewhat more during the day. The ridge was so amplified that easterly flow had developed underneath the ridge from central Texas to southern California. This easterly flow provided one of the important ingredients toward the eventual development of the Palomar storm. The easterly flow helped to advect large amounts of mid-level moisture from southern Arizona into the mountains where the storms developed. In addition, the flow aloft remained rather weak throughout the day; at 700 mb ranging from light and variable to 10 knots. At 500 mb winds were easterly at only 5 knots on the morning of the 13th. Even at 200 mb winds were only 10 to 15 knots. The weakness of the flow contributed to the slow movement of the MCS and allowed the storm to take on the characteristic shape of an MCS circular system.

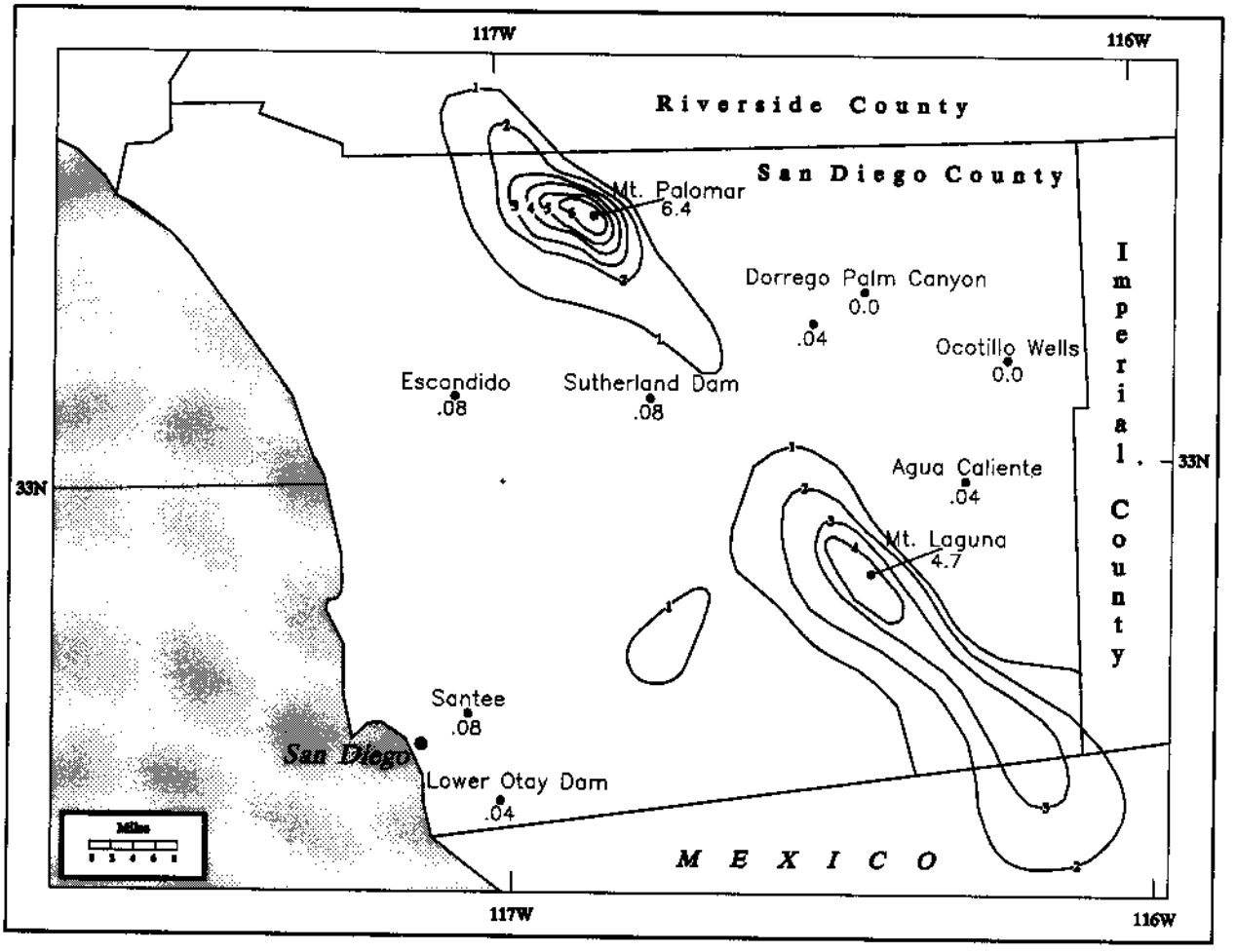

Figure 9.2. *Isohyets and recorded amounts, in inches, from the Palomar Mountain storm of August 13, 1992.*

Despite warm temperatures at the 500-mb level, ranging from -5 to -7°C over southern California and Arizona, convection was widespread indicating that there was no cap to inhibit convective development.

At the surface, a thermal trough (also referred to as a *heat low*) was located from Baja, California northward to the central part of the state, a more or less semipermanent feature in this area during the summer months. Circulation patterns associated with a strongly-developed (i.e., through a thick layer of the atmosphere) thermal trough can be conducive to drawing subtropical moisture northward into the eastern side of the trough (Hill 1993). In addition, convergence in the trough is often an aid in thunderstorm initiation, and may have played a role in the development of thunderstorms which affected southern and southeastern California over the three-day period, August 12-14, 1992. Surface temperatures well in excess of 100°F were recorded from the California desert areas northward to the Central Valley each day during this period, providing plenty of destabilizing energy to the lower atmosphere.

Low-level moisture was also extremely high in the period leading up to the Palomar storm. Surface dewpoints were well into the 70s across southern California; at Imperial, California dewpoints reached 79°F and 80°F at 1500 UTC and 1800 UTC on the 13th. These reading are at the extreme upper limit of moisture believed possible in southern California in August as shown in Figure 9.11. San Diego recorded a dewpoint of 70°F at 1500 UTC and 1800 UTC, just several hours prior to the onset of precipitation both there and at Palomar. The maximum three-hour persisting dewpoint for August at San Diego is 73°F. Precipitable water was also well above normal; at 1200 UTC (0500 PDT) on August 13 Miramar NAS, near San Diego, measured 1.64 inches or 164% of normal for the date. By the afternoon, 0000 UTC (1700 PDT) August 14, it had increased to 1.89 inches or 188% percent of normal (1700 PDT). This extremely high moisture had tropical origins in the Gulf of California and is visible on sequences of satellite water-vapor images for the day.

Scofield and Robinson (1992) have demonstrated the relationship between heavy convective rainfall and tropical water-vapor plumes. The plumes are tongues or streams of moisture, detectable on water-vapor imagery at 6.7 microns, and can indicate high moisture between the 700- and 200-mb levels, with a peak sensitivity near the 400-mb level. These plumes form a connection that links the Intertropical Convergence Zone (ITCZ) with areas

further north. Such plumes are often associated with the Southwest United States monsoon pattern (Adang and Gall 1989) and are closely tied to flash flood-producing thunderstorms that occur during the monsoon (Fleming and Spayd 1986). That such a tropical moisture plume occurred on the day of the Palomar storm is supported by the analysis sent out over Automation of Field Operations Services (AFOS) provided by the Synoptic Analysis Branch of the National Environmental Satellite, Data and Information Services (NESDIS) on the day of the storm. The AFOS remarks describe the meteorological effects of the deepening central U.S. trough, which has served to force a "dark dry slot south-southwestward into eastern Arizona and New Mexico ...and this in turn has forced a tropical moisture plume southward into Mexico and extending into Southwest Arizona and southern California" (NESDIS 1992). The statement also said that tremendous diffluence aloft was helping to maintain the thunderstorm activity. According to the same statement, satellite precipitation estimates over portions of Imperial County were 2.3 to 2.6 inches for the three-hour period from 00 UTC to 03 UTC. Over San Diego County, satellite estimates were somewhat less, about 1.2 inches in the same three-hour period. It is important to note that this time period is somewhat after the most intense rain observed at Palomar and Laguna.

An examination of the satellite imagery and radar summaries on the day of this storm shows that thunderstorm activity was widespread in southern and southeastern California on August 13. Morning activity began over parts of Riverside and Imperial counties and was evident on radar and satellite by 1630 UTC (930 PDT). This activity showed a slow westward movement with time, and produced some heavy rainfall in the desert (see NESDIS statements in previous paragraph), although the sparsity of stations precludes any real knowledge of how much rain fell from the morning system. The Palomar storm evidently developed quite separately from this system. Mostly clear skies prevailed in the early morning hours over extreme southwestern California, but by around 1800 UTC, the beginning stages in the development of the Palomar storm can be seen on the visible and infrared imagery. Very rapid expansion of cold cloud tops occurs during the two half-hour images, and continued expansion can be seen over the next several hours until about the 2230 UTC image, after which time there is noticeable cooling of cloud tops. The heaviest precipitation occurred during the hours from 2015 to 2115 UTC, when cloud tops appeared to be at their coldest, indicating the period of most intense convection. The rapid expansion of cold cloud tops is one of the key ingredients in the convective -precipitation-estimation technique used by NESDIS (Juying and Scofield 1989). In addition, the Palomar area is

close to the center of the visible anvil, an area where the heaviest precipitation is usually found in storms with weak vertical shear, which, as noted earlier, was the case for this event.

Given the extremely high moisture in place and a very unstable air mass, all that was needed to cause significant convection was a lifting mechanism. The importance of having such a mechanism cannot be understated. For instance, despite the high moisture at San Diego noted earlier, only .05 inches fell that day. Lifted indices in southern California fell from +1 at 00 UTC on August 13 to -4 at 00 UTC on August 14. K-indices were also quite high, 36 for both time periods, a value associated with about an 80 to 90 percent probability of thunderstorm occurrence in the western United States (Lee 1973). The lifting mechanism for the development of this storm is not immediately apparent from an inspection of the synoptic weather maps. There is no organized low pressure area or front traversing the region on August 13. The baroclinic model (Aviation) analysis for 1200 UTC August 13 to 00 UTC August 14 does show a weak (8 unit) vorticity maximum moving from western Arizona to southern California. Such positive vorticity advection is associated with upward vertical motion. This vorticity maximum may in fact be a reflection of a westward-moving tropical wave (often referred to as an *easterly wave*). The possible role of tropical waves in producing extreme rainfall in southern California has not been fully explored, but might provide some interesting findings.

Perhaps the simplest lifting explanation is the orographic effect of the mountains. The highest rainfall amounts at Palomar and Mt. Laguna are centered over the highest local terrain, strongly suggesting that orographic uplift was responsible for producing the critical lift necessary for these extreme thunderstorms. Another possible factor is that outflow boundaries from the morning thunderstorm activity over portions of Riverside and San Bernardino counties helped to initiate new convection further west over and near the mountains east of San Diego.

9.5 Adjustment for Maximum Moisture

9.5.1 Maximum Persisting 3-Hour Dewpoints

As in all previous PMP studies, surface dewpoint temperatures were used as a measure of the moisture available for a particular storm and to estimate the theoretical upper limit to moisture for storms occurring at a specific time and place. The rationale for using surface dewpoints, as opposed to other measures of atmospheric water vapor such as precipitable water or humidity at various levels, has been discussed in several other HMRs. It is easily the most widely available measure of atmospheric moisture in terms of both spatial and temporal coverage. PMP studies have long employed the concept of maximum-persisting dewpoints to provide an upper-limit moisture availability index. The maximum-persisting dewpoint temperature is defined as the maximum dewpoint temperature which is equaled or exceeded at any observation point for the specified period. For a 3-hour period with hourly dewpoints of 70, 71, and 72 °F, the maximum persisting dewpoint would be 70°F; that being the highest reading not undercut at any observation point during the sequence.

HMR 57 was the first study to use 3-hour, instead of 12-hour maximum persisting dewpoints for local-storm analysis. It is hypothesized in that report that the moisture necessary for local storms does not need to be as widespread or persistent as for general storms. Further, it was felt that the duration of the representative dewpoint for a storm should be correlated with the storm duration. Local storms are by definition much shorter in duration than 12 hours, with 3 hours being close to the median for local storms in the western United States Because HMR 49 used 12-hour persisting dewpoints for its local-storm study, it was necessary to develop a new climatology of 3-hour persisting dewpoints for the current study.

Table 9.2 shows the list of surface observation stations used in the development of this new dewpoint climatology, while Figure 9.3 shows the location of these stations. As in the general-storm situation, high dewpoint episodes while rain was falling, or when there was virtually no chance of rain, were not used. An example of a no-rain situation is the existence of an inversion where low-level moisture becomes trapped near the surface, and

Table 9.2. *Surface airway stations for dewpoint climatology.*

Station Name	Latitude	Longitude	Elevation (ft)	Years
Camp Pendleton MCAS	33°18'	-117°21'	76	18
Lemoore Reeves NAS	36°20'	-119°57'	240	27
Long Beach WSCMO	33°49'	-118°09'	25	43
Bakersfield Meadows	35°25'	-119°03'	495	44
Bishop AP	37°22'	-118°22'	4108	44
Daggett FAA AP	34°52'	-116°47'	1922	44
Los Angeles Intl AP	33°56'	-118°24'	97	45
San Diego Lindbergh	32°44'	-117°10'	13	44
Santa Barbara FAA AP	34°26'	-119°50'	9	28
Blue Canyon	39°17'	-120°42'	5280	41
Oakland Metro AP	37°44'	-122°12'	6	36
Sacramento Exec AP	38°31'	-121°30'	18	45
San Francisco Int AP	37°37'	-122°23'	8	44
Stockton Metro AP	37°54'	-121°15'	22	36
Alameda NAS	37°44'	-122°19'	16	43
Crows Landing	37°24'	-121°08'	164	7
Moffett Field NAS	37°25'	-122°03'	39	43
Santa Maria AP	34°54'	-120°27'	254	38
Mount Shasta	41°19'	-122°19'	3590	38
Red Bluff FSS	40°09'	-122°15'	349	39
Redding Mun AP	40°30'	-122°18'	502	6
Arcata AP	40°59'	-124°06'	203	43
El Toro MCAS	33°40'	-117°44'	381	43
China Lake Armitage	35°41'	-117°41'	2220	43
Miramar NAS	32°52'	-117°08'	459	41
Point Mugu NF	34°07'	-119°07'	10	42
San Diego North Isl.	32°42'	-117°12'	49	43
Tustin MCAF	33°42'	-117°50'	59	40
Imperial Beach REAM	32°34'	-117°07'	20	40
San Nicholas Isl.	33°15'	-119°27'	568	42
San Clemente I. NAAS	33°01'	-118°35'	171	28
Twentynine Palms NAAS	34°13'	-116°03'	1765	5
Fresno Air Term.	36°47'	-119°43'	336	44
Yuma, Arizona	32°40'	-114°36'	213	7
Las Vegas, Nevada	36°05'	-115°10'	2162	45
Reno, Nevada	39°30'	-119°47'	4409	43
Medford, Oregon	42°23'	-122°53'	1300	44

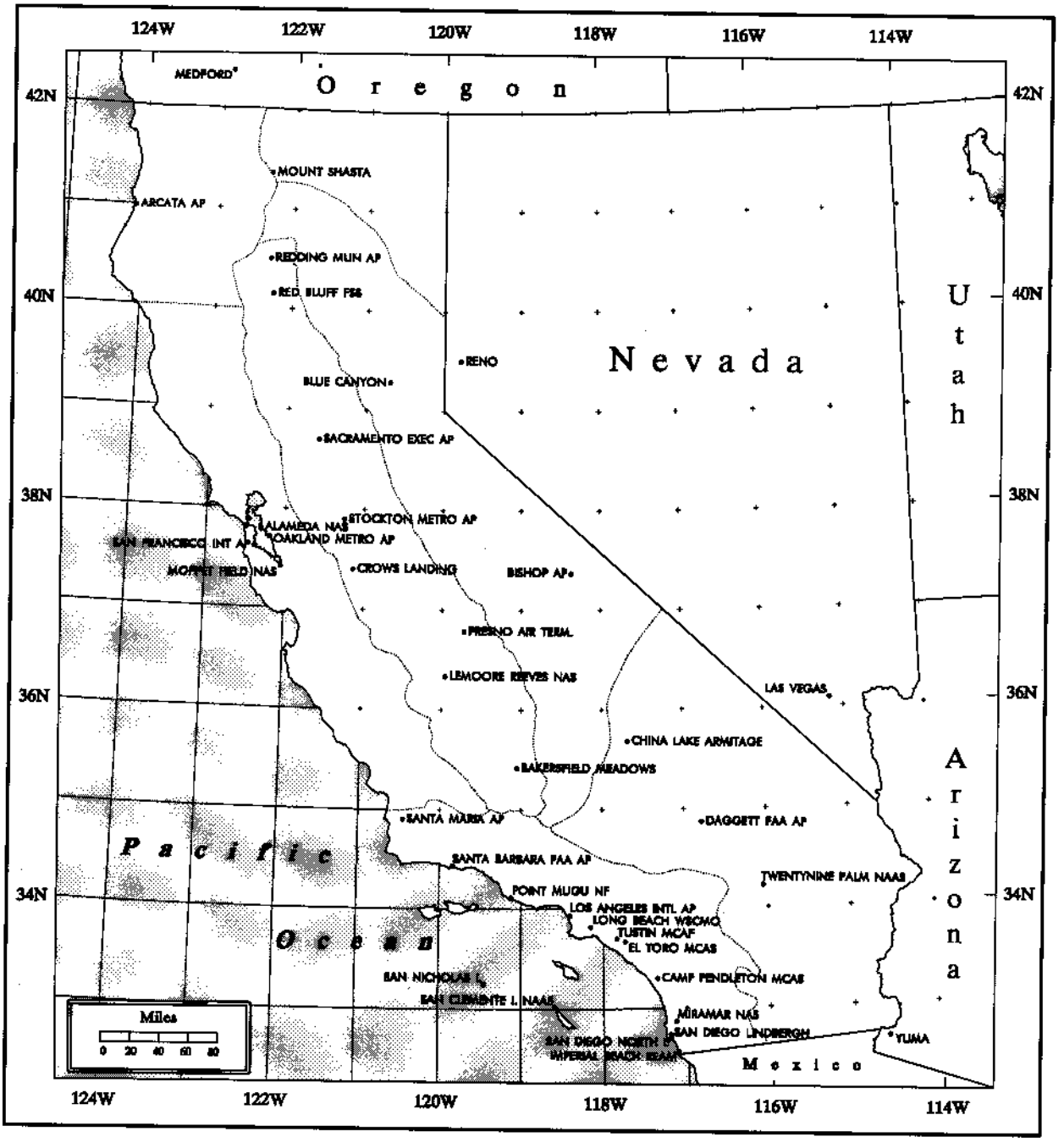

Figure 9.3. *Surface observation stations used in the development of the three hour persisting dewpoint maps (Figures 9.4 to 9.15).*

does not reflect a saturated air mass through the depth of the atmosphere. Such capping of the lower atmosphere is common under calm, anticyclonic conditions. Table 9.2 shows 37 stations in California and adjacent states of Oregon, Nevada and Arizona that were used in the analysis. The period of record was variable, but the majority of stations had at least 30 years of data. The earliest records date from the mid-1940's, while the latest cover through early 1992.

The stations used in the dewpoint analysis ranged in elevation from near sea level to over 5000 feet, requiring that all values be adjusted to a common reference value. As in previous PMP studies, the 1000-mb level was used and all dewpoints were adjusted using a saturated pseudo-adiabatic atmosphere, with data from Technical Paper No. 14 (U.S. Weather Bureau 1951), which provides precipitable water and other moisture-related factors for a saturated pseudo-adiabatic atmosphere. After the data were adjusted to 1000 mb, software was developed that extracted a limited number of the highest dewpoint sequences. The actual number was based on whether or not *good* meteorological sequences could be found, i.e., those not contaminated by rainfall or unusual moisture stratification (admittedly a difficult condition to identify in the absence of nearby atmospheric soundings). Data outliers were checked and discarded if found to be in error or clearly defied the prevailing data pattern. The highest (maximum dewpoints) accepted sequences were then plotted for each station and the general pattern of isodrosotherms (contours of equal dewpoint) drafted. The initial spatial paradigm was based on several previously existing maximum dewpoint climatologies (United States Department of Commerce, 1948, HMR 36) and of course on the data field itself. In addition, the 12-hour dewpoint analysis contained in the present report (see Chapter 4) was compared to the results of the 3-hour analysis, as an additional check on the pattern and magnitude of the final map values. The difference between isodrosotherms at common reference points on the 3- and 12-hour maps varied from as little as 1°F to a maximum of about 5°F, with an average difference of 2 to 3°F.

A comparison of the 3-hour dewpoint maps in the current study with the 3-hour values shown in HMR 57 along the California border do show some minor differences. Interestingly, the isodrosotherms, in this study, are slightly lower than in HMR 57. The reason for this discrepancy is that HMR 57 used no stations in California to extrapolate the

isolines southward across the Oregon border. The use of Arcata and Mount Shasta in the current study, with 43 and 38 years of data, respectively, enabled the spatial pattern to be better defined in the northern California area, resulting in a slight decrease in the maximum-persisting values.

Figures 9.4 to 9.15 show the mid-monthly analysis of 3-hour maximum persisting dewpoints for California. These dewpoints are used to provide upper-limit moisture fields for maximizing local storms. The seasonal progression of these maps reflects the evolution of the large-scale temperature and moisture variations across the country. During the winter months, from December through April, the highest dewpoints occur in southern California along a roughly north-south gradient. The main moisture source during this season for nearly all of California is the Pacific Ocean. The presence of the cool California current along the immediate coast keeps surface dewpoints lower than might be expected at these latitudes. However, under certain flow patterns subtropical Pacific Ocean moisture is drawn into California beneath strong Southwest flow aloft. Meteorologists have at times referred to this as the *pineapple express*, alluding to the source of moisture over the Hawaiian Islands. This pattern is usually responsible for the highest dewpoint episodes. In the winter months, the dewpoint gradient is quite small over the state, especially in January where the difference across the entire state is less than 3°F.

A transitional period in April to May sees a complete reversal of the pattern with the highest dewpoints now coming from the east. One of the reasons for this pattern is the northward movement of the North Pacific subtropical anticyclone to its summer position and the development of the inland thermal low over southwestern United States, combine to create northerly flow along the west coast, causing significant upwelling of cooler ocean water. These waters modify overlying air masses, and reduce their boundary-layer dewpoint temperatures. This pattern becomes more pronounced as the warm season progresses, reaching a maximum in August, when a strong west to east gradient exists and extreme southeastern California reaches a 3-hour maximum persisting value of 79°F. Such very high dewpoints are likely associated with the intrusion of extremely moist air from the Gulf of California. Hales (1972) was among the first to document the northward movement of moisture from the Gulf of California, while Hansen (1975) demonstrated the importance of such moisture to the development of extreme rainfall events in the west. Douglas (1995)

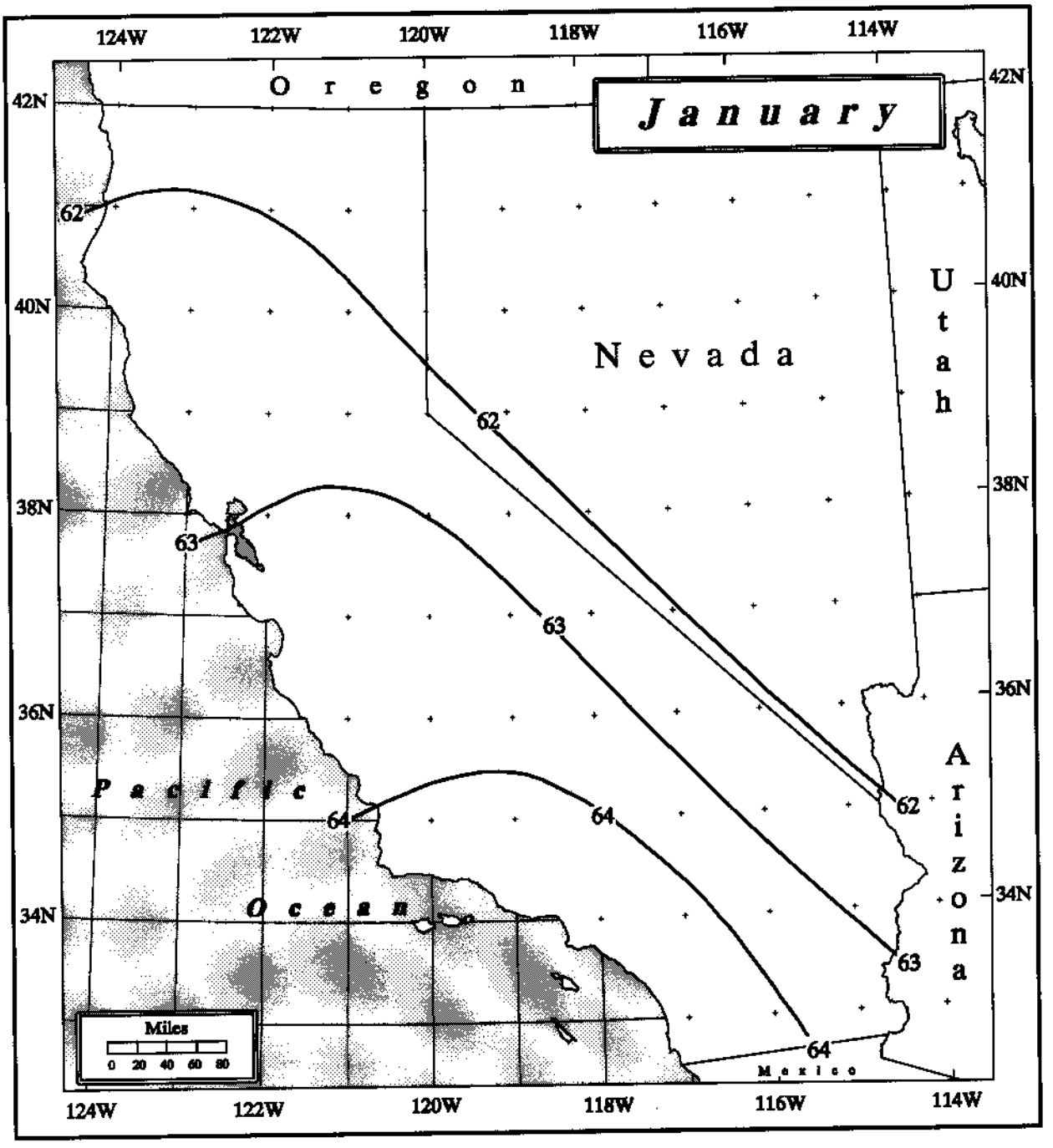

Figure 9.4. *Three-hour maximum persisting 1000-mb local-storm dewpoints for January (°F).*

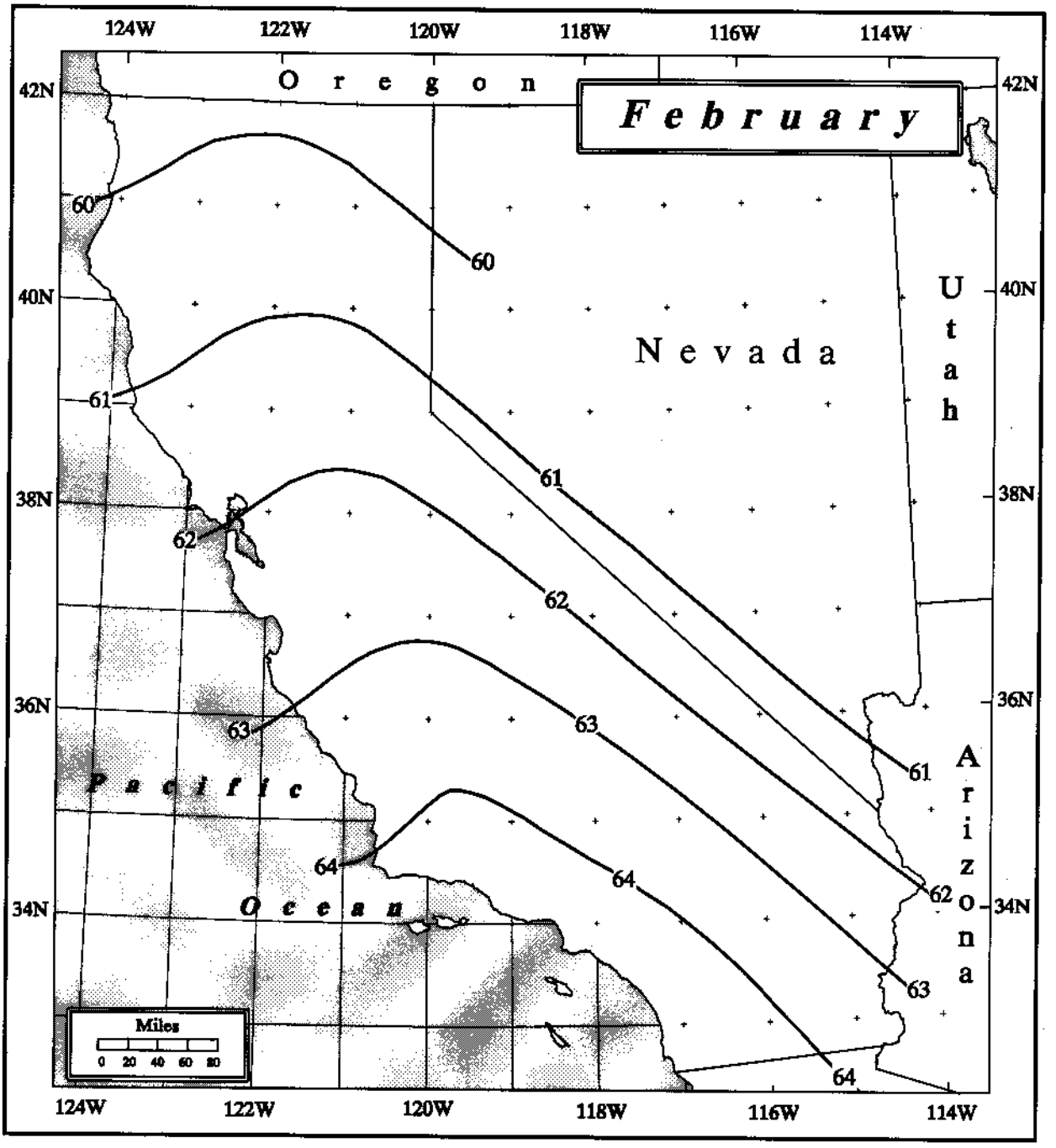

Figure 9.5. *Three-hour maximum persisting 1000-mb local-storm dewpoints for February (°F).*

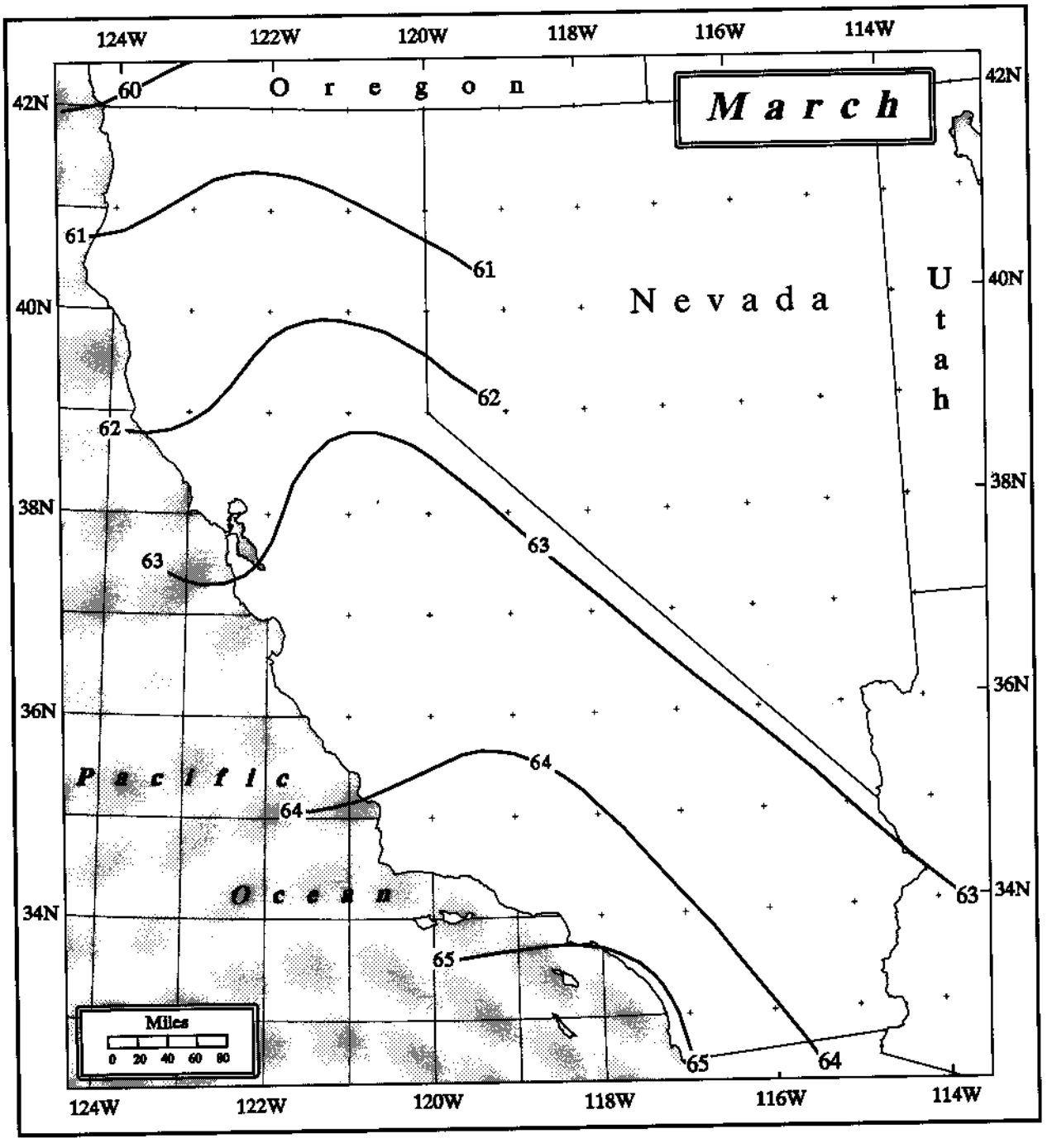

Figure 9.6. *Three-hour maximum persisting 1000-mb local-storm dewpoints for March (°F).*

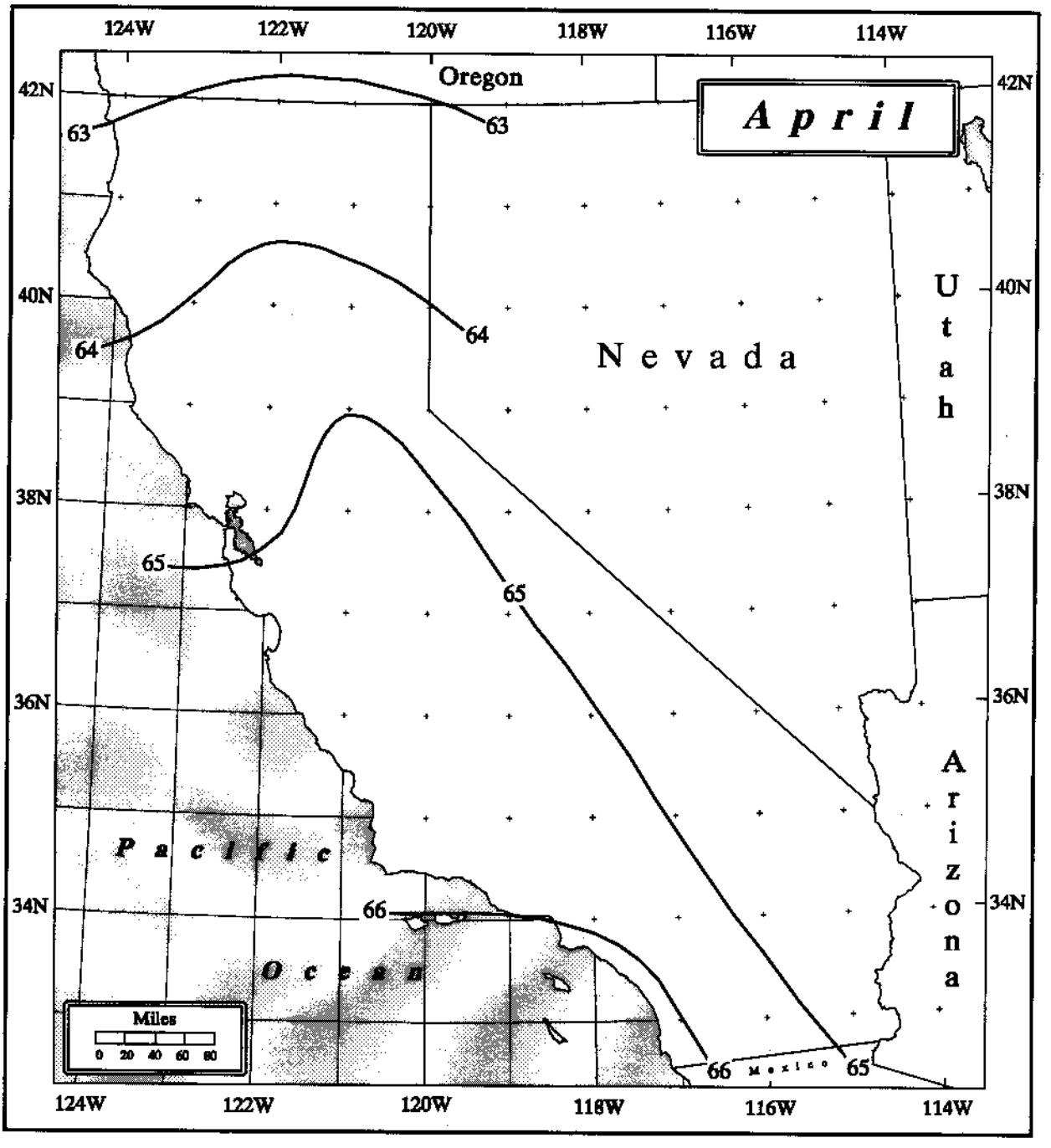

Figure 9.7. *Three-hour maximum persisting 1000-mb local-storm dewpoints for April (°F).*

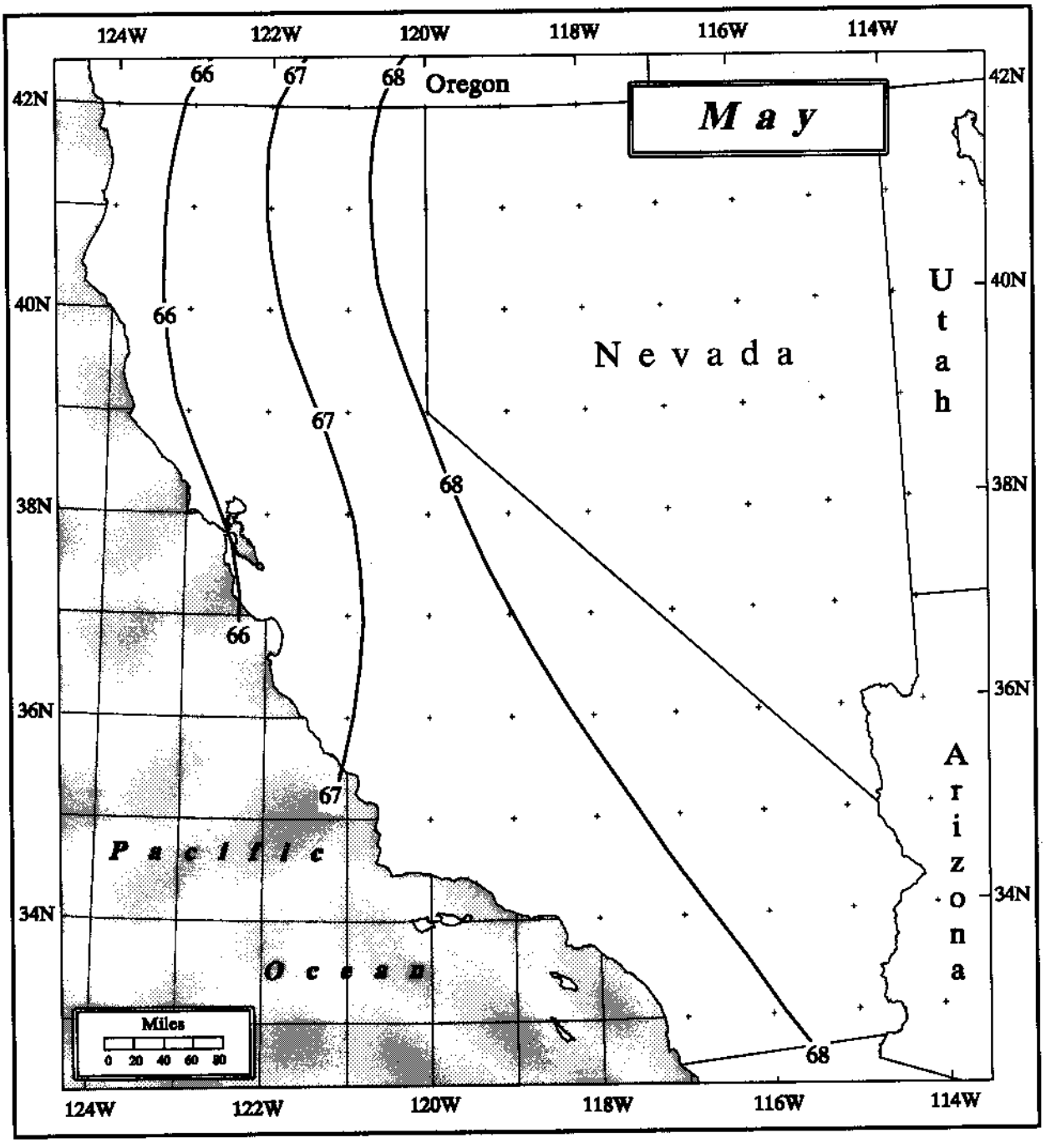

Figure 9.8. *Three-hour maximum persisting 1000-mb local-storm dewpoints for May (°F).*

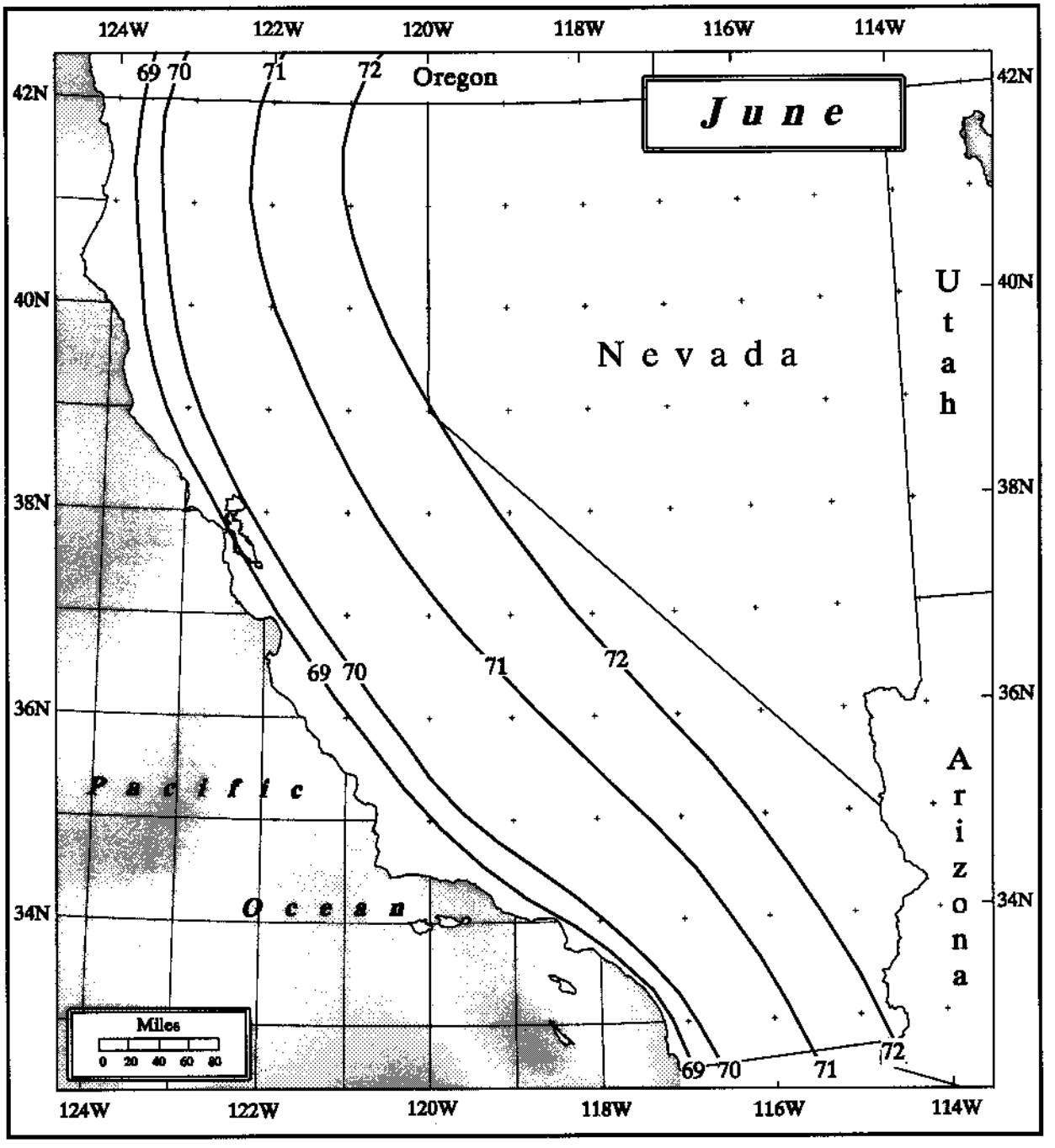

Figure 9.9. *Three-hour maximum persisting 1000-mb local-storm dewpoints for June (°F).*

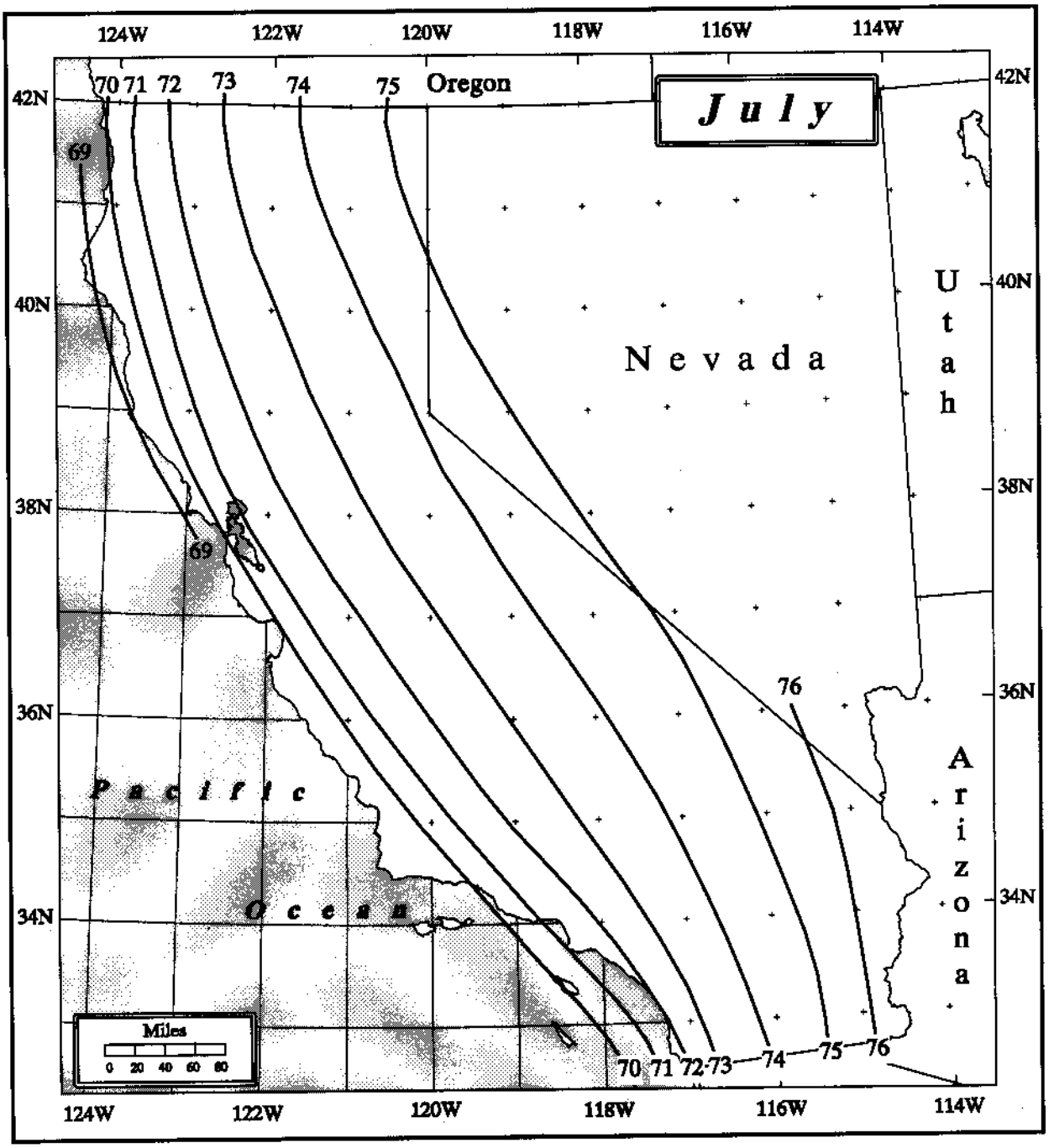

Figure 9.10. *Three-hour maximum persisting 1000-mb local-storm dewpoints for July (°F).*

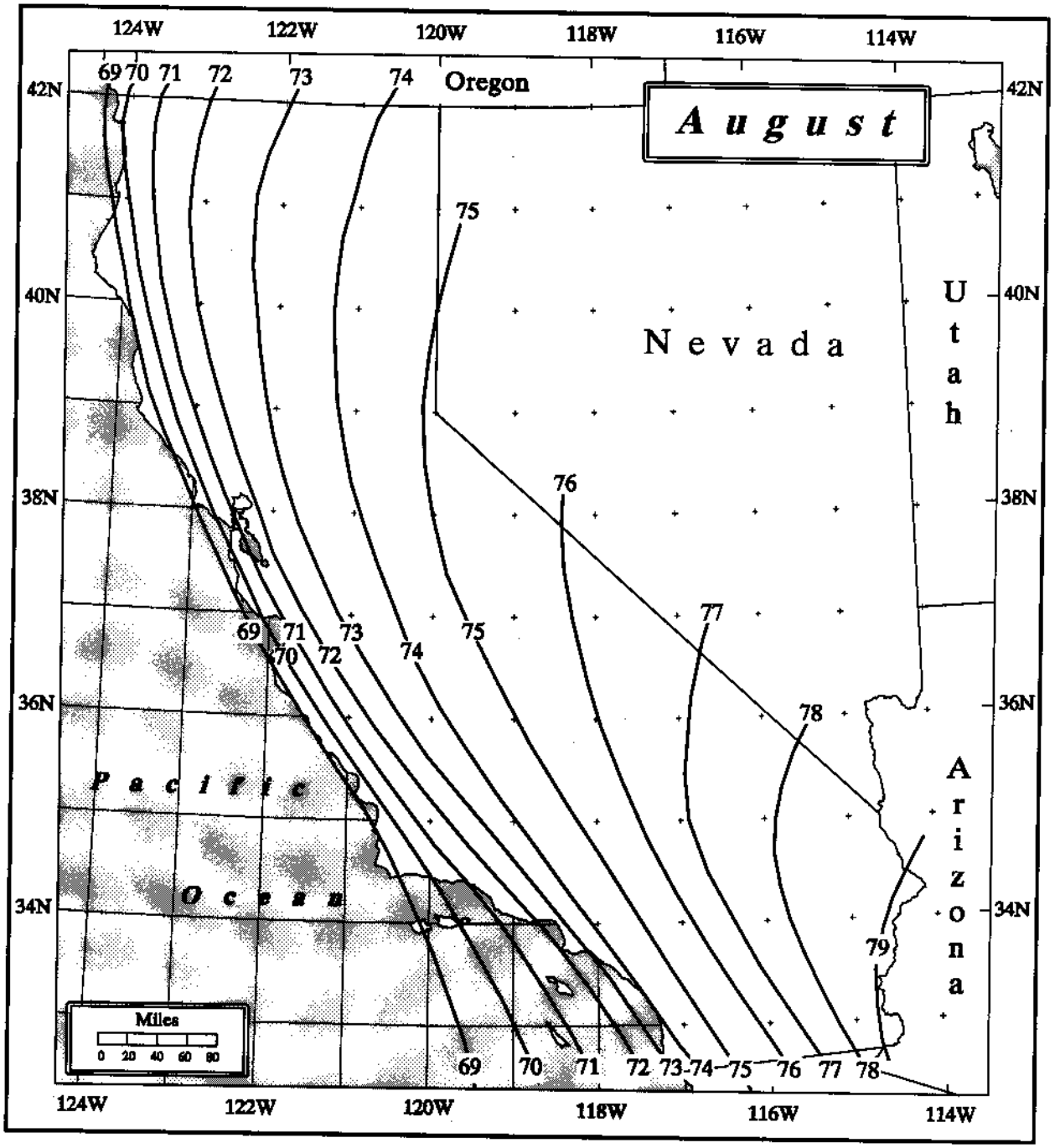

Figure 9.11. *Three-hour maximum persisting 1000-mb local-storm dewpoints for August (°F).*

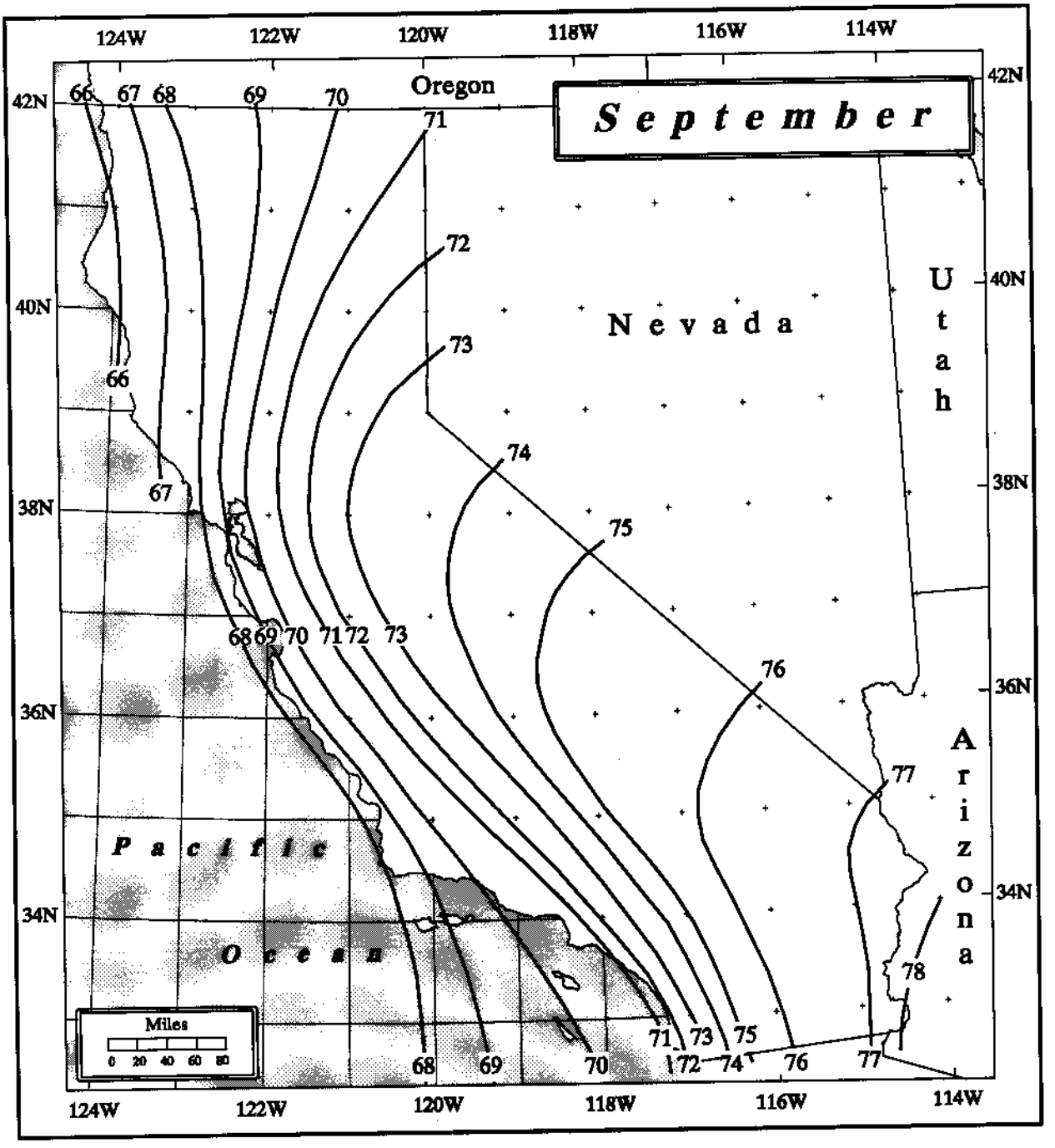

Figure 9.12. *Three-hour maximum persisting 1000-mb local-storm dewpoints for September (°F).*

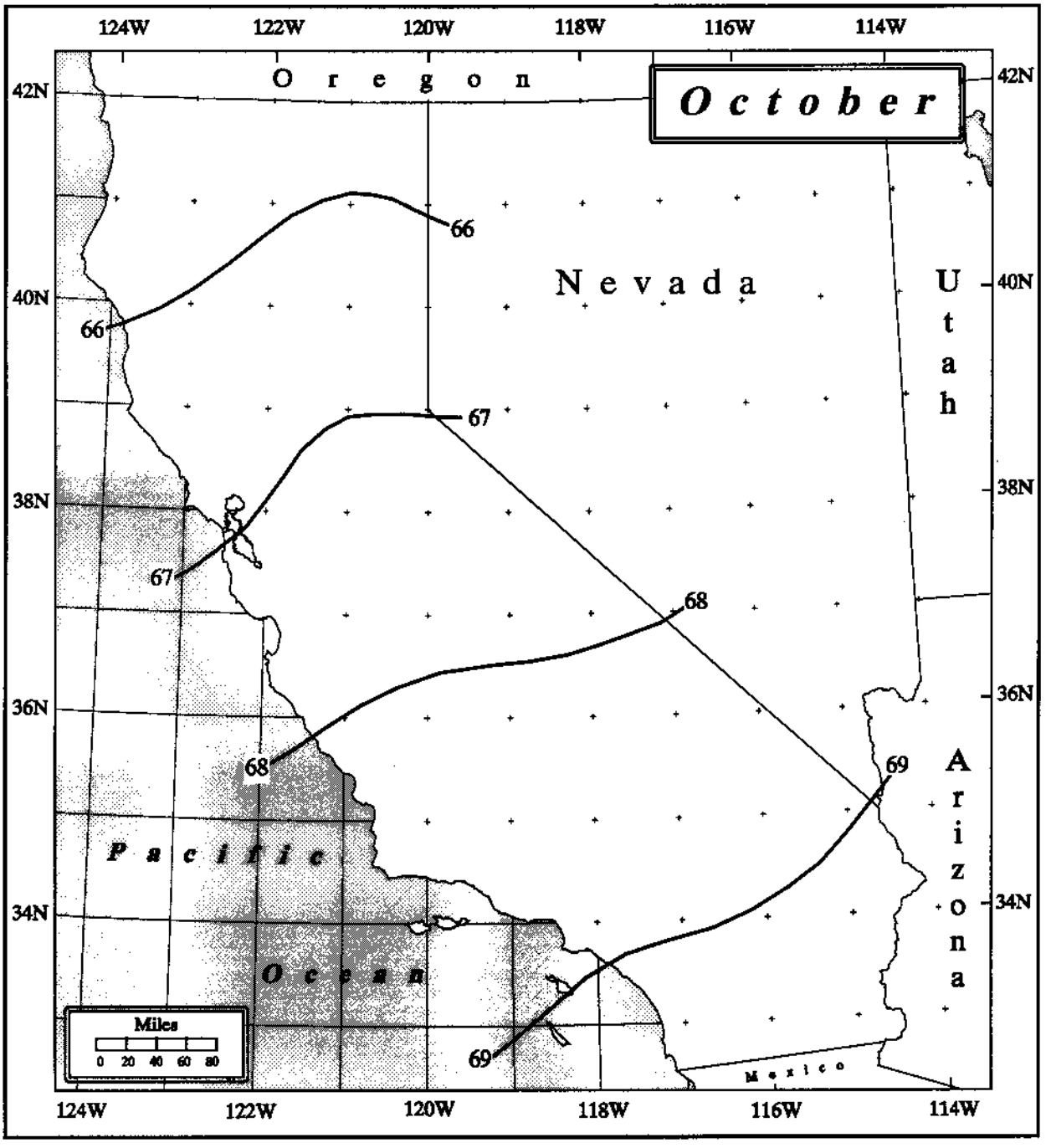

Figure 9.13. *Three-hour maximum persisting 1000-mb local-storm dewpoints for October (°F).*

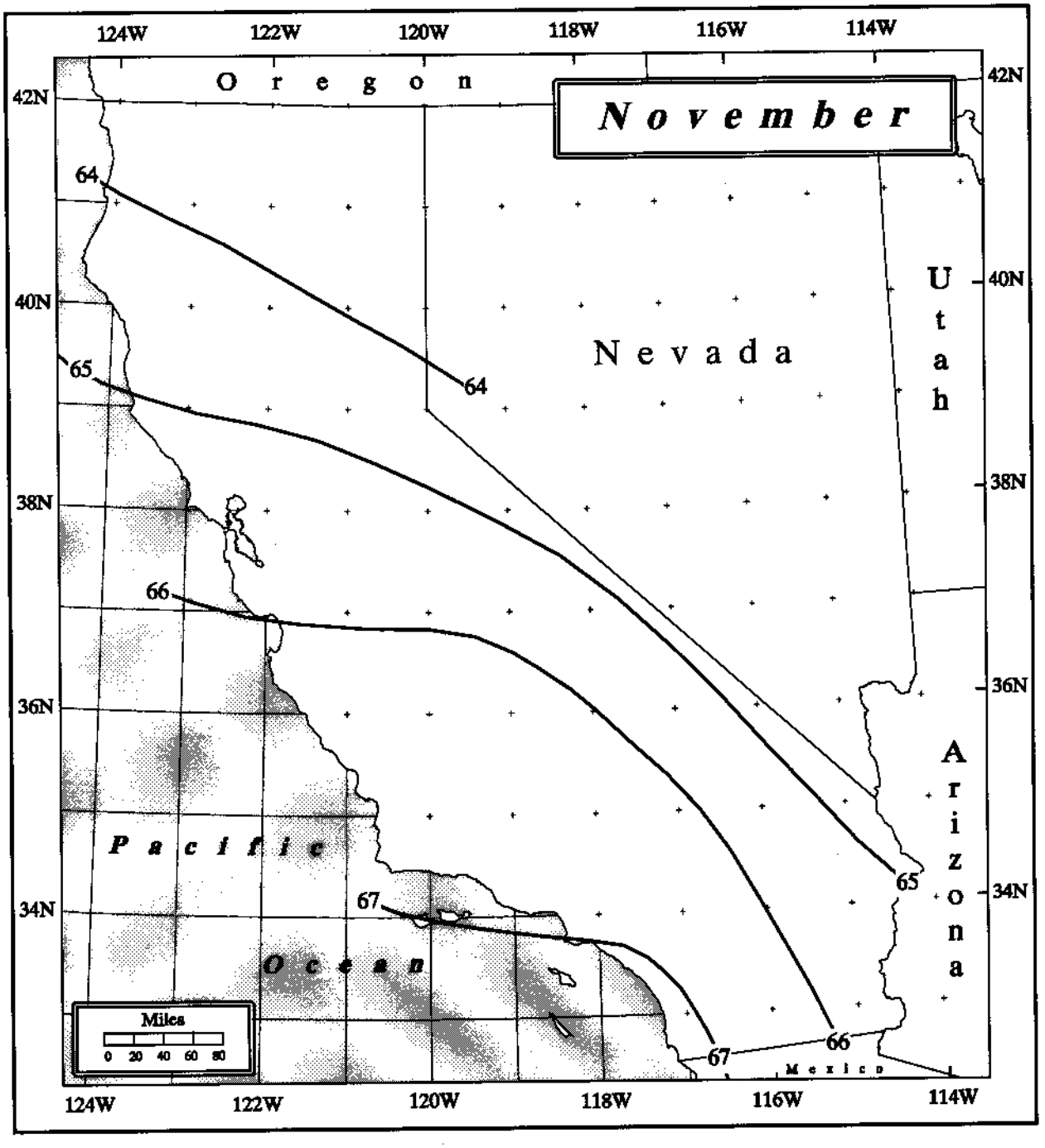

Figure 9.14. *Three-hour maximum persisting 1000-mb local-storm dewpoints for November (°F).*

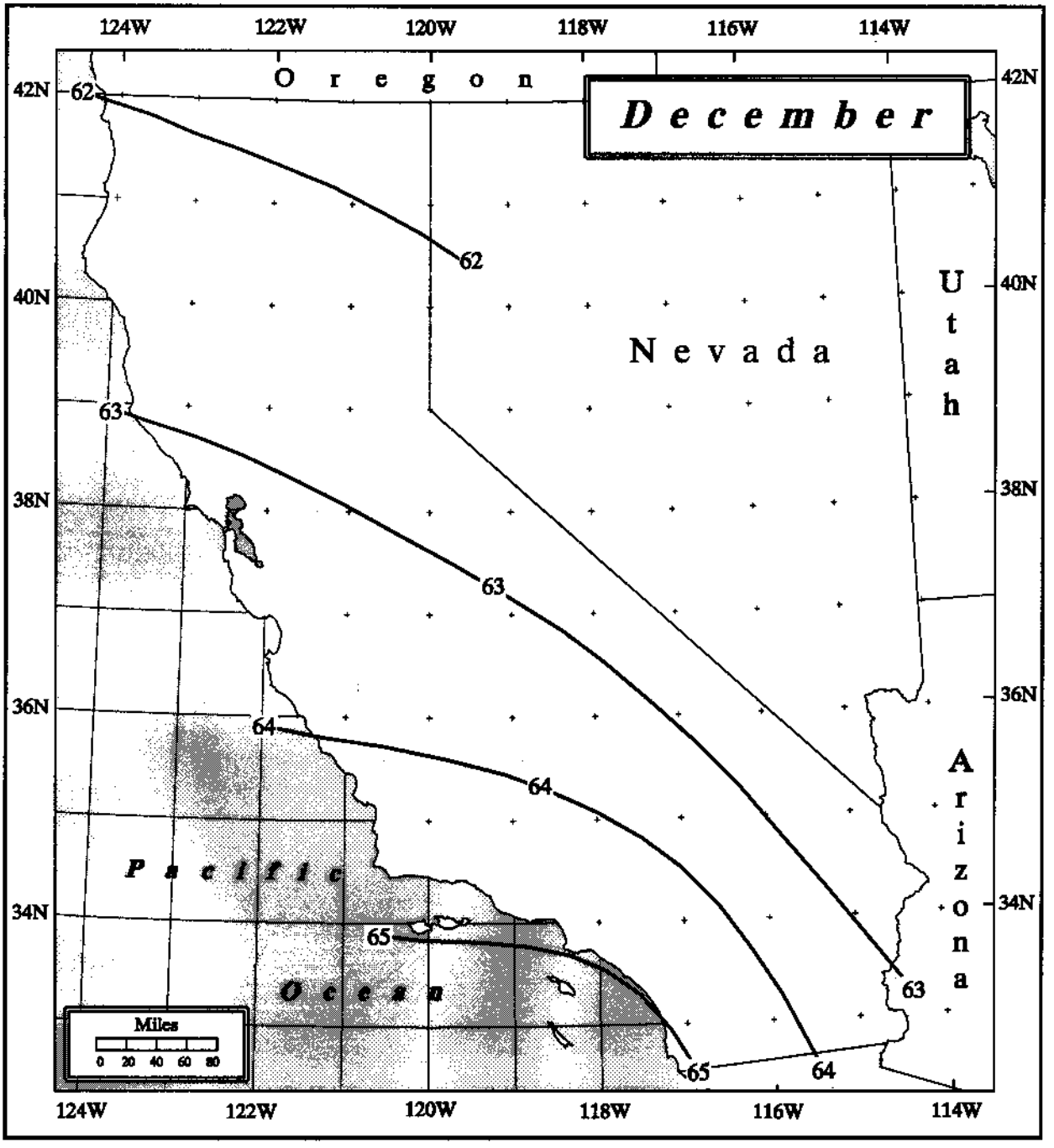

Figure 9.15. *Three-hour maximum persisting 1000-mb local-storm dewpoints for December (°F).*

has confirmed in very recent research the existence of a low-level jet at around 300 meters in the southerly flow over the Gulf of California and adjacent areas. The low-level jet is found to occur under different synoptic flow regimes and is certainly responsible for transporting some of the highest dewpoint air into southeastern California. These low-level intrusions of extremely moist air are probably responsible for the most extreme thunderstorm activity in the deserts of southeastern California. Another very recent study of a severe MCS in central Arizona (McCollum et al. 1995) confirmed that the low-level moisture responsible for the destabilization of the air mass had its roots in the southerly low-level flow from the Gulf of California.

Several studies have detailed the importance of the Southwest monsoon pattern to summertime rainfall over the southwestern United States, mainly during July and August (Carleton 1985, 1986). This pattern, which brings moisture into the Southwest from a westward expansion of the Bermuda High, is also responsible for the advection of significant moisture into California, but most of this moisture is transported in the southeasterly flow at midlevels, from about 700 mb and higher (Watson et al. 1994). It appears, however, that the highest dewpoints are probably associated with the Gulf of California low-level jet. The general pattern with the highest dewpoints over southeastern California with decreasing dewpoints to the northwest, maintains itself during September; but by late October and November, the cool season pattern has reasserted itself, and dewpoints again decrease from west to east.

9.5.2 Adjustment for In-Place Maximization

The in-place adjustment for moisture maximization of local storms is similar to the process for general storms, with some important differences. The adjustment is in the ratio of the precipitable water for the 3-hour maximum persisting dewpoint at the storm location (Figures 9.4 to 9.15) to that for the 3-hour maximum persisting dewpoint for the storm in question. It has been the practice since HMR 55A for the local-storm adjustment procedure not to indicate a specific inflow direction to obtain the storm dewpoint, as is done in general storms. In local storms, the inflow can be specified in any direction from the storm location, because of the assumption that local storms can develop independently of large-scale moisture inflows which sustain extreme general storms. The much smaller scale of local storms in fact makes this practice a necessity, due to the paucity of observations near the

actual location of most extreme storms. Preferably, observations within 50 miles of the storm site are used, although even this proximity is not always possible.

A second important difference between the general- and local-storm moisture adjustment procedure is the limitation of 1.50 placed on the maximization of local storms. This upper limit was not imposed on the storms in HMR 49, but only the Avalon, California storm in October 1941 exceeded the upper limit. The most compelling reason for establishing this limitation is lack of dewpoint data for some of the local storms. Using stations too far removed from the local source of moisture for a storm may lead to representative storm dewpoints too low, thus causing unreasonably high moisture adjustments.

9.6 Horizontal Transposition

As in the general storm procedure, local storms are transposed from their location to other areas where storms of equal magnitude or intensity have not been observed, but where the storm dynamics might be reasonably expected to occur. Once a transposition has been made it is only the available moisture which limits the amount of rainfall which this hypothetical storm could produce. Hence, it is necessary to assess the mechanism or dynamics in major storms in order to determine the validity of transposition. The dynamics involved in the formation of extreme local storms in California are discussed in Section 9.4. The limits to the transposition of a particular storm are somewhat subjective, but essentially reflect the analyst's judgement as to what is meteorologically possible. Generally, storms are not transposed across major ridgelines, a large distance from significant moisture sources, or into different climatic zones. For example, Fleming and Spayd (1986) indicated that MCSs did not develop west of the Mojave desert and the adjacent mountains.

9.7 Adjustment for Elevation

Most convective storms rely on an abundant supply of moisture, primarily at lower levels of the atmosphere, for their formation and maintenance. There is, however, a relatively steep decrease in moisture availability as elevation increases. For instance, in a saturated air column with a surface (1000-mb) dewpoint of 65°F, about half of the water vapor is concentrated in the lowest 6,000 feet of the atmosphere and almost 80 percent in the

lowest 12,000 feet. The depletion of moisture with altitude implies that there would be a reduction in rainfall at higher elevations. A specific height at which this reduction occurs is not obvious from the limited available data, and research has been inconclusive in answering this question. The problem is complicated in that while moisture is less, elevated terrain also acts to increase rainfall by several mechanisms, including increased vertical velocities, orographic lifting, differential heating of mountain slopes and enhanced convergence.

The effect of topography on the development of extreme local storms is not at all clear. In HMR 50, of 35 events that met the definition of local storms in the West (Arizona, California, Colorado, Nevada, and Utah) 18 occurred over ridges and slopes in what was classified as orographic terrain. The other 17 occurred on basically flat terrain. In addition, many of the storms that occur over flat terrain are initiated as convective clouds over nearby mountains and then move out over nearby flat areas. There are numerous examples of storms that developed over both mountainous and flat terrain. Randerson (1976) found that the very heavy rainfall at Las Vegas, Nevada in July 1975 had its origins over flat terrain; whereas the Bakersfield storm of July 1972 was triggered over nearby mountains and moved out over the adjacent flatlands.

Several studies (Banta and Schaaf 1987, Schaaf et al. 1988) have employed GOES satellite imagery to confirm the existence of so-called thunderstorm genesis zones within mountainous areas, where storms are initiated. They show that such mountain-initiated thunderstorms can stay in their genesis zones or dissipate near the edge of the mountains; but their gust fronts or outflows often spill onto the adjacent plains and aid in the initiation of new storms. Other research has confirmed the existence of increased convection over mountainous terrain. Abbs and Pielke (1986) found that areas of upslope flow and increased convergence of moist unstable air became preferred regions for convective development. Toth and Johnson (1985), using Colorado data, found that elevated locations were zones of convergence maxima and correlate well with areas favored for convective storms.

Although there seems to be little doubt that elevated terrain can lead to increased frequency of convective development, this does not say that the intensity of storms is any greater, especially at the extreme upper end of the intensity spectrum. The lack of data at very high elevations makes this a particularly difficult question to answer. One of the early

studies by Cooper (1967) used 93 gages ranging in elevation from 3600 to 7200 feet in a Southwest Idaho dense network. The study found no discernible relationship between elevation and peak intensity or total amount of rainfall for this range of elevations. According to a more recent study (Henz and Kelly 1989) there were 24 cases of high elevation heavy rains (above 7500 feet, with an intensity of 2 inches per hour or greater) in the Colorado Front Range from 1965 to 1988. Many of these occurred at least partially above 8000 feet. Some research (Jarrett 1989, Jarrett and Costa 1986) has employed paleohydrologic techniques to estimate the frequency of high-elevation flood-producing storms in the Colorado Rockies. They found little evidence for very heavy rainfall above 8000 feet, while stating that such storms are not infrequent below 7500 feet. This suggests that there may be a rather abrupt transition zone in rainfall intensity over a small range in elevation.

Terrain can also act as a channeling or barrier mechanism for low-level moisture, thus affecting the location of some storms. Hansen (1975) in a study of several extreme local storms in the intermountain West demonstrated the manner in which low-level moisture tends to follow paths of least resistance through valleys and around large mountains. Blocking terrain abounds in California, as a look at any topographic map of the state will show. Pacific Ocean moisture is prevented from easy penetration to the interior by coastal ranges extending nearly the entire length of the coast, through breaks in this mountain chain occur most notably around the San Francisco Bay region. Penetration of Pacific Ocean air into the interior Central Valley is possible through this area. There is, however, no explicit adjustment for local storms for effects of barrier elevations on moisture. The rationale is that short-duration storms do not necessarily require a prolonged period of uninterrupted inflow. This follows World Meteorological Organization procedures (WMO 1973) and previous PMP studies.

The relationship between elevation and rainfall was examined for the 31 extreme storms in Table 9.1. The storms occurred over a wide range of elevations (from below sea level to above 10,000 feet), but no significant correlation could be established between rainfall amounts and elevation.

In a further attempt to define the rainfall-elevation relationship in California local storms, the list of storms in Appendix 3, Table A3.1, was used. The 137 storms in this list

were plotted against elevation and the results are shown in Table 9.3. No clear trend emerges from an inspection of this table and regression analysis confirms that there is no significant rainfall-elevation relationship in this dataset. Nine of the ten storms equaling or exceeding 2 inches in one hour occurred below 5000 feet but a large majority of the 137 storms also occurred below this elevation. There is, however, a distinct bias for the cooperative climate observing stations to be at lower elevations where people tend to live. In 1992, the last year for which data were analyzed for this study, California had 238 observing stations in the Hourly Precipitation Data Station Index. Table 9.3 shows the percentage occurrence of these observing stations by 1000-foot elevation zones. For example, nearly 42 percent of the stations were located in Zone 1 or below 1000 feet. By contrast only about 9 percent were located at elevations greater than 5000 feet. This table also compares the frequency of extreme storms within each elevation zone. The comparison must be considered a *rough* one, because the storms in the extreme storm list are drawn from the period from 1948-1992, while the NCDC station list is just from 1992. The actual composition of the NCDC list changes slightly from year to year as stations drop off or are added, although it is unlikely that the elevation profile of the list has altered much. In a randomly selected year, 1955, the composition of station elevations differed from 1992 by no more than 2.5 percent (although the total number of stations dropped from 277 to 238). The most interesting feature of Table 9.3 is the preponderance of extreme storms in elevation zone 5, 4,000 to 4,999 feet. Stations in this zone are three times more likely to experience heavy rainfalls. The other high-elevation zones, 6, 7, and 8, also had more heavy storms than number of observing stations would suggest. By contrast, stations in the lowest elevation zone (below 1,000 feet) saw far fewer extreme storms (less than half) than their frequency in the population of stations. The conclusion to be drawn from this limited survey suggests very strongly that elevated terrain does indeed play a strong role in increasing the overall frequency of heavy local storms in California. It is, however, difficult to conclude that the few storms at the extreme tail of a distribution (i.e., the PMP storm) will in fact produce more rainfall at higher elevations than storms at lower elevations. It should be reiterated that PMP, as it is currently formulated, is not a statistical construct. Rather it is derived solely from observational and theoretical considerations that do not expressly recognize anything about the probability of an event.

Table 9.3. *Percent of observing stations (1992) and extreme storms (1948-1992) by elevation zone (ft).*

	Zone 1 (<1000)	Zone 2 (1000+)	Zone 3 (2000+)	Zone 4 (3000+)	Zone 5 (4000+)	Zone 6 (5000+)	Zone 7 (6000+)	Zone 8 (7000+)
NCDC Stations (N=238)	41.6	18.1	13.4	8.4	9.2	5.5	2.9	<1
Storms (N=137)	17.5	13.1	14.6	9.5	27.0	10.2	4.3	3.6

Previous PMP studies, including HMR 43, HMR 49, HMR 55A, and HMR 57, also investigated the elevation-rainfall relationship in local storms. Several different solutions were adopted, but all centered around the idea of decreasing the PMP above a specified elevation at a rate consistent with the decrease in moisture availability. The first two studies make no moisture adjustments from sea level up to 5,000 feet, above which a decrease in the level of PMP would be expected. The rate of decrease was set at 5 percent per 1000 feet of elevation increase above that threshold. HMR 55A, which provides PMP estimates from the Continental Divide to the 103rd meridian, uses a slightly different procedure. Because of the high terrain throughout most of this study area, the PMP Index map in HMR 55A was established at 5,000 feet, rather than sea level, with moisture adjustments made at locations at least 1,000 feet below (adjust up) or above (adjust down) that level. The magnitude of the adjustment is determined from a nomogram which gives a variation of 5 to 10 percent per 1000-foot elevation change and is also dependent on the maximum-persisting dewpoint temperature for the drainage in question.

In HMR 57, the PMP Index map for the Pacific Northwest was prepared for sea level and an elevation adjustment not imposed until 6,000 feet. Above that elevation a decrease at approximately the pseudo-adiabatic rate for a saturated atmosphere was assumed. However, rather than use the actual pseudo-adiabatic rate, which varies non-linearly with elevation, the rate of reduction was set at 9 percent per 1000-foot increment in order to ease calculations for the user. Similar to the analysis for California, extreme storms in the Northwest showed no significant relation between elevation and storm intensities. Again, the almost total lack of high-elevation data was a hindrance in terms of developing an accurate assessment of the variation of extreme rainfall with altitude.

For the current California study, the elevation adjustment procedure is exactly the same as that used in HMR 57. No adjustments to PMP are made in the first 6,000 feet and a 9 percent reduction is made for each 1000 feet (or percentage thereof) above that level.

9.8 Depth-Duration Relationships

In keeping with the practice and procedures developed in previous HMRs, local-storm duration is limited to a maximum of six hours, with relationships developed in the form of a ratio to the Index 1-hour 1-mi^2 storm. This ratio is expressed in the form of a 6-hour to 1-hour ratio (6-:1-hour), with interim ratios also available. The assumptions, methodology and data sources used in the current study differ considerably from those used in HMR 49, which provided local-storm PMP for California. These differences have resulted in substantial changes in the depth-duration relations for California.

The biggest change was in the data selection process. In HMR 49 the base 6-:1-hour ratio depth-duration relationship was established as 1.44 using data from a variety of sources, including storms in the central and eastern United States The current study uses data only from California storms: 1- to 6-hour storms in California with a return frequency of 50 years or more were accepted for the depth-duration analysis. A total of 231 storms were found to meet this criterion and were used for the depth-duration analysis. In addition, HMR 49 employed a larger number of storms by accepting a much lower precipitation threshold in order to study the spatial variation of depth-duration ratios across the state. The criteria in HMR 49 vary from 0.2 inches per hour along the coast to 0.5 inches in the interior. These numbers are substantially lower than the threshold used to develop depth-duration relationships in the current study. The higher threshold was selected in an effort to provide a more realistic assessment of extreme storms, rather than using a larger number of storms which would include more *run of the mill* events.

The outcome of these changes in the criteria for storm selection was a dramatic reduction in 6-:1-hour ratios from those appearing in HMR 49. Figure 9.16 shows the 6-:1-hour ratios for California which have been adopted for this study. To see the differences compare this map with HMR 49, Figure 4.7. Reductions are found throughout the state, with the greatest declines along the coast and in the northwest areas. In cases where a basin straddles a boundary line, the analyst may use their judgement or take the

areal number in which the bulk of the basin exists. It is very important to state that the 6-hour to 1-hour ratio is based on the most intense one-hour period of precipitation, not necessarily for the first hour of rainfall. Although the vast majority of storms in California are *front-loaded*, meaning the bulk of the rain occurs in the first two hours of the storm, there are storms where the heaviest rain occurs later in the six hours.

In the PMP storm the bulk of the rainfall falls in the first hour of the storm (see Figure 9.17), so it is important to know the distribution of rainfall during that hour. A first-guess relationship for durations less than one hour was established using Hourly Precipitation Data: forty-eight storms from 1948-1992 that met the intensity criteria stated above (50-year return period) and that had data for less than one hour were analyzed. For these 48 storms, the mean 15-minute to one-hour ratio was 0.49; for 30 min/1 hour 0.76; and 45 min/1 hour 0.90. These results show that below one hour there is also a strong tendency for storms to be front-loaded.

Unfortunately, the most intense storms such as those used to set PMP, rarely have detailed depth-duration information available. Of the storms in Table 9.1, only the Palomar Mountain and Forni Ridge storms have detailed information. At Forni Ridge, the first five minutes produced 34 percent of the 1-hour total and the first 15 minutes 63 percent. It is believed that applying the Forni Ridge depth-duration curve to the index PMP map across the entire state would lead to unrealistic rates of precipitation in some areas. For instance, in southern California over the region east of San Diego, where the 1-hr 1-mi^2 index PMP is 12 inches, the 5-minute rainfall would reach 4.08 inches and the 15-minute amount would total 7.56 inches. At the Palomar Mountain storm, which is located within this part of southern California, the maximum 15-minute amount was 1.40 inches, representing only 29 percent of the 1-hour amount and the 30-minute total was 2.70 inches, or 57 percent of the 1-hour. Note that these rates of precipitation are significantly less than those at Forni Ridge. Based on the fact that no comparable rainfall amounts have yet been observed in extreme storms in any of the western United States, it was felt that the Forni Ridge curves below one hour were too extreme for adoption statewide.

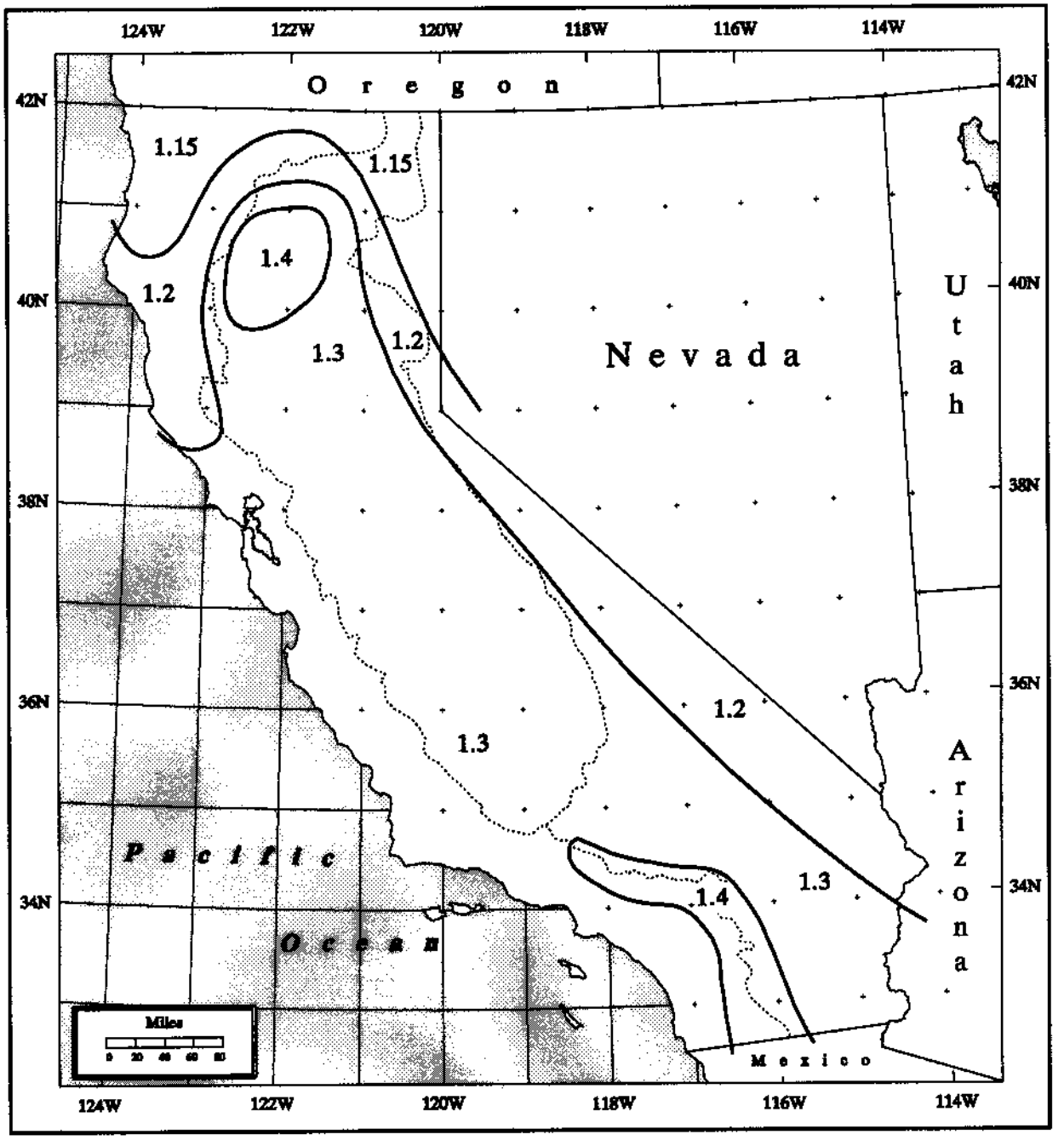

Figure 9.16. *California local-storm PMP 6-hour to 1-hour ratios for 1 mi². For use with Figure 9.17; A = 1.15, B = 1.2, C = 1.3, D = 1.4. Dashed lines are drainage divides. Same as Figure 13.24.*

At durations below one hour a single relationship was adopted for the entire state, hence the single curve shown in Figure 9.17. The curve shows that 55% of the one-hour rainfall occurs in the first 15 minutes, 79% in the first 30 minutes and 91% in the first 45 minutes. This is a somewhat less steep curve (less intense in the early portions of the storm) than the most extreme ratios found in HMR 49. That report provided a family of curves below one hour which varied the intensity of the rainfall over that first hour. Areas with low 6-:1-hour ratios had a steeper curve in the early part of the storm than areas with higher 6-:1-hour ratios. As discussed above, the 48 storms analyzed for California for this report did not show ratios as intense as most of the curves in HMR 49. For durations beyond 1 hour, the single curve (Figure 9.17) branches four ways corresponding to the four classes of 6-:1-hour ratios found for California local storms. The four types of depth-duration relationships (beyond 1 hour) are shown in Figure 9.17 by letter designators as in the following chart:

	Designator			
	A	B	C	D
6-:1-hour Ratio	1.15	1.20	1.30	1.40

Table 9.4 contains the percentages at the key durations upon which the four curves of Figure 9.17 are based.

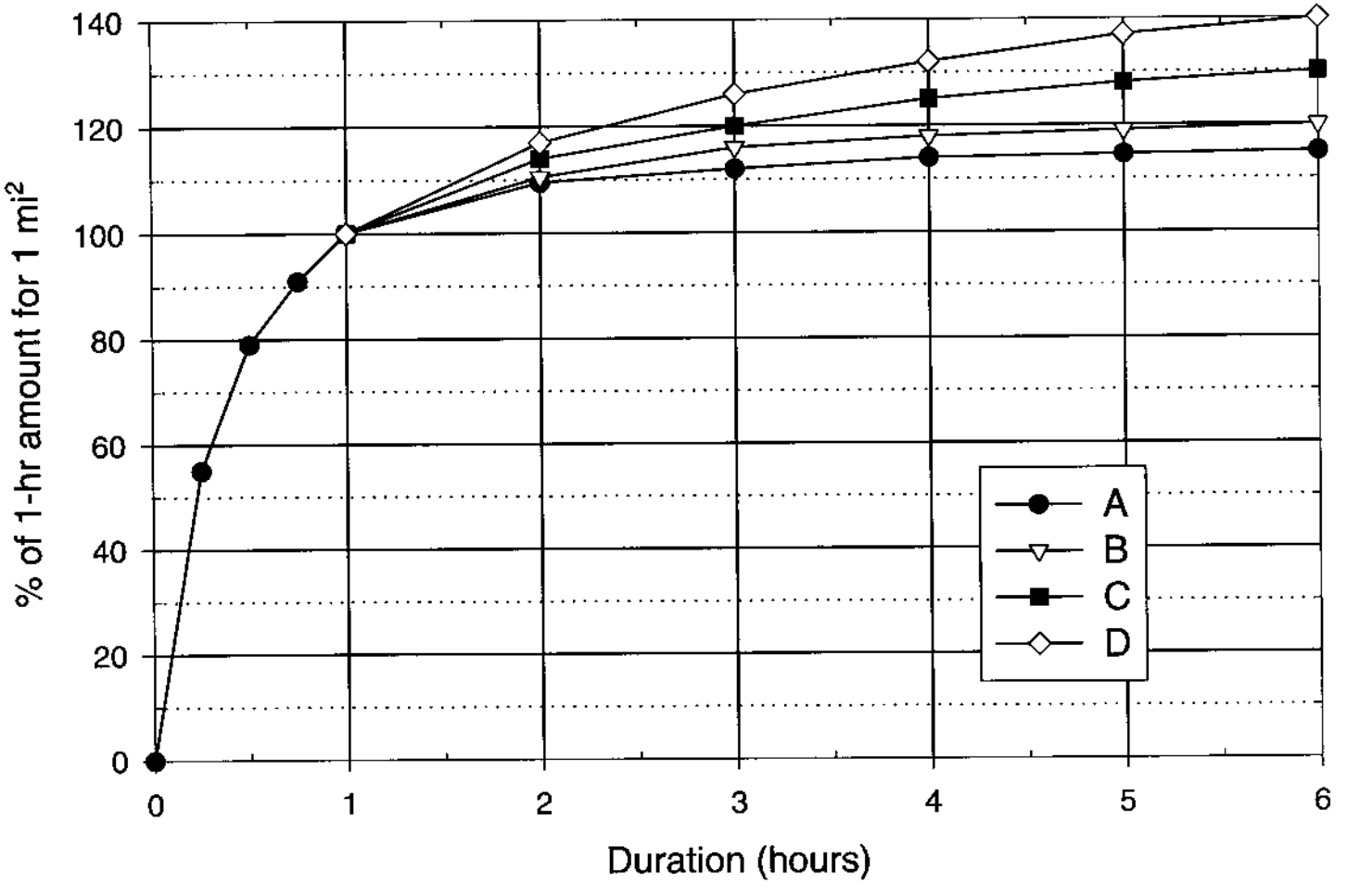

Figure 9.17. *Depth-duration relations for California for 6-hour to 1-hour ratios. These ratios are mapped in Figure 9.16; A = 1.15, B = 1.16, C = 1.3, D = 1.4. Same as Figure 13.23.*

Table 9.4. *Depth-duration relations (percent of 1-hour amount) for 1-mi² PMP for California local storms.*

Duration (hours)	Relationship Designator (see Figure 9.17) A	B	C	D
0	0	0	0	0
1/4	55	55	55	55
1/2	79	79	79	79
3/4	91	91	91	91
1	100	100	100	100
2	109.5	110.5	114	117
3	112	116	120	126
4	114	118	125	132
5	114.5	119	128	137
6	115	120	130	140

The recommended chronology for incremental local-storm amounts will be mentioned in Chapter 13, Sections 13.4.2 and 13.5.2 to follow.

9.9 Depth-Area Relationships

9.9.1 Spatial Aspects

One of the most critical aspects of the PMP problem is how the storm varies spatially. Since the index map for local-storm is drawn for a 1 square mile area, it is necessary to develop relationships for areas out to the limits of the storm. Perhaps no segment of PMP research is subject to more uncertainty, owing once again to the almost total lack of reliable data. The small-scale of most intense thunderstorms and the broadly spaced conventional rainfall observing network ensures that these storms will be poorly sampled, if not missed altogether. A relatively few studies using dense rain gage networks have provided insight into the spatial distribution of heavy rainfall in intense convective storms and much of what

has been learned comes from these few studies. A review of much of this research can be found in the section on local-storm depth-area relations in HMR 57 and is not repeated here.

In an attempt to look at spatial patterns, the isohyetal patterns from all 137 local storms listed in Table A3.1 (Appendix 3) were plotted. To ensure complete coverage of the storms, the rainfall center and all stations within a 1-degree radius of latitude and longitude were mapped. This provided an area (over 11,000 mi^2) of coverage for each storm, well in excess of the rainfall production from any local storm. This proved to be a relatively unproductive exercise, in that the wide spacing of the observing network did not allow for a detailed evaluation of depth-area relationships. In a few cases, with storm centers located in highly populated areas, some spatial patterns could be identified. The mapping of the isohyetal patterns of these storms did provide some rudimentary information on the areal extent of rainfall in these storms, especially at the edges of the rain shield. In many cases the closest gage to the storm center is 20 or more miles away, meaning there is only one observation within the 500 square miles around the center, if in fact the true center has even been measured. If nothing else, the isohyetal patterns in these 137 storms provide support to the concept of the local storm covering an area of up to at least 500 mi^2. While the majority cover a lesser area size there are a substantial number with precipitation covering an area of this size or greater. With the poor resolution allowed by the gage spacing it is difficult to determine the *real* isohyetal pattern, but certainly it can inferred to some degree. Storms in Appendix 3 (Table A1.3) that cover an area of at least 500 mi^2 include those of August 22, 1951, August 23, 1955, August 4, 1961, August 7, 1963, August 25, 1982, and June 7, 1989. The density of gages in these storms was such that it seems fairly certain that the storms covered an area of at least 500 mi^2. In many other cases it was difficult to determine whether observed amounts represent multiple storm centers or if there was a systematic decrease in rainfall away from the nominal storm center. Again, the resolution of the network simply precludes a more detailed and informative analysis.

9.9.2 Additional Depth-Area Analysis

The adopted depth-area relationship for this study draws heavily on the few extreme storms that have been thoroughly documented in terms of rainfall distribution. In California the storms include Tehachapi (9/30/32), Vallecito (7/18/55), and Bakersfield (6/7/72). These storms were also available when HMR 49 was prepared and were used in conjunction

with other Southwestern United States extreme local storms, to establish a series of depth-area curves (Figure 4.8, page 121 of HMR 49) which were applied to the entire Great Basin and California. The final depth-area curves for HMR 49 for durations from 15 minutes to 6 hours are shown in Figure 4.9 (page 123) of that report. Since HMR 49 was published in 1977, several important storms have occurred in California and other parts of the Southwest which provide some important support to the depth-area relationships contained in that report. In addition, the Hydrometeorology Branch undertook a reanalysis of the depth-area curves for the storms that were used in HMR 49 in an attempt to validate the results of that study.

The new storms analyzed for depth-area relations include the previously discussed Palomar Mountain storm (storm #30 in Table and Figure 9.1), the Borrego storm (#26), and a storm near Ute, Nevada that occurred on August 10, 1981, and does not appear on the California storm list.

The Palomar storm discussed in Section 9.4.3 was also analyzed for depth-area using the published isohyetal pattern in a storm report prepared by the Flood Control Division, County of San Diego (1992). The storm pattern was digitized and a depth-area analysis was determined. The values from the depth-area analysis of the Palomar storm at 4 hours are only slightly larger than those from the HMR 49 depth-area curve for area sizes up to about 50 mi^2 and only slightly below at greater area sizes.

The Ute, Nevada storm, a well-documented MCC in August, 1981 (Randerson 1986) provided strong supporting data for the validity of depth-area relationships found in HMR 49. This storm occurred close enough to California (about 75 miles) for it to be considered transposable to the state. A comparison between the three-hour depth-area pattern from this storm and the three-hour curve in HMR 49 shows that the two patterns are remarkably close for all area sizes out to 500 mi^2.

The isohyetal patterns for the storms contained in HMR 49 were re-analyzed for depth-area relationships in order to document their accuracy and homogeneity using digital techniques not available in that study. The storms which were re-analyzed included all seven of those shown in HMR 49, Figure 4.8, three of which were California storms also shown here in Table 9.1. The results were reassuring in that there was little substantial

variation between the two sets of analyses for most of the storms, and where there were large differences, the underestimates were in HMR 49. Differences ranging from about 2 percent to 14 percent were found in the Bakersfield storm, with the largest difference at an area size of a little over 10 mi^2. Larger departures from the analysis in HMR 49 were found for the Phoenix, Arizona storm of June 22, 1972. Differences of greater than 20 percent were found to occur at some area sizes, the largest at about 100 mi^2. It is unclear as to why such discrepancies were found, but the new analysis was performed using the isohyetal pattern contained in the Corps of Engineers study of October 1972 (USCOE 1972), which is the most definitive study on this storm.

9.9.3 Areal Distribution Procedure

The first step in this procedure is to set the rainfall pattern for the local storm. That is, both the shape of the pattern and its distribution (number and gradient of isohyets) need to be fixed. For this study, there are four distinctive local-storm distributions corresponding to the four distinct groups of 6-hour to 1-hour depth-duration ratios found for California local storms discussed in Section 9.8. The isohyetal pattern shown in Figure 9.18 is considered to be representative of the pattern for each of the four groups of local storms. The assigned isohyetal values are specified by the percentages shown in Tables 9.5 to 9.8. These gradient specifying values illustrate the transition from the characteristic northwest states local-storm model in HMR 57 to the local-storm model valid for the Colorado River and Great Basin drainages in HMR 49.

Given the 2 to 1 ratio of major to minor axis of the elliptical isohyetal local-storm pattern in Figure 9.18 and the four sets of rainfall gradient specifying values, it is a straightforward matter to calculate the average depth-area relationship necessary to produce the isohyetal labels shown in Tables 9.5 to 9.8. The results from these calculations are shown in Tables 9.9 to 9.12 and are also shown in graphical form in Figures 9.19 to 9.22. Tables 9.9 to 9.12 are not reproduced in Chapter 13 since Figures 13.25 to 13.28 contain all the information necessary to make depth-area adjustments. The use of these tables and figures is outlined in Chapter 13, the local-storm procedure.

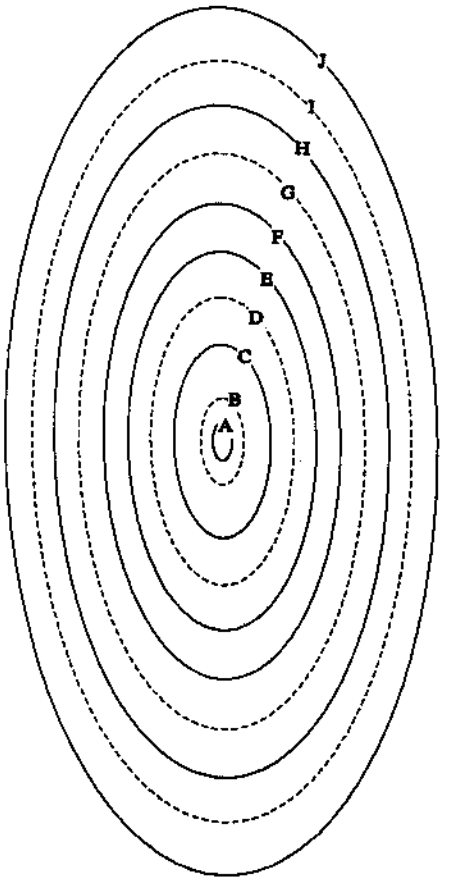

ISOHYET	ENCLOSED AREA AREA (MI^2)	(KM^2)
A	1	2.6
B	5	13
C	25	65
D	55	142
E	95	246
F	150	388
G	220	570
H	300	777
I	385	997
J	500	1295

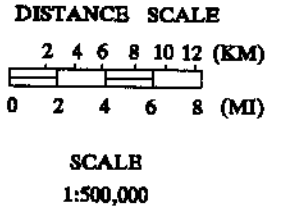

Figure 9.18. *Idealized isohyetal pattern for local-storm PMP areas up to 500 mi². Same as Figure 13.20.*

Table 9.5. *Isohyetal label values (percent of 1-hour, 1-mi² average depth) to be used with the isohyetal pattern of Figure 9.18 and basin average depths from Figure 9.19.*

	Duration (hours)								
Isohyet	1/4	1/2	3/4	1	2	3	4	5	6
A	55	79	91	100	109.5	112	114	114.5	115
B	35	57	68	74.8	83.5	85.5	87.5	88	88.5
C	24	40	49	56	62.9	4.5	66	66.5	67
D	18.5	30.5	39	43	48	49.5	50.6	51.1	51.5
E	13	22.5	29	32.2	36.6	37.7	38.6	39	39.5
F	7.5	14.0	19	22.4	25	25.7	26.3	26.7	27.0
G	4.5	8.5	12	14.0	16.2	16.8	17.4	17.9	18.2
H	1.8	3.5	5	6.5	8.3	8.8	9.3	9.8	10.3
I	0.4	0.7	0.9	1.1	2.2	2.7	3.2	3.7	4.1
J	0.1	0.3	0.5	0.7	1.2	1.7	2.2	2.6	2.9

Table 9.6. *Isohyetal label values (percent of 1-hour, 1-mi² average depth) to be used with the isohyetal pattern of Figure 9.18 and the basin average depths from Figure 9.20.*

	Duration (hours)								
Isohyet	1/4	1/2	3/4	1	2	3	4	5	6
A	55	79	91	100	110.5	116	118	119	120
B	35.5	55	68	78	88	95	99	101	102.5
C	24	39	49	57	66	72	75	77	78.5
D	19	30	39	44	51.5	56	58.5	60	61
E	13.5	22	28	33	39	42.7	44.5	46	47
F	8.5	15	20	23	28	31.5	33.5	35	36
G	5.5	9.5	13	15	19	22	24	25	26
H	2	4.5	6.0	7.5	11.5	14.5	16.5	17.5	18.5
I	1	2	3	4	8	11	13	14.5	15.5
J	1	2	3	4	7	10	12	13.5	14.5

Table 9.7. *Isohyetal label values (percent of 1-hour, 1-mi^2 average depth) to be used with the isohyetal pattern of Figure 9.18 and the basin average depths from Figure 9.21.*

	Duration (hours)								
Isohyet	1/4	1/2	3/4	1	2	3	4	5	6
A	55	79	91	100	114	120	125	128	130
B	44	66	77.6	86	100	106	111	114	116
C	26	44	53.6	61	74	81	86	89	91
D	17	31	40.2	46.5	58	65	70	73	75
E	11	20	26.8	32.5	42	49	54	57	59
F	6.6	13	19	24	32	38	43	46	48
G	6.5	11	14	16	23	28	33	36	38
H	5	8	10.5	12	17.5	21.5	25.5	29	31
I	3	6.0	8.5	10.5	16	20	24	27.5	30
J	2.5	5.5	8	10	15	19	23	26.5	29

Table 9.8. *Isohyetal label value (percent of 1-hour, 1-mi^2 average depth) to be used with the isohyetal pattern of Figure 9.18 and the basin average depths from Figure 9.22.*

	Duration (hours)								
Isohyet	1/4	1/2	3/4	1	2	3	4	5	6
A	55	79	91	100	117	126	132	137	140
B	39	61	74	84	100	109	115	120	123
C	24	42	52	60	76	85	91	96	99
D	15	28	37	44	59	67	73	78	81
E	9	19	26	32	44	52	58	63	67
F	6	13.5	19	24	34	40	45	50	54
G	6	10	13.5	16	24	30	35	39	42
H	4	7	10	13	19	24	28	32	35.5
I	3.3	6.5	9	11	18	23	27	31	34.5
J	3	5.5	8	10	17	22	26	30	33.5

Table 9.9. *Average depth of local-storm PMP (percent of 1-mi² average depth) for area size and duration where the 6-hour to 1-hour, 1-mi² depth-duration ratio is less than 1.2.*

Area (mi²)	Duration (hours)								
	1/4	1/2	3/4	1	2	3	4	5	6
1	100.0	100.0	100.0	100.0	100.0	100.0	100.0	100.0	100.0
5	85.4	88.8	89.8	90.0	90.4	90.5	90.7	90.8	90.8
25	60.0	66.8	69.3	70.4	71.3	71.7	72.0	72.2	72.3
55	48.3	54.8	57.9	59.0	59.9	60.3	60.6	60.8	61.0
95	40.0	45.8	49.2	50.0	50.9	51.3	51.6	51.8	52.0
150	32.4	37.7	40.9	41.7	42.5	42.9	43.1	43.3	43.5
220	25.9	30.6	33.3	34.2	34.9	35.3	35.5	35.7	35.9
300	20.7	24.6	27.0	27.8	28.6	28.9	29.2	29.4	29.6
385	16.6	19.8	21.7	22.5	23.3	23.7	23.9	24.2	24.5
500	12.9	15.4	16.9	17.5	18.3	18.7	19.0	19.3	19.6

Table 9.10. *Average depth of local-storm PMP (percent of 1-mi² average depth) for area size and duration where the 6-hour to 1-hour, 1-mi² depth-duration ratio of 1.2.*

Area (mi²)	Duration (hours)								
	1/4	1/2	3/4	1	2	3	4	5	6
1	100.0	100.0	100.0	100.0	100.0	100.0	100.0	100.0	100.0
5	85.8	87.9	89.9	91.2	92.0	92.8	93.6	94.0	94.2
25	60.3	65.2	69.4	72.2	74.4	76.2	77.8	78.6	79.2
55	48.1	53.3	57.8	60.4	62.9	64.7	66.2	67.1	67.7
95	39.7	44.6	48.9	51.2	53.8	55.4	56.7	57.6	58.1
150	32.1	36.7	40.6	42.7	45.2	46.8	48.0	48.9	49.5
220	25.7	29.9	33.4	35.1	37.7	39.3	40.5	41.4	42.0
300	20.6	24.3	27.3	28.8	31.3	33.0	34.3	35.1	35.7
385	16.6	19.8	22.3	23.7	26.4	28.1	29.5	30.3	31.0
500	13.2	15.8	18.0	19.2	21.9	23.8	25.1	26.1	26.7

Table 9.11. *Average depth of local-storm PMP (percent of 1-mi² average depth) for area size and duration where the 6-hour to 1-hour, 1-mi² depth-duration ratio of 1.3.*

Area (mi²)	Duration (hours)								
	1/4	1/2	3/4	1	2	3	4	5	6
1	100.0	100.0	100.0	100.0	100.0	100.0	100.0	100.0	100.0
5	92.0	93.4	94.1	94.4	95.1	95.3	95.5	95.6	95.7
25	69.3	74.4	76.5	77.7	80.1	81.4	82.1	82.6	82.8
55	52.8	59.7	62.9	64.6	68.0	70.2	71.4	72.0	72.5
95	41.3	48.2	51.9	54.0	57.9	60.6	62.2	63.1	63.7
150	32.0	38.2	42.1	44.6	48.6	51.7	53.6	54.7	55.4
220	25.2	30.6	34.4	36.8	40.8	44.0	46.2	47.5	48.3
300	20.7	25.3	28.7	30.7	34.7	37.8	40.1	41.6	42.5
385	17.4	21.5	24.6	26.4	30.3	33.2	35.7	37.3	38.3
500	14.3	18.1	20.9	22.7	26.4	29.3	31.8	33.6	34.7

Table 9.12. *Average depth of local-storm PMP (percent of 1-mi² average depth) for area size and duration where the 6-hour to 1-hour, 1-mi² depth-duration ratio of 1.4.*

Area (mi²)	Duration (hours)								
	1/4	1/2	3/4	1	2	3	4	5	6
1	100.0	100.0	100.0	100.0	100.0	100.0	100.0	100.0	100.0
5	88.4	90.9	92.5	93.6	94.2	94.6	95.5	95.6	95.7
25	63.5	70.3	73.9	76.3	79.0	81.4	82.1	82.6	82.8
55	45.2	56.1	60.2	63.1	67.4	70.2	71.4	72.0	72.5
95	33.1	45.0	49.4	52.5	57.5	60.6	62.2	63.1	63.7
150	26.0	35.8	40.3	43.5	48.7	51.7	53.6	54.7	55.4
220	20.9	28.8	33.0	36.0	41.1	44.0	46.2	47.5	48.3
300	17.3	23.8	27.5	30.3	35.0	37.8	40.1	41.6	42.5
385	14.7	20.3	23.7	26.3	30.8	33.2	35.7	37.3	38.3
500	12.4	17.2	20.3	22.6	27.1	29.3	31.8	33.6	34.7

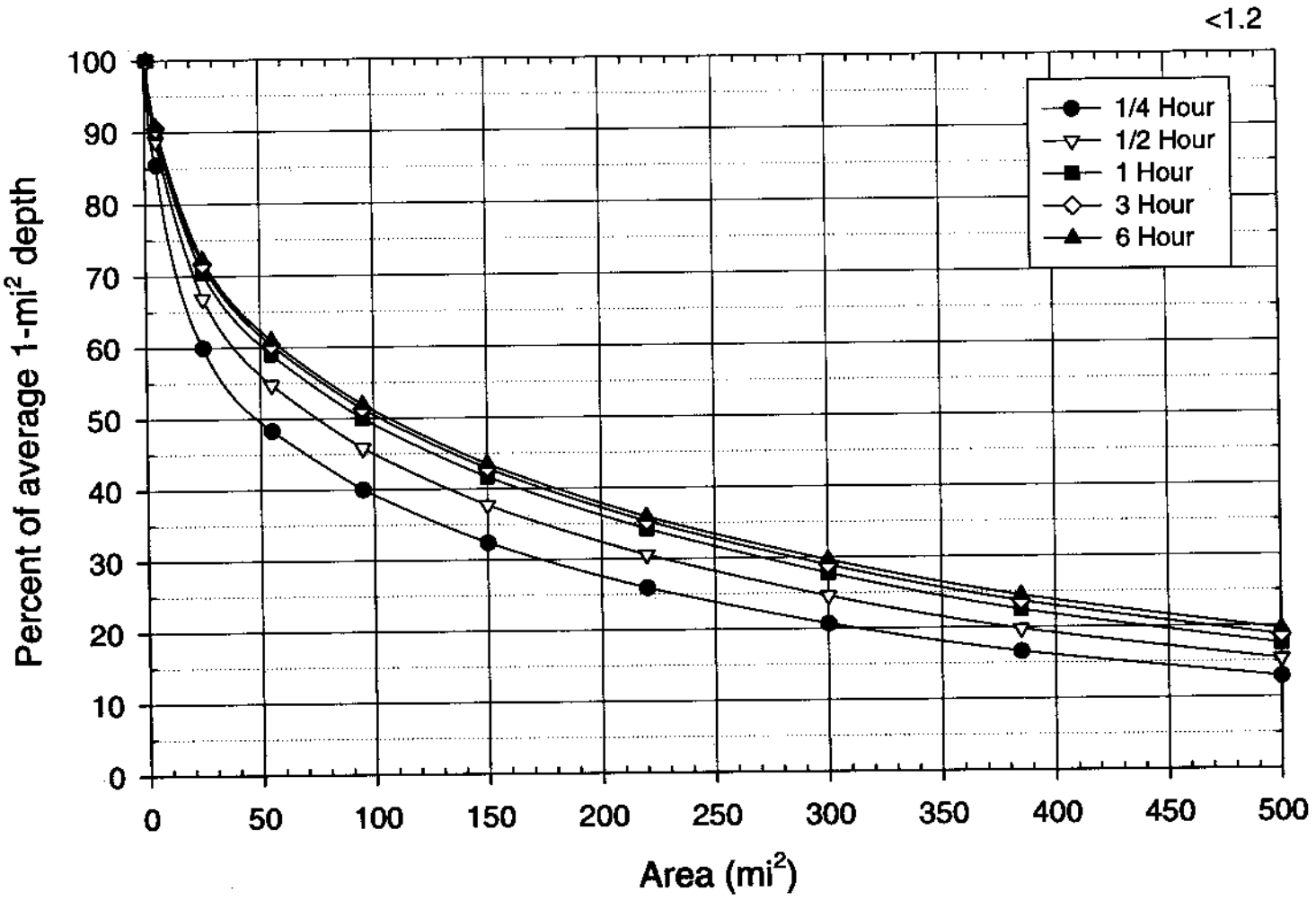

Figure 9.19. *Depth-area relations for California local-storm PMP for a 1-mi², 6-hour, to 1-hour depth-duration ratio less than 1.2. Same as Figure 13.25.*

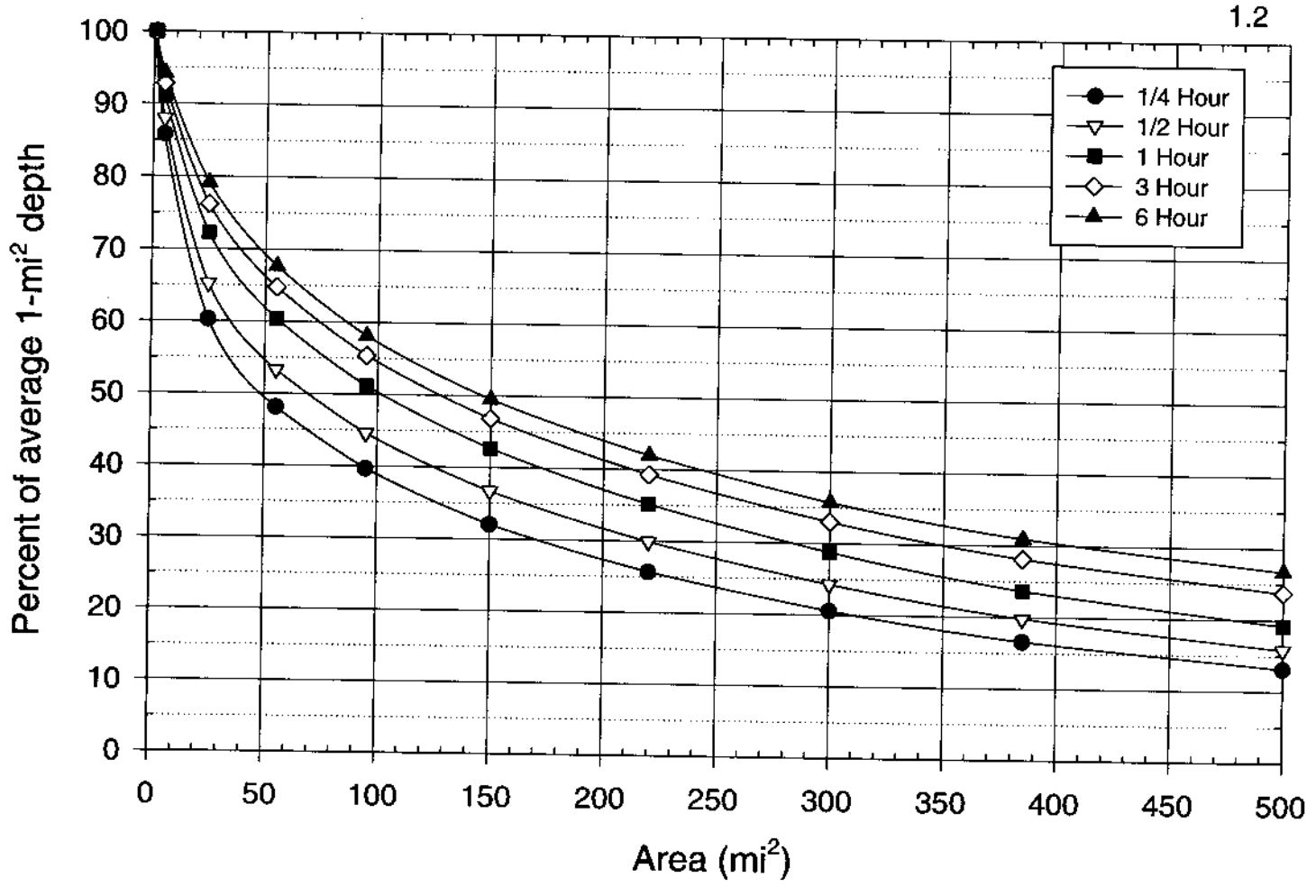

Figure 9.20. *Depth-area relations for California local-storm PMP for a 1-mi², 6-hour, to 1-hour depth-duration ratio equal to 1.2. Same as Figure 13.26.*

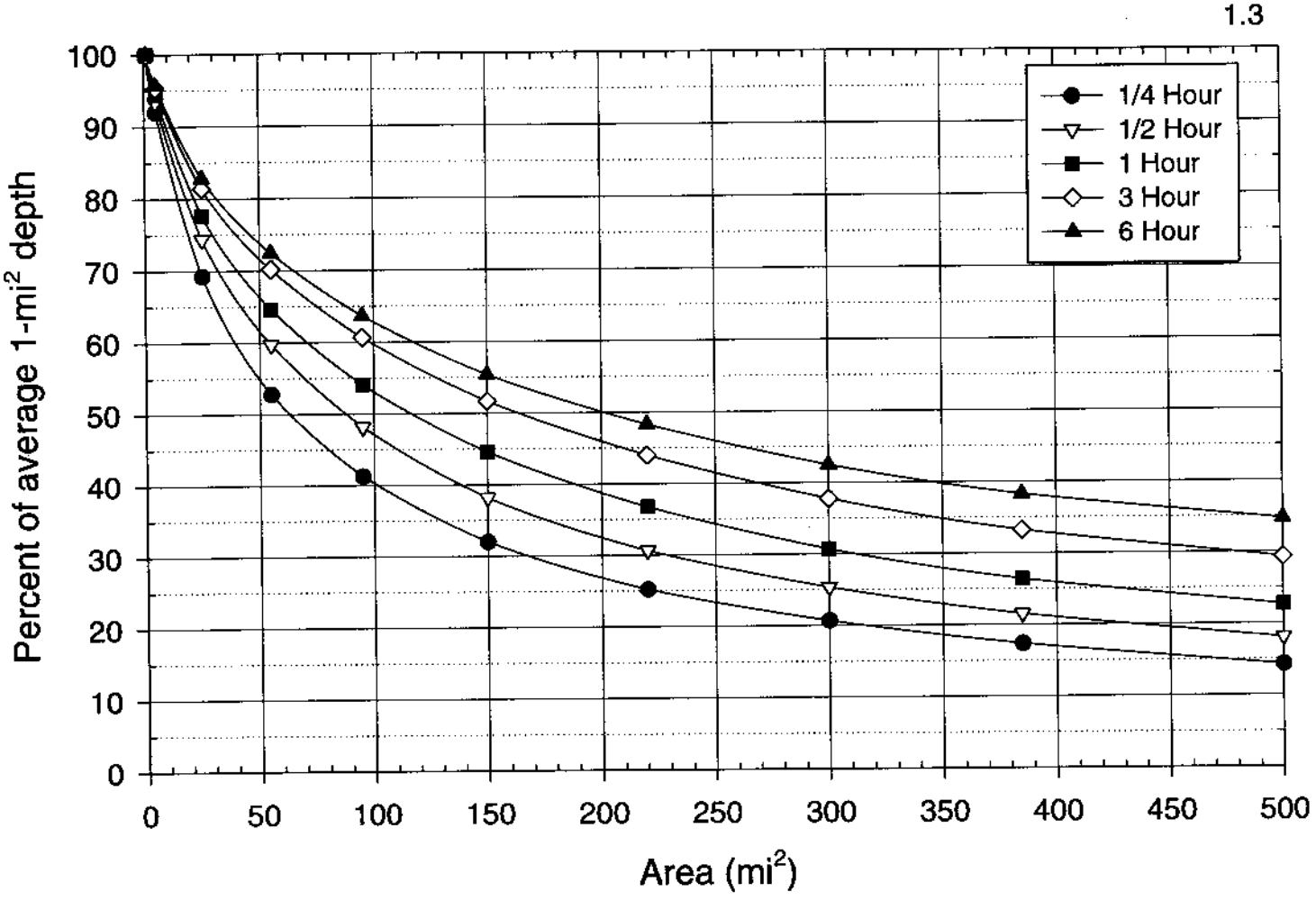

Figure 9.21. *Depth-area relations for California local-storm PMP for a 1-mi², 6-hour, to 1-hour depth-duration ratio equal to 1.3. Same as Figure 13.27.*

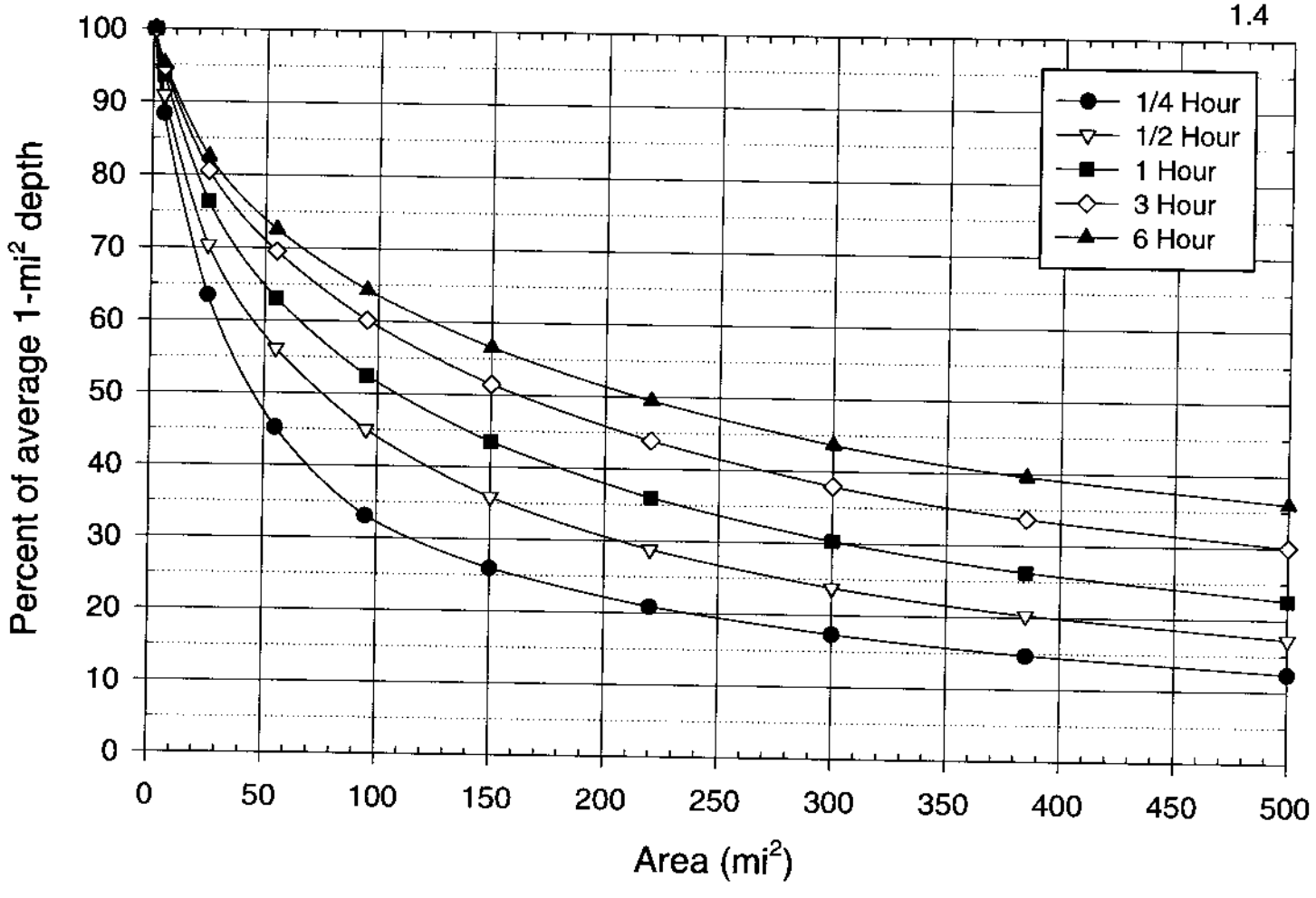

Figure 9.22. *Depth-area relations for California local-storm PMP for a 1-mi², 6-hour, to 1-hour depth-duration ratio equal to 1.4. Same as Figure 13.28.*

9.10 Local-storm Index Maps

The local storm or 1-hour, 1-mi^2 PMP Index map, shown in Figure 9.23, used the HMR 49 Index map as a starting point. As discussed in Section 9.3, 14 storms were added to the extreme storm list since HMR 49. As obviously the terrain is unchanged, any new storms and changes in the way the moisture field was drawn (the basis for storm maximization) would provide justification for Index map changes.

The Index map shows a PMP maximum of 12 inches over southern California, including much of the Imperial Valley and adjacent mountains to the west. The preponderance of extreme storms in this part of the state (Figure 9.1) provides strong evidence that it is a favored location for the development of intense storms. Proximity to the rich moisture source of the Gulf of California, a southerly latitude allowing for maximum solar insolation, a tendency for low-level jets to form in this area, and the possibility of mesoscale systems to propagate westward out of Arizona into this region (e.g., the Palomar Mountain storm) are all factors for heavy rainfall event occurrence in this area.

A much more widespread maximum of more than 11 inches covers the desert area of southern and southeastern California, with the 11-inch isoline bulging northwest into the San Bernardino Mountains east of Los Angeles. Again, this entire area is open to periodic incursions of subtropical moisture from the Gulf of California or Pacific Ocean. The rare hurricanes, tropical storms or more likely their remnants, into this part of California is a major source of heavy rainfall during these infrequent events (e.g., the Indio storm of September 1939 or the Borrego storm of September 1976).

Local-storm PMP decreases rather sharply along the coastal plain of southern California, falling to around 7 inches in the San Diego and Los Angeles metropolitan areas, a value only about 55 to 65 percent of that in the mountains only a short distance away. This dramatic change indicates the importance of terrain in helping to initiate convection and in anchoring some storms in stationary positions, which can lead to very heavy local rainfall. The Palomar Mountain storm is an excellent example of this type of terrain influence on extreme storm formation and maintenance. The extreme storms that do occur

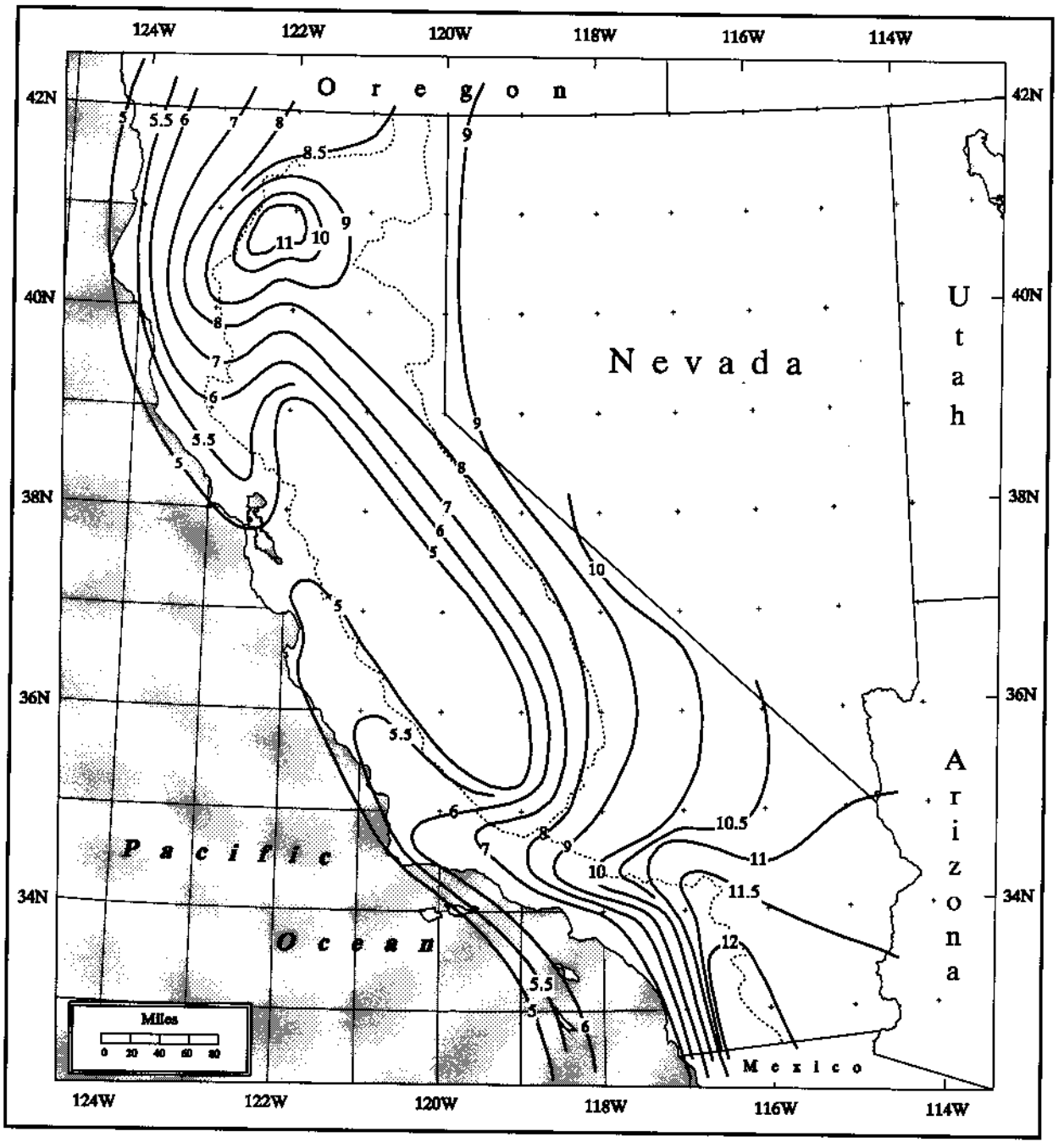

Figure 9.23. *California local-storm PMP precipitation estimates for 1 mi², 1 hour (inches). Dashed lines are drainage divides. Same as Figure 13.21.*

along the coast are more often the result of embedded convection within mesoscale rainbands in large-scale storms. Good examples are both Santa Barbara storms of February 1958 and January 1978.

Moving north and west from the southern California mountains, PMP continues to decrease steadily, reaching a broad minimum over the Central Valley. PMP within this broad, flat area is about only about 5 inches, for reasons that are primarily terrain-related. Moisture inflow is sharply limited from the southeast, where the highest moisture sources exist and also from the west where the coastal ranges block Pacific Ocean air from reaching the Valley easily, except for a small opening through the San Francisco Bay area. In addition, no natural terrain features exist to enhance uplift or channel the moisture flows within the valley itself.

A secondary PMP maximum of 11 inches is found over the northern end of the Sacramento River valley and in the adjacent high terrain near Shasta Lake. One of the factors involved in the existence of this PMP center includes the frequent development of a low-level jet which transports moisture northward very efficiently. In addition, the terrain is also favorable for storm development. The Valley narrows near its northern end, causing increased local convergence and uplift, and elevations increase abruptly in the foothills surrounding the upper end of the Valley. Ample extreme storm evidence supports the location of this maximum (Figure 9.1), including the relatively recent Redding storm, discussed in Section 9.4.1.

9.11 Comparisons with Previous Work

PMP updates have used the results from earlier antecedent studies as a basis for evaluating newer results. For local-storm PMP in California the only antecedent study was HMR 49, so comparisons are obviously limited. However, a comparison was also made with HMR 57 along the Oregon-California border. As a first step in the comparison, both HMR 49, Figure 4.5 and the new local-storm PMP Index maps, Figure 9.23, were digitized and a raster field generated for each. The results showed that the largest differences between HMR 49 and the new local-storm Index map are concentrated in the northwestern part of California, mostly in the Eel and Russian River basins. Increases of up to 30 percent occur over a very small part of that area, but a more general increase of 10 to 15 percent is

found over most of California north of about 40°N latitude. Over most of the state the ratio between the two maps is actually quite close to one (i.e., no difference), falling within plus or minus 5 percent. In a few isolated spots, the percentage is around 90, and a broad area of 95 percent or less occurs over the Mojave Desert and surrounding areas.

Individual basin comparisons were also carried out for 50 basins across the state, ranging in size from less than 1 mi^2 up to nearly 500 mi^2. These basin comparisons were carried out for both the 1- and 6-hour durations. The most important differences occur at the 6-hour duration, which was expected since the depth-duration ratios in HMR 49 were lowered, quite significantly in some parts of the state (Section 9.9 - Depth-Duration Relationships). At 1-hour, the basin PMP differences are fairly limited, with the variations reflecting the pattern discussed above. As an example, for Santa Monica Creek, a small basin near the coast, the HMR 49 PMP was 94 percent of the new PMP at 1 hour (5.67 inches versus 6.05 inches). At 6 hours, however, the HMR 49 PMP was 123 percent of the new PMP (10.06 inches versus 8.20 inches). Numerous test basins showed a similar pattern of close agreement at the 1-hour duration, with much wider differences at 6 hours.

Another comparison was made along the Oregon-California border where the new local-storm Index map, Figure 9.23, joins the HMR 57 Index map. Here, the differences are slight, amounting to less than a half inch at the intersection of the California coast and the border of Oregon (5.1 inches in Figure. 9.23 vs. 5.5 inches in HMR 57 Figure 11.19). The differences decrease steadily to the east, reaching essentially zero at the northeast corner of California. The new values are consistently just slightly lower than the HMR 57 values, until the difference reaches zero. Considering that the same methodology and the same major storm data base was available for both studies, the reason for these minor differences may be ascribed to the slight variation in the 3-hour maximum-persisting dewpoint fields between the two studies (Section 9.5.1). This difference resulted in a lower storm maximization in the current California study than in HMR 57, thus causing the border discrepancies. Since the elevation and depth-duration relationships for this study are the same as those in HMR 57 no greater deviations between the two reports may be expected to occur at the 6-hour time frame or in high elevation basins.

10. INDIVIDUAL DRAINAGE PMP COMPARISONS

An important final step was to compare probable maximum precipitation (PMP) estimates for individual drainages from the present study, HMR 59, with those defined in HMR 36 (1961). Many differences, some quite profound, have appeared and thus, have reflected the need for the new data and revised methodologies. Some of the changes will have an immediate impact on present and future water control projects.

Thirty eight basins which were examined to compare HMR 59 PMP estimates to HMR 36 PMP values. Table 10.1 shows the results for each basin, listed in order of increasing basin size. The basins are shown on the map, Figure 10.1. All of the basins drain, at least partially, from mountainous regions and are impacted by orographic precipitation. Most PMP estimates from the smaller basins (less than 200 mi^2) have increased substantially from HMR 36 at all durations, to HMR 59. For example, Los Banos Basin, 156 mi^2, shows an increase of 22 percent at 6 hours and an increase of 39.7 percent at 72 hours. Basins of 200 mi^2 and 1000 mi^2 trend toward decreasing PMP values, in relation to HMR 36. Generally, at short durations (1, 6, 12 hours) PMP values have increased and at longer durations (24, 48, 72 hours) PMP values have remained constant or decreased in most instances. In basins greater than 1000 mi^2, HMR 59 PMP values decrease substantially as compared with HMR 36 PMP values. For instance, the basin PMP above Twitchell Dam, 1135 mi^2, decreases from 22.5 percent at 12 hours to 31.9 percent less than HMR 36 at 24 hours.

Differences in PMP values between the two reports relate to the differences in how the depth-area-duration (DAD) relations were determined. HMR 59 DADs were based upon storm-based relations, whereas, HMR 36 DADs were based upon a mass-conservation model combining air speed, wind direction and resulting moisture off the Pacific. Table 10.2 provides an overall comparison of the percentage changes in general-storm PMP between values computed for this study versus those values determined in HMR 36.

Table 10.1. *Comparison of various California basin-average PMP depths (inches) from HMR 59 to HMR 36 for selected durations. Associated percentage changes also shown.*

Site	mi^2	Study	1 hr	6 hr	12 hr	24 hr	48 hr	72 hr
Ortega	.0063	HMR 59	3.08	10.56	16.72	22.00	31.02	34.98
		HMR 36	3.22	9.73	15.13	22.49	31.22	36.29
		% change	-4.30	8.50	10.50	-2.20	-0.60	-3.60
Lauro	0.44	HMR 59	3.64	12.48	19.76	26.00	36.66	41.34
		HMR 36	3.20	9.61	14.94	22.21	30.83	35.84
		% change	13.80	29.90	32.30	17.10	1.89	15.30
Glen Anne	0.55	HMR 59	3.71	12.72	20.14	26.50	37.37	42.14
		HMR 36	3.08	8.90	13.64	20.02	27.56	31.07
		% change	20.40	42.90	47.70	32.40	35.60	35.60
Contra Loma	1.07	HMR 59	1.82	5.88	9.10	14.00	20.72	24.50
		HMR 36	2.28	5.69	8.20	11.47	15.40	18.01
		% change	-20.20	3.30	11.00	22.10	34.50	36.00
Sly Park	17	HMR 59	2.83	8.54	13.26	20.52	32.15	36.49
		HMR 36	2.19	6.69	10.64	16.61	24.50	29.46
		% change	29.20	27.70	24.60	23.50	31.20	23.90
Casitas	39	HMR 59	3.76	12.96	20.78	27.55	39.35	44.89
		HMR 36	3.25	10.91	17.48	26.63	37.50	43.69
		% change	5.70	18.80	18.90	3.50	4.90	2.70
Sutherland	50	HMR 59	2.64	9.10	14.64	19.39	27.79	31.68
		HMR 36	-----	10.06	16.22	24.60	34.23	39.37
		% change		-9.50	-9.70	-21.20	-18.80	-19.50
San Vincente	76	HMR 59	1.72	5.98	9.59	12.82	18.40	20.96
		HMR 36	-----	6.89	10.57	15.37	20.92	24.17
		% change		-13.20	-9.30	-16.60	-12.00	-13.30
Little Panoche	82	HMR 59	1.32	4.57	7.49	11.01	16.42	19.70
		HMR 36	1.77	4.48	6.28	8.46	10.99	12.83
		% change	-25.40	2.00	19.30	30.10	49.40	53.50
San Luis	83	HMR 59	1.78	6.22	10.33	14.58	21.60	25.77
		HMR 36	1.78	4.48	7.21	10.33	14.12	16.63
		% change	0.00	38.80	43.20	41.10	53.00	55.00
Sweetwater	88	HMR 59	1.68	6.02	9.71	12.97	18.54	21.31
		HMR 36	-----	6.39	9.74	14.01	18.95	21.95
		% change		-5.80	-0.30	-7.40	-2.20	-2.90

Table 10.1. *Comparison of various California basin-average PMP depths (inches) from HMR 59 to HMR 36 for selected durations. Associated percentage changes also shown.*

Site	mi^2	Study	1 hr	6 hr	12 hr	24 hr	48 hr	72 hr
Lower Otay	93	HMR 59	1.81	6.35	10.23	13.66	19.57	22.45
		HMR 36	-----	6.43	9.83	14.23	19.31	22.35
		% change		-1.20	4.10	-4.00	1.30	0.40
Loveland	94	HMR 59	2.64	9.22	14.87	19.82	28.53	32.76
		HMR 36	-----	7.77	12.35	18.49	25.55	29.47
		% change		18.70	20.40	7.20	11.70	11.20
Morena	109	HMR 59	2.85	9.94	16.09	21.60	30.98	35.54
		HMR 36	-----	7.41	11.93	18.09	25.16	29.00
		% change		34.10	34.90	19.40	23.10	22.60
Barrett Lake	124	HMR 59	2.45	8.61	13.93	18.57	26.71	30.71
		HMR 36	-----	7.40	11.79	17.66	24.42	28.17
		% change		16.40	18.20	5.20	9.40	9.00
Stampede	130	HMR 59	1.73	5.33	8.42	13.24	21.18	24.50
		HMR 36	-----	4.47	7.69	12.86	19.92	24.29
		% change		19.30	9.50	3.00	6.30	0.90
Los Banos	156	HMR 59	1.50	5.37	9.10	12.58	18.74	22.46
		HMR 36	-----	4.40	6.67	9.78	13.59	16.08
		% change		22.00	36.40	28.60	37.90	39.70
Sepulveda	156	HMR 59	2.60	9.14	14.79	19.89	28.67	33.01
		HMR 36	-----	7.04	11.06	16.35	22.45	25.96
		% change		29.80	33.70	21.70	27.70	27.20
Hansen	157	HMR 59	3.75	13.19	21.36	28.72	41.41	47.68
		HMR 36	-----	9.91	16.20	24.79	34.65	39.90
		% change		33.10	31.90	15.90	19.50	19.50
Seven Oaks	177	HMR 59	3.37	11.86	19.16	25.71	37.17	42.75
		HMR 36	-----	10.10	19.10	29.70	41.70	47.50
		% change		17.40	0.30	-13.40	-10.90	-10.00
El Capitan	189	HMR 59	2.41	8.52	13.77	18.55	26.80	30.93
		HMR 36	-----	8.24	13.25	20.09	27.96	32.26
		% change		3.40	3.90	-7.70	-4.10	-4.10
Whiskeytown	202	HMR 59	1.85	7.64	14.28	20.04	30.54	37.04
		HMR 36	-----	8.37	14.39	24.09	37.36	45.60
		% change		-8.70	-0.80	-16.80	-18.30	-18.80

Table 10.1. *Comparison of various California basin-average PMP depths (inches) from HMR 59 to HMR 36 for selected durations. Associated percentage changes also shown.*

Site	mi^2	Study	1 hr	6 hr	12 hr	24 hr	48 hr	72 hr
Henshaw	203	HMR 59	2.27	8.00	12.96	17.44	25.23	29.13
		HMR 36	-----	7.32	11.87	18.10	25.26	29.16
		% change		9.30	9.20	-3.60	-0.10	-0.10
Santa Fe	248	HMR 59	3.87	13.70	22.26	29.96	43.41	47.68
		HMR 36	-----	11.57	19.18	29.67	41.70	39.90
		% change		18.40	16.10	1.00	4.10	19.50
Lake Hodges	253	HMR 59	1.64	5.80	9.38	12.66	18.35	21.19
		HMR 36	-----	6.94	10.83	16.19	22.38	25.94
		% change		-16.40	-9.20	-21.80	-18.00	-18.30
Whittier Narrow	307	HMR 59	2.37	8.39	15.43	18.42	26.68	30.98
		HMR 36	-----	8.09	12.96	19.62	27.29	31.57
		% change		3.70	19.10	-6.10	-2.20	-1.90
Bradbury	417	HMR 59	3.19	11.41	18.54	25.09	36.54	42.52
		HMR 36	-----	10.74	18.18	28.88	41.67	48.81
		% change		6.20	2.00	-13.10	-12.30	-12.90
Monticello	566	HMR 59	2.26	8.26	14.07	19.70	29.51	35.49
		HMR 36	-----	6.11	10.16	16.36	24.57	29.78
		% change		35.20	38.50	20.40	20.10	19.20
Trinity	692	HMR 59	1.42	5.96	11.30	15.89	24.55	30.02
		HMR 36	-----	5.53	9.47	16.54	25.89	31.68
		% change		7.80	19.30	-3.90	-5.20	-5.20
Santa Margarita	714	HMR 59	1.38	4.97	8.20	11.19	16.29	19.10
		HMR 36	-----	6.01	9.76	14.88	20.81	24.19
		% change		-17.30	-16.00	-24.80	-21.70	-21.00
Clear Lake	735	HMR 59	0.95	3.27	4.53	6.77	9.81	11.16
		HMR 36	-----	2.58	4.08	6.31	9.25	11.06
		% change		26.70	11.00	7.30	6.10	0.90
New Melones	904	HMR 59	1.75	5.50	8.89	14.21	23.42	27.62
		HMR 36	-----	5.80	10.15	17.02	26.22	31.85
		% change		-5.20	-12.40	-16.50	-10.70	-13.30
Auburn	973	HMR 59	2.20	6.90	11.21	17.72	29.56	34.64
		HMR 36	-----	6.48	11.43	19.39	30.25	36.99
		% change		6.48	-1.90	-8.61	-2.28	-6.35

Table 10.1. *Comparison of various California basin-average PMP depths (inches) from HMR 59 to HMR 36 for selected durations. Associated percentage changes also shown.*

Site	mi²	Study	1 hr	6 hr	12 hr	24 hr	48 hr	72 hr
Twitchell	1135	HMR 59	1.24	4.70	7.90	10.97	16.24	19.06
		HMR 36	-----	6.08	10.20	16.12	23.25	27.42
		% change		-22.70	-22.50	-31.90	-30.20	-30.50
Friant	1591	HMR 59	1.68	5.28	8.62	13.98	23.13	27.33
		HMR 36	-----	5.31	9.35	15.60	23.70	28.56
		% change		-0.60	-7.80	-10.40	-2.40	-4.30
Folsom	1861	HMR 59	1.68	5.47	8.95	14.56	23.84	28.57
		HMR 36	-----	5.68	9.90	16.64	25.75	31.48
		% change		-3.70	-9.60	-12.50	-7.40	-9.20
Prado Dam	2245	HMR 59	1.37	5.24	8.75	12.19	18.04	21.36
		HMR 36	-----	5.60	10.60	16.50	23.10	26.30
		% change		-6.40	-17.50	-26.10	-21.90	-18.80
Shasta	3027	HMR 59	1.27	4.50	7.85	12.29	20.02	24.32
		HMR 36	-----	5.36	9.69	16.64	26.15	32.09
		% change		-16.00	-19.00	-26.10	-23.40	-24.20

Table 10.2. *Total percentage change in all drainages from Table 10.1 for each duration (HMR 59 vs. HMR 36). Negative percentages indicate that PMP computed from HMR 59 is less than that obtained from HMR 36.*

	1 hr	6 hr	12 hr	24 hr	48 hr	72 hr
Range of %	-25 to 29	-23 to 43	-23 to 48	-32 to 41	-30 to 53	-31 to 53
Mean %	2	9	10	0	4	4

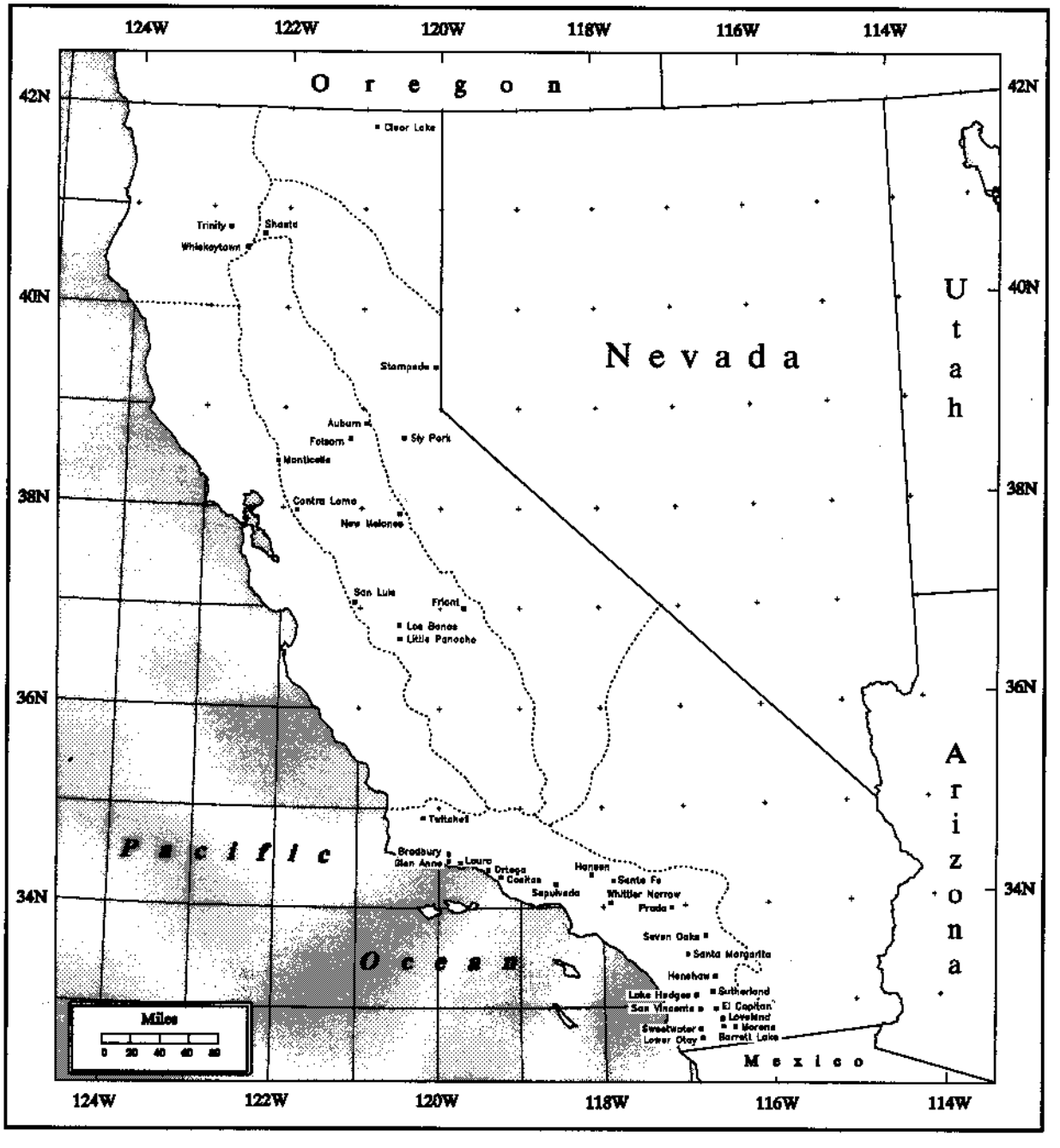

Figure 10.1. *Locations of basins used to compare HMR 59 and HMR 36 general-storm estimates. Dashed lines are regional DAD boundaries.*

11. COMPARISONS

The comparisons used to assess PMP estimates derived in this study are similar to evaluations made for previous hydrometeorological reports. However, with advanced computer technology, a more comprehensive and detailed approach is possible. In the past, comparisons between maps were made by choosing points from a grid (such as quarter degrees), manually calculating the values and then computing the differences or ratios. Now it is possible, in most cases, to determine differences or ratios by using the computer to extract values using a geographic information system (GIS). This information can be compared precisely at all locations or areas down to .08 mi^2 (where the raster cells have a 15-second resolution). As in recent Hydrometeorological Reports, comparisons are made between the PMP estimates and 1) 100-year precipitation frequency amounts (NOAA Atlas 2), 2) previous PMP studies for the same (HMR 36 1961) and neighboring regions (HMR 57 1994 and HMR 49 1977), 3) observed extreme rainfall, and 4) the relationship between general-storm PMP and local-storm PMP.

11.1 Comparison to NOAA Atlas 2

General-storm PMP was compared to the 100-year precipitation frequency analyses for 24 hours, 10 mi^2 from NOAA Atlas 2. As mentioned above, the ability to compare and contrast the two layers of information at every point was available and the map that represents the ratio between PMP and NOAA Atlas 2 is shown in Figure 11.1.

By definition, PMP is larger than the 100-year precipitation frequency amounts for all storm types, therefore, the ratios are always greater than one. The smallest ratio of PMP to the 100-year frequency was 1.7 which occured in the south-central Sierra Nevada mountains. Conversely, the highest ratio 4.5, was located in southeastern California near the Salton Sea, in the lee of the Sierra Nevada near Owens Valley (Figure 11.1). Most of the ratios across the state range from about 2.5 to 3.3. However, large areas of southeast California and the Central Valley are not within this range. Values reach 4.1 in the Central Valley and 4.5 in the desert southeast. In mountainous regions the trend is toward lower

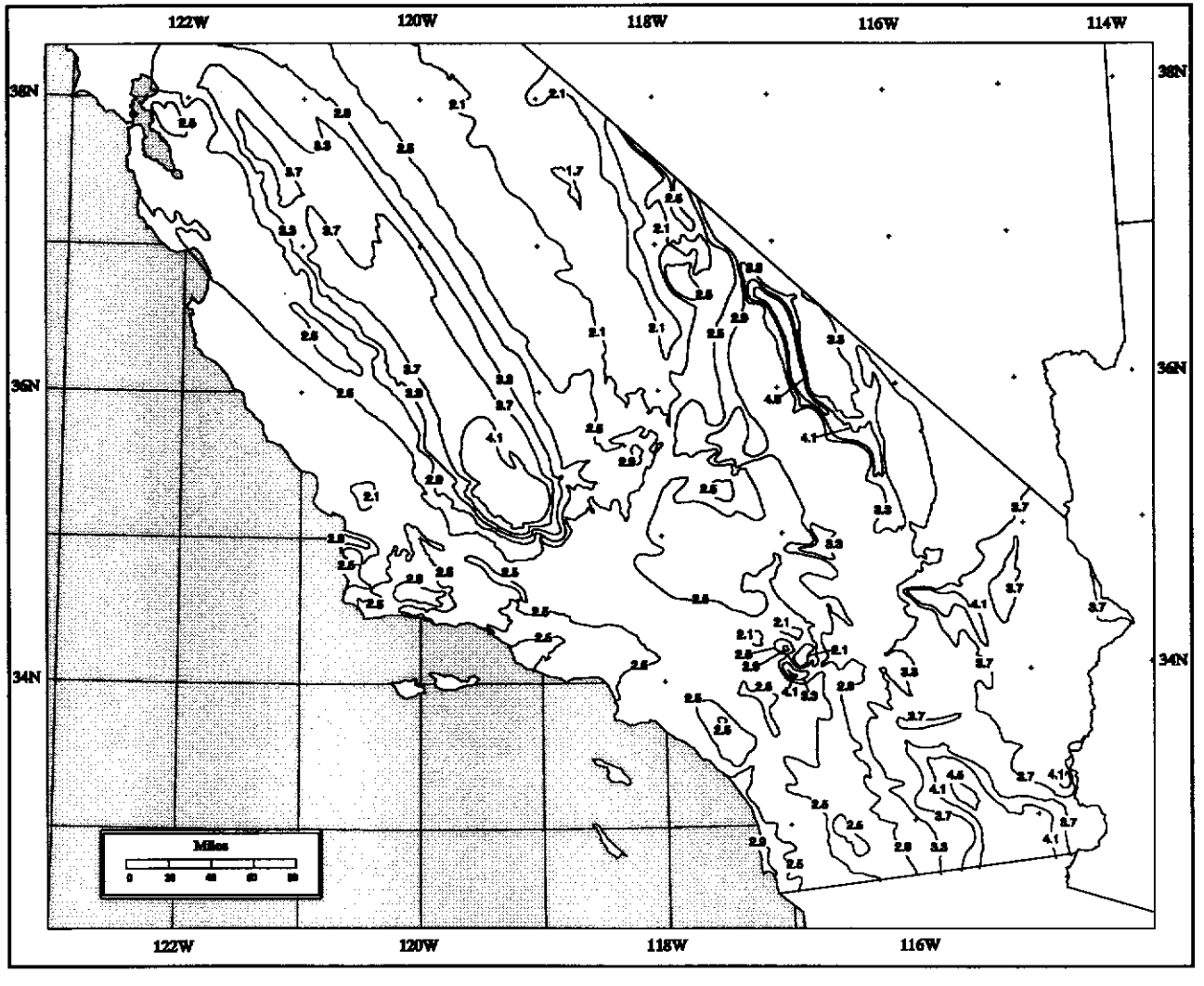

Figure 11.1. *Ratio of 10 mi^2, 24-hour PMP Index map to 100-year, 24-hour precipitation frequency analysis from NOAA Atlas 2 for California south of 38 °N (non-dimensional ratios).*

ratios where PMP estimates are less than twice as large as the 100-year precipitation frequency values.

Overall, the comparison indicates that larger ratios are in lower elevations where short-duration, convective precipitation predominates, and smaller ratios in higher elevations where general-storm, long-duration precipitation is prevalent. The precipitation over lower elevations and the desert southeast is much more sporadic with high levels of cloudburst activity. It should be noted that NOAA Atlas 2 combines all types of precipitation events together and it is impossible to know exactly which category of storm (general or local) generated the values for the 100-year frequency analyses. Nevertheless, this study has accepted the 100-year data from NOAA Atlas 2 as the best precipitation frequency information currently available, and it is used extensively throughout (see Chapters 5 and 7) as a basis for PMP development.

11.2 Comparison to HMR 36

PMP estimates were also compared with estimates from HMR 36. The PMP Index map was compared with a computer-calculated raster layer derived from HMR 36 at 24 hours, 10 mi^2. Creating a raster layer of HMR 36 was a complex process since it was based upon a 6-hour, 200-mi^2 convergence map and a 6-hour, 200-mi^2 orographic map that needed to be combined and converted to 24-hour, 10-mi^2 format. Other area sizes and durations were also computed and compared for specific basins. They are shown in Table 11.1 and are discussed in Section 11.3.

Instead of finding the ratio between the two studies, the difference was calculated by subtracting HMR 36 PMP from HMR 59 PMP estimates. HMR 36 does not include the entirety of California; therefore, regions to the east of the Sierra Nevada mountains and most of the desert southeast could not be compared.

The results for the 24-hour, 10-mi^2 comparison, shown in Figure 11.2, indicate that HMR 59 PMP estimates are anywhere from 12 inches less than to 24 inches greater than HMR 36 PMP. The area covered by positive values was several times larger than that covered by negative amounts. The areas of greatest increase were generally confined to

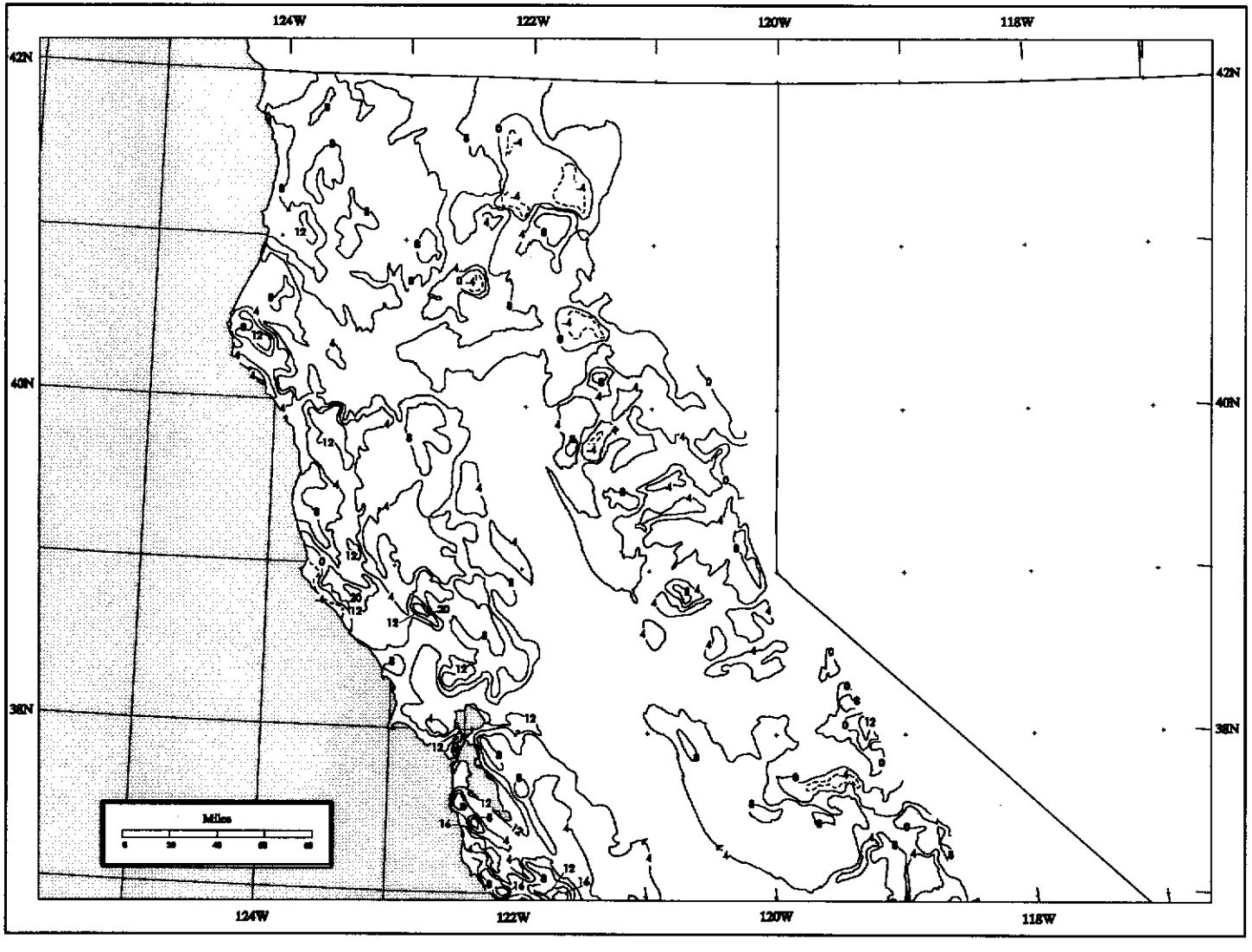

Figure 11.2a. *HMR 59 general-storm PMP values minus HMR 36 general-storm values at 24 hours, 10 mi² for northern California. Negative values are shown by dashed lines and positive values are solid lines. Due to the complex nature of this figure, some lines were removed for legibility.*

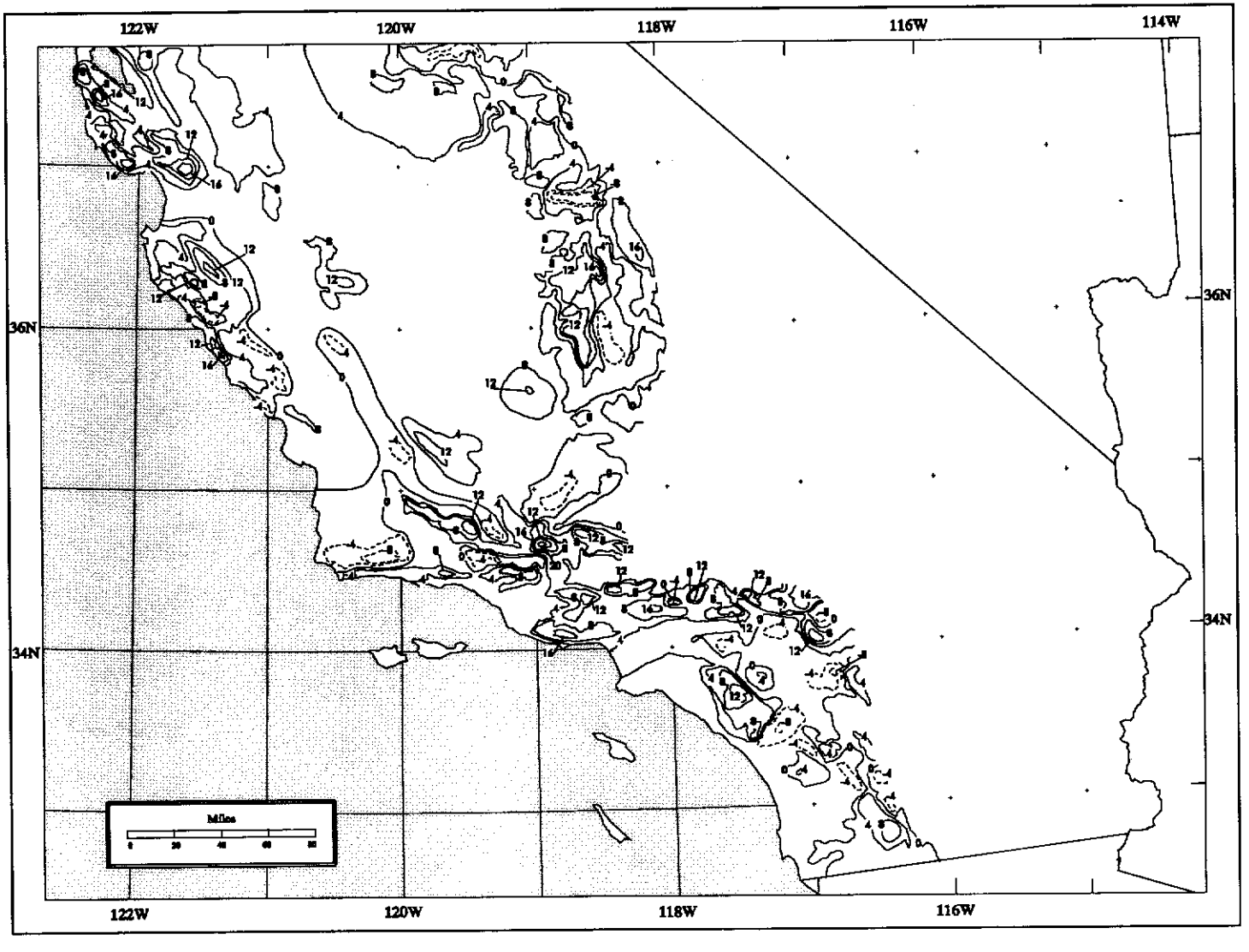

Figure 11.2b. *HMR 59 general-storm values minus HMR 36 general-storm values at 24 hours, 10 mi² for southern California. Negative results are shown by dashed lines and positive results are solid lines. Due to the complex nature of this figure, some lines were removed for legibility.*

orographic regions. Results showed localized increases of up to 24 inches in the San Gabriel and San Bernardino mountains from HMR 36 PMP to HMR 59 PMP. This trend of increased PMP values continues along the length of the Sierra Nevada mountains where the positive differences reach 12 inches in isolated areas. Along the Coastal range, in southern California, there are few positive differences; however, north of San Francisco most of the region had positive values reaching 24 inches in spots.

Areas with negative values, where HMR 59 PMP estimates are lower than HMR 36 estimates, are confined spatially to sheltered (downwind of major orographic regions) and non-orographic regions. There are a few valleys in the Sierra Nevada mountains where negative values reach 12 inches. Other areas of negative, but minimal differences are found in the northernmost Sierra Nevada mountains, most of the Shasta River drainage, areas just east of the Coastal mountains south of Monterey, and in portions of the non-orographic region east and south of Los Angeles.

Differences between the two reports can be attributed to several factors: to changes in technique, a longer and updated storm sample, and a better understanding of the physical mechanisms responsible for precipitation over orographic and non-orographic terrain. As HMR 59 PMP estimates are based upon the 100-year precipitation frequency, which is very detailed in mountainous regions, the complex terrain was better defined and more accurate than in HMR 36. For example, some of the negative values in the Sierra Nevada mountains occur where 100-year frequency values are relatively low compared to their surrounding values. This makes qualitative sense since these valleys are protected from moisture inflow due to their orientation, placement of other surrounding barriers, and prevailing storm inflow moisture. Most of the HMR 59 PMP increases from HMR 36, as noted previously, were in orographic regions. The explanation for this behavior again can be attributed to the use of the 100-year precipitation frequency analysis that increased the values of PMP in the higher elevations in proportion to the lower elevations. HMR 36 PMP used a mass-conservation model to create the orographic effect which created different results and less precipitation in orographic areas. The HMR 36 model was unable to describe local convergence, convection, or any of the *seeder feeder* effects that are common in mountainous areas (Browning 1980, Hobbs 1989).

11.3 Comparison to Extreme Rainfalls

Records from major or extreme storms listed in Chapter 2, Table 2.1 have also been compared with general-storm PMP estimates for HMR 59 and are shown in Table 11.1. The comparison is expressed as a percentage of PMP. The records are observed values from both daily and hourly stations. Again, the 24-hour, 10-mi^2 PMP Index map was compared, this time, with the 24-hour maximum precipitation for each station within the critical precipitation period for that storm. The critical precipitation period is defined as the portion of a storm considered most important for depth-area-duration analysis. Locations with ratios exceeding 49 percent (i.e. 24-hour maximum is one half or more of the 24-hour, 10-mi^2 HMR 59 PMP estimate for that point) are shown in Table 11.1. Storms without values greater than 49 percent were not included in Table 11.1.

Figure 11.3 shows 138 observations of 24-hour precipitation that exceed 49 percent of HMR 59 PMP scattered throughout California. The only region not well represented by recorded extreme rainfall is the desert Southeast. This region is under-represented due to the scarcity of stations and a lack of recorded observations. Just two storms were significant in the southeast, August 15 - 17, 1977 and July 27-29, 1984, and neither produced enough precipitation to exceed the 49-percent threshold of HMR 59 PMP.

A couple of ratios, reaching nearly 100 percent of HMR 59 PMP, did occur and are detailed below. For comparison sake, the HMR 36 PMP values are printed as well in Table 11.1. The highest ratio found from the storm list data is 92 percent of PMP at Johnsondale, California from the December 4-6, 1966 storm in the southern Sierra. Other high values include an 89 percent at Oakland Rishell Dr., near the San Francisco Bay that occurred in the October 10-14, 1962 storm, and 87 percent at Indian Rock, California just north of Lake Tahoe in the December 19-24, 1964 event.

Besides examining the data for the extreme events included in the storm list in Chapter 2, Table 2.1, maximum 24-hour precipitation values from Technical Paper No. 16 (1952) and NOAA Technical Report NWS 25 (1980) were compared. Also records from hourly and daily values, available from 1948 through 1994, were compared to HMR 59 PMP estimates. Only observations from storms not on the storm list, Chapter 2, Table 2.1, were

Table 11.1. *24-hour station precipitation from extreme storms and associated ratios for HMR 36 and HMR 59 PMP at 24 hour, 10 mi^2. Only ratio values greater than 49 percent are given for HMR 59.*

Storm Date	Site	Precipitation (inches)	% of HMR 36	% of HMR 59
12/8-12/1937	Lookout	5.11	<50	60
	Trimmer Experiment Sta	7.85	55	57
	Lake City	5.13	<50	56
	Montgomery Creek	5.11	<50	51
2/27-3/3/1938	Santa Rosa Rch	9.38	<50	68
1/20-24/1943	Hoegees Camp	25.83	102	75
	Glenn Camp	22.93	77	75
	Camp Leroy Hoegees	26.07	102	74
	Lancaster	5.53	NA	69
	Ontario	8.30	<50	60
	Santa Anita RS	15.41	65	56
	San Gabriel Dam 2	22.65	63	55
	Agua Dulce Canyon	8.78	54	54
	Santa Barbara	7.34	<50	52
	Saugus State Hwy	10.19	54	52
	Sierra Madre	14.47	62	52
	Big Pines Park	10.17	62	52
	Salinas Dam	8.32	<50	51
	Saugus Substation	9.94	53	51
	Big Santa Anita Dam	15.36	62	51
	Monrovia Falls	15.87	63	51
	San Gabriel Dam 1	16.97	59	51
	San Gabriel Dam 1a	17.20	65	51
	Lytle Creek Headworks	17.99	63	50
11/17-21/1950	Mono Lake	6.66	NA	59
	Springville Tule Headwk	15.04	74	54
12/21-24/1955	Long Valley Res	5.87	NA	57
	Woodacre	10.68	<50	56
	Mono Lake	5.99	NA	53
	Bowman Dam	12.97	52	53
	Donner Memorial St Park	8.21	58	52
	Topaz Lake	4.44	NA	52
	Paicines Ohrwall Ranch	6.73	56	50

Table 11.1. (continued)

Storm Date	Site	Precipitation (inches)	% of HMR 36	% of HMR 59
10/10-14/1962	Oakland Rishell Dr	13.09	93	89
	Radio KAHI-KAFI	11.59	94	71
	Smartsville	9.98	116	69
	Verona	6.83	71	67
	Oakland 39th Ave	9.55	69	61
	Bear River Ranch	10.24	86	60
	Hayward High School	9.47	<50	60
	Country Club Center	5.39	<50	59
	Aerojet Fire Dept	6.53	73	58
	Nicolaus	5.87	64	58
	Central Valley Hatchery	6.06	66	57
	Arden & Mission	6.15	67	57
	Taylorsville	8.20	55	57
	Mather AFB	6.08	67	56
	Dewey & Winding Way	6.06	67	55
	Marysville	6.67	76	55
	Milford	6.07	NA	55
	Westwood	6.67	51	55
	Hedge & Fruitridge	5.72	62	54
	Sierraville R S	6.41	<50	54
	Jamesville	6.22	NA	54
	Rocklin	6.48	73	53
	Lincoln	6.76	77	53
	Cohasset 1 NNE	11.40	<50	53
	Orangevale	6.51	71	52
	Coloma	6.78	75	52
	Colfax	10.02	56	52
	Town & Country Mitchell	5.45	59	51
	Applegate	8.57	56	51
	Sacramento FAA AP	5.59	60	50
	Hidden Valley Ranch	9.49	69	50
	Las Plumas	10.40	<50	50
12/19-24/1964	Indian Rock	10.49	NA	87
	Lookout 3 WSW	4.97	NA	58
	Garberville	12.45	52	54
	Tahoe City	7.18	NA	54
	Donner Memorial St Park	8.13	57	51
	Harris 10 SE	14.53	61	51

Table 11.1. (continued)

Storm Date	Site	Precipitation (inches)	% of HMR 36	% of HMR 59
12/4-6/1966	Johnsondale	16.67	96	92
	Big Pine 13 SE	6.61	NA	71
	Independence	6.46	NA	68
	Greenhorn Mtn Park	11.57	68	67
	Kern River PH 3	7.28	<50	62
	Tinemaha	5.66	NA	61
	Camp Nelson	15.23	73	55
	Lone Pine 13 SE	5.87	NA	53
	Wofford Heights	6.15	<50	51
	Paso Robles	5.86	<50	51
	Milo 5 NE	13.28	74	50
	Springville 7 N	9.61	65	50
1/11-18/1974	Greenview	6.94	69	53
1/3-5/1982	S 96	9.97	65	73
	S 76	9.87	72	72
	S 390	23.64	86	71
	S 401	12.92	79	70
	S 99	9.02	59	70
	S 348	23.31	79	69
	S 382	11.84	79	68
	S 432	13.11	80	67
	S 167	13.81	77	64
	S 100	8.59	56	63
	S 443	11.56	68	61
	S 430	11.60	65	60
	S 124	14.64	104	60
	S 97	8.31	57	60
	S 368	10.74	70	59
	S 398	10.88	66	59
	S 1038	11.05	66	59
	S 383	11.88	70	57
	S 361	11.35	62	57
	S 159	10.50	70	57
	S 364	10.58	64	56
	S 358	12.17	64	56
	S 360	10.31	60	55
	S 371	12.00	63	55
	S 1051	7.54	52	55
	S 98	7.57	51	55
	S 151	11.72	64	55

Table 11.1. (continued)

Storm Date	Site	Precipitation (inches)	% of HMR 36	% of HMR 59
1/3-5/1982 cont.	S 139	9.57	64	55
	S 478	10.87	82	55
	S 440	9.83	58	54
	S 350	19.14	57	54
	S 290	11.34	55	54
	S 74	7.24	53	54
	S 72	7.24	52	54
	S 169	9.06	63	54
	S 362	11.43	63	53
	S 354	19.63	56	53
	S 126	7.11	53	53
	S 130	12.29	61	53
	S 128	10.93	54	53
	S 140	8.88	61	53
	S 365	12.35	66	52
	S 431	15.76	66	51
	S 185	6.28	<50	51
	S 120	9.31	59	51
	S 429	9.05	53	50
	S 428	16.77	63	50
	S 372	20.95	62	50
	S 154	11.38	62	50
	S 413	9.83	61	50
2/14-19/1986	Bucks Lake	17.65	69	63
	Four Trees	17.82	<50	59
	Atlas Road	16.35	103	56
	Sagehen Creek	6.97	52	50

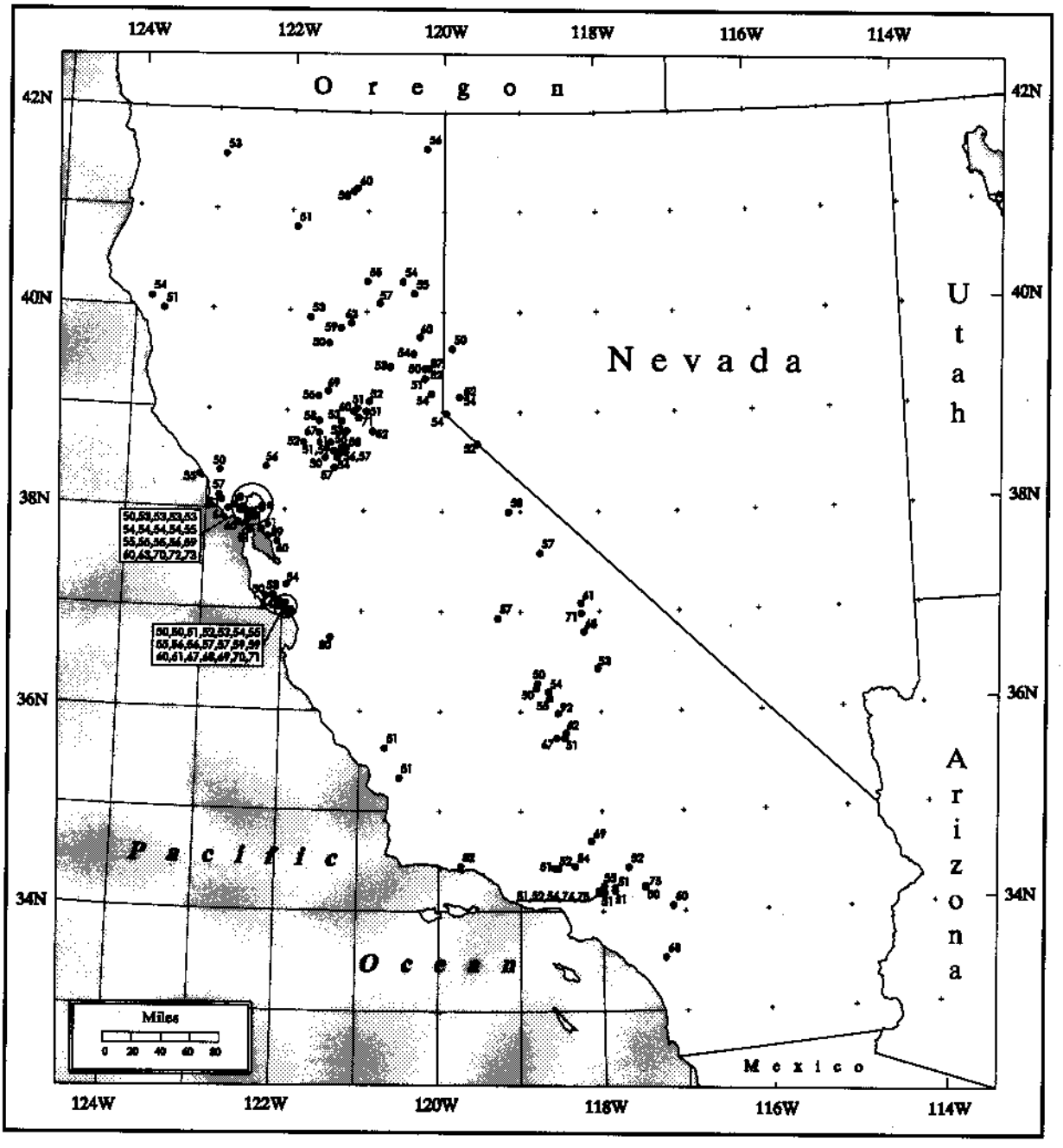

Figure 11.3. *Comparison between maximum point, 24-hour storm precipitation and general-storm PMP estimates at 24 hours, 10 mi². The values represent the ratio of storm precipitation to PMP. Only values greater than 49 percent of PMP are shown.*

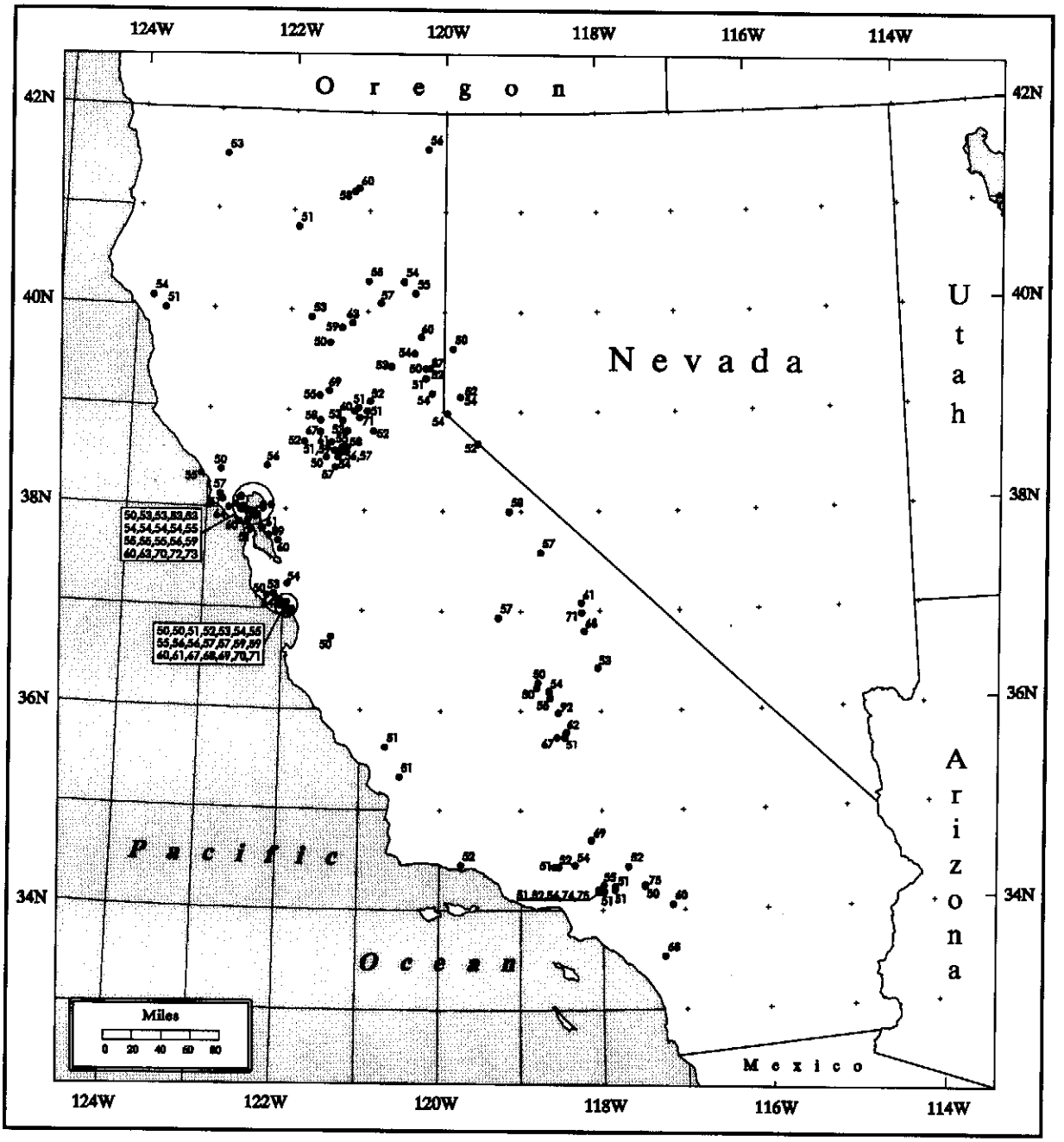

Figure 11.3. *Comparison between maximum point, 24-hour storm precipitation and general-storm PMP estimates at 24 hours, 10 mi². The values represent the ratio of storm precipitation to PMP. Only values greater than 49 percent of PMP are shown.*

used in this station data comparison. The most outstanding ratio from this investigation was at Ferguson Ranch, in the northern Central Valley, on December 4, 1980 where 87 percent of PMP was observed, listed in Table 11.2 and shown in Figure 11.4. This event was embedded in a large-scale heavy rainfall event. This storm was not included in Chapter 2, Table 2.1 since the precipitation associated with the storm at other surrounding stations was not nearly as significant.

Tables 11.1 and 11.2 also show the comparison of station records with HMR 36 PMP. In most cases, the percentages from HMR 36 PMP were higher than those from HMR 59. This suggests that HMR 36 PMP values are lower in most circumstances when compared directly to HMR 59 PMP. In the January 1943 storm, two stations, Hoegees Camp and Camp Leroy Hoegees, surpassed HMR 36 PMP at 102 percent. In the October 1962 storm, one station, Smartsville, registered 116 percent of PMP and two stations were in the 90 percent range. The Johnsondale storm, mentioned previously as 92 percent of HMR 59 PMP, was 96 percent of HMR 36 PMP. The January storm of 1982 had an observation of 104 percent of HMR 36 PMP and February storm of 1986 had a station report of 103 percent of HMR 36 PMP. The comparable values for HMR 59 were 60 and 56 percent respectively. It becomes clear that the revision of HMR 36 is necessary since the PMP values within it were less than those recorded in several events.

11.4 Comparison between General-storm and Local-storm PMP

At small area sizes (< 500 mi^2) and short durations (< 6 hours) local-storm PMP is often larger than general-storm PMP. Chapter 9 has the complete definition. Two sets of ratios were derived using general- and local-storm PMP values at 1 hour and 10 mi^2 and at 6 hours and 10 mi^2. Table 11.3 shows 48 grid-point locations throughout California and the associated ratios of general-storm to local-storm PMP values.

The ratios of general to local PMP values, at 1 hour and 10 mi^2, indicate a fairly consistent relationship, showing slightly higher ratios at the coast and lesser values inland, as seen in Figure 11.5. The exception to this tendency to decrease inland is the area of larger ratios along the central Sierra. The maximum ratio was 71 percent (not shown) along the

Table 11.2. *Maximum 24-hour precipitation values from stations in California. Only ratios greater than 49% of HMR 59 PMP estimates for 24-hours, 10 mi^2 are shown. The same stations were compared to HMR 36 where possible.*

Site	Date	Precipitation (inches)	% of HMR 36	% of HMR 59
Ferguson Ranch	12/4/1980	12.30	85	87
Campo	8/12/1891	11.50	77	82
Nellie	1/17/1916	11.24	70	77
Ship Mountain	1/12/1980	24.23	100	75
Harrison Gulch R.S.	12/3/1970	12.60	70	74
Bieber	3/31/1978	6.40	NA	72
Forest Lake	12/11/1906	6.07	<50	71
Henshaw Dam	2/16/1927	14.48	55	68
Boca	3/20/1907	6.00	NA	65
Sacramento	4/20/1880	7.24	79	63
Benton Inspect Sta.	2/24/1969	5.18	NA	61
Marysville	12/25/1983	7.29	83	60
Fort Ross	11/22/1874	14.72	86	59
White Mountain	1/25/1967	6.90	NA	59
Yreka	1/2/1901	6.30	68	59
Encinitas	10/12/1889	6.42	56	57
San Miguel	1/18/1914	5.32	<50	57
Oakdale Woodard	4/3/1958	5.72	75	56
San Francisco	12/19/1866	7.48	56	56
McCloud	1/23/1915	14.15	52	55
Stirling City	12/30/1913	16.23	59	55
Tehachapi R.S.	3/2/1983	5.30	<50	55
Indio	9/24/1939	6.45	NA	54
Mono Lake	1/31/1963	6.13	NA	54
Raywood Flats	2/10/1927	18.87	67	54
Sierraville	12/30/1913	5.50	<50	52
Independence	12/6/1966	4.95	NA	52
Meeks Bay	1/11/1909	11.99	55	52
San Luis Obispo Poly.	1/19/1969	7.90	60	52
Lakeshore	12/20/1955	15.34	52	51
Platina	12/31/1964	8.00	<50	51
Covina Temple	2/17/1927	10.62	54	50
Kelsey	1/24/1983	9.00	56	50
Upper Snowcreek	11/23/1965	9.50	54	50

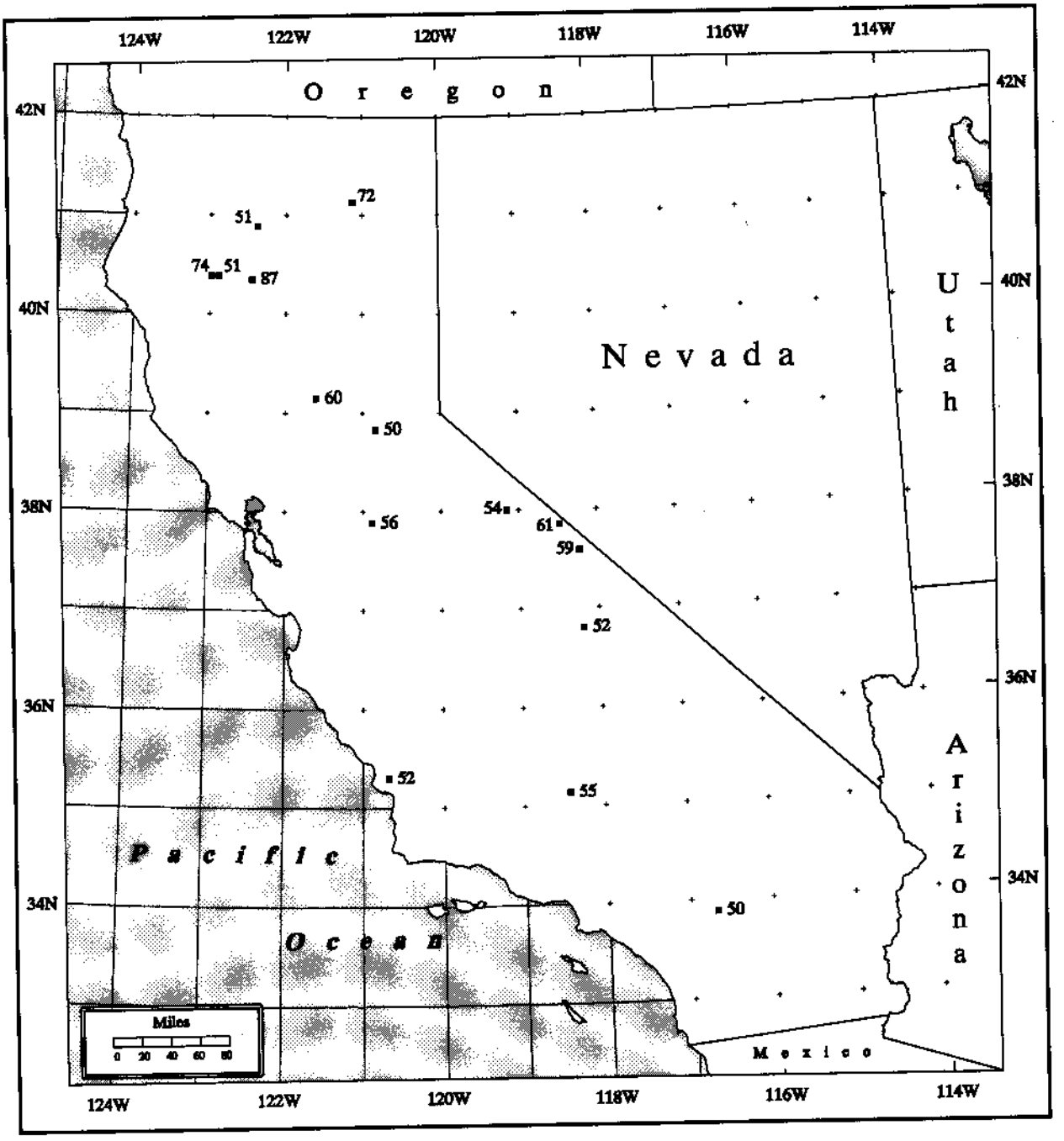

Figure 11.4. *Comparison between maximum recorded point rainfall at cooperative and first-order stations and general-storm PMP estimates at 24 hours, 10 mi^2. The values represent the ratio of historic station data to PMP. Only values greater than 49 percent of PMP are shown.*

Table 11.3. *Comparison of general-storm to local-storm PMP estimates (inches) for various grid-point locations at 1 and 6 hours, 10 mi².*

Lat Lon	Local 1 hr, 10 mi²	General 1 hr, 10 mi²	General/Local 1-hr ratio	Local 6 hr, 10 mi²	General 6 hr, 10 mi²	General/Local 6-hr ratio
42° -124°	4.77	3.05	0.64	5.72	12.18	2.13
42° -123°	6.03	1.45	0.24	7.24	5.87	0.81
42° -122°	7.27	1.41	0.19	8.72	4.59	0.53
42° -121°	7.57	1.34	0.18	9.08	4.35	0.48
42° -120°	7.97	1.34	0.17	9.56	4.36	0.46
41° -124°	5.02	2.49	0.50	6.02	9.98	1.66
41° -123°	7.56	2.58	0.34	9.45	10.34	1.09
41° -122°	9.95	3.58	0.36	13.93	10.74	0.77
41° -121°	7.83	1.34	0.17	9.79	4.37	0.45
41° -120°	8.01	1.33	0.17	9.61	4.34	0.45
40° -124°	4.95	3.52	0.71	6.19	13.01	2.10
40° -123°	7.83	3.10	0.40	10.18	11.45	1.12
40° -122°	7.11	1.76	0.25	9.95	5.67	0.57
40° -121°	7.65	2.23	0.29	9.95	6.68	0.67
40° -120°	8.01	1.34	0.17	9.61	4.36	0.45
39° -123°	5.31	3.20	0.60	6.90	11.07	1.60
39° -122°	4.46	1.31	0.29	5.80	4.25	0.73
39° -121°	6.30	2.39	0.38	8.19	7.18	0.88
39° -120°	7.65	1.19	0.16	9.56	3.57	0.37
38° -123°	4.46	2.21	0.50	5.80	7.65	1.32
38° -122°	4.41	1.62	0.37	5.73	5.62	0.98
38° -121°	4.32	1.51	0.35	5.62	4.88	0.87
38° -120°	6.12	3.30	0.54	7.96	9.90	1.24
38° -119°	7.88	1.29	0.16	9.85	3.87	0.39
37° -122°	4.46	2.78	0.62	5.80	9.61	1.66

Table 11.3. (continued)

Lat Lon	Local 1 hr, 10 mi²	General 1 hr, 10 mi²	General/Local 1-hr ratio	Local 6 hr, 10 mi²	General 6 hr, 10 mi²	General/Local 6-hr ratio
37° -121°	4.41	1.71	0.39	5.73	5.51	0.96
37° -120°	4.32	1.18	0.27	5.62	3.82	0.68
37° -119°	6.21	3.13	0.50	8.07	9.40	1.16
37° -118°	7.92	1.30	0.16	9.90	3.89	0.39
36° -121°	4.86	1.76	0.36	6.32	6.08	0.96
36° -120°	4.32	1.39	0.32	5.62	4.48	0.80
36° -119°	4.46	1.32	0.30	5.80	4.26	0.73
36° -118°	7.43	1.72	0.23	9.66	5.17	0.54
36° -117°	8.73	3.76	0.43	11.35	7.51	0.66
36° -116°	9.45	2.96	0.31	11.81	5.93	0.50
35° -120°	5.36	3.82	0.71	6.97	13.09	1.88
35° -119°	6.03	1.09	0.18	7.84	3.52	0.45
35° -118°	8.15	2.38	0.29	10.60	4.76	0.45
35° -117°	9.09	2.65	0.29	11.82	5.30	0.45
35° -116°	9.54	2.71	0.28	12.40	5.42	0.44
35° -115°	9.90	4.41	0.45	12.87	8.81	0.68
34° -118°	6.75	2.77	0.41	9.45	9.48	1.00
34° -117°	10.22	2.69	0.26	14.31	9.23	0.65
34° -116°	10.40	3.76	0.36	14.56	7.51	0.52
34° -115°	10.22	3.88	0.38	13.29	7.76	0.58
33° -117°	8.10	1.87	0.23	11.34	6.40	0.56
33° -116°	10.85	3.76	0.35	15.19	7.52	0.50
33° -115°	10.56	4.01	0.38	13.73	8.03	0.58

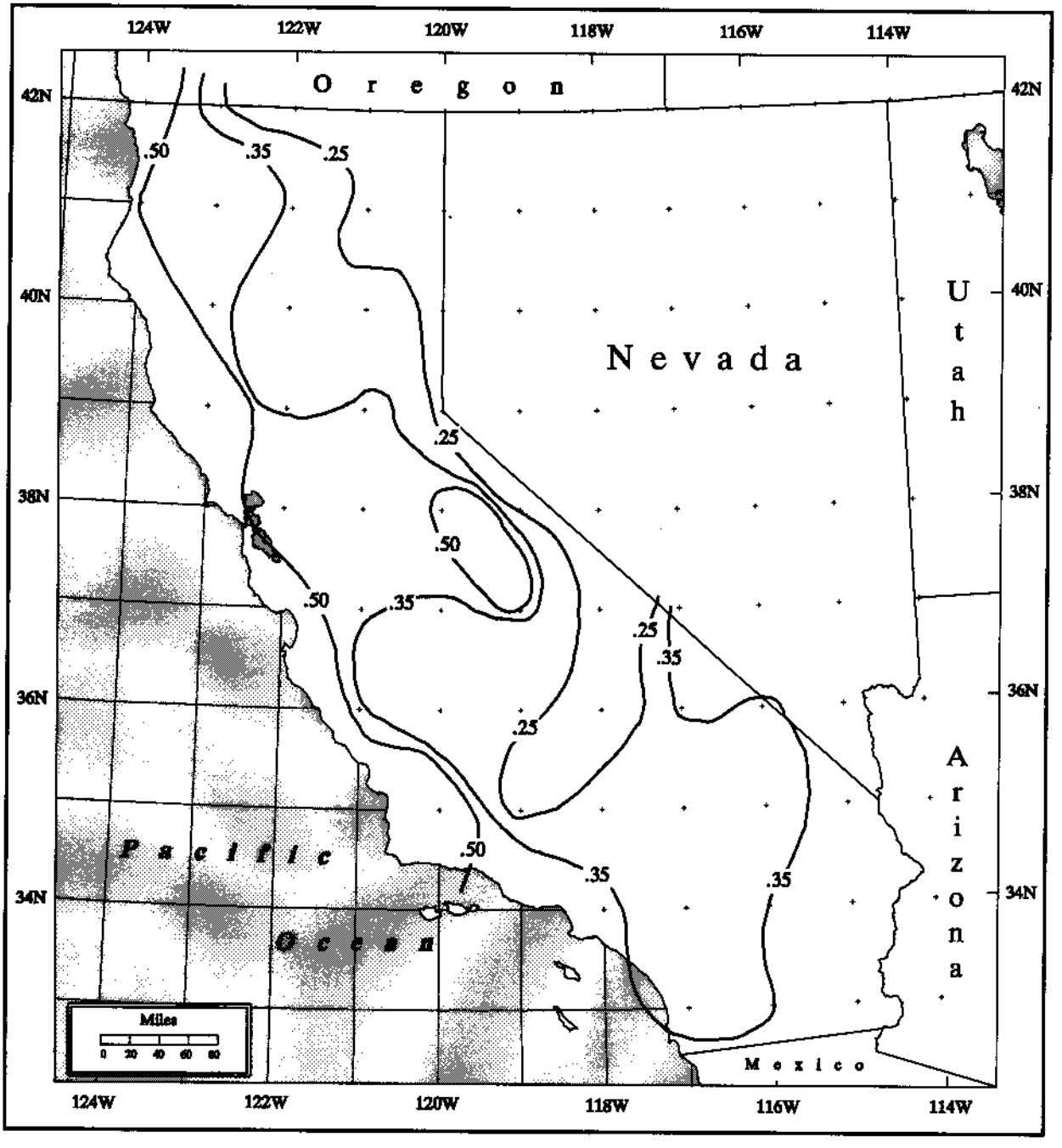

Figure 11.5. *Ratios of general-storm to local-storm PMP estimates at 1 hour, 10 mi².*

coast where local-storm values are at their lowest and general-storm values are relatively high. At 6 hours, 10 mi^2 the differences between general-storm and local-storm PMP become larger, as seen in Figure 11.6. Along the coast general-storm to local-storm ratios are well over one, but quickly fall off inland. Again a secondary maximum (> 1.0) occurs along the Sierra Nevada mountains. The maximum ratio values stretch along the northwestern coast of California and reach a high of 2.13.

These comparisons are somewhat forced or artificial in that for all but the southeastern region, (Chapter 3, Figure 3.2), the general-storm values are usually from wintertime storms, whereas local-storm values come from summertime events. Had the comparisons been made during the summertime months alone, one could expect the ratios shown in Figure 11.5 and 11.6 to be somewhat lower. Both figures demonstrate the need to examine both types of storms when trying to determine PMP for a specific location. These figures show a small sample of the range of possible PMP comparisons.

11.5 Comparison to Adjoining PMP Studies

The California study region is surrounded by the Pacific Ocean, Oregon, Nevada, Arizona, and Mexico. HMR 57 for Oregon and Washington borders the region on the north and HMR 49 not only borders on the east but applies to the areas east of the Sierra Nevada mountains and the desert southeast. This section will examine how the results of the new PMP agree with these two studies.

11.5.1 Comparison to HMR 57

Although this report was developed independently of neighboring studies, many of the same techniques were applied from earlier hydrometeorological reports to prepare HMR 59. HMR 57 borders HMR 59 on the north along 42°N and storms that have centers in northern California were also used for PMP calculations in Oregon and Washington. Likewise, storms used in HMR 57 were used in California. Thus, the two studies used some of the same data. In addition, the means of analysis and methodology were similar, allowing a certain level of continuity.

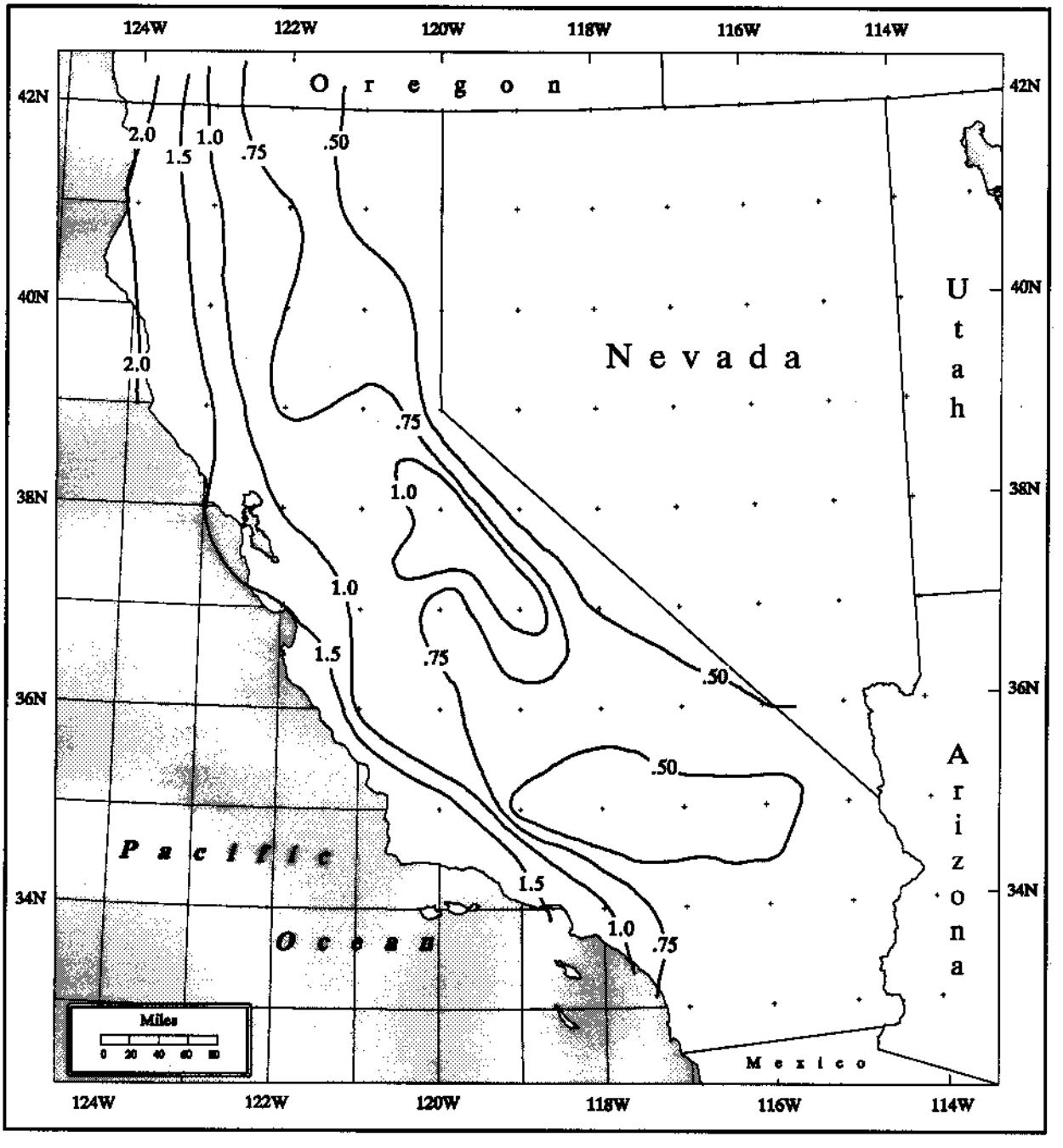

Figure 11.6. *Ratios of general-storm to local-storm PMP estimates at 6 hours, 10 mi².*

The 24-hour, 10-mi^2 PMP Index analysis from HMR 59, with a few minor adjustments, agrees with HMR 57 rather closely. This is to be expected since HMR 57 was recently completed (as far as HMRs are concerned) and the methods used were very similar to those used for this study. At all area sizes and durations, the differences are minor due to the similarity of methodology and data. Table 11.4 shows the relative differences in percent between the HMR 59 and HMR 57 depth-area-duration relations. The greatest differences appear at area sizes of 500 mi^2 and less. Negative differences (HMR 59 less than HMR 57) up to 8.7 percent, at 6 hours, 100 mi^2 are noted. At area sizes of 2000 to 5000 mi^2 and durations equal or greater than 24 hours, the relations actually reverse slightly so that by 48 hours, 5000 mi^2, HMR 59 values are one percent higher than HMR 57. In all other cases, the values in HMR 59 are zero or slightly less than HMR 57 along the border between Oregon and California.

Table 11.4. *Percent differences in depth-area factors at 42° N (HMR 59 minus HMR 57).*

mi^2	1 hr	6 hr	24 hr	48 hr	72 hr
10	0.0	0.0	0.0	0.0	0.0
50	-7.0	-7.7	-6.1	-4.75	-3.8
100	-7.0	-8.7	-5.7	-5.2	-3.8
200	-6.5	-8.0	-5.9	-4.8	-3.15
500	-3.1	-5.7	-3.95	-2.6	-1.3
1000	-2.2	-3.8	-1.7	-0.5	+0.3
2000	-0.4	-1.3	+0.1	-0.2	0.0
5000	-0.3	-0.3	+0.8	+1.0	+0.2
10000	-0.2	-0.3	-0.2	0.0	0.0

11.5.2 Comparison to HMR 49

HMR 49 covers the Colorado and Great Basin drainage that includes a large portion of eastern California. More specifically, HMR 49 includes areas just east of the Sierra Nevada mountains and the deserts of southeast California. Comparisons were conducted throughout the region for various area sizes and durations where HMR 59 and HMR 49 overlap and are shown in Table 11.5. The depth-area-duration (DAD) regions from HMR

59 (Chapter 3, Figure 3.2) that are also covered in HMR 49 include the Northeast, Sierra, Southeast, and Southwest.

Table 11.5. *Average percentages of HMR 59 Index values compared to HMR 49. The Northeast region consists of 5 data points, the Sierra has 6 data points, and the Southeast has 33 data points.*

Region	mi^2	6 hr	12 hr	24 hr	48 hr	72 hr
Northeast	10	125	114	118	119	113
	200	125	111	112	114	109
	1000	132	111	110	112	107
	5000	127	98	96	96	93
Sierra	10	84	87	93	105	103
	200	81	83	88	100	100
	1000	82	82	86	98	100
	5000	81	79	82	93	96
Southeast	10	88	95	89	85	87
	200	89	96	89	85	88
	1000	88	94	87	82	85
	5000	79	85	77	71	73

As for methodology, HMR 49 was not based exclusively upon storm-derived DAD as were HMR 57 and HMR 59 . Therefore, agreement between HMR 59 and HMR 49 PMP values were not expected to be as close as those found between HMR 59 and 57. Another difference is that HMR 49 does not permit 1-hour general-storm PMP estimates to be determined directly so comparisons cannot be made at this duration. Furthermore, the relationship between HMR 59 and HMR 49 differs markedly from the variation reported between HMR 59 and HMR 36. As noted above, HMR 59 PMP is larger than HMR 36 at small-area sizes. However, differences decrease as area sizes increase. Differences between HMR 59 and HMR 49 are not nearly as consistent. In general, HMR 59 PMP values, at all area sizes from north to south, transition from greater than HMR 49 PMP values in the north to less in the south. Within the regions themselves the most prevalent tendency is for HMR 59 values to decrease with respect to area size.

For the three regions adjacent to HMR 49 composite averages were made using data points from each area. Clearly, in the Northeast region, HMR 59 values are larger at most durations and area sizes (Table 11.5). The largest positive differences occur at 10 mi^2 and slowly decrease with increasing area size and to some extent with duration. At 5000 mi^2, however, HMR 59 values become slightly less than HMR 49.

In the Sierra region, along the east side of the Sierra Nevada mountains HMR 59 PMP values, for the most part, fall below HMR 49 levels. However, PMP values in HMR 59 are nearly equal to or larger than HMR 49 at 48 and 72 hours for all of the Sierra regions. HMR 49 is greater at all 6-hour and 12-hour areas and nearly equal otherwise.

In the Southeast region, HMR 59 PMP values are less than HMR 49 PMP values. These differences tend to increase with increasing area size (i.e., ratios are smaller) and to a lesser extent with duration. Most comparisons in this region show that changes are less than 25 percent except in a few areas along the region boundaries where some larger variations do exist due to the classification of regions.

12. CONCLUSIONS AND RECOMMENDATIONS

This report, HMR 59, presents principles and development of probable maximum precipitation (PMP) for California. It is a revision of HMR 36 (1961) and the California area of HMR 49 (1977). The methodology is much the same as in HMR 55A (Colorado River Basin, 1988) and HMR 57 (northwestern United States, 1994). PMP estimates from this study are compared with its predecessors, HMR 36 (California) and HMR 49 (Colorado River and Great Basin Drainages), and with other indices, such as record storms in other parts of the world in order to evaluate the results. HMR 59 includes all of the procedures for calculating PMP and describes the principles and development of PMP estimates for 10 mi^2 to 10,000 mi^2 and 1 to 72 hours. Local-storm PMP estimates are described for 1 mi^2 to 500 mi^2 and 15 minutes to 6 hours. HMR 58 (1998), its immediate predecessor contains, in entirety, the PMP calculation procedures, including snowmelt, which are found here in Chapter 13 and Appendix 4. HMR 58 and HMR 59 are different presentations of the same study, with HMR 58 containing calculation procedures only, and HMR 59 containing a description of the complete study, including the calculation procedures.

Among the important achievements and conclusions set by this study are:

1. HMR 58 (1998), Calculation Procedures for California PMP is the first Hydrometeorological Report available in full on the world wide web. HMR 58 is a section of HMR 59.

2. Established a digital storm analysis procedure to routinely analyze major storms in an objective, consistent, and timely manner. A geographic information system (GIS) was employed to develop spatial and temporal relationships important for depth-area-duration (DAD) analysis and finally for PMP estimate calculations.

3. All-season, general-storm PMP estimates and monthly variations are provided for area sizes of 10 to 10,000 mi^2 and durations up to 72 hours. Besides the all-season general-storm PMP Index values, seasonal adjustments were prepared for all months of the year.

4. New climatologies of 3-hour and 12-hour maximum persisting dewpoints were developed.

5. PMP for California was established that is consistent with PMP for the Pacific Northwest (HMR 57).

6. In comparison with HMR 36 Index values Index PMP (10-mi^2, 24-hour) has increased substantially in certain sections of the Coastal Mountains, and along the length of exposed portions of the Sierra Nevada; and decreased in limited areas in non-orographic regions and locations downwind of significant mountains.

7. Short-duration, general-storm PMP values (1, 6, 12 hours) are higher than HMR 36; while longer-duration (24, 48, 72 hours) values have remained constant or decreased for the most part.

8. As a function of area size, general-storm PMP values have increased substantially for drainages smaller than 200 mi^2, while for areas greater than 200 mi^2 PMP values are generally less than in HMR 36.

9. The ratios between PMP values at 24 hours and 100-year precipitation values from NOAA Atlas 2 were found to be consistent with similar comparisons made in other parts of the western United States.

10. Local-storm PMP estimates were provided for all of California, including the northwest corner of the state which had not been covered by HMR 49.

11. A synoptic climatology for local storms was developed and was used to set 6-hour to 1-hour ratios of point rainfall for California local storms.

12. Local-storm PMP values are about 10 to 15 percent higher in California north of 40°, compared with HMR 49; while changes over most of the rest of the state were plus or minus 5 percent. Durationally, little change was found at 1 hour, but a wider range of decrease was found at 6 hours.

13. The PMP estimates derived for this report are the best available for California, and should be applied to all future design studies.

14. The estimates available from this report represent storm-centered, average depths of PMP that form the basis for site-specific applications.

15. The procedures provided in Chapter 13 are relatively simple to apply, and cover both general-storm and local-storm PMP applications.

As a consequence of this study, the following recommendations are made:

1. That future effort be made to determine how best to areally and chronologically distribute average PMP values from this study.

2. That climatological data be reviewed to determine whether the recommended time sequences of temperature, dewpoints, winds and precipitation used in Appendix 4 (Snowmelt) continue to be appropriate; that future study on the probable maximum snowpack and corresponding maximum rainfall be done.

3. Although storm analysis was accomplished relatively quickly, work towards a more automated system should be continued. This will enhance the ability to archive more storm events as they happen.

4. That effort be made towards applying radar precipitation data to current and future analysis, both storm spatial and durational. A bridge towards radar data and away from the Theissen polygon approach would be a positive step. Since much of the country is covered by WSR-88D radar, and data collection procedures are in place, data transfer to a GIS system is possible.

5. Work with model developments to enhance the understanding of physical processes assumed in this and other PMP studies.

6. That studies be carried out for California considering basin and storm area sizes, seasonality at the geographic variation of antecedent precipitation.

13. COMPUTATIONAL PROCEDURE

13.1 Introduction

The steps to calculate probable maximum precipitation (PMP) for general and local storms in California are provided in this chapter. All tables, figures, and plates are included here. As in the procedures recommended in HMR 55A (1988) and HMR 57 (1994), these steps produce storm-centered, average depths of PMP applicable to a specific drainage.

General-storm PMP may be determined for durations from 1 to 72 hours over areas from 10 to 10,000 mi^2, and local-storm PMP may be determined for durations from 15 minutes to 6 hours over areas between 1 and 500 mi^2. When making PMP estimates for basins less than 500 mi^2, it is recommended that both general and local-storm PMP be calculated. The larger of these estimates represents the basin PMP. The decision as to which of these results is most critical for the basin involves hydrological considerations related to flooding, and are beyond the scope of this report. The final selection of PMP, local- or general-storm value, is a choice for the user. Seasonal variation of general-storm PMP has been included to aid the user when other hydrologic factors have a bearing on water management decisions. The seasonal information is shown in Figures 13.1 to 13.10.

We have attempted to keep the computational procedure in this report simple and straightforward. The Index PMP map was drawn for the general storm at 1:1,000,000 scale for northern and southern sections of California, with an overlap of at least one degree of latitude. The maps contain latitude and longitude markings, county boundaries, and selected cities or towns. In addition, each index map contains regional boundaries for use with DAD relations. These maps accompany this report, Plates 1 and 2. See Endnote[1] for map supplement requests.

If calculations are being made for a drainage which encompasses more than one DAD region (Figure 13.11, and also outlined on Plates 1 and 2), use proportionally-weighted

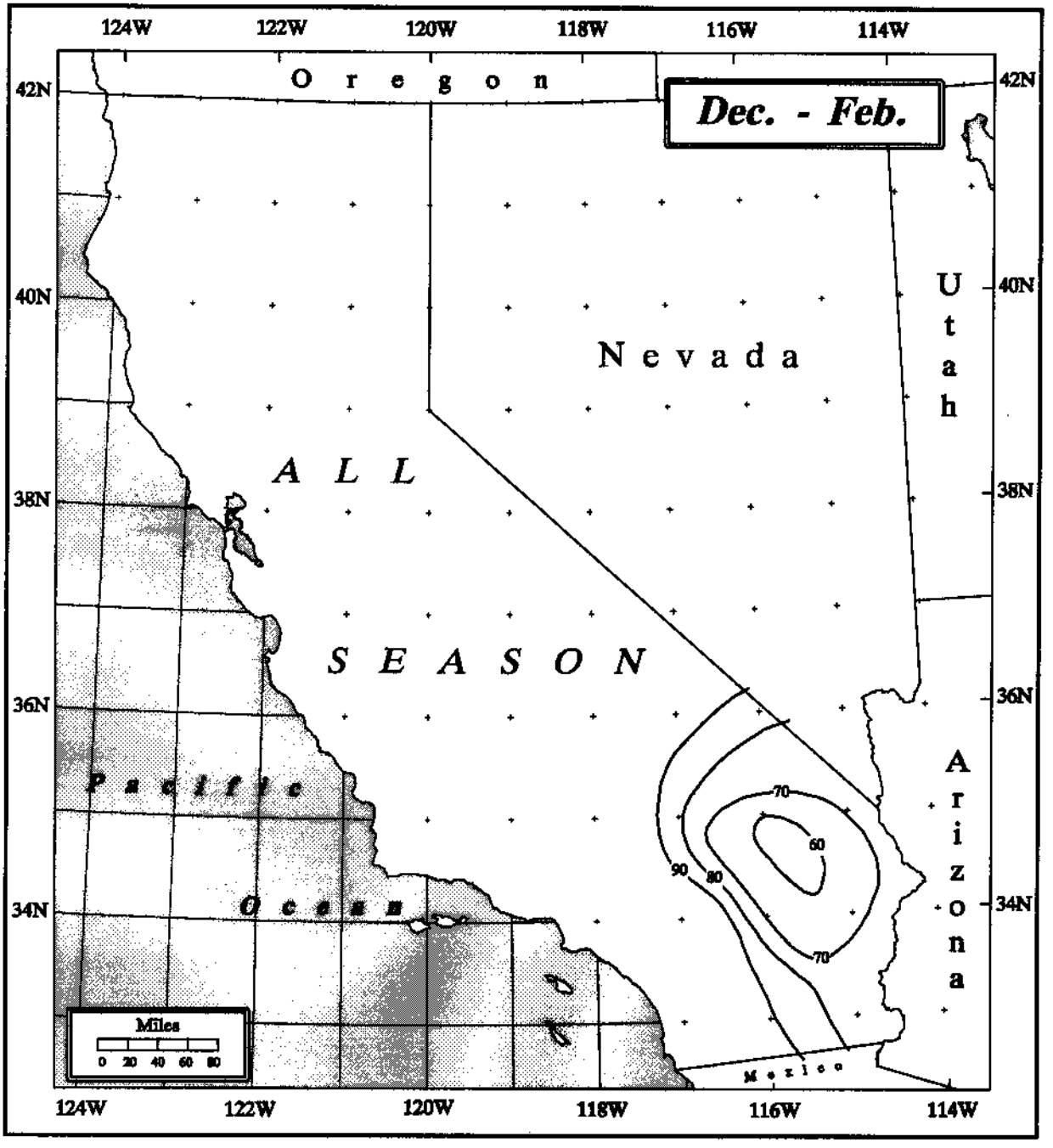

Figure 13.1. *10-mi² 24-hour general-storm PMP for December through February in California as a percent of all-season PMP (Plates 1 and 2). Same as Figure 7.2.*

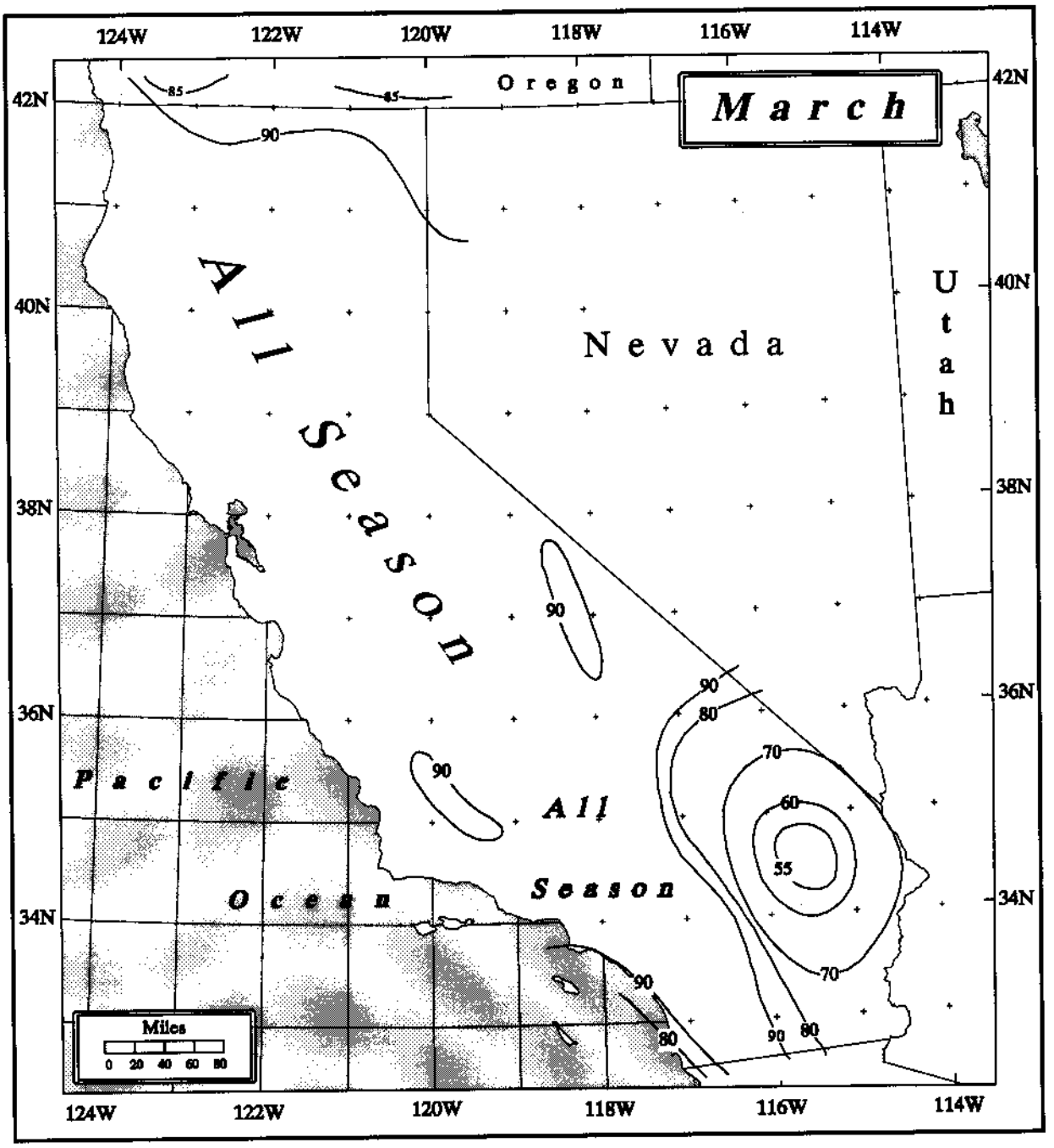

Figure 13.2. *10-mi² 24-hour general-storm PMP for March in California as a percent of all-season PMP (Plates 1 and 2). Same as Figure 7.3.*

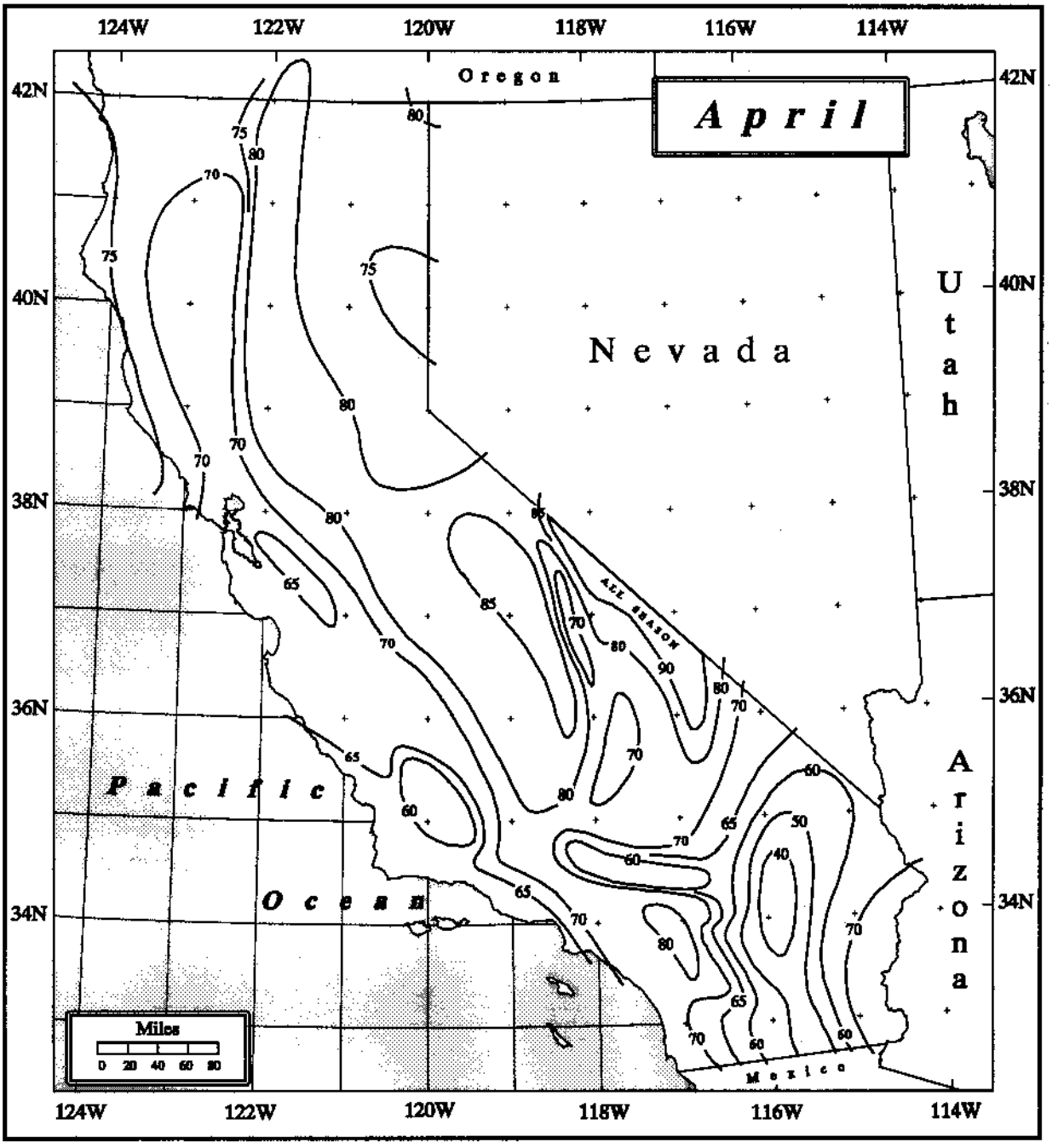

Figure 13.3. *10-mi² 24-hour general-storm PMP for April in California as a percent of all-season PMP (Plates 1 and 2). Same as Figure 7.4.*

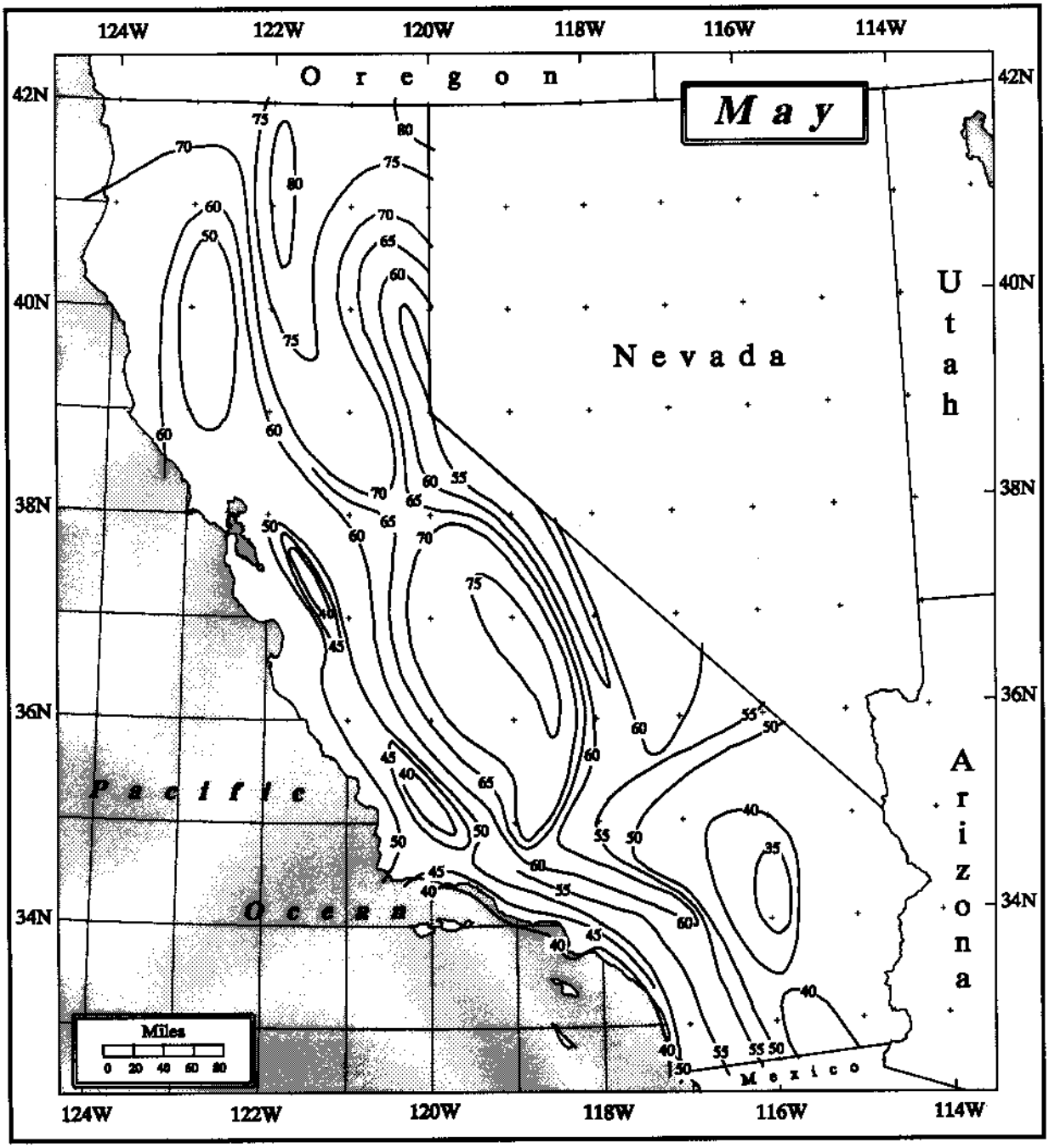

Figure 13.4. *10-mi² 24-hour general-storm PMP for May in California as a percent of all-season PMP (Plates 1 and 2). Same as Fiure 7.5.*

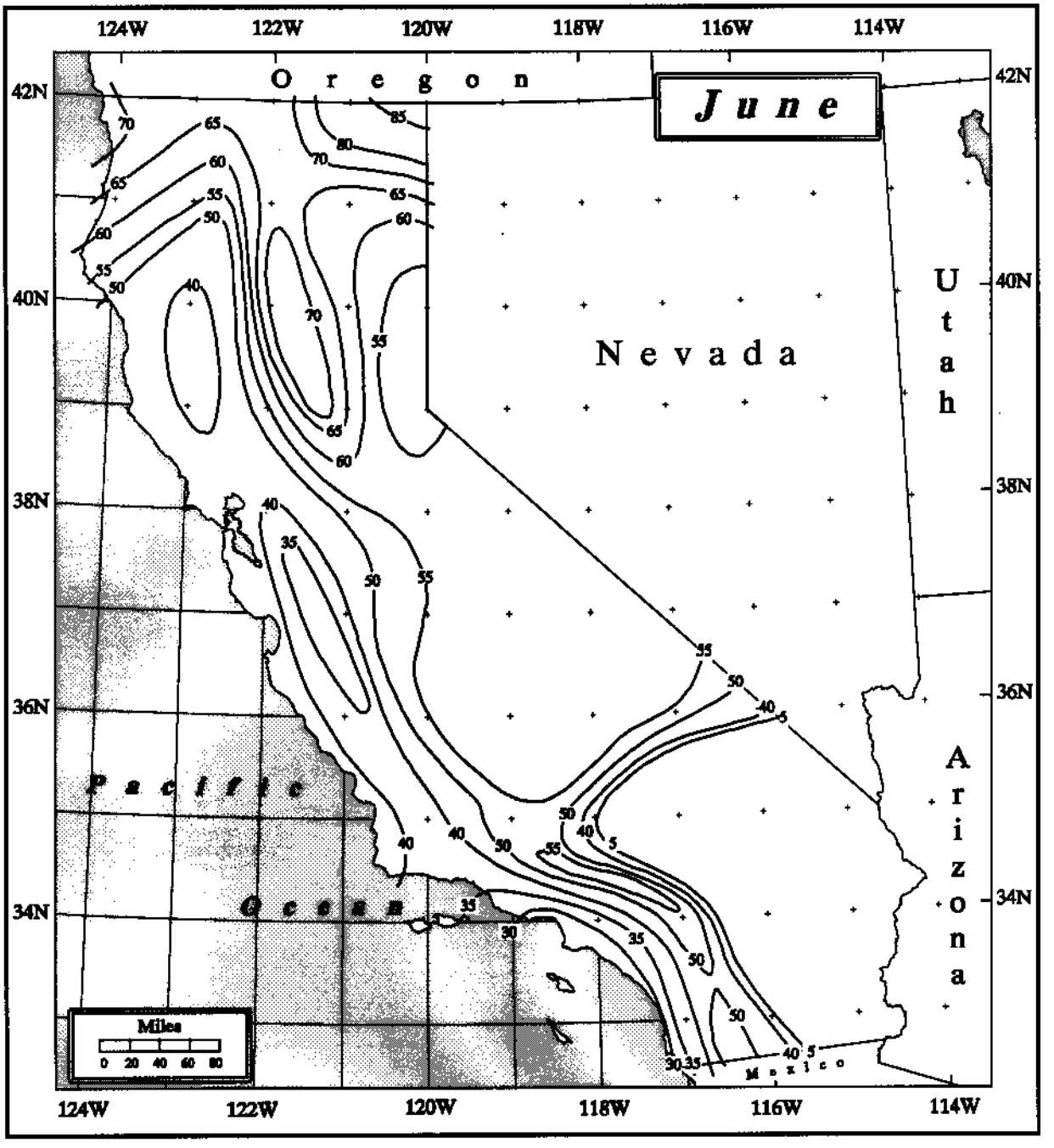

Figure 13.5. *10-mi² 24-hour general-storm PMP for June in California as a percent of all-season PMP (Plates 1 and 2). Same as Figure 7.6.*

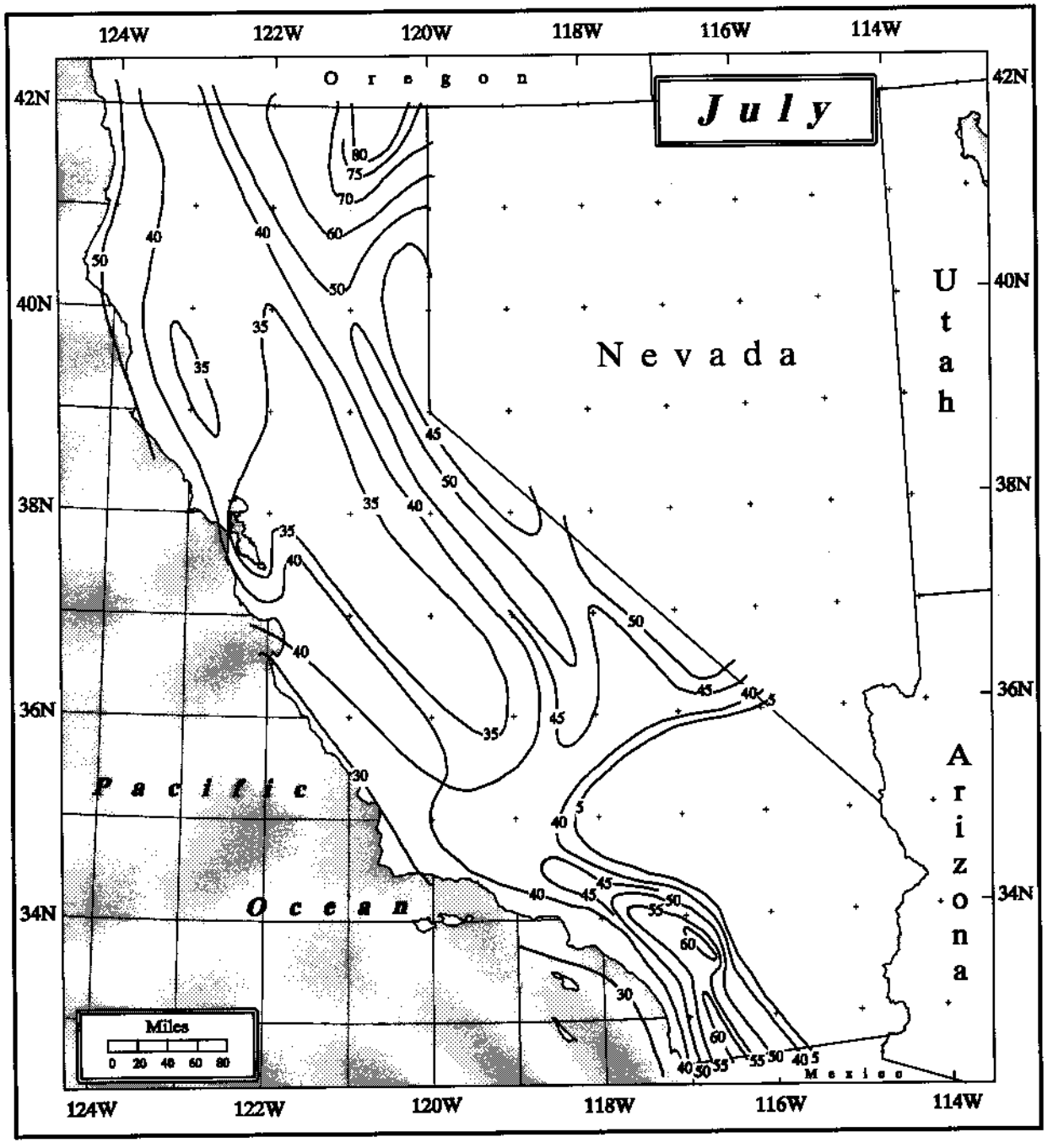

Figure 13.6. *10-mi² 24-hour general-storm PMP for July in California as a percent of all-season PMP (Plates 1 and 2). Same as Figure 7.7.*

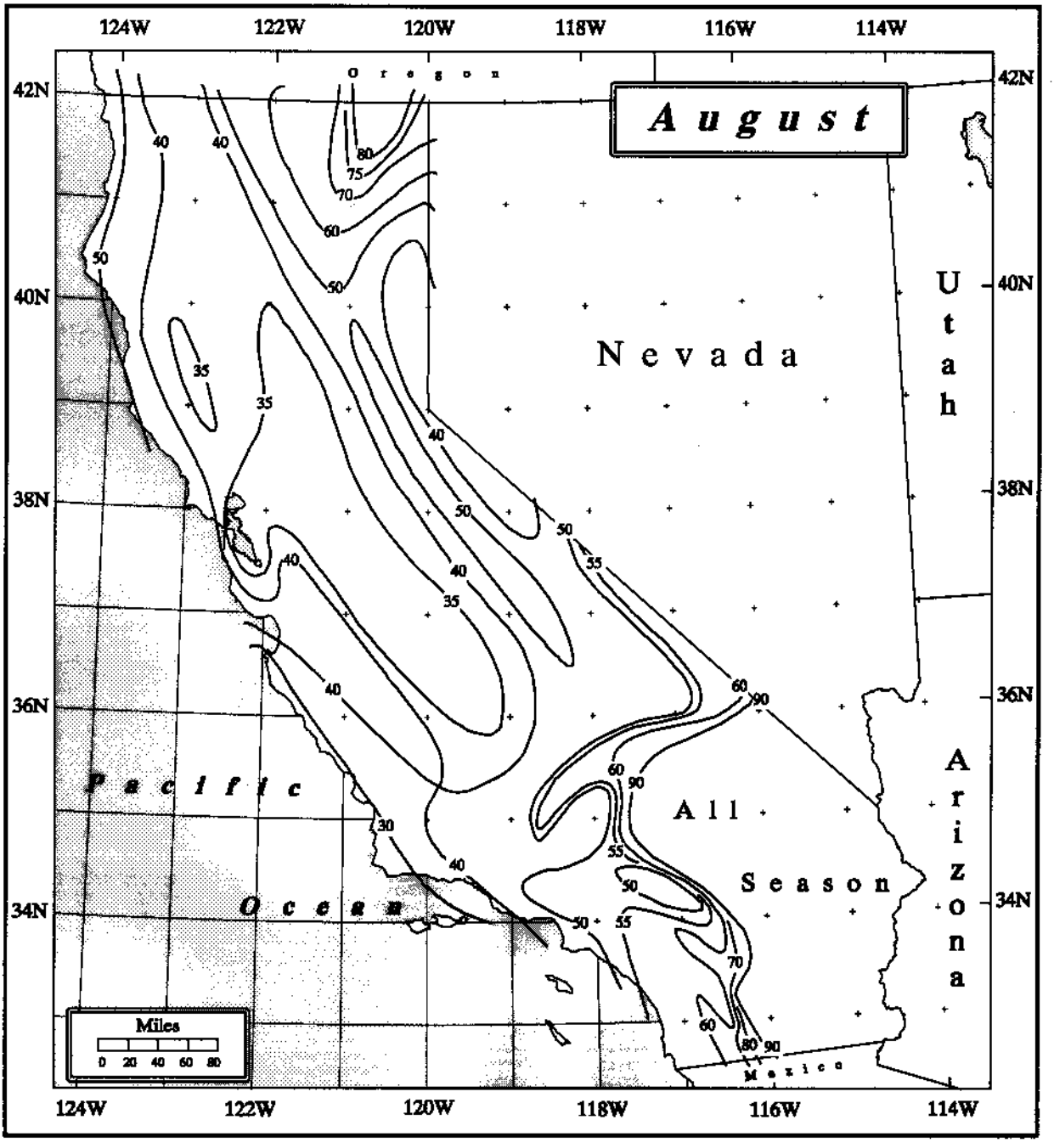

Figure 13.7. *10-mi² 24-hour general-storm PMP for August in California as a percent of all-season PMP (Plates 1 and 2). Same as Figure 7.8.*

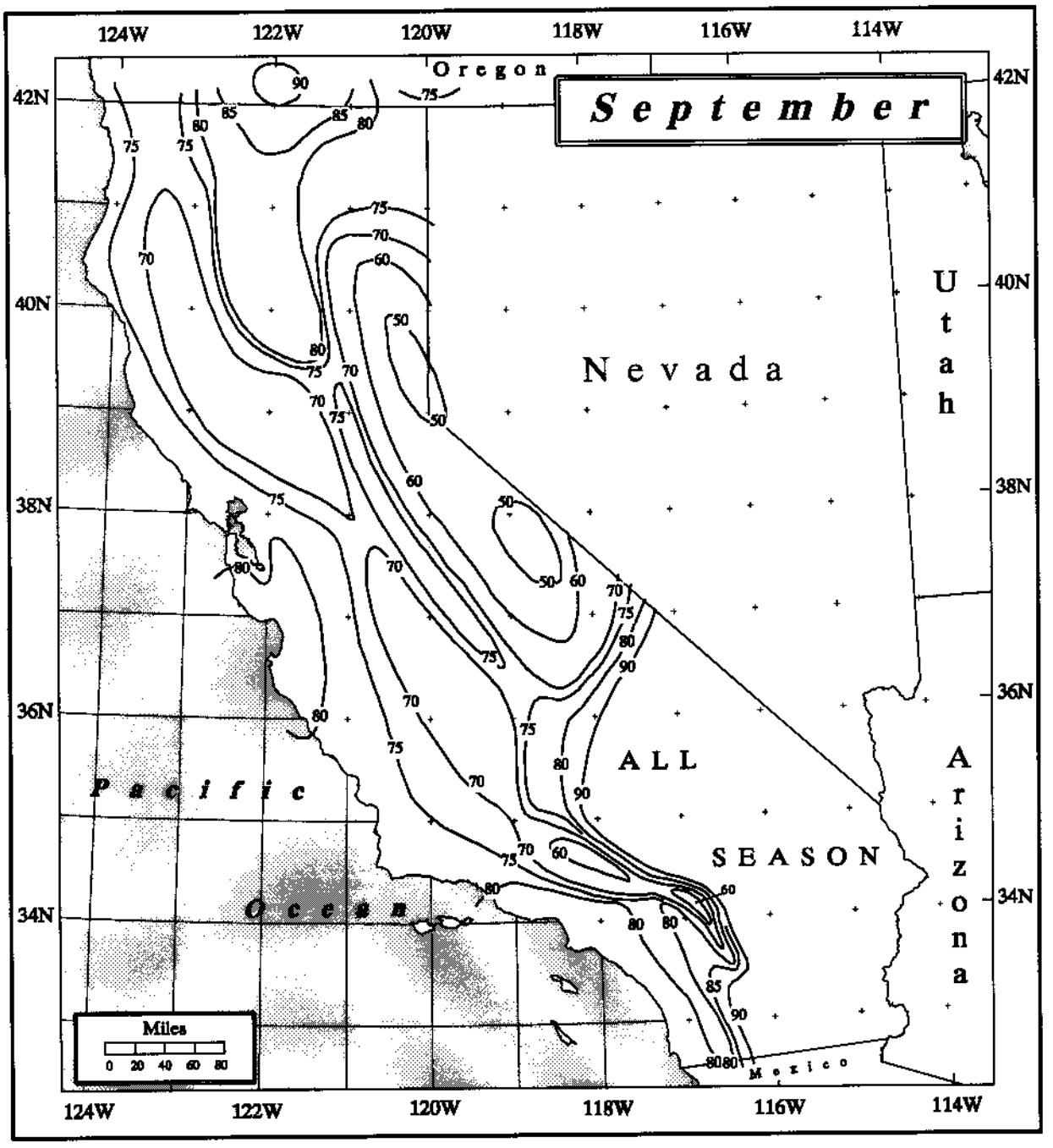

Figure 13.8. *10-mi² 24-hour general-storm PMP for September in California as a percent of all-season PMP (Plates 1 and 2). Same as Figure 7.9.*

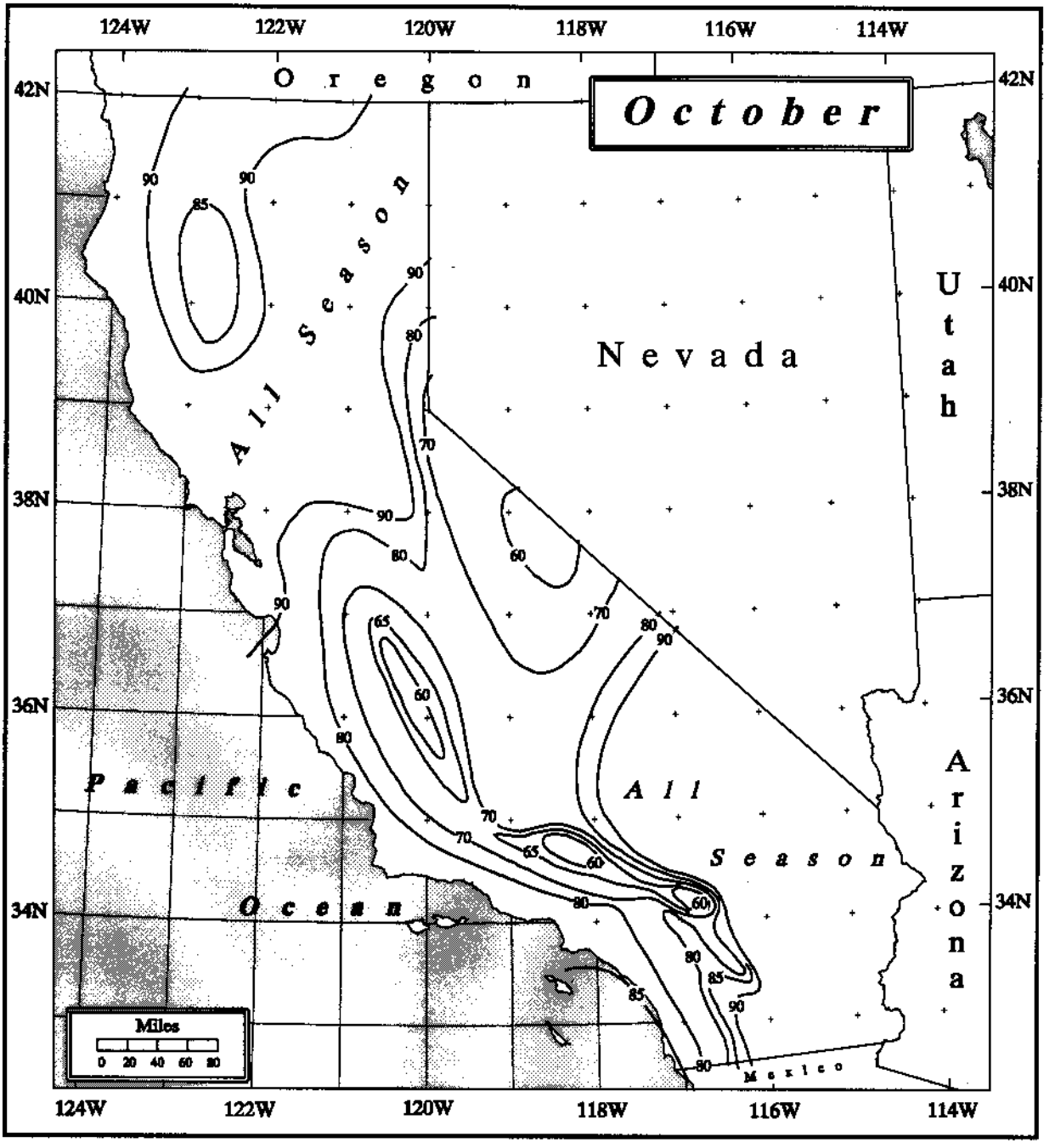

Figure 13.9. *10-mi² 24-hour general-storm PMP for October in California as a percent of all-season PMP (Plates 1 and 2). Same as Figure 7.10.*

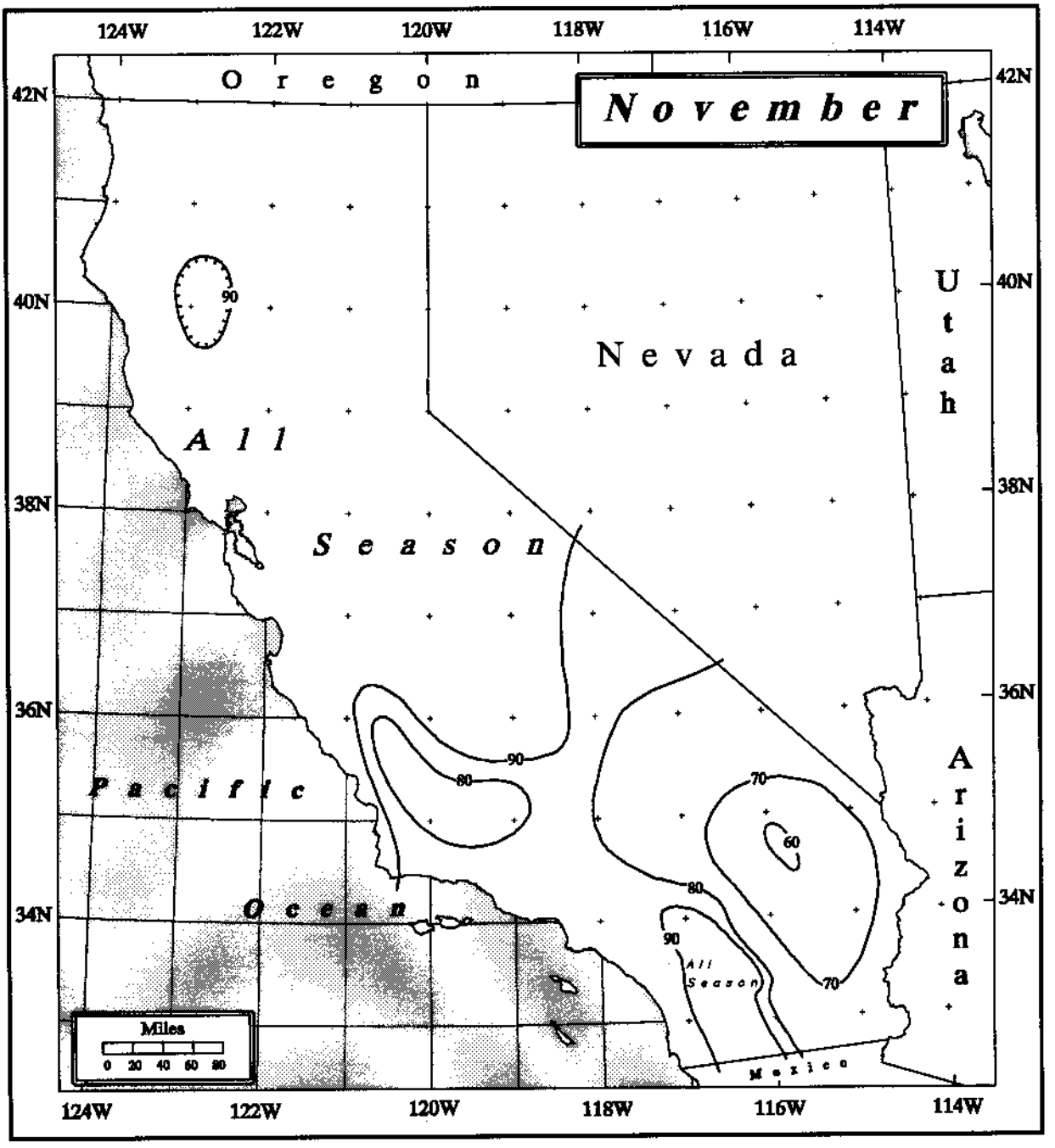

Figure 13.10. *10-mi² 24-hour general-storm PMP for November in California as a percent of all-season PMP (Plates 1 and 2). Same as Figure 7.11.*

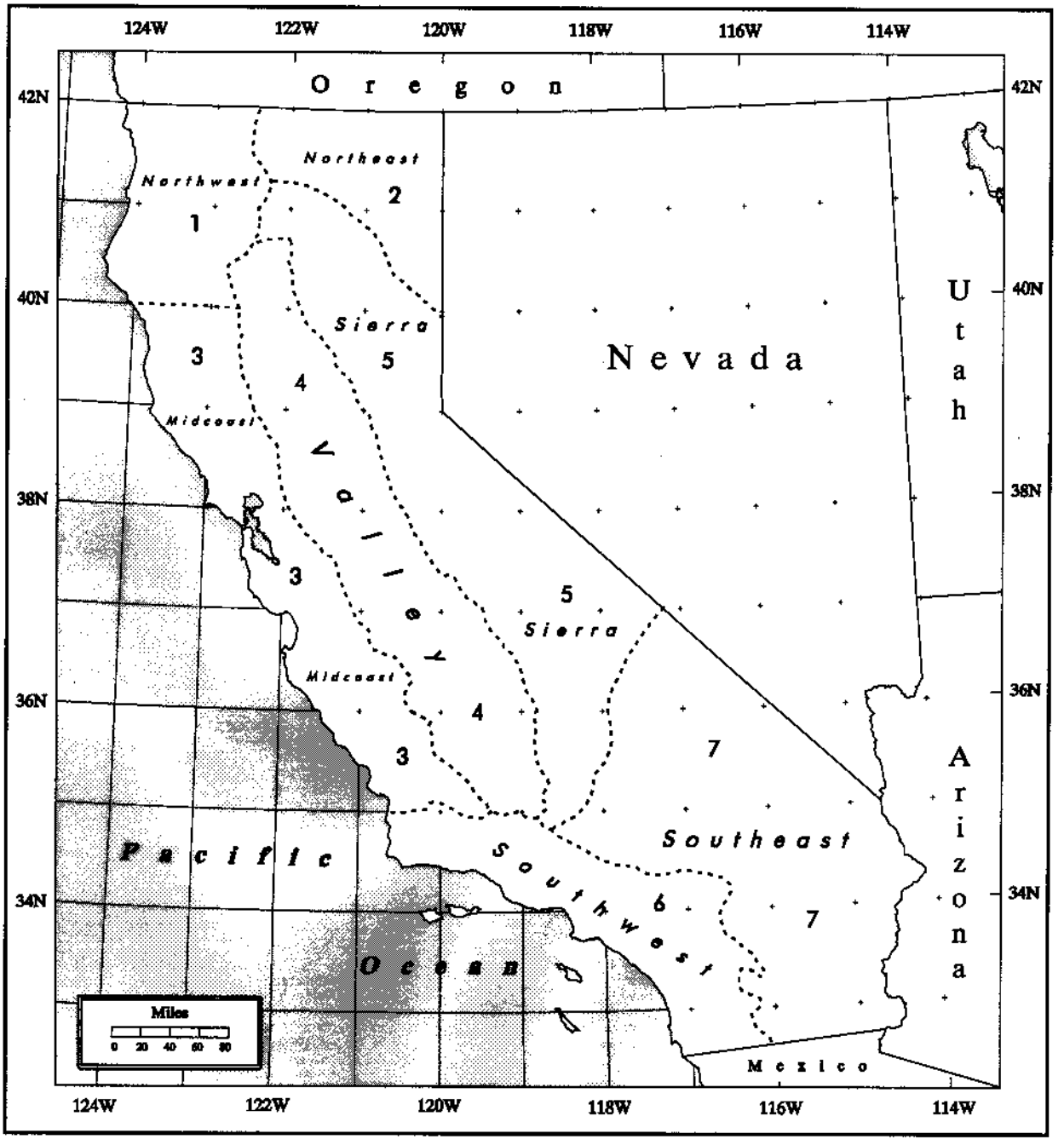

Figure 13.11. *Regional boundaries for development of depth-area-duration relations. Same as Figure 3.3.*

results; i.e., calculate results for each subregion separately and then combine the PMP values in a manner proportional to the area of each subregion. For example, for a drainage of 100 area units which encompasses three subregions each having areas of 70, 20, 10 units respectively, the resulting average value for the drainage, R, is:

$$R = ((R_1)\ 70 + (R_2)20 + (R_3)10)/100$$

where R_1, R_2, and R_3 are the average PMP values within each of the subregions within the drainage.

The following sections present the detailed steps needed to specify PMP either for all-season, i.e., an annual maximum, or for any individual month of the year. These steps are comprehensive, in the sense that they are applicable for any and every drainage in California. The procedures outlined here, along with the general-storm Index map, have been peer-reviewed. If a user finds that these steps, with their supporting maps, figures, or diagrams, do not account for some unique hydrometeorological aspect of a particular drainage, he or she should consult the Hydrometeorological Design Studies Center staff of the National Weather Service to determine the best course of action.

13.2 General Storm Procedure

Step

1. Drainage Outline

   Trace the outline of the perimeter of the drainage of concern (at 1:1,000,000 scale) onto a transparent overlay, or define the basin boundary using a Geographic Information System (GIS).

2. User Decision

   Decide whether an all-season (annual) PMP value is needed or seasonal PMP is required.

3. All-Season Index PMP Estimate

Place the drainage overlay on the appropriate all-season index map and make a uniform grid that covers the drainage. Obtain index map estimates of PMP for each grid point and determine the drainage average index PMP amount. The grid separation size should take into account the gradient of PMP across the drainage, so that reasonably representative results will be obtained. This step can also be done using a GIS or other commercial software. In areas with extreme gradients, such an analysis would be more accurate when using the digital file of Plates 1 or 2, which is available from the Hydrometeorological Design Studies Center.

4. Seasonal Index PMP Estimates

Skip to Step 5 if all-season PMP alone is required. Figures 13.1 to 13.10 are the starting point for seasonal PMP estimates. Determine the average value for each month to the nearest whole percent within the drainage and plot them on graph paper at the midpoint of each month. Draw a smooth curve through the points. In doing this a range of plus or minus 5 percent is allowed for any percentage at or below 85 percent. Select the percentage at any point in the selected month(s) from the smoothed curve. Any month with a selected percentage higher than 90 percent is treated as a month in which the all-season value of PMP applies, i.e., 100 percent applies to such a month. Multiply the all-season, average value of PMP from Step 3 by the percentage from this step.

For each month of interest determine the value of the monthly offset from the all-season envelope (90% or greater) for that month. The offset is determined by "taking the shorter path" or by counting the number of months from the nearest all-season month.

5. Depth-Duration Relations

The depth-duration subregions for California are shown on Figure 13.11. These subregions are also delineated on Plates 1 and 2. For the subregion containing the drainage of interest, read the corresponding depth-duration ratios from Table 13.1

(all-season) or Table 13.2 (seasonally adjusted) and multiply each by the 24-hour result obtained from Step 3 (all-season) or Step 4 (seasonally-adjusted). Use proportionally-weighted results if more than one subregion is subtended by a drainage boundary.

Table 13.1. *All-season PMP depth-duration ratios for 10mi² for California regions.*

	Duration					
Region	**1**	**6**	**12**	**24**	**48**	**72**
Northwest	0.10	0.40	0.73	1.00	1.49	1.77
Northeast	0.16	0.52	0.69	1.00	1.40	1.55
Midcoastal	0.13	0.45	0.74	1.00	1.45	1.70
C. Valley	0.13	0.42	0.65	1.00	1.48	1.75
Sierra	0.14	0.42	0.65	1.00	1.56	1.76
Southwest	0.14	0.48	0.76	1.00	1.41	1.59
Southeast	0.30	0.60	0.86	1.00	1.17	1.28

6. Areal Reduction Factors

Obtain the all-season reduction factors from either Table 13.3, or from Figures 13.12 to 13.17, as appropriate. For a specific month, however, use Tables 13.4 to 13.9 (interpolate to the required drainage area size) using the monthly offset for seasonal PMPs selected in step 4. Multiply the applicable reduction factors by the corresponding 10-mi² amounts from Step 5. If the drainage includes more than one subregion, again use proportionately-weighted results.

7. Incremental Estimates

If incremental values for the various durations are needed, plot the results from Step 6 on graph paper and draw a smooth curve to obtain intermediate

Table 13.2. *Seasonally adjusted 10-mi² depth-duration ratios (monthly offsets).*

Northwest

Offset	1 hr	6 hr	12 hr	24 hr	48 hr	72 hr
1	0.102	0.404	0.734	1.000	1.445	1.682
2	0.106	0.416	0.745	1.000	1.386	1.558
3	0.112	0.428	0.759	1.000	1.341	1.469
4	0.121	0.448	0.774	1.000	1.296	1.416
5	0.127	0.464	0.788	1.000	1.267	1.381

Northeast

Offset	1 hr	6 hr	12 hr	24 hr	48 hr	72 hr
1	0.163	0.525	0.693	1.000	1.358	1.473
2	0.170	0.541	0.704	1.000	1.302	1.364
3	0.179	0.556	0.718	1.000	1.260	1.287
4	0.194	0.582	0.731	1.000	1.218	1.240
5	0.203	0.603	0.745	1.000	1.190	1.209

Midcoastal

Offset	1 hr	6 hr	12 hr	24 hr	48 hr	72 hr
1	0.133	0.455	0.744	1.000	1.407	1.615
2	0.138	0.468	0.755	1.000	1.349	1.496
3	0.146	0.482	0.770	1.000	1.305	1.411
4	0.157	0.504	0.784	1.000	1.262	1.360
5	0.165	0.522	0.799	1.000	1.233	1.326

Central Valley

Offset	1 hr	6 hr	12 hr	24 hr	48 hr	72 hr
1	0.133	0.424	0.653	1.000	1.436	1.663
2	0.138	0.437	0.663	1.000	1.376	1.540
3	0.146	0.449	0.676	1.000	1.332	1.453
4	0.157	0.470	0.689	1.000	1.288	1.400
5	0.165	0.487	0.702	1.000	1.258	1.365

Table 13.2. (cont.) *Seasonally adjusted 10-mi² depth-duration ratios (monthly offsets).*

Sierra

Offset	1 hr	6 hr	12 hr	24 hr	48 hr	72 hr
1	0.143	0.424	0.653	1.000	1.513	1.672
2	0.148	0.437	0.663	1.000	1.451	1.549
3	0.157	0.449	0.676	1.000	1.404	1.461
4	0.169	0.470	0.689	1.000	1.357	1.408
5	0.178	0.487	0.702	1.000	1.326	1.373

Southwest

Offset	1 hr	6 hr	12 hr	24 hr	48 hr	72 hr
1	0.143	0.485	0.764	1.000	1.368	1.511
2	0.148	0.499	0.775	1.000	1.311	1.399
3	0.157	0.514	0.790	1.000	1.269	1.320
4	0.169	0.538	0.806	1.000	1.227	1.272
5	0.178	0.557	0.821	1.000	1.199	1.240

Southeast

Offset	1 hr	6 hr	12 hr	24 hr	48 hr	72 hr
1	0.294	0.594	0.856	1.000	1.206	1.347
2	0.283	0.577	0.843	1.000	1.258	1.455
3	0.268	0.561	0.827	1.000	1.300	1.542
4	0.248	0.536	0.811	1.000	1.345	1.600
5	0.236	0.517	0.796	1.000	1.376	1.641

Table 13.3. *All-season depth-area relations for California by region.*

Northwest / Northeast

Area (mi²)	1 hr	6 hr	12 hr	24 hr	48 hr	72 hr
10	100.00	100.00	100.00	100.00	100.00	100.00
50	87.50	88.50	90.00	91.50	93.00	94.00
100	82.00	84.00	86.00	88.00	89.50	91.00
200	77.00	79.50	82.00	84.00	86.00	87.75
500	69.50	73.00	76.25	78.25	81.00	83.00
1000	63.00	67.50	71.00	73.50	76.50	79.00
2000	55.50	60.50	64.00	67.00	69.50	72.00
5000	42.50	49.50	52.50	56.00	59.00	62.00
10000	32.00	40.00	43.50	47.00	51.00	54.00

Midcoastal

Area (mi²)	1 hr	6 hr	12 hr	24 hr	48 hr	72 hr
10	100.00	100.00	100.00	100.00	100.00	100.00
50	87.50	88.75	90.00	91.00	92.00	93.00
100	81.75	83.75	85.50	87.00	88.50	90.00
200	75.75	78.25	80.50	82.50	84.50	86.25
500	67.50	71.00	73.50	76.00	78.50	80.50
1000	60.75	65.50	68.00	70.50	73.00	75.50
2000	53.00	58.50	61.50	64.00	67.00	70.00
5000	38.00	44.50	48.50	52.00	55.00	59.00

Central Valley

Area (mi²)	1 hr	6 hr	12 hr	24 hr	48 hr	72 hr
10	100.00	100.00	100.00	100.00	100.00	100.00
50	84.50	87.25	89.50	91.50	92.75	94.00
100	77.25	81.00	84.00	86.50	88.50	90.50
200	70.00	74.50	78.00	81.00	83.00	85.00
500	59.75	64.75	68.75	72.00	74.50	77.00
1000	51.00	56.50	61.00	64.50	67.00	69.50
2000	41.00	47.50	52.00	55.50	58.50	61.50
5000	27.00	33.75	38.50	42.00	45.25	48.50
10000	14.00	21.00	26.00	30.00	33.00	36.50
10000	25.00	34.00	38.00	42.00	45.00	49.00

Table 13.3 (cont.) *All-season depth-area relations for California by region.*

Sierra

Area (mi^2)	1 hr	6 hr	12 hr	24 hr	48 hr	72 hr
10	100.00	100.00	100.00	100.00	100.00	100.00
50	88.00	89.00	90.00	91.00	92.50	94.00
100	82.50	84.00	85.50	87.00	89.25	91.25
200	76.75	78.75	80.75	82.75	85.50	88.25
500	69.25	71.75	74.25	77.00	80.50	83.50
1000	63.25	66.25	69.25	72.25	76.25	79.75
2000	57.00	60.00	63.50	67.00	71.25	75.25
5000	47.50	51.00	55.00	59.00	63.50	68.00
10000	40.00	44.00	48.00	52.50	57.50	62.00

Southwest

Area (mi^2)	1 hr	6 hr	12 hr	24 hr	48 hr	72 hr
10	100.00	100.00	100.00	100.00	100.00	100.00
50	87.75	88.50	89.50	90.50	91.75	92.75
100	81.75	83.25	84.75	86.25	87.75	89.25
200	75.75	78.00	79.75	81.50	83.75	85.75
500	67.50	70.50	72.50	75.00	77.50	80.00
1000	60.00	63.50	66.00	69.00	71.75	74.75
2000	51.00	56.00	59.00	62.00	65.00	68.00
5000	35.00	41.00	46.00	50.00	52.50	56.00
10000	22.00	30.00	34.00	38.00	42.00	46.00

Southeast

Area (mi^2)	1 hr	6 hr	12 hr	24 hr	48 hr	72 hr
10	100.00	100.00	100.00	100.00	100.00	100.00
50	89.00	90.50	91.75	93.00	94.50	96.00
100	83.50	85.25	87.25	89.00	90.75	92.50
200	76.50	79.75	82.00	84.00	86.00	88.00
500	66.00	70.75	74.00	76.50	78.75	81.00
1000	56.50	63.25	67.00	70.00	72.50	75.00
2000	46.00	54.75	59.00	62.00	64.75	67.50
5000	31.25	41.50	47.00	50.00	52.50	55.50
10000	19.00	30.00	36.00	39.50	42.50	45.00

Table 13.4. *Seasonally adjusted areal reduction factors for the Northeast and Northwest regions.*

Offset 1 Month						
Area (mi^2)	**1 hr**	**6 hr**	**12 hr**	**24 hr**	**48 hr**	**72 hr**
10	1.000	1.000	1.000	1.000	1.000	1.000
50	0.913	0.930	0.948	0.960	0.967	0.975
100	0.861	0.883	0.905	0.928	0.945	0.960
200	0.785	0.818	0.847	0.871	0.900	0.919
500	0.677	0.725	0.769	0.798	0.835	0.859
1000	0.582	0.644	0.690	0.730	0.762	0.790
2000	0.480	0.559	0.608	0.650	0.680	0.709
5000	0.340	0.436	0.478	0.524	0.561	0.595
10000	0.240	0.338	0.372	0.418	0.467	0.502
Offset 2 Months						
Area (mi^2)	**1 hr**	**6 hr**	**12 hr**	**24 hr**	**48 hr**	**72 hr**
10	1.000	1.000	1.000	1.000	1.000	1.000
50	0.894	0.921	0.939	0.952	0.959	0.965
100	0.831	0.868	0.892	0.916	0.929	0.941
200	0.753	0.802	0.834	0.858	0.880	0.892
500	0.641	0.702	0.746	0.778	0.806	0.825
1000	0.544	0.617	0.658	0.697	0.728	0.751
2000	0.447	0.528	0.570	0.610	0.639	0.666
5000	0.313	0.401	0.436	0.484	0.519	0.552
10000	0.218	0.302	0.335	0.381	0.428	0.459
Offset 3 Months						
Area (mi^2)	**1 hr**	**6 hr**	**12 hr**	**24 hr**	**48 hr**	**72 hr**
10	1.000	1.000	1.000	1.000	1.000	1.000
50	0.883	0.916	0.933	0.944	0.950	0.955
100	0.809	0.859	0.882	0.904	0.916	0.926
200	0.729	0.789	0.821	0.844	0.867	0.878
500	0.619	0.687	0.726	0.757	0.785	0.803
1000	0.522	0.596	0.636	0.671	0.697	0.719
2000	0.425	0.500	0.541	0.576	0.605	0.634
5000	0.294	0.374	0.412	0.451	0.481	0.512
10000	0.205	0.284	0.320	0.355	0.393	0.424

Table 13.4. (cont.) *Seasonally adjusted areal reduction factors for the Northeast and Northwest regions.*

Offset 4 Months						
Area (mi^2)	**1 hr**	**6 hr**	**12 hr**	**24 hr**	**48 hr**	**72 hr**
10	1.000	1.000	1.000	1.000	1.000	1.000
50	0.865	0.902	0.926	0.940	0.946	0.952
100	0.787	0.837	0.869	0.890	0.901	0.913
200	0.696	0.760	0.800	0.821	0.842	0.853
500	0.576	0.649	0.695	0.721	0.747	0.765
1000	0.474	0.555	0.601	0.633	0.658	0.679
2000	0.375	0.464	0.502	0.536	0.563	0.590
5000	0.244	0.337	0.375	0.412	0.435	0.459
10000	0.162	0.248	0.283	0.317	0.354	0.383
Offset 5 Months						
Area (mi^2)	**1 hr**	**6 hr**	**12 hr**	**24 hr**	**48 hr**	**72 hr**
10	1.000	1.000	1.000	1.000	1.000	1.000
50	0.851	0.893	0.917	0.931	0.946	0.955
100	0.770	0.823	0.851	0.874	0.886	0.898
200	0.672	0.743	0.778	0.801	0.822	0.833
500	0.551	0.627	0.667	0.697	0.722	0.740
1000	0.448	0.538	0.572	0.607	0.635	0.660
2000	0.347	0.445	0.480	0.516	0.546	0.572
5000	0.216	0.322	0.352	0.392	0.425	0.453
10000	0.141	0.228	0.261	0.298	0.339	0.367

Table 13.5. *Seasonally adjusted areal reduction factors for the Midcoastal region.*

Offset 1 Month

Area (mi^2)	1 hr	6 hr	12 hr	24 hr	48 hr	72 hr
10	1.000	1.000	1.000	1.000	1.000	1.000
50	0.903	0.915	0.928	0.943	0.957	0.975
100	0.846	0.868	0.886	0.908	0.930	0.949
200	0.775	0.804	0.832	0.856	0.885	0.909
500	0.663	0.710	0.750	0.778	0.815	0.838
1000	0.564	0.630	0.671	0.706	0.738	0.770
2000	0.458	0.536	0.584	0.621	0.655	0.690
5000	0.308	0.392	0.441	0.486	0.523	0.566
10000	0.188	0.287	0.325	0.374	0.412	0.456

Offset 2 Months

Area (mi^2)	1 hr	6 hr	12 hr	24 hr	48 hr	72 hr
10	1.000	1.000	1.000	1.000	1.000	1.000
50	0.885	0.906	0.919	0.935	0.949	0.965
100	0.817	0.853	0.872	0.896	0.914	0.931
200	0.743	0.787	0.820	0.843	0.866	0.882
500	0.627	0.688	0.727	0.758	0.786	0.805
1000	0.527	0.603	0.639	0.673	0.704	0.732
2000	0.427	0.506	0.547	0.582	0.616	0.648
5000	0.283	0.360	0.403	0.450	0.484	0.525
10000	0.170	0.257	0.293	0.340	0.378	0.417

Offset 3 Months

Area (mi^2)	1 hr	6 hr	12 hr	24 hr	48 hr	72 hr
10	1.000	1.000	1.000	1.000	1.000	1.000
50	0.874	0.902	0.913	0.927	0.940	0.955
100	0.795	0.844	0.862	0.885	0.901	0.917
200	0.719	0.775	0.807	0.830	0.852	0.869
500	0.606	0.673	0.708	0.739	0.766	0.784
1000	0.505	0.583	0.619	0.648	0.674	0.701
2000	0.405	0.480	0.520	0.550	0.583	0.616
5000	0.266	0.336	0.381	0.419	0.448	0.487
10000	0.160	0.241	0.279	0.317	0.347	0.385

Table 13.5. (cont.) *Seasonally adjusted areal reduction factors for the Midcoastal region.*

Offset 4 Months

Area (mi^2)	1 hr	6 hr	12 hr	24 hr	48 hr	72 hr
10	1.000	1.000	1.000	1.000	1.000	1.000
50	0.855	0.888	0.907	0.923	0.936	0.952
100	0.774	0.823	0.850	0.871	0.887	0.903
200	0.688	0.746	0.786	0.807	0.827	0.843
500	0.564	0.636	0.677	0.703	0.729	0.747
1000	0.459	0.543	0.584	0.612	0.637	0.662
2000	0.358	0.445	0.483	0.512	0.543	0.574
5000	0.220	0.303	0.347	0.382	0.406	0.437
10000	0.126	0.211	0.247	0.284	0.313	0.348

Offset 5 Months

Area (mi^2)	1 hr	6 hr	12 hr	24 hr	48 hr	72 hr
10	1.000	1.000	1.000	1.000	1.000	0.000
50	0.842	0.879	0.897	0.915	0.936	0.000
100	0.757	0.809	0.832	0.855	0.872	0.000
200	0.664	0.730	0.765	0.787	0.808	48.000
500	0.539	0.614	0.650	0.679	0.705	1.016
1000	0.434	0.526	0.556	0.587	0.615	0.919
2000	0.331	0.427	0.461	0.493	0.526	0.875
5000	0.196	0.289	0.325	0.364	0.396	0.834
10000	0.110	0.194	0.228	0.267	0.299	0.749

Table 13.6. *Seasonally adjusted areal reduction factors for the Central Valley region.*

Offset 1 Month

Area (mi^2)	1 hr	6 hr	12 hr	24 hr	48 hr	72 hr
10	1.000	1.000	1.000	1.000	1.000	1.000
50	0.828	0.886	0.918	0.940	0.952	0.970
100	0.752	0.823	0.866	0.893	0.915	0.934
200	0.663	0.750	0.798	0.832	0.860	0.889
500	0.536	0.638	0.701	0.739	0.775	0.803
1000	0.437	0.541	0.608	0.652	0.683	0.715
2000	0.333	0.440	0.504	0.548	0.582	0.616
5000	0.207	0.295	0.350	0.393	0.432	0.466
10000	0.113	0.182	0.222	0.267	0.302	0.339

Offset 2 Months

Area (mi^2)	1 hr	6 hr	12 hr	24 hr	48 hr	72 hr
10	1.000	1.000	1.000	1.000	1.000	1.000
50	0.812	0.877	0.909	0.932	0.944	0.960
100	0.726	0.809	0.853	0.882	0.899	0.916
200	0.636	0.734	0.786	0.819	0.841	0.862
500	0.507	0.618	0.679	0.720	0.748	0.771
1000	0.408	0.518	0.580	0.622	0.652	0.679
2000	0.310	0.415	0.472	0.514	0.547	0.578
5000	0.190	0.271	0.320	0.363	0.400	0.432
10000	0.102	0.162	0.200	0.243	0.277	0.310

Offset 3 Months

Area (mi^2)	1 hr	6 hr	12 hr	24 hr	48 hr	72 hr
10	1.000	1.000	1.000	1.000	1.000	1.000
50	0.802	0.872	0.903	0.924	0.935	0.951
100	0.707	0.801	0.843	0.870	0.886	0.902
200	0.615	0.723	0.774	0.806	0.828	0.849
500	0.490	0.605	0.661	0.701	0.729	0.751
1000	0.391	0.500	0.561	0.599	0.624	0.651
2000	0.295	0.394	0.448	0.486	0.518	0.550
5000	0.179	0.253	0.302	0.338	0.371	0.400
10000	0.096	0.153	0.191	0.227	0.254	0.287

Table 13.6. (cont.) *Seasonally adjusted areal reduction factors for the Central Valley region.*

Offset 4 Months						
Area (mi^2)	**1 hr**	**6 hr**	**12 hr**	**24 hr**	**48 hr**	**72 hr**
10	1.000	1.000	1.000	1.000	1.000	1.000
50	0.785	0.859	0.897	0.920	0.931	0.947
100	0.688	0.780	0.831	0.857	0.873	0.889
200	0.588	0.696	0.753	0.784	0.804	0.825
500	0.456	0.572	0.633	0.668	0.694	0.716
1000	0.355	0.466	0.529	0.565	0.590	0.615
2000	0.260	0.365	0.416	0.452	0.482	0.513
5000	0.148	0.228	0.275	0.309	0.336	0.359
10000	0.076	0.133	0.169	0.203	0.229	0.259
Offset 5 Months						
Area (mi^2)	**1 hr**	**6 hr**	**12 hr**	**24 hr**	**48 hr**	**72 hr**
10	1.000	1.000	1.000	1.000	1.000	1.000
50	0.772	0.850	0.888	0.912	0.931	0.951
100	0.673	0.768	0.813	0.841	0.858	0.874
200	0.568	0.681	0.733	0.764	0.785	0.805
500	0.436	0.552	0.608	0.645	0.670	0.692
1000	0.336	0.451	0.504	0.542	0.569	0.597
2000	0.241	0.350	0.398	0.435	0.467	0.497
5000	0.131	0.218	0.258	0.294	0.328	0.354
10000	0.066	0.123	0.156	0.191	0.219	0.248

Table 13.7. *Seasonally adjusted areal reduction factors for the Sierra region.*

Offset 1 Month

Area (mi^2)	1 hr	6 hr	12 hr	24 hr	48 hr	72 hr
10	1.000	1.000	1.000	1.000	1.000	1.000
50	0.908	0.920	0.933	0.950	0.962	0.985
100	0.851	0.868	0.886	0.908	0.930	0.960
200	0.775	0.799	0.822	0.851	0.880	0.919
500	0.667	0.706	0.745	0.778	0.820	0.859
1000	0.582	0.630	0.676	0.715	0.762	0.810
2000	0.493	0.550	0.603	0.650	0.699	0.749
5000	0.385	0.449	0.501	0.552	0.608	0.653
10000	0.300	0.372	0.410	0.472	0.531	0.577

Offset 2 Months

Area (mi^2)	1 hr	6 hr	12 hr	24 hr	48 hr	72 hr
10	1.000	1.000	1.000	1.000	1.000	1.000
50	0.889	0.911	0.924	0.942	0.954	0.975
100	0.821	0.853	0.872	0.896	0.914	0.941
200	0.743	0.782	0.810	0.839	0.861	0.892
500	0.632	0.684	0.722	0.758	0.791	0.825
1000	0.544	0.603	0.644	0.683	0.728	0.770
2000	0.459	0.519	0.565	0.610	0.658	0.703
5000	0.354	0.413	0.457	0.510	0.563	0.605
10000	0.272	0.332	0.370	0.429	0.487	0.527

Offset 3 Months

Area (mi^2)	1 hr	6 hr	12 hr	24 hr	48 hr	72 hr
10	1.000	1.000	1.000	1.000	1.000	1.000
50	0.878	0.907	0.918	0.934	0.945	0.965
100	0.800	0.844	0.862	0.885	0.901	0.926
200	0.719	0.770	0.797	0.825	0.847	0.878
500	0.611	0.669	0.703	0.739	0.771	0.803
1000	0.522	0.583	0.623	0.657	0.697	0.737
2000	0.436	0.492	0.537	0.576	0.622	0.669
5000	0.333	0.385	0.432	0.475	0.522	0.561
10000	0.256	0.312	0.353	0.400	0.447	0.487

Table 13.7. (cont.) *Seasonally adjusted areal reduction factors for the Sierra region.*

Offset 4 Months

Area (mi^2)	1 hr	6 hr	12 hr	24 hr	48 hr	72 hr
10	1.000	1.000	1.000	1.000	1.000	1.000
50	0.860	0.893	0.912	0.930	0.941	0.961
100	0.778	0.823	0.850	0.871	0.887	0.913
200	0.688	0.742	0.777	0.802	0.823	0.853
500	0.568	0.632	0.673	0.703	0.734	0.765
1000	0.474	0.543	0.588	0.621	0.658	0.697
2000	0.385	0.456	0.498	0.536	0.579	0.623
5000	0.276	0.347	0.393	0.434	0.472	0.503
10000	0.202	0.273	0.312	0.358	0.403	0.440

Offset 5 Months

Area (mi^2)	1 hr	6 hr	12 hr	24 hr	48 hr	72 hr
10	1.000	1.000	1.000	1.000	1.000	1.000
50	0.846	0.883	0.902	0.922	0.941	0.965
100	0.761	0.809	0.832	0.855	0.872	0.898
200	0.664	0.725	0.756	0.783	0.803	0.833
500	0.543	0.610	0.646	0.679	0.709	0.740
1000	0.448	0.526	0.560	0.595	0.635	0.676
2000	0.356	0.438	0.476	0.516	0.561	0.604
5000	0.245	0.332	0.369	0.413	0.461	0.496
10000	0.176	0.251	0.288	0.337	0.386	0.422

Table 13.8. *Seasonally adjusted areal reduction factors for the Southwest region.*

Offset 1 Month

Area (mi^2)	1 hr	6 hr	12 hr	24 hr	48 hr	72 hr
10	1.000	1.000	1.000	1.000	1.000	1.000
50	0.893	0.915	0.928	0.940	0.952	0.965
100	0.837	0.863	0.881	0.898	0.920	0.939
200	0.770	0.799	0.818	0.842	0.870	0.899
500	0.658	0.696	0.730	0.758	0.795	0.828
1000	0.555	0.611	0.647	0.686	0.723	0.760
2000	0.441	0.513	0.561	0.601	0.636	0.670
5000	0.284	0.361	0.419	0.468	0.499	0.538
10000	0.165	0.254	0.291	0.338	0.384	0.428

Offset 2 Months

Area (mi^2)	1 hr	6 hr	12 hr	24 hr	48 hr	72 hr
10	1.000	1.000	1.000	1.000	1.000	1.000
50	0.875	0.906	0.919	0.932	0.944	0.955
100	0.807	0.848	0.867	0.887	0.904	0.921
200	0.739	0.782	0.805	0.829	0.851	0.872
500	0.623	0.674	0.708	0.739	0.767	0.795
1000	0.519	0.585	0.616	0.655	0.690	0.722
2000	0.411	0.484	0.525	0.564	0.598	0.629
5000	0.261	0.332	0.382	0.433	0.462	0.498
10000	0.150	0.227	0.262	0.308	0.353	0.391

Offset 3 Months

Area (mi^2)	1 hr	6 hr	12 hr	24 hr	48 hr	72 hr
10	1.000	1.000	1.000	1.000	1.000	1.000
50	0.864	0.902	0.913	0.924	0.935	0.946
100	0.786	0.840	0.858	0.875	0.891	0.907
200	0.715	0.770	0.793	0.815	0.838	0.859
500	0.602	0.660	0.689	0.720	0.747	0.775
1000	0.497	0.566	0.596	0.630	0.661	0.692
2000	0.390	0.459	0.499	0.533	0.566	0.598
5000	0.245	0.310	0.361	0.403	0.428	0.462
10000	0.141	0.213	0.250	0.287	0.323	0.361

Table 13.8. (cont.) *Seasonally adjusted areal reduction factors for the Southwest region.*

Offset 4 Months						
Area (mi^2)	**1 hr**	**6 hr**	**12 hr**	**24 hr**	**48 hr**	**72 hr**
10	1.000	1.000	1.000	1.000	1.000	1.000
50	0.846	0.888	0.907	0.920	0.931	0.942
100	0.765	0.818	0.845	0.861	0.877	0.894
200	0.683	0.742	0.772	0.793	0.813	0.834
500	0.560	0.624	0.659	0.685	0.712	0.738
1000	0.451	0.527	0.563	0.595	0.624	0.654
2000	0.344	0.426	0.463	0.496	0.527	0.558
5000	0.203	0.279	0.329	0.368	0.387	0.414
10000	0.111	0.186	0.221	0.257	0.292	0.327
Offset 5 Months						
Area (mi^2)	**1 hr**	**6 hr**	**12 hr**	**24 hr**	**48 hr**	**72 hr**
10	1.000	1.000	1.000	1.000	1.000	1.000
50	0.833	0.879	0.897	0.912	0.931	0.946
100	0.748	0.805	0.827	0.846	0.863	0.879
200	0.660	0.725	0.751	0.774	0.794	0.814
500	0.536	0.602	0.633	0.662	0.688	0.713
1000	0.427	0.510	0.536	0.571	0.602	0.635
2000	0.319	0.409	0.443	0.477	0.510	0.541
5000	0.180	0.267	0.308	0.350	0.378	0.409
10000	0.097	0.171	0.204	0.241	0.279	0.313

Table 13.9. *Seasonally adjusted areal reduction factors for the Southeast region.*

Offset 1 Month

Area (mi^2)	1 hr	6 hr	12 hr	24 hr	48 hr	72 hr
10	1.000	1.000	1.000	1.000	1.000	1.000
50	0.902	0.935	0.945	0.952	0.964	0.970
100	0.838	0.877	0.894	0.912	0.920	0.929
200	0.779	0.832	0.848	0.874	0.880	0.891
500	0.713	0.760	0.776	0.807	0.820	0.837
1000	0.643	0.702	0.725	0.745	0.763	0.780
2000	0.561	0.622	0.647	0.655	0.675	0.690
5000	0.389	0.477	0.522	0.535	0.553	0.573
10000	0.253	0.355	0.427	0.444	0.464	0.484

Offset 2 Months

Area (mi^2)	1 hr	6 hr	12 hr	24 hr	48 hr	72 hr
10	1.000	1.000	1.000	1.000	1.000	1.000
50	0.921	0.944	0.954	0.960	0.972	0.980
100	0.869	0.892	0.908	0.924	0.936	0.947
200	0.813	0.849	0.861	0.887	0.900	0.918
500	0.753	0.785	0.800	0.828	0.850	0.871
1000	0.688	0.733	0.761	0.781	0.799	0.821
2000	0.602	0.659	0.691	0.698	0.717	0.735
5000	0.423	0.519	0.572	0.578	0.597	0.618
10000	0.279	0.397	0.474	0.488	0.506	0.529

Offset 3 Months

Area (mi^2)	1 hr	6 hr	12 hr	24 hr	48 hr	72 hr
10	1.000	1.000	1.000	1.000	1.000	1.000
50	0.932	0.949	0.960	0.968	0.982	0.990
100	0.892	0.902	0.918	0.936	0.950	0.962
200	0.840	0.862	0.874	0.902	0.914	0.933
500	0.779	0.802	0.822	0.850	0.872	0.894
1000	0.718	0.759	0.787	0.811	0.834	0.857
2000	0.634	0.695	0.728	0.738	0.759	0.773
5000	0.450	0.556	0.605	0.621	0.644	0.667
10000	0.297	0.423	0.497	0.523	0.552	0.573

Table 13.9. (cont.) *Seasonally adjusted areal reduction factors for the Southeast region.*

Offset 4 Months						
Area (mi^2)	**1 hr**	**6 hr**	**12 hr**	**24 hr**	**48 hr**	**72 hr**
10	1.000	1.000	1.000	1.000	1.000	1.000
50	0.952	0.964	0.967	0.972	0.986	0.994
100	0.917	0.926	0.932	0.951	0.965	0.976
200	0.879	0.896	0.898	0.927	0.941	0.961
500	0.838	0.849	0.859	0.893	0.916	0.939
1000	0.791	0.815	0.833	0.859	0.883	0.907
2000	0.719	0.750	0.783	0.794	0.815	0.829
5000	0.543	0.618	0.664	0.680	0.711	0.743
10000	0.376	0.484	0.562	0.585	0.612	0.634
Offset 5 Months						
Area (mi^2)	**1 hr**	**6 hr**	**12 hr**	**24 hr**	**48 hr**	**72 hr**
10	1.000	1.000	1.000	1.000	1.000	1.000
50	0.968	0.974	0.977	0.981	0.986	0.990
100	0.938	0.941	0.952	0.968	0.981	0.993
200	0.910	0.916	0.923	0.951	0.964	0.984
500	0.876	0.880	0.894	0.924	0.948	0.971
1000	0.836	0.841	0.875	0.896	0.915	0.934
2000	0.776	0.781	0.820	0.825	0.841	0.855
5000	0.612	0.646	0.709	0.714	0.729	0.753
10000	0.432	0.526	0.608	0.622	0.639	0.662

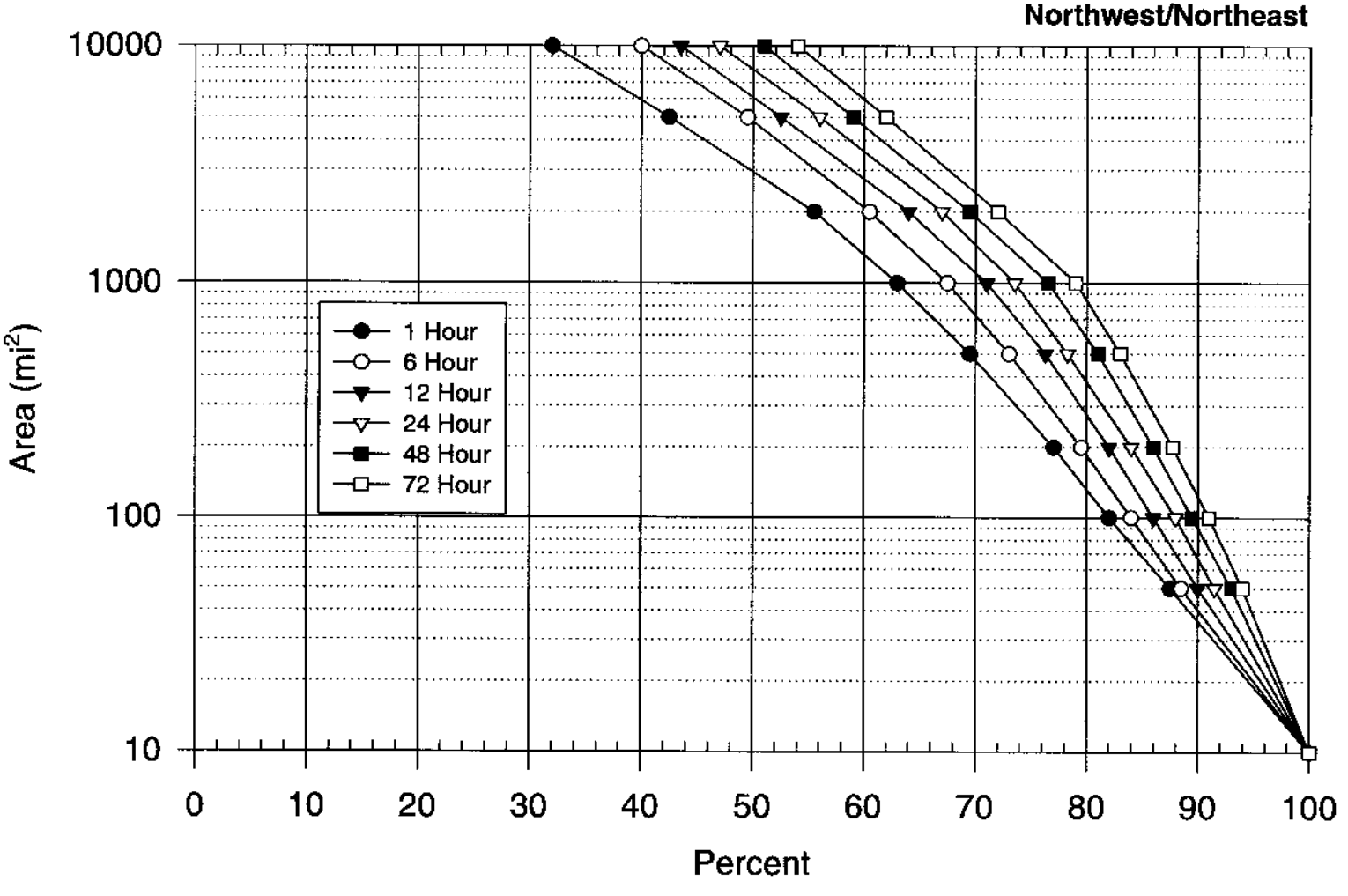

Figure 13.12. *Depth-area relations for the California Northwest/Northeast region for 1 to 72 hour durations. Same as Figure 8.1.*

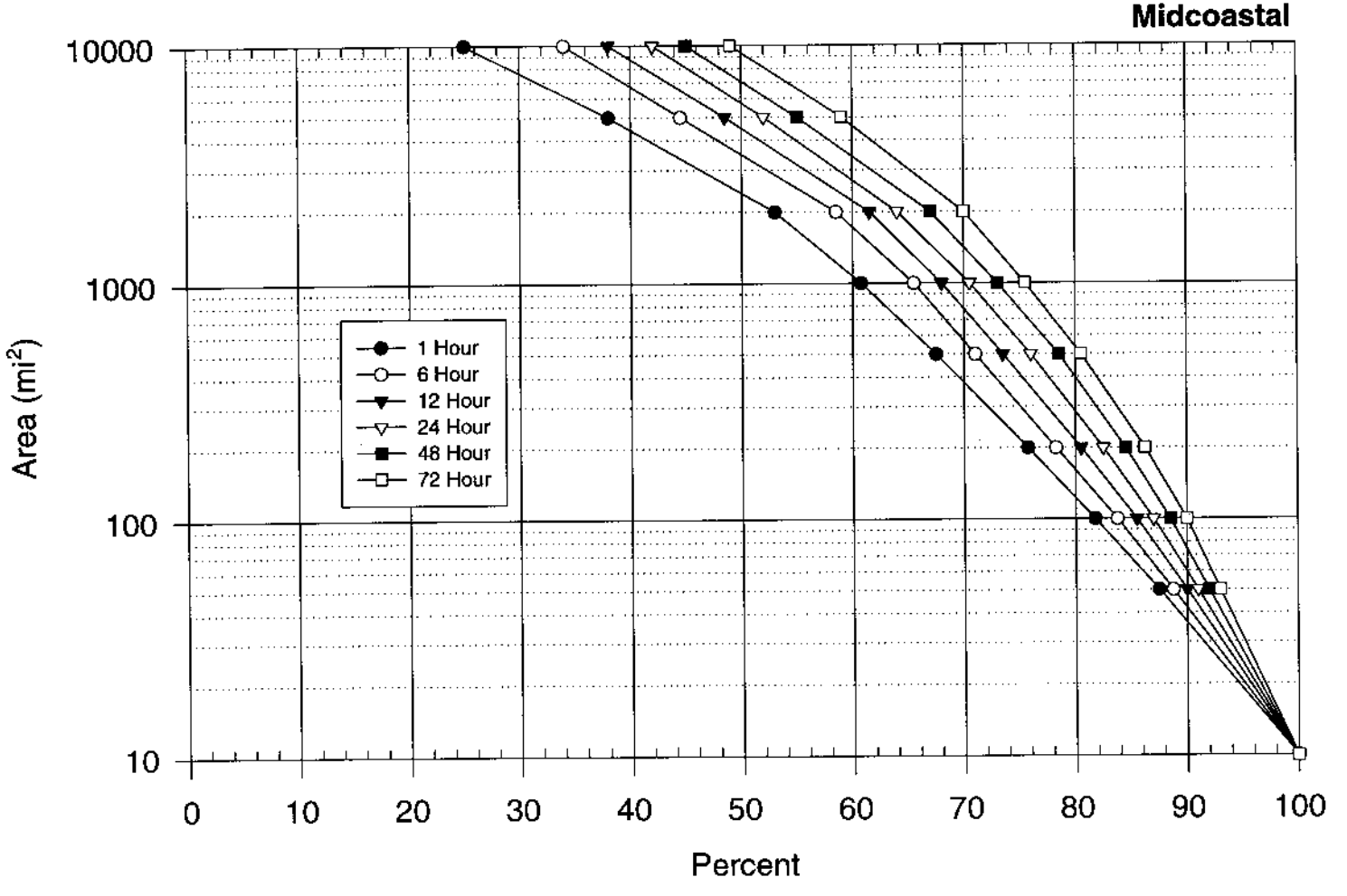

Figure 13.13. *Depth-area relations for the California Midcoastal region for 1 to 72 hour durations. Same as Figure 8.2.*

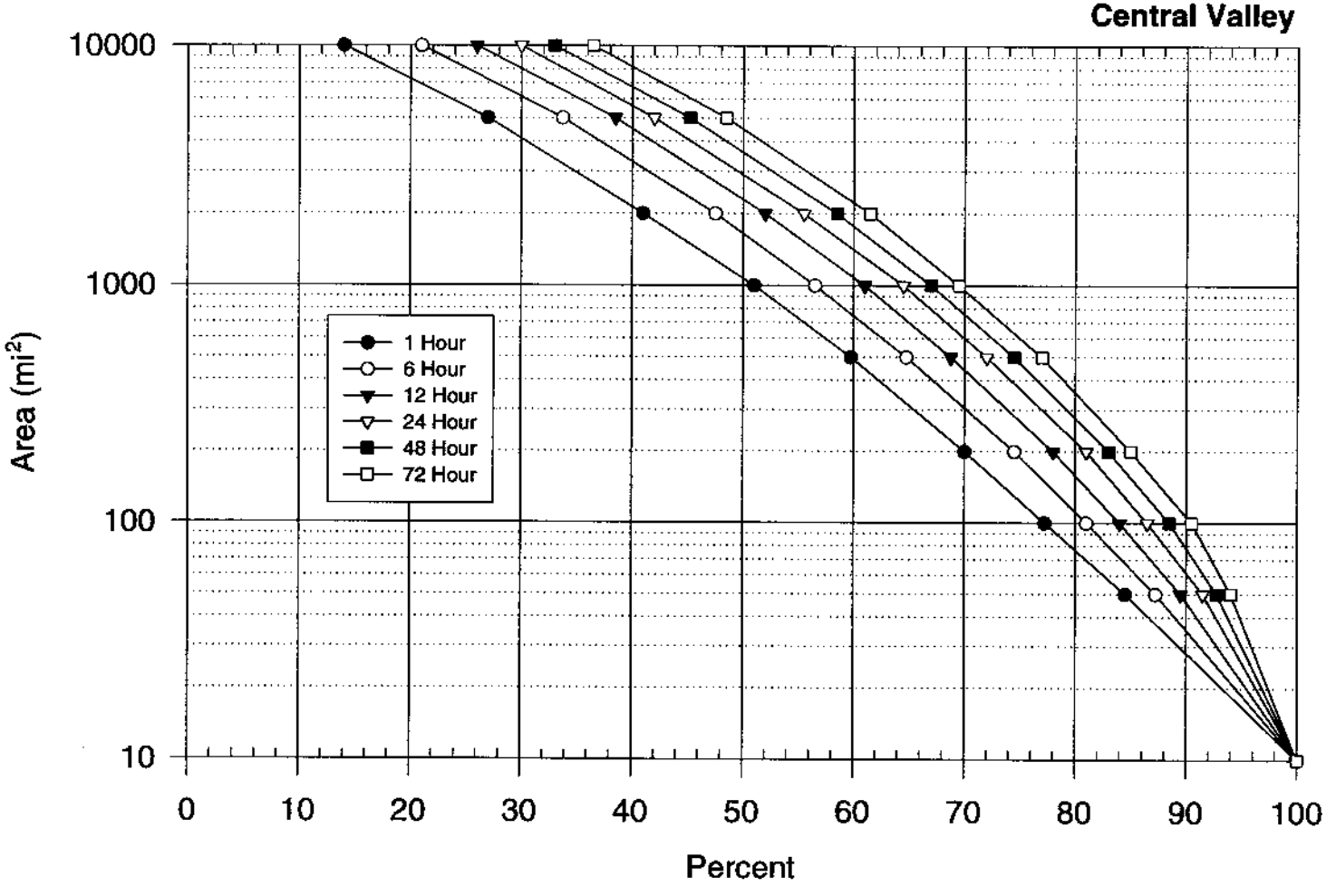

Figure 13.14. *Depth-area relations for the California Central Valley region for 1 to 72 hour durations. Same as Figure 8.3.*

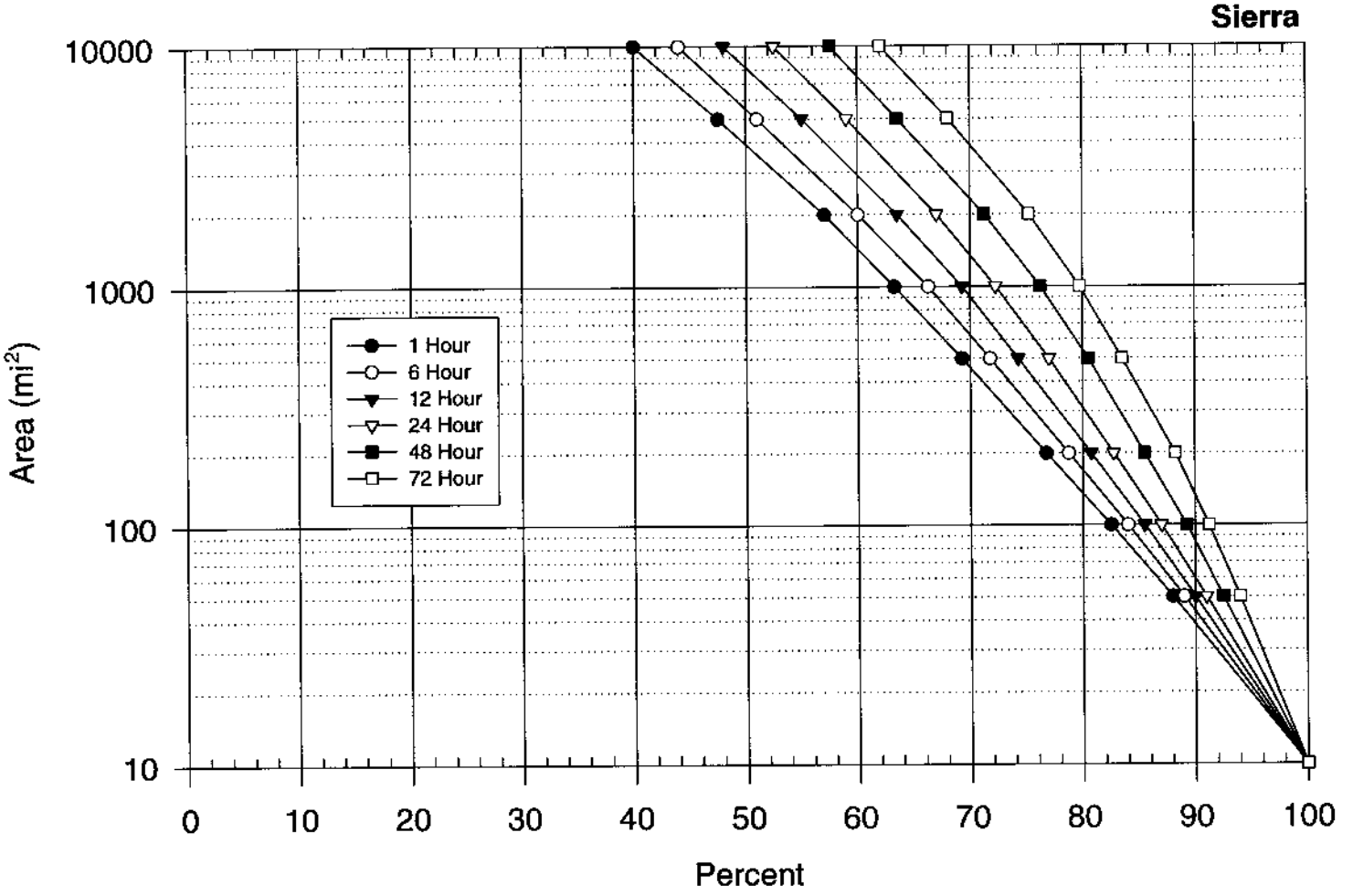

Figure 13.15. *Depth-area relations for the California Sierra region for 1 to 72 hour durations. Same as Figure 8.4.*

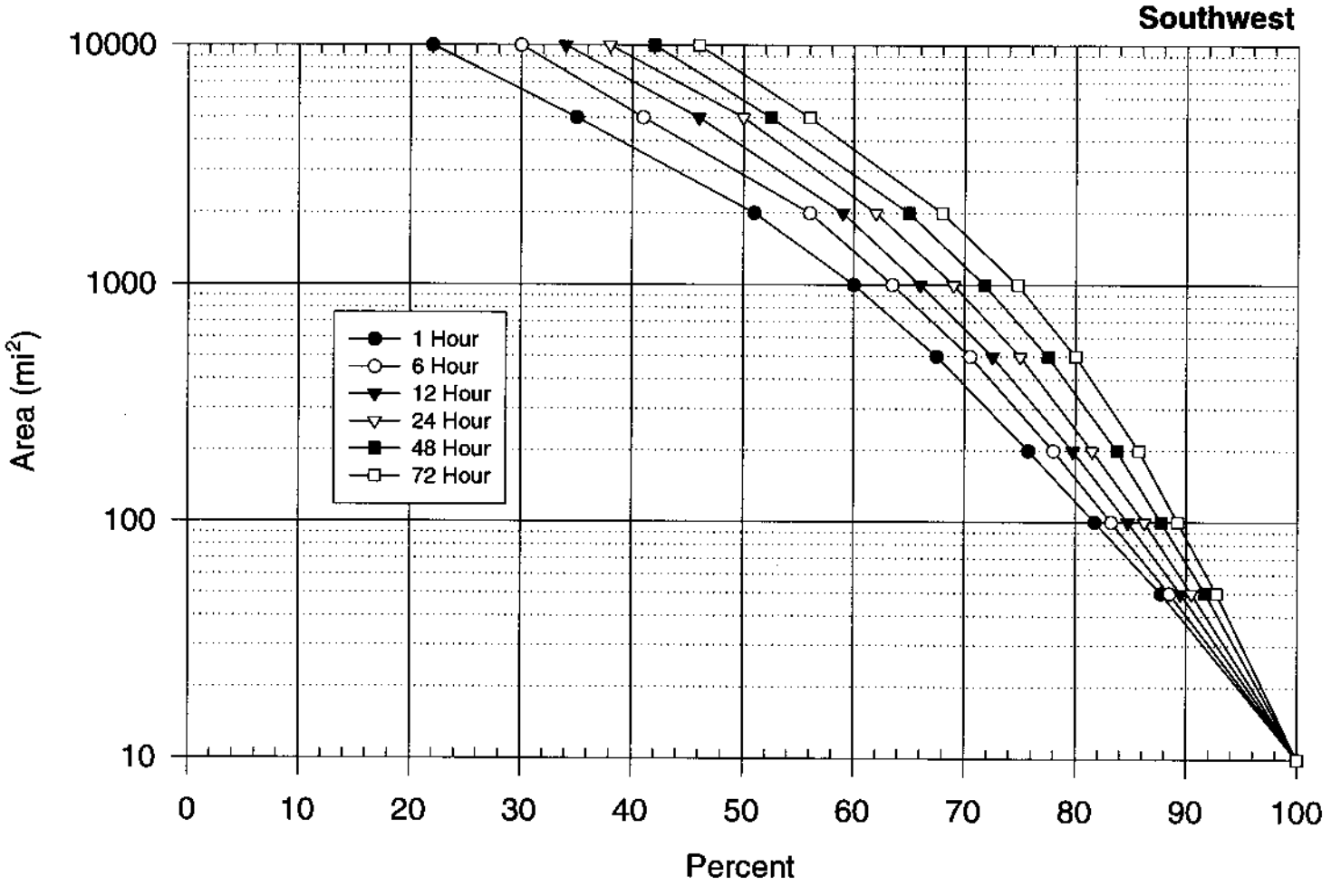

Figure 13.16. *Depth-area relations for the California Southwest region for 1 to 72 hour durations. Same as Figure 8.5.*

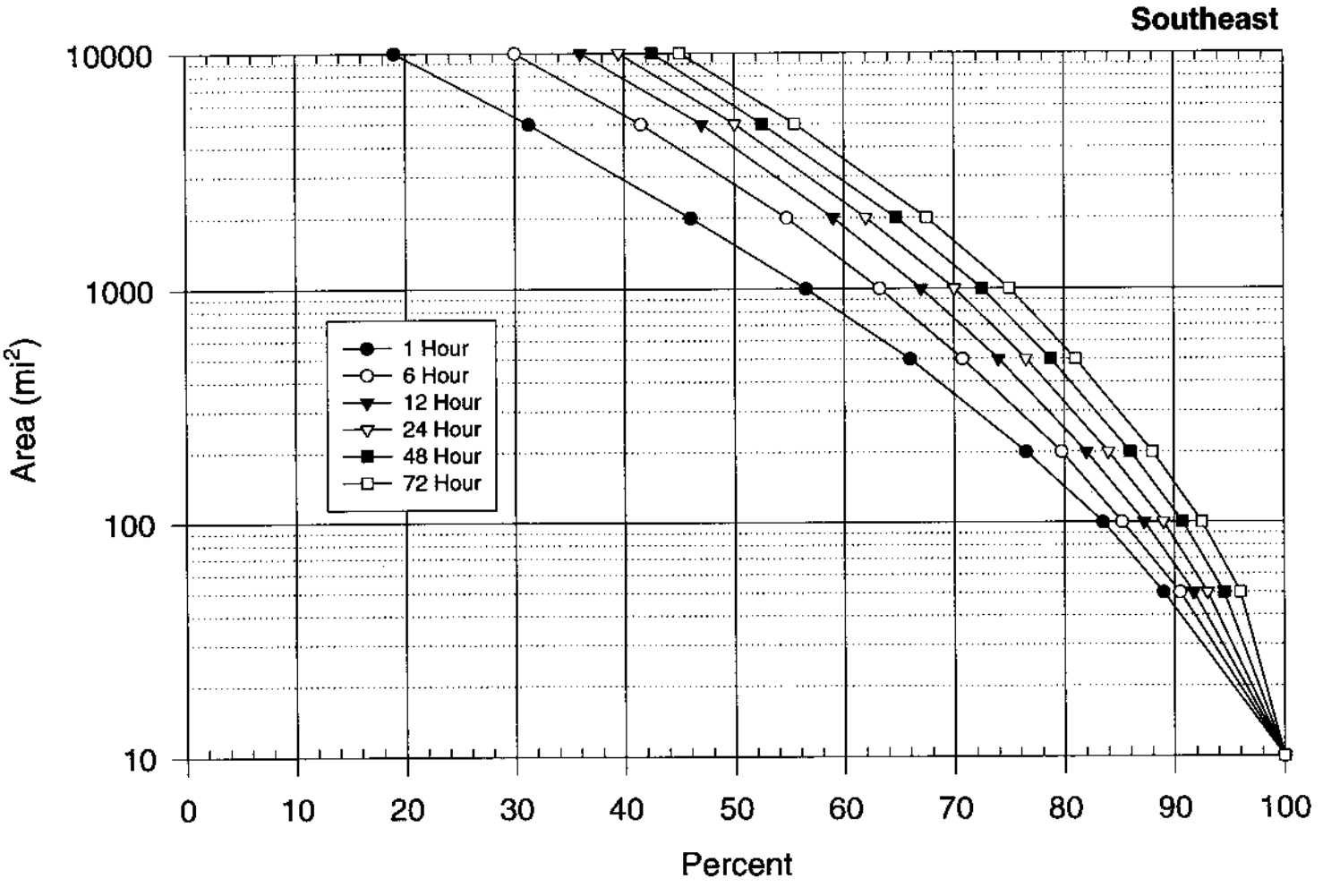

Figure 13.17. *Depth-area relations for the California Southeast region for 1 to 72 hour durations. Same as Figure 8.6.*

cumulative 6-hour values. A margin of plus or minus 0.5 inch is permissible in drawing this curve due to various roundings in Steps 1 to 6. Subtract each cumulative 6-hour depth from the depth of the next longer cumulative 6-hour duration. Some applications may require hourly increments. If this is the case, the smooth curve is subdivided into 72 cumulative hourly amounts and each cumulative hourly depth is subtracted from the depth at the next cumulative 1-hour longer duration.

8. Snowmelt parameters, temporal, and areal distributions.

During peer review a consensus recommendation was to include some procedures in the report to deal with these items. These items had not been within the scope originally formulated for the study. The snowmelt procedure from HMR 36 (1961) is incorporated in this report and found in Appendix 4.

Chronological partitioning of the PMP and its areal distribution were not studied in this report We would recommend that the user employ historical storms or divide the 72-hour PMP into 6-hour increments. Then arrange the final storm configuration into a front-, middle-, or end-loaded temporal distribution depending on the water management decisions that are required. One possible way of doing this is as follows:

A. For DAD regions 1-6 (Figure 13.11), group the four heaviest 6-hour values of the 72-hour PMP in a 24-hour sequence.

B. Within the maximum 24-hour period arrange the four 6-hour values as follows. Place the second highest 6-hour values next to the highest, the third highest on either side of the first two 6-hour values, and the fourth highest at either end.

C. The 24-hour largest 6-hour values may be positioned anywhere in the 72-hour storm period. The remaining eight 6-hour amounts may be positioned anywhere else.

A hydrologist may experiment with different temporal sequences to uncover any factors that would make a particular sequence more critical than another for a basin

of concern. Selection of a particular sequence for a basin is a decision for the user.

One way of distributing the storm spatially is by developing an isopercental analysis based on the 100-year precipitation frequency maps from NOAA Atlas 2 (1973). This approximation was used to develop the individual storm analyses for this study, and has been used on other occasions to represent storm distributions.

Another approximation can be made by using a significant storm with a sufficient number of observations to draw a storm pattern over the basin of interest. If such a storm has been observed, then the storm pattern can be used to define an isopercental analysis for the PMP distribution. However, only a few California storms have sufficient detail to define a storm pattern over the complex terrain.

13.3 Example of General-Storm PMP Computation

The 973-mi^2 Auburn drainage above Folsom Lake is used as an example for the general-storm PMP. The Auburn drainage is located in the Sierra subregion or region 5. In this example, we will use the steps of Section 13.2. First, we will calculate the all-season PMP for the drainage, and then the PMP for the *off-season* month of May.

All-Season Calculation

Step

1. Drainage Outline

   The Auburn drainage is outlined on a section of the 24-hour, general-storm PMP Index in Figure 13.18, at a scale of 1:1,000,000.

2. User Decision

   We will do an all-season PMP calculation.

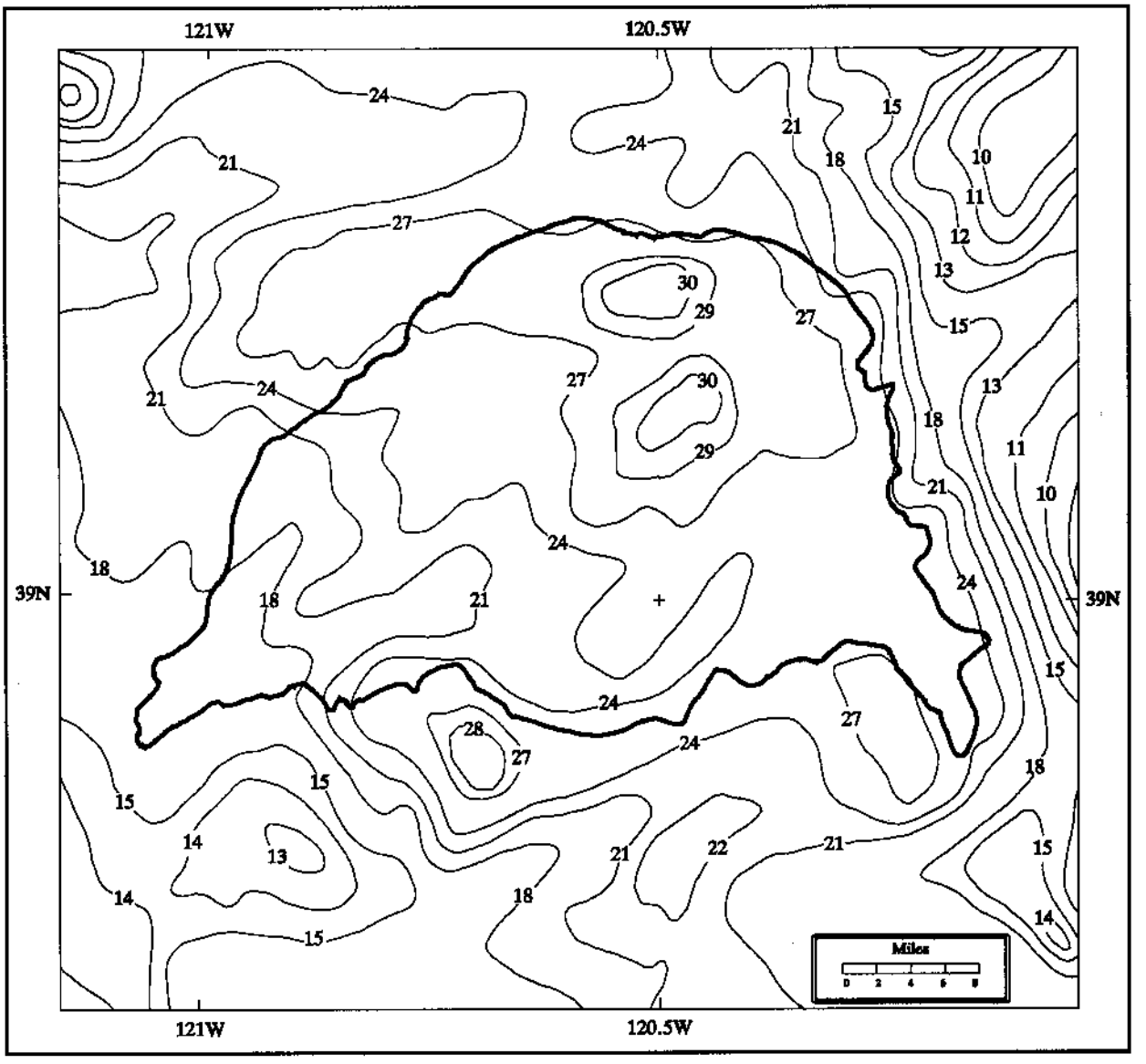

Figure 13.18. *Contours of general-storm index PMP in and around the 973-mi^2 Auburn drainage (heavy solid line) in California.*

3. All-Season Index PMP Estimate

Figure 13.18 shows the contours of index (10-mi^2, 24-hour) PMP superimposed on the outline of the Auburn drainage. It's average value is 24.6 inches.

4. Seasonal Index PMP Estimates

Skip this step.

5. Depth-Duration Relations

The Auburn drainage is within the Sierra classification (region 5) except for a very small portion near the dam site which may be regarded as inconsequential. Table 13.1 gives the ratios for durations from 1 hour to 72 hours.

Ratios for Auburn drainage						
	Duration (hours)					
	1	6	12	24	48	72
All-Season	.14	.42	.65	1.00	1.56	1.76

Multiply the result from Step 3, the average 10-mi^2, 24-hour PMP of 24.6 inches, by these ratios to produce the following 10-mi^2 depths of all-season PMP for Auburn:

Auburn drainage 10-mi^2 PMP						
	Duration (hours)					
	1	6	12	24	48	72
All-Season Depth (inches)	3.4	10.3	16.0	24.6	38.4	43.3

6. Areal Reduction Factors

Using the Auburn drainage area of 973 mi^2 and Figure 13.15, we get the following reduction ratios:

Reduction factors for Auburn drainage						
	Duration (hours)					
	1	6	12	24	48	72
All-Season	.64	.67	.70	.72	.77	.80

The depths from Step 5 are multiplied by these ratios to obtain the all-season, storm-centered average depths of PMP for the 973-mi^2 area of the Auburn drainage:

Auburn drainage average PMP depths						
	Duration (hours)					
	1	6	12	24	48	72
All-Season Depth (inches)	2.2	6.9	11.2	17.7	29.6	34.6

The results are plotted in Figure 13.19 as a solid line.

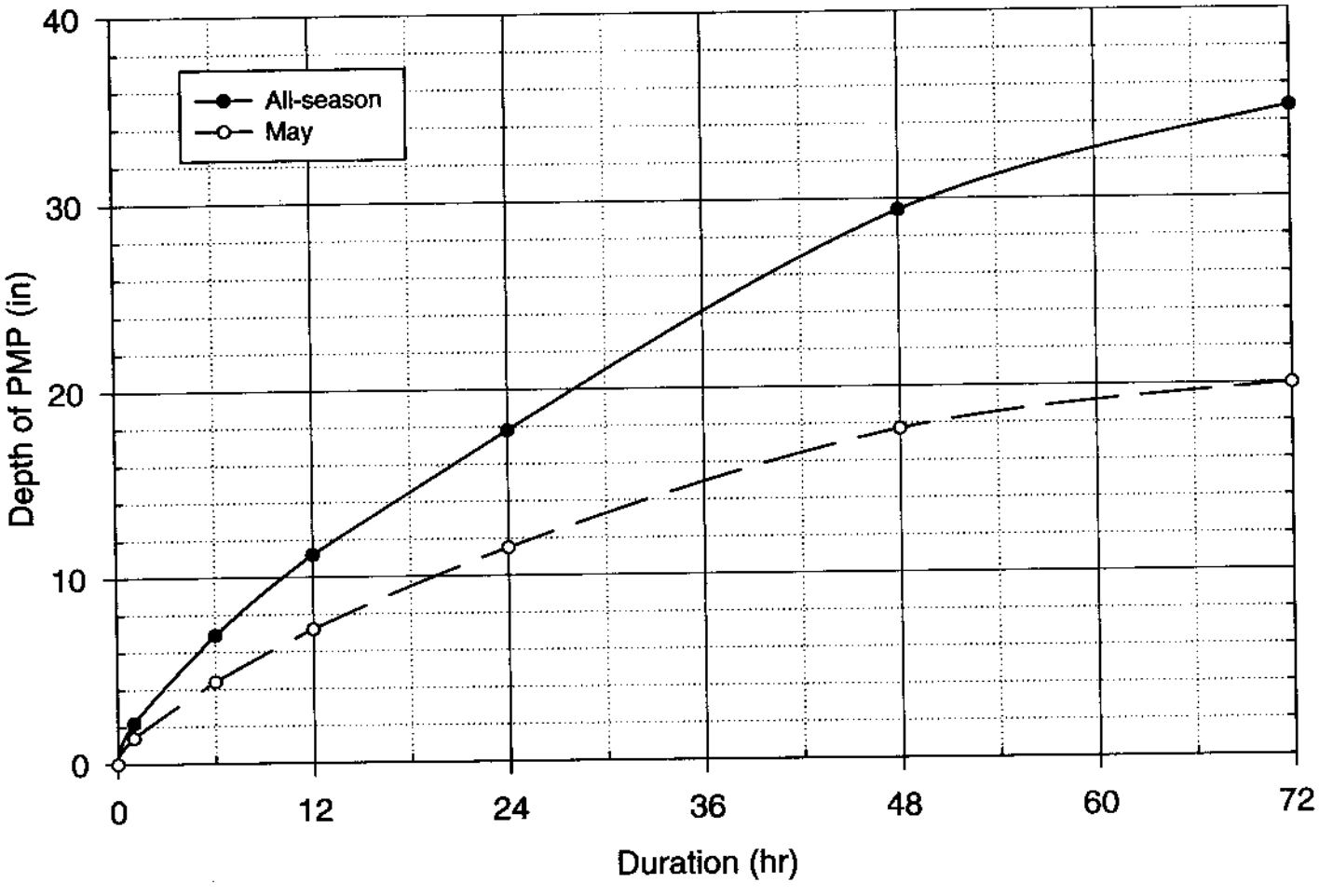

Figure 13.19. *Depth-duration curves for storm-centered, average depth of all-season (solid) and May (dotted) PMP for the 973-mi^2 Auburn drainage in California.*

7. Incremental Estimates

Cumulative depths at 6-hour increments, extracted from the curve of Figure 13.19 are:

6-hour cumulative depths												
	Duration (hours)											
	6	12	18	24	30	36	42	48	54	60	66	72
All-Season PMP (inches)	6.9	11.2	14.6	17.7	20.8	23.8	26.7	29.6	31.6	32.7	33.7	34.6

The 6-hour incremental amounts are obtained by subtracting each (cumulative) durational amount from the next larger amount to get:

6-hour incremental depths												
	Duration (hours)											
	6	12	18	24	30	36	42	48	54	60	66	72
All-Season PMP Increment (inches)	6.9	4.3	3.4	3.1	3.1	3.0	2.9	2.9	2.0	1.1	1.0	0.9

8. Temporal Distribution, Areal Distribution, and Snowmelt Parameters

Using the rules from Step 8 the twelve 6-hour increments from Step 7 could be distributed as following: 3.1, 3.0, 2.9, 2.9, 3.1, 4.3, 6.9, 3.4, 1.1, 0.9, 2.0, 1.0

The areal distribution can be found by following Step 8 in Section 13.2.

For snowmelt parameters see Appendix 4. A completed example for the all-season month of November may be found there.

Seasonal or Monthly PMP Calculation

Step

1. Drainage Outline

   As with the all-season example, the outline of the drainage depicted nominally at a scale of 1:1,000,000 in Figure 13.18 is the of Auburn drainage.

2. User Decision

   We will calculate seasonal PMP for the month of May.

3. All-Season Index PMP Estimate

   Even though we are doing PMP for May which is not an all-season month, we need an all-season index value as a starting point. As with the previous all-season example, Figure 13.18 shows the average depth to be 24.6 inches.

4. Seasonal Index PMP estimates

   Figure 13.4 shows the variation of general-storm PMP for the month of May as a percentage of all-season PMP (Plates 1 and 2). We determined an average value of 68 percent (to the nearest whole percent) for the Auburn drainage. This percentage was multiplied by the average depth from Step 3, and gives an average value of PMP of 16.7 inches for May. The nearest all-season month is March (Figure 13.2), and the monthly offset is 2.

5. Depth-Duration Relations

   As indicated earlier, the Auburn drainage is within the Sierra classification (region 5) except for a very small portion near the dam site which is inconsequential. Table 13.2 shows that the seasonally adjusted 10-mi^2 depth-duration ratios for May or a two-month offset are:

Ratios for Auburn drainage						
	Duration (hours)					
	1	6	12	24	48	72
May	.148	.437	.663	1.00	1.451	1.549

The 10-mi^2 depth of May PMP is obtained by multiplying the average 24-hour, 10-mi^2 PMP for May (16.7 inches) at Auburn by ratios for 1 hour to 72 hours. These are shown below:

Auburn drainage 10-mi^2 PMP						
	Duration (hours)					
	1	6	12	24	48	72
May Depth (inches)	2.5	7.3	11.1	16.7	24.2	25.9

6. Areal Reduction Factors

Interpolating to 973 mi^2 from Table 13.7 (Sierra region, offset of 2), we obtain the following reduction ratios:

Reduction factors for Auburn drainage						
	Duration (hours)					
	1	6	12	24	48	72
May	.548	.607	.648	.687	.731	.773

Multiplying these ratios by the corresponding May PMP depths from Step 5 gives the following storm-centered average depths of PMP across the 973-mi^2 Auburn drainage for May:

Auburn average drainage (973-mi^2) PMP depths						
	Duration (hours)					
	1	6	12	24	48	72
May Depth (inches)	1.4	4.4	7.2	11.5	17.7	20.0

7. Incremental Estimates

The results from Step 6 are also plotted in Figure 13.19 and a curve (dotted line) is drawn for these results. Cumulative depths at 6-hour increments to the nearest tenth of an inch, extracted from the curves, are as follows:

6-hour cumulative depths												
	Duration (hours)											
	6	12	18	24	30	36	42	48	54	60	66	72
May PMP (inches)	4.4	7.2	9.4	11.5	13.3	15.0	16.4	17.7	18.5	19.1	19.6	20.0

To obtain 6-hour PMP values, subtract each (cumulative) amount from the next larger amount to get:

6-hour incremental depths												
	Duration (hours)											
	6	12	18	24	30	36	42	48	54	60	66	72
May PMP Increment (inches)	4.4	2.8	2.2	2.1	1.8	1.7	1.4	1.3	0.8	0.6	0 .5	0.4

8. Temporal Distribution, Areal Distribution, and Snowmelt Parameters

A possible temporal precipitation (inches) sequence for the twelve 6-hour increments in May is: 0.6, 0.8, 2.2, 4.4, 2.8, 2.1, 1.8, 1.7, 1.4, 1.3, 0.5, 0.4

This is a possible sequence from the guidelines mentioned is Step 8 of Section 13.2. The areal distribution of isohyets can be obtained using the guidance from Step 8 of Section 13.2. No snowmelt parameters are required for May, since they are only valid for October through April.

13.4 Local Storm Procedures

Two options are available for obtaining the local-storm PMP values. They are:

A. Obtain the average depth of PMP for a drainage without specifying its areal distribution, or

B. Specify the areal distribution of the precipitation from a PMP storm within a drainage.

Option A requires Steps 1-5 below; Option B requires that Steps 1 and 2 are used followed by Step 6. If Option B is selected, a drainage average depth of the isohyetal precipitation pattern for various PMP storm placements must be chosen. There will be as many average depths for the drainage as there are placements for the PMP storm. The average depths of precipitation in a drainage obtained from Option B will be less than the average depth of PMP from Option A unless the drainage has the exact boundary shape shown in Figure 13.20.

Step

1. One-hour, 1-mi^2 local-storm PMP

   Locate the basin on Figure 13.21 and determine the basin-average, 1-hour, 1-mi^2, local-storm index value of PMP. Use linear interpolation.

2. Adjustment for Mean Drainage Elevation

   Determine the mean elevation of the drainage. No adjustment is necessary for elevations of 6,000 feet or less. If the mean elevation is greater than 6,000 feet,

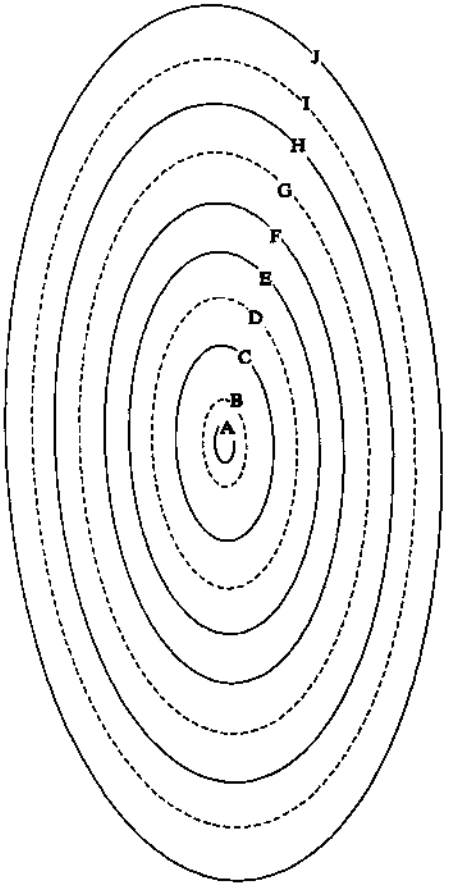

ISOHYET	ENCLOSED AREA AREA (MI^2)	(KM^2)
A	1	2.6
B	5	13
C	25	65
D	55	142
E	95	246
F	150	388
G	220	570
H	300	777
I	385	997
J	500	1295

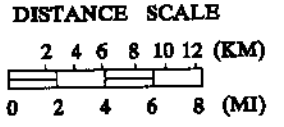

SCALE
1:500,000

Figure 13.20. *Idealized isohyetal pattern for local-storm PMP areas up to 500 mi^2. Same as Figure 9.18.*

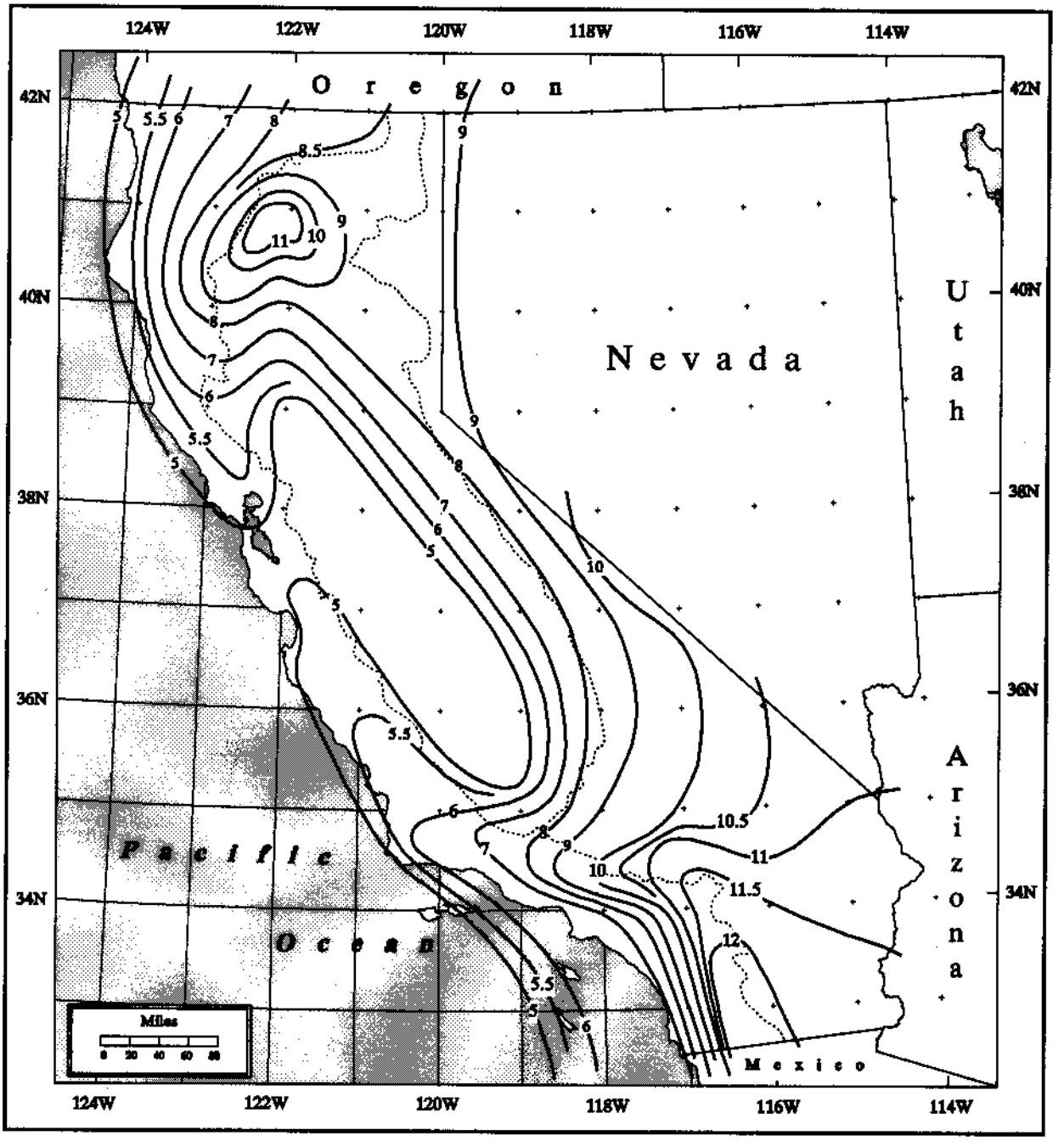

Figure 13.21. *California local-storm PMP precipitation estimates for 1 mi², 1 hour (inches). Dashed lines are drainage divides. Same as Figure 9.23.*

reduce the PMP from Step 1 by 9 percent for every 1,000 feet above the 6,000-foot level. Figure 13.22 can be used to graphically determine this value.

As an example of the elevation adjustment let us assume we have a basin with a mean elevation of 8,700 feet (2,700 feet above 6,000 feet). The reduction factor would be 24.3 percent (2.7 times .09), giving an elevation-adjusted PMP of 76 percent (rounded) of full 1-hour, 10-mi^2 PMP. Had Figure 13.22 been used, a value of about 76 percent is read off the line labeled pseudo-adiabat for an elevation of 8,700 feet.

3. Adjustment for Duration

The 1-mi^2 local-storm PMP estimates for durations less than 1 hour are obtained from Figure 13.23, as a percentage of the 1-hour amount from Step 2. For durations greater than 1 hour, determine the location of the basin on Figure 13.24, which provides a 6-hour to 1-hour ratio of the local-storm PMP. Multiply this ratio by the 1-hour local-storm PMP to obtain the 6-hour local-storm PMP. The four multipliers on Figure 13.24 are defined as A (1.15), B (1.2), C (1.3), and D (1.4) and correspond to the A, B, C, and D of Figure 13.23. Local-storm PMP amounts for durations of 1 to 6 hours can be obtained from Figure 13.23 or Table 13.10 for specific durations.

4. Adjustment for Basin Area

Figures 13.25 to 13.28 give the area reductions to 500 mi^2 depending on the 6-hour depth-duration ratio used in Step 3. The reductions obtained for the selected durations and area of the basin then are multiplied respectively by the results from Step 3, and a smooth curve is drawn on graph paper for the plotted values to get estimates for durations not specified.

5. Temporal Distribution

Review of local-storm temporal distributions for this region show that most local storms have durations less than 6 hours and that the greatest 1-hour amount occurs

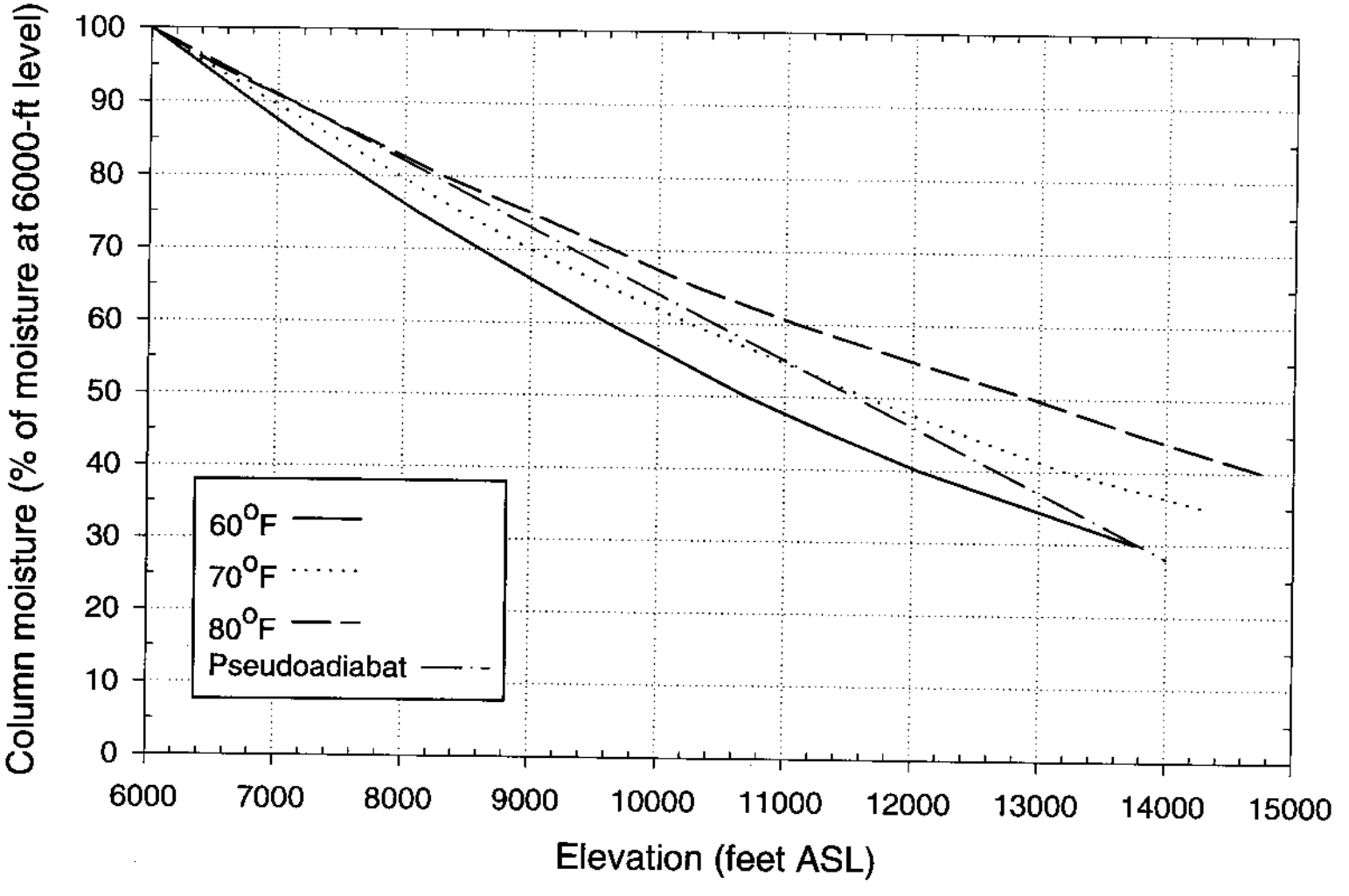

Figure 13.22. *Pseudoadiabatic decrease in column moisture for local-storm basin elevations.*

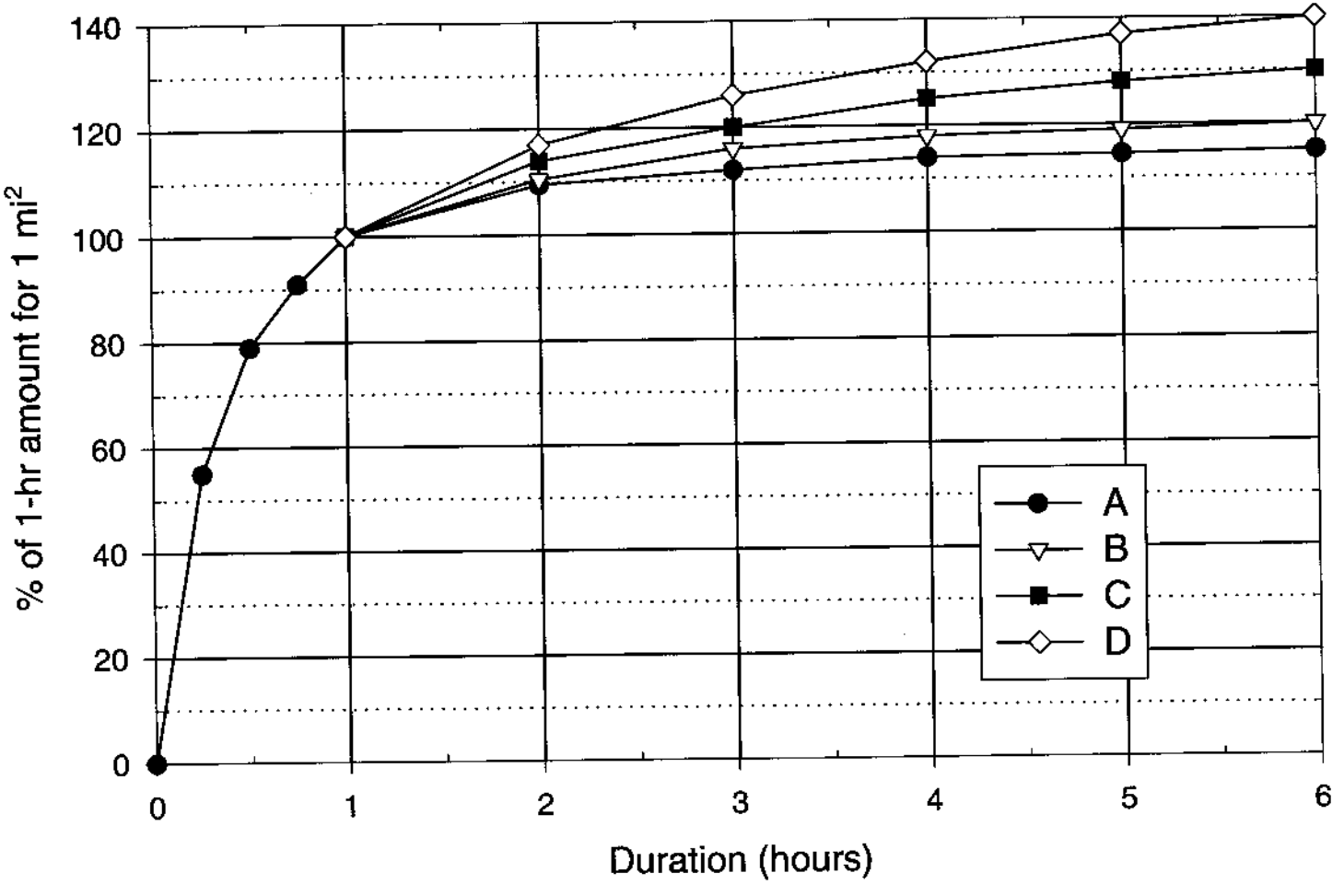

Figure 13.23. *Depth-duration relations for California for 6-hour to 1-hour ratios. The ratios are mapped in Figure 13.24; A = 1.15, B = 1.2, C = 1.3, D = 1.4. Same as Figure 9.17.*

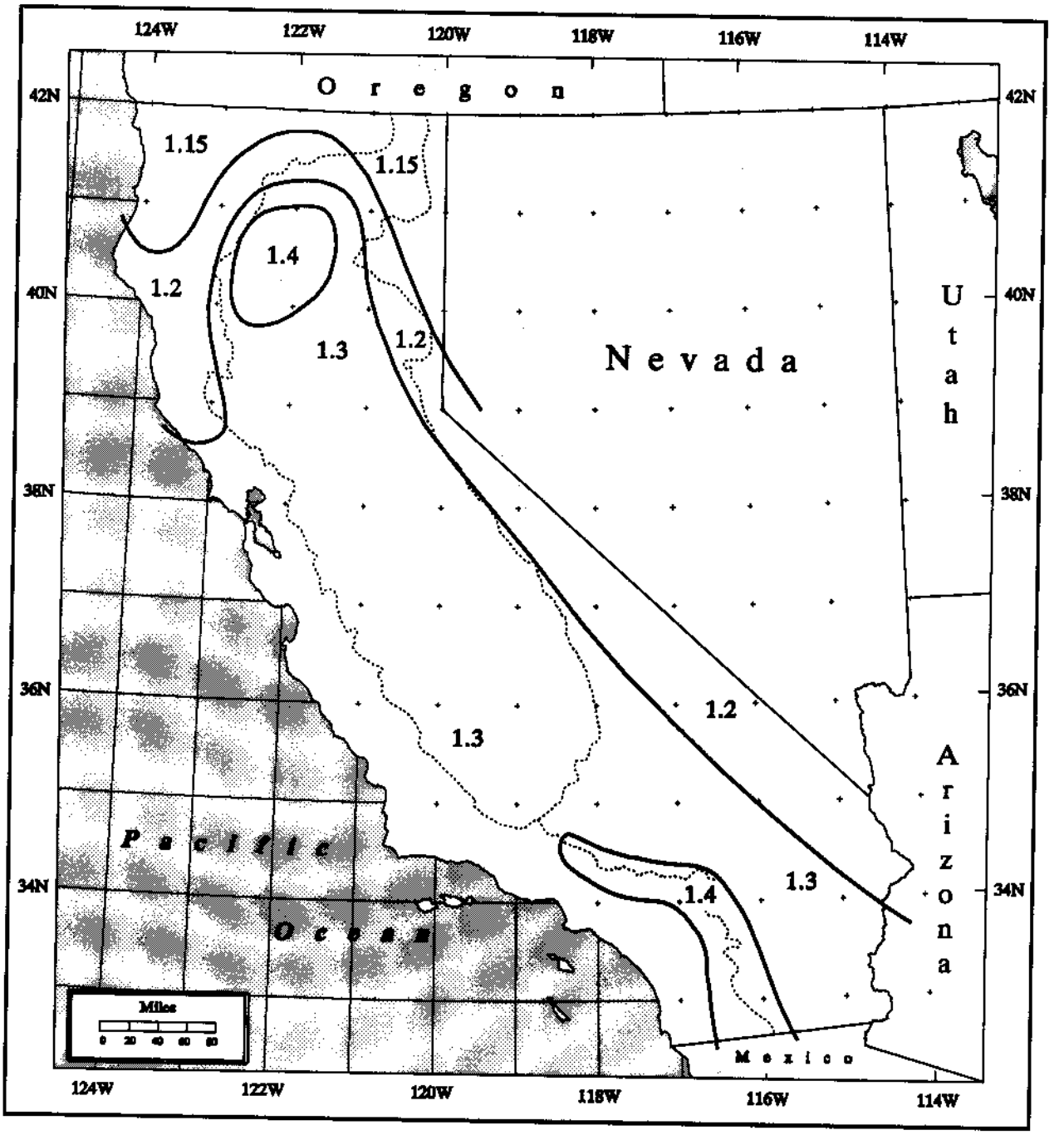

Figure 13.24. *California local-storm PMP 6-hour to 1-hour ratios for 1 mi². For use with Figure 13.23; A = 1.15, B = 1.2, C = 1.3, D = 1.4. Dashed lines are drainage divides. Same as Figure 9.16.*

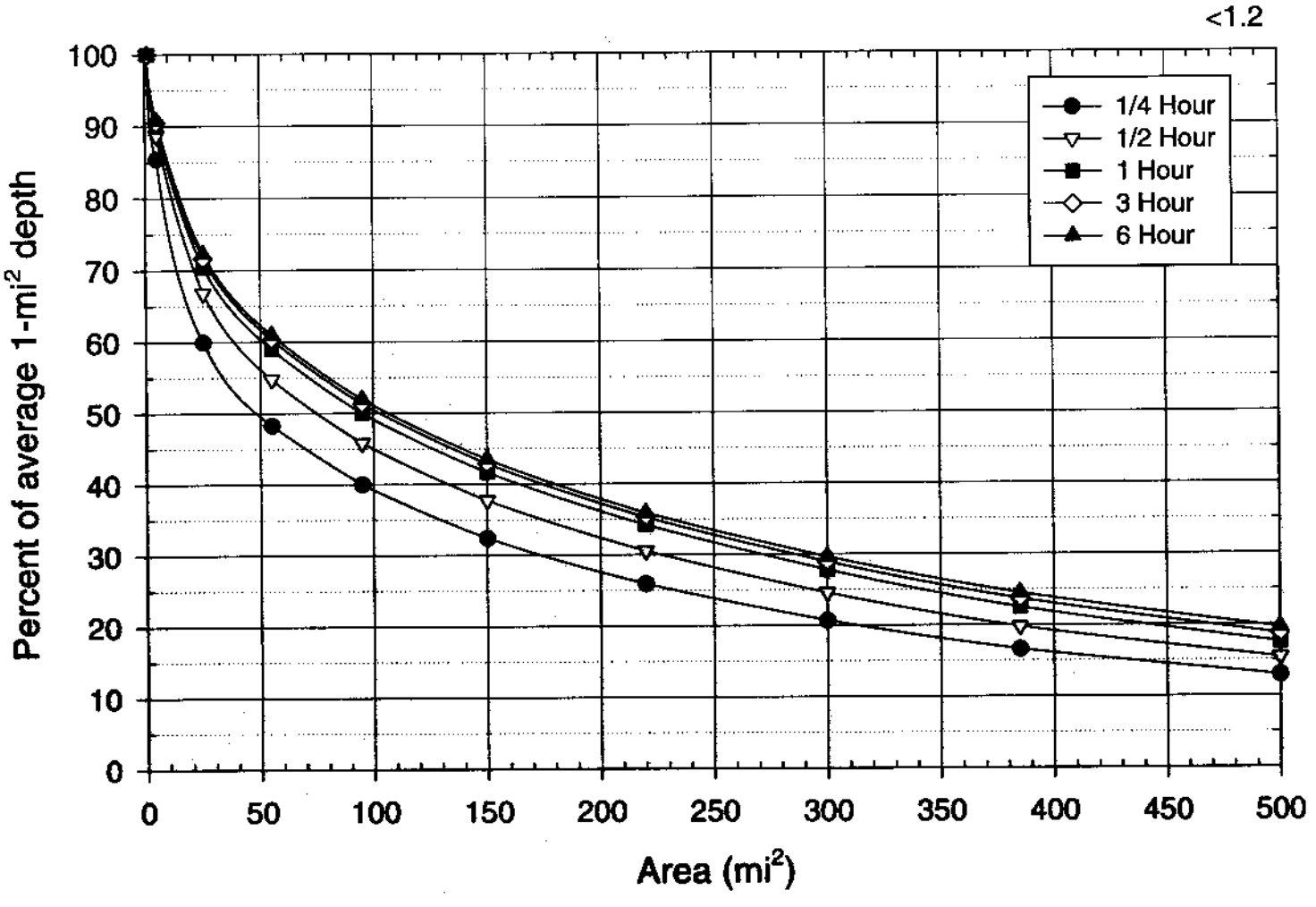

Figure 13.25. *Depth-area relations for California local-storm PMP for a 1-mi², 6-hour to 1-hour depth-duration ratio less than 1.2. Same as Figure 9.19.*

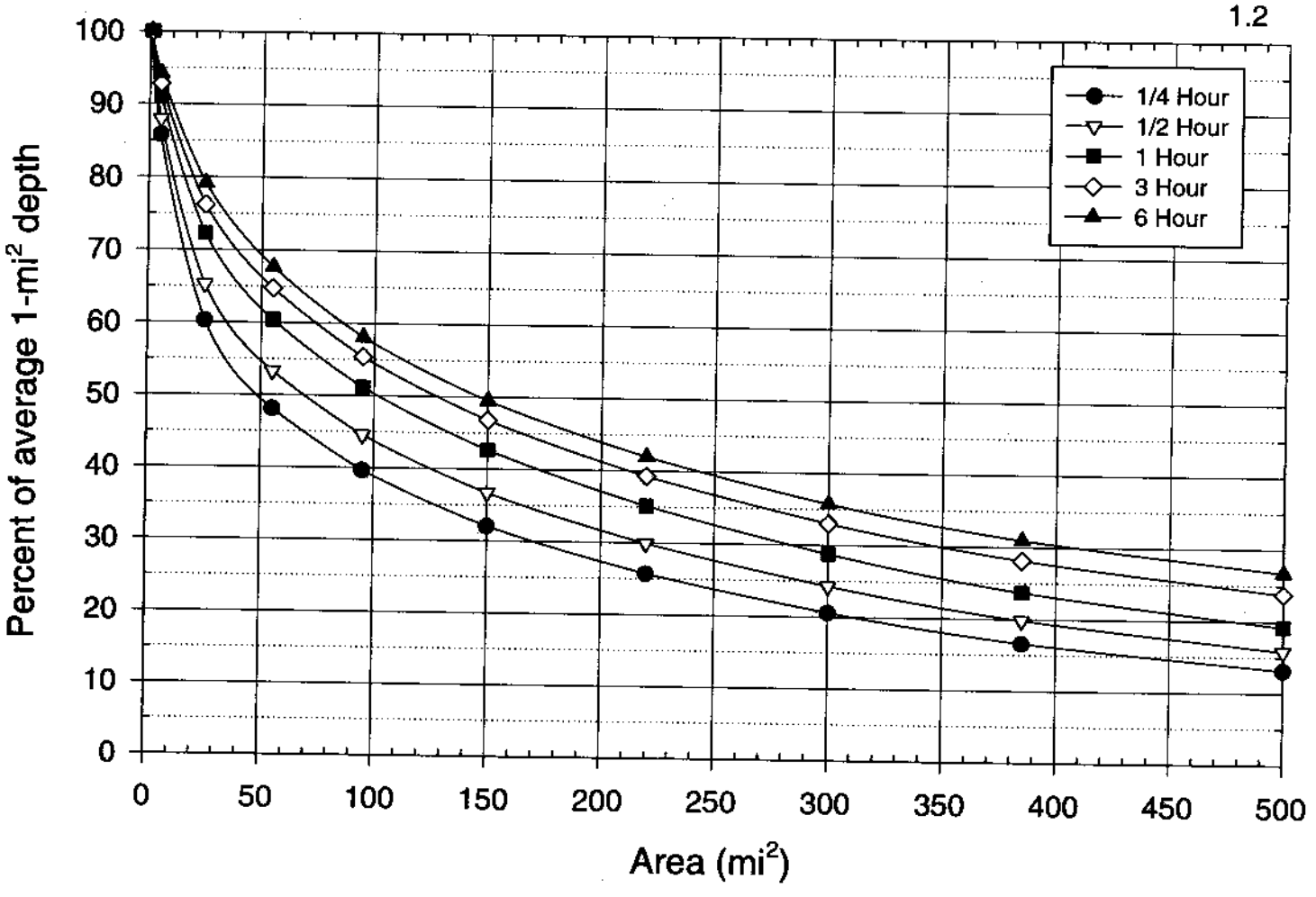

Figure 13.26. *Depth-area relations for California local-storm PMP for a 1-mi², 6-hour to 1-hour depth-duration ratio equal to 1.2. Same as Figure 9.20.*

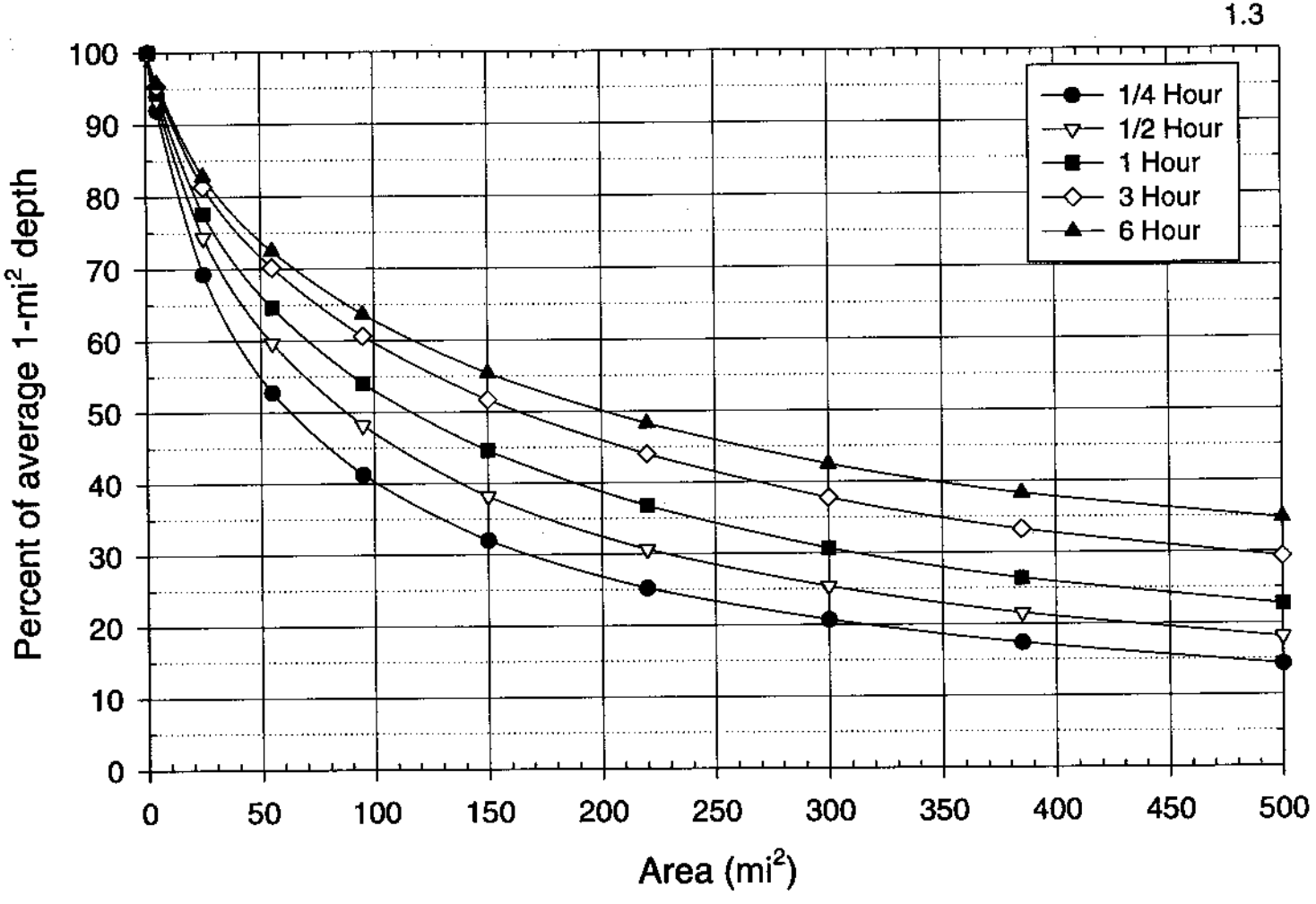

Figure 13.27. *Depth-area relations for California local-storm PMP for a 1-mi², 6-hour to 1-hour depth-duration ratio equal to 1.3. Same as Figure 9.21.*

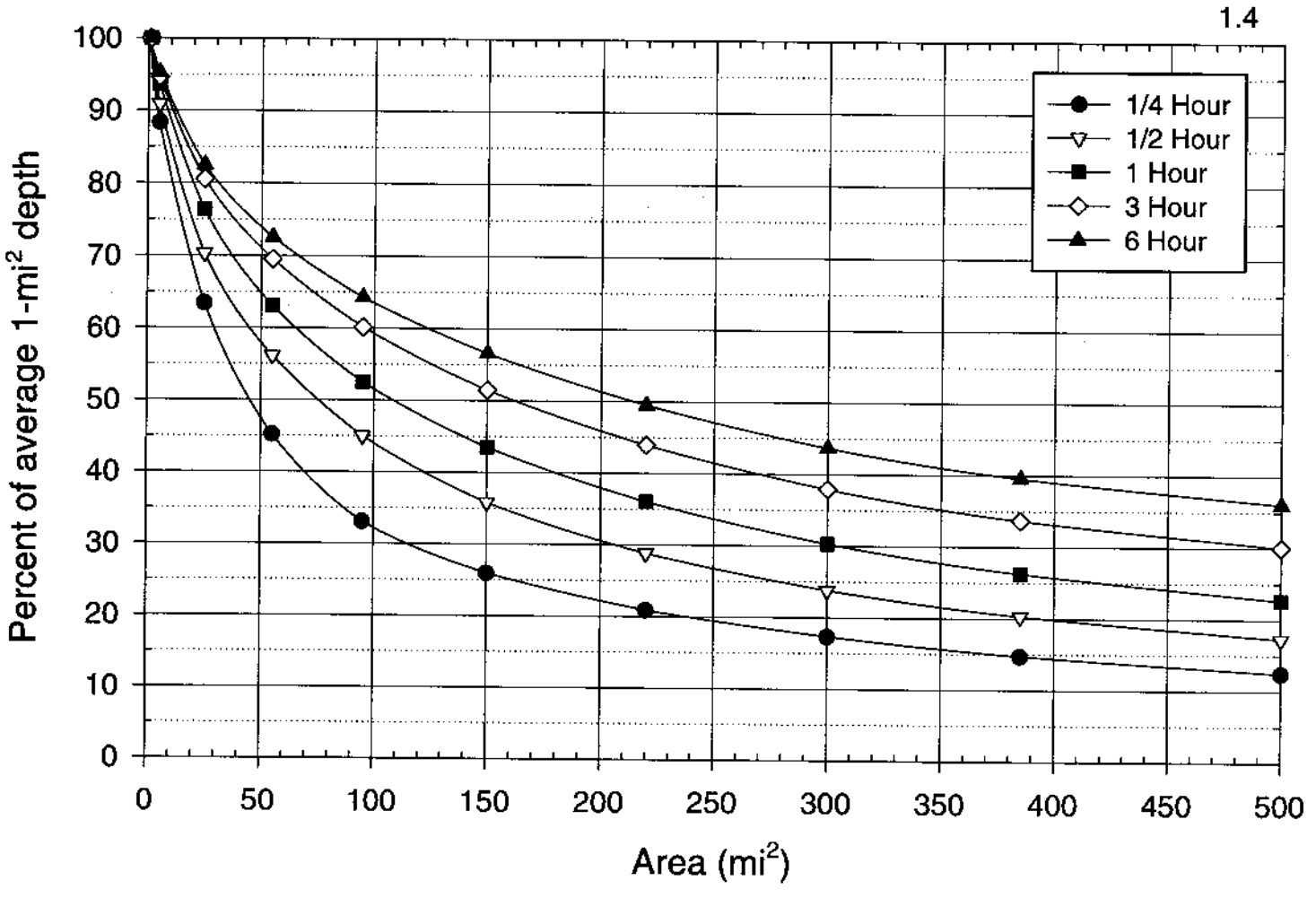

Figure 13.28. *Depth-area relations for California local-storm PMP for a 1-mi², 6-hour to 1-hour depth-duration ratio equal to 1.4. Same as Figure 9.22.*

in the first hour. The recommended sequence of hourly increments is as follows: arrange the hourly increments from largest to smallest as obtained directly by successive subtraction of values read from the smoothed depth-duration curve. The most intense 1-hour of precipitation occurs in the first hour of the storm, the second most intense hour in the second hour, and so forth.

Table 13.10.
Depth-duration relations (percent of 1-hour amount) for 1-mi² PMP for California local storms.

	Relationship Designator (see Figure 13.23)			
Duration (hours)	A	B	C	D
0	0	0	0	0
1/4	55	55	55	55
1/2	79	79	79	79
3/4	91	91	91	91
1	100	100	100	100
2	109.5	110.5	114	117
3	112	116	120	126
4	114	118	125	132
5	114.5	119	128	137
6	115	120	130	140

6. Areal Distribution for Local-Storm PMP

The elliptical pattern in Figure 13.20 and the tabulated percentages in Tables 13.11 to 13.14, are used to describe the areal distribution of precipitation of a local PMP storm. The 2:1 ratio of the major to minor axis of Figure 13.20 should be used or *placed* only on a map at a 1:500,000 scale. The average index value from Step 2 (or Step 1 if no elevation adjustment is made) is multiplied by each of the percentages from the appropriate table (Tables 13.11 to 13.14) to obtain the value for each

Table 13.11. *Isohyetal label values (percent of 1-hour, 1-mi² average depth) to be used in conjunction with isohyetal pattern of Figure 13.20 and basin-average depths from Figure 13.25.*

	Duration (hours)								
Isohyet	1/4	1/2	3/4	1	2	3	4	5	6
A	55	79	91	100	109.5	112	114	114.5	115
B	35	57	68	74.8	83.5	85.5	87.5	88	88.5
C	24	40	49	56	62.9	4.5	66	66.5	67
D	18.5	30.5	39	43	48	49.5	50.6	51.1	51.5
E	13	22.5	29	32.2	36.6	37.7	38.6	39	39.5
F	7.5	14.0	19	22.4	25	25.7	26.3	26.7	27.0
G	4.5	8.5	12	14.0	16.2	16.8	17.4	17.9	18.2
H	1.8	3.5	5	6.5	8.3	8.8	9.3	9.8	10.3
I	0.4	0.7	0.9	1.1	2.2	2.7	3.2	3.7	4.1
J	0.1	0.3	0.5	0.7	1.2	1.7	2.2	2.6	2.9

Table 13.12. *Isohyetal label values (percent of 1-hour, 1-mi² average depth) to be used in conjunction with the isohyetal pattern of Figure 13.20 and basin-average depths from Figure 13.26 .*

	Duration (hours)								
Isohyet	1/4	1/2	3/4	1	2	3	4	5	6
A	55	79	91	100	110.5	116	118	119	120
B	35.5	55	68	78	88	95	99	101	102.5
C	24	39	49	57	66	72	75	77	78.5
D	19	30	39	44	51.5	56	58.5	60	61
E	13.5	22	28	33	39	42.7	44.5	46	47
F	8.5	15	20	23	28	31.5	33.5	35	36
G	5.5	9.5	13	15	19	22	24	25	26
H	2	4.5	6.0	7.5	11.5	14.5	16.5	17.5	18.5
I	1	2	3	4	8	11	13	14.5	15.5
J	1	2	3	4	7	10	12	13.5	14.5

Table 13.13. *Isohyetal label values (percent of 1-hour, 1-mi² average depth) to be used in conjunction with the isohyetal pattern of Figure 13.20 and basin-average depths from Figure 13.27.*

	Duration (hours)								
Isohyet	1/4	1/2	3/4	1	2	3	4	5	6
A	55	79	91	100	114	120	125	128	130
B	44	66	77.6	86	100	106	111	114	116
C	26	44	53.6	61	74	81	86	89	91
D	17	31	40.2	46.5	58	65	70	73	75
E	11	20	26.8	32.5	42	49	54	57	59
F	6.6	13	19	24	32	38	43	46	48
G	6.5	11	14	16	23	28	33	36	38
H	5	8	10.5	12	17.5	21.5	25.5	29	31
I	3	6.0	8.5	10.5	16	20	24	27.5	30
J	2.5	5.5	8	10	15	19	23	26.5	29

Table 13.14. *Isohyetal label value (percent of 1-hour, 1-mi² average depth) to be used in conjunction with the isohyetal pattern of Figure 13.20 and basin-average depths from Figure 13.28.*

	Duration (hours)								
Isohyet	1/4	1/2	3/4	1	2	3	4	5	6
A	55	79	91	100	117	126	132	137	140
B	39	61	74	84	100	109	115	120	123
C	24	42	52	60	76	85	91	96	99
D	15	28	37	44	59	67	73	78	81
E	9	19	26	32	44	52	58	63	67
F	6	13.5	19	24	34	40	45	50	54
G	6	10	13.5	16	24	30	35	39	42
H	4	7	10	13	19	24	28	32	35.5
I	3.3	6.5	9	11	18	23	27	31	34.5
J	3	5.5	8	10	17	22	26	30	33.5

lettered isohyet (A - J). Once the labels have been determined for each application, the pattern can be moved to different placements on the basin. In most instances, the greatest volume of precipitation will be obtained when the pattern is centered in the drainage. However, peak flows may actually occur with placements closer to the drainage outlet. The basin-averaged depth of precipitation is obtained for chosen local PMP storm placements, by using planimetry, a GIS, or other area-averaging methods.

13.5 Example of Local-Storm PMP Calculation

We have selected a small area in southeastern California known as the McCoy Wash to illustrate the steps for calculating local-storm PMP. The Wash has an area size of 167 mi^2 and its boundary, along with selected contours of elevation, is shown in Figure 13.29. We will illustrate both options A and B referenced in the previous section.

Local-Storm PMP for McCoy Wash

Step

1. One-hour, 1-mi^2 PMP

   The centroid of the Wash is near latitude 33.75° N and longitude 114.75° W. Interpolation to this centroid on Figure 13.21 gives an average local PMP value (1-hour, 1-mi^2) of 11.4 inches to the nearest tenth of an inch. Interpolation was appropriate here since there is little, if any, gradient of index values across the Wash. For locations where significant gradients of index values exist, an average index value should be found.

2. Adjustment for Mean Drainage Elevation

   The mean elevation of the Wash is well below 6,000 feet as shown on Figure 13.29. No elevation adjustment is needed, and the local-storm PMP from Step 1 remains at 11.4 inches.

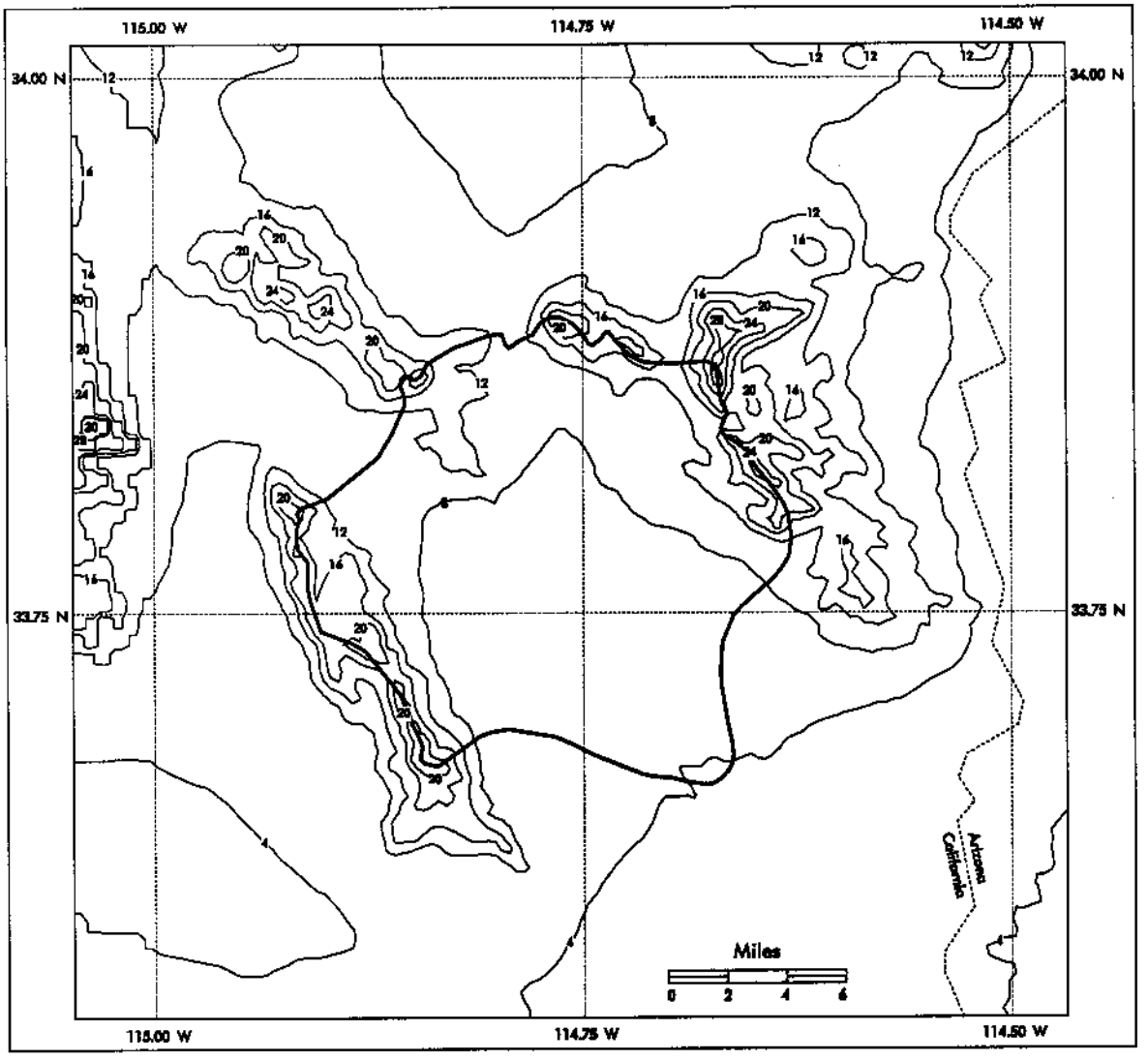

Figure 13.29. *McCoy Wash, California drainage boundary (solid, heavy line) with elevation contours (solid, thin lines) in hundreds of feet.*

3. Adjustment for Duration

The value of the 6-hour to 1-hour ratio near the Wash's centroid found in Figure 13.24 is 1.3. The depth-duration curve which applies here is curve *C* from Figure 13.23, and column *C* from Table 13.10 is also applicable.

Multiplication of the column *C* percentages by the average depth from Step 2 gives the average 1-mi^2 values for the Wash:

	Duration (hours)								
	1/4	1/2	3/4	1	2	3	4	5	6
1-mi^2 Average Depth (inches)	6.3	9.0	10.4	11.4	13.0	13.7	14.3	14.6	14.8

4. Adjustment for Basin Area

Figure 13.27 gives the depth-area relations for a 6-hour to 1-hour ratio of 1.3 The reduction ratios used to obtain average depths basin from 1-mi^2 depths for the 167 mi^2 and their depths are:

	Duration (hours)				
	1/4	1/2	1	3	6
Reduction Ratio	.31	.37	.43	.50	.54
167-mi^2 Average Depth (inch)	2.0	3.3	4.9	6.9	8.0

These results are shown, and a smooth curve fitted to these depths as shown in Figure 13.30.

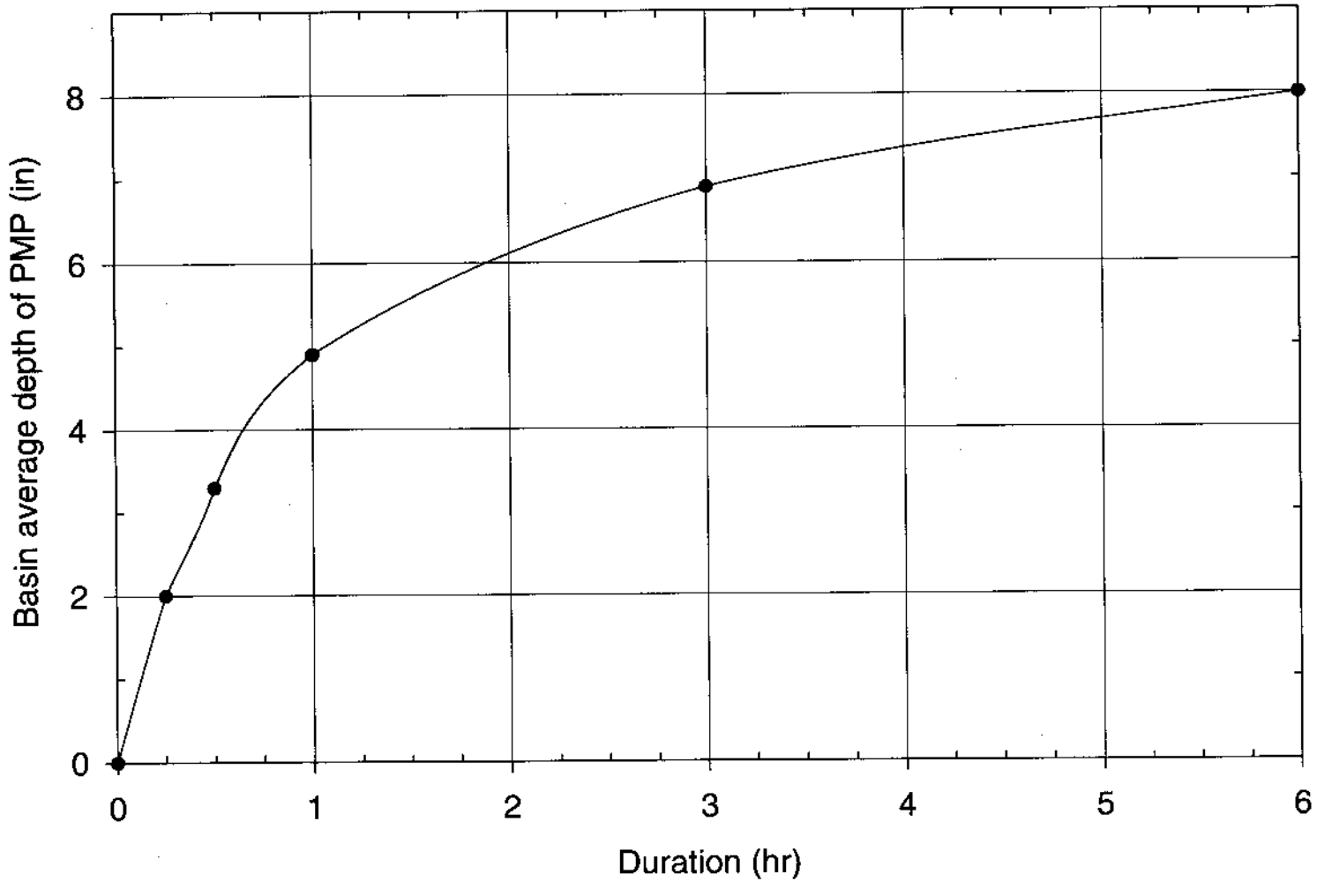

Figure 13.30. *Average depth of local-storm PMP for the 167-mi² McCoy Wash, California.*

5. Temporal Distribution

The smoothed cumulative hourly values from Step 4 and the incremental hourly values resulting from successive subtractions are:

Hourly Intervals						
	1	2	3	4	5	6
Cumulative PMP (inch)	4.9	6.1	6.9	7.4	7.7	8.0
Incremental PMP (inch)	4.9	1.2	0.8	0.5	0.3	0.3

The highest increment to lowest increment sequence shown above is the recommended chronology for local-storm PMP at McCoy Wash.

6. Areal Distribution of Local-Storm PMP

The areal distribution of local-storm PMP is given by the isohyets of Figure 13.20. Remember these isohyets are meant to be placed within a basin boundary at the 1:500,000 map scale. For this example, the percentages from Table 13.13 apply for a basin with a 6-hour to 1-hour ratio of 1.3. When the 6-hour to 1-hour ratio is 1.15, 1.2, or 1.4, Tables 13.11, 13.12, or 13.14 apply respectively.

It is important to note that when Tables 13.11 to 13.14 are used in a particular case, that the percentages from the selected table apply only to the 1-mi^2, 1-hour average local-storm PMP from Step 2, and NOT to the values from Step 3. In this example, the average depth is 11.4 inches, and the isohyetal labels of Table 13.15 result. An average 6-hour depth of 8.0 inches for the 167-mi^2 McCoy Wash Basin is given (Step 4). Using Figure 13.20 the isohyetal labels range from 14.82 inches enclosing 1 mi^2 to 4.33 inches enclosing 220 mi^2 for that duration.

Remember that the isohyetal labels in Step 6 produce the average depths from Step 4 only if the basin in consideration is elliptical with a 2:1 ratio of the major to minor

axis and the ellipses are centered in a *perfect* drainage. The ellipses with the indicated values from this step when placed in an irregularly shaped drainage and then averaged, will produce average depths less than those resulting from Step 4. The PMP level for the drainage comes from Step 4, with the isohyetal labels of Step 6 giving an idea of a possible areal distribution for the storm.

Table 13.15. *Isohyetal label values for local-storm PMP, McCoy Wash, California (167 mi^2).*

Isohyetal Tag (mi^2)	Duration (hours) 1/4	1/2	3/4	1	2	3	4	5	6
A (1)	6.27	9.01	10.37	11.40	13.00	13.68	14.25	14.59	14.82
B (5)	5.02	7.52	8.85	9.80	11.40	12.08	12.65	13.00	13.22
C (25)	2.96	5.02	6.11	9.65	8.44	9.23	9.80	10.15	10.37
D (55)	1.94	3.53	4.58	5.30	6.61	7.41	7.98	8.32	8.55
E (95)	1.25	2.28	3.06	3.71	4.79	5.59	6.16	6.50	6.72
F (150)	.75	1.48	2.17	2.74	3.65	4.33	4.90	5.24	5.47
G (220)	.74	1.25	1.60	1.82	2.62	3.19	3.76	4.10	4.33
H (300)	.57	.91	1.20	1.37	2.00	2.45	2.91	3.31	3.53
I (385)	.34	.68	.97	1.20	1.82	2.28	2.74	3.14	3.42
J (500)	.29	.63	.91	1.14	1.71	2.17	2.62	3.02	3.31

Endnote[1]

Plates 1 and 2 have limited detail in some regions. The Hydrometeorological Design Studies Center will provide supplemental map(s) containing a more complete set of isohyets or digital values for specific drainages areas, upon request.

ACKNOWLEDGMENTS

This report was prepared under the direction of John Vogel, formerly Chief of the Hydrometeorological Design Studies Center and presently Director of the National Weather Service Training Center, and subsequently by Lesley T. Julian, Program Manager of the Hydrometeorological Design Studies Center. Other contributors include: Julie Daniel, Tania Davila, Susan Gillette, John McGovern, Dan Romberger, Barbara Turner, and Michael Yekta.

This report was submitted to and reviewed by the following: Catalino Cecilio, Robert Collins, Dennis Marfice, Douglas Morris, John Riedel, Maurice Roos, Louis Schreiner, Ronald Spath, and Richard Stodt. The following individuals from the U.S. Army Corps of Engineers provided valuable insights and guidance during review of this report: Earl Eiker, Richard DiBuono, Frank Krhoun. All of the above are thanked for their invaluable contributions.

REFERENCES

Abbs, D.J. and R.A. Pielke, 1986: Thermally forced surface flow and convergence patterns over northeast Colorado, *Monthly Weather Review*, Vol. 114, 2281-2296.

Adang, T.C. and R.L. Gall, 1989: Structure and dynamics of the Arizona monsoon boundary, *Monthly Weather Review,* Vol. 117, 1423-1438.

American Meteorological Society, 1959: *Glossary of Meteorology*, Boston, MA, 638 pp.

Australian National Committee on Large Dams, 1988: Workshop on spillway design floods, *Conference proceedings for workshop,* held February 4, 1988 in Canberra, Australia, published by the Water Authority of Western Australia, Leederville, Australia, 81 pp.

Banta R.M. and C.B. Schaaf, 1987: Thunderstorm genesis zones in the Colorado Rocky Mountains as determined by traceback of geosynchronous satellite images, *Monthly Weather Review*, Vol. 115, 463-476.

Bolsenga, S.J., 1965: The relationship between total atmospheric water vapor and surface dewpoint on a mean daily and hourly basis, *Journal of Applied Meteorology*, Vol. 4, 430-432.

Browning, K.A., M.E. Hardman, T.W. Harrold, and C.W. Pardoe, 1973: The structure of rainbands within a midlatitude depression, *Quarterly Journal of the Royal Meteorological Society*, Vol. 99, 215-231.

Browning, K.A., 1980: On the low-level redistribution of atmospheric water caused by orography, *Proceedings International Cloud Physics Conference*, Tokyo, Supplement, pp 96-100.

Bryant, W.C., 1972: Report on the Bakersfield storm, June 7, 1972, prepared by Kern County Water Agency, Bakersfield, California, July, 1972.

Carleton, A.M., 1985: Synoptic and satellite aspects of the southwestern United States summer "monsoon," *Journal of Climatology*, Vol. 5, 389-402.

Carleton, A.M., 1986: Synoptic-dynamic character of 'bursts' and 'breaks' in the South-west U.S. summer precipitation singularity, *Journal of Climatology*, Vol. 6, 605-622.

Changery, M.J., 1981: National thunderstorm frequencies for the contiguous United States, National Climatic Data Center, Asheville, NC, 22 pp. plus appendices.

Cooper, C.F., 1967: Rainfall intensity and elevation in southwestern Idaho, *Water Resources Research*, Vol. 3, 131-137.

Corrigan, P., D.D. Fenn, D.R. Kluck, and J.L. Vogel, 1998: Probable maximum precipitation for California – calculation procedures, *Hydrometeorological Report Number 58*, National Weather Service, National Oceanic and Atmospheric Administration, U. S. Department of Commerce, Silver Spring, MD, 92 pp.

Cotton, W.R., and R.A. Anthes, 1989: *Storm and Cloud Dynamics*, Academic Press, San Diego, CA, 883 pp.

Crutcher, H.L. and J.M. Meserve, 1970: *Selected Level Heights, Temperatures and Dewpoints for the Northern Hemisphere*, Naval Weather Service Command, Washington DC.

Cudworth, A.G., Jr., 1989: *Flood Hydrology Manual*, United States Government Printing Office, Denver, CO, 243 pp.

Douglas, M.W., 1995: The summertime low-level jet over the Gulf of California, *Monthly Weather Review*, Vol. 123, 2334-2346.

Environmental Data Service, 1896-1976: *Climate and Crop Service*, 1896-1910; *Monthly Weather Review*, 1910-13; *Climatological Data by Sections*, 1914-76, National Oceanic and Atmospheric Administration, U.S. Department of Commerce, Asheville, NC.

Federal Emergency Management Agency, 1990: Probable maximum precipitation and probable maximum flood workshop, *proceedings of workshop*, held May 1-4, 1990, Berkeley Springs, WV, Washington, DC, 25 pp.

Fenn, D.D., 1985: Probable maximum precipitation estimates for the drainage above Dewey Dam, John's Creek, Kentucky, *NOAA Technical Memorandum, NWS HYDRO #41*, National Weather Service, U.S. Department of Commerce, Silver Spring, MD, 33 pp.

Fleming, E.L. and L.E. Spayd, Jr., 1986: Characteristics of Western Region Flash Flood Events in GOES Imagery, *NOAA Technical Memorandum NESDIS 13*, Washington, D.C., 82 pp.

Fontana, Christopher E., 1977: Study of a heavy precipitation occurrence in Redding, California, *NOAA Technical Memorandum NWS WR-123*, 19 pp.

Goodridge, J.D., 1992: A study of 1000-year storms in California, *Ninth Annual PACLIM Workshop*, Asilmoar Conference Center, Pacific Grove, California, April 21-24, 1992, 67 pp.

Hales, J.E., Jr., 1972: Surges of maritime tropical air northward over the Gulf of California, *Monthly Weather Review,* Vol. 100, 298-306.

Hansen, E.M., 1975: Moisture source for three extreme local rainfalls in the southern intermountain region, *NOAA Technical Memorandum NWS HYDRO-26*, Silver Spring, MD, 57 pp.

Hansen, E.M., F.K. Schwarz, and J.T. Riedel, 1977: Probable maximum precipitation estimates, Colorado River and Great Basin drainages, *Hydrometeorological Report Number 49*, National Weather Service, National Oceanic and Atmospheric Administration, U. S. Department of Commerce, Silver Spring, MD, 161 pp.

Hansen, E.M., and F.K. Schwarz, 1981: Meteorology of important rainstorms in the Colorado and Great Basin drainages, *Hydrometeorological Report Number 50*, National Weather Service, National Oceanic and Atmospheric Administration, U.S. Department of Commerce, Silver Spring, MD, 167 pp.

Hansen, E.M., D.D. Fenn, L.C. Schreiner, R.W. Stodt, and J. F. Miller, 1988: Probable maximum precipitation estimates--United States between the Continental Divide and the 103rd meridian, *Hydrometeorological Report Number 55A*, National Weather Service, National Oceanic and Atmospheric Administration, U.S. Department of Commerce, Silver Spring, MD, 242 pp.

Hansen, E.M., D.D. Fenn, P. Corrigan, J.L. Vogel, L.C. Schreiner, and R.W. Stodt, 1994: Probable maximum precipitation–Pacific northwest states, *Hydrometeorological Report Number 57*, National Weather Service, National Oceanic and Atmospheric Administration, U. S. Department of Commerce, Silver Spring, MD, 338 pp.

Henz, J.F. and R.A. Kelly, 1989: Survey of thunderstorm rainfall characteristics in the Colorado Central Front Range above 7500 feet from 1979 to 1988 (storm data), *Report for Colorado Water Conservation Board*, Denver, CO.

Hill, Christopher D., 1993: Forecast problems in the western region of the National Weather Service: An overview, *Weather and Forecasting*, Vol. 8, 158-165.

Hobbs, P., 1978: Organization and structure of clouds and precipitation on the mesoscale and microscale in cyclonic storms, *Review of Geophysics and Space Physics*, Vol. 16, 741-755.

Hobbs, P.V., 1989: Research on clouds and precipitation: past, present, and future, Part 1, *Bulletin of the American Meteorological Society*, Vol. 70, 282-285.

Jarrett, R.D. and J.E. Costa, 1986: Evaluation of the flood hydrology in the Colorado Front Range using streamflow records and paleoflood data for the Big Thompson River basin, *International Symposium on Flood Frequency and Peak Analyses*, May 14-17, 1986, American Water Resources Association.

Jarrett, R.D., 1990: Hydrology and paleohydrology used to improve the understanding of flood hydrometeorology in Colorado, in *Design of Hydraulic Structures 89: Proceedings of the Second International Symposium on Design of Hydraulic Structures*, Fort Collins, CO, June 26-29 1989, Maurice L. Alberston and Rahim A. Kia, [eds.], A.A. Balkema, Rotterdam, Netherlands, and Brookfield, Vermont 489 pp.

Jennings, A.H., 1952: Maximum 24-hour precipitation in the United States, *Technical Paper Number 16*, U.S. Weather Bureau, U.S. Department of Commerce, Washington, DC, 284 pp.

Junker, Norman W., 1992: *Heavy Rain Forecasting Manual*, National Weather Service Training Center, Kansas City, 91 pp.

Juying, X. and R.A. Scofield, 1989: Satellite-derived rainfall estimates and propagation characteristics associated with mesoscale convective systems (MCSs), *NOAA/NESDIS Technical Memorandum NESDIS 25*, U.S. Department of Commerce, Washington, DC, 49 pp.

Katzfey, J.J., 1995: Simulation of extreme New Zealand precipitation events, Part II: Mechanisms of precipitation development, *Monthly Weather Review*, Vol. 123, 755-775.

Kesseli, J.E. and C.B. Beaty, 1959: Desert flood conditions in the White Mountains of California and Nevada, *Technical Report EP-108*, Headquarters Quartermaster R & E Command, U.S. Army, Natick, MS, 120 pp.

Kuehn, M.H., 1983: Effects of exceeding probable maximum precipitation on a severely burned watershed, *Earth Resources Monograph 12*, United States Department of Agriculture Forest Service, Pacific Southwest Region, San Francisco, CA, 27-39.

Lee, R.F., 1973: A refinement of the use of K-values in forecasting thunderstorms in Washington and Oregon, *NOAA Technical Memorandum NWS WR-87*, 21 pp.

Maddox, R.A., 1983: Large-scale meteorological conditions associated with midlatitude, mesoscale convective complexes, *Monthly Weather Review*, Vol. 111, 1475-1493.

Maddox, R.A., L.R. Hoxit, and F. Canova, 1980: Meteorological characteristics of heavy precipitation and flash flood events over the western United States, *NOAA Technical Memorandum,* ERL APCL-23, Boulder, Colorado, 87 pp.

Martin, J.E., J.D. Locatelli, P.V. Hobbs, P. Wang, and J.A. Castle, 1995: Structure and evolution of winter cyclones in the central United States and their effects on the distribution of precipitation, part 1: A synoptic-scale rainband associated with a dryline and lee trough, *Monthly Weather Review*, Vol. 123, 241-264.

McCollum, D.M., R.A. Maddox, and K.W. Howard, 1995: Case study of a severe mesoscale convective system in central Arizona, *Weather and Forcasting*, September 1995, Vol. 10, 643-665.

Meitin, J., K.W. Howard, and R.A. Maddox, 1991: SW area monsoon project: *Daily Operations Summary*, National Severe Storms Laboratory, Norman, OK, 115 pp.

Miller, J.F., R.H. Frederick, and R.J. Tracey, 1973: Precipitation frequency atlas of the western United States, Vol. XI, California, *NOAA Atlas 2*, National Weather Service, National Oceanic and Atmospheric Administration, U. S. Department of Commerce, Silver Spring, MD, 71 pp.

Miller, J.F., E.M. Hansen and D.D. Fenn, 1984: Probable maximum precipitation for the Upper Deerfield River drainage, Massachusetts/Vermont, *NOAA Technical Memorandum, NWS HYDRO 39*, National Weather Service, U.S. Department of Commerce, Silver Spring, MD, 36 pp.

National Climatic Data Center (NCDC), 1948- : *Local Climatological Data (Station)*, NESDIS, U.S. Department of Commerce, Asheville, NC (ongoing publication.)

National Climatic Data Center, 1951- : *Hourly Precipitation Data (State)*, NESDIS, U.S. Department of Commerce, Asheville, NC (ongoing publication.)

National Climatic Data Center, 1992: Maps of annual 1961-1990 normal temperature, precipitation and degree days, *Climatography of the United States Number 81 - Supplement Number 3*. U.S. Department of Commerce, Asheville, NC, 6 pp.

National Oceanic Atmospheric Administration Environmental Research Laboratory, 1985: *Comprehensive Ocean-Atmosphere Data Set Release 1*, Boulder, Colorado.

National Research Council, 1985: *Safety of Dams, Floods, and Earthquake Criteria*, Water Science and Technology Board, National Academy Press, Washington, DC, 321 pp.

National Research Council, 1988: *Estimating Probabilities of Extreme Floods, Methods, and Recommended Research*, Water Science and Technology Board, National Academy Press, Washington, DC, 141 pp.

National Research Council, 1994: *Estimating Bounds on Extreme Precipitation Events--A Brief Assessment*, Committee on Meteorological Analysis, Prediction, and Research, Board on Atmospheric Sciences and Climate, National Academy Press, Washington DC, 29 pp.

National Weather Service, 1995: *National Weather Summary*, National Severe Storms Forecast Center, Kansas City, MO, July 22, 1995.

Office of Water Data Coordination, 1986: *Feasibility of Assigning a Probability to the Probable Maximum Flood*, Hydrology Subcommittee of the Interagency Advisory Committee on Water Data, Washington, PC, 79 pp.

Peck, E.L., J.C. Monro and M.L. Snelson, 1977: Hydrometeorological data base for the United States, *Proceedings of the Second Conference on Hydrometeorology*, October 25-27, 1977, Toronto, Ontario, Canada, 75-78.

Pyke, C.B., 1975: The Indio California thunderstorm of 24 September 1939. *Proceedings of National Symposium on Precipitation Analysis for Hydrologic Modeling, June 26-28, 1975, Davis, California*, American Geophysical Union, 143-152.

Randerson, D., 1976: Meteorological Analysis for the Las Vegas, Nevada, Flood of 3 July 1975, *Monthly Weather Review*, Vol. 104, 719-727.

Randerson, D., 1986: A mesoscale convective complex type storm over the desert southwest, *NOAA Technical Memorandum NWS WR-196*, Salt Lake City, UT, 54 pp.

Reitan, C.H., 1963: Surface dewpoint and water vapor aloft, *Journal of Applied Meteorology*, Vol. 2, 776-779.

Riedel, J.T. and L.C. Schreiner, 1980: Comparison of generalized estimates of PMP with greatest observed rainfalls, *NOAA Technical Report NWS-25*, 66 pp.

Riedel, J.T., 1985: Probable maximum precipitation estimates for northeast California, *Report for the Civil Engineering Department of the Pacific Gas and Electric Company*, San Francisco, CA, 44 pp.

San Diego County, 1992: *Storm Report - August 12-14, 1992*, Department of Public Works, Flood Control Division - Alert Storm/Data, 10 pp.

Schaaf, C.B., J. Wurman, and R.M. Banta, 1988: Thunderstorm-producing terrain features, *Bulletin of the American Meteorological Society*, March 1988, Vol. 69(3), 272-277.

Schreiner, L.C. and J.T. Riedel, 1978: Probable maximum precipitation estimates--United States east of the 105th meridian. *Hydrometeorological Report Number 51*, National Weather Service, National Oceanic and Atmospheric Administration, U. S. Department of Commerce, Silver Spring, MD, 87 pp.

Scofield, R.A. and J. Robinson, 1992: The "water vapor plume/potential energy axis connection" with heavy convective rainfall, *Proceedings of the Symposium on Weather Forecasting and the Sixth Conference on Satellite Meteorology and Oceanography*, January 5-10, 1992, Atlanta, GA, American Meteorological Society, J36-J43.

Shapiro M.A. and D.A. Keyser, 1990: Fronts, jet streams and the tropopause, *Extratropical Cyclones: The Erik Palmen Memorial Volume*, C. Newton and E. Holopainen, [eds], American Meteorological Society, 167-189.

Showalter, A.K. and S.B. Solot, 1942: Computation of maximum possible precipitation, *Trans. American Geophysical Union 1942*, 258-274.

Smith, W.P. and R.L. Gall, 1989: Tropical squall lines of the Arizona monsoon, *Monthly Weather Review*, Vol. 117, 1553-1569.

Thiao, W., R.A. Scofield, and J. Robinson, 1993: The relationship between water vapor plumes and extreme rainfall events during the sumer season, *NOAA/NESDIS Technical Report 67*, U.S. Department of Commerce, Washington, DC, 69 pp.

Thiessen, A.H., 1911: Precipitation averages for large areas, *Monthly Weather Review*, Vol. 39.

Toth J.J. and R.H. Johnson, 1985: Summer surface flow characteristics over northeast Colorado, *Monthly Weather Review*, Vol. 113, 1458-1469.

Tubbs, A.M., 1972: Summer thunderstorms over California, *Monthly Weather Review,* Vol. 100, 799-807.

U.S. Army Corps of Engineers, 1945-1980: *Storm rainfall in the United States, depth-area-duration data*, Washington, D.C.

U.S. Army Corps of Engineers, 1955: *Report on flood of 18 July 1955 near Vallecito, California*, Los Angeles District, Los Angeles.

U.S. Army Corps of Engineers, 1957: *Hydrology, Tachevah Creek, Whitewater River Basin*, California, Los Angeles District, Los Angeles, CA, 11 pp.

U.S. Army Corps of Engineers, 1961: Flood control hydrology - Caliente Creek stream group, California, *Office Report*, U.S. Army Engineer District, Sacramento.

U.S. Army Corps of Engineers, 1972: *Report on the flood of 22 June, 1972 in Phoenix metropolitan area, Arizona*, U.S. Army Corps of Engineers, Los Angeles District, 57 pp. and 19 plates

U.S. Army Corps of Engineers, 1977: *Flood damage report, San Bernardino, Riverside, Imperial counties California; floods of September 1976*, Los Angeles District, 34 pp.

U.S. Department of Commerce, 1948: Highest persisting dewpoints in western United States for durations of 12 to 120 hours, *Weather Bureau Technical Paper Number 5*, Washington D.C., 27 pp.

U.S. Navy Marine Climatic Atlas of the World (NAVAIR50-1C-65), Volume IX, Naval Oceanographic Command Detachment, Asheville, NC, May 1981.

U.S. Weather Bureau, 1896- : *Climatological Data (State)*, NOAA, U.S. Department of Commerce, Asheville, NC (ongoing publication).

U.S. Weather Bureau, 1951: Tables of precipitable water and other factors for a saturated pseudo-adiabatic atmosphere, *Technical Paper Number 14*, U.S. Department of Commerce, Washington, DC, 27 pp.

U.S. Weather Bureau, 1960: Generalized estimates of probable maximum precipitation for the United States west of the 105th meridian, *Technical Paper Number 38*, U.S. Department of Commerce, Washington, DC, 66 pp.

U.S. Weather Bureau, 1961, 1969: Interim report, probable maximum precipitation in California, *Hydrometeorological Report Number 36*, U.S. Department of Commerce, Washington, DC, 202 pp.

U.S. Weather Bureau, 1966: Probable maximum precipitation, Northwest States, *Hydrometeorological Report Number 43*, Environmental Science Services Administration, U.S. Department of Commerce, Washington, DC, 228 pp.

Vogel, J.L., 1993: New PMP estimates for the Pacific northwest, *1993 Annual Conference Proceedings*, Association of State Dam Safety Officials, Lexington, KY, pp 41-46.

Watson, A.I., R.L. Holle, R.E. López, D.R. MacGorman, R. Ortiz, and W.D. Otto, 1994: The life cycle of lightning and severe weather in a 3-4 June 1985 Pre-storm mesoscale convective system, *Monthly Weather Review*, Vol. 122, 1798-1808.

Watson, A.I., R.E. Lopez, and R.L. Holle, 1994: Diurnal cloud-to-ground lightning patterns in Arizona during the Southwest monsoon, *Monthly Weather Review*, Vol. 122, 1716-1725.

Weaver, R.L., 1962: Meteorology of hydrologically critical storms in California. *Hydrometeorological Report Number 37*, U.S. Department of Commerce, Washington DC, 207 pp.

World Meteorological Organization, 1973: Manual for estimation of probable maximum precipitation, *Operational Hydrology Report Number 1, WMO Number 332*, Geneva, Switzerland, 190 pp.

World Meteorological Organization, 1986: Manual for estimation of probable maximum precipitation, *Operation Hydrology Report Number 1, WMO Number 332*, Geneva, Switzerland, 269 pp.

Zipser, E.J., 1982: Use of a conceptual model of the life-cycle of mesoscale systems to improve very-short range forecasts, *Nowcasting*, K.A. Browning, Ed., Academic Press, 191-204.

APPENDIX 1

Depth-Area-Duration Tables

Appendix 1 contains depth-area-duration (DAD) tables, also referred to as pertinent data sheets, computed through the storm analysis procedure for each of the storms listed in Chapter 2, Table 2.1. The storm analysis procedure is covered in Chapter 5. These 31 storms were believed to be the most significant storms affecting California, based upon magnitude, location, and season of occurrence. Synoptic descriptions for each storm are in Appendix 2.

The DAD results are given for the center with the greatest precipitation amount. If more than one center was analyzed for a particular storm, only the one with the maximum DAD amounts is shown. Each center was determined from a combination of the total-storm isohyetal map and DAD curves. Latitude and longitude (in degrees/minutes), storm number, storm date, and a location description are included on the DAD sheets for convenience.

The pertinent data sheets have a standard format in which the areal component ranges from 1 mi^2 to 30,000 mi^2 and the durational component ranges from 1 hour to 96 hours. Often storms do not cover the entire area or last 96 hours.

STORM 40 - (12/9 - 12/1921)
ENTIRE STORM
48° 01' N 121° 32' W

Area (mi^2) Duration (hours)

	1	6	12	18	24	30	36	42	48	54	60	66	72
1	1.30	3.58	5.35	6.79	8.61	10.66	11.82	12.57	12.57	13.92	16.14	17.67	19.31
10	1.30	3.58	5.35	6.79	8.58	10.66	11.82	12.57	12.57	13.92	16.14	17.67	19.31
50	1.27	3.48	5.26	6.68	8.34	10.36	11.49	12.24	12.24	13.53	15.69	17.17	18.76
100	1.23	3.37	5.12	6.50	8.16	10.14	11.24	11.96	11.96	13.19	15.31	16.76	18.29
200	1.16	3.19	4.89	6.22	7.89	9.80	10.87	11.56	11.56	12.64	14.72	16.09	17.52
500	1.01	2.77	4.60	5.89	7.47	9.28	10.28	10.96	10.96	11.58	13.64	14.87	16.05
1000	0.90	2.54	4.38	5.64	7.21	8.95	9.92	10.60	10.60	10.90	12.94	14.06	14.98
2000	0.78	2.36	4.16	5.37	6.91	8.57	9.56	10.20	10.20	10.36	12.29	13.27	13.93
5000	0.63	2.06	3.59	4.62	5.91	7.39	8.33	8.92	8.92	8.95	10.63	11.43	11.90
10000	0.46	1.66	2.93	3.85	4.86	6.09	6.90	7.45	7.50	7.53	8.80	9.41	9.80
20000	0.31	1.36	2.50	3.43	4.35	5.39	6.19	6.89	6.94	6.95	7.98	8.44	8.73
27253	0.25	1.22	2.28	3.17	3.99	4.92	5.66	6.35	6.41	6.42	7.30	7.68	7.93

STORM 88 - (12/26 - 30/1937)
ENTIRE STORM
44° 55' N 123° 38' W

Area (mi^2) Duration (hours)

	1	6	12	18	24	30	36	42	48	54	60	66	72
1	1.17	3.38	5.90	8.40	10.94	13.35	15.31	16.47	17.56	17.56	17.56	19.83	20.71
10	1.17	3.32	5.80	8.26	10.76	13.13	15.05	16.19	17.26	17.26	17.26	19.49	20.36
50	1.12	3.23	5.64	8.03	10.46	12.76	14.63	15.74	16.78	16.78	16.78	18.95	19.79
100	1.02	3.07	5.40	7.66	9.98	12.21	14.01	15.07	16.05	16.05	16.05	18.13	18.95
200	0.90	2.84	4.96	6.95	9.09	11.14	12.80	13.75	14.62	14.62	14.62	16.51	17.31
500	0.74	2.44	4.20	5.72	7.40	9.12	10.53	11.37	12.02	12.06	12.14	13.64	14.58
1000	0.58	2.18	3.58	4.84	6.43	7.72	8.91	10.15	10.72	11.04	11.59	12.53	13.27
2000	0.54	2.02	3.19	4.43	5.89	7.17	8.19	9.10	9.60	9.85	10.39	11.23	12.00
5000	0.45	1.69	2.59	3.70	4.87	5.95	6.82	7.59	7.99	8.07	8.51	9.17	9.92
10000	0.34	1.33	2.31	3.33	4.31	5.23	6.00	6.65	7.00	7.13	7.54	8.18	8.99
13869	0.29	1.16	2.18	3.16	4.04	4.89	5.63	6.22	6.55	6.70	7.10	7.72	8.57

Area (mi^2) Duration (hours)

	78	84	90	96
1	22.67	24.80	26.80	27.08
10	22.28	24.38	26.34	26.61
50	21.67	23.71	25.62	25.88
100	20.80	22.78	24.63	24.88
200	19.10	20.95	22.67	22.90
500	16.12	17.75	19.25	19.49
1000	14.55	15.97	17.24	17.71
2000	13.13	14.51	15.70	16.15
5000	10.92	12.15	13.22	13.55
10000	9.90	10.93	11.81	12.18
13869	9.44	10.37	11.16	11.55

STORM 126 - (10/26 - 29/1950)
ENTIRE STORM
41° 52' N 123° 58'W

Area (mi^2)	Duration (hours)												
	1	6	12	18	24	30	36	42	48	54	60	66	72
1	1.84	6.44	11.47	13.47	15.84	16.50	17.96	18.96	19.37	19.98	20.69	20.93	21.17
10	1.84	6.44	11.47	13.47	15.84	16.50	17.96	18.96	19.37	19.98	20.69	20.93	21.17
50	1.77	6.20	11.05	13.00	15.31	15.98	17.42	18.46	18.89	19.47	20.19	20.46	20.72
100	1.58	5.63	10.12	11.98	14.21	14.95	16.47	17.68	18.30	18.88	19.56	19.97	20.35
200	1.31	4.80	8.76	10.51	12.62	13.49	15.14	16.61	17.51	18.19	18.71	19.33	19.89
500	1.01	3.91	7.05	9.03	11.02	11.78	13.69	15.65	16.88	17.71	17.90	18.73	19.18
1000	0.86	3.13	5.57	7.52	9.29	9.99	12.19	14.55	15.97	17.02	17.17	17.90	18.29
2000	0.72	2.68	4.85	6.32	7.77	9.00	11.34	13.24	14.57	15.73	15.90	16.62	17.03
5000	0.56	2.30	4.14	5.40	6.59	8.02	9.62	10.96	12.17	13.17	13.39	14.17	14.57
10000	0.45	1.89	3.41	4.58	5.68	7.02	8.41	9.51	10.56	11.26	11.47	12.23	12.65
20000	0.34	1.49	2.71	3.83	4.88	6.17	7.44	8.35	9.25	9.74	9.96	10.67	11.15
50000	0.20	1.02	1.93	2.79	3.65	4.42	5.29	5.93	6.54	6.89	7.11	7.67	8.18
80511	0.14	0.75	1.42	2.09	2.75	3.28	3.88	4.36	4.75	5.02	5.34	5.78	6.21

STORM 149 - (11/21 - 24/1961)
ENTIRE STORM
42° 10' N 123° 56' W

Area (mi^2)	Duration (hours)												
	1	6	12	18	24	30	36	42	48	54	60	66	72
1	1.11	3.91	6.80	9.35	11.18	12.22	13.10	13.96	15.12	15.72	16.68	16.93	17.00
10	0.94	3.55	6.27	8.89	10.90	12.01	13.00	13.67	14.72	15.46	16.43	16.74	16.85
50	0.78	3.34	5.89	8.38	10.56	11.66	12.77	13.34	14.18	15.06	16.01	16.38	16.51
100	0.74	3.22	5.67	8.12	10.18	11.24	12.34	12.93	13.75	14.66	15.56	15.96	16.09
200	0.70	3.06	5.42	7.68	9.47	10.48	11.64	12.36	13.12	14.18	14.97	15.41	15.53
500	0.63	2.86	5.10	7.05	8.86	10.00	11.35	12.16	12.83	13.89	14.64	15.01	15.13
1000	0.58	2.70	4.86	6.58	8.38	9.59	11.06	11.93	12.55	13.63	14.34	14.67	14.79
2000	0.49	2.47	4.53	6.10	7.57	8.71	10.02	10.87	11.71	12.78	13.43	13.71	13.80
5000	0.34	1.94	3.62	4.95	6.42	7.61	8.57	9.40	10.30	11.22	11.81	12.09	12.17
10000	0.28	1.61	2.98	4.21	5.64	6.76	7.62	8.46	9.17	9.96	10.57	10.86	10.97
20000	0.23	1.30	2.40	3.38	4.65	5.66	6.42	7.19	7.74	8.32	8.90	9.20	9.32
20850	0.23	1.28	2.36	3.32	4.57	5.58	6.33	7.09	7.63	8.19	8.77	9.07	9.20

STORM 156 - (12/21 - 24/1964)
ELK VALLEY REGION, NORTHWESTERN CALIFORNIA CENTER
41° 52' N 123° 40' W

Area (mi^2) Duration (hours)

	1	6	12	18	24	30	36	42	48	54	60	66	72
2	2.05	5.35	7.62	10.02	14.05	15.83	17.10	20.33	21.11	22.56	23.23	25.04	26.28
10	2.05	5.35	7.62	10.02	14.05	15.83	17.10	20.33	21.11	22.56	23.23	25.04	26.28
50	1.93	5.21	7.39	9.81	13.83	15.44	16.64	19.93	20.78	22.03	22.64	24.37	25.60
100	1.72	5.11	7.23	9.65	13.67	15.24	16.31	19.64	20.55	21.75	22.26	23.87	25.16
200	1.59	4.90	6.96	9.33	13.25	14.74	15.74	19.05	19.94	21.09	21.56	23.05	24.36
500	1.27	4.28	6.27	8.50	12.11	13.39	14.48	17.56	18.36	19.37	19.80	20.94	22.37
1000	0.97	3.63	5.64	7.86	11.04	12.14	13.42	16.12	16.90	17.83	18.25	19.11	20.57
1932	0.72	2.98	5.02	7.25	9.83	10.81	12.26	14.51	15.30	16.15	16.57	17.27	18.69

STORM 165 - (1/14 - 17/1974)
GIBSON HWY MTCE STATION REGION, NORTHWESTERN CALIFORNIA CENTER
41° 08' N 122° 16'W

Area (mi^2) Duration (hours)

	1	6	12	18	24	30	36	42	48	54	60	66	72
1	1.13	3.85	5.99	8.88	10.52	11.20	12.33	13.79	14.95	15.67	17.10	17.20	17.20
10	1.13	3.85	5.90	8.65	10.27	11.20	12.33	13.79	14.95	15.67	17.10	17.20	17.20
50	1.00	3.38	5.65	8.25	9.75	11.08	12.23	13.56	14.66	15.38	16.70	16.79	16.79
100	0.92	3.20	5.55	8.14	9.63	10.86	12.00	13.23	14.28	15.01	16.23	16.32	16.32
200	0.79	3.09	5.32	7.81	9.27	10.33	11.57	12.65	13.64	14.49	15.54	15.64	15.64
500	0.65	2.68	4.85	7.09	8.42	9.32	10.63	11.61	12.49	13.43	14.33	14.44	14.44
1000	0.57	2.36	4.41	6.43	7.63	8.52	9.60	10.66	11.47	12.25	13.20	13.40	13.42
2000	0.46	2.08	4.01	5.82	6.96	7.70	8.65	9.74	10.40	11.15	12.07	12.32	12.36
2272	0.44	2.03	3.93	5.70	6.81	7.52	8.49	9.56	10.19	10.94	11.84	12.09	12.13

STORM 175 - (12/24 - 26/1980)
ENTIRE STORM
44° 55' N 123° 44' W

Area (mi^2) Duration (hours)

	1	6	12	18	24	30	36	42	48
1	0.97	2.93	4.99	7.07	9.22	10.84	11.27	11.27	11.27
10	0.97	2.93	4.99	7.07	9.22	10.84	11.27	11.27	11.27
50	0.95	2.88	4.89	6.94	9.05	10.66	11.12	11.12	11.12
100	0.87	2.76	4.59	6.56	8.53	10.11	10.62	10.63	10.63
200	0.80	2.62	4.11	5.90	7.63	9.09	9.65	9.67	9.67
500	0.70	2.24	3.22	4.66	5.96	7.17	7.80	7.82	7.82
1000	0.58	2.06	2.77	3.99	5.08	6.18	6.84	6.87	6.87
2000	0.47	1.76	2.46	3.57	4.56	5.64	6.29	6.32	6.32
5000	0.36	1.36	2.00	2.95	3.78	4.78	5.38	5.41	5.41
10000	0.29	1.11	1.67	2.52	3.16	4.04	4.55	4.60	4.60
20000	0.23	0.90	1.43	2.19	2.68	3.48	3.95	4.03	4.03
24865	0.21	0.83	1.35	2.08	2.53	3.30	3.77	3.85	3.86

STORM 508 - (1/15 - 19/1906)
NORTHERN SIERRA CENTER
39° 54' N 121° 34' W

Area (mi^2) Duration (hours)

	1	3	6	12	18	24	36	48	60	72	84
1	2.16	4.46	8.07	12.51	15.33	15.33	15.33	15.33	22.70	27.80	30.51
10	2.00	4.28	7.57	12.00	14.77	14.77	14.77	14.77	20.90	26.72	29.23
50	1.78	3.88	6.92	10.96	13.65	13.65	13.65	13.65	19.30	24.38	26.63
100	1.66	3.64	6.39	10.17	12.74	12.74	12.74	12.74	17.93	22.50	24.66
200	1.58	3.30	5.79	9.10	11.52	11.52	11.52	11.52	16.20	20.21	22.06
500	1.40	2.88	5.00	7.89	10.21	10.21	10.21	10.21	14.73	18.45	20.00
1000	1.22	2.58	4.51	7.07	9.24	9.24	9.51	9.51	13.43	16.92	18.60
2000		2.15	3.75	5.84	7.72	7.72	8.19	8.19	11.37	14.25	15.66
5000			2.55	4.00	5.26	5.26	6.75	6.75	8.81	10.70	12.11
10000				2.49	3.52	3.54	5.05	5.05	6.54	7.85	9.01

STORM 523 - (5/8 - 10/1915)
NORTHERN VALLEY CENTER
40° 42' N 122° 26' W

Area (mi^2) Duration (hours)

	1	3	6	12	18	24	36	48	60	72
1	2.30	5.02	7.67	9.37	9.50	11.46	12.80	14.32	14.51	14.54
10	2.22	4.81	7.50	9.22	9.38	10.51	12.54	13.89	14.30	14.35
50	2.19	4.61	7.37	8.82	8.96	10.32	12.16	13.33	13.80	13.82
100	1.98	4.36	6.80	8.21	8.35	9.49	11.17	12.37	12.78	12.80
200	1.76	3.86	5.92	7.20	7.29	8.38	9.69	10.87	11.28	11.31
500	1.40	2.97	4.62	5.56	5.67	6.55	7.90	8.87	9.22	9.26
1000		2.28	3.62	4.37	4.47	5.11	6.52	7.15	7.50	7.54
2000		1.61	2.70	3.31	3.38	3.77	4.95	5.38	5.62	5.65
5000					2.15	2.92	3.39	3.75	4.45	4.49
10000					1.76	2.30	2.82	3.16	3.56	3.60
20000						1.68	2.15	2.47	2.64	2.69

STORM 525 - (1/1 - 4/1916)
NORTHERN SIERRA CENTER
39° 48' N 121° 36' W

Area (mi^2) Duration (hours)

	1	3	6	12	18	24	36	48	60	72
1	1.22	3.37	5.45	7.47	9.22	10.35	11.52	12.36	13.18	13.49
10	1.17	3.34	5.38	7.22	8.77	10.12	11.26	12.04	12.85	13.26
50	1.13	2.89	4.80	6.70	7.90	9.17	10.20	10.71	11.50	11.80
100	1.12	2.68	4.55	6.26	7.20	8.40	9.36	9.51	10.50	10.75
200	1.11	2.41	4.09	5.79	6.90	7.70	8.89	9.02	9.50	9.87
500		1.88	3.60	5.21	6.36	6.94	8.36	8.43	8.73	9.10
1000		1.54	3.30	4.79	5.81	6.58	7.62	7.68	8.15	8.50
2000		1.49	2.98	4.40	5.43	6.22	6.99	7.02	7.65	7.90
5000		1.48	2.56	3.80	4.62	5.26	6.16	6.21	6.56	6.94
10000			2.07	3.13	3.76	4.38	5.11	5.21	5.57	5.88
20000					2.70	3.35	3.95	4.17	4.45	4.80
30000					2.19	2.66	3.30	3.49	3.69	4.10

STORM 544 - (12/9 - 12/1937)
NORTHERN SIERRA CENTER
40° 11' N 121° 26' W

Area (mi^2)	Duration (hours)									
	1	3	6	12	18	24	36	48	60	72
1	2.28	4.45	6.51	10.53	13.14	15.37	20.13	22.02	22.28	22.30
10	2.20	4.36	6.46	10.37	13.11	15.29	19.83	21.73	22.03	22.15
50	2.19	4.29	6.41	10.31	12.70	14.50	18.91	20.76	21.00	21.20
100	2.14	4.13	6.21	9.89	12.20	13.80	17.97	19.81	20.12	20.32
200	1.99	3.91	5.81	9.30	11.50	12.86	16.75	18.63	18.96	19.25
500	1.80	3.41	5.19	8.26	10.52	11.50	14.45	16.82	17.52	18.13
1000	1.64	2.97	4.53	7.05	8.89	10.41	13.62	16.60	16.99	17.65
2000	1.49	2.52	3.89	5.65	7.72	9.53	13.15	15.65	16.35	16.59
5000		1.92	3.01	4.25	6.39	8.19	11.33	13.80	14.40	14.76
10000			2.31	3.66	5.14	6.66	9.18	11.23	11.77	12.13
20000				2.80	3.75	4.80	6.69	8.35	8.69	8.89

STORM 572 - (12/21 - 24/1955)
SOUTHERN SIERRA CENTER
37° 59' N 119° 20' W

Area (mi^2)	Duration (hours)									
	1	3	6	12	18	24	36	48	60	72
1	2.57	5.39	7.57	11.18	12.02	13.53	18.75	21.12	22.53	23.79
10	2.49	5.23	7.38	11.14	11.70	13.42	18.58	20.89	22.46	23.56
50	2.38	5.05	7.15	10.65	11.38	12.83	17.93	20.06	21.12	22.10
100	2.36	4.80	6.80	10.15	10.87	12.28	17.07	19.19	20.60	21.29
200	2.22	4.50	6.34	9.35	10.02	11.25	15.35	18.25	20.08	20.94
500			4.78	6.23	8.85	10.37	14.33	17.13	19.23	20.16
1000			3.75	5.91	8.02	9.78	13.13	16.47	18.45	19.54
2000			3.26	5.62	7.67	9.48	12.30	15.55	18.01	18.85
5000			2.92	5.17	7.11	8.77	11.21	14.68	16.62	17.05
10000			2.50	4.28	6.05	7.53	9.78	12.77	14.55	14.85
20000				3.19	4.50	5.55	7.13	9.48	10.45	10.70
30000					3.50	4.36	5.50	7.24	8.20	8.35

STORM 575 - (10/10 - 14/1962)
NORTHERN SIERRA CENTER
40° 02' N 121° 29' W

Area (mi^2)	Duration (hours)											
	1	3	6	12	18	24	36	48	60	72	84	96
1	2.60	4.56	7.30	11.85	14.45	20.70	27.00	27.90	29.28	29.49	31.05	31.39
10	2.50	4.47	6.85	11.05	13.77	19.71	25.79	26.60	29.18	29.41	30.79	31.29
50	2.42	4.37	6.40	10.28	12.70	18.30	24.02	24.92	28.57	28.80	30.28	30.69
100	2.40	4.31	5.88	9.55	11.79	16.94	22.20	24.89	28.22	28.42	29.97	30.30
200	2.30	4.05	5.44	8.50	10.40	14.97	19.65	24.00	27.04	27.35	28.80	29.34
500	1.70	3.38	4.67	6.78	8.31	11.95	16.73	20.85	24.00	24.52	25.89	27.07
1000		2.64	3.69	5.49	7.64	10.50	14.22	18.65	22.51	23.59	24.52	26.31
2000		1.75	2.82	5.02	7.19	9.50	13.06	17.71	21.51	22.97	23.73	25.63
5000				4.13	6.01	8.19	11.03	14.75	18.35	19.42	20.00	21.38
10000				3.12	4.98	6.44	8.90	11.35	14.06	14.95	15.40	16.63

STORM 630 - (1/3 - 5/1982)
COASTAL BAY CENTER
37° 05 N 122° 01'W

Area (mi^2)	Duration (hours)								
	1	3	6	12	18	24	36	48	60
1	2.10	5.51	9.29	15.93	23.11	24.90	25.53	25.53	25.56
10	1.63	4.85	7.86	13.27	19.00	20.65	21.73	21.75	21.76
50	1.31	3.82	6.37	11.79	17.01	19.08	20.02	20.03	20.05
100	1.25	3.39	6.02	10.99	15.75	17.55	18.42	18.43	18.45
200		2.90	5.19	9.92	14.15	15.76	16.47	16.48	16.50
500		2.06	3.95	7.70	11.05	12.46	13.28	13.29	13.30
1000		1.65	3.12	5.99	8.38	9.10	10.28	10.31	10.32
2000			2.25	4.94	7.00	8.00	8.01	8.03	8.04
5000			1.89	3.65	5.22	6.49	7.47	7.51	7.51
10000				2.62	3.84	4.78	5.59	5.78	5.80
20000						3.45	4.10	4.27	4.29

STORM 1000 - (2/1 - 6/1905)
SOUTHWEST CENTER
34° 30' N 119° 10 W

Area (mi^2)	Duration (hours)											
	1	3	6	12	18	24	36	48	60	72	84	96
1	1.26	3.45	5.66	7.28	8.61	9.54	9.67	11.00	12.63	13.60	14.42	14.94
10	1.25	3.31	5.40	7.22	8.50	9.34	9.59	10.70	12.48	12.93	14.22	14.28
50	1.23	3.02	4.96	6.61	7.87	8.66	8.83	9.86	11.82	12.16	13.30	13.40
100	1.11	2.72	4.24	5.94	6.99	7.79	7.94	8.85	11.11	11.33	12.48	12.69
200	0.98	2.44	4.00	5.30	6.33	7.00	7.10	8.00	10.50	10.71	11.77	11.85
500	0.88	2.19	3.52	4.71	5.49	6.21	6.25	6.99	9.39	9.67	10.50	10.55
1000	0.77	1.97	3.20	4.22	4.94	5.52	5.63	6.33	8.48	8.81	9.50	9.63
2000	0.70	1.71	2.83	3.75	4.48	4.95	5.06	5.67	7.00	7.70	7.90	8.61
5000	0.64	1.51	2.41	3.23	3.78	4.46	4.50	4.99	5.65	6.42	6.50	7.10
10000	0.48	1.23	1.84	2.54	3.04	3.42	3.64	4.41	4.91	5.40	5.50	6.14
20000			1.05	1.84	2.00	2.59	2.60	3.43	3.77	4.31	4.45	4.87

STORM 1002 - (2/27 - 3/3/1938)
SOUTHWEST CENTER
34° 14' N 117° 32' W

Area (mi^2)	Duration (hours)											
	1	3	6	12	18	24	36	48	60	72	84	96
1	2.72	6.62	10.68	17.37	20.05	21.74	21.79	27.94	31.60	35.00	36.33	37.25
10	2.68	6.00	9.62	15.85	18.91	20.25	20.45	25.71	29.42	32.63	33.53	34.29
50	2.50	5.77	9.04	14.35	18.00	19.30	19.55	22.25	24.43	27.14	28.05	29.76
100	2.41	5.54	8.60	13.74	17.22	18.37	18.65	21.20	22.59	24.03	26.75	28.32
200	2.20	4.98	7.77	12.44	15.50	16.57	16.87	19.20	20.35	22.29	24.15	25.60
500	1.82	4.10	6.34	10.45	12.76	13.75	13.96	16.30	17.95	20.08	21.69	22.52
1000	1.30	3.10	5.14	9.82	11.88	13.18	13.38	15.45	16.60	18.30	20.01	21.12
2000	0.88	2.60	4.65	8.02	9.75	10.49	10.80	12.55	13.75	15.28	16.62	17.40
5000		1.77	3.16	5.73	6.95	7.89	8.34	9.90	10.60	11.80	12.77	13.53
10000		1.23	2.26	4.28	5.39	6.16	6.72	7.40	8.66	9.46	10.10	10.80
20000			1.25	2.60	3.64	4.17	4.50	5.20	5.88	6.40	6.87	7.41

STORM 1003 - (1/20 - 24/1943)
SOUTHWEST CENTER
34° 12' N 118° 03' W

Area (mi^2)	Duration (hours)											
	1	3	6	12	18	24	36	48	60	72	84	96
1	2.90	5.50	9.50	16.05	20.52	25.70	33.18	36.10	36.51	36.52	36.54	36.65
10	2.43	4.78	8.55	14.62	17.80	22.90	28.76	31.60	32.28	32.30	32.86	33.00
50	2.14	4.25	7.85	13.15	16.38	20.62	26.32	28.82	29.91	30.63	30.81	30.95
100	1.97	3.92	7.25	11.77	15.42	19.60	24.96	27.63	28.56	29.19	29.25	29.38
200	1.80	3.57	6.63	10.80	14.70	18.38	23.41	26.18	26.91	27.11	27.23	27.31
500	1.65	3.20	5.91	10.28	13.38	16.62	21.13	23.55	24.16	24.52	24.62	24.65
1000	1.30	2.78	5.02	8.60	11.25	14.25	18.45	20.51	21.27	21.54	21.55	21.56
2000	0.97	2.04	4.59	7.55	9.70	12.00	16.02	17.33	18.69	18.79	18.83	18.84
5000	0.62	1.80	3.50	5.78	7.50	9.50	13.32	14.79	15.60	15.78	15.86	15.88
10000			2.67	4.38	5.75	7.25	10.21	11.45	12.01	12.40	12.78	12.80
20000				3.00	4.17	4.92	7.14	7.90	8.77	9.05	9.28	9.45
30000					3.00	3.20	5.36	6.30	6.78	7.20	7.32	7.40

STORM 1004 - (11/17 - 21/1950)
NORTHERN SIERRA CENTER
39° 08' N 120° 20' W

Area (mi^2)	Duration (hours)												
	1	3	6	12	18	24	36	48	60	72	84	96	102
1	1.30	3.39	4.52	7.71	10.13	12.38	14.40	14.76	18.18	23.76	26.14	26.53	26.67
10	1.19	2.98	4.29	7.51	9.78	12.01	14.03	14.51	17.91	23.56	25.80	26.42	26.54
50	1.13	2.56	4.19	7.36	9.53	11.54	13.50	14.09	17.27	22.80	24.91	25.24	25.81
100	0.91	2.40	4.01	7.14	9.29	11.26	13.24	13.84	16.82	22.03	24.07	24.77	25.00
200	0.64	2.05	3.81	6.82	8.92	11.00	12.92	13.67	16.49	21.24	23.25	23.99	24.21
500	0.35	1.61	3.44	6.27	8.39	10.42	12.27	12.96	15.68	20.13	22.43	23.00	23.27
1000	0.11	1.56	2.84	5.74	7.80	9.63	11.38	12.04	14.65	18.71	21.11	21.71	22.07
2000		1.42	2.37	5.16	7.07	8.65	10.29	10.84	12.96	16.59	18.90	19.73	19.96
5000		1.05	1.63	4.25	5.88	7.31	8.75	9.39	11.00	13.71	15.53	16.21	16.22
10000		0.64	1.00	3.18	4.44	5.60	6.68	7.23	8.49	10.52	11.90	12.45	12.54
20000			0.43	2.69	2.80	3.60	4.27	4.73	6.51	6.99	7.63	8.00	8.01

STORM 1005 - (1/25 - 27/1956)
SOUTHWEST CENTER
34° 13' N 117° 31'W

Area (mi^2)	Duration (hours)							
	1	3	6	12	18	24	36	48
1	1.38	3.37	5.07	8.11	10.21	11.65	14.45	16.17
10	1.33	3.34	4.87	7.77	9.91	11.45	14.25	15.96
50	1.22	3.05	4.42	7.23	9.09	10.70	12.95	14.49
100	1.09	2.75	4.08	6.78	8.57	10.33	12.63	13.86
200	0.92	2.30	3.91	6.42	8.12	10.00	12.24	13.32
500	0.75	1.95	3.56	5.64	7.40	9.17	11.16	12.48
1000	0.65	1.68	3.03	5.25	6.82	8.17	10.06	11.38
2000	0.47	1.31	2.64	4.60	5.76	7.00	9.12	9.98
5000	0.35	0.96	1.80	3.63	4.86	5.83	7.80	8.80
10000					3.48	4.39	5.82	6.80

STORM 1006 - (9/17 - 20/1959)
NORTH VALLEY CENTER
40° 43' N 122° 16' W

Area (mi^2)	Duration (hours)							
	1	3	6	12	18	24	36	48
1	3.48	7.73	10.78	12.81	16.75	18.47	18.63	18.77
10	3.27	7.44	10.49	12.02	16.58	17.83	18.19	18.29
50	2.93	6.20	9.05	10.75	15.06	16.45	16.89	17.00
100	2.75	4.39	6.57	10.11	13.38	14.90	15.74	15.81
200	2.27	3.34	5.14	8.27	10.75	12.82	14.02	14.40
500		2.27	3.57	5.95	7.45	9.27	10.70	11.81
1000		1.69	3.01	4.39	5.59	6.80	8.13	8.96
2000		1.44	2.68	3.55	3.70	3.86	5.09	6.19
5000			2.16	3.00	3.36	3.50	3.78	4.50
10000			1.76	2.82	3.06	3.22	3.43	3.50
20000			1.65	2.32	2.57	2.71	2.90	3.05
30000				2.03	2.30	2.42	2.66	2.77

STORM 1007 - (12/4 - 6/1966)
SIERRA CENTER
36° 17'N 118° 36'W

Area (mi^2)	Duration (hours)								
	1	3	6	12	18	24	36	48	54
1	4.15	8.35	13.30	16.47	18.78	22.22	32.88	35.90	35.99
10	4.00	8.19	12.80	16.00	18.21	21.69	31.48	34.38	34.51
50	3.70	7.52	11.85	14.82	16.80	19.90	28.54	31.35	31.49
100	2.69	6.14	10.05	12.22	16.15	18.75	27.55	30.59	30.61
200	2.20	4.66	8.40	10.90	15.70	18.20	26.36	29.62	29.89
500	1.47	3.82	6.14	9.50	13.98	16.20	23.22	26.11	26.28
1000		2.81	4.32	7.78	11.78	13.89	19.97	22.64	22.77
2000		2.00	3.32	5.95	9.05	11.02	15.53	17.98	18.22
5000			2.18	4.00	6.02	7.48	10.17	12.42	12.53
10000			1.88	3.22	4.75	5.55	7.80	9.32	9.41
20000				2.48	3.50	4.25	6.08	7.30	7.39
30000					2.75	3.42	4.98	5.98	6.01

STORM 1008 - (1/23 - 26/1969)
SOUTHWEST REGION
34° 13' N 117° 35' W

Area (mi^2)	Duration (hours)										
	1	3	6	12	18	24	36	48	60	72	80
1	3.13	5.75	9.38	14.00	17.45	19.53	26.68	33.60	36.08	36.61	37.10
10	2.84	5.13	8.34	13.41	16.83	19.07	25.75	31.98	34.50	35.22	35.48
50	2.35	4.24	7.42	12.56	15.75	18.23	24.14	29.95	32.30	33.03	33.10
100	1.90	4.14	7.02	11.60	14.50	17.21	21.40	26.68	28.72	29.27	29.60
200	1.69	3.80	6.46	10.54	13.34	15.76	18.56	23.25	25.15	25.79	25.85
500	1.41	3.30	5.70	9.00	11.16	13.22	14.95	18.95	20.88	21.50	21.55
1000	1.00	2.76	4.98	8.35	10.02	12.28	14.10	17.58	19.00	19.43	19.65
2000	0.86	2.35	4.17	6.80	9.13	9.47	11.50	12.77	14.77	15.46	15.55
5000	0.65	1.78	3.33	5.72	7.18	8.35	9.30	10.99	11.91	12.58	12.70
10000	0.32	1.13	2.29	4.13	5.29	6.98	7.20	8.10	9.00	9.49	9.65
20000			0.68	2.60	3.60	4.23	4.80	5.40	5.92	6.32	6.37

STORM 1010 - (2/14 - 19/1986)
SIERRA REGION
39° 54' N 121° 12' W

Area (mi^2) Duration (hours)

	1	3	6	12	18	24	36	48	60	72	84	96	108	120
1	2.02	4.18	5.45	10.19	14.30	18.48	24.68	29.31	29.72	32.61	34.84	36.40	38.68	40.40
10	1.90	3.75	5.40	9.87	13.87	18.12	24.28	28.21	28.99	31.91	34.56	35.70	38.24	39.81
50	1.71	3.35	5.34	9.41	13.16	17.09	22.78	26.59	27.56	30.66	33.09	34.17	36.53	37.96
100	1.63	3.17	4.99	8.90	12.46	16.11	21.41	25.04	25.86	28.98	31.38	32.24	34.57	35.80
200	1.54	2.98	4.62	7.99	11.04	14.50	19.26	22.44	23.12	25.82	28.19	29.21	31.48	32.72
500	1.18	2.47	3.97	6.69	9.43	12.39	16.50	19.68	20.70	23.42	25.60	26.78	29.08	30.20
1000	0.92	1.81	3.43	5.80	8.52	10.90	15.46	17.79	19.13	21.50	23.50	25.39	27.39	29.83
2000		1.52	2.86	5.14	7.63	9.70	13.87	15.95	17.90	20.18	22.00	23.99	25.83	27.00
5000		0.53	2.23	3.99	6.10	7.92	11.29	13.02	14.89	17.92	18.53	20.83	22.20	23.31
10000			1.82	3.38	4.87	6.39	9.01	11.47	12.43	14.00	15.60	17.31	18.50	19.37
20000			0.80	2.35	3.50	4.64	6.58	7.58	9.03	10.24	11.15	12.73	13.57	14.34
30000			0.10	0.72	2.32	3.38	5.11	5.73	7.00	7.76	8.51	9.88	10.65	11.07

STORM 1011 - (9/25 - 26/1939)
SOUTHWEST CENTER
34° 16' N 118°04' W

Area (mi^2) Duration (hours)

	1	3	6	12	18	24	36	42
1	2.15	3.95	6.10	7.75	9.70	10.50	11.85	12.42
10	1.87	3.60	5.59	7.48	9.30	10.08	11.29	11.72
50	1.41	3.32	4.52	6.21	8.74	9.50	10.36	10.57
100		2.80	3.89	5.63	8.01	8.77	9.47	9.76
200		2.21	3.09	4.89	7.30	7.72	8.49	8.78
500		1.59	2.73	4.78	6.46	6.80	7.38	8.09
1000			2.60	4.51	5.80	6.12	6.81	7.22
2000				4.01	5.13	5.57	6.14	6.28
5000						3.72	4.22	4.26

STORM 1012 - (5/18 - 19/1957)
SIERRA CENTER
39° 57' N 121°27 W

Area (mi^2) Duration (hours)

	1	3	6	12	18	24	36	48	60
1	1.15	1.60	3.13	4.63	6.70	7.27	7.82	8.47	8.60
10	1.08	1.50	3.00	4.55	6.60	7.23	7.68	8.30	8.48
50		1.38	2.75	4.45	6.50	7.19	7.58	7.90	8.30
100		1.35	2.70	4.34	6.48	6.92	7.54	7.57	8.00
200		1.33	2.52	4.29	6.30	6.66	7.33	7.47	7.75
500		1.28	2.44	3.96	5.83	6.26	6.97	7.19	7.43
1000		1.25	2.15	3.75	5.18	5.93	6.61	6.94	7.20
2000			1.80	3.42	4.78	5.51	6.19	6.59	6.93
5000				2.72	3.77	4.21	5.02	5.41	5.69
10000					2.80	3.40	4.03	4.36	4.50
20000							2.72	3.03	3.08

STORM 1013 - (6/1 - 2/1958)
NORTHWEST CENTER
42° 15' N 123° 25' W

Area (mi^2) Duration (hours)

	1	3	6	12	18	24	36	48
1	1.20	3.00	3.76	4.25	4.40	4.55	4.65	4.67
10	1.15	2.95	3.60	4.05	4.20	4.33	4.55	4.57
50	1.10	2.81	3.45	3.87	4.02	4.17	4.40	4.45
100	1.01	2.53	3.15	3.45	3.74	4.02	4.30	4.35
200	0.95	2.27	2.70	3.05	3.35	3.62	4.10	4.17
500	0.70	1.67	2.19	2.68	2.90	3.12	3.75	3.85
1000	0.60	1.25	1.70	2.15	2.40	2.65	3.10	3.20
2000		0.75	1.20	1.60	1.80	2.05	2.48	2.67
5000			0.50	0.80	0.92	1.04	1.48	1.75

STORM 1014 - (7/8 - 10/1974)
SIERRA CENTER
38° 50' N 120° 41' W

Area (mi^2)	Duration (hours)							
	1	3	6	12	18	24	36	48
1	2.25	3.20	4.10	4.57	5.30	6.25	7.35	7.50
10	1.86	2.90	3.95	4.48	5.25	6.20	7.25	7.40
50	1.55	2.52	3.80	4.40	5.12	5.85	7.10	7.15
100	1.43	2.45	3.67	4.37	4.95	5.58	6.97	7.02
200	1.28	2.25	3.55	4.25	4.60	5.33	6.78	6.85
500		2.00	3.15	3.85	4.25	4.97	6.55	6.61
1000		1.87	2.60	3.40	3.95	4.65	6.10	6.20
2000		1.65	2.20	2.97	3.50	4.30	5.54	5.70
5000				2.15	2.67	3.30	4.50	4.55
10000						2.35	3.50	3.55

STORM 1015 - (8/13 - 16/1976)
SIERRA CENTER
40° 43' N 122° 16' W

Area (mi^2)	Duration (hours)							
	1	3	6	12	18	24	36	48
1	1.86	2.86	4.33	4.81	4.85	5.21	5.54	5.67
10	1.84	2.83	4.24	4.65	4.72	5.11	5.39	5.44
50	1.75	2.80	4.13	4.47	4.67	4.87	5.28	5.35
100	1.73	2.67	4.00	4.40	4.60	4.73	5.18	5.28
200	1.54	2.39	3.86	4.33	4.47	4.60	5.00	5.13
500	1.11	1.87	3.43	3.93	4.12	4.25	4.73	4.88
1000		1.51	2.80	3.29	3.42	3.60	4.33	4.50
2000		1.10	1.95	2.53	2.80	2.93	3.70	3.90
5000				1.57	1.87	2.02	2.63	2.79
10000						1.33	1.85	1.98

STORM 1016 - (9/9 - 11/1976)
SOUTHWEST CENTER
34° 20' N 117° 03' W

Area (mi^2) Duration (hours)

	1	3	6	12	18	24	36	48
1	2.15	3.42	5.80	10.15	13.58	15.55	17.20	17.20
10	2.07	3.15	5.62	9.77	13.15	15.10	16.65	16.70
50	1.79	2.86	5.10	8.71	11.60	13.30	14.60	15.10
100	1.50	2.67	4.66	7.90	10.63	12.15	13.32	14.05
200	1.28	2.51	4.02	7.13	9.50	10.90	11.80	12.60
500	1.02	2.10	3.12	6.00	8.00	9.02	9.60	10.60
1000		1.76	2.73	5.08	6.67	7.60	8.40	9.02
2000		1.50	2.41	4.40	5.67	6.30	7.02	7.60
5000		1.35	2.24	3.50	4.42	4.90	5.45	5.80
10000			2.03	2.77	3.30	3.90	4.40	5.55
20000						2.95	3.33	3.50

STORM 1017 - (8/15 - 17/1977)
SOUTHEAST CENTER
34° 50' N 115° 41' W

Area (mi^2) Duration (hours)

	1	3	6	12	18	24	36	48	60
1	2.39	2.77	3.45	5.33	5.33	5.86	5.86	6.24	6.25
10	2.27	2.65	3.34	5.26	5.26	5.70	5.70	6.16	6.17
50	2.21	2.55	3.30	5.18	5.18	5.59	5.59	6.12	6.12
100	2.07	2.51	3.27	5.17	5.17	5.53	5.53	6.03	6.03
200	1.89	2.48	3.26	4.92	4.92	5.49	5.49	5.82	5.82
500	1.65	2.44	2.89	4.53	4.53	5.02	5.02	5.28	5.28
1000	1.49	2.10	2.60	4.01	4.01	4.44	4.44	4.81	4.81
2000	1.31	1.69	2.11	3.16	3.16	3.52	3.53	3.85	3.85
5000		1.49	1.55	2.10	2.10	2.47	2.57	2.88	2.88
10000				1.63	1.68	1.80	1.89	2.37	2.39
20000				1.23	1.39	1.63	1.70	1.86	1.91

STORM 1018 - (7/27 - 29/1984)
SOUTHEAST CENTER
34° 58' N 115° 31' W

Area (mi^2)	Duration (hours)						
	1	3	6	12	18	24	36
1	5.05	5.58	5.78	5.89	5.89	5.89	5.90
10	4.98	5.48	5.68	5.79	5.79	5.79	5.80
50	4.79	5.36	5.51	5.70	5.70	5.70	5.71
100	4.70	5.21	5.36	5.51	5.51	5.51	5.52
200	4.51	4.96	5.12	5.32	5.32	5.32	5.34
500	4.02	4.47	4.66	4.75	4.75	4.75	4.78
1000	3.30	3.67	3.80	3.93	3.93	3.93	4.09
2000	2.52	2.80	3.00	3.34	3.34	3.34	3.40
5000	0.78	1.70	2.20	2.46	2.50	2.50	2.56
10000			1.45	1.87	1.96	1.96	2.09
20000				1.28	1.31	1.39	1.49

APPENDIX 2

Synoptic Descriptions

The following synoptic descriptions cover storms considered most significant to this study (Chapter 2, Table 2.1), and are included to give insight to the types of conditions supporting these major events. These nine storms provided the greatest non-orographic precipitation for the regions indicated in Chapter 6, Figure 6.2. These synoptic discussions are brief, qualitative analyses in which no detailed cross-sections or isentropic examination were conducted. Such analysis was determined to be beyond the scope of this project and was not possible in some cases due to limited data. Various maps and discussions from other hydrometeorological reports, i.e. HMR 37 (1962) and HMR 50 (1981), were available but were not included for sake of brevity.

The first four storm descriptions are nearly identical to those in HMR 57 (1994). The only differences that may arise are due to the selection of a different precipitation center than that used in HMR 57. In some cases, mesoscale meteorological factors occurring further south played a more significant role in California, as than in Oregon and Washington.

STORM: 40
DATE: 12/9 - 12/1921
LOCATION: North Central Cascades
DURATION: 72 hours

SYNOPTIC DESCRIPTION: A broad area of surface high pressure extended from the Great Basin southwestward into the Pacific off California. A plume of moist air, on the backside of this ridge, followed a trajectory from near Hawaii to the coastal area of Washington on the 9th. Over the Aleutians, a low pressure system moved to the north-northeast, with a trailing cold front. The cold front became occluded as it pushed onshore through British Columbia, with surface winds increasing to more than 30 knots along the Washington coast. The

low-pressure system intensified very quickly as it moved toward the northeast on the 10th. A secondary cold front moved onshore on the 11th. This caused a wind shift to the west before shifting back to the southwest ahead of the next system.

By the 12th, winds increased to 40 knots along the coast as the occluded front brought an intensified pressure gradient along with it. This appeared to have produced the heaviest core precipitation in the core region. Rainfall ended on the 13th.

The cause of the heavy rainfall was attributed to the strong southwesterly flow encountering the coastal and Cascade Mountains during the 10th and 11th, supported by a strong pressure gradient. The rainfall occurred in two surges; the first and lesser surge was from the afternoon of the 9th to the morning of the 10th, while the heavier surge occurred between late on the 10th through the morning of the 12th. At Silverton, Washington a rainfall amount of 15.38 inches was recorded.

STORM: 88
DATE: 12/26 - 30/1937
LOCATION: Coastal Mountains of Washington, Oregon
DURATION: 96 hours

SYNOPTIC DESCRIPTION: This storm brought moist flows into the coastal mountains of Oregon and Washington, with numerous rainfall centers in excess of 10 inches. The largest observed amount occurred near Valsetz, Oregon, where some 25 inches fell on the southwest facing slopes. The mountains in this region rise to levels between 3500 and 4000 feet.

The primary storm of the 28th to 30th followed a series of quick moving, low pressure centers that passed through western Washington to the east. On the 26th, a low pressure system moved into the Gulf of Alaska and rapidly deepened during the next 30 hours. This resulted in both a slowing of movement and an intensification of the onshore gradient that increased the winds to the coastal mountains. A quasi-stationary front developed along the Washington/Oregon border. Several short waves passed along this frontal surface that provided rain impulses during the storm. Movement of the frontal surface south and then

back north may have contributed to the maximum rains occurring in Oregon since the boundary was over the same region twice.

By the 30th, the front had been displaced eastward and the rains ceased along the coastal mountains except for a few showers. Most of the mass curves for this storm show rain occurring in two bursts separated by nearly 30 hours. It is apparent from these curves that little convective activity was associated with this event.

From the Northern Hemisphere Daily Weather Maps, dewpoints are in the low 40's, with air temperatures ranging between 55° and 61° F. Temperatures at this level are indicative of trajectories from subtropical latitudes at this time of year.

STORM: 149
DATE: 11/21 - 24/1961
LOCATION: Southwestern Oregon
DURATION: 72 hours

SYNOPTIC DESCRIPTION: A deep low pressure center, located over southwestern Alaska on the 20th, moved toward the southeastern Alaskan coast by the 21st. Central pressure was less than 970 mb, and an occluded front trailed southward along the coast to the southern end of Vancouver Island. Here, a warm front branched off and into the Oregon coast that initiated a three-day period of rainfall over western Washington and Oregon. On the 22nd, the warm front was replaced by a cold front that rotated clockwise to align itself east-west across the coast by the end of the 23rd. The tight gradient through this sequence pulled strong southwesterly winds onshore into the coastal mountains. Heavy snow was reported throughout the mountains, causing power outages and some road closings. The heaviest rains were noted along the coast with Brookings, Oregon, recording over 10 inches. Precipitation ended the morning of the 24th, as a wave passed along the front, pulling it southward into California.

It is possible that some moisture entering this storm was pulled northward from the remnants of tropical storm Dot; however, available synoptic analyses were insufficiently

clear off the coast to support this claim. Moisture from such a source would more than account for the heavy rains observed.

Most of the precipitation fell in the western portions of the two states. It was believed that the combination of strong convergent flows and orographic lifting concentrated most of the heavy rains against the major mountain slopes. Unseasonably cold temperatures preceded the passage of the warm front into the region. This undoubtedly accounted for the heavy snows reported in the mountains.

STORM: 165
DATE: 1/13 - 17/1974
LOCATION: Coastal Washington and Oregon
DURATION: 72 hours

SYNOPTIC DESCRIPTION: A strong high-pressure system prevailed over the Gulf of Alaska, representing a block to storms and the jet stream entering the west coast on the 10th. An arctic airmass was centered to the north and northeast of the storm location. Large negative temperature departures were observed over portions of Washington and Oregon, with below-zero temperatures reported throughout the region east of the Cascades. The blocking high began to regress westward by the 11th, allowing a surge of warm air to enter the coast at the southern end of the region. Both temperatures and dewpoint temperatures rose significantly during a 24-hour period beginning the 12th. Rapid cyclogensis developed in the Gulf in place of the high-pressure system, and a number of short waves moved around the trough at the time of increasing temperature and moisture flows. Early snowfall changed to rain that intensified with time as the gradient increased and as the orographic influences took over.

Coastal winds were reported at 60 mph along the Washington coast, increasing to 75-100 mph along the Oregon coast. Winds of such magnitude cause considerable damage but also support the strong orographic effects noted in the precipitation pattern for this storm. Beginning on the 16th, a second short wave began to push through the region, bringing an end to this period of heavy rains.

Mount Shasta, California, set an all-time 24-hour rainfall of 6.97 inches during this storm, and Sexton Summit, Oregon, set 12-, 24-, and 72-hour records of 3.39, 5.98, and 11.52 inches, respectively. More than 9 inches fell on a large portion of western Oregon, while a few stations had maxima of nearly 13 inches.

STORM: 630
DATE: 1/3 - 5/1982
LOCATION: Mid-coast California
DURATION: 60 Hours

SYNOPTIC DESCRIPTION: The upper-level features preceding and during this January event were such that prolonged advection of warm moist subtropical air over modified polar air at the surface was certain. A low-amplitude trough, situated over the Pacific Northwest and eventually sagging southward, steered short waves into the Northern California coast. The trough by itself allowed polar air continually to refresh the California interior with new cooler air. A split jet stream beginning much further to the west, due to a blocking pattern at 500 mb, caused the northern branch of the jet stream to steer north into Alaska and the other branch to track far to the south over subtropical ocean waters. The southern stream dipped to near Hawaii and recurved to meet the northern branch nearly over California where the flow was closer to westerly.

From January 1 through the 2nd, a strong short wave moved along the northern branch through Alaska and down into the Pacific Northwest. The short wave brought cold and damp conditions to northern and central California. Freezing levels were down to sea level in the northern California region and were near 2500 feet in the San Francisco Bay area. Winds were northerly with reinforcing cold air advection occurring the rest of the day. Another shot of cold air slid across the area with the next wave, that also originated in the Gulf of Alaska. This wave moved well north of California on the 3rd but had the effect of keeping the surface airmass much colder than normal and strengthening the temperature gradient between the approaching southern-stream wave and the continental air. An additional effect of the temperature gradient was steering the jet stream nearly parallel to the coast of California near the San Francisco Bay thus *locking* in a pattern.

Meanwhile, a southern-stream short wave was strengthening just northeast of Hawaii. This wave was able to entrain large amounts of moisture as it developed and moved east-northeast toward the coast. As this disturbance approached California, precipitation began along the coast on the afternoon of the 3rd. A surface warm front, associated the low pressure system, stalled along and nearly parallel the coast as the subtropical airmass collided with the cold air in place. For at least the next 24 hours, the front sat acting as a ramp for overrunning precipitation in California. The corresponding short wave moved over northwest California and into Oregon leaving the quasi-stationary warm front essentially intact along the California coast.

A secondary low formed offshore and it too moved northeast eventually through central California pulling a cold front behind it, virtually shutting down the precipitation mechanism responsible for the extreme rainfall over the San Francisco Bay area. As it moved slowly toward the coast, however, it kept the flow of warm moist maritime air focused on the same area that had received the brunt of the heavy precipitation thus far. By early on the 5th of January the second low pressure system had moved well inland and only scattered precipitation was left over.

Observed rainfalls were extremely high over the coastal regions and much less not far inland. The persistence of the warm front just offshore and the frictional convergence of the coastal mountains both combined to make the rainfall spectacular along these uplift areas. Rainfall totals for 30 to 36 hours were more than 24 inches in localized spots and well over 10 inches over a broad area of the coast just west of San Francisco. Mass curves near or along the coast show a constant stream of precipitation through the storm period with few interruptions or pulses of rainfall. The rainfall seemed very general and consistent in behavior and not extremely convective, just very constant.

STORM: 1003
DATE: 1/20 - 24/1943
LOCATION: Southwest California
DURATION: 96 hours

SYNOPTIC DESCRIPTION: Major Pacific coast storms have several important characteristics in common. These include blocking patterns in the central or eastern Pacific, which split the jet stream and steer disturbances north and south for days or weeks, abundant cold polar or arctic air over the intermontaine region, a tropical/subtropical connection, and a strong southwesterly flow that continues for an extended time. All these factors came into play in January 1943 over California. First, a series of three low-pressure systems were pushed further and further south by a large-scale blocking pattern situated to the north and west of California. The first system moved southeasterly out of the Gulf of Alaska and into Washington on the 19th and 20th of January before weakening and continuing east. The corresponding cold front moved south down the coast through northern California and stalled between San Francisco and Los Angeles. The cold air associated with the front filtered down through most of the state. To the west, the stalled remnant front extended west-southwest over the ocean and set the stage for the next developing storm system that would track along the frontal boundary.

The second low-pressure system developed along the southern branch of the jet stream near Hawaii. It intensified rapidly upon moving northeast and into contact with the colder polar air to the north of the frontal boundary. The center of the second low moved into southern Oregon and continued northeast, weakening rapidly. The third and final wave followed quickly after the second short wave but did not deepen as much as the preceding one as it moved into northern California.

Meanwhile throughout the storm's history, rainfall progressed further and further south, as each succeeding low-pressure system pulled the cold-front boundary further south. Flow ahead of each wave shifted from westerly to southwesterly and became increasingly warm and moist. Extremely strong winds carried the subtropical air into the mountain barriers along the southern coast of California. Very low pressure associated with the

disturbances and the subtropical high poised to the south caused a tight gradient to form over the West coast.

Strong and persistent southwesterly flow over southern California ushered in the extreme precipitation values recorded over much of the south. The most prodigious precipitation began early on the 21st, in the central part of the state, and quickly moved south to where the front had slowed considerably until the front associated with the third, and final, low-pressure system came through on the 23rd. Generally, precipitation over most of the southwestern portions of California was due to coastal convergence, instability, and orographic lifting. *Perfect* flow trajectories (i.e., the Pineapple Express) with high winds focused the rainfall on those orographic zones aligned perpendicular to mean flow from the surface to 700 mb. More than 26 inches was recorded at Hoegee's Camp, high in the San Gabriel's, over 24 hours and more than 36 inches in four days of rainfall.

In many ways this was similar to storm 1002 (2/27 - 3/3/1938). Both storms tapped the warm moist maritime tropical air of the central Pacific and pulled it north into southern California. Sustained high winds transported the moisture to the coast and inland due to large pressure differences north-south across the region. More than one short wave developed and moved onshore in each storm throughout the rainy period as well. Another commonality was the slow moving or stationary front in the vicinity of the extreme rainfall as well as lingering polar (maritime) air entrenched before the rains began. The most intense precipitation, in both storms, fell in the mountains north and east of Los Angeles making both storms primarily orographically driven.

STORM: 1004
DATE: 11/17-21/1950
LOCATION: Sierra Center
DURATION: 102 hours

SYNOPTIC DESCRIPTION: A series of short waves and their corresponding fronts over a relatively short period, combined with a moist tropical connection caused excessive precipitation to fall over north-central California. A blocking ridge did exist during this

storm, but the block was weak, centered around 180° W, allowing short waves to travel both north and south of the ridge. Those disturbances traveling south of the ridge were also weak and did not intensify much before they crossed the coast line. A significant quasi-stationary upper-level low churned away for most of the storm duration just off the coast of southwestern Canada. An upper-level trough moved northeast from its position near the Hawaiian Islands toward the Pacific coast thereby providing a track for the southern-stream low pressure systems to follow up the Pacific coast and extending to the low already off the coast of Canada.

The storm period began with a cold front moving southeast out of the Gulf of Alaska on November 15th and 16th into northern California where the front became stationary. The front stretched back west-southwest where the next short wave was evolving and moving northeast toward the Pacific coast. Tropical flow preceding the next rapidly intensifying short wave crashed into California on the 18th and dumped very heavy rains and snows in the coastal mountains, as well as in the central and southern Sierra. Meso-lows moved along the stationary east-west oriented front during the day increasing rainfall totals. By the next morning the front was slowly moving south of Sacramento and dissipating as high pressure built in from the south.

As the ridge began to move toward the east another disturbance began to organize southwest of California and in the northern stream another cold front approached from the northwest. Again the convergence of the frontal boundary and the southwest short wave caused rapid intensification just offshore on November 19th. The frontal boundary, swinging southeastward again, slowed to a nearly stationary position just north of where the first front became stationary on the 17th. A ridge aloft, began to build rapidly to the northwest on the 20th effectively cutting off the narrow warm moist plume to the southwest thus ending the precipitation in California. The stationary front slowly edged south and became indistinct as the pressure rose across California and into the Pacific.

The heaviest precipitation fell in two general areas, the southern and central Sierra mountains early in the storm period (November 18th) and the northern Sierra mountains (primarily November 20th) with the second bout of rainfall. Most 24-hour rainfall totals from early on the 18th in the central Sierra region exceeded 8 inches with several stations recording more than 10 inches during this period. At Hetch Hetchy over 13 inches fell for

this duration. Later on the 20th, as the next precipitation surge hit the Sierra, heavy rains fell over some of the same areas inundated two days before. At Blue Canyon, for example, more than 8.5 inches fell over the 24-hour period beginning at midnight on the 19th.

While other more extreme storms have hit the Sierra mountains, none has centered so distinctly in such a remote location as this storm (see Chapter 6). Due to a constricted moisture source to the west-southwest and a nearly stationary front draped east-west across northern California, most of the extreme precipitation fell in narrow bands across the mountains. Winds, although strong, were not as severe as many comparable storms to the region.

STORM: 1010
DATE: 2/14 - 19/1986
LOCATION: Sierra Center
DURATION: 120 hours

SYNOPTIC DESCRIPTION: The conditions resulting in the February 1986 extended heavy precipitation event over California were a result of a blocking pattern upstream of the Pacific west coast. A strong high-pressure ridge formed over the eastern Pacific early in February, essentially diverting flow around to the north and south of it. Through time the ridge strengthened and eventually became cut off in the Gulf of Alaska. As the ridge developed and slowly progressed northeast, much of the upper-level flow undercut the block, near latitude 30° to 40° N, entraining air from the warm tropical ocean surrounding Hawaii.

Although some rains began on February 11th, the heavier rainfall began on the 14th as the first major low-pressure system tracked into Washington. The trailing strong cold front brought widespread heavy rains and gusty winds. Behind the front the rains continued as the warm moist inflow continued to pump up and over the colder polar air at the surface. The next major disturbance influenced the state on February 16th as the second major short wave exploded off the Pacific coast. The cold front that had moved into southern California on the 15th stalled and began moving northward on the 16th as a warm front. Overrunning rains continued over the central and northern portions of California. Snow levels during the

entire event were quite high as the warm moist air, originating as far south as 5° to 10° N, was advected northeast ahead of the low-pressure system. The rain continued through the 17th and 18th as the next and final short wave in the series smashed into the coast. By the 19th snow levels had dropped as a dry cool airmass moved into place and a more westerly wind cut off the tropical moisture that had brought so much precipitation to the Pacific west coast.

Throughout the storm period precipitation fell over a broad area of California and the west coast. As each short wave intensified, occluded, and moved onshore, it brought heavy rainfall with it. The rainfall, however, focused on the northern and central Sierra mountains and coastal regions from central to northern California. From February 12th to 21st, more than 45 inches fell over parts of the Sierra and more than 18 inches fell at Bucks Lake in 24 hours from the morning of the 16th. Although individual stations show heavy 24-hour amounts, the storm is more remarkable for its length of heavy rainfall duration.

The source region of tropical air, south of Hawaii, makes this storm extraordinary as does the duration of that connection. Other factors include strong jet stream winds that were reflected down to the surface. The strong southwesterly winds allowed the rapid and uninterrupted transport of tropical moisture to central and northern California even after a cold front at the surface (February 14 -15) had moved south of the area. Finally, since the overall flow was perpendicular to the prevailing mountain orientation, orographic forcing became the rule.

STORM: 1017
DATE: 8/15 - 17/1977
LOCATION: Southeast Region
DURATION: 60 hours

SYNOPTIC DESCRIPTION: For southeast California the most extreme rainfall events occur during the summer months mainly July through September. These storms are commonly the result of tropical storms or the residue of a tropical storm that has drifted northward near or into southern California. In this case, tropical storm Doreen was the cause

of the terrific rains recorded across the deserts of California and the areas around Los Angeles. However, in locations along the coast and the adjacent mountains, west of the desert, the rainfall associated with Doreen, pales in comparison to the all-season amounts recorded during the winter in these same regions.

A *typical* summer regime set up over the southwestern United States with a heat low centered over the deserts at the surface and high pressure aloft. Low-level moisture was advected to the north and east of the surface low circulation centered near Death Valley. Evidence of the very high dewpoints in southeastern California can be noted long before the storm actually began. These dewpoints may be partially related to the moisture shield surrounding the tropical storm off the Baja coast. The moisture appeared at least 24 hours before the heavy rains began on the 15th of August.

As Doreen made her way north, moisture became more abundant and widespread. Dewpoints in the 70's covered most of southeastern California by August 16th. Due to limited observations, coverage in this part of the region and the chaotic manner in which the rains fell, detailed analysis at the mesoscale level proved difficult. Suffice to say, heavy convective elements developed late on the 15th and early on the 16th. This precipitation, however, was primarily confined to the United States-Mexican border. The following 24-hours resulted in the more widespread rainfall as the tropical storm, still west of Baja, moved closer causing more instability. Heavy rains began by the afternoon of the 16th and lasted through most of the night as they slowly worked north over the southeastern portion of California.

More than 6 inches were recorded at Mitchell Caverns late August 16th into early on the 17th. Heavy rains similar to these rains fell across other parts of the desert during this period. West of the coastal mountains, heavy tropical rains fell almost 24 hours later as the remnant tropical depression worked its way northward along the coast. The tropical moisture and heavy rains were eventually pulled northeast into central Nevada essentially ending the precipitation in California by the 19th.

Although not obvious, several factors could have caused this storm to release its potential over southeast California. Diurnal heating patterns contributed to the moisture flow into the area. The tropical storm provided a deeper than normal moisture column and

increased dynamics as it approached. Some orographic factors may also be linked but discerning it with the lack of records is hard. Mitchell Caverns is higher (3700 feet) than much of the area surrounding it especially to the south. It is therefore possible that some orographic influence held sway in some localized regions of rapid upslope. The mountains around Los Angeles had greater precipitation than in the city; therefore, some orographic factors were definitely involved there.

APPENDIX 3

Local Storm List

This list of 137 storms represents all the additional local storms examined for HMR 59. The storm locations are shown on the map in Figure A3.1. While the storms listed in Chapter 9, Figure 9.1 were considered the most extreme, these additional storms were considered important for this study. The local storms provided below are included for the benefit of the user and for future study. All latitudes are degrees north, negative longitudes are degrees west. A 24-hour clock is used for the hour of maximum rainfall.

Table A3.1. *Extreme local storms in California.*

#	Location	Latitude (degrees)	Longitude (degrees)	Elevation (feet)	Date	Hour of maximum rainfall	Max 1-hour rainfall (inches)	Max 6-hour rainfall (inches)
1	IRON MOUNTAIN	34°08'	-115°08'	922	7/22/1948	22	1.19	1.20
2	KYBURZ STRAWBERRY	38°48'	-120°09'	5700	7/31/1949	14	1.04	1.06
3	HEMET RESERVOIR	33°40'	-116°40'	4360	10/15/1949	10	1.18	1.43
4	MILL CREEK INTAKE	34°05'	-116°56'	4945	7/6/1950	13	1.02	1.31
5	TRINITY CENTER RS	41°00'	-122°41'	2300	9/15/1950	18	1.02	1.03
6	POINT ARENA	38°54'	-123°42'	100	4/16/1951	14	1.03	1.32
7	TERMO 1 E	40°52'	-120°26'	5300	6/20/1951	15	1.03	1.03
8	SIERRAVILLE RS	39°35'	-120°22'	4975	8/19/1951	14	1.02	1.22
9	BLYTHE FAA AP	33°37'	-114°43'	390	8/20/1951	19	1.08	1.46
10	TRINITY CENTER RS	41°00'	-122°41'	2300	8/22/1951	17	1.01	1.43
11	CRAWFORD RANCH	32°53'	-116°17'	1500	8/26/1951	16	1.99	2.50
12	SANTA FE DAM	34°07'	-117°58'	427	4/19/1952	14	1.18	1.70
13	ALTURAS RS	41°30'	-120°33'	4400	6/6/1952	14	1.13	1.20
14	BIG BEAR LAKE DAM	34°14'	-116°58'	6820	7/24/1952	15	1.17	1.94
15	HARRISON GULCH RS	40°22'	-122°58'	2750	8/1/1952	20	1.29	1.30
16	FLORENCE LAKE	37°16'	-118°58'	7325	8/12/1953	14	1.82	2.07
17	MILFORD LAUFMAN RS	40°08'	-120°21'	4860	6/11/1955	20	1.05	1.05
18	JULIAN	33°05'	-116°36'	4220	8/23/1955	15	2.58	2.83
19	RUNNING SPRINGS RS	34°12'	-117°05'	5970	7/26/1956	17	1.00	1.00
20	SHASTA DAM	40°43'	-122°25'	1075	6/2/1958	2	1.14	3.55
21	THE GEYSERS	38°48'	-122°50'	1668	6/10/1958	16	1.40	1.77
22	SUSANVILLE 1 WNW	40°26'	-120°40'	4555	7/24/1958	17	1.02	1.02
23	MILFORD LAUFMAN RS	34°05'	-116°56'	4860	7/29/1958	15	2.10	2.24
24	CUYAMA RS	34°51'	-119°29'	2750	8/16/1958	16	1.32	2.80
25	HEMET RESERVOIR	33°40'	-116°36'	4360	8/16/1958	12	1.00	1.03
26	FLORENCE LAKE	37°16'	-118°58'	7330	8/9/1959	14	1.18	1.96
27	SLACK CANYON	36°05'	-120°40'	2500	9/12/1959	16	1.14	1.20

Table A3.1. *Extreme local storms in California.*

#	Location	Latitude (degrees)	Longitude (degrees)	Elevation (feet)	Date	Hour of maximum rainfall	Max 1-hour rainfall (inches)	Max 6-hour rainfall (inches)
28	JULIAN	33°05'	-116°36'	4220	9/13/1959	14	1.68	1.94
29	MILL CREEK INTAKE	34°05'	-116°56'	4945	9/13/1959	13	1.14	1.68
30	MILL CREEK INTAKE	34°05'	-116°56'	4945	7/22/1960	15	1.80	1.84
31	CRAWFORD RANCH	32°53'	-116°17'	1500	8/21/1960	17	1.00	1.06
32	MILL CREEK INTAKE	34°05'	-116°56'	4945	9/10/1960	16	1.15	1.55
33	OROVILLE RS	39°32'	-121°34'	300	5/30/1961	16	2.08	2.32
34	SANTA ANA RIVER PH	34°06'	-117°06'	1970	8/4/1961	17	1.30	1.35
35	JULIAN	33°05'	-116°36'	4220	8/4/1961	16	1.27	2.04
36	CRAWFORD RANCH	32°53'	-116°17'	1500	8/18/1961	16	2.19	2.66
37	CAMP ANGELUS	34°09'	-116°59'	5768	8/21/1961	13	1.25	1.37
38	TUJUNGA MILL FC	34°23'	-118°05'	4650	8/22/1961	13	1.28	1.80
39	WELDON 1 WSW	35°40'	-118°18'	2680	8/22/1961	16	1.14	1.37
40	MILL CREEK INTAKE	34°05'	-116°56'	4945	8/23/1961	13	1.74	1.79
41	FINLEY 5 SW	38°58'	-122°57'	1750	8/27/1961	17	1.18	1.28
42	MC CLOUD	41°15'	-122°08'	3280	5/29/1963	18	1.21	1.29
43	ETNA	41°28'	-122°54'	2950	6/13/1963	19	1.20	1.43
44	HENSHAW DAM	33°14'	-116°46'	2700	8/7/1963	13	1.79	1.99
45	TEHACHAPI AIRPORT	35°08'	-118°26'	3960	8/8/1963	12	1.20	2.19
46	MILL CREEK INTAKE	34°05'	-116°56'	4945	8/14/1963	14	1.22	1.90
47	CRESTLINE LAKE GREGORY	34°14'	-117°16'	4530	9/18/1963	6	2.01	2.89
48	LUCIA WILLOW SPRINGS	35°53'	-121°27'	360	3/6/1965	4	1.17	1.79
49	JULIAN	33°05'	-116°36'	4220	7/15/1965	13	1.17	1.26
50	KYBURZ STRAWBERRY	38°48'	-120°09'	5700	7/17/1965	14	1.14	1.23
51	HETCH HETCHY	37°57'	-119°47'	3870	8/14/1965	15	1.58	1.87
52	SODA SPRINGS 1 E	39°19'	-120°22'	6890	8/14/1965	12	1.10	1.10
53	BIG PINES PARK FC	34°23'	-117°41'	6850	8/16/1965	14	1.33	3.35
54	CLEARLAKE 4 SE	38°54'	-123°36'	1350	8/17/1965	14	1.08	1.15
55	LOS ANGELES CIVIC CTR.	34°03'	-118°14'	270	9/18/1965	14	1.28	1.39
56	EL CAPITAN DAM	32°53'	-116°49'	600	3/24/1966	15	1.20	1.70
57	REDDING 5 SSE	40°30'	-122°22'	425	4/9/1966	19	2.40	3.51
58	JULIAN WYNOLA	33°06'	-116°39'	3650	7/30/1966	11	1.03	1.30
59	CHUCHUPATE RS	34°48'	-119°01'	5260	8/2/1966	15	1.25	1.27
60	RUNNING SPRINGS 1 E	34°12'	-117°05'	5970	10/6/1966	8	1.10	1.10
61	FALLBROOK	33°21'	-117°15'	660	4/5/1967	13	1.00	1.00
62	ROBBS PEAK PH	38°54'	-120°22'	5120	5/12/1967	10	1.00	1.00
63	FORT JONES 6 ESE	41°35'	-122°43'	3320	6/20/1967	17	1.58	2.13
64	BIG PINES PARK FC	34°23'	-117°41'	6850	7/13/1967	12	1.02	1.37
65	TUJUNGA MILL FC	34°23'	-118°05'	4650	8/23/1967	16	1.29	1.71
66	WARNER SPRINGS	33°17'	-116°38'	3180	8/31/1967	1	1.09	1.90
67	NEEDLES	34°50'	-114°36'	150	7/22/1968	20	2.07	2.23
68	HURKEY CREEK PARK	33°41'	-116°41'	4390	7/23/1968	11	1.18	1.59
69	SAN JOSE	37°21'	-121°54'	67	8/21/1968	13	1.25	1.92
70	IRON MOUNTAIN	34°08'	-115°08'	922	10/3/1968	17	1.72	2.08
71	MOUNT DANAHER	38°42'	-120°40'	3410	4/2/1969	20	1.10	1.50
72	MILL CREEK INTAKE	34°05'	-116°56'	4945	8/8/1969	15	1.15	1.35

Table A3.1. *Extreme local storms in California.*

#	Location	Latitude (degrees)	Longitude (degrees)	Elevation (feet)	Date	Hour of maximum rainfall	Max 1-hour rainfall (inches)	Max 6-hour rainfall (inches)
73	IDYLLWILD FIRE DEPT.	33°45'	-116°43'	5380	8/15/1970	10	1.10	1.60
74	BRIDGEPORT RS	38°15'	-119°14'	6441	7/20/1971	15	1.05	1.25
75	WARNER SPRINGS	33°17'	-116°38'	3180	8/4/1971	14	1.40	1.42
76	MARKLEEVILLE	38°42'	-119°47'	5530	8/12/1971	15	1.12	1.12
77	PALOMAR MTN. OBSY	33°21'	-116°52'	5550	6/5/1972	14	1.00	1.09
78	HUNTINGTON LAKE	37°14'	-119°13'	7020	6/7/1972	15	2.00	2.90
79	LORAINE	35°18'	-118°26'	2720	5/14/1973	16	1.39	1.55
80	NEEDLES	34°50'	-114°36'	150	7/19/1974	19	1.72	2.33
81	CUYAMACA	32°59'	-116°35'	4640	7/19/1974	13	1.10	1.30
82	TUJUNGA MILL FC	34°23'	-118°05'	4650	7/23/1974	14	1.14	1.24
83	WELDON 1 WSW	35°40'	-118°18'	2680	7/24/1974	18	1.65	1.80
84	FORT JONES 6 ESE	41°35'	-122°43'	3320	7/12/1975	15	1.00	1.40
85	FERGUSON RANCH	40°21'	-122°27'	800	8/18/1975	23	1.10	1.50
86	WARNER SPRINGS	33°17'	-116°38'	3180	9/3/1975	13	1.40	1.40
87	CUYAMACA	32°59'	-116°35'	4640	9/4/1975	14	1.00	1.10
88	HURKEY CREEK PARK	33°41'	-116°41'	4390	9/7/1975	13	1.10	1.40
89	HENSHAW DAM	33°14'	-116°46'	2700	7/25/1976	16	1.10	1.70
90	ETNA	41°28'	-122°54'	2950	6/7/1977	16	1.40	1.80
91	MILL CREEK INTAKE	34°05'	-116°56'	4945	8/22/1977	15	1.30	1.30
92	SANTA MARGARITA BOOSTE.	35°22'	-120°38'	1100	9/4/1977	24	1.30	1.30
93	MILL CREEK INTAKE	34°05'	-116°56'	4945	8/6/1979	12	1.20	1.60
94	BLYTHE 7 W	33°37'	-114°43'	390	8/11/1979	18	1.34	1.74
95	HAYFIELD PUMPING PLANT	33°42'	-115°38'	1370	8/12/1979	4	1.30	2.10
96	REDDING 5 SSE	40°30'	-122°22'	425	8/28/1979	19	1.40	1.80
97	DEL MONTE	36°36'	-121°52'	45	5/5/1980	13	1.30	2.20
98	BLYTHE 7 W	33°37'	-114°43'	390	8/14/1981	5	1.11	1.71
99	CUYAMACA	32°59'	-116°35'	4640	8/14/1981	13	1.00	1.00
100	CUYAMACA	32°59'	-116°35'	4640	9/7/1981	15	2.30	3.00
101	NORTH BLOOMFIELD	39°22'	-120°54'	3280	6/19/1982	16	1.10	1.60
102	HURKEY CREEK PARK	33°41'	-116°41'	4390	7/25/1982	14	1.20	1.50
103	RUNNING SPRINGS 1 E	34°12'	-117°05'	5970	7/26/1982	9	1.30	1.90
104	SAN JACINTO RS	33°47'	-116°58'	1560	8/25/1982	18	1.20	1.30
105	OAK GROVE RS	33°23'	-116°48'	2750	8/7/1983	15	1.40	1.40
106	FLORENCE LAKE	37°16'	-118°58'	7325	8/8/1983	15	1.80	2.60
107	HENSHAW DAM	33°14'	-116°46'	2700	8/9/1983	14	1.00	1.10
108	SEPULVEDA DAM	34°10'	-118°28'	670	8/16/1983	17	1.20	1.49
109	LYTLE CRK FTHILL BLVD.	34°06'	-117°20'	1160	8/17/1983	15	2.65	5.79
110	BEAUMONT	33°56'	-116°58'	2613	7/13/1984	15	1.20	1.50
111	ELSINORE	33°40'	-117°20'	1285	7/15/1984	18	1.10	1.20
112	HUNTINGTON LAKE	37°14'	-119°13'	7020	7/17/1984	18	1.30	1.40
113	BIG PINES PARK FC	34°23'	-117°41'	6845	7/18/1984	14	1.40	1.50
114	BLYTHE 7 W	33°37'	-114°43'	390	7/21/1984	16	1.06	1.08
115	MORENA DAM	32°41'	-116°31'	3075	7/27/1984	16	1.50	1.60
116	OZENA GUARD STN.	34°41'	-119°21'	3590	7/31/1984	16	1.20	1.40
117	HOLLISTER 9 ENE	36°55'	-121°14'	2600	8/8/1984	14	1.20	1.20

Table A3.1. *Extreme local storms in California.*

#	Location	Latitude (degrees)	Longitude (degrees)	Elevation (feet)	Date	Hour of maximum rainfall	Max 1-hour rainfall (inches)	Max 6-hour rainfall (inches)
118	HAYFIELD PUMPING PLANT	33°42'	-115°38'	1370	8/19/1984	16	1.10	1.70
119	BATTLE CREEK ADR	40°24'	-122°08'	420	5/28/1985	21	1.10	2.50
120	HAYFIELD PUMPING PLANT	33°42'	-115°38'	1370	7/19/1985	17	1.00	1.40
121	PORTOLA	39°48'	-120°28'	4850	7/25/1985	16	1.10	1.41
122	COFFEE CREEK RS	41°05'	-122°42'	2500	7/30/1985	17	1.40	1.80
123	SHASTA DAM	40°43'	-122°25'	1075	5/20/1986	18	1.50	2.70
124	NEEDLES	34°50'	-114°36'	480	8/11/1986	20	1.10	1.90
125	CALAVERAS BIG TREES	38°17'	-120°19'	4695	9/1/1986	7	1.30	1.50
126	DOWNIEVILLE	39°34'	-120°50'	2915	7/26/1988	16	1.40	1.70
127	COVELO EEL RIVER RS	39°50'	-123°05'	1514	8/14/1988	17	1.00	1.60
128	OAK GROVE RS	33°23'	-116°48'	2750	8/23/1988	13	1.30	1.60
129	MILFORD LAUFMAN RS	40°08'	-120°21'	4860	6/7/1989	16	1.40	1.40
130	HAYFIELD PUMPING PLANT	33°42'	-115°38'	1370	7/10/1989	15	1.20	1.30
131	HURKEY CREEK PARK	33°41'	-116°41'	4390	8/24/1988	2	1.70	1.80
132	BOWMAN DAM	39°27'	-120°39'	5385	7/14/1990	15	1.00	1.20
133	SUSANVILLE 1 WNW	40°26'	-120°40'	4555	7/18/1990	18	1.40	2.00
134	OAK GROVE RS	33°23'	-116°48'	2750	4/9/1990	13	1.20	1.40
135	BIEBER	41°10'	-121°08'	4125	7/18/1991	20	1.40	1.40
136	EL CENTRO 2 SSW	32°46'	-115°34'	-30	7/31/1991	15	1.10	1.10
137	IDYLLWILD FIRE DEPT.	33°45'	-116°43'	5380	7/31/1991	7	1.30	1.80

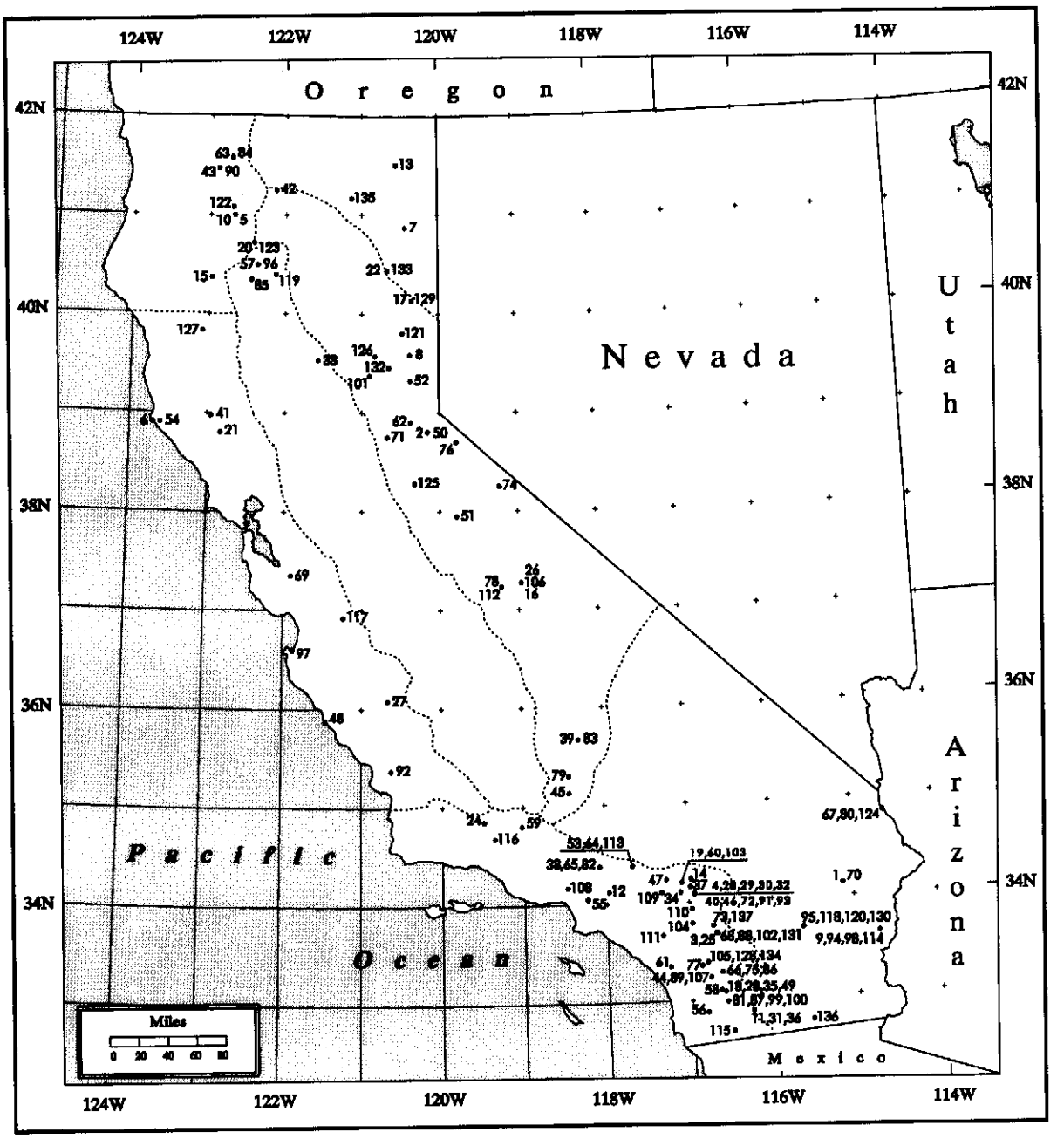

Figure A3.1. *Locations of the 137 local storms from in Table A3.1. The dotted lines indicate the regions specified for depth-area-duration, Chapter 3, Figure 3.3.*

APPENDIX 4

Snowmelt Parameters

In HMR 36 (1961) a snowmelt procedure was provided. Information was included for determination of temperatures, dewpoints, precipitation, and winds during and prior to a PMP storm. The development of new snowmelt parameters was beyond the scope of this report. However, during peer review, inclusion of snowmelt parameter procedures was mentioned by most reviewers as highly desirable. This Appendix is in response to those requests.

The core of the Appendix is a worksheet consisting of five sections (A-E). It is essentially the same worksheet that appeared in HMR 36. An example for the Auburn drainage above Folsom Dam is provided for mid-November. The figures referenced in Chapter X of HMR 36 dealing with variation of precipitable water, temperature/elevation relations, temperature prior to a PMP storm, and winds have not been changed except for new figure numbers. The seasonal variation of maximum moisture table (Table 4-1 in HMR 36) was replaced by Table A4.1. The revision of this table was based on new dewpoint data. The durational variation of maximum moisture, Table A4.2, is unchanged. The seasonal variation of maximum moisture, Table A4.1, is a function of the regional DAD boundaries for Chapter 3, Figure 3.3.

An important part of this methodology is the wind speed expected at the surface of a snow pack; these winds and reduction factors are needed in Steps D.1 and D.2 of the worksheet. The recommended factors for basins not sheltered from the winds by topographic features in advance of a PMP storm are a function of regions.

The factors for the regions are:

Region	Factor
1, 3, 6	.80
2, 5	.75

In cases where basins are sheltered from the winds the reduction factors should reduce the surface winds speeds even more. The amount of the reduction should be decided by the user.

We have assumed that snowmelt is not an important factor for basins in regions 4 and 7. If snowmelt parameters are needed for basins in these regions, use the factor in the above list from the region closest to the basin of concern.

Data values from Figures A4.1 to A4.7 may vary, and there will be some difference from user to user. Figure A4.8 gives the dewpoint temperatures for February over California.

Table A4.1. *Monthly variation of maximum moisture (percent/100 of February maximum). See Chapter 3, Figure 3.11 for region boundaries.*

	Month						
Region	October	November	December	January	February	March	April
3, 4, 6	1.22	1.13	1.08	1.03	1.00	1.03	1.06
7	1.35	1.11	1.03	0.97	1.00	1.03	1.06
1, 2	1.29	1.14	1.12	1.05	1.00	1.00	1.08
5	1.29	1.17	1.11	1.03	1.00	1.03	1.09

Table A4.2. *Durational variation of maximum moisture (percent of 12-hour precipitable water).*

Duration (Hour)	6	12	18	24	30	36	42	48	54	60	66	72
Percent	104	100	97	95	93	91	89	88	86	85	84	83

Snowmelt Parameters Worksheet

Drainage:_____ Average elevation (nearest 100 feet):_____

Month:_____ Region:_____

A. Temperatures and Dewpoints During PMP Storm

1) Average 12-hour February 1000 mb persisting dewpoint over basin (Figure A4.8): _____

2) Precipitable water (W_p) for temperature from Step A.1 (Figure A4.1): _____

3) Seasonal adjustment for month selected (Table A4.1): _____

4) Line 2 _____ x line 3 = _____

	6-Hour Period											
	1	2	3	4	5	6	7	8	9	10	11	12
5) W_p corresponding to 6-hour temperature increments during PMP storm. Line 4 x %'s of Table A4.2 (inches).												
6) 6-hour incremental sea-level temperatures and dewpoints from Figure A4.1 (°F).												
7) Sea-level temperatures and dewpoints adjusted to average basin elevation. Figure A4.2 (°F).												
8) Height of 32°F above mean sea-level. Figure A4.2 (1000's feet). Use dewpoints from line 6.												

9) The temperatures and elevations in Steps A.7 and A.8 should be arranged in time sequence corresponding to the selected PMP storm sequence (see E.3).

B. Temperatures Prior to PMP Storm

	Hours Prior to Storm Onset							
	48	42	36	30	24	18	12	6
1) Differences between temperature at the beginning of storm and at indicated hours prior to storm. From Figure A4.3, in range from curve A_1 to curve B (°F).								

2) The above differences are added to the initial temperature determined in Step A.9.

C. Dewpoints Prior to PMP Storm

	Hours Prior to Storm Onset							
	48	42	36	30	24	18	12	6
1) Differences between dewpoint at the beginning of storm and at indicated hours prior to storm. Figure A4.3, curve C (°F).								

2) The above differences are subtracted from the initial temperature (dewpoint) determined in Step A.9.

D. Snowmelt Winds

	6-Hour Period											
	1	2	3	4	5	6	7	8	9	10	11	12
1) Winds from Figure A4.5 (Regions 1, 3, 6) or A4.6 (Regions 2, 5) and interpolations at average basin elevation (feet msl) reference Figure A4.4 (mph).												
2) Winds reduced to surface conditions. See text for factor to be used. Step D.1 winds x factor (mph).												
3) Surface winds adjusted to month selected. Step D.2 winds x _____ (from Figure A4.7) (mph).												

4) Arrange 6-hour winds (Step D.3) in time sequence similar to arrangement of precipitation and temperatures in PMP storm (see E.4).

E. Time Sequence of Temperatures, Winds and Precipitation During PMP Storm

	6-Hour Period											
	1	2	3	4	5	6	7	8	9	10	11	12
1) Month of concern 6-hourly PMP increments for the selected drainage obtained by procedures of Chapter 13 (inches).												

	Time in Hours From Beginning of Storm											
	6	12	18	24	30	36	42	48	54	60	66	72
2) 6-hour PMP increments arranged according to sequence adopted in Section 13.2, Step 8 (inches).												
3) 6-hour temperatures from A.7 arranged in same sequence (°F).												
4) 6-hour winds from D.3 arranged in same sequence (mph).												
5) Height of freezing level from A.8 in same sequence (1000's feet).												

	Hours Prior to Storm Onset								
	48	42	36	30	24	18	12	6	0
6) Temperature prior to storm. Differences of B.1 added to the temperature from E.3, 6-hour column.									
7) Dewpoints prior to storm. Differences of C.1 subtracted from the temperature from E.3, 6-hour column.									

8) Winds prior to storm may be assumed to be the 72-hour duration value from D.3 for two days prior to storm.

Snowmelt Parameters Worksheet
(Example)

Drainage: Auburn
Month: Mid-November

Average elevation (nearest 100 feet): 4700
Region: Sierra (5)

A. Temperatures and Dewpoints During PMP Storm

1) Average 12-hour February 1000 mb persisting dewpoint over basin (Figure A4.8): 60° F

2) Precipitable water (W_p) for 60° F (Figure A4.1): 1.38

3) Seasonal adjustment for November (Table A4.1): 1.17

4) 1.38 times 1.17 = 1.61 inches

	6-Hour Period											
	1	2	3	4	5	6	7	8	9	10	11	12
5) W_p corresponding to 6-hour temperature increments during PMP storm. 1.61 x %'s of Table A4.2 (inches).	1.67	1.61	1.56	1.53	1.50	1.47	1.43	1.42	1.38	1.37	1.35	1.34
6) 6-hour incremental sea-level temperatures and dewpoints from Figure A4.1 (°F).	63.8	63.0	62.3	62.0	61.6	61.1	60.8	60.6	60.0	59.9	59.6	59.3
7) Sea-level temperatures and dewpoints adjusted to 4700 feet elevation. Figure A4.2 (°F).	51.5	50.7	49.8	49.4	49.0	48.4	48.0	47.6	47.3	47.0	46.7	46.3
8) Height of 32° F above mean sea level. Figure A4.2 (1000's feet). Use dewpoints from line 6.	11.6	11.3	10.9	10.8	10.7	10.4	10.2	10.1	9.9	9.8	9.7	9.6

9) The temperatures and elevations in Steps A.7 and A.8 should be arranged in time sequence corresponding to the selected PMP storm sequence (see E.3).

B. Temperatures Prior to PMP Storm

	Hours Prior to Storm Onset							
	48	42	36	30	24	18	12	6
1) Differences between temperature at the beginning of storm and at indicated hours prior to storm. From Figure A4.3, selecting curve A_1 (°F).	10.0	9.5	9.0	8.0	7.0	6.0	4.5	3.5

2) The above differences are added to the initial temperature determined in Step A.9.

C. Dewpoints Prior to PMP Storm

	Hours Prior to Storm Onset							
	48	42	36	30	24	18	12	6
1) Differences between dewpoint at the beginning of storm and at indicated hours prior to storm. Figure A4.3, curve C (°F).	3.5	2.5	2.0	2.0	1.5	1.0	1.0	0.5

2) The above differences are subtracted from the initial temperature (dewpoint) determined in Step A.9.

D. Snowmelt Winds

	6-Hour Period											
	1	2	3	4	5	6	7	8	9	10	11	12
1) Winds from Figure A4.6 and interpolations at 4700 feet msl (4700 feet = 840 mb) reference Figure A4.4 (mph).	78	69	64	60	57	54	52	50	49	48	47	46
2) Winds reduced to surface conditions similar to Auburn. Step D.1 winds x 0.75 (mph).	59	52	48	45	43	40	39	38	37	36	35	35
3) Surface winds adjusted to November. Step D.2 winds x 0.82 (from Figure A4.7) (mph).	48	42	39	37	35	33	32	31	30	30	29	29

4) Arrange 6-hour winds (Step D.3) in time sequence similar to arrangement of precipitation and temperatures in PMP storm (see E.4).

E. Time Sequence of Temperatures, Winds and Precipitation During PMP Storm

	6-Hour Period											
	1	2	3	4	5	6	7	8	9	10	11	12
1) November 6-hourly PMP increments for the selected drainage obtained by procedures of Chapter 13 (inches).	6.9	4.3	3.4	3.2	3.0	2.9	2.9	2.8	2.1	1.2	1.1	1.0

	Time in Hours From Beginning of Storm											
	6	12	18	24	30	36	42	48	54	60	66	72
2) 6-hour PMP increments arranged according to sequence adopted in Section 13.2, Step 8 (inches).	3.0	2.9	2.8	2.9	3.2	4.3	6.9	3.4	1.2	1.0	2.1	1.1
3) 6-hour temperatures from A.7 arranged in same sequence (°F).	49.0	48.4	47.6	48.0	49.4	50.7	51.5	49.8	47.0	46.3	47.3	46.7
4) 6-hour winds from D.3 arranged in same sequence (mph).	35	33	31	32	37	42	48	39	30	29	30	29
5) Height of freezing level from A.8 in same sequence (1000's feet).	10.7	10.4	10.1	10.2	10.8	11.3	11.6	10.9	9.8	9.6	9.9	9.7

	Hours Prior to Storm Onset								
	48	42	36	30	24	18	12	6	0
6) Temperature prior to storm. Differences of B.1 added to the temperature from E.3, 6-hour column.	59.0	58.5	58.0	57.0	56.0	55.0	53.5	52.5	49.0
7) Dewpoints prior to storm. Differences of C.1 subtracted from the temperature from E.3, 6-hour column.	45.5	46.5	47.0	47.0	47.5	48.0	48.0	48.5	49.0

8) Winds prior to storm may be assumed to be 29 mph for two days prior to storm.

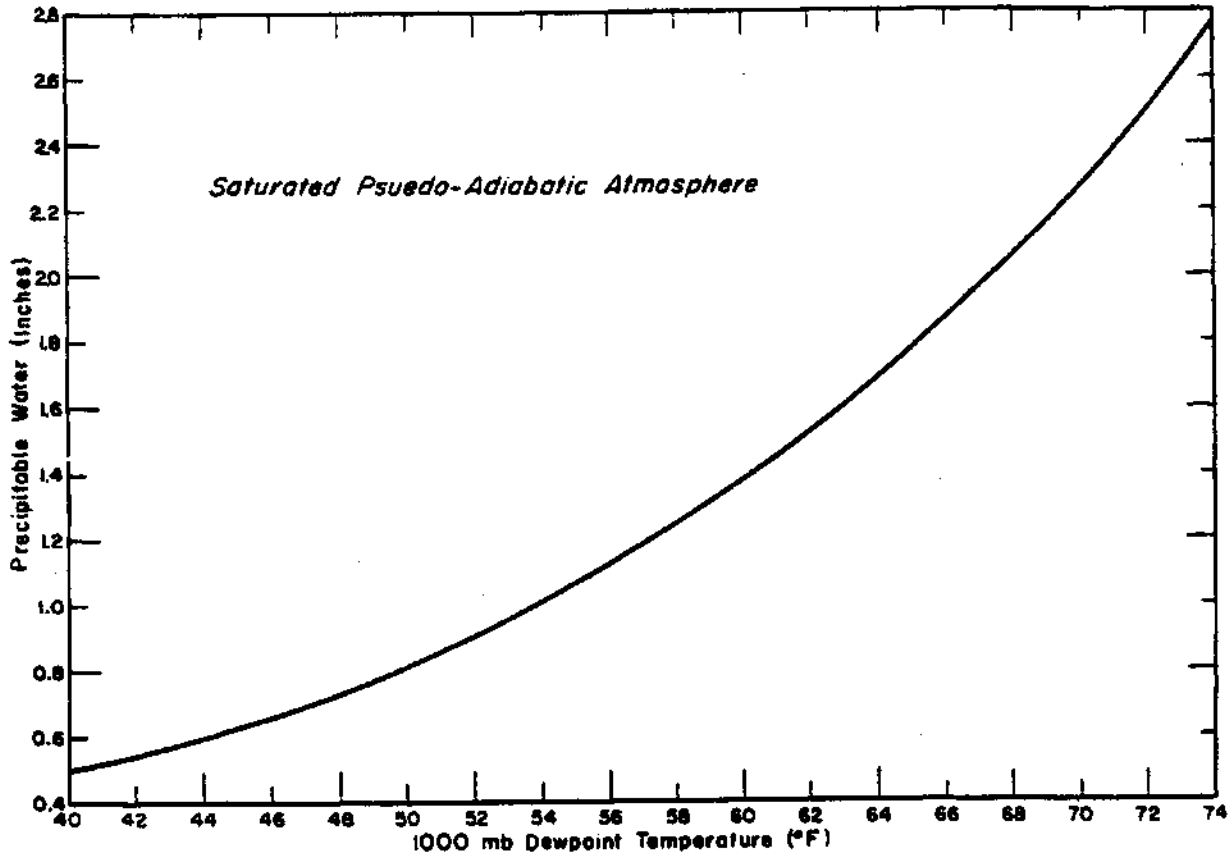

Figure A4.1. *Variation of precipitable water with 1000-mb dewpoint temperature.*

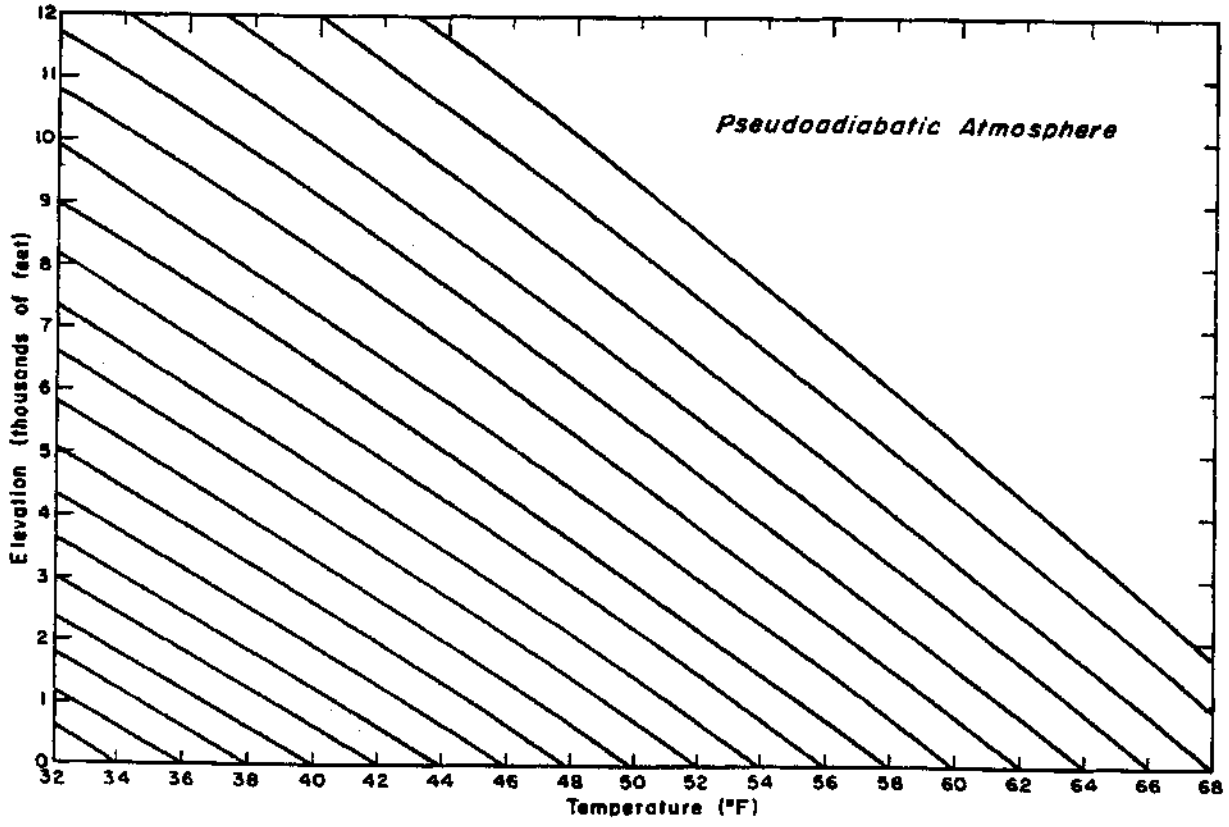

Figure A4.2. *Decrease of temperature with elevation.*

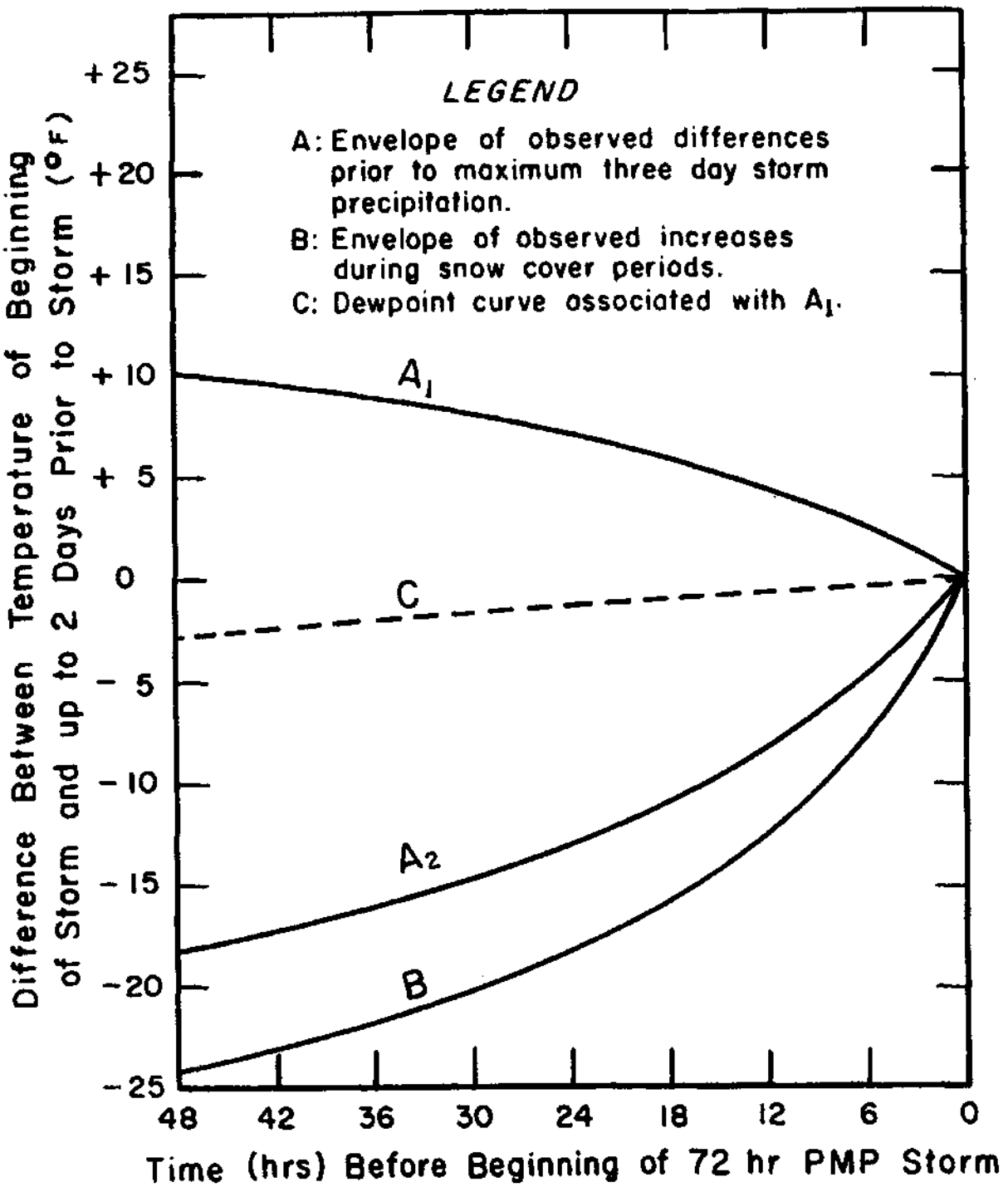

Figure A4.3. *Temperature prior to a PMP storm.*

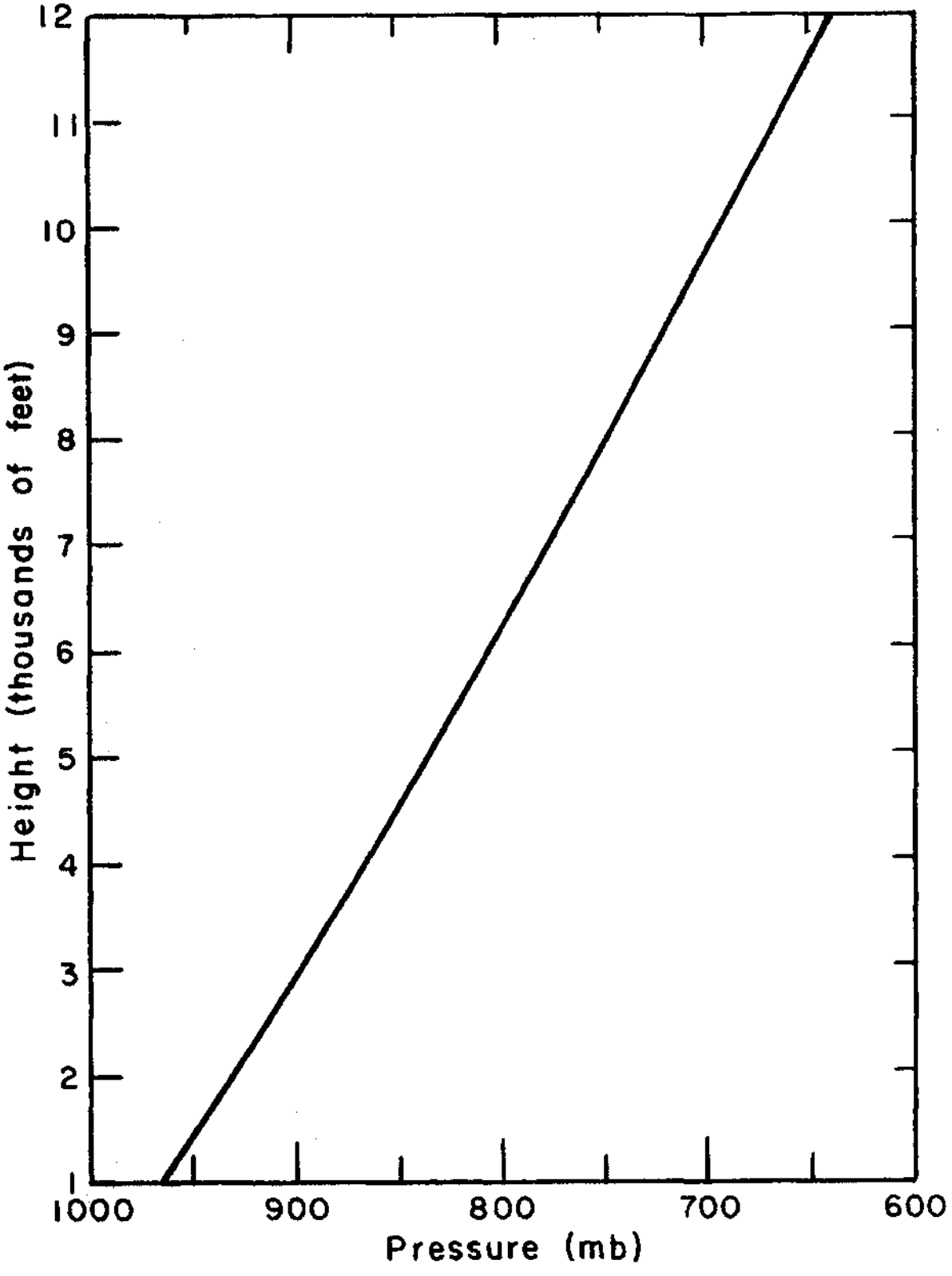

Figure A4.4. *Pressure-height relation.*

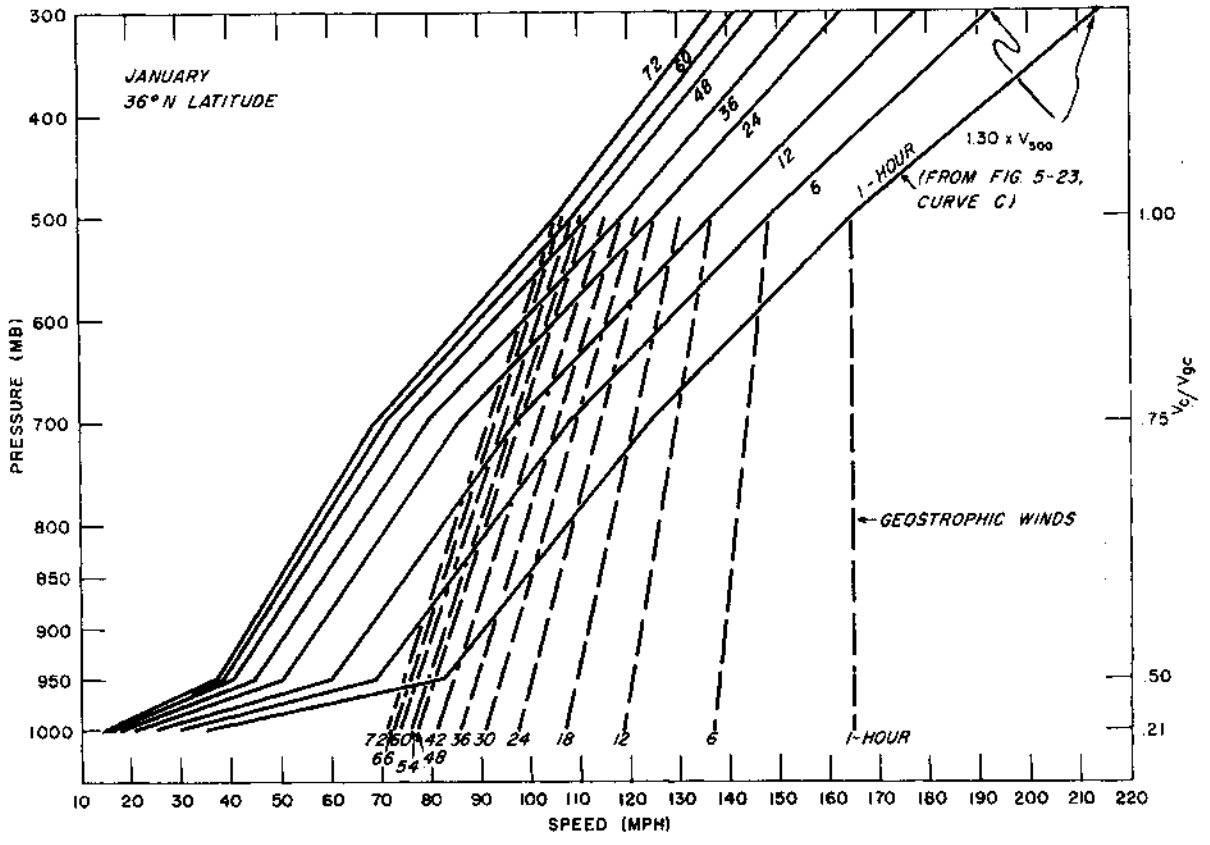

Figure A4.5. *Maximum winds normal to coast range.*

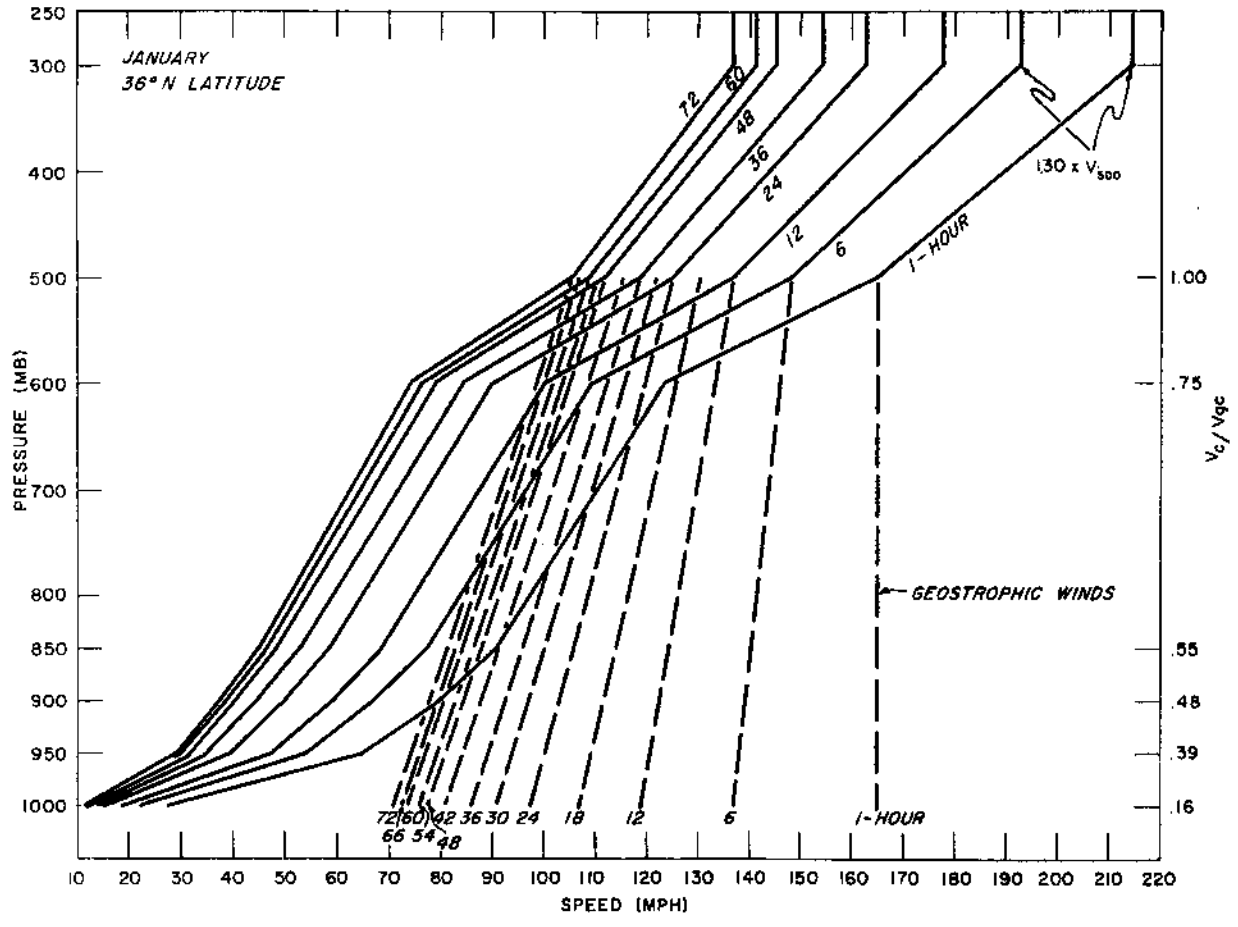

Figure A4.6. *Maximum winds normal to the Sierra mountains.*

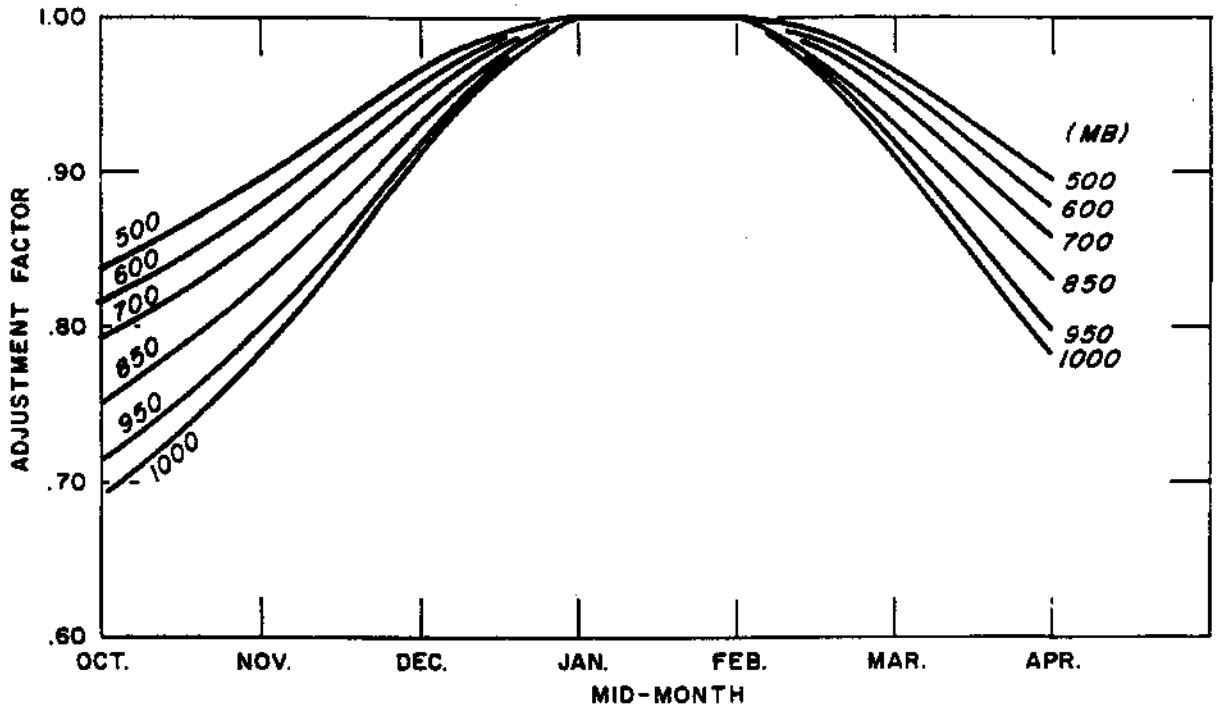

Figure A4.7. *Seasonal variation of maximum winds.*

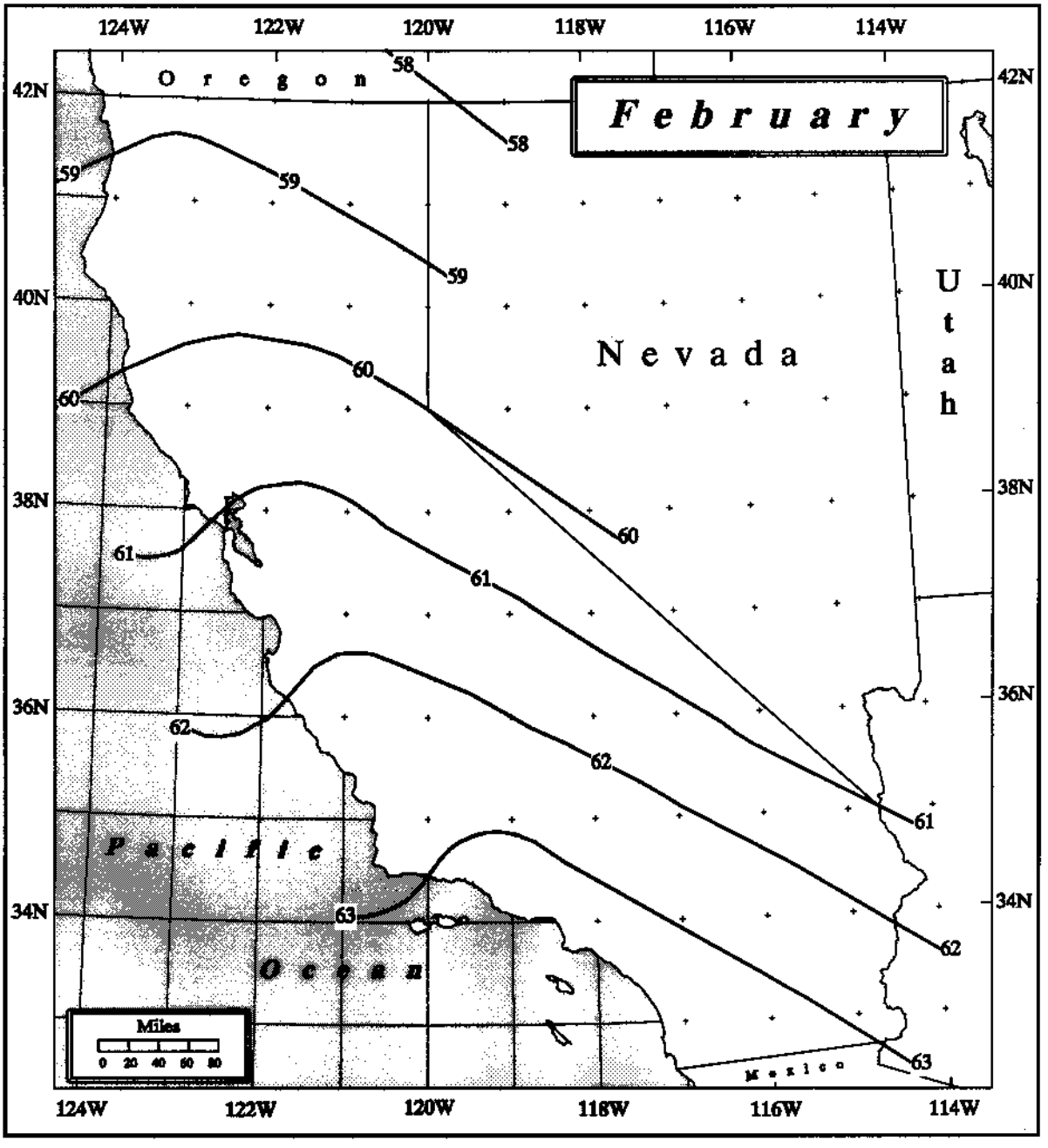

Figure A4.8. *Twelve-hour maximum persisting 1000-mb dewpoints for February (°F). Same as Figure 4.2.*

APPENDIX 5

Storm Separation Method

The storm separation method (SSM) was devised for HMR 55A (1988) as a technique that would identify orographic and non-orographic components of precipitation produced by storms over regions of varied topographic characteristics. The identification was achieved by using all the various kinds and amounts of available information about the storms to answer a uniform series of questions. The original version of the SSM and updates to it were printed in HMR 57 (1994).

It was decided that users of this report (HMR 59) might want to review the original and updated material constituting the SSM in connection with their reading of Chapter 5, Section 5.4. These materials are reproduced here; the material from HMR 55A coming first, and the updated material from HMR 57 following it. References in each of these groups of material to figures, chapters, or sections in the parent reports have been retained rather than masked out in the reproductions. We hope that these references, may be useful to those who wish to dig deeper into such matters.

7. STORM SEPARATION METHOD

7.1 Introduction

In order to establish PMP in the CD-103 region, it was considered necessary to find a property of observed major storm precipitation events that is only minimally effected by terrain so transposition of observed precipitation amounts would not be limited to places where the terrain characteristics are the same as those at the place where the storm occurred. The name given to this idealized property is "free atmospheric forced precipitation" (FAFP) which has been called "convergence only" precipitation in publications such as HMR No. 49 (Hansen et al. 1977). For a more complete definition of FAFP, see the Glossary of Terms in section 7.2. It is emphasized that FAFP is an idealized property of precipitation since no experiment has yet been devised to identify in nature which raindrops were formed by orographic forcing and which by atmospheric forcing. This chapter explains how FAFP may be estimated for specific storms. Background information is provided on the development of the storm separation method (SSM).

7.2 Glossary of Terms

Terms frequently used in the SSM are listed alphabetically.

A_o: See P_a. It is the term for the effectiveness of orographic forcing used in module 3.

AI: The analysis interval, in inches, for the isohyets drawn for a storm.

B_i: See PCT2. It is the term representing the "triggering effects" of orography. It is used in module 2. B_i is a number between 0 and 1.0 representing the degree of FAFP implied by the relative positioning of the 1st through i-th isohyetal maxima with those terrain features (steepest slopes, prominences, converging upslope valleys) generally thought to induce or "stimulate" precipitation. A high positive correlation between terrain features and isohyetal maxima yields a low value for B_i. For each isohyetal maximum there is just one B-type correlation and, thus, if the area covered by a given maximum is extensive enough so that more than one area category is contained within its limits, the B correlations are determined using all isohyets comprising a particular maximum. For the larger-area/shorter-duration categories, the B_1 correlation may need to be made in widely separated, noncontiguous areas.

When available, the chart of maximum depth-area-duration curves from the Part II Summary of the storm analysis*, along with its associated documentation, is the primary source for determining how many centers (n) and which isohyetal maxima were used to determine the average depth for the area being considered.

BFAC: 0.95 (RCAT). It represents an upper limit for FAFP in modules 2 and 5. See also the definition for PX.

DADRF: The depth-area-duration reduction factor is the ratio of two average depths of precipitation.

$$DADRF = RCAT/MXVATS$$

DADFX: DADFX = (HIFX)(DADRF). It is used in module 2 to represent the largest amount of nonorographic precipitation caused by the same atmospheric mechanism that produced MXVATS.

F_i: See PCT2. It is the term for the "upsloping effects" of orography and it is used in module 2. It is a number between 0 and 1.0, which represents the degree of atmospheric forcing implied by the orientation of the applicable upwind segments of the isohyets with elevation contours (high positive correlation of these parameters means a low value for F_i) for the 1st through i-th maxima. For an isohyetal maximum there is just one F-type correlation, and if the area covered by a given maximum is extensive enough so that more than one area category is contained within its limits, the F correlations are the same for each of the area categories. F-type correlations are determined using all isohyets comprising a particular maximum. As with B-type correlations, maximum depth-area-duration curves from the Part II of the storm report should be used to determine which precipitation centers are involved in the isohyetal maximum.

*A depth-area-duration storm analysis is separated into two parts. The first part develops a preliminary isohyetal map and mass curves of rainfall for all stations in the storm area. The second part includes a final isohyetal map, computation of the average depth of rainfall over all isohyetal areas and determination of the maximum average depth for all area sizes up to the total storm area. The complete procedure used for making depth-area-duration analysis is described in "Manual for Depth-Area-Duration Analysis of Storm Precipitation" (World Meteorological Organization 1986).

FAFP: Free Atmospheric Forced Precipitation is the precipitation not caused by orographic forcing; i.e., it is precipitation caused by the dynamic, thermodynamic, and microphysical processes of the atmosphere. It is all the precipitation from a storm occurring in an area where terrain influence or forcing is negligible, termed a nonorographic area. In areas classified as orographic, it is that part of the total precipitation which remains when amounts attributable to orographic forcing have been removed. Factors involved in the production of FAFP are: convergence at middle and low tropospheric levels and often, divergence at high levels; buoyancy arising from heating and instability; forcing from mesoscale systems, i.e., pseudo fronts, squall lines, bubble highs, etc.; storm structure, especially at the thunderstorm scale involving the interaction of precipitation unloading with the storm sustaining updraft; and lastly, condensation efficiency involving the role of hydroscopic nuclei and the heights of the condensation and freezing levels.

HIFX: The largest isohyetal value in the nonorographic part of the storm. The same atmospheric forces (storm mechanism) must be the cause of precipitation over the areas covered by the isohyet used to determine HIFX and MXVATS.

I_m: That part of RCAT attributed solely to atmospheric processes and having the dimension of depth. Since it is postulated that FAFP cannot be directly observed in an orographic area, some finite portion of it was caused by forcing other than free atmospheric. The FAFP component of the total depth must always be derived by making one or more assumptions about how the precipitation was caused. The subscript "m" identifies the single assumption or set of assumptions used to derive the amount designated by I. For example, a subscript of 2 will refer to the assumptions used in module 2. The key assumptions of all the modules are detailed in section 7.3.1. Refer to the schematic for each module in figures 7.3 to 7.6 for the specific formulation for each I_m.

LOFACA: LOFACA is the lowest isohyetal value at which it first becomes clear to the analyst that the topography is influencing the distribution of precipitation depths. Confirmation of this influence is assumed to occur when good correlation is observed between the LOFACA isohyet and one or more elevation contours in the orographic part of the storm.

How is LOFACA found? A schematic isohyetal pattern is shown by the solid lines in figure 7.1 to illustrate this procedure. Start at the storm center and follow the inflow wind direction out to the lowest valued isohyet in the analysis (no lower than 1 in.) located in the orographic part of the storm. If the storm pattern is oddly shaped, it may be necessary to use a direction slightly different from the exact inflow direction. Any direction within ± 22.5 degrees either side of the inflow direction which allows comparisons of the sort described above is acceptable. The vector CL in the schematic of figure 7.1 represents the path in this storm that is parallel to the inflow wind and directed at the lowest valued isohyet. Next, draw

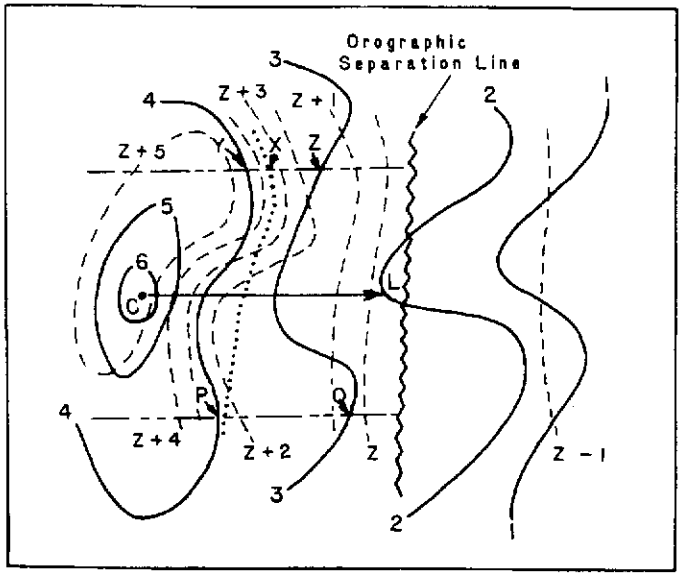

Figure 7.1.—Schematic illustrating determination of LOFACA.

two lines parallel to and either side of the vector CL. Each of the parallel lines will be drawn at a distance from CL of 1/2 the length of CL. These lines are the dash-dot lines in figure 7.1. These lines will be called "range lines." The range lines end at the orographic separation line (the saw-toothed line in figure 7.1) since only correlations in the orographic part of the storm are important in determining LOFACA.

The next step is to examine those isohyets which intersect the range lines down wind of the storm center of isohyetal maximum. Such segments are considered candidate isohyetal segments (CIS) and they are depicted by the segments of the isohyets PY and QZ in figure 7.1. The objective is to determine which CIS has a good correlation with topographic features indicated by the dashed lines. A good correlation is a CIS that parallels one of the smoothed elevation contours along one-half or more of its length. When no isohyet is found meeting the criterion, LOFACA is defined to be zero. As depicted in the schematic, the 4-in. CIS indicated by the solid line (from P to Y) shows a good correlation with the Z + 2 and Z + 3 contours, so the value of LOFACA is 4 in. If the 4-in. isohyet in figure 7.1 had been along the dotted line from P to X,

there would have been a poor correlation and the value of LOFACA would have been zero for this storm.

The significance of LOFACA is that precipitation depths at and below this value are assumed to have been produced solely by atmospheric forces without any additional precipitation resulting from topographic effects; i.e., they represent the "minimum level" of FAFP for the storm. If more than one isohyetal center exists for the area size selected, the procedure is followed for each center. If the value of LOFACA is different for two or more of these centers, the lowest of the values is used as the one and only value of LOFACA for that storm and area size.

LOFAC: $LOFAC = LOFACA + \frac{AI}{2}\left(PB^{\frac{(AI)}{2}} - 1\right)$.

It is a refinement to LOFACA based on the concept that AI may prejudice the assigning of a minimum level of FAFP.

MXVATS: The average depth of precipitation for the total storm duration for the smallest area size analyzed, provided that it is not larger than 100 mi^2. It is obtained from the pertinent data sheet (P.D.S.) for the storm included in "Storm Rainfall" (Corps of Engineers 1945 -). It is used in several modules to calculate percentages of FAFP. If the area criterion cannot be met, the storm is not used in the study.

n: When used in module 2 it is the number of analyzed isohyetal maxima used to set the average depth of precipitation for a given area size.

OSL: Orographic Separation Line is a line which separates the CD-103 region into two distinct regions, where there are different orographic affects on the precipitation process. In one region, the nonorographic, it is assumed no more than a 5-percent change (in either increasing or decreasing the precipitation amount for any storm or series of storms) results from terrain effects. In contrast, the other region is one where the influence of terrain on the precipitation process is significant. An upper limit of 95 percent and a lower limit of no less than 5 percent is allowed. The line may exist anywhere from a few to 20 miles upwind (where the wind direction is that which is judged to prevail in typical record setting storms) of the point at which the terrain slope equals or exceeds 1,000 ft om 5 miles or less with respect to the inflowing wind direction (sec. 3.2).

P_a: P_a (and A_o) is a ratio in which the effectiveness of an actual storm in producing precipitation is compared with a conceptualized storm of "perfect" effectiveness. In such a conceptual model, features known by experience to be highly correlated with positive vertical motions, or an efficient storm structure, would be numerous and exist at an optimum (not always the largest or strongest) intensity level.

Thus,

$$P_a = \frac{\text{Effectiveness of Actual Atmospheric Mechanisms}}{100}$$

where the numerator is a number between 5 and 95

$$A_o = \frac{\text{Effectiveness of Actual Orographic Mechanisms}}{100}$$

where the numerator is a number between 0 and ≤95.

It would have been desirable to express both P_a and A_o in physically meaningful units; however, this was not considered practical because the available meteorological data for most of the storms of concern are generally extremely limited. Hence, the present formulation is expressed in terms of subjective inferences about physical parameters known to be effective in the production of precipitation either in major storms in nonorographic regions or by considering the results of flow of saturated air against orographic barriers. This type of formulation is required, because of the limited availability of meteorological information for the storms, but is considered adequate for the purposes of this report. Mechanically, the effectiveness of the particular storm is derived by using the checklists in module 3.

PA: The ratio of the nonorographic area containing precipitation to the total storm precipitation area is given by PA. Its inverse is used when setting a realistic upper limit for I_2 and I_5 (see definition for PX on the following page). Areas in which the depth of precipitation is less than 1 in. are not used in forming the ratio. In contrast to PC, PA does not depend upon the area size being considered in the storm separation method.

PB: When the LOFACA isohyet does not extend from the orographic part into the nonorographic part of the storm, it is the ratio of the sum of the areas in the nonorographic part containing amounts equal to or greater than LOFACA (the numerator) to the total nonorographic area in which precipitation depths associated with the storm are 1 in. or more. When the LOFACA isohyet does extend into the nonorographic part of the storm, the numerator is increased by an amount representing the area bounded by the LOFACA isohyet and the OSL. It is used in module 2 in setting a value for LOFAC. Note: when LOFACA is zero, PB will be one and LOFAC will also equal zero.

PC: It is used in the formulations of PCT1, PCT2, and PCT3 to take into account the contribution of nonorographic precipitation to total FAFP (which includes FAFP contributions from orographic areas). It is expressed as a number between 0 and 0.95 The value of the upper limit is 0.95 because no storm in which more than 95 percent of the precipitation fell in nonorographic areas was considered. Thus, some storms from the list of important storms were not considered since they occurred in the nonorographic region.

If, for the area size being considered, part of the total volume of precipitation occurred in a nonorographic area, PC is the ratio of

that partial volume to the total volume. If none of the total volume was nonorographic, PC = 0. The ratio of volumes is obtained by forming the ratio of the corresponding area sizes first, then multiplying that ratio by an estimate of the average depth in the nonorographic area, and finally dividing this result by the average depth for the total area, both of these depths occurring at maximum duration.

PX: is the smaller of either BFAC or DADFX multiplied by $(PA)^{-1}$ except when PA = 0, in which case PX = BFAC. Once selected, PX serves to define what is a realistic upper limit for I_2 and I_5.

PCT1: $$PCT1 = PC + \frac{RNOVAL}{MXVATS}(0.95-PC).$$

MXVATS is used only for the smallest area size on the P.D.S. (provided that it is not greater than 100 mi^2) because the average depth at larger area sizes is influenced by how isohyets were drawn.

PCT2: $$PCT2 = PC + \left(\frac{\sum_{i=1}^{n}(F_i + B_i)}{2n}\right)(0.95 - PC)$$

It is a number between 0 and 0.95 where n is the number of isohyetal maxima in the orographic part of the storm applicable to the area/duration category being considered. Estimates of F- and B-type correlations are dependent upon the quality of the isohyetal analysis and upon proper identification of the precipitation centers involved in the area category under consideration. When there is no Part II storm study information available, the analyst must decide whether a reasonable estimate can be made for n. When there are just a few maxima, each at a different depth, a reasonable estimate is likely, whereas when there are numerous maxima all of which are for the same depth and which enclose about the same area, it is less likely that a reliable value for PCT2 can be calculated. When the latter is the case, the answer to question 13 in module 2 will be "no" and the analyst documents this situation in module 5 after completing modules 3 and 4.

PCT22: This is the ratio I_2/RCAT where I_2 is the total amount of RCAT that is FAFP. I_2 is defined by the relationship:

$$I_2 = [LOFAC + (MXVATS - LOFAC)PCT2]DADRF$$

Substitution of these terms into the definition for PCT22 leads to the relationship:

$$PCT22 = PCT2 + \left(\frac{LOFAC}{MXVATS}\right)(1-PCT2)$$

PCT3: $$PCT3 = PC + \left(\frac{P_a}{P_a + A_o}\right)(0.95-PC)$$

It is a dimensionless number usually between 0.05 and 0.95, representing the percent of the total depth of precipitation for a given area/duration category attributable to the atmospheric processes alone. It is obtained not only by considering primarily meteorological information, but also by considering the following minimal list of additional information: a P.D.S. for the storm (DAD data) including the location of the storm center; a chart of smoothed contours of terrain elevation; and precipitation data sufficient to define where precipitation did or did not occur. More detailed precipitation information is used, when available.

The range of 0.05 to 0.95 is considered reasonable, because it is postulated that the orographic influence never completely vanishes, and when the orographic influence is predominant, precipitation would not continue without some contribution from atmospheric forcing mechanisms. Though not expected to occur, it is conceivable that PCT3 may exceed 0.95 if the estimated orographic forcing was downslope, actually decreasing the total possible precipitation. This matter is discussed further in the section dealing with module 3. The formulation for PCT3 is meant to apply only to major storms and definitely not to minor storms where negative terrain forcing on lee slopes might approach, or exceed, the magnitude of the atmospheric forcing.

RCAT: The average depth of precipitation for the selected category. The "CAT" indicates that the parameter R is a variable depending on category definition.

RNOVAL: Representative nonorographic value of precipitation. It is the highest observed amount in the nonorographic part of the storm. The value of RNOVAL is not adjusted to the elevation at which MXVATS is believed to have occurred. RNOVAL and MXVATS must result from the same atmospheric forces (storm mechanism).

7.3 Background

The SSM was developed in the present format because four distinct sets of precipitation information were available for record-setting storms in the CD-103 region. These were:

1. Reported total storm precipitation, used in module 1.
2. Isohyet and depth-area-duration analyses of total storm precipitation, including Part I and Part II Summaries, used in module 2.
3. Meteorological data and analyses therefrom, used in module 3.
4. Topographic charts, used in all modules.

Since the quantity and quality of the information in the first three of these sets would vary from storm to storm, it was concluded that a method which relied on just one of the first three sets (along with topographic charts) might be quite useless for certain storms. Alternatively, one could have a SSM which always combined information from the first three sets. This choice was rejected since, for most of the storms, one or more of the sets might contain no useful information and bogus data would have to be used. Clearly, the SSM depends on the validity of the input information.

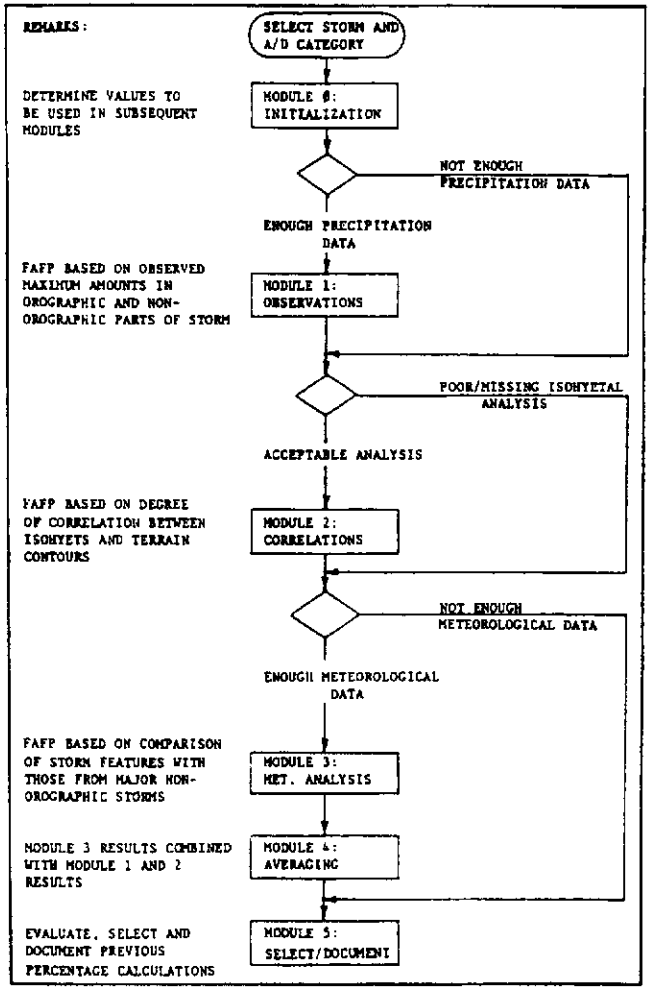

Figure 7.2.—Main flowchart for SSM.

Four sets of information are used in the SSM to produce up to five estimates c FAFP for area categories up to 5,000 mi^2 and durations up to 72 hr for storm with major rainfall centers in areas classified as "orographic." The mechanic of the procedure used to arrive at one numerical value of FAFP for any relevan area/duration (A/D) category for any qualifying storm are accomplished b completing the tasks symbolically represented in a MAIN FLOWCHART for the SS (fig. 7.2) along with its associated SSM MODULE FLOWCHARTS (fig. 7.3 to 7.7) wit references to the following items:

1. Glossary of Terms (sec. 7.2).

2. Concepts for use of the modules (sec. 7.3.1).

3. Specific questions to be answered in the MAIN FLOWCHART and the MODUL FLOWCHARTS.

7.3.1 Basic Concepts

The validity of the techniques in the SSM depends on the validity of th concepts upon which they are based. Evaluation of these concepts is crucial i the application of the procedure. A relative evaluation of the validity of th concepts underlying the individual modules will govern which of the five possibl values will be used for FAFP for a given A/D category. The evaluation i formalized in module 5 (column E) of the SSM based on the analysts evaluation o the various concepts. Several concepts are basic to acceptance of the procedur as a whole (all modules) while others relate to the evaluation of individua modules.

7.3.1.1 Overall Method. The total depth of precipitation for a given A/ category is composed of precipitation that results from atmospheric forces an from the added effect of orography. The method assumes that the effect o orography may either contribute to or take away from the amount of precipitatio that is produced by the atmosphere. When the orographic effect is positiv (expressed as a percentage contribution to total precipitation), it may not b less than 5 percent. If it is also assumed that the terrain surrounding th location where a given storm of record occurred had been transparent; i.e., ha no effect on the atmospheric forces acting there, the resulting total precip- itation would be the same as the free air forced component of precipitation fo the actual storm.

It is assumed that the FAFP never completely disappears in storms of record and the total volume may contain contributions over both the orographic an nonorographic areas. The further assumption is made that, when no other information is available at the shorter durations, inferences made fro precipitation depths valid at maximum storm duration for a given area are equall valid for the same area at shorter durations down to and including the minimu duration category.

7.3.1.2 Module 1. There are three components that underlie the use o precipitation observations in the estimation of the contribution of th atmosphere to the precipitation amounts in storms. These are:

1. If free atmospheric forcing in the nonorographic part of the storm ha been smaller that it was, the value of the maximum depth o precipitation would have been proportionally less.

2. The FAFP in the orographic region of the storm is approximated by the maximum precipitation depths in the nonorographic region, as long as the same atmospheric forces are involved at each location.

3. Estimates of the FAFP based on assumptions 1 and 2 are better for small rather than intermediate or large area sizes.

7.3.1.3 **Module 2.** This module uses an isohyetal analysis of the precipitation data to evaluate the free air forced component of precipitation. Inherent in the use of this module is the existence of an isohyetal analysis based on adequate precipitation information and prepared without undue reliance on normal annual precipitation or other rainfall indices which may induce a spurious correlation between the precipitation amounts and topography. In addition, there are five other concepts underlying this module. These are:

1. One or more than one level of LOFACA may exist in the orographic part of a storm. When more than one storm center is contained in a given area category, the lowest level of LOFACA found is used for that area size.

2. LOFACA exists when there is a good correlation between some isohyet and elevation contours.

3. Upsloping and triggering (F- and B-type correlations) are of equal significance in determining the percentage of precipitation above LOFACA which is terrain forced.

4. For an orographic storm (centered in th orographic portion of the region), the larger the nonorographic portion becomes (in relation to the total storm area), the more likely that the observed largest rainfall amount in the nonorographic portion (as represented by DADFX) is the "true" upper limit to FAFP in the orographic part of the storm.

5. Estimates of FAFP using the above assumptions are better at intermediate and large rather than small area sizes.

7.3.1.4 **Module 3.** This module makes use of the meteorological analysis and the evaluation of the interaction of dynamic mechanisms of the atmosphere with terrain to estimate the FAFP. There are seven basic concepts underlying the use of this module. These are:

1. Estimates of FAFP made using the techniques of this module may be of marginal reliability if the storms considered are those producing moderate or lesser precipitation amounts.

2. A variety of storms exist, each one of which has an optimum configuration for producing extreme precipitation.

3. The more closely the atmospheric forcing mechanisms for a given storm approach the ideal effectiveness for that type of storm, the larger the effectiveness value (P_a) for that storm becomes.

4. The FAFP is directly proportional to the effectiveness of atmospheric forcing mechanisms and inversely proportional to the effectiveness of orographic forcing mechanisms.

5. If the effectiveness of the orographic forcing mechanisms is of opposite sign to the effectiveness of the atmospheric forcing mechanisms and of equal or larger magnitude, little or no precipitation should occur.

6. The FAFP of storms of record is arbitrarily limited to no more than 100 percent of the maximum precipitation depth for the area/duration category under consideration.

7. Estimates of FAFP using the above assumptions are better at large rather than at intermediate or small area sizes.

7.3.1.5 **Module 4.** A basic assumption underlying the use of module 4 is that better results can be obtained by combining information; i.e., averaging the percentages obtained from the isohyetal analysis with the meteorological analysis and those obtained from analysis of the precipitation observations with the meteorological analysis. Better estimates are produced by averaging when there is little difference in the expressed preference for any one of the techniques or sources of information and, also, when the calculated percentage of FAFP from each of the modules exhibits wide differences.

Little is to be gained from use of the averaging technique over estimates produced by one of the individual analyses of modules 1, 2, or 3 when:

1. There are large differences in the expressed preference for the techniques of one module.

2. The sources of information for one of the individual modules is definitely superior.

3. The calculated percentages among the modules are in close agreement.

7.4 Methodology

The SSM was developed in a modular framework. This permits the user to consider only those factors for which information is available for an individual storm. A MAIN FLOWCHART of the SSM is shown in figure 7.2.

The MAIN FLOWCHART gives the user an overview of the SSM. Modules 1, 2, and 3 are designed to use the first three information sets mentioned in section 7.3 as indicated by the remarks column at the left side of the flowchart. A decision must be made initially for any storm and category as to which modules can be appropriately used, module 1, 2, or 3. The decision is based on a minimum level of acceptability of the information required by the module in question. The decisions are formalized for each of these three modules in module 0. The heart of the SSM procedure is module 5 where documentation is made of the SSM process, thereby permitting traceability of results. Though module 5 can be reached on the flowchart only after passing through each of the other modules, it is recommended that the steps in each module be documented in the record sheet of module 5 as the analyst proceeds. Transposition and moisture maximization of the index value of precipitation follows the completion of the SSM and will be discussed in chapter 8.

7.4.1 Module Flowcharts

There is a flowchart for each module. These were developed to aid the analyst in following the procedures in the SSM.

7.4.1.1 **Module 0 Procedure (fig. 7.3).** It is important in this module to decide on the adequacy of the available data. The results of this assessment are entered in column D of figure 7.8. The following rules concerning criteria are used:

1. For modules 1, 2, or 3, if there are no data available for the given technique (module), assign 0 to column D.

2. If the data are judged to be highly adequate, assign a value of either 7, 8, or 9, where 9 is the most adequate.

3. If the quantity, consistency, and accuracy of the information are judged to be adequate, assign a value of either 4, 5, or 6 to column D.

4. If the input information are judged as neither highly adequate, adequate, or missing, a value of either 1, 2, or 3 must be assigned to column D. A value of 1 is the lowest level of adequacy consistent with affirmative responses to questions 3, 5, and 7 in module 0.

An evaluation of a technique is not appropriate when there is insufficient information available for it to be used. Assigning an effective value of zero to column D under these circumstances eliminates the possibility.

The Glossary of Terms provides all required information needed to give numerical values to the five variables in the first step of the module 0 procedure. Note: In this module and in modules 1, 2, and 3, the connector symbol (C) applies only within the given module; i.e., when one is sent to a connector symbol it is always the one that is found in that module.

The following questions need to be answered in this module:

Q.1. Is PC equal to or greater than 0.95?

Q.2. Is there a HXVATS for an area size equal to or less than 100 mi^2 on the Pertinent Data Sheet for this storm?

Q.3. Are the quantity, quality, and distribution of the nonorographic observations sufficient to select a reliable value for RNOVAL?

Q.4. Is an isohyetal analysis available?

Q.5. Is the isohyetal analysis reliable?

Q.6. Is a reliable isohyetal analysis easily accomplished?

Q.7. Are the meteorological data sufficient to make a reliable estimate of P_a and A_o?

Q.8. Is RNOVAL equal to zero?

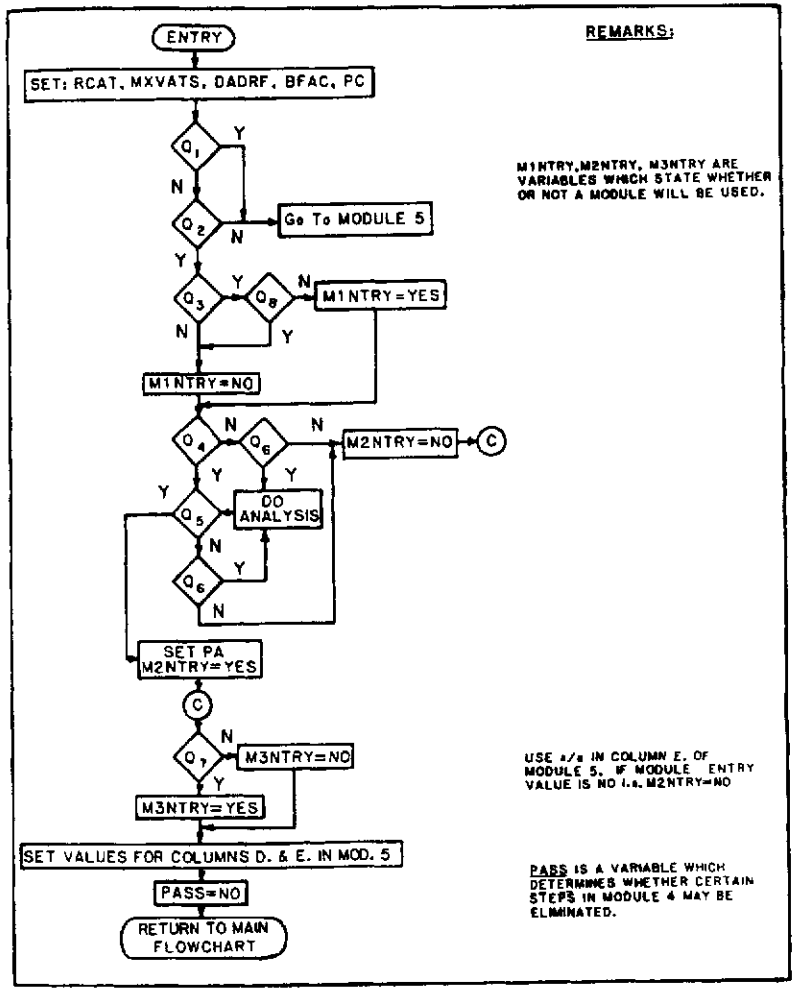

Figure 7.3.—Flowchart for module 0, SSM.

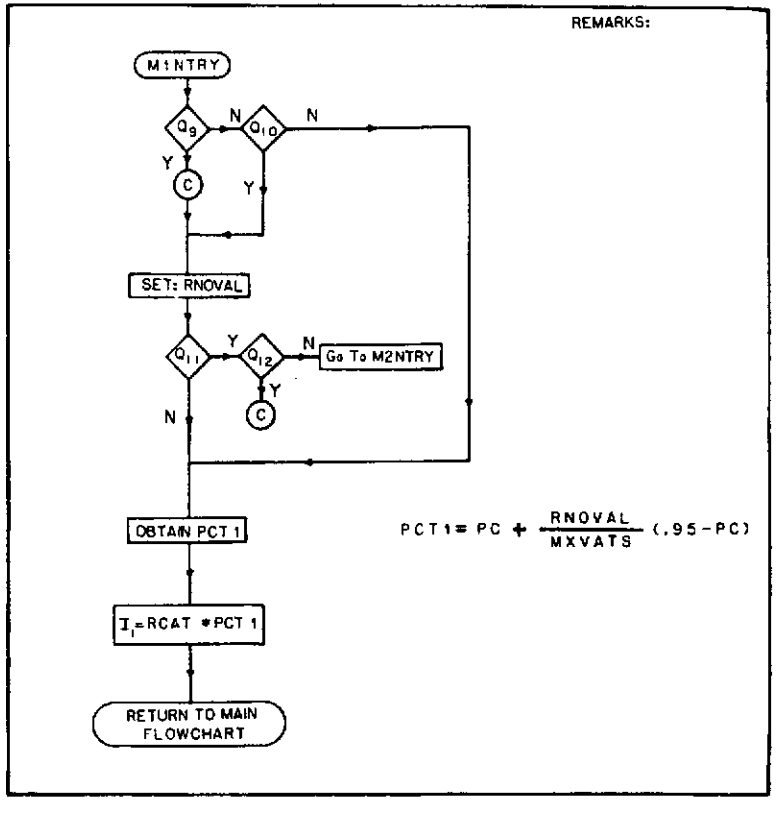

Figure 7.4.—Flowchart for module 1, SSH.

7.4.1.2 **Module 1 Procedure (fig. 7.4).** This module comes closer than any other in estimating a value for FAFP based on observed precipitation data. The key variables RNOVAL and MXVATS are based on direct observation, even though in some circumstances uncertainty surrounds the accuracy of these observations. The actual values selected depend on the placement of the DSL (sec. 3.2.1) in the vicinity of the storm under consideration. Additionally, an analytical judgment must be made concerning the storm mechanism that resulted in MXVATS and RNOVAL. If there is more than one storm mechanism involved in the storm, the value selected for RNOVAL must result from the same mechanism that produced MXVATS.

The following questions are asked in module 1:

Q.9. Is this the first time in this module for this storm?

Q.10. Has the analyst just arrived here from module 4 to do a review?

Q.11. Is RNOVAL equal to MXVATS?

Q.12. Is a review of the data and assigned values for the variable needed?

If it is a good assumption that RNOVAL will usually be observed at a lower elevation than MXVATS, then there is a bias toward relatively large values for PCT1 in relation to the other percentages from the other modules, since total or cumulative precipitable water usually decreases with increasing elevation. The viability of PCT1 depends on the density of good precipitation observations on the date the storm occurred.

7.4.1.3 **Module 2 Procedure (fig. 7.5).** In this module, the average depth of precipitation for a given area-duration category is conceived of as a column of water composed of top and bottom sections (where the bottom section can contain from 0 to 95 percent of the total depth of water). The limit to the top of the bottom section is set by the parameter LOFAC. The bottom section is conceived to contain only a minimum level of FAFP for the storm. The top section contains precipitation that results from orographic forcing, and perhaps additional atmospheric forcing. The percent (if any) of the top section that results from atmospheric forcing is determined by the F-type and B-type correlations. The value computed for LOFAC is sensitive to the accuracy of the isohyetal analysis for the storm. This sensitivity must be taken into account when evaluating module 2 procedures in column E of module 5.

The procedure in which the precipitation is divided into two sections, is represented also in the expression for PCT22, which may be rewritten as:

$$PCT22 = PCT2\left(1 - \frac{LOFAC}{MXVATS}\right) + \frac{LOFAC}{MXVATS}$$

There are three terms on the right-hand side of the above equation. The rightmost of these terms is the minimum level of FAFP for the whole column expressed as a percent of the total and is the bottom section of the idealized column described above. The product of the first two terms on the right-hand side of the equation describes the top section of the idealized column, where PCT2 is the percent of the top section arising from atmospheric forcing and the second term is the depth of total precipitation minus the minimum level of FAFP expressed as a percent.

LOFACA is set to zero and LOFAC becomes zero when a good correlation cannot be found between any of the isohyets and the elevation contours upwind of the storm center. Zero is the numerical value that is appropriate for a minimum level of FAFP for the storm. Here it is assumed that the bottom section of the idealized

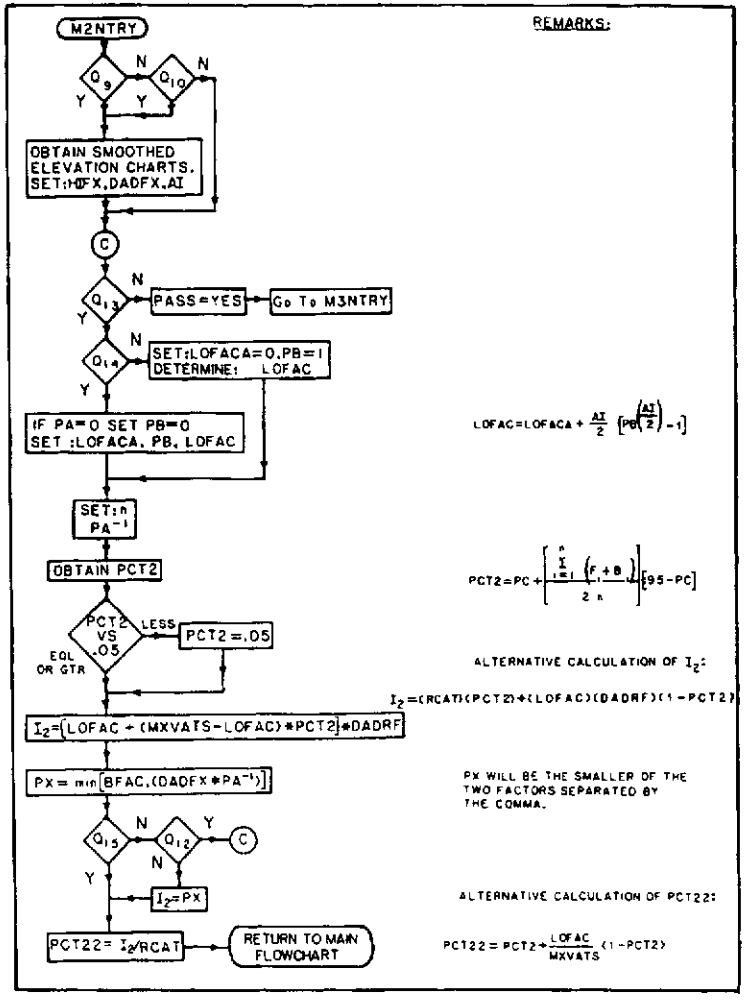

Figure 7.5.--Flowchart for module 2, SSM.

column is empty (minimum level of FAFP = 0), and both F-type and B-type correlations will determine the appropriate level of FAFP for the storm. The F and B correlations, to properly establish the appropriate FAFP, are determined nearby and upwind from the storm center.

As in module 1, an analytical judgment must be made on storm mechanism. In module 1, it was required that MXVATS and RNOVAL are the result of the same dynamic process. In module 2, it is necessary to determine that RNOVAL and HIFX are the result of the same atmospheric forces (storm mechanism).

The following questions are asked in module 2:

Q.9. Is this the first time in this module for this storm?

Q.10. Has the analyst just arrived here from module 4 to do a review?

Q.12. Is a review of the data and assigned values for the variable needed?

Q.13. Can it be determined which isohyetal maxima control(s) the average depth for the category selected?

Q.14. Is there good correlation between some isohyet and the elevation contours in the orographic part of the storm near the storm center?

Q.15. Is I_2 less than or equal to PX?

A feature of module 2 not to be overlooked is the consequence of a negative response to question 15 accompanied by a negative response to question 12. In this case an arbitrarily defined upper limit is set on PCT22 and I_2. The upper limit will be the smaller of two numbers. The selection of BFAC as one of these numbers is obvious when one considers that orographic forcing may be either positive or negative. The second factor is a consequence of the concept that the larger PA becomes, the more likely the second factor represents the true level of FAFP, since with a large value of PA the largest observed rainfall amount in the nonorographic portion is more likely to represent a true upper limit.

LOFAC is always a number equal to or slightly less than LOFACA. This is so because it is possible that the minimum level of FAFP is reached before the arbitrarily set analysis interval allows it to be "picked up." It is reasoned that the larger the area "occupied" by the LOFACA isohyet in the nonorographic part of the storm, the more likely that the analysis interval has "picked up" the described depth. When there is no nonorographic portion to the storm, the parameter PB, used to set a value for LOFAC, becomes undefined (see definition of PB). Consequently, in the module 2 FLOWCHART it must be determined whether a nonorographic portion of the storm exists when there is an affirmative response to question 14. If so, a reasonable value for PB is zero. The consequence of a negative response to question 14 is that LOFACA must be zero. Regardless of whether or not a nonorographic part of the storm exists, LOFAC must not be less than zero and this is ensured by setting PB equal to 1.

7.4.1.4 **Module 3 Procedure (fig. 7.6).** This module uses meteorological and terrain information to evaluate an appropriate level of FAFP. This is accomplished through evaluation of P_a and A_o.

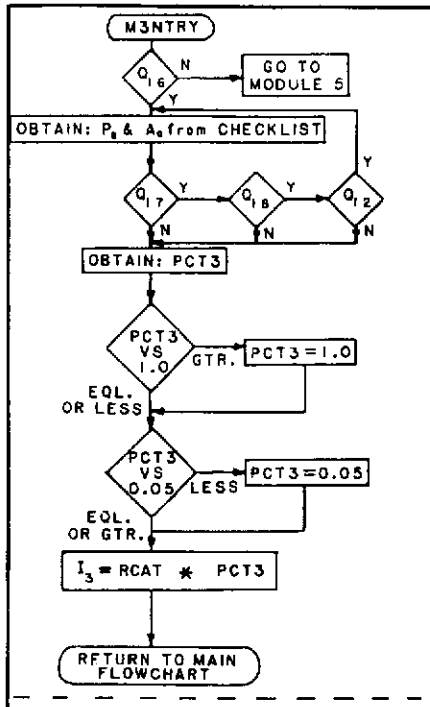

P_a CHECKLIST

Cat. Data	Parameter	A (✓)	B .05-.95	C 1-3	D B*C
Surface	Iso. Ptn. Fronts Waves Sq.Ln. Other				
Upper Air	PVA/SW Cutoff Blocking JetStm Other				
Rawinsonde	Stability Shear Other				
Satellite	Diver. Merger MCC Other				
Radar	LEWP Merger Others				
Other					
Duration (%)					
Totals =					
P_a = Total D/Total C =					

A_o CHECKLIST

Parameter	A Phys. Val.	B 0-±.95	C 1-3	D B*C
Inflow Direct				
Inflow Speed				
Gradient of Elevation				
Stability				
Other				
Duration (%)				
Totals =				
A_o = Total D/Total C =				

REMARKS

$$PCT3 = PC + \frac{P_a}{P_a + A_o}(.95 - PC)$$

LEGEND

PVA = Positive Vorticity Advection
MCC = Mesoscale Convective Complex
LEWP = Line Echo Wave Pattern

Figure 7.6.—Flowchart for module 3, SSM.

The following guidelines are provided to aid in the evaluation of P_a on the checklist given in the flowchart (fig. 7.6):

1. Use column A to indicate (by a checkmark) the presence of one or more features which infer positive vertical motion, or which may contribute toward an efficient storm structure.

2. Take as a basis for comparison an idealized storm which contains the same features or phenomena that were checked off in column A and indicate in column B, by selecting a number between 0.05 and 0.95, the degree to which the effectiveness of the selected actual storm features/phenomena (in producing precipitation) approaches the effectiveness of the same features/phenomena in the idealized storm. Where more than one feature/phenomenon is selected for a given category of meteorological information, it is the aggregate effectiveness which is considered and recorded in column B.

3. Repeat steps 1. and 2. for each category (surface, upper air,..., others) of meteorological data.

4. If the quantity and quality of the information permits, the degree of convective-scale forcing may be distinguished from forcing due to larger scale mechanisms. If convective-scale forcing predominates for some area/duration categories and larger scale forcing at others, then the value assigned in column B may vary by area/duration category; i.e., the same effectiveness value may be different for each category of a given storm.

5. In column C an opportunity is given to assign one category a greater influence on P_a in relation to the others by assigning weighted values. For each applicable category the value in column D is the product of columns B and C. P_a is obtained by dividing the total of column D by the total of column C.

6. Meteorological data categories, for which there is not sufficient information from a particular storm, are disregarded in P_a calculations for that storm.

7. When effectiveness changes with the selected duration, the resulting value in column B is weighted by duration; this process is to be distinguished from the weighting mentioned in (5) above.

A_o is a measure of the effectiveness of the orographic forcing effects. The following guidelines are used to aid in evaluating A_o:

1. Indicate in column A the value (in physical units) for the first five parameters. If any of these parameters change significantly during the duration category selected, indicate in the duration box the percent of time each of the values persists. To obtain the largest value in column B (largest effectiveness) observe the joint occurrence of tightly packed isobars (high wind speed) perpendicular to steep slopes for 100 percent of the duration category selected. Another way to look at this is to combine the first three parameters into a vertical displacement parameter, W_o, from the formula $W_o = V * S$, where V is the

component of the wind perpendicular to the slopes for the duration being considered in kt and S is the slope of the terrain in ft/mi. The effectiveness of W_o is then compared with an idealized value representing 100 percent effectiveness. The measured steepness of the slopes in the CD-103 region depends on the width across which the measurement is made. For a small distance (less than 5 mi.) a value of 0.25 is about the largest to be found, while for a large distance (greater than 80 mi.) a value of 0.06 is about the largest. A component of sustained wind normal to such slopes of 60 kt is assumed to be about the largest attainable in this region. Therefore, a W_o of 15 kt for small areas and of 3.5 kt for large areas are the values which would be considered highly effective.

None of the orographic storms studied occurred in places where the measured steepness of the slopes came near to the values just mentioned. Consequently, the vertical displacements observed for small areas were from .02 kt up to near 2 kt and proportionally smaller for the larger areas for these storms. Therefore, the effectiveness value used in the top box in column B was scaled to the values observed in the storms of record; i.e., a W_o of close to 2 kt was considered highly effective for small areas.

The inflow level for the storm is assumed to be the gradient wind level, and it is further assumed that the surface isobaric pattern gives a true reflection of that wind; i.e., the direction of the inflow wind is parallel to the surface isobars and its speed proportional to the spacing of the isobars as measured at the storm location. When rawinsonde observations are available in the immediate vicinity of the storm, they are used as the primary source of information for wind direction and speed.

When there is a sufficiently large number of wind observations, the average values of direction and speed are used for the duration considered. If the level of wind variability is large for the duration considered, the representativeness of the data is scored low in column C of module 5.

The fourth parameter, stability, must be considered in combination with the first three or W_o. Highly stable air can have a dampening effect on the height reached by initially strong vertical displacement (and consequently, the size to which cloud droplets can grow). In a highly unstable condition, vertical displacements of less than 2 kt can, through buoyancy, reach great height, thereby producing rainfall-sized droplets. The effectiveness value for stability is placed in the second box from the top in column B. Weighted values corresponding to the two top boxes of column B are placed in the two top boxes of column C to reflect the combined effects of W_o and stability; i.e., in the case where instability causes moderately weak displacements to grow, the stability "effectiveness" would be weighted strongly (given a 3) and the combined first three parameters weighted weakly (given a 1).

Entries in the other considerations box (for example, the shape of terrain features which may cause "fixing" of rainfall) need not be considered as dependent on the first four parameters.

2. The value for A_o is then obtained in the same manner as described in guideline 5 for P_a.

3. When evidence indicates that the orographic influence is negative; i.e., taking away from total possible precipitation, the values in column B are made negative and when the conditions are borderline between positive and negative, they are made zero. Negative orographic influence, when occurring in a storm where the atmospheric forcing approaches its conceptually optimum state, may cause some category values of PCT3 to exceed 1.0 resulting in FAFP larger than the total storm average depth for that category. The conventions of module 3, however, do not permit values of PCT3 to exceed 1.0.

4. The remarks section of module 5 should be used to document where the elevation gradients (ΔZ) were measured. For small areas, this would typically be at a point upwind of the largest report/isohyet. For larger areas, the average value from several locations may be used, or if one location is representative of the average value, it alone may be used. Sometimes the gradient is measured both upwind and downwind of the storm center (where inflow wind is used) if the vertical wind structure is such that a storm updraft initiated downwind may be carried back over the storm location by the winds aloft to contribute additional amounts to the "in place" amounts.

The overriding importance of applying this module only to major storms cannot be overstressed. The consequence of "running through" a frequently observed set of conditions is that, by definition, the values for <u>both</u> P_a and A_o will have to be quite small. When both parameters are small (less than about .4) a sensitivity study (not included here) showed that small differences in the values assigned to P_a and A_o (the independent variables) would produce large differences in the value of the dependent variable (PCT3). However, it does not follow that the definition of P_a which permits a lower limit of zero is incorrect. A storm can reasonably be postulated in which the extreme amounts were traceable to exceptional orographic forcing and, thus, <u>both</u> terms would not be small (PCT3 in this case is 5 percent). Not only are "infinite" values for PCT3 removed by the FLOWCHART constraints, but a value of zero in the denominator of the ratio $P_a/(P_a + A_o)$ is a violation of the concept that if the orographic forcing negated the atmospheric forcing, no matter how large, little or no precipitation should occur.

The "model" envisioned in module 3 (as distinguished from the "model" of module 2 just discussed) follows from the concept that FAFP is directly proportional to the effectiveness of atmospheric forcing and inversely proportional to the effectiveness of the orographic forcing mechanisms. The rate at which an imaginary cylinder fills up (whose cross-sectional area is the same as the area category being used) is directly proportional to the condensation rate producing the precipitation which falls into the cylinder. The paramount factor determining the condensation rate is the vertical component of the wind resulting from both atmospheric (P_a) and orographic (A_o) forcing.

The following questions are asked in this module:

Q.12. Is a review of the data and assigned values for the variable needed?

Q.16. Does there exist, or is there sufficient information available to construct, a map of where at least 1 in. of precipitation did or did not occur for this storm?

Q.17. Is A_0 less than zero?

Q.18. Is (are) the storm center(s) incorrectly located on the terrain map?

The remaining portions of the module 3 FLOWCHART, not discussed above, are simple and straightforward.

7.4.1.5 **Module 4 Procedure (fig. 7.7).** It is not contemplated that a computer program will be coded from the MAIN or MODULE FLOWCHARTS because the determination of the appropriate PCT's and I's is done easily manually. There is no real requirement for the variable PASS to be in the module 4 FLOWCHART. It is included only to make it obvious that the first part of the FLOWCHART should be skipped when returning to module 4 from a review of data in modules 1 and 3. The purpose of this module is simply to create two additional indices of FAFP on the assumption that an averaged value may be a better estimate than one produced in modules 1, 2, or 3.

A preliminary test of the SSH by six analysts each using six different storms showed that it was quite rare that one analyst would select a high (low) value for a PCT when other analysts were selecting low (high) values given that the interval range was the one shown in the right-hand remarks section of the module 4 FLOWCHART. Thus, a review is required of relevant information when an average percentage is to be created from individual percentages differing by two intervals.

PCT1 was not averaged with PCT2 because modules 1 and 2 conceive of the idealized column of precipitation representing the average depth for a given area-duration category in different ways; i.e., there is no minimum level of FAFP considered in module 1.

The following questions are asked in this module:

Q.12. Is a review of the data and assigned values for the variable needed?

Q.19. Is I_5 less than or equal to PX?

Those concepts of the module 4 FLOWCHART not discussed above are straightforward.

7.4.1.6 **Module 5 Documentation (fig. 7.8).** It should be noted again that even though the MAIN FLOWCHART shows that module 5 is not used until module 2 and/or module 4 have been completed, this was done only to keep the diagramming of the MAIN FLOWCHART and the MODULE FLOWCHARTS relatively uncluttered by variables not related to the task at hand. Even though documentation can await completion of module 2 and/or module 4, it is preferable to document the value assigned to a variable as soon as it is determined.

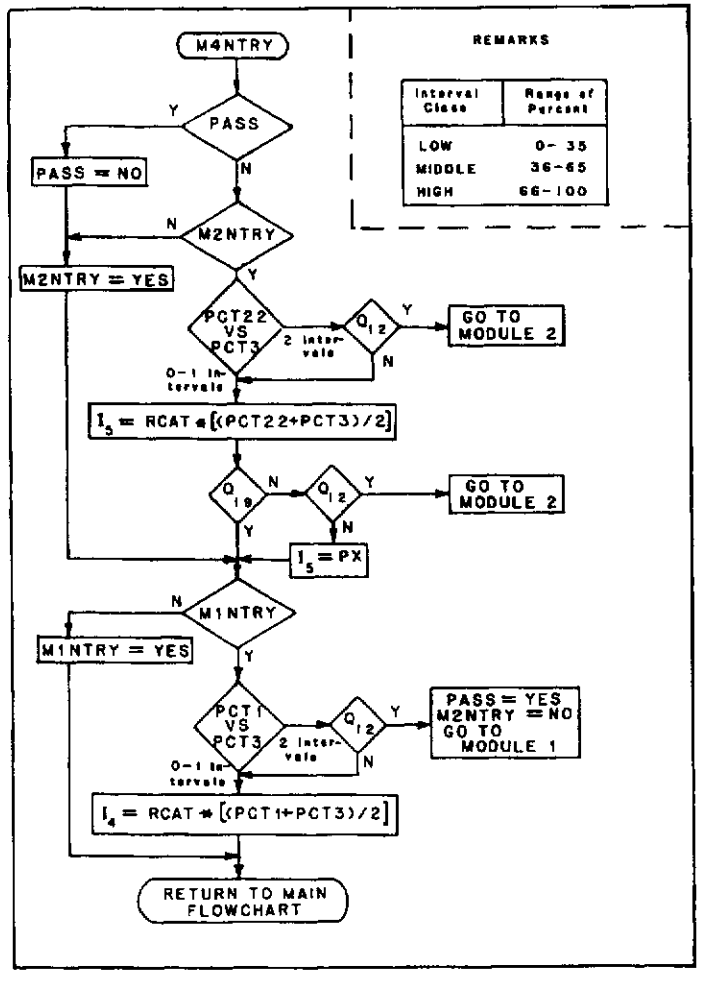

Figure 7.7.—Flowchart for module 4, SSH.

Obviously, the scheme is designed to permit selection of I_1, I_2 or I_3 when there is a strong preference for one of them and to select I_4 or I_5 when there is little overall preference. In the case where there is some preference for a given module and some agreement between the index values generated therefrom, the analyst must make a decision as to which index is to be preferred. The range of values used to represent index agreement categories was based on values actually selected in a test involving six different analysts working with six different storms.

The final value selected for FAFP is determined by the largest value in column F. If the same value has been computed for more than one index value, the index with the largest subscript is selected (I_2 over I_1, I_3 over I_2).

7.5 Example of Application of SSM

One of the most critical storms for determining the PMP in the CO-103 region occurred at Gibson Dam, MT on June 6-8, 1964 (75). Figure 7.9 shows the completed module 5 worksheet for this storm for the 24-hr 10-mi^2 precipitation. The final percentage selected for this storm was 61 percent for PCT5. This gave an FAFP of 9.1 in.

7.6 Application of SSM to this Study

The SSM was used in this study to estimate FAFP for just one category, 10 mi^2 and 24 hr. This category was selected as the key (index) category for this study for several reasons. The first reason relates to area size. In determination of the effects of orography on precipitation, it is easiest to isolate these effects for the smaller areas. In addition, if larger area sizes were used, the determination of the orographic effects for computation of the final PMP values would have been very complicated. At some transposed location, the increase in precipitation as a result of orographic effects for a very small area can be determined with little ambiguity. If a larger area (e.g., 1,000 mi^2) was used, the effect of terrain at a transposed location would be related directly to the shape and orientation of the 1,000-mi^2 area selected. This factor, therefore, indicated use of the 10-mi^2 area as most appropriate.

The 24-hr duration was selected because of the reliability of data for this duration. For storms before 1940, the amount of recording raingage information is relatively sparse. Determination of amounts for durations less than 24 hr for these storms is based on only limited data. This indicates use of a storm duration of 24 hr or longer. A review of the important storms in this region shows several that did not last the entire 72-hr time period of interest in the present study. Most notable of these are the Gibson Dam, MT storm (75) and the Cherry Creek (47), Hale (101), CO storms. These two factors made selection of the 24-hr duration most appropriate. Selection of this duration also had the advantage of minimizing the extrapolation required to develop PMP estimates for the range of durations required in the study.

DOCUMENTATION AND INDEX SELECTION

STORM ID/DATE, REMARKS: Gibson Dam, MT (75) 6/6-8/64

MODULE	PARAMETER	VALUE			EVALUATION SCALE: COL.D 0-9; COL.E 1-9 MODULES 1-3: COL.F: IS THE SUM OF COLS. D&E. COL.D: HOW ADEQUATE IS THE INPUT INFORMATION FOR THE REQUIREMENTS SET BY MODULE'S TECHNIQUE. COL.E: HOW LIKELY IT IS THAT THIS TECHNIQUE WILL ESTIMATE THE CORRECT INDEX VALUE BASED ON ITS ASSUMPTIONS? FOR MODULE 4 SEE SELECTION RULE. OVERALL RULE: SELECT INDEX VALUE WITH LARGEST COL. F SCORE. LARGEST SUBSCRIPT BREAKS TIES.			
					REMARKS	D	E	F
5	CATEGORY	10mi²/24 hr						
	RCAT	10.7						
	BFAC	14.2						
	MXVATS	16.4						
	DADRF	.91						
	PA	.40						
	PC	0						
1	RNOVAL	7.5						
	PCT1	.43						
	I_1	6.4				7	7	14
2	AI	1.0						
	LOFACA	6.0						
	PB	.1						
	LOFAC	5.7						
	HIFX	6.0						
	DADFX	5.5						
	PA^{-1}	2.5						
	PX	13.7				7	6	13
	n	1						
	$\sum(F_i+B_i)$	.8+.4 = 1.2						
	PCT2	.57						
	I_2	10.7						
	PCT22	.72						
3	COLUMN	A	B	C	ma = moist adiabatic saturated na = not applicable Grad. Elev measured upwind of isohyetal max between 1000 and 7000 ft			
	INFLOW DIR.	090						
	INFLOW SPD	23mi						
	GRAD. ELEV.	.045	.8	1				
	W_o	1.0						
	STABILITY	ma	.6	1				
	A_o	.7				8	7	15
	SURFACE		.7	1				
	UPPER AIR		.85	2				
	RADB		.6	1				
	SATELLITE		na					
	RADAR		na					
	F_a	.75						
	PCT3	.49						
	I_3	7.3						
4	(PCT22 + PCT3)/2	.61						
	I_5	9.1						15
4	(PCT1 + PCT3)/2	.46						
	I_4	6.9			RETURN TO MAIN FLOWCHART			15

Figure 7.9.—Completed module 5 documentation form for Gibson Dam, MT storm (75) of June 6-8, 1964.

HMR 57 CHAPTER 6. STORM SEPARATION METHOD

6.1 Introduction

The storm separation method (SSM) is an outgrowth of practices that were initiated in the late 1950's for PMP studies in orographic regions. HMR 36 (USWB, 1961) is one of the earliest reports to discuss PMP development in terms of orographic and convergence precipitation components. Convergence precipitation in this context is the product of atmospheric mechanisms acting independently from terrain influences. Conversely, orographic precipitation is defined as the precipitation that results directly from terrain influences. It is recognized that the atmosphere is not totally free from terrain feedback (the absolute level and variability of precipitation depths in some storms can only be accounted for by the variability of the terrain); but cases can be found where the terrain feedback is either too small or insufficiently varied to explain the storm precipitation patterns and in these cases, the precipitation is classified as pure convergence or non-orographic precipitation.

PMP studies, such as HMR 36, 43, and 49, were based on determination of convergence and orographic components through procedures that varied with each report. With the development of HMR 55A (Hansen et al., 1988), a technique was utilized that had some similarities to previous studies, but was based on determination of convergence amounts from observed storms. Convergence precipitation in that report was referred to as free-atmospheric forced precipitation (FAFP). The technique used in HMR 55A is complex and involves the analyst tracking through a set of modules in which knowledge of observed conditions and experience are used to arrive at estimates of the FAFP. The estimates are in turn weighted, based on the analyst's judgment of the amount and quality of overall information, to obtain a result. This process has been referred to as the storm separation method (SSM) and is described at considerable length in HMR 55A.

Since the development of the SSM in HMR 55A, the procedure has been applied in a number of subsequent studies (Fenn, 1985; Miller et al., 1984; Kennedy, 1988; and Tomlinson and Thompson, 1992). Through these various developments, the SSM has undergone minor refinements. The entire development discussed in HMR 55A will not be repeated here, but readers interested in these details will find a reprint of the pertinent chapter (Chapter 7) from HMR 55A in Appendix 3 of this report. Similar information is contained in the 1986 edition of the WMO Manual for Estimation of Probable Maximum Precipitation (WMO, 1986).

The process of estimating FAFP from a storm for a given area size and duration is achieved by using the hydrometeorological information available for the storm to answer certain questions. These questions are contained within several modules which constitute the body of the SSM.

The hydrometeorological information about a storm may be missing over large areas with respect to the storm's full precipitation pattern; or the information when available may be unevenly distributed; or it may be biased or contradictory. In view of such informational dilemmas, a decision about the level of FAFP for a storm may have to accommodate a fair amount of uncertainty. The questions asked in the SSM modules are formulated in such a way that analysts with different levels of experience could estimate different amounts of FAFP. Under such circumstances a consensus among analysts often leads to the best FAFP estimate for a storm, but the consensus process is not a necessary part of the SSM.

Because of the extensive information provided by the storm analysis program and the number of storms studied, the SSM technique was considered most appropriate for the present study. The technique was applied directly according to the original guidance, subject to the modifications described in the following section.

6.2 Changes to the Previously Published SSM

The remainder of this Chapter covers modifications to the modular development presented in Appendix 3. This discussion covers specific changes in detail that may be beyond the casual reader's interest.

Several details concerning questions and procedures used in the SSM were changed in this report from their formulation in HMR 55A. For example, in Module 0, which provides guidance to the analyst regarding decisions on the adequacy of available data, the adjective "reliable" was replaced by "unbiased" in questions 5 and 6 (see Appendix 3). This was done to clarify the fact that isohyetal analyses derived from the isopercental technique, even though reliable, are created based on an assumption which Module 2 attempts to prove. The need to avoid such a fallacy is made more clear by use of the adjective "unbiased" and, consequently Module 2 was not used to analyze any of the storms in this study.

Maximization of the index values was accomplished on the storm separation worksheet (Module 5, see Figure 6.1). This figure is an updated version of Figure 7.8 from HMR 55A (Appendix 3). Some new terms introduced in Figure 6.1 of this report are explained as follows:

$IMAX_n^{1000}$ = the index value of non-orographic precipitation for the storm center, adjusted to 1000 mb and moisture maximized as obtained from the module (n) indicated by the subscripts 1, 2, 3, 4, and 5,

IPMF(SC) = In-place maximization factor applicable at the storm center,

V.ADJC(SC) = A factor used to adjust values (to sea level) of precipitation obtained at elevations above sea level,

IPMF(NO) = In-place maximization factor at the location of RNOVAL[1],

BE(SC)
BE(NO) = Barrier elevation at the storm center (SC) and at the location of RNOVAL (NO),

V.ADJ(NO) = A vertical adjustment factor used to adjust the value of RNOVAL to sea level,

DP/SST(X)
DP/SST(0) = The upper limit (X) and observed storm day (0) values representing storm moisture content,

H.ADJ = Horizontal adjustment factor,

I_1^{EL} = The value of RNOVAL, not yet reduced to sea level, and

I_2^{EL} = The calculated value of non-orographic precipitation at the storm center, not yet reduced to sea level.

Module 1 considers the observed precipitation data, where the value of RNOVAL (the highest non-orographic rainfall representative of the storm center) was adjusted to a common barrier elevation (sea level). This avoided the bias toward large values for PCT 1 (percent of storm rainfall that is non-orographic) mentioned in paragraph 7.4.1.2 of HMR 55A. If there was a gradient in the field of maximum 12-hour persisting dew points (see section 4.2) between the location of the storm center and the locations of RNOVAL, a horizontal adjustment factor, H.ADJ, was applied to RNOVAL. It has been assumed that RNOVAL is an appropriate depth of non-orographic precipitation for the area category selected in Module 0. This observation (RNOVAL) is acceptable for an area of 10 mi^2, but this assumption becomes less reliable for larger area sizes. This assumption is compatible with assumption 3 stated in Section 7.3.1.2 of HMR 55A.

---

[1]See GLOSSARY, Table 6.1, for definition of terms extracted from HMR 55A Chapter 7 (enclosed as Appendix 3).

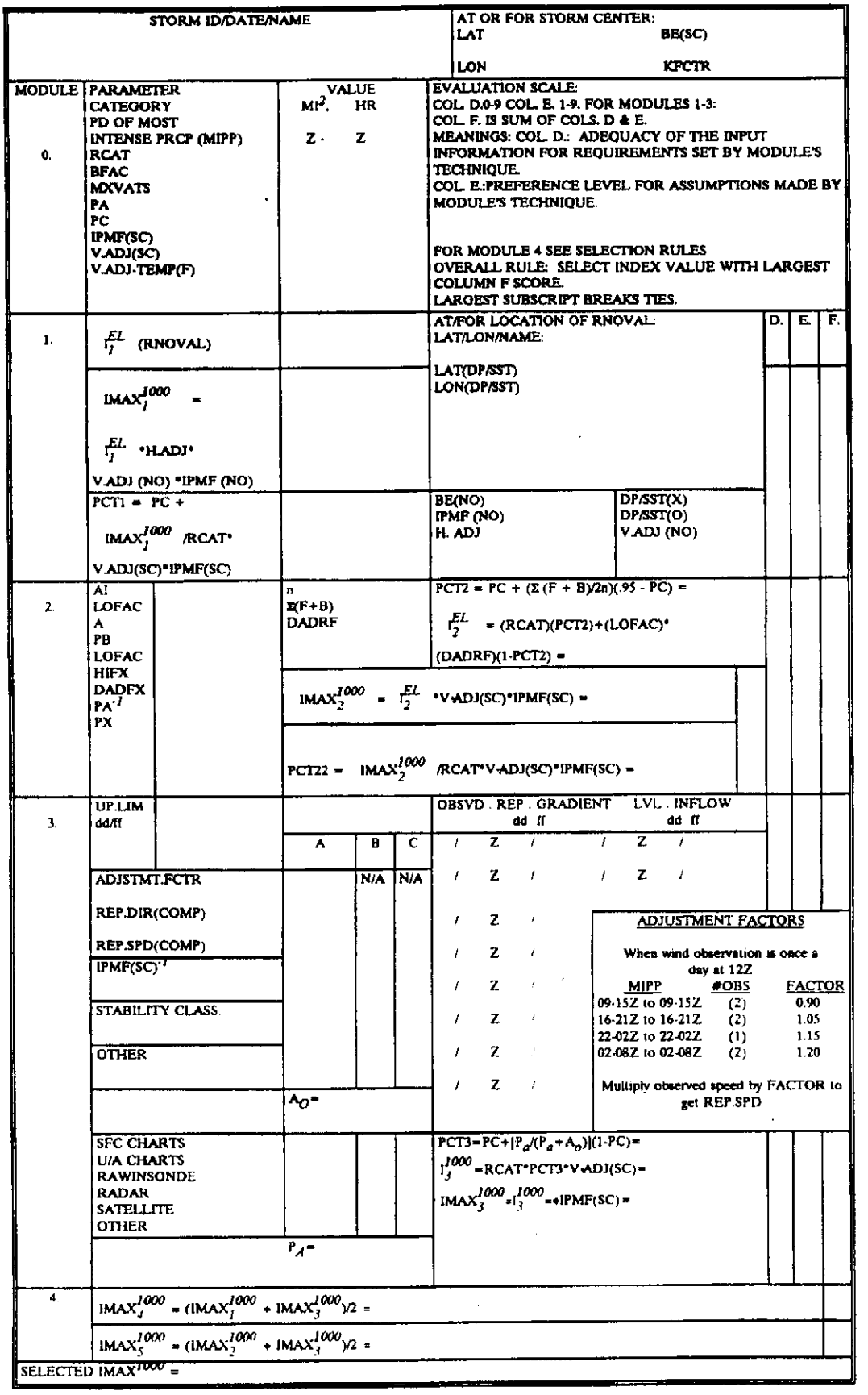

Figure 6.1 -- Storm separation method worksheet; Module 5.

Table 6.1.-- Glossary of terms modified in storm separation method.	
A_o:	Term for effectiveness of orographic forcing used in Module 3, (see also P_a). Varies between 0 and 95 percent.
MXVATS:	Average depth of precipitation for the total storm duration for the smallest analyzed area less than 100 mi^2 (from pertinent data sheet for storm).
I_1:	That part of RCAT attributed solely to atmospheric processes and has the dimensions of depth. Subscript 1 associates application to Module 1.
P_a:	Term for effectiveness of actual atmospheric mechanisms in producing precipitation as compared to conceptual "perfect" effectiveness. Varies between 5 and 95 percent.
PC:	Used in calculations of modules to take into account the contribution of non-orographic precipitation to total FAFP (that includes contribution from orographic areas). Varies between 0 and 95 percent.
PCT 3:	The percentage of non-orographic precipitation in a storm from the third module based on comparison of storm features with those from major non-orographic storms.
RCAT:	The average precipitation depth for storm area size and duration being considered.
RNOVAL:	Representative non-orographic precipitation value that is the highest observed amount in the non-orographic part of the storm.
W_o:	A vertical displacement parameter, the product of the wind component perpendicular to the slope (for duration considered) and the slope in feet/miles.

The flowchart used for Module 1 is shown in Figure 6.2, and modified only slightly from that used in HMR 55A to reflect adjustments to sea level. Since hourly values of precipitation were available from automated analysis procedures, PCT1 did not have to be calculated from the variables RNOVAL and MXVATS. Consequently, the value of PCT1 for the total storm duration could be assumed to be the same as the index duration (24-hours). The index depth of non-orographic precipitation from Module 1, was therefore obtained directly from the depth for the index duration at the site selected for RNOVAL. However, since PCT1 is necessary in Module 4, it was derived from the relationship

$$PCT1 = PC + \frac{IMAX_1^{1000}}{(RCAT * V.ADJ(SC) * IPMF(SC))(0.95 - PC))}.$$

The ratio, $IPMF(SC)^{-1}$, listed in Module 3 in Figure 6.1, is relatively large when "observed" storm moisture is close to its upper limit and vice versa. Thus, from a strictly moisture content point of view, values in Column B would be relatively large when this parameter is relatively large and vice versa.

In Module 3 shown in Figure 6.3, the orographic parameter, A_o, was derived using a somewhat revised procedure, when compared to that in Appendix 3. The vertical displacement parameter, W_o, and the elevation gradient were not used. But, the upper-limit wind speed, which was a constant in HMR 55A, was allowed to vary across the region. The variation was based on extreme wind speed data (Simiu et al., 1979) for 10 United States locations in the northwest and five locations nearby. The optimum inflow direction for orographic storms, used in setting the barrier elevations, was determined for each of the 15 locations. Then at each location, the series of annual maximum speeds and their associated directions were searched to find the largest annual wind speed coinciding with the optimum inflow wind direction. This speed became the first approximation of the upper-limit speed for the optimum inflow direction at the site. This first approximation wind speed was changed only if certain conditions were found, as given in the following rules:

(a) If the first approximation speed was less than the mean speed for all directions in the total sample, the mean speed became the upper-limit speed, while the optimum inflow direction remained the same.

(b) If the first approximation speed was larger than the sample mean but less than the 100-year speed, it was compared with the sample mean plus one standard deviation speed, and the larger of these two became the upper-limit speed, while the optimum inflow direction remained the same.

(c) If the first approximation speed was greater than the 100-year speed, the 100-year speed became the upper limit speed, while the optimum inflow direction remained the same.

An analysis of 30-year return period wind speeds, prepared by Donald Boyd for the National Building Code of Canada (Newark, 1984), and kindly supplied to us by D.J. Webster, Atmospheric Environment Service, Canadian Climate Centre, provided a basis for extrapolating the upper-limit isotachs into Canada.

The component of the wind speed along the direction of optimum inflow, representative of the 24 hours of most intense precipitation, was obtained for each storm being analyzed. This speed was modified by empirical adjustment factors shown in Module 3 of the storm separation worksheet, Figure 6.1.

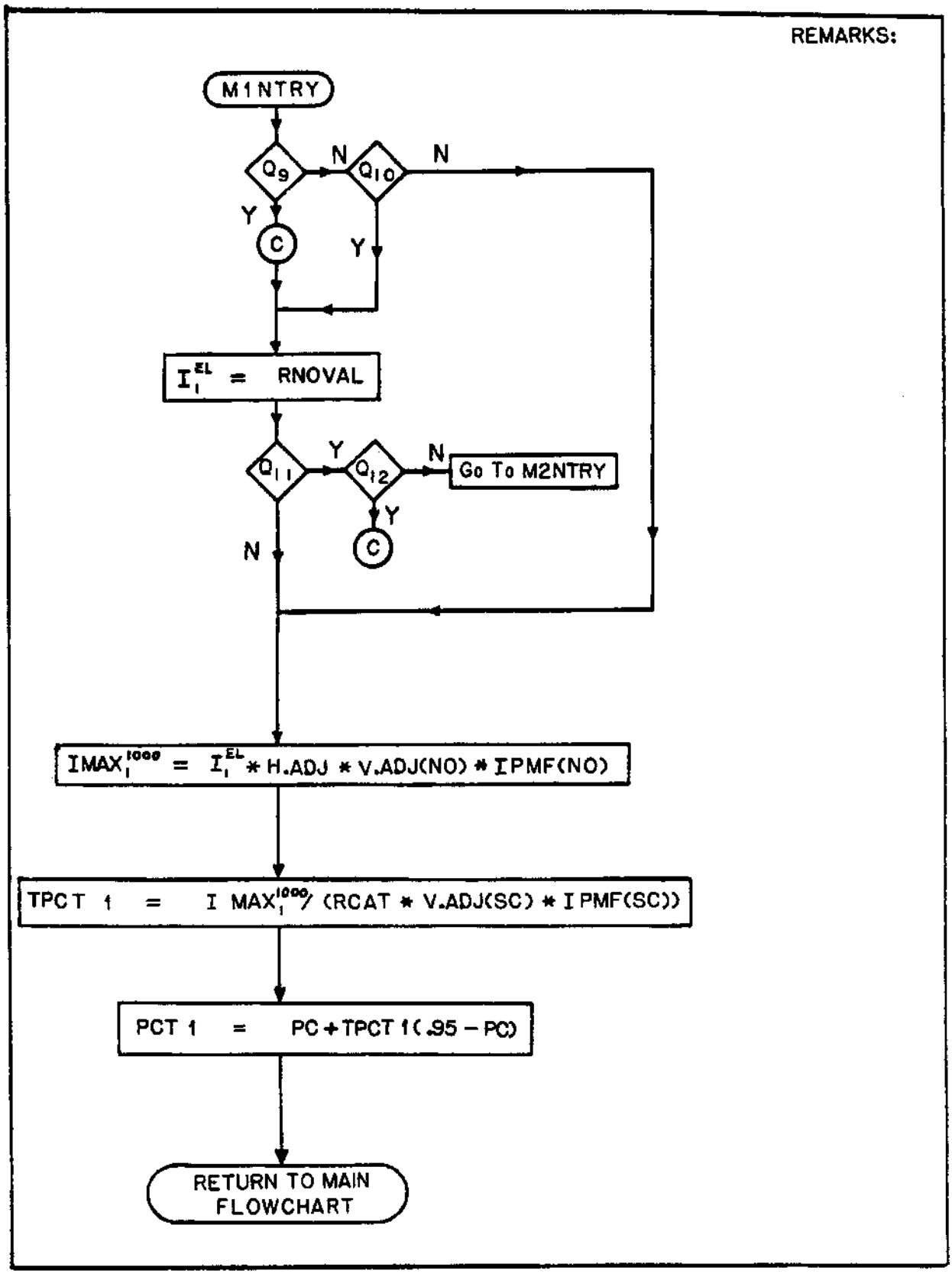

Figure 6.2 -- Module 1 flowchart.

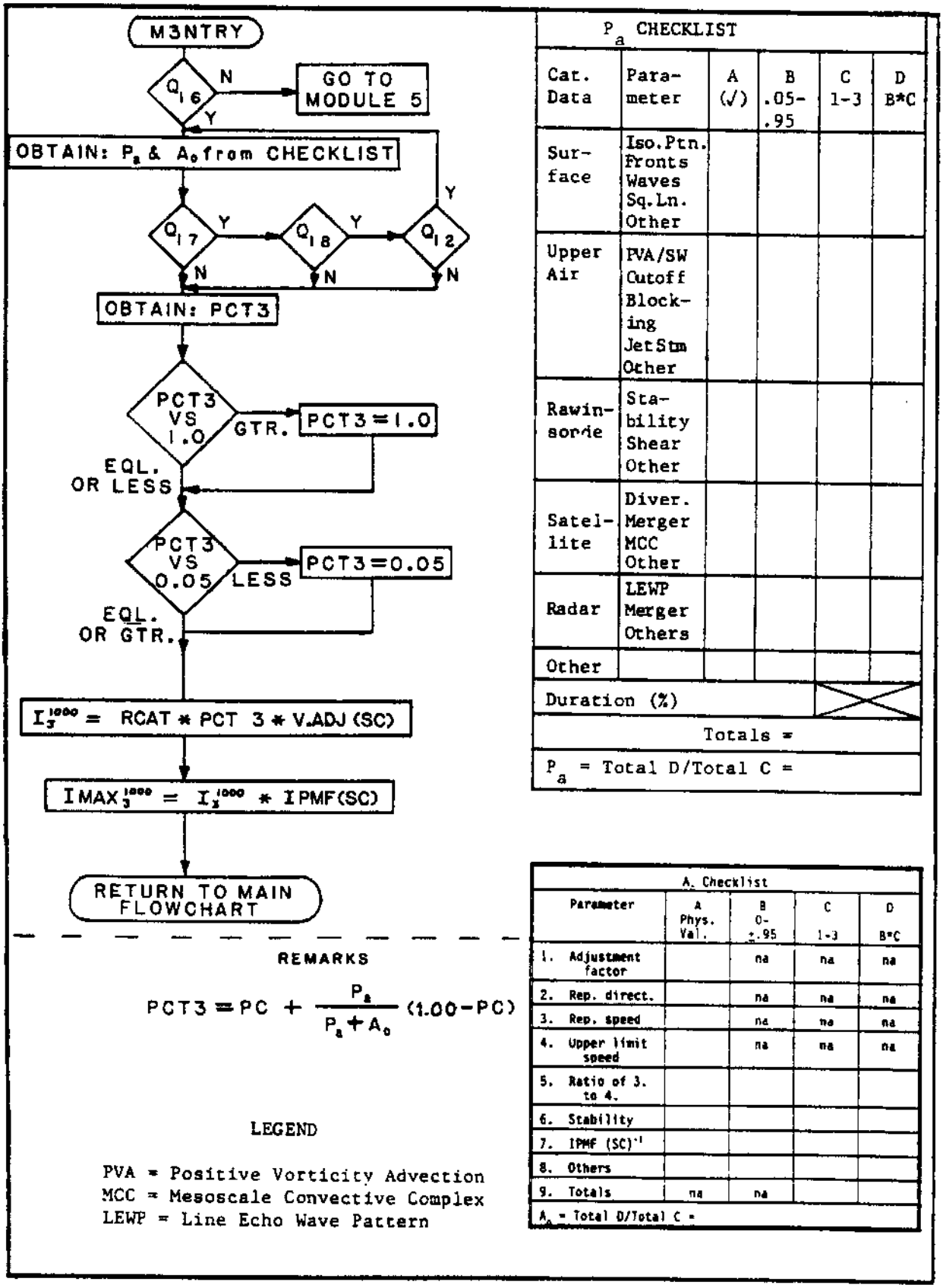

P_a CHECKLIST

Cat. Data	Parameter	A (√)	B .05-.95	C 1-3	D B*C
Surface	Iso.Ptn. Fronts Waves Sq.Ln. Other				
Upper Air	PVA/SW Cutoff Blocking Jet Stm Other				
Rawinsonde	Stability Shear Other				
Satellite	Diver. Merger MCC Other				
Radar	LEWP Merger Others				
Other					
Duration (%)					
Totals =					
P_a = Total D/Total C =					

A. Checklist

Parameter	A Phys. Val.	B 0-±.95	C 1-3	D B*C
1. Adjustment factor		na	na	na
2. Rep. direct.		na	na	na
3. Rep. speed		na	na	na
4. Upper limit speed		na	na	na
5. Ratio of 3. to 4.				
6. Stability				
7. IPMF (SC)$^{-1}$				
8. Others				
9. Totals	na	na		
A_o = Total D/Total C =				

Figure 6.3 -- Module 3 flowchart.

These factors were applied when, during the most intense 24 hours of precipitation, there were only one or two wind observations available at 1200 UTC. These empirical adjustment factors are in the form of ratios based on relations observed in eight recent storms from the storm list in Appendix 1.

These ratios compare the 1200 UTC wind speed(s) noted above to the average wind speeds (when all eight 3-hourly observations are available for the 24 hours of most intense precipitation). This ratio was then divided by the upper-limit speed and the resulting quotient multiplied by 0.95 and put in column B alongside the wind parameter in the A_o portion of Module 3. Because both upper-limit speed and direction (which incorporates moisture availability) are involved in the evaluation of the inflow parameter, the weight assigned to it in column C of Module 3 should be higher than for the stability parameter, assuming a good sample of inflow winds for a storm is available. Here again, the decision to use wind speeds in this section that are at a level less than the theoretical maximum was made as an attempt at limiting the compounding of maxima.

The formulation for PCT3, shown in HMR 55A (Appendix 3) as equal to the sum of the non-orographic rainfall component and a term that accounts for the effectiveness of the storm's atmospheric mechanism to produce precipitation was changed to:

$$PCT3 = PC + \frac{P_a}{P_a + A_o}(1.00 - PC).$$

This was done because, by original definition, P_a and A_o could never exceed a value of 0.95. The formulation used previously had a bias toward lower estimates of FAFP built into it in the term (0.95 - PC). This bias was eliminated by replacing 0.95 by 1.00 in this term.

Figure 6.4 attempts to clarify the use of stability in setting a value for A_o in Module 3. The evaluation of the influence of the stability set in column B of the module is related to variations from the pseudo-adiabatic lapse rate and ranges from 0 to 0.95. This range may be subdivided as follows (see Figure 6.4): 0.65 to 0.95 when the observed lapse rates are optimum for producing orographic enhancement of FAFP, 0 to 0.45 when the lapse rates are least conducive for producing orographic enhancement of FAFP, and 0.45 to 0.65 for the remaining cases. The optimum cases are those where the lapse rates on average are in the range 1°C more stable to 2°C less stable than pseudo-adiabatic within 100-mb layers from the surface to 300 mb. The largest value in column B of Figure 6.3 should be associated with the less stable of these cases. Lapse rates least conducive for producing orographic enhancement of FAFP (i.e., those of greatest instability) would be those greater than -4°C from pseudo-adiabatic. The cases greater than +4°C from pseudo-adiabatic, i.e., the most stable cases, would be given the lowest scores in column B.

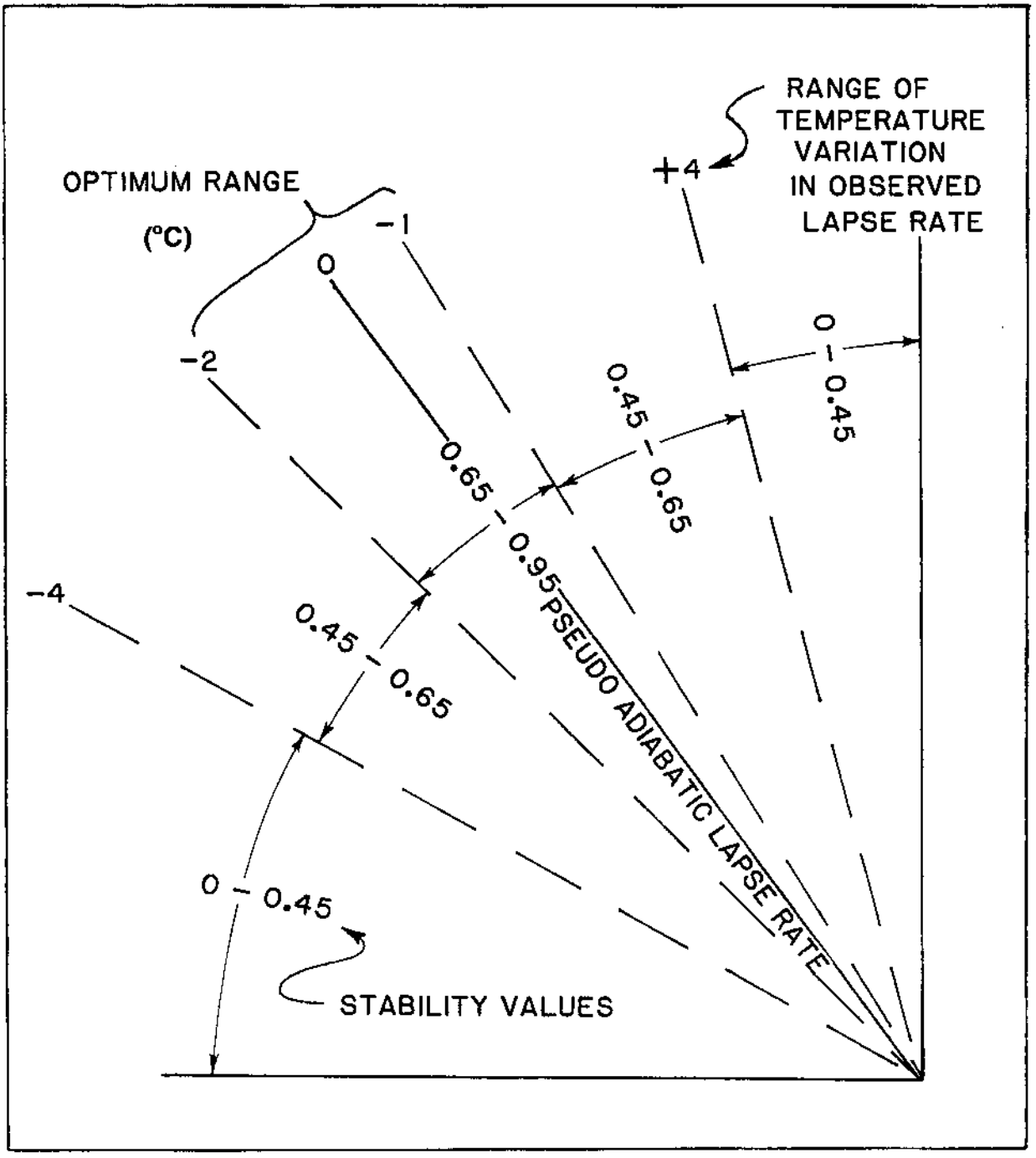

Figure 6.4 -- Schematic diagram to show relative range of stability values compared to the pseudo-adiabatic lapse rate.

It is reasoned that orographic enhancement of FAFP should increase up to some limit with decreasing stability. Beyond that limit (set subjectively at 2°C more unstable than pseudo-adiabatic) as lapse rates approach the dry adiabatic, there should begin decreases in moisture content sufficient to weaken the production of purely orographic precipitation.

Cotton and Anthes (1989) noted that the orographic (described as orogenic precipitation in that report) enhancement of precipitation involves complex problems in the formulation of atmospheric scale interactions and phase changes. The procedures followed to obtain A_o in Module 3 (Figure 6.3) barely scratch the surface of these problems, but a more sophisticated approach awaits the results of continuing research by atmospheric scientists, and no change is offered here.

It is recognized that the lack of upper-air information for most of the earlier storms of record may make use of the stability parameter impossible in the formulation of A_o. For more recent storms, however, if less than complete information was available, this condition limits the value of the weighting assigned to the stability parameter in column C of Module 3.

Finally, a routine was added to each module which asked the analyst the following question. Once a value for FAFP had been obtained, is the implied orographic factor at the storm center satisfactory in relation to the K factor, derived independently from 100-year precipitation-return intensity at the same location? If significant differences in orographic factor could not be resolved, a low valuation would be given in column D to the estimation of FAFP for the module being used. Apart from these changes, use of the SSM in this report was the same as in HMR 55A (see Appendix 3).

As mentioned above, a process related to, but not part of the SSM, was the reconciliation of differing estimates of FAFP by different analysts. Another procedure adopted for this report and related to the SSM, but not part of it was adjustment of finalized FAFP values to a common reference level of the atmosphere for all storms. The reference level used was 1000 mb. Based on the maximum persisting 12-hour 1000-mb dew point at the location of the derived FAFP, the FAFP was changed in the same proportion as the change in water available for precipitation in a saturated, pseudo-adiabatic atmosphere. No change was made in FAFP; however, for storms occurring between sea level and 1000 feet above sea level. This procedure was adopted so that direct comparisons of FAFP could be made easily among all 30 storms analyzed, and so that the sea-level analysis of the 100-year non-orographic component could be used as guidance for analysis of the field of FAFP. It was also the procedure used as part of storm transposition used in creating the index map of FAFP (refer to Chapter 7).

Since we were dealing with FAFP at sea level, the precipitation depth at the elevation of the largest enclosed isohyet might be potentially as large as the depth at a somewhat smaller valued enclosed isohyet, provided that the second center was

located at a higher elevation. In such cases, both centers were evaluated for FAFP, and the results adjusted to sea level.

From the 28 storms centered in the United States and the two storms located in Canada, FAFP values for 50 isohyetal maxima were set. At least one value was set for each storm. In five of the United States storms, one or more centers for which DAD relationships were developed were not analyzed, either because the central value was significantly smaller than that at the principal center or because the centers were very close to one another with no significant difference in value. Depth-area-duration analyses were not done for all of the isohyetal maxima examined by the storm separation method, but were done for all centers which provided controlling values in the analysis of FAFP (Appendix 2).